THE CLIVAR-SPAIN REPORT

ON THE

CLIMATE IN SPAIN

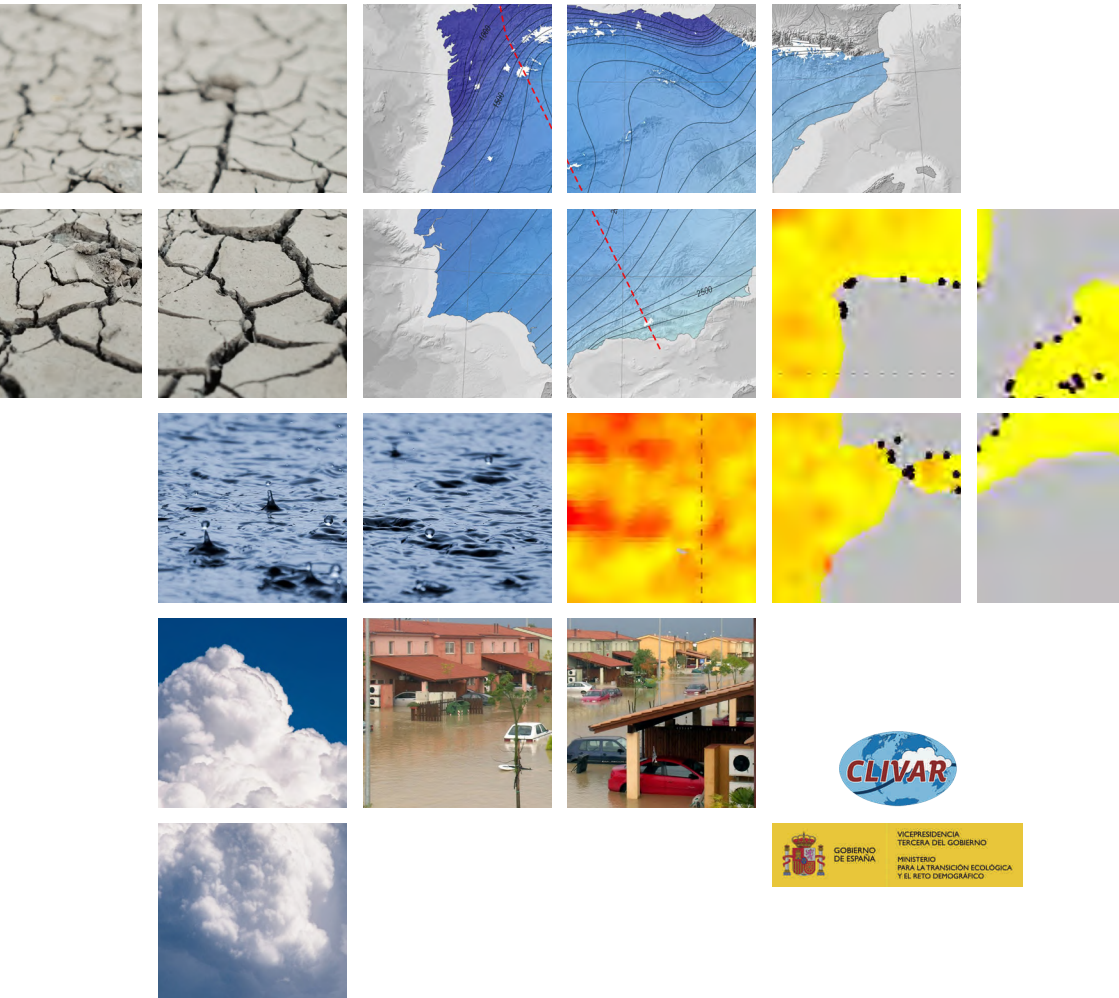

CLIVAR

GOBIERNO DE ESPAÑA

VICEPRESIDENCIA TERCERA DEL GOBIERNO

MINISTERIO PARA LA TRANSICIÓN ECOLÓGICA Y EL RETO DEMOGRÁFICO

Catálogo de publicaciones del Ministerio: https://www.miteco.gob.es/es/ministerio/servicios/publicaciones/
Catálogo general de publicaciones oficiales: https://cpage.mpr.gob.es/

Title: THE CLIVAR-SPAIN REPORT ON THE CLIMATE IN SPAIN
2024 edition

Report coordination by the CLIVAR-Spain committee:
Gabriel Jordà, Isabel Cacho, Daniel Argüeso, Blanca Ayarzagüena, Joaquim Ballabrera-Poy, Omaira E. García-Rodríguez, Alfonso Hernanz, Sixto Herrera, Ana Moreno, Raquel Nieto, Marc Prohom, Jose C. Sánchez-Garrido, Raquel Somavilla

MINISTERIO PARA LA TRANSICIÓN ECOLÓGICA
Y EL RETO DEMOGRÁFICO

® MINISTERIO PARA LA TRANSICIÓN ECOLÓGICA Y EL RETO DEMOGRÁFICO (MITECO)

Edita:
© SUBSECRETARÍA
Gabinete Técnico (MITECO).
Plaza de San Juan de la Cruz 10. 28003, Madrid. ESPAÑA

© De los textos e imágenes: sus autores

NIPO (papel): 665-24-088-7
NIPO (en línea): 665-24-089-2
Depósito legal: M-26880-2024
ISBN (papel): 978-84-18778-48-3
ISBN (en línea): 978-84-18778-49-0
Maquetación: LOTA COMUNICACIÓN INTEGRAL, S.L.
Impresión: LOTA COMUNICACIÓN INTEGRAL, S.L.

FSC
MIXTO
Papel
FSC® C103654

ACKNOWLEDGEMENTS

Chapter 1

We acknowledge our research groups and the funding from various international and national projects. MM was supported by the PID2020-117768RB-I00 project of MCIN/AEI/10.13039/501100011033. AH is supported by the Spanish Ministry of Science and Innovation through the Ramón y Cajal Scheme [RYC2020-029253-I] and the PID2022-139775OB-I00 MEDIATIC - project funded by MCIN/AEI/10.13039/501100011033 and "ERDF A way of making Europe". B. A. acknowledges the funding from the European Research Council under the Horizon Europe program (PASSAGE, 101039348). JFGR was funded by PID2021-126696OB. AM acknowledges the funding from TEMPURA project (ref PID2022-139101OB-I00) and AGA projects ID2021-125619OB-C21 and PID2021-125619OB-C22 and the support from the research group RNM-190 (Junta de Andalucía)

Chapter 2

We acknowledge the support received by the "Gobierno de Aragón" research group "Geomorfología y Cambio Global (E02_23R)" and the "Agència de Gestio d'Ajuts Universitaris i de Recerca of the Government of Catalonia" research group "ANTALP (Antarctic, Arctic, Alpine Environments; 2021 SGR 00269)". The work has been partially supported by LIFE PYRENEES4CLIMA - Towards a climate resilient cross-border mountain community in the Pyrenees (LIFE22/101104957). We also thank the PTI Polar-CSIC for the network created around cryosphere studies. AM acknowledges the funding from National Parks Autonomous Agency (OAPN) (OCHESTRA ref. 2552/2020). MB is supported by the HORIZON TMA MSCA Postdoctoral Fellowships – Global Fellowships 2022 project (no. 101107943) funded by the European Union.

Chapter 3

R.S-N is supported by grant RYC2021-034330-I, funded by MCIN/AEI/10.13039/501100011033 and by "European Union Next-Generation EU/PRTR". R.N. was funded by Xunta de Galicia and EU/ERDF, under project ED431C 2021/44 "Programa de Consolidación e Estructuración de Unidades de Investigación Competitivas". J.C.F-A. is supported by the Xunta de Galicia postdoctoral grant (IN606B2024/016). R.N. and J.C.F-A. also acknowledge the Ministerio de Ciencia e Innovación with funding from "European Union Next-Generation EU/PRTR" (PRTR-C17·I3) under project TED2021-129152B-C43. S.B.V is granted by the Santiago Grisolía grant (CIGRIS/2021/131). E.U.-C. was supported by the FPI fellowship (PRE2019-090148). S.J.G.R acknowledges support from the Oeschger Centre for Climate Change Research and from project PID2020-116153RB-I00 funded by MCIN/AEI/10.13039/501100011033. S.H. acknowledge support the support of the Spanish Government through the Agencia Estatal de Investigación (project PID2019-111481RB-I00 - Contribución española al Atlas del IPCC-AR6; Desarrollo y problemas científicos). A.M-N was supported by the FPU program of the Spanish Ministerio de Universidades (FPU20/01220). T.L. acknowledges support from project PID2021-125806NB-I00 funded by MCIN/AEI. M.C.A-C was funded by the Spanish Ministry of Universities through the Beatriz Galindo Programme (BG22/00102). J.C-G was supported by the FPU program of the Spanish Ministerio de Universidades (FPU22/02606). The research of sections

5, “Wind”, and partially section 6, “Atmospheric Moisture”, were developed in the framework of the CSIC Interdisciplinary Thematic Platform (PTI) Clima (PTI+ CLIMA) and the RED-CLIMA 2 project (LINCGLOBAL - CSIC, LINCG24042). Section 3 “Temperature” was partially based in the framework of the research projects PID2020-118797RB-I00 (MCIN/AEI/10.13039/501100011033) from the Ministry of Science and Innovation, and PROMETEO/2021/016 from the Generalitat Valenciana.

Chapter 4

R.S. acknowledges the funding from ThinkInAzul programme supported by MCIN with funding from European Union NextGenerationEU (PRTR-C17.I1) and by Gobierno de Cantabria. M.M acknowledges a grant from the Spanish Ministry of Universities through the European Union - Next Generation EU programme, and from” Pla de recuperació, transformació i resiliència” and the University of the Balearic Islands, and also support by the agreement between the Spanish Ministry for Ecological Transition and Demographic Challenge and CSIC, funded by the European Union-Next Generation EU Program. MF was funded by PTA2022-021307-I, MCIN/AEI/10.13039/501100011033 and by FSE+.

Chapter 5

J.B., A.C and J.F. acknowledge support from project CORDyS (PID2020-116595RB-I00), funded by MICIU/AEI/10.13039/501100011033. A.C. acknowledges support from Project COMPOUND (TED2021-131334A-I00) funded by MCIN/AEI/10.13039/501100011033 and by the European Union NextGenerationEU/PRTR. S.H. acknowledge support the support of the Spanish Government through the Agencia Estatal de Investigación (project PID2019-111481RB-I00 - Contribución española al Atlas del IPCC-AR6; Desarrollo y problemas científicos). D.A. acknowledges support from Grant CNS2022-135323 funded by MCIN/AEI/10.13039/501100011033 and by the European Union NextGenerationEU/ PRTR. J.A. acknowledges support from projects PID2020-116873GB-I00 and TED2021-130702B-I00 funded by MCIN/AEI/10.13039/501100011033 and Unión Europea NextGenerationEU; and Research Group E46_20R funded by Gobierno de Aragón. A.G. and J.C.P.D. thank the Government of the Canary Islands, Consejería de Transición Ecológica, Lucha contra el Cambio Climático y Planificación Territorial, for their support (published agreement: B.O.C. No. 238, November 20, 2020). M.M-D. and M.I. acknowledge support from project LIFE-URBANKLIMA2050 (Ref. LIFE18 IPC/ES/000001). J.C.F-A. acknowledges support from the Xunta de Galicia under the Postdoctoral grant IN606B2024/016, and by Ministerio de Ciencia e Innovacion with funding from European Union NextGenerationEU (PRTR-C17·I3) under project TED2021-129152B-C43. C.G, R.V. and W.C. acknowledge support from project SIHROCO (PID2021-128656OB-I00), funded by MICIU/AEI/10.13039/501100011033 and FEDER, EU.

Chapter 6

G.J. acknowledges support from project SEAFRONT (TED2021-132132B-C21) funded byr MCIN/AEI /10.13039/501100011033 and for UE NextGenerationEU/ PRTR

PROLOGUE

Climate change is already affecting our lives and entails one of the most significant risks facing humanity. The sixth report of the Intergovernmental Panel on Climate Change (IPCC), published in 2022, reflected once again that changes in the climate system generated by human activity represent an increasingly serious threat to our well-being and the planet's health. The recently published analysis of climate impacts and risks for Europe, known as the EUCRA report, also alerts that we are facing multiple and concurrent hazards related to climate change, some of them with catastrophic effects. Our continent is the fastest warming (since the 1980s, it has warmed up about twice as much as the rest of the world) and, within Europe, the southern region is particularly affected by heat and prolonged drought, with especially severe risks expected that require urgent action.

The scientific evidence on climate change, and the risks and associated impacts, leaves no room for doubt and is the driving force to continue developing ambitious policies and measures that will allow us to move towards a low-emission climate-resilient future. Science confirms, once again, that we are facing a climate emergency, in which it is urgent to act to restrain this process and avoid its worst consequences. We must build on the science, which is alerting us about the problem, but also provides the solutions and the ambition which we must strive towards.

The generation of scientific knowledge on climate change is based on an understanding of how the climate system works, how it has evolved in the past, and the possible climate scenarios we will face in the future. Scientific research on the physics of climate, therefore, is a major strand for building adequate responses to climate change.

The CLIVAR-Spain Committee and Thematic Network has become, since its creation in 2004, a reference in the generation of knowledge on physical processes related to climate and climate change. This third report on Spain's climate continues the trajectory initiated in the previous reports, published in 2004 and 2010, and represents an update on the state of the art of climate research in Spain. The report strategically complements the global conclusions of the sixth IPCC assessment report, allowing us to better comprehend our climate and reflecting the new knowledge available for the development of climate science in Spain.

In addition, this publication is a recognition of the climate science community in our country, whose research allows us to continue advancing in a better understanding of our environment and to adopt measures to face challenges as relevant as climate change. For this reason, I would like to express my support and gratitude to the CLIVAR-Spain Committee and Thematic Network and to the entire scientific community that has participated in the preparation of this report, and to extend it to all the scientists who contribute from Spain to the generation of knowledge on climate change. It is in our hands to listen to science and be guided by it with ambitious climate action.

D. Hugo Morán Fernández

Secretary of State for the Environment

INDEX

Pag.

INTRODUCTION

The CLIVAR Spain committee is an entity that is part of the international CLIVAR effort (Climate and Ocean: Variability, Predictability, and Change, https://www.clivar.org/). CLIVAR is a project of the World Climate Research Program (WCRP), which aims to improve the understanding of climate variability and change, as well as the interactions between the ocean and the atmosphere.

In Spain, the CLIVAR Spain Committee (http:// http://clivar.es/) began its journey in 1999-2000, as the National CLIVAR Committee, sponsored by the Ministry of the Environment, to become, through a special action of the National Research Plan, a CLIVAR thematic network. Its initial objective was to structure, foster and coordinate the research groups of the different scientific lines on climate in Spain, covering both paleoclimatic studies, instrumental observations or numerical modeling of the atmosphere and ocean, to reach regionalized projections on the western Mediterranean, which had already been identified as a region of great impact for climate change in the IPCC (Intergovernmental Panel on Climate Change) reports.

From that moment on, the thematic committee/network worked intensively and in parallel on several lines: (i) the search for funding to consolidate the coordination work in the climate scientific community in Spain, (ii) the relationship with other committees that existed, with a low degree of activity, to try to merge their activities and serve as a common reference for the country's research community; (iii) the relationship with national and international institutions, and in particular, with CLIVAR International (which was specified in two support documents, in 2011 and 2018) and with the Spanish Office of Climate Change; and (iv) the ambitious goal of replicating, on a regional scale, the philosophy and tasks of the IPCC report work cycles. Since its creation, the CLIVAR committee has issued three reports (2006, 2010 and 2017) and one executive report (2019) on the state of the art of climate in Spain, compiling its main advances.

This CLIVAR-Spain 2024 report aims to synthesize the state of the art of climate studies in Spain, identifying the main recent advances in understanding past, present and future climate change and variability in the country. The report is divided into six chapters, each of which focuses on a different area of knowledge, and for each chapter, the authors have identified the most notable or outstanding aspects, which are indicated below.

CLIVAR-SPAIN 2024 ASSESSMENT REPORT - HIGHLIGHTS

CHAPTER 1 - Atmospheric and oceanic changes since the last glacial maximum: Review of proxy-based and climate model simulation reconstructions in the Iberian Peninsula

- **Regional Variability and Record Scarcity Hinder Iberian Peninsula Climate Reconstruction Since Last Glacial Maximum.** Past climate variability in the Iberian Peninsula recorded by marine and terrestrial records is regionally heterogeneous, from north to south and from the Mediterranean to the Atlantic sectors, partly explained by the imprint of seasonal signals on the different proxies. The scarcity of available records

prevents a proper spatial reconstruction of the climate changes since the Last Glacial Maximum (LGM).

- **Northern Hemisphere Climate Synchronicity Evident in Iberian Peninsula During Last Deglaciation and Holocene**. Synchronicity with major climate variations in the Northern Hemisphere, attributed to ocean-atmospheric teleconnection mechanisms, is clearly evidenced especially during abrupt climate changes of the last deglaciation and the Holocene. Improvements in the resolution of proxy records have allowed exploring the intra-event variability of key climate events of the last deglaciation (eg. Younger Dryas) and Holocene interglacial (e.g., 8200 year event).
- **Advances in Proxy Calibration and Novel Paleothermometers Enhance Reliability of Past Climate Reconstructions**. The efforts carried out in the last decade on climate proxies' calibration, applicability, and limitations have reduced the uncertainty associated with the quantitative estimation of environmental variables (e.g., temperature reconstructions have significantly improved over the last decade due to the discovery and implementation of novel paleothermometers). The adoption of statistically robust methods and the creation of innovative transfer functions that enable the quantitative estimation of past climate variables are important steps to develop more reliable climate reconstructions.
- **AMOC's Role in Abrupt Climate Changes During Last Glacial Period**. Modeling studies provide insight into the role of reorganizations of the Atlantic Meridional Overturning Circulation in abrupt climate changes of the last glacial period, both Dansgaard-Oeschger and Heinrich events, as well as into the links between both types of events.
- **Last 2000 Years Crucial for Contextualizing Present Warming**. In recent times, the last 2000 years have emerged as a period of pivotal importance to contextualise the magnitude and velocity of present warming offering a unique opportunity for proxy and model validation.
- **Enhancing Proxy-Model Collaboration Key to Understanding Climate System**. Future efforts are required to enhance collaboration between the paleoclimate communities focusing on proxy data and those making use of climate models, which will give a crucial understanding of the climate system.
- **Short-Term Climatic Changes Coincide with Societal Shifts in Holocene Iberian Peninsula**. Changing climate has affected terrestrial and marine ecosystems throughout Earth's history, including human population dynamics in the Quaternary. Important societal changes have occurred coeval with short-term climatic changes in the Iberian Peninsula during the Holocene (e.g., around 8.2 and 4.2 ka PB).
- **Post-LGM Landscape Evolution Driven by Insolation, Abrupt Events, and Human Impact**. Long-term terrestrial landscape evolution since the LGM has mainly been driven by insolation changes, interrupted by abrupt events triggered by atmospheric, oceanic, and solar dynamics. This landscape evolution, primarily evidenced by vegetation distribution, shows significant differences between the Late Holocene and the end of the previous interglacial period, probably due to the impact of anthropogenic activities in the last millennia that have reduced forested areas. Similarly, natural fire dynamics since the LGM changed in the Late Holocene, when fire activity increased despite the fuel availability decline as a consequence of the expansion of shrublands.

CHAPTER 2 – The study of the Cryosphere in the Iberian Peninsula

- **Advances in Cryosphere Studies Reveal Expansion and Contraction Patterns in Iberian Peninsula**. Understanding of the evolution of the cryosphere in the Iberian Peninsula has significantly improved over the last decades, showing evidence of expanding the domain of the cold processes during cold periods and shrinking during warmer phases.
- **Cold-Climate Processes Shift to Higher Altitudes in Response to Warming Trends**. The cryosphere is responding rapidly to recent climate trends, with all its components (glaciers, permafrost, seasonal frozen ground, snow, ice caves) being affected. In response to the warming trend, cold-climate processes on the Iberian Peninsula are moving to higher altitudes.
- **Rapid Decline of Glaciers: Loss in Extent, Thickness, and Evolutionary Processes**. Glaciers have shown a fast decline in the last decade, with remarkable loss in both extent and thickness. This has led to a reduction in the number of glaciers and also in the occurrence of distinct processes that characterise the evolution of glaciers in their last stages before their final disappearance.
- **Urgent Need for Guidelines to Mitigate Risks from Permafrost Degradation in Spanish Mountain Ranges**. Permafrost, which is permanently frozen ground, is practically disappearing in Sierra Nevada and showing signs of warming at the summits of the Pyrenees. Its degradation accelerates rockfalls and avalanches, posing risks to mountaineers and hikers in the highest massifs of this mountain range. In this regard, it is evident that it is necessary to develop guidelines for local and regional administrations to reduce potential risks to people and infrastructure.
- **Long-Term Records Show Decreasing Snow Cover Duration and Accumulation in Iberian Peninsula**. The snow phenomena in the Iberian Peninsula is characterised by a high interannual variability, which makes the identification of short-term trends difficult. However, the longest snow records show a decrease in snow cover duration and its maximum accumulation. The high dependence that water resources have on snow accumulation in mountain areas shows the relevance of better understanding and managing snow processes under climate change scenarios.
- **Ice Caves in the Pyrenees and Picos de Europa: Vanishing Archives of Paleoenvironmental Data**. Ice caves from the Pyrenees and Picos de Europa host perennial ice bodies providing highly valuable paleoenvironmental information covering the last millennia and based on the study of geochemical, and biological proxies; unfortunately; most of those sequences are disappearing. The reduction of ice currently observed is primarily regulated by the decline in winter precipitation and the rise in winter temperatures.

CHAPTER 3. Revisiting the atmospheric variables in Spain during the observational period: variability, trends and drivers

- **Trend Variability and Intensification of Heat Waves in Spain Over the Past Six Decades**. Temperature trends in Spain during the instrumental period (approximately the last 100 years) are positive, with a clear acceleration since the 1980s, however, the spatial variability is large and the significance in shorter periods is variable. Heat waves have increased in frequency, duration and intensity throughout the last six decades.

- **Implications of a Warming Mediterranean Sea on Convective Events and High Precipitation in Spain:**. Precipitation in the instrumental period, and also in shorter and more recent cycles, does not show significant changes. However, there are large regional and seasonal differences, with the Mediterranean area being the most sensitive to extremes. Extreme precipitation trends are not clear for the whole territory or temporal period, but an increase of convective events has been observed, leading to an increase of high precipitation events, especially in the end of autumn, probably related to a warmer Mediterranean sea.

- **Longer and Intensified Droughts in last decades Linked to Increased Atmospheric Evaporative Demand.** The 21st century has experienced the greatest frequency of severe droughts of the last 150 years. While precipitation amounts have been around average values, higher temperatures pushed a higher atmospheric evaporative demand, leading to longer and more intense droughts.

- **Decline in Near-Surface Wind Speeds in the Iberian Peninsula from 1960s to 2010.** Near-surface wind speed in the Iberian Peninsula has declined from the early 1960s to 2010 at an annual rate of about -0.15 ms^{-1} $decade^{-1}$ ($p < 0.05$), being followed by a cessation of the stilling or a weak and non-significant wind strengthening period. The Iberian Peninsula wind stilling may have been caused by an increase in atmospheric thermal stability and a northward shift of the jet stream. No other cause was found for the cessation of stilling than a change in the trend of the western Mediterranean oscillation.

- **Impact of Moisture Transport Reductions on Summer Precipitation in the Iberian Peninsula.** The Iberian Peninsula shows a strong relationship between moisture transport and hydrometeorological extremes, such as extreme precipitation or meteorological drought. The remarkable decrease in recent summer precipitation over the Iberian Peninsula can be attributed to reductions in moisture contributions from the Iberian Peninsula, and to the west (North Atlantic) and the east (Mediterranean and Western Europe) of the precipitation shed, accounting for 26 %, 57 % and 17 % of the main source supply reduction, respectively.

- **Atmospheric Variability over the Iberian Peninsula: Beyond the North Atlantic Oscillation.** Although the North Atlantic Oscillation (NAO) is the main source of atmospheric variability over the Iberian Peninsula, weather regimes such as the Scandinavian Blocking, the Atlantic Ridge and the Atlantic Low or remote patterns as El Niño - Southern Oscillation (ENSO), Tropical Atlantic modes and even extreme polar vortex events can also have a significant impact.

- **Climate Trends in Spanish Islands: Rising Temperatures and a Slight Decrease in Precipitation.** The Canary Islands are experiencing higher temperatures especially in summer, leading to a higher frequency of heatwaves. Precipitation trends are not homogeneous, but a general decrease in total amounts has been observed. Balearic Islands temperature records show that both minimum and maximum temperatures have increased above 0.50 ºC per decade over the period 1976-2006. They also experienced a notable negative trend in annual rainfall of 1.63 mm per year over the period 1951-2006, although it was not stable along the entire period.

- **Impacts of Climate Change on Spanish Mountain Systems: Accelerated Snowmelt and Glacier Decline.** The Spanish mountain systems suffer from the same impacts as the rest of the territory (droughts, heat waves, etc.), triggered by a subtle decrease in annual precipitation and a clear increase in temperatures. However, these are accelerating snowmelt processes

that will make the glaciers disappear in the next decades. Water resources have already been affected, with a significant impact on mountain ecosystems.

- **Impact of Urban Heat Island Effect on Spain: Rising Temperatures and Urban Design Challenges.** Spain is especially sensitive to the Urban Heat Island (UHI) effect, given that a high percentage of its population resides in urban areas (approximately 81%). In the last decade, most populated cities in Spain have experienced unprecedented temperature records driven by climate change and exacerbated by urban factors such as the UHI effect, giving rise to a growing awareness of the importance of designing sustainable and resilient urban environments, considering local climatic conditions.

CHAPTER 4. Physical and biogeochemical changes in the ocean around Spain during the observational period: variability, trends and drivers

- **All Oceanic Waters Surrounding the Iberian Peninsula and Archipelagos are Warming Faster than the Global Average.** The average rate of warming is 0.25°C/decade, that is 67% faster than the global average (0.15°C/decade).
- **Less Warming in Some Coastal Areas.** Upwelling regions in the west and north coast of the Iberian Peninsula and the Canary Island upwelling system seem to be a 'reducto' of global warming, and depending on the area even cooling trends are observed.
- **Mediterranean Warming is 2-3 Times the Global Rate Since the 1980s, Affecting the Entire Water Column.** Since the beginning of the 1980s decade, this warming has been two or three times larger than that observed for the rest of the world ocean and has been accompanied by an increase in the frequency, intensity and duration of heat waves and the increase of the salinity of surface waters. The warming and salting process of the Mediterranean Sea has affected the whole water column.
- **Observed Trends in Stratification and Mixing at Odds with the Expectation of Concurrent Stratification Strengthening and Mixed Layer Shoaling Brought About by Anthropogenic Global Warming.** Despite the warming observed in surface waters around the Iberian Peninsula, observations in Spanish waters along with other global studies have shown that this warming occurs together with a generalised stratification increase of 1-9%/dec and mixed layer deepening of several meters per decade. Such a finding is at odds with the expectation. The Mediterranean sea seems not affected by changes in stratification and/or mixed layer depths.
- **Regional Sea Level Rise Patterns.** Satellite altimetric observations since the early 1990s show a steady mean sea level rise over 3 mm/yr along the Spanish coasts. In-situ tide gauge records reveal significant interannual to multi-decadal sea level variability, superimposed to the long-term trends, and driven by large scale climate patterns.
- **Observed Changes in Extreme Sea Level Events.** The frequency and intensity of coastal extreme sea levels, triggered by atmospheric perturbations, are largely modulated by changes in mean sea level. Along the Spanish Atlantic coasts, the 50-year return levels for the atmospheric contribution (excluding mean sea level) ranges between 20 cm to 60 cm, increasing northwards, and between 40 cm and 50 cm along the Mediterranean coasts.

- **Unabated Ocean Acidification from Surface to Depth.** The pH decrease in surface waters, upper, and intermediate water masses near the Iberian Peninsula and Canary Islands unequivocally point to anthropogenic carbon dioxide influence as the main forcing agent. There exists large regional variability, with coastal and shallower areas experiencing more complex and dynamic changes than oceanic regions due to land discharges and productivity.
- **Detecting Ocean Deoxygenation is Challenging.** The unequivocal detection of ocean deoxygenation in many regions requires consistent long-term observations as natural oxygen variability complicates the attribution of deoxygenation to specific drivers. Currently, there is no statistically significant deoxygenation beyond natural variability in the waters surrounding the Iberian Peninsula and Canary Islands. In coastal areas the observed deoxygenation is mainly affected by eutrophication due to anthropogenic pressures rather than temperature increases or reduced ventilation.

CHAPTER 5. An updated review of regional atmospheric climate change over Spain: model evaluation and projections

- **Projected Decline in Mean Precipitation with Increased Extreme Events Throughout the 21st Century.** Mean precipitation is projected to decline along the century, but precipitation extremes are projected to increase.
- **Uncertainties in Near-Surface Wind Speed Projections over the Iberian Peninsula.** Both Global (GCM) and Regional (RCM) climate models poorly simulate the observed wind speed changes and multidecadal variability over the Iberian Peninsula. GCMs generally project a decline of near-surface wind speed (NSWS) for the end of the century for the Iberian Peninsula, remarkable for high anthropogenic forcing scenarios; while some RCMs indicate reinforcement of NSWS for the same periods. Given the large uncertainties found, NSWS projections should be taken with caution and further efforts are needed to accurately simulate NSWS.
- **No Clear Signal in Atmospheric Circulation Indices and Blocking Frequency Projections over the Iberian Peninsula.** Internal variability is the main uncertainty source for future projections of the atmospheric circulation. The projected wintertime East Atlantic (EA), Scandinavian (SCA) and East Atlantic-Western Russia (EA-WR) indices derived from sea level pressure do not exhibit significant changes towards their positive or negative phase along the 21st century. Depending on the considered GCMs, the North Atlantic Oscillation (NAO) index also remains stable or will exhibit a slight trend towards its positive phase. Atmospheric blocking over the Iberian Peninsula is projected to become less frequent in winter and no significant change is to be expected in summer.
- **Significant Reduction in Relative Humidity Across Iberian Peninsula Linked to Summer Oceanic Evaporation Increase.** A remarkable reduction of relative humidity over the Iberian Peninsula during all seasons and all climate scenarios is found, but particularly during summer caused mainly by the increase of oceanic evaporation.
- **Projected Increase in Arid Climates and Water Scarcity Across Iberian Peninsula and Southern Europe.** Together with increasing temperatures and decreasing precipitation, the water scarcity over already dry areas will be exacerbated. Thus, a tendency toward more arid climates is projected over the Iberian Peninsula and southern Europe. The contribution of

moisture from the North Atlantic Ocean to Europe and the Iberian Peninsula will be reduced and will have an impact on the precipitation regime and a reduction in rainfall, especially during winter and autumn by the end of the century. Atmospheric rivers' frequency will increase by 50% under the high-emission scenario, and the more extreme water vapour transports will increase by 20%.

- **Rising Fire Danger and Heat Exposure in 21st Century Climate Projections.** Climate projections point to an increase in fire danger conditions, consisting in more frequent fires, more extreme events and longer danger seasons, which are expected to expand to June and, to a lesser extent, to September. Environmental heat exposure is projected to rise in the course of the 21st century, with exceedances of impact-relevant thresholds increasing non-linearly with the magnitude of future warming.
- **Climate Change Impact on Tourism and Agriculture in Spain: Shifts in Seasons and Variability Effects.** Optimal conditions for tourism in summer will deteriorate, with an improvement in shoulder seasons and a northward shift. Climate change may lead to a reduction in some cultivars production (including grapes), which could be accentuated due to an enhanced inter-annual variability.
- **Projected Climate Changes Increase Aridity and Drought Severity in Southern Iberian Peninsula** A projected reduction in precipitation over southern Iberian Peninsula, combined with an enhanced increase of atmospheric evaporative demand, may lead to a decrease in surface evapotranspiration and an increase in aridity conditions. Changes in drought conditions are also projected to increase in both frequency and severity, consistently in global and regional studies.
- **Combining Wind and Solar Energy for Enhanced Reliability During Droughts.** Hybrid systems combining wind and solar energies may be useful to reduce energy storage requirements and periods of low productivity (drought days).
- **Challenges and Opportunities in High-Resolution Climate Modeling for the Canary Islands.** The Canary Islands are expected to experience significant temperature increases (up to 4.2°C by the end of the century under the Representative Concentration Pathway 8.5 (RCP8.5) scenario) and a substantial decrease in precipitation (around 30%). This will exacerbate drought conditions, especially at higher altitudes. The fire season will lengthen, with more extreme fire risk days and a larger area susceptible to fires due primarily to reduced precipitation. While high-resolution climate modelling for the Canary Islands is challenging, due to the high computational demand, their unique characteristics present a valuable opportunity to study convection-permitting simulations. International collaboration is crucial for further climate research in the archipelagos.

CHAPTER 6. Regional oceanic climate change projections around Spain

- **Projected Upwelling Increase Along Western Iberian and Canary Coasts, with Decreased Downwelling in Northern Iberia.** The circulation around the Iberian Atlantic waters and the Canary Islands is expected to be intensified due to the enhancement of the density gradients and the increase of winds. The upwelling along the western Iberian coasts and the Canary region will also increase while a decrease of the downwelling in the northern Iberian coasts is also expected.

- **Stable General Circulation in the Mediterranean with Projected Reduction in Deep Water Convection.** No large changes in the general circulation of the Mediterranean have been reported, but a large reduction in the deep-water convection is foreseen as well as a moderate increase in the mesoscale activity.
- **Climate Trends in Spanish Waters: Enhanced Summer Heat and Intensified Marine Heatwaves.** Temperature will increase in all Spanish waters in the whole water column, especially in the Mediterranean. The warming will be higher in summer, and the intensity of marine heatwaves will be strongly enhanced. It is expected a freshening of northeast Atlantic waters due to the advection of waters from the Arctic. In coastal areas, that freshening will be partially damped by the increased coastal upwelling
- **Projected Changes in Mediterranean Salinity.** The salt content in the Mediterranean will increase due to the enhancement of water losses. However, the salinity in the shallower waters of the Western basin may decrease due to the entrance of fresher Atlantic Waters.
- **Sea-Level Rise Dominates Future Extreme Events.** Mean sea level around Spain will roughly follow the same evolution of global mean sea level as regional differences produced by changes in the circulation and mass redistribution almost compensate each other. Up to 90% of the changes in extreme sea levels by 2100 are explained by future sea-level rise, compared to 10% due to changes in extreme sea levels associated with storm surges and waves. Historical centennial events are expected to occur several times per year.
- **Ocean Acidification and Oxygen Decline Linked to Climate Change Drivers.** Robust surface acidification trends are driven by the absorption of anthropogenic carbon emissions. The projected reduction in dissolved oxygen concentration is attributed to enhanced upper-ocean stratification, weaker ventilation of subsurface waters, and warming-induced reduction in O_2 solubility.
- **Projected Nutrient Scarcity in Euphotic Zone Due to Upper-Ocean Stratification Impacts Net Primary Production in Atlantic Iberia and Canary Islands.** Diminished nutrient availability in the euphotic zone is expected; nutrients supply from the deep ocean will be likely impeded by stronger upper-ocean stratification. Projected negative changes of net primary production in the Atlantic sector of the Iberian Peninsula and off the Canary Islands, but with large inter-model uncertainty. Changes of net primary production in the Mediterranean are largely uncertain across models.

CHAPTER 1

ATMOSPHERIC AND OCEANIC CHANGES SINCE THE LAST GLACIAL MAXIMUM: REVIEW OF PROXY-BASED AND CLIMATE MODEL SIMULATION RECONSTRUCTIONS IN THE IBERIAN PENINSULA.

Coordinators: Isabel Cacho[1], Ana Moreno[2]

Authors: Blanca Ausín[3], Antonio García-Alix[4], Armand Hernández[5], Fidel González Rouco[6], Marisa Montoya[6]

Collaborators: Daniel Abel-Schaad[7], Francisca Alba-Sánchez[7], Roberto Bao[5], Xavier Benito[8], Jon Camuera[9], Alba de la Vara[10], Fernando Domínguez Castro[2], David Domínguez-Villar[3], Isabel Dorado Liñan[11], Felix García Pereira[6], Fernando Gázquez Sánchez[12], Juan José Gómez-Navarro[13], Penelope González-Sampériz[2], Concepción Jiménez de Cisneros[14], Francisco Jiménez Espejo[14], Gonzalo Jiménez-Moreno[4], Prabodha Lakrani[3], Susana Lebreiro[15], Charo López-Blanco[4], José Antonio López-Sáez[16], Javier Martin-Chivelet[17], Francisca Martínez Ruiz[14], Belen Martrat[18], Mario Morellón[17], Carles Pelejero[19], Javier P. Tarruella[3], Xabier Pontevedra-Pombal[20], Marta Rodrigo Gámiz[4], Teresa Rodrigues[21], Fernando S. Rodrigo[22], Francisco Javier Sierro[3], Ernesto Tejedor[23], José M Vaquero[24], Antje Voelker[21].

[1] Department of Earth and Ocean Dynamics, Faculty of Earth Sciences, University of Barcelona, Barcelona, Spain

[2] Department of Geoenvironmental Processes and Global Change, Pyrenean Institute of Ecology (IPE-CSIC), Zaragoza, Spain

[3] Institute of Natural Resources and Agobiology of Salamanca (IRNASA), CSIC, Salamanca, Spain

[4] Department of Stratigraphy and Paleontology, Faculty of Sciences, University of Granada, Granada, Spain

[5] Interdisciplinary Center for Chemistry and Biology (CICA), Faculty of Sciences, University of A Coruña, A Coruña, Spain

[6] Department of Earth Physics and Astrophysics, Complutense University of Madrid (CSIC-UCM), Madrid, Spain

[7] Department of Botany, Faculty of Sciences, University of Granada, Granada, Spain

[8] Marine and Continental Waters Program, Institute of Agrifood Research and Technology (IRTA), La Rapita, Spain

[9] Unit of Botany, Facultad de Pharmacy, Complutense University of Madrid, Spain

[10] Kveloce (Senior Europa S.L.), Valencia, Spain

[11] Systems and Natural Resources Department, Technical University of Madrid, Madrid, Spain

[12] Department of Biology and Geology, Faculty of Experimental Sciences, University of Almería, Almería, Spain

[13] Department of Development and Applications, State Meteorological Agency, Barcelona, Spain

[14] Andalusian Earth Science Institute (IACT-CSIC), Granada, Spain

[15] Department of Geological Hazards and Climate Change, National Geological and Mining Institute (CN IGME-CSIC), Madrid, Spain

[16] Department of Archaeology and Social Processes, Institute of History (IH-CSIC), Madrid, Spain

[17] Department of Geodynamics, Stratigraphy, and Paleontology, Faculty of Geological Sciences, Complutense University of Madrid, and Institute of Geosciences (CSIC-UCM), Madrid, Spain

[18] Institute of Environmental Assessment and Water Research (IDAEA-CSIC), Barcelona, Spain

[19] ICREA and Institute of Marine Sciences (ICM-CSIC), Barcelona, Spain

[20] Departament of Soil Science and Agricultural Chemistry, Faculty of Biology, University of Santiago de Compostela, Santiago de Compostela, Spain

[21] Marine Geology and Georesources Division, Portuguese Institute for Sea and Atmosphere, Algés, Portugal, and the Algarve Centre of Marine Sciences (CCMAR), University of Algarve, Faro, Portugal

[22] Department of Chemistry and Physics, School of Experimental Sciences, University of Almería Almería, Spain

[23] Department of Geology, National Museum of Natural Sciences (MNCN-CSIC), Madrid, España

[24] Department of Physics, Faculty of Sciences, University of Extremadura, Badajoz, Spain

1. Introduction

Understanding how and why the Earth's climate changed prior to instrumental measurements is essential to frame the current climate change in the context of natural climate variability. Assessing changes in past climate variability from proxy-based records and model simulations provides insight into mechanisms that operate on timescales longer than the instrumental period. Also, it helps to disentangle mechanisms of natural variability that contributed to past climate changes from the causes of the current anthropogenically induced climate change.

Two main tools for characterising past climate variability are proxy-based reconstructions and simulations using a range of climate models of different levels of complexity. Among these, Earth System Models (ESMs) stand as the tools including the highest number of Earth system components, which are represented with the highest possible level of realism. Reconstructing past climate variability is particularly challenging due to the complexity of factors controlling how climatic variables are recorded in the different climate archives and proxy-based records. Similarly, climate modelling faces important challenges regarding the representation of climate forcings and the accurate simulation of regional variability. Both approaches target slightly different objectives: while proxy-based reconstructions aim at representing the actual evolution of past climate variability, model experiments provide a sequence of climate states that are consistent with the estimations of past changes in external forcings. Therefore, the realisation of internal climate variability can, and will likely be, different from reality and from climate reconstructions. In turn, hybrid products assimilating climate reconstructions in model experiments attempt to provide a physically based interpolation that is consistent both with proxy-based reconstructions of external forcing and past climate variability. Still, both scientific fields have advanced enormously

in recent decades. On the side of past climate reconstructions, substantial improvements have been achieved in both quality and quantity. On the modelling side, computational resources have improved enormously, allowing the use of higher model resolutions, and important efforts have been made to incorporate more realistic representations of all Earth system components in ESMs. As a result, the last IPCC report (AR6) has successfully framed most of the currently observed and future projected climatic evolution within a long-time geological perspective. This exercise also allows for extending model-data comparison of reconstructions and simulations to regional scales. The current chapter aims to provide an updated view of the large effort in reconstructing and modelling past climate variability, with a specific focus on the Iberian Peninsula (IP), conducted over the last few decades. This effort establishes the foundation for evaluating current and future regional climate conditions.

During the Quaternary (the past 2.6 Ma), the Earth's climate has fluctuated between glacial and interglacial states in response to orbital cycles. Long-term climate records, as predicted by Milutin Milankovitch, have proved that changes in insolation driven by orbital cycles are the main triggers of this glacial-interglacial variability, but the climate system does not show a linear response to this forcing (Hodell, 2016). Decades of palaeoclimatic research indicate that the intensity of glacial-interglacial cycles was ultimately shaped by climate feedbacks that operate within the Earth system itself. Among many factors, changes in the Earth's albedo in response to changes in the extension of ice sheets or greenhouse gas concentrations were key elements altering the radiative balance of the Earth and thus, responsible for a significant part of the glacial-interglacial thermal changes and its rapid character. While orbital cycles act over time scales of 20 to 100 ka, inducing relatively smooth changes in insolation distribution over the Earth, feedbacks often lead to a threshold behaviour. For instance, ice melting or changes in ocean circulation react on time scales of decades to centuries, rapidly destabilising after crossing certain thresholds (Barker and Knorr, 2021). These processes have been crucial in the development of millennial time-scale climate variability that was particularly intense during most of the Quaternary glacial periods. The end of these glacial periods, known as deglaciations, constitute the top example of non-linearity between the actual trigger (orbital forcing) and the rapid and enhanced response within the climate system. The interplay between slow insolation changes and rapid ice melting phases, coupled with the reorganisation of ocean currents and impacts on atmospheric carbon dioxide (CO_2) concentration, acted as strong feedbacks in deglaciations, pulling the Earth out of ice ages (Clark et al., 2012). The drivers of these phases of global warming were very different from those at present, but associated feedbacks are common to "tipping point" processes that need to be understood at global and regional scales (Brovkin et al., 2021; Lenton et al., 2019).

The last deglaciation (ca. 18-11 ka Before Present - BP- being Present the year 1950) is the most extensively studied end of an ice age because of the number of available records and the overall higher accuracy of the chronologies. The interplay of external forcing and ice-albedo and ocean feedbacks bears policy-relevant implications relative to the current warming and hence constitutes one of the targets of this chapter. Paradoxically, the onset of this deglaciation was interrupted by an extreme cooling event in the North Atlantic Ocean, adjacent continents, and most of the Northern Hemisphere. This event, associated with a major delivery of icebergs and a weakening or even shutdown of the Atlantic Meridional Overturning Circulation (AMOC), is known as Heinrich Stadial 1 (HS1; (Hodell et al., 2017)). In contrast, the Southern Hemisphere started to warm at the same time, while sea ice retreated in the Southern Ocean. This led to enhanced upwelling of deep water, with the consequent release of CO_2 to the atmosphere, stored in the glacial deep

ocean, providing a strong warming feedback (Clark et al., 2012). At about 14.5 ka BP, the AMOC reactivated, leading to the first rapid deglacial warming in the Northern Hemisphere, marking the onset of the Bölling-Allerød (B-A) interstadial period, also known as the Greenland Interstadial 1 (GI-1). Yet, at 12.9 ka BP, the AMOC abruptly switched back into a weak state, during the so-called Younger Dryas period (YD), or Greenland Stadial 1 (GS-1). This event led again to an overall cooling in most of the Northern Hemisphere, with impacts also evident in the Southern Ocean. Finally, at 11.8 ka BP, a very rapid AMOC resumption led to the second rapid deglacial warming of the Northern Hemisphere, entering the current Holocene interglacial period. The tight link between this deglacial evolution and AMOC dynamics becomes particularly relevant when considering the currently ongoing warming. Future projections for the AMOC, as presented in the last IPCC report, predict a significant reduction of this circulation system by the end of the century, with enhanced impact for those scenarios with larger emissions. Recent work inducing tipping in ESM simulations for the first time endorses the current course towards an AMOC collapse (van Westen et al., 2024). Such situation was identified in the last IPCC report as an analogue to that occurred during the YD period (AR6: Chapter 8), highlighting the interest of this period to understand the widespread impacts that an AMOC shutdown would have, in particular on the climate of the IP.

Throughout the Holocene, the Earth's climate has experienced significant regional and temporal variability, although Greenland ice cores recorded rather stable temperatures compared to the previous glacial period (Rasmussen et al., 2014). Reconstructions of global temperature anomalies have allowed the identification of an Early to Middle Holocene Thermal Maximum (HTM; ~10 to 6 ka BP) and a subsequent cooling trend towards the present (Kaufman et al., 2020) owed mostly to orbital changes. On the contrary, climate models show evidence of lower temperatures during the early Holocene and continuous warming until ~2 ka BP in the Northern Hemisphere (Marsicek et al., 2018). This contradictory temperature evolution derived from models and some proxy-based records is known as the "Holocene temperature conundrum" (Hopcroft et al., 2023). Achieving a robust Holocene temperature reconstruction would facilitate identifying the forcing factors and feedbacks that played a major role during this period, and could have implications for model simulations in climate change scenarios. The hydrological responses during the Holocene are even more complex than the thermal ones and imply a higher spatial and temporal variability (Fernández-Montes et al., 2017). Nevertheless, a general pattern of increased humidity during the well-documented HTM and a drying trend thereafter has been identified in various records from the Northern Hemisphere, including Iberian sites. Furthermore, although the Holocene is climatically more stable than the last deglaciation, it is also punctuated by abrupt events, such as the 8.2 ka event associated with the decline of the AMOC (Bauer et al., 2004). Other events during the Middle and Late Holocene were not related to freshwater pulses in the North Atlantic, as the Laurentide ice sheet had completely melted by this time. On the contrary, their causes were likely related to internal climate variability, perhaps modulated by the overall reduction in summer insolation across the Northern Hemisphere due to orbital changes, generally considered the cause of the Late Holocene neoglaciation (Bradley and Bakke, 2019). One of the most prominent events during this period is the 4.2 ka event, which is reported to have occurred in many regions worldwide, - although with more evidence available within the Mediterranean region - and was generally characterised by dry and cool climatic conditions (Bini et al., 2019).

Advancing our understanding of past climate variations in the IP requires high-quality (including quantitative) proxy-based records capable of reconstructing rapid climate changes with sufficient resolution to discern decadal, annual, or even seasonal changes. This is essential for determining

whether the current changes are unprecedented compared to the natural baseline conditions defined by previous periods. Moreover, new calibration methods have been developed to better quantify temperature or precipitation changes in the past using diagnostic proxies combined with an improved mechanistic understanding of the climate system gained from modelling exercises. In the IP, the past decade has seen the production of new records from both marine and terrestrial environments, aimed at exploring climate variability during rapid past climate transitions like the YD or characterising internal variability within climate events, such as phases within HS1. Moreover, the application of new climate proxies, backed by rigorous calibration exercises, enables the precise quantification of past climate changes, contributing to contextualising current warming trends. In modelling research, efforts have been focused on incorporating all significant forcings (e.g., solar, volcanism, aerosol, anthropogenic) to advance the understanding of processes and feedbacks. Simulations of the Last Millennium spanning over the period 850-1850 within the Common Era (CE), in the terminology of the Coupled/Paleo Model Intercomparison Project (CMIP/PMIP; (Eyring et al., 2016; Jungclaus et al., 2017)) and of the complete CE have extended back the use of solar, volcanic, greenhouse gases and land use land cover changes (LULC hereafter). Conversely, simulations extending beyond the CE still lack a full representation of forcings and often focus on solar and orbital changes while missing LULC and important feedbacks like those including dynamic ice-sheets, dynamic vegetation, etc.

Thus, there is still much work to be done. Some areas in the IP and the surrounding ocean lack information on past climates, as most research has focused on specific marine locations and in mountain regions where lake sediments, peat bogs, caves, and glacial deposits are more frequent and more continuous. Furthermore, some periods or transitions remain underexplored due to low sedimentation rates, particularly in marine records, resulting in inadequate temporal resolution. Finally, a more comprehensive understanding of the different climate indicators is necessary for land-sea comparison. These indicators often describe the climate under different seasons and with varying resolutions. They are frequently non-quantitative, making their comparison with or their integration into model simulations challenging. Future palaeoclimate research in the IP will strive to integrate new information from long, robust, and quantitative proxy-based records along with modelling outputs. This integration aims to identify the dynamics involved in past rapid environmental and climate changes and their impacts. Such efforts will provide an opportunity to better understand and predict potential future impacts of present anthropogenic warming on the planet by achieving improved knowledge on the role of external forcings and climate system feedbacks on long-term climate variability.

2. IP climate variability and associated large-scale oceanic and atmospheric patterns since the Last Glacial Maximum (LGM)

2.1. LGM and Deglaciation

The LGM occurred approximately from 23 to 19 ka BP and is typically defined as the period when global ice sheets reached their maximum extent within the last glaciation, as indicated by both data (Rasmussen et al., 2014) and models (Alvarez-Solas et al., 2019; Blasco et al., 2019; Tabone et al., 2018). Globally, cold and arid conditions resulted from strongly reduced Northern Hemisphere summer insolation and atmospheric CO_2 concentrations, as indicated by model studies (e.g. (Montoya and Levermann, 2008)). However, the LGM was

not necessarily the coldest and the most arid period of this glacial cycle, either globally or regionally, as suggested by lake sediments from the IP (Camuera et al., 2019; González-Sampériz et al., 2006; Jambrina-Enríquez et al., 2014; Morellón et al., 2009a, 2009b; Moreno et al., 2012a; Oliva et al., 2019) and Iberian Central System glaciers (Domínguez-Villar et al., 2013). Because of the LGM low sea level (minimum values about 130 m below present), marine productive cells or upwelling centres in the Western Iberian margin migrated offshore (Salgueiro et al., 2014). Yet, the Western Iberian margin was more productive and colder than during the Late Holocene (Martins et al., 2015; Salgueiro et al., 2014). Despite the prevailing influence of the cold Portugal Current in the Western Iberian margin (Maiorano et al., 2023), the latitudinal gradient, characterised by a ~4 °C increase from the Galician margin to the Gulf of Cadiz, up to ~18 °C (Salgueiro et al., 2014), was reversed in the Western Mediterranean Sea, with surface temperatures oscillating around 15 °C in the Alboran Sea (Blanca Ausín et al., 2015; Morcillo-Montalbá et al., 2021; M. Rodrigo-Gámiz et al., 2014). In Figure 1.1 some palaeoclimate reconstructions from IP are shown covering the last 20 ka.

Both models and data indicate much larger climate variability on millennial timescales during the last glacial period than during the Holocene, as a result of substantial variability of the AMOC (e.g., (Banderas et al., 2018, 2015, 2012)). The same applies to the last deglaciation. The last deglacial melting started with the occurrence of the HS1 at about 18 ka BP, characterised by cold conditions in the North Atlantic realm and a major weakening or even shutdown of the AMOC (Figure 1.2). Modelling studies suggest an important feedback of the AMOC reduction on ice sheets: the weakened AMOC led to subsurface warming in the Nordic and Labrador Seas resulting in the rapid melting of the Hudson Strait and Labrador ice shelves. The lack of buttressing by the Laurentide ice shelves caused a substantial ice-stream acceleration, enhanced ice discharge, and subsequent sea level rise (Alvarez-Solas et al., 2013; Álvarez-Solas et al., 2011). A similar mechanism applies during ice discharges of the last glacial period (Alvarez-Solas et al., 2013). The AMOC weakening during these events led to a cold phase in the Northern Hemisphere and the southward migration of the oceanic thermal fronts (i.e., Polar, Subpolar, and Subtropical Fronts), resulting in a southward shift in the storm track (Eynaud et al., 2009; López-Martínez et al., 2006; Luetscher et al., 2015).

The IP proxy-based records indicate that the HS1 was colder and more arid than the LGM (Moreno et al., 2012b). Quantitative mean air temperature reconstructions estimated minimum values of 12 ºC for the HS1 followed by the HS3, HS2 and then by the LGM, in the Padul lake record from the southern IP (Rodrigo-Gámiz et al., 2022). A pollen assemblage study from the same record presented a new climatic subdivision of the HS1 alternating humid and arid sub-phases, identifying three sub-stages with milder arid conditions during the middle one (HS1b), supported by temperature oscillations from the Mediterranean Sea (Figure 1.1; (Camuera et al., 2021)). Because of the AMOC collapse, the oceanic Polar Front migrated as far south as 42°N, reorganising the hydrography of the whole Western Iberian margin (Martins et al., 2015). Sediment cores from the Western Iberian margin reveal that Antarctic Bottom Water (AABW) reached these north latitudes between 2500 and 3100 m (Voelker and De Abreu, 2011). On the surface, marine temperatures dropped but showed a meridional gradient of ~10 °C from the north to the south Iberian margin (Salgueiro et al., 2014), possibly influenced by the warmer Azores Current in the south (Martins et al., 2015).

Melting icebergs transported coarse mineral grains, named Ice Rafted Debris (IRDs), from the European and Laurentide ice sheets that deposited along the west Iberian margin (Ausín et al., 2020; Plaza-Morlote et al., 2017). Fresh and cold melting waters entered the Western Mediterranean Sea, transporting fine detrital carbonate from Laurentine sources into the Alboran Sea ((Hodell et al., 2017); Figure 1.1). Consistent with the terrestrial records, marine records also identify three distinct phases within HS1. In the northern margin (Bay of Biscay), deep waters progressed from cold to extremely cold during the first two phases while the third phase was dominated by ocean bottom anoxia and warmer waters (Pascual et al., 2020).

Sea surface temperature (SST) records from the western and southern IP show a "w-shape" structure for HS1, with a central warmer episode (HS1b) that interrupted the overall extreme cold conditions of this stadial period (Martrat et al., 2014; Mesa-Fernández et al., 2022; Morcillo-Montalbá et al., 2021; Singh et al., 2023). This intra-HS1 warming episode preceded the arrival of IRDs in the Iberian margin and the influx of fresh meltwaters into the Mediterranean Sea, suggesting a causality between this subtropical heat accumulation and the subsurface warming that triggered the largest HS1 ice destabilisation phase (Figure 1.1; (Hodell et al., 2017; Jiménez-Amat and Zahn, 2015; Sierro et al., 2020)). Such variability also had an apparent impact on upwelling intensity, nutricline depth, and primary productivity (Ausín et al., 2020). The inflowing fresh melting waters into the western Mediterranean promoted an overall stratification that led to a slowdown in deep convection, reducing oxygen content in the deep basin and weakening the Mediterranean Outflow Water (MOW; (Lebreiro et al., 2018; Mesa-Fernández et al., 2022; Pérez-Asensio et al., 2020a; Sierro et al., 2020)). But at the same time, MOW became deeper, being detected down to >2600 m in the western Iberian margin (Ausín et al., 2021; Sierro et al., 2020). During the third phase of the HS1, when the surface freshwater anomaly became diluted, and climate conditions on land reached their maximum aridity (Camuera et al., 2021), MOW increased its oxygen content and intensity, particularly at shallow sites. This situation should have injected heat and salt into shallower depths of the North Atlantic Ocean, contributing to the reactivation of the AMOC that marked the end of this episode (Sierro et al., 2020).

The B-A or GI-1 (14.5-12.9 ka BP) period started with the resumption of a strong AMOC linked to the northward migration of the oceanic thermal fronts that led to an overall rapid warming in the Northern Hemisphere. The B-A climate in the whole IP is usually characterized by generally warm and wet conditions, in contrast to the previous LGM and HS1 periods (Bernal-Wormull et al., 2021; Camuera et al., 2019, 2021; García-Alix et al., 2014; González-Sampériz et al., 2010, 2017; Jambrina-Enríquez et al., 2014; Jiménez-Moreno et al., 2023a; Moreno et al., 2010; Muñoz Sobrino et al., 2013; Rodrigo-Gámiz et al., 2022; Singh et al., 2023). Temperatures in the ocean also confirm an overall warming from the Bay of Biscay to the western Mediterranean (Català et al., 2019; Martrat et al., 2014; Morcillo-Montalbá et al., 2021; Pascual et al., 2020; Marta Rodrigo-Gámiz et al., 2014; Rodrigues et al., 2010), with warmer waters in the Mediterranean sector than in the Atlantic one. However, the IP transition toward warmer and wetter conditions from the HS1 to the B-A, despite several regional/record heterogeneities, can be described as a more gradual transition than that identified in northern latitudes, such as in Greenland (Camuera et al., 2021; Moreno et al., 2012b; Naughton et al., 2016; Rodrigo-Gámiz et al., 2022). The B-A period was not stable, and both marine and continental records indicate

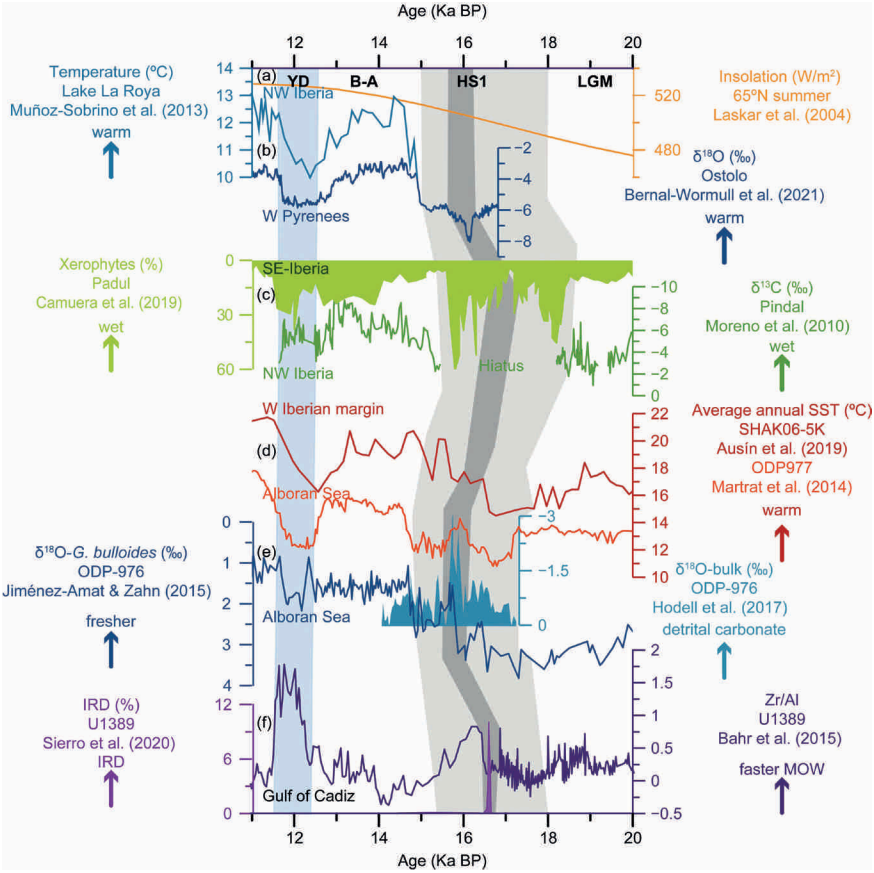

Figure 1.1. Deglacial records for proxies sensitive to temperature, humidity, and oceanographic conditions in and around the IP: a) Summer Insolation at 65ºN, climate forcing that triggered the last deglaciation; b) July air temperatures based on Chironomid from La Roya Lake (NW IP; Muñoz Sobrino et al., 2013) and a speleothem $\delta^{18}O$ record from Ostolo cave as an indicator of air temperatures (northern IP; Bernal-Wormull et al., 2021); c) Records for hydrological changes based on Pollen percentages of the xerophytes group from Padul wetland (SE IP; Camuera et al., 2019) and a $\delta^{13}C$ speleothem record from Pindal Cave (NW IP; Moreno et al., 2010); d) Records of annual averaged SST based on alkenones from the W Iberian Margin (Ausín et al., 2019) and the Alboran Sea (Martrat et al., 2014); e) Alboran Sea records of $\delta^{18}O$ as an indicator of saltier/fresher surface inflowing waters into the Mediterranean Sea (Jiménez-Amat and Zahn, 2015) and a proxy for the arrival of fine carbonates associated with IRD (Hodell et al., 2017); f) Gulf of Cadiz records of IRD and also Zr/Al as an indicator for intensity of the outflowing Mediterranean waters (Sierro et al., 2020). LGM: Last Glacial Maximum, HS1: Heinrich Stadial 1, B-A: Bølling-Allerød, YD: Younger Dryas. Records are plotted on their original chronologies, note that due to the intrinsic uncertainties of each of the archives and dating methods, the climatic periods do not always present homogeneous ages.

short-lived oscillations (GI-1a-GI-1e; (Camuera et al., 2021; Moreno et al., 2012b)). For instance, higher resolution studies have identified a rapid cooling event during the second half of the B-A (Intra-Allerød Cold Period; e.g., (Carrasco et al., 2015; Hernández et al., 2023; Jambrina-Enríquez et al., 2014; Muñoz Sobrino et al., 2013; Turu et al., 2021, 2018)). In more detail, (Muñoz Sobrino et al., 2013) identified up to three intra-B-A short regional cold events linked to the Greenland isotopic sub-stages GI-1d, GI-1c2, and GI-1b. Hydrological reconstructions also indicate some B-A variability, suggesting a gradual increase in precipitation from early to later phases of the B-A period resulting from a southward migration of the westerly winds (i.e., negative NAO (North Atlantic Oscillation) -like conditions), steadily extending its influence with wetter and milder conditions over the IP (Costas et al., 2016; García-Alix et al., 2014; Moreno et al., 2010; Naughton et al., 2016; Rodrigo-Gámiz et al., 2022, 2011). In the ocean, records from the western Iberian margin have confirmed that the early B-A warming preceded meltwater pulse mwp-1A, the fastest phase of deglacial sea level rise concomitant with the northward displacement of the Azores Front (Ausín et al., 2020; Rodrigues et al., 2010). These changes led to the development of extremely dysoxic conditions in the eastern part of the northern Iberian margin (Pascual et al., 2020) and primary productivity increased all over the margin compared to the previous HS1 (Ausín et al., 2020; Morcillo-Montalbá et al., 2021). This sea level rise also had consequences in the Mediterranean circulation, which promoted vertical stratification, weakening the thermohaline convection in the Gulf of Lion and led to the dominance of poorly ventilated intermediate and deep waters that formed the last Organic Rich Layer (ORL) in the Alboran Sea between 14.4 and 8.9 ka BP ("Martínez-Ruiz et al 2015 QSR_resumen," n.d.; Pérez-Asensio et al., 2020b; Rodrigo-Gámiz et al., 2011). A high-resolution study of seven marine records from a transect from the Algero-Balearic basin to the Alboran Sea pointed to different phases within the Organic Rich Layer 1 (ORL1), an interval characterised by organic-rich sediments in the Western Mediterranean marine sediments: the ORL1a (15-11.7 ka BP) and ORL1b (11.7-9 ka BP), characterised by different bottom water oxygen conditions (Mesa-Fernández et al., 2022).

The YD or GS-1 (12.9-11.7 ka BP) period represented an interruption in the deglacial warming of the Northern Hemisphere driven by a subtle weakening in the AMOC intensity that returned the Atlantic region to a cold stadial (Naughton et al., 2016) (Figure 1.2).

In the marine realm around the IP, this cold period is commonly described as a two-phase event: a coldest first phase followed by warmer conditions during the second half (Blanca Ausín et al., 2015; Ausín et al., 2020; Rodrigo-Gámiz et al., 2011; Marta Rodrigo-Gámiz et al., 2014) while, on land, a first dry phase has been observed, followed by an increase in humidity (Baldini et al., 2019; Bartolomé et al., 2015). A longitudinal front between colder offshore and warmer onshore waters was located at 10°W by the western Iberian margin, possibly due to the influence of the subtropical Paleo-Iberian Poleward Current (Salgueiro et al., 2014). At the same time, a meridional gradient of about 9 ºC has been described from the Galician margin to the Gulf of Cadiz, as for the HS1, this gradient reversed in the Alboran Sea, which was several degrees colder. The latter further supports the amplifying effect of the Mediterranean Sea (Blanca Ausín et al., 2015; Morcillo-Montalbá et al., 2021; Marta Rodrigo-Gámiz et al., 2014; Salgueiro et al., 2014). These conditions were clearly associated with a more southerly and zonal storm track linked to the southern shift of the Polar Front and Jet Stream (Costas et al., 2016; Gázquez et al.,

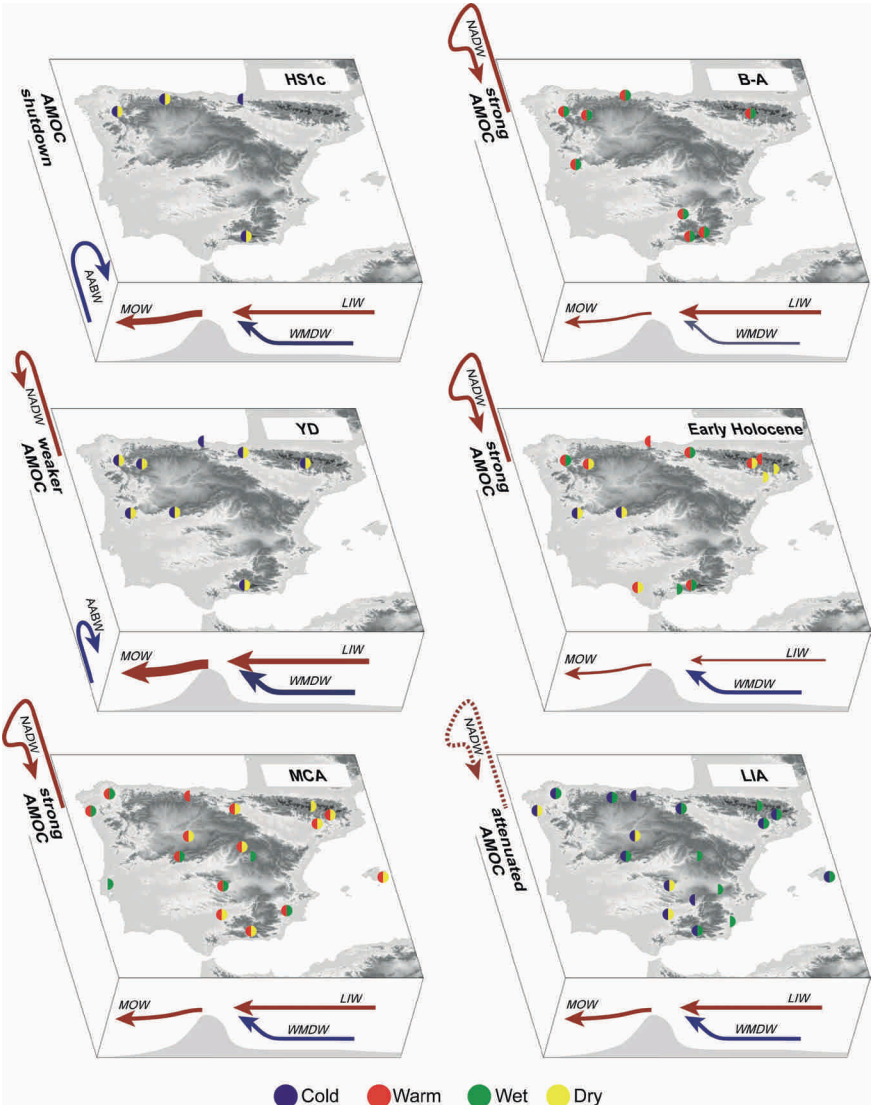

Figure 1.2. Schematic representation of climate periods in the IP and adjacent seas. Dots indicate local climate conditions (blue-cold, red-warm, green-wet, and yellow-dry) from selected available proxy-based records (see text for references). Blue and red arrows indicate main water masses and circulation: AMOC: Atlantic Meridional Overturning Circulation; NADW: North Atlantic Deep Water; AABW: Antarctic Bottom Water; MOW: Mediterranean Outflowing Water; LIW: Levantine Intermediate Water; WMDW: Western Mediterranean Deep Water. Climate periods: HS1c: Heinrich Stadial 1c; B-A: Bølling-Allerød; YD: Younger Dryas; MCA: Mediaeval Climate Anomaly, and LIA: Little Ice Age.

2018; Moreno et al., 2023; Naughton et al., 2019, 2016). This atmospheric configuration mirrors the modern Scandinavian pattern (SCA), marked by a blocking high pressure over Scandinavia influencing storm tracks (Rea et al., 2020). As a consequence, the IP climatic conditions were mostly dry and, according to existing estimations, around ~30–35 % drier than today (Gázquez et al., 2018). Continental records, including lakes and cave records, also confirm the previously described double phase of the YD, consisting in this case of a cooling and drying followed by a warmer and wetter second phase (Bartolomé et al., 2015; Camuera et al., 2021; Hernández et al., 2023; Naughton et al., 2019; Rodrigo-Gámiz et al., 2022; Turu et al., 2021). Evidence from the Duero River basin indicates that the YD started with a dry spell followed by a phase of moderate-magnitude floods between 11.6 and 11.5 ka BP (Benito et al., 2023). The YD was also a period of glacier reactivation in the Iberian mountains (Carrasco et al., 2015; Hernández et al., 2023; Jambrina-Enríquez et al., 2014; Oliva et al., 2019). These YD dry climatic conditions dominated over the entire Mediterranean region and induced a strong reinforcement of the thermohaline circulation in the eastern Mediterranean Sea that led to an enhanced westward outflow of east source waters, about double the present-day influx into the western Mediterranean (Trias-Navarro et al., 2023). This influx is coherent with the observed invigoration of MOW in the Gulf of Cadiz (Bahr et al., 2015; Lebreiro et al., 2018; Sierro et al., 2020). At the same time, the deep Alboran basin was still poorly ventilated, maintaining the formation of the ORL, dominated by reduced oxygen conditions (ORL1a; (Mesa-Fernández et al., 2022)), but deep intermediate depths (at 900 m) suddenly became reventilated, suggesting an invigoration of intermediate convection in the western Mediterranean basin (Pérez-Asensio et al., 2020b; Trias-Navarro et al., 2023). At the end of the YD, a sharp surface temperature increase is observed in just a few decades, parallel to the sea level rise associated with meltwater pulse mwp-1B (Bernal-Wormull et al., 2021; Rodrigues et al., 2010).

2.2. The Holocene

Long-term climate variability in the IP during the Holocene is primarily attributed to precession-driven insolation changes (Hernández et al., 2020b; Wanner et al., 2008). Superimposed on this orbital-scale climate evolution, other forcings such as solar activity and atmospheric modes of variability drove Holocene centennial-scale climate oscillations (e.g., (Hernández et al., 2021; Moffa-Sánchez et al., 2014)). Periods of high Total Solar Irradiance (TSI) commonly result in blocking-like patterns over mid-latitudes, which lead to increased aridity over the IP (NAO-like positive pattern). Thus, periods of decreased (increased) TSI correspond to regional wetter (drier) conditions. Furthermore, Holocene climate variability in the IP was also closely related to circulation changes in the North Atlantic Ocean, the westerlies position, dynamics of atmospheric circulation patterns, and Mediterranean storm activity (Di Rita et al., 2018; Fletcher et al., 2013; Martin-Puertas et al., 2023). These factors can be modulated by TSI variations and the strength and/or position of the Azores High (e.g., (Cresswell-Clay et al., 2022; Hernández et al., 2021)). According to well-known mechanisms governing present-day variability in the North Atlantic region, changes in the position and extent of the Azores High, impacting the NAO variability, are one of the main controllers for the Holocene position of North-Atlantic westerly winds (Goslin et al., 2018; Hu et al., 2022; Mellado-Cano et al., 2019). In addition, rainfall variability in winter and spring are well explained by the southwest-northeast-defined index between

the Iberian and Italian peninsulas, the Western Mediterranean Oscillation (WeMO; (Moreno et al., 2017)). Therefore, variations in both synoptic-scale climate patterns and large-scale atmospheric circulation indexes (e.g., NAO and WeMO) have been useful to explain the high spatial Holocene climate variability and complexity in the IP (Moreno et al., 2017). Some proxy records covering the Holocene period in the IP are represented in Figure 1.3.

2.2.1. Early Holocene (Greenlandian)

During the Early Holocene (or Greenlandian, 11.7-8.2 ka BP) the orbital configuration led to high summer insolation in the Northern Hemisphere. This period started with an overall warming across the whole IP, supported by consistent records available from the north to the south and surrounding seas (Figure 1.3), setting the end of the cold and arid conditions of the YD, and leading to the more stable climate conditions of the Holocene (e.g., (Bernal-Wormull et al., 2023; Gázquez et al., 2018; González-Sampériz et al., 2017; Jambrina-Enríquez et al., 2014; Jiménez-Moreno et al., 2023a; López-Avilés et al., 2022; María J. Ramos-Román et al., 2018; Rodrigo-Gámiz et al., 2022; Tarrats et al., 2018)). However, records from the northeastern part, specifically the northern Mediterranean Iberia (i.e., the Pyrenees), indicate a delayed temperature increase at the Holocene onset. This delay is attributed to the strong seasonal contrast between high summer and low winter temperatures (Tarrats et al., 2018). Vegetation types also reflect harsh environmental conditions, particularly attributed to cold winter temperatures (González-Sampériz et al., 2017). A rise in winter temperatures across the Pyrenean range occurred around 9.8–9.5 ka BP (Tarrats et al., 2018), whereas alpine palaeoclimatic records from Sierra Nevada (southern IP) indicate an earlier temperature maximum, after 10.5 ka BP (Camuera et al., 2019; Jiménez-Moreno et al., 2023a; López-Avilés et al., 2022; Mesa-Fernández et al., 2018; Toney et al., 2020). Marine temperature reconstructions show rather a rapid warming at the onset of the Greenlandian, likely attributed to more annually averaged estimates (Ausín et al., 2019; Català et al., 2019; Gomes et al., 2020; Martínez-García et al., 2015; Marta Rodrigo-Gámiz et al., 2014). In the Alboran Sea, multi-proxy quantitative SST reconstructions oscillated between 18 and 23 °C (Morcillo-Montalbá et al., 2021; Marta Rodrigo-Gámiz et al., 2014).

A weakening of the Azores High enhanced the steering of storm tracks to the south and resulted in an overall increase of rainfall across IP (Thatcher et al., 2020; Wanner et al., 2011). This weakened Azores High during the Early Holocene partially explains why this period was relatively wet (with a southern migration of the westerlies) compared to the Middle and Late Holocene (Gomes et al., 2020; Thatcher et al., 2020). Moreover, differences in summer and winter insolation defined the climate seasonality, argued to be an important driver of hydroclimate variability, particularly in the southern IP, promoting enhanced winter precipitation from Mediterranean source areas (García-Alix et al., 2021; Wagner et al., 2019; Zielhofer et al., 2017). In the context of the whole IP, this period shows a complex regional pattern in the timing and intensity of the hydrological changes (Finné et al., 2019; Morellón et al., 2018), forming two spatial clusters: i) for northwestern areas, a near-instantaneous rise in humidity, and ii) for eastern and southern

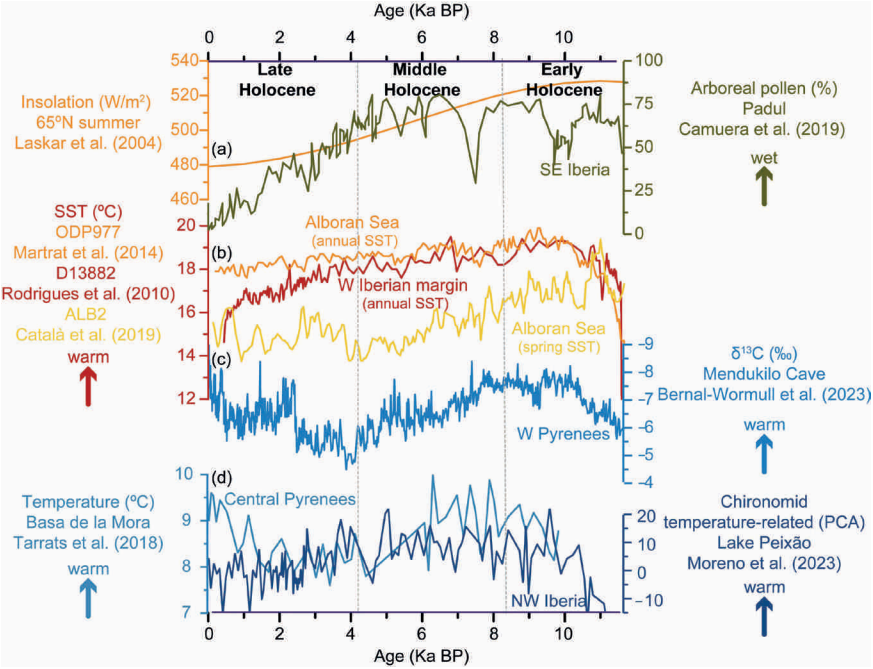

Figure 1.3. Holocene records for proxies sensitive to temperature and humidity conditions in, and around, the IP. a) Summer Insolation at 65ºN and speleothem $\delta^{18}O$ record as indicator of % of recycled precipitation in northwestern IP (Domínguez-Villar et al., 2017); b) % of arboreal pollen from wetland deposits as proxy of hydrological conditions (Padul, southeastern IP: Camuera et al., 2019); c) SST records based on alkenones (represent annual average values) for the western Iberian margin (red; Rodrigues et al., 2010), for the Alboran Sea (orange; Martrat et al., 2014) and based on Mg/Ca ratios on G. bulloides (represent spring values) for the Alboran Sea (orange; Català et al., 2019); d) A speleothem $\delta^{13}C$ record as proxy of air temperature from Mendukilo cave (northern IP; Bernal-Wormull et al., 2023); e) Chironomid based air temperature reconstruction from Basa de la Mora Lake (northeastern IP; Tarrats et al., 2018) and Chironomid temperature related record from Lake Peixao (western IP; Moreno et al., 2023).

sites, the persistence of prolonged arid conditions, similar to the preceding YD, followed by a generally abrupt increase in moisture ca. 10-9 ka BP (Morellón et al., 2018). Before 9.7 ka BP in northern Iberia, hydrological conditions and vegetation responses displayed an E–W pattern linked to Atlantic vs Mediterranean-influenced areas (Gomes et al., 2020) and an altitudinal gradient in the Central Pyrenees (González-Sampériz et al., 2017). While lowland lakes experienced the lowest levels throughout the entire Holocene (Morellón et al., 2009b; Pellicer et al., 2016), high-altitude lakes reached almost their highest levels due to increased winter

snowpack and subsequent summer snowmelt (Pérez-Sanz et al., 2013). After 9.7 ka BP, this pattern shifted to milder temperatures and an increase in water availability (Pellicer et al., 2016; Pérez-Sanz et al., 2013). At this time, southern IP entered what is called the Western Mediterranean Humid Period, representing the wettest stage of the Holocene (García-Alix et al., 2021; Toney et al., 2020). Lacustrine and marine records from the western and southern IP prove a stepwise increase in moisture during this transition (Finné et al., 2019; Gázquez et al., 2018; Ilvonen et al., 2022; Morellón et al., 2018).

These relatively warm and humid conditions were punctuated by various short-lived centennial-scale events with a cold climate signature (B. Ausín et al., 2015). These events generally tracked North Atlantic SST variability, with warmer (cooler) Atlantic SSTs corresponding to more humid (drier) conditions in the Atlantic IP (Sánchez Goñi et al., 2016; Sánchez-Goñi et al., 2013). Some of these events were related to floods over the IP and aligned with North Atlantic meltwater pulses (Baldini et al., 2019; Benito et al., 2023; Bernal-Wormull et al., 2023; Smith et al., 2016). The occurrence of some events remains ambiguous along the IP, but two of the most studied events occurred at 9.2 and 8.2 ka BP, and they have been recognized in several marine and continental IP records (Bernal-Wormull et al., 2023; Ilvonen et al., 2022; Singh et al., 2023). The 9.2 ka event was generally recorded as dry and cold across the IP (e.g., Baldini et al., 2019; Bernal-Wormull et al., 2023; María J Ramos-Román et al., 2018; Turu et al., 2021), whereas the 8.2 ka event was recognized as cold elsewhere, but dry (e.g., Domínguez-Villar et al., 2009; Pérez-Sanz et al., 2013; Schröder et al., 2020) or wet, when it appears undistinguished of the general "Western Mediterranean Humid Period" of Early Holocene (Rodrigo-Gámiz et al., 2022; Tarrats et al., 2018; Thatcher et al., 2020; Toney et al., 2020).

The variability of the hydrological cycle in the IP during this time period recorded millennial oscillations with a periodicity of ca. 1 ka, supporting that ocean conditions in the northern North Atlantic control long-term climate hydroclimate variability in the IP (Domínguez-Villar et al., 2017; Fletcher et al., 2013). Circulation conditions in the Mediterranean were dominated by a major stagnation phase in the eastern Mediterranean that led to the formation of the last sapropel (S1: 10.8-6 ka BP; Checa et al., 2020). This situation induced a major reduction in the westward flow of eastern Mediterranean waters, resulting in a weakening of the MOW strength (Sierro et al., 2020; Trias-Navarro et al., 2023). In contrast, the deep Alboran Sea became well-ventilated at 9 ka BP, ending the formation of the ORL or ORL-1b (Mesa-Fernández et al., 2022; Pérez-Asensio et al., 2020b) that was initiated during the B-A period.

2.2.2. Middle Holocene (Northgrippian)

During the Middle Holocene or Northgrippian (8.2-4.2 ka BP), northern summer insolation decreased while winter insolation progressively increased due to changes in eccentricity. However, temperature reconstructions in the IP do not strictly agree with these changes in orbital forcing (González-Sampériz et al., 2017). Some terrestrial records from north IP show maximum Holocene temperature values during this period (ca. 8-6.5 ka BP; Figure 1.3; Tarrats et al., 2018), but most

continental and marine IP records indicate a declining trend in temperatures consistent with the North Atlantic Neoglacial period that followed the progressive reduction in summer insolation (Bernal-Wormull et al., 2023; Català et al., 2019; Leunda et al., 2019; Sancho et al., 2018). Off Portugal, similar general trends are observed in SST records (Ausín et al., 2019), interrupted by brief cold events at 8.2, 7.1, and 5.5 ka BP (Singh et al., 2023).

Orbital changes resulted in a net decrease in annual insolation in the Northern Hemisphere inducing cooling and a southward migration of the Intertropical Convergence Zone (ITCZ) with the Azores High (Wanner et al., 2011). This situation led to overall drier conditions in the IP for the Northgrippian compared to the Greenlandian, but these changes were complicated by land-surface feedbacks that resulted in complex changes in IP moisture (Liu et al., 2023). Consequently, some discrepancies exist between records, with proxy-based data indicating wet conditions until 6 ka BP (Gil-Romera et al., 2010; Ilvonen et al., 2022; Pérez-Obiol et al., 2012; Pérez-Sanz et al., 2013), while other proxy datasets show dry conditions between 8.2 and 5.5 ka BP (Benito et al., 2023; Jambrina-Enríquez et al., 2014; Moreno et al., 2011), likely reflecting Atlantic versus Mediterranean influences. Although the west–east gradient in moisture appears to have been less pronounced during the Northgrippian than at present (Liu et al., 2023), the central IP was mostly wet during this period (Aranbarri et al., 2014; Moreno et al., 2017). The Azores High gradually migrated southward since ca. 7 ka BP, and the NAO-like pattern was largely in a positive mode in the Middle Holocene, resulting in less winter precipitation in the IP (Jambrina-Enríquez et al., 2014; Wanner et al., 2008). The establishment of the current western Mediterranean dynamics occurred after ca. 7-6 ka BP (B. Ausín et al., 2015; García-Alix et al., 2021; Toney et al., 2020; Zielhofer et al., 2017). Hydroclimate conditions in alpine southern Iberia records (i.e., Sierra Nevada) were wet, including a transition to dry conditions after ca. 6-5 ka BP (Jiménez-Moreno et al., 2023a; López-Avilés et al., 2022), whereas they were mostly dry in southern Iberia lowlands records (Fletcher et al., 2013; García-Alix et al., 2022; Rodrigo-Gámiz et al., 2022; Walczak et al., 2015). After 5 ka BP, some records show a general increase in precipitation (Benito et al., 2015; Castro et al., 2015; Dessandier et al., 2018), but central Iberia underwent a marked shift towards a more arid climate (Thatcher et al., 2020). Thatcher et al., 2020 proposed discernible wetter intervals for 7.5–7.1, 6.9–6.5, 6.4–6.0, and 5.5–5.2 ka BP, separated by drier periods. During the Middle Holocene, the millennial variability of the hydrological cycle changed its periodicity from ca. 1 ka to the ca. 2 ka that continued until nowadays (Domínguez-Villar et al., 2017; Fletcher et al., 2013; Jiménez-Moreno et al., 2022). Thus, until the large ice masses in Europe and North America were not melted completely, their impact on the northern North Atlantic had a strong teleconnection at millennial timescales (with a periodicity of ca. 1 ka) with the hydrological cycle in the IP. However, once those ice caps were deglaciated, the Tropical North Atlantic transferred its millennial climate oscillations (with a ca. 2 ka periodicity) to the hydrological cycle variability in the IP.

The Middle Holocene ended with the so-called 4.2 ka event. Although it remains insufficiently resolved in many IP records, an increasing number of studies identify

it as a rapid climate event (e.g., Bernal-Wormull et al., 2023; Moreno et al., 2017; María J Ramos-Román et al., 2018; Schirrmacher et al., 2019; Schröder et al., 2018). There are indications of severe aridification centred around 4.2 ka BP in the western IP (Thatcher et al., 2020), whereas the manifestation of this event in the southern IP showed very arid conditions (Lillios et al., 2016; Schröder et al., 2020). However, it appears to be shorter compared to the prolonged dry episode observed in other regions (Schirrmacher et al., 2019). In the northern IP, the climate around 4.2 ka BP was the driest of the full Holocene (Baldini et al., 2019; Domínguez-Villar et al., 2017). Temperature reconstructions from both north and south IP indicate this event as one of the coolest within the Holocene, with temperatures below those observed at 8.2 ka event, which also involved a period of intense ventilation in the Western Mediterranean Sea (Baldini et al., 2019; Bernal-Wormull et al., 2023; Català et al., 2019).

2.2.3. Late Holocene (Meghalayan)

A southward shift of westerlies marked the onset of the Late Holocene or Meghalayan (4.2-0 ka BP), coinciding with prevailing negative NAO-like phases (maximum winter precipitation) between 4 and 2 ka BP (Jambrina-Enríquez et al., 2014). However, around 4.2 ka BP, the transition to the cold Neoglacial period occurred (Wanner et al., 2011), characterised by increased TSI values and likely positive NAO conditions (e.g., Repschläger et al., 2017), potentially driving increased aridity throughout the region. The overall climate picture in the IP during the Meghalayan is not geographically homogeneous, as several short (centennial-scale) events introduced a complex heterogeneity in the regional climate responses. Northern IP records suggest substantial centennial-scale temperature variability from 4 to 2.5 ka BP and exhibit a pronounced warming event at ~3 ka BP (Baldini et al., 2019; Català et al., 2019; Martín-Chivelet et al., 2011). According to Martín-Chivelet et al., 2011, the main climatic periods are: i) ca. 4–3 ka BP, a warm period punctuated by cool events around 4, 3.6 and 3.3 ka BP; ii) 2.9–2.5 ka BP, a cold interval (Iron Age Cold Period); and iii) 2.5–1.7 ka BP, a moderately warm period (Iberian Roman Warm Period), with maximum temperatures between 2.2 and 1.8 ka BP. However, the validity of the proxy data from these speleothems used as palaeothermometer has been questioned (Domínguez-Villar, 2013). The lowest temperature values throughout the Holocene have been reconstructed during the period ca. 4.2–2.5 ka BP, coinciding with the first part of the Meghalayan period (Schirrmacher et al., 2020; Tarrats et al., 2018; Toney et al., 2020; Turu et al., 2021). In southern IP, despite the limited number of reconstructions of temperature for this period, a temperature minimum around 4.1-4 ka BP and a maximum between ca. 2.5-2.0 ka BP have been described (Ilvonen et al., 2022; Jiménez-Moreno et al., 2023a; Toney et al., 2020). In contrast, off Portugal, a brief cold event was recorded at 2.5 ka (Singh et al., 2023), whereas in the Bay of Biscay Martínez-García et al., 2015 proposed the intrusion of colder polar surface and bottom waters, which retreated during the Late Holocene.

The long-term aridification that characterises the Late Holocene in southern Europe (Corella et al., 2011; Cruz et al., 2015; Ilvonen et al., 2022; Martín-Puertas et al.,

2010; Morellón et al., 2009b; Nieto-Moreno et al., 2011) triggered the transition from permanent to shallow or ephemeral lakes in the western Mediterranean region (García-Alix et al., 2022, 2021; Jiménez-Espejo et al., 2014; Jiménez-Moreno et al., 2023b). Dry conditions also prevailed in northern IP until at least, 2.5 ka BP (Bernal-Wormull et al., 2023; Cruz et al., 2015; González-Sampériz et al., 2017; Pérez-Sanz et al., 2013). However, in the northwest, Jambrina-Enríquez et al., 2014 identified a wetter interval between 4.8 and 3.3 ka BP, with a relative decline in rainfall afterward. Similar increases in humidity between ca. 5-3 ka BP were also interpreted in Roñanzas peatbog (Ortiz et al., 2010) and Enol Lake (Moreno et al., 2011), whereas dry conditions occurred in Galician offshore (NW Iberia) of up to 3.3 ka BP (Bernárdez et al., 2008), followed by more humid conditions between 3.3 and 1.7 ka BP (Bernárdez et al., 2008; Diz et al., 2002). Pena et al., 2010 suggested events of reduced rainfall between 3.7 and 2.9 ka BP in the Ría de Muros (NW Iberia), and Muñoz Sobrino et al., 2012 identified short cold and dry events at about 4.6-4.3 and 3.8-3.6 ka BP, interspersed with warmer and wetter periods in Ría de Vigo (NW Iberia). Also in NW Iberia, Castro et al., 2015 defined wet conditions until 3.9 ka BP, between 3.6 and 3.4 ka BP, 3.3-3.1 ka BP, and 2.7–2.5 ka BP, previously recognized in other mires in northern Iberia (Ortiz et al., 2010). Interspersed between these wet periods of Pena da Cadela bog, three dry periods were recorded (3.9-3.7 ka BP; 3.3-2.7 ka BP; 2.4-2.3 ka BP). From a hydroclimate perspective, there is a clear consensus at the scale of the IP that arid conditions prevailed between ca. 4 ka BP and 2.7 ka BP, whereas wetter conditions dominated between 2.7 and 1.5 ka BP (Cisneros et al., 2021; Martín-Puertas et al., 2011; Nieto-Moreno et al., 2011). The most humid episode was recorded at 2.5-1.7 ka BP and was characterised by weaker winds from Africa (García-Alix et al., 2021; Jiménez-Moreno et al., 2013). Additionally, periods of flooding occurred at 3.5–3.3, ca. 2.6, ca. 2 ka BP (Santisteban et al., 2019).

2.3. The Common Era (CE)

The CE refers to the past 2 ka BP (Figure 1.4), usually expressed in calendar years and divided into four main climate phases, excluding the instrumental period: the Roman Warm Period (RWP), the Early Middle Ages (EMA), the Medieval Climate Anomaly (MCA), and the Little Ice Age (LIA). The main drivers governing climate variability at these timescales include climate modes of variability, i.e., large-scale atmospheric patterns, including orbital changes, solar and volcanic activity, LULC and anthropogenic greenhouse gases and aerosols; all these agreed to be used as boundary conditions for ESM last millennium simulations (Jungclaus et al., 2017; Schmidt et al., 2011).

In the northwest Iberian margin, upwelling variability during the last millennia has been connected to North Atlantic climate patterns such as the Atlantic Multidecadal Oscillation (AMO) on a decadal scale (Abrantes et al., 2011). However, this link decoupled after CE 1850, indicating a substantial anthropogenic influence for the last 150 yr, in line with a noticeable sea surface warming observed from 1970 off Portugal (Abrantes et al., 2017). Thus, comparing these periods with the industrial period (1850-Present), or the so-called historical period in PMIP terminology, aids in understanding the interplay between human-induced and natural climate variability.

The RWP (ca. 0 – 500 CE) is the warmest interval in the marine Iberian realm over the last two millennia (Abrantes et al., 2017, 2011; Cisneros et al., 2016). This period also exhibited warm inland conditions (Martín-Chivelet et al., 2011; Ramos-Román et al., 2018). Moreover, in the Western Mediterranean Sea, it was the most productive period of the last 4 ka BP (see Nieto-Moreno et al., 2011), characterised by intense deep-water formation (Cisneros et al., 2019). However, the hydroclimate during this period showed a complex pattern, with aridity in the north (Bartolomé et al., 2024; Morellón et al., 2011; Moreno et al., 2011), alternating conditions in the central region (Currás et al., 2012; Sánchez-López et al., 2016), prevailing humidity in the southwest (Martín-Puertas et al., 2010, 2008; Nieto-Moreno et al., 2011), and aridity in the southeast (Gázquez et al., 2020), indicating a significant spatial variability. Temperature conditions and hydroclimate gradients, with a humid trend towards southern IP, suggest that the prevalent climate was dominated by the combination of negative NAO and positive East Atlantic (EAP) patterns. Hernández et al., 2015 indicated that this combination led to wet and warm winters and warm summers (Abrantes et al., 2017; Sánchez-López et al., 2016).

The EMA (ca. 500 – 900 CE) is characterised by a relatively homogeneous cooling trend and cold conditions across the IP (María J. Ramos-Román et al., 2018). Nevertheless, complex spatial climate patterns arise. For instance, the northwestern IP experienced colder and more humid conditions (Bartolomé et al., 2024; Jambrina-Enríquez et al., 2014), in contrast to the more arid conditions in the eastern IP (Corella et al., 2012; Currás et al., 2012) and a shift from wet to dry conditions in Balearic Islands (Cisneros et al., 2021). The aridity gradient towards western and southern IP, combined with generally cold conditions, indicates that the positive NAO and negative EAP phases dominated the main climate variability, leading to dry and cold winters and cold summers (Abrantes et al., 2017; Sánchez-López et al., 2016). Moreover, based on documentary sources and observations at seasonal-to-annual timescales, Domínguez-Castro et al., 2014 identified three severe droughts during 748–754 CE, 812–823 CE, and 867–879 CE, particularly affecting southern IP.

The abundance of climate studies covering the last millennium has increased with the increase in the spatial distribution of proxy samples, allowing for a more detailed reconstruction of the MCA (ca. 900 – 1300 CE; Bartolomé et al., 2024; Ludwig et al., 2019; Moreno et al., 2012; Roberts et al., 2012; see also Figure 1.2). While most records suggest warmer and drier conditions (Cisneros et al., 2021; Corella et al., 2013), some studies indicate spatial hydroclimate heterogeneity (López-Blanco and Romero-Viana, 2019; Moreno et al., 2012). For example, Moreno et al., 2012 highlighted records from northwest Iberia that indicate increased humidity during the MCA, reflecting a behaviour opposite to that of Mediterranean Iberia, which was predominantly under drying conditions. Moreover, Abrantes et al., 2017 proposed two climate intervals along the western Iberian margin: i) the early MCA (900– 1100 CE) with warm and dry winters (Castro et al., 2020), cool summers, and extreme flooding (Machado et al., 2011), suggesting a link between the AMO and a high-pressure blocking system over northwestern Europe (positive-like mode of the SCA) as well as positive phases of NAO and EAP; ii) the late MCA (1200–1300 CE) with a wet and dry phase (Castro et al., 2020), along with cold stormy winters and warm summers resulting from a shift in SCA to its negative phase. Overall, relatively higher primary productivity off Lisbon characterised the whole period (Bartels-Jónsdóttir et al., 2015) and a decrease in bottom-water oxygenation in the Western Mediterranean Sea (Cisneros et al., 2016; Nieto-Moreno et al., 2011).

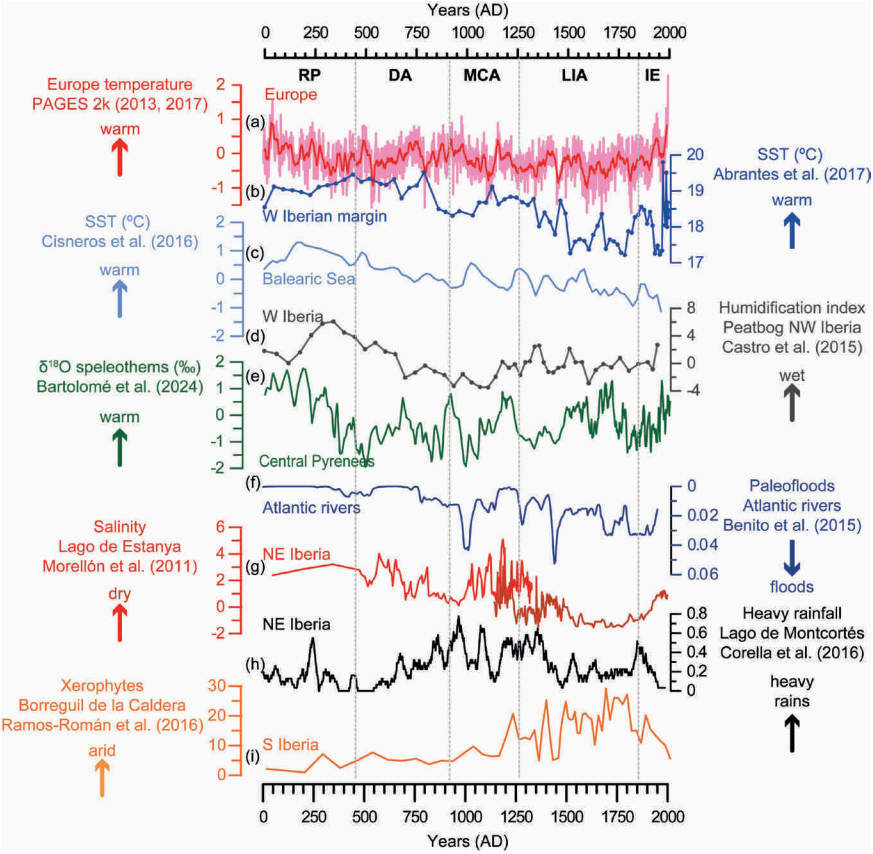

Figure 1.4. Proxy records sensitive to temperature and humidity conditions in and around the IP for the last 2000 years. a) temperature reconstruction from Europe, compiled by the PAGES2k group (pink line, running average width window = 15 years) (PAGES 2k Consortium, 2013); SST reconstructed from b) western Iberian marine cores (Abrantes et al., 2017) and c) Mediterranean cores offshore Balearic islands (Cisneros et al., 2016); d) detrended humidity index from a peatbog in western Iberia (Castro et al., 2015); e) Central Pyrenean $\delta^{18}O$ composite record based on eight stalagmites from four caves (Bartolomé et al., 2024); f) probability of palaeofloods in Atlantic rivers from Iberian Peninsula (Benito et al., 2015); g) salinity reconstructed from geochemical data from Estanya lake in the Pre-Pyrenees (González-Sampériz et al., 2017; Morellón et al., 2012, 2011); h) rainfall reconstructed from calcite layers from Montcortés Lake in the Pre-Pyrenees (Corella et al., 2012); i) abundance of xerophytes from alpine lakes in southern Iberia (Ramos-Román et al., 2016). RP: Roman Period, DA: Dark Ages, MCA: Mediaeval Climate Anomaly, LIA: Little Ice Age, IE: Industrial Era.

The LIA (ca. 1300 – 1850 CE), preceding anthropogenic warming, is characterised by colder continental and oceanic conditions (Abrantes et al., 2017; Cisneros et al., 2021; Nieto-Moreno et al., 2011; Oliva et al., 2018) with the advection of subpolar waters in the Portuguese margin (Abrantes et al., 2017; Bartels-Jónsdóttir et al., 2015) and a two-step event in the Western Mediterranean (Cisneros et al., 2016) that reflects a first warmer phase with intense deep-water formation, and a second colder phase with weaker deep-water formation. The available continental records confirm this double structure with transitions from warmer to colder (Dorado Liñán et al., 2015) and wetter to drier (Gardoki et al., 2023) conditions. However, regional differences in timing and intensity are evident (Barreiro-Lostres et al., 2014; Oliva et al., 2018). For example, (Castro et al., 2020) presented a highly resolved peat record, suggesting sub-phases for the LIA in NW Iberia: i) a wet period, with a first wet maximum and some relatively dry episodes that lasted until 1610 CE; ii) a less humid phase, with a clear tendency to very cold conditions, from 1610 to 1735 CE, iii) a short phase (1735–1815 CE) with increased dryness relative to the previous period, with alternating drought and rainfall episodes, and, iv) a second wet maximum until 1850 CE. In more detail, periods of higher flood incidence have been reconstructed (Bullón, 2011; Corella et al., 2012; Sánchez-García and Schulte, 2023). Nevertheless, there is a distinct difference in the behaviour of catastrophic floods in the northern series compared to southern ones (Blöschl et al., 2020; Machado et al., 2011). The northern floods appear to be associated with the atmospheric dynamics of cold episodes. But these oscillations are not as clearly observed in the southern series, where oscillations manifest with different temporal patterns. This complexity arises because the Western Mediterranean is situated in a transitional zone with a prevalence of air mass circulation (Barriendos et al., 2019). Additionally, despite the LIA was a predominantly wet period (Figure 1.2; Rodrigo, 2018), it also witnessed extreme droughts (Esper et al., 2015; Tejedor et al., 2016), as exemplified by reconstructions across the entire IP at the end of the 17th century (Romero-Viana et al., 2011; Vegas-Vilarrúbia et al., 2022). Some of these extreme droughts coincide with solar minima, such as the Maunder and Dalton minima (1645-1715 and 1790-1820, respectively), suggesting a relationship between solar activity and extreme climate events (Bartolomé et al., 2024; Domínguez-Castro et al., 2010; Gil-Guirado et al., 2019; Morellón et al., 2011; Rodrigo et al., 2012; Romero-Viana et al., 2011; Sánchez-García and Schulte, 2023, p. 202; Tejedor et al., 2017; Vegas-Vilarrúbia et al., 2022). Conversely, although some studies have explored the relationship between volcanic eruptions and climate patterns (Tejedor et al., 2019; Trigo et al., 2009), this link is less clear (Domínguez-Castro et al., 2012). Only a few reconstructed cold extremes (536 CE, 1453 CE, 1601 CE, 1816 CE) coincide with large volcanic eruptions (Bartolomé et al., 2024; Esper et al., 2020; Tejedor et al., 2019), suggesting that the severe cooling events in Iberia are mostly influenced by internal dynamics and solar activity rather than volcanic forcing (Esper et al., 2020; Hernández et al., 2020a). Thus, the LIA was dominated by the negative phases of the NAO and EAP, leading to cold and wet winters and cold summers (Mellado-Cano et al., 2019; Rodrigo, 2019; Sánchez-López et al., 2016; Sicre et al., 2016).

ESM simulations of the last millennium (850-1850 CE), continued during the historical period, 1850-2014 (in PMIP/CMIP terminology; Eyring et al., 2016), use as boundary conditions specifications of natural (orbital, solar and volcanic) as well as anthropogenic (LULC, greenhouse gases and aerosols) forcings (Jungclaus et al., 2017). However, it should be recalled that greenhouse gases also include natural changes before industrialization and the anthropogenic effects in LULC extend back well before 1850. Estimates of solar and

volcanic variability as well as CO_2 concentrations used in PMIP4 and in recent simulations of the CE, are represented in Figure 1.5 and are implemented with relatively minor differences across models and simulations.

Reconstructions of the NAO variability (Hernández et al., 2020; Ortega et al., 2015) suggest, as discussed above, slightly higher NAO values during the MCA and lower during the LIA, but with considerable variability within those periods. In fact, model simulations (Figure 1.5) produce a wide range of model responses, comparable or wider than the NAO variability within each simulation. Nevertheless, consistently with reconstructions, for each simulation, the index values tend to be slightly larger during the MCA, in response to higher TSI and lower volcanic activity (Roldán-Gómez et al., 2020). Simulated NAO multi-decadal variability is model and simulation dependent, which suggests that internal variability, rather than external forcing, dominates at these timescales. Consistently with this, analyses of hydroclimate variability in PMIP3,4 simulations for different regions have evidenced long-term responses to external forcing, but with internal variability playing a major role in mid-latitude decadal and multi-decadal variability (Roldán-Gómez et al., 2023). Nevertheless, some studies (Fernández-Montes et al., 2017; Gómez-Navarro et al., 2012) have focused on the precipitation-temperature relationships in experiments with regional climate model simulations driven by boundary conditions provided by global climate model simulations of the last millennium (González-Rouco et al., 2009), that included yearly variations in natural and anthropogenic forcings. These analyses have found that increases in model resolution through dynamical downscaling can enhance forced responses in seasonal precipitation for certain areas, and thus precipitation-temperature relationships, by orographically affecting the convection level or during summer through changes in convective activity. Therefore, future developments in improving model resolution can bear implications for our understanding of hydroclimate variability in response to external forcing and thus, for model-data comparison (Rodrigo, 2012).

Modelled temperature variability varies across regions and depends on the ESM realisation, which also suggests a role of internal variability. However, it shows more coherent responses to external forcing (Figure 1.5) with multi-decadal cooling coinciding with decreases in solar variability and the occurrence of volcanic activity; conversely for relatively warm periods. As found in reconstructions of summer temperature variability in the Pyrenees (Dorado Liñán et al., 2012) and Cazorla (Dorado Liñán et al., 2015), for which extended higher temperatures are found in the MCA before a LIA cooling well after the 16th century, additional to temperature minima aligned with solar minima and volcanic cooling. Warmth in the 20th century seems to be overstated by model simulations in comparison to reconstructions (Dorado Liñán et al., 2012), likely a result of some PMIP3 model experiments missing aerosol and LULC forcings.

3. Impacts

Climate change is predicted to threaten biodiversity (Dawson et al., 2011) operating at different ecological scales from species to populations, ecosystems, and biomes. Most models and empirical data indicate that many species might shift their climatic niches not only along the space axis by showing large geographic displacements and widespread extinctions, but also by altering their

life history in time or their physiology to survive under the new climatic conditions (Bellard et al., 2012). Therefore, the impact of climate change on ecosystems, and thus on human beings, is one of the greatest challenges that our society is currently facing (IPCC, 2023, 2022). While the present human-induced climate change is affecting ecosystems more abruptly than in the past, understanding the impact of climate on ancient environments and its subsequent influence on the evolution, dispersion, and distribution of hominin species is crucial (deMenocal, 2011; Gosling et al., 2022; Margari et al., 2023; Stewart and Stringer, 2012; Timmermann et al., 2022). Therefore, the reconstruction of past ecosystem responses to external disturbances is essential to understand the consequences of the ongoing climate change and those of possible future scenarios (Harrison and Bartlein, 2012; IPCC, 2023; Lear et al., 2021).

3.1. Marine environments

One of the most important landscape modifiers in coastal areas is sea-level change, with recent global warming emerging as its main driver in the last few decades (IPCC, 2023, 2022). Under non-anthropogenically forced conditions, global sea level has risen ca. 130 m since the LGM lowstand (Lambeck et al., 2002). Sea level started to rise as a consequence of the ice sheet melting at ~19.5–19 ka BP (Carlson and Clark, 2012) and almost stabilised after ~7–6 ka BP (Lambeck et al., 2014). However, regional factors have modulated sea level variations at the regional scale. In this context, northwestern Iberia showed fluctuating sea levels, and although a decrease and stabilisation were detected after 6.8 ka, there was a slight increase after 4.2 ka BP (Alonso Millán and Pagés Valcarlos, 2010; García-Artola et al., 2018). Additionally, occasional but significant sea level rises occurred in the Iberian Mediterranean coast in the latest Holocene, e.g., between 1.6 and 0.2 ka BP (Ejarque et al., 2016). The general stabilisation of sea-level rise in the Middle Holocene allowed for the identification of regional climatic effects on coastal areas. For example, the development of the Ebro delta in northeastern Iberia during the Early-Mid Holocene transition, as other Mediterranean deltas, showed progradational deposits under moderate-to-reduced rising sea level and highstand conditions, associated with significant fluvial sediment inputs (enhanced precipitation; Cearreta et al., 2016). Moreover, sand coastal barriers protecting lagoons, marshlands and back-barrier perched lakes in Iberian coasts experienced significant instability, and even breaks, as a consequence of palaeostorms since the Middle Holocene, specially under NAO negative phases (López-Belzunce et al., 2022; Marco-Barba et al., 2013; Ruiz et al., 2020; Sáez et al., 2018). Finally, a new modifier agent, anthropogenic activity, has played an important role on Iberian coasts during the Late Holocene, especially in the last millennium, overprinting the effect of climatic conditions on sea level fluctuations (López-Belzunce et al., 2022; Muñoz Sobrino et al., 2014; Ruiz-Pérez and Carmona, 2019; Sáez et al., 2018).

Coccoliths and planktonic foraminifera assemblages evidenced that ocean upwelling patterns, and thus, productivity have changed since the LGM in the western Iberian Margin. Sea-level minima during the LGM could have forced a westward migration of the coastal upwelling centres, possibly accompanied by a strengthening of northward winds, promoting high productivity. On the contrary, a general upwelling reduction in the Holocene, caused by a weaker subtropical Azores High pressure system and the northward displacement of the Azores Current, gave rise to low productive conditions in the area (Palumbo et al., 2013; Salgueiro et al., 2014).

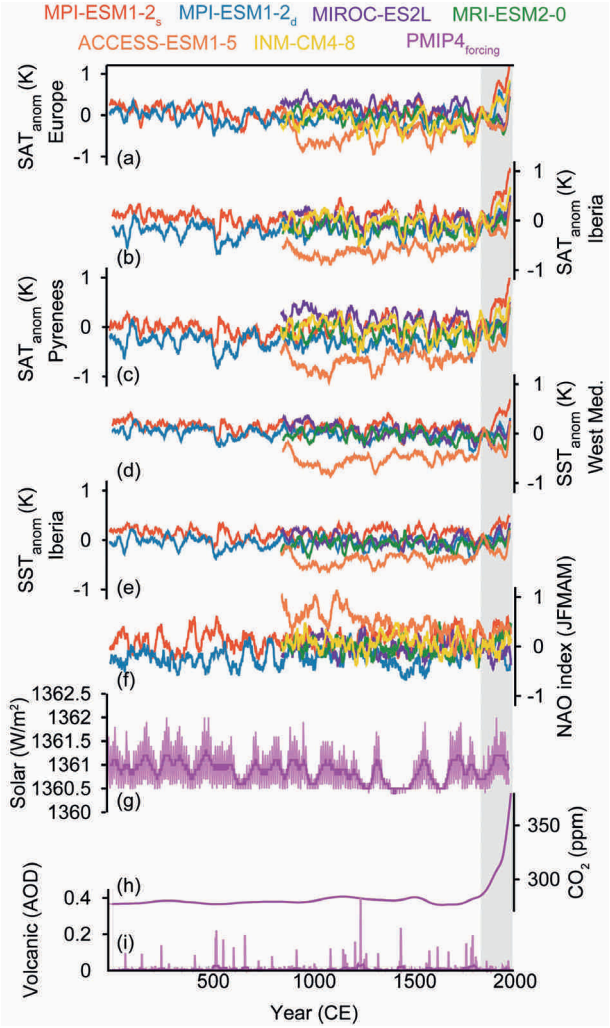

Figure 1.5. Simulated climate in the IP and North Atlantic context during the CE as well as some of the external forcing (solar, CO_2, and volcanic forcings) boundary conditions used in PMIP4 ESM simulations (see legend for colors). SAT anomaly (K) during the historical period (1850-2014, shaded gray) in: (a) Europe (10ºW-40ºE, 35ºN-70ºN); (b) Iberia (9.5ºW-3.2ºE, 36ºN-43.5ºN); and (c) the Pyrenees (2ºW-3ºE, 42ºN-44ºN). (d) Same as (a, b, c) but for SST anomalies (K) in the West Mediterranean basin (2ºW-13ºE, 34ºN-45ºN), and (e) the sea areas surrounding the Iberian Peninsula (12ºW-5ºE, 34ºN-46ºN). (f) NAO index in JFMAM, computed as the standardized pressure gradient between Reykjavik (22ºW, 64ºN) and Gibraltar-Cádiz (5.4ºW, 36.2ºN). (g) Solar forcing (W/m^2) in the last two millennia; yearly (31-year moving average) values are depicted in clear (dark) pink. (h) Same as (g), but for CO_2 (ppm) atmospheric concentration. (i) Same as (g, h), but for volcanic forcing, given as the stratospheric aerosol optical depth (AOD). CE: Common Era.

The alternation between suboxic and oxic conditions in Atlantic marine environments at the end of the last glacial cycle, corresponding to abrupt climate changes such as LGM, HS1, B-A and YD, controlled the development of benthic assemblages, especially foraminifera. Subsequently, these faunas adapted to well-oxygenated waters during the Holocene, probably influenced by the Northeast Atlantic Deep Water, seasonally-pulsed organic matter fluxes to the seafloor and high productivity (Grunert et al., 2015; Rodriguez-Lazaro et al., 2017). In specific areas, such as the Tagus pro-delta in the Iberian margin, Holocene benthic foraminifera communities responded to river discharge dynamics for at least the last 6 ka BP, showing increased benthic productivity with enhanced Tagus discharges, eventually controlled by the climatic evolution of western Iberia (Bartels-Jónsdóttir et al., 2015; Dessandier et al., 2018). More recently, the main changes in the Western Iberian Upwelling system and phytoplankton (dinoflagellate) associations have been observed since the second half of 20th century. These changes are attributed to regional climate variability (i.e., warming, increased water stability, and nutrient availability), possibly exacerbated by anthropogenic nutrient inputs (Ribeiro et al., 2016, 2012).

3.2. Terrestrial Environments

Past landscape and vegetation dynamics in the IP have been controlled by both long and short term climate changes, but human activities have emerged as an additional transformative agent in the Middle-Late Holocene, and particularly since Mediaeval times (Carrión et al., 2010 and references therein; Aranbarri et al., 2020, 2015; Camuera et al., 2019, 2018; Corella et al., 2012, 2011; González Sampériz et al., 2019; González-Sampériz et al., 2017; López-Sáez et al., 2017, 2014b, 2014a; Morales-Molino and García-Antón, 2014; Morellón et al., 2011; Moreno et al., 2011). Landscape transformation is more intense in arid/semiarid regions, which currently prevail in most areas of the IP except for those close to the north and west coast (Paniagua et al., 2019). In these Iberian arid/semiarid areas, mainly in those dominated by the Mediterranean climate, changing climate not only controls precipitation but also influences the vegetative cover, a main driver of potential soil development and erosion (Barreiro-Lostres et al., 2017; Pérez-Lambán et al., 2018). Erosion events impacted riverine tufa environments, causing major changes in fluvial dynamics that destroyed and constructed tufa barriers through the Holocene, a key ecological niche in Mediterranean and semiarid landscapes (Domínguez-Villar et al., 2013). During long-term arid periods, the vegetation cover retracted, intensifying the potential erosive conditions. In this way, glacial/stadial and/or overall arid periods, such as the Late Holocene, with reduced forest cover and sparse vegetation, registered stronger catchment weathering and/or erosion in southern Iberia (Camuera et al., 2019, 2018) as well as poor soil development in some areas of northern Iberia (Pérez-Lambán et al., 2018). Within the overall arid context of the Late Holocene, very short-term humid conditions resulted in significant erosion, sediment delivery, and floodings during the last millennium. However, a clear relationship between these enhanced periods of sediment delivery into lakes also agrees with periods of significant changes in land use and land clearing in the catchments (Barreiro-Lostres et al., 2017; Corella et al., 2011). This is a common Late Holocene duality that is difficult to disentangle: the potential role of human activities amplifying natural climatic impacts (e.g., (García-Alix et al., 2017; Vicente de Vera García et al., 2023).

The different cycles of glacier advance/retreat, ultimately controlled by Northern Hemisphere atmospheric and oceanic dynamics, have modelled the Quaternary glacial and periglacial

landscapes in the Iberian mountain ranges (i.e., Pyrenees, Cantabrian, northwestern, central, Iberian, and Betic Ranges; Oliva et al., 2019). Although glacier retreat was not continuous or uniform after the LGM in the IP under increasing summer insolation conditions (García-Ruiz et al., 2016), the depressions formerly occupied by glaciers in some mountain ranges gave rise to lakes and/or peatlands, especially during the B-A and the earliest Holocene (Castillo Martín, 2016). The sedimentary records of these highly climate-sensitive remote alpine wetlands constitute exceptional archives of climate change (Catalan et al., 2017, 2013; Zamora and Oliva, 2022).

Post-glacial, long-term productivity in several Iberian lakes was controlled by temperatures, highly dependent on insolation in alpine systems (Jiménez-Moreno et al., 2023a; Muñoz Sobrino et al., 2013). Similarly, the long-term evolution of hydrology was driven by insolation changes since the LGM (Camuera et al., 2022, 2018; García-Alix et al., 2021; González-Sampériz et al., 2020; Santisteban et al., 2019). However, the response of lake levels to these insolation changes, modulated by the local precipitation/evapotranspiration balance, was not uniform in the different sectors of the IP (Camuera et al., 2018; Morellón et al., 2018). Both long- and short-term lake level variations eventually conditioned the development of wetland and riparian vegetation in freshwater environments (Camuera et al., 2019).

3.3. Vegetation and fires

Vegetation and regional fire reconstructions in the IP have traditionally been conducted through pollen and sedimentary charcoal/microcharcoal analyses in both marine and continental records, as they provide high-resolution archives documenting terrestrial ecosystem changes. There are very few vegetation reconstructions using plant macrofossil remains, which are particularly useful in peatlands (Castro et al., 2020, 2015). During the last glacial-interglacial cycle, insolation dominated by orbital-scale precession, and to a lesser extent eccentricity, were the most important factors controlling long-term climatic changes in the IP, forcing regional responses of vegetation cover (Camuera et al., 2019; González-Sampériz et al., 2020). At shorter time scales, vegetation responded to millennial-to-centennial-scale climate variability since the LGM, (cold-arid events/ stadials and warm-humid interstadials, such as the HS1, B-A, YD, or the Dansgaard-Oeschger (DO) events), driven by atmospheric, oceanic and solar dynamics (Camuera et al., 2021, 2019; William J Fletcher et al., 2010; W J Fletcher et al., 2010; Gomes et al., 2020; González-Sampériz et al., 2020, 2017; Jiménez-Moreno et al., 2023b; López-Sáez et al., 2020, 2014a; Moreno et al., 2012a; María J Ramos-Román et al., 2018; Ramos-Román et al., 2016; Vegas et al., 2010). These high and low frequency climate oscillations also controlled fire activity, as wildfires depend on the biomass availability. Thus, wildfires usually developed more intensely in humid and warm periods such as the B-A or the Early-Middle Holocene, when higher fuel biomass (enhanced vegetation development) was available (Burjachs and Expósito, 2015; Gil-Romera et al., 2014; Jiménez-Moreno et al., 2023b), and less intensely in cold and dry intervals such as HS1 or YD (Genet et al., 2021; Gil-Romera et al., 2014; Jiménez-Moreno et al., 2023b).

At the end of the last glacial cycle, during the Marine Isotope Stage (MIS) 2, some mesothermophilous taxa found refuge in Mediterranean coastal shelves and intramountainous

valleys, recovering and dispersing again in the Holocene (González-Sampériz et al., 2010). Overall, the IP registered low/moderate mesophyte vegetation and forest development after the LGM that abruptly rose when summer isolation increased, at the onset of the B-A, and especially during the Early Holocene, when warmer and more humid conditions prevailed. In any case, the specific features of vegetation depended on the geographical location, and for example, forested vegetation exhibited more temperate and less Mediterranean forest components in northern Iberia than in southern areas since the LGM (Camuera et al., 2019; Gomes et al., 2020; González-Sampériz et al., 2020, 2017). Lower values of summer insolation in the Middle Holocene are concurrent with an overall trend towards less forested areas in the IP after ca. 6 ka BP, or even earlier in high-sensitive alpine areas. This retraction was more noticeable in the Late Holocene (Alba-Sánchez et al., 2021; Gomes et al., 2020; González-Sampériz et al., 2017; Jiménez-Moreno et al., 2022; López-Sáez et al., 2014a; Manzano et al., 2019; Morales-Molino and García-Antón, 2014; María J. Ramos-Román et al., 2018). The decrease in forested areas in the Middle Holocene was also evidenced by a decrease of ~200-400 m in the tree line in the Pyrenees after 5.7 ka BP (Leunda et al., 2019). A transitional period between the humid Early-Middle Holocene (before ~7 ka) and the arid Middle-Late Holocene (after 5.5 ka BP) has been suggested to differentiate this Middle Holocene phase of vegetation transformation in the Mediterranean Iberia (Pérez-Obiol et al., 2011).

The fire scenario is intricate in the Holocene when wildfire events were not always simultaneous, even within the same region. This complexity is due to the complicated natural interactions between fire, climate, landscape, and vegetation, in addition to the human activities that disturbed Late Holocene natural dynamics (Anderson et al., 2011; Burjachs and Expósito, 2015; García-Alix et al., 2013; Genet et al., 2021; Gil-Romera et al., 2014, 2010; Jiménez-Moreno et al., 2023b, 2013; Leunda et al., 2020; Pérez-Obiol et al., 2011). However, overall, the Early and Early-Middle Holocene registered moderate-to-high fire activity under high summer insolation, warm and humid conditions and the expansion of mesophytes, providing high loads of fuel biomass. This contrasts with a decrease in fire activity resulting from the retraction of forested areas in the Middle Holocene (Anderson et al., 2011; Burjachs and Expósito, 2015; Gil-Romera et al., 2014, 2010; Leunda et al., 2020; Morales-Molino et al., 2018). More specifically, studies in southwestern Iberia suggested Early Holocene recurrent fires of low intensity affecting closed vegetation and infrequent fires of high intensity after 8 ka BP. This was contemporaneous with the degradation of the Mediterranean forest and the expansion of open vegetation (Ericaceae-dominated shrubland; Genet et al., 2021). In this regard, climate and natural fire activity are supposed to be the main factors influencing vegetation development during the Early and Middle Holocene (Gil-Romera et al., 2014; Mighall et al., 2023), although vegetation has demonstrated to be highly resilient to fire disturbances in some areas of Iberia (e.g., central Iberia; López-Sáez et al., 2014).

In addition to climate, another significant agent determining vegetation dynamics after the Middle-Late Holocene transition was human activity (Carrión et al., 2010; Mighall et al., 2023). However, fires (natural or human-induced) could still have played an important role in vegetation turnover (Brisset et al., 2020; González Sampériz et al., 2019), since forests were unable to completely recover after fire events (López-Sáez et al., 2014a). In this regard, the vegetation succession after wildfire events in Mediterranean areas, where

Mediterranean forest/maquis usually recovered after woodland decline, evolved into a shrubland replacement in the Late Holocene (Burjachs and Expósito, 2015). Despite the overall Late Holocene arid conditions and shrubland expansion reducing available fuel biomass, especially in the last millennia, natural fire occurrence was masked by human activities such as metallurgy, mining, smelting, forest clearance, pasturing, or agriculture, that intensified fire development (Anderson et al., 2011; Burjachs and Expósito, 2015; García-Alix et al., 2013; Genet et al., 2021; Gil-Romera et al., 2014, 2010; Jiménez-Moreno et al., 2023b, 2022, 2013; Leunda et al., 2020; Luelmo-Lautenschlaeger et al., 2019; Morales-Molino et al., 2018; Pérez-Obiol et al., 2011).

Annual-to-decadal forest dynamics in the last millennium can be investigated through tree ring analyses. Subalpine Pyrenean forests over the last 700 yr have mainly been controlled by temperature (Garcés-Pastor et al., 2018), driven by solar variability and volcanism at multi-decadal time scales during preindustrial times (Dorado Liñán et al., 2012). However, the controls over temperature variability in the 20th century are unclear (Dorado Liñán et al., 2012). Other kinds of forests are more dependent on water availability. This is the case of juniper trees in the Iberian System Mountain Range that responded to the interplay between Atlantic Westerlies and Mediterranean depressions over the last 200-300 yr, being especially sensitive to late spring-early summer droughts (Esper et al., 2015). Similarly, rear-edge birch populations in central Iberia negatively responded to the summer water deficit in the last 60 yr, exhibiting a declining growth trend since the early 21st century (de Andrés et al., 2023). In some cases, the combined effect of climate and human pressure has affected the distribution and resilience of some forests, such as the *Abies pinsapo* forests in southern Iberia during the last millennium (Alba-Sánchez et al., 2019).

3.4. Climate, environment and human populations

Although overall the dynamics of Paleolithic and Neolithic populations were highly dependent on climate and natural environmental fluctuations, abrupt climatic oscillations and harsh environmental conditions at the end of the last glacial cycle such as during the HS2, the LGM, HS1, and even the YD, did not seem to severely impact human occupations in northern-northeastern and central IP (Alcaraz-Castaño et al., 2021; Alday et al., 2018; López-Sáez et al., 2017, 2014a, 2014b; Montes et al., 2016; Pérez Díaz and López-Sáez, 2019). This would reinforce the hypothesis that SW Europe served as a refuge area during the Upper Paleolithic (Pérez Díaz and López-Sáez, 2019). However, harsh conditions at centennial scale caused by short-term climatic events, such as the 8.2 ka or the 4.2 ka events, triggered Iberian social crises; e.g., depopulation in the Ebro Basin during the 8.2 ka event (González-Sampériz et al., 2009), changes in subsistence strategies in southern Iberia between 8.2 ka and 7.3 ka (Cortés Sánchez et al., 2012), or demographic transformations and migrations around the 4.2 ka event (Lillios et al., 2016), among others.

Human populations in southern IP have used coastal resources since Neanderthal times. This consumption increased during the deglaciation, especially since the HS1 - B-A transition, decreased during the YD and increased throughout the Holocene until the Chalcolithic (Cortés-Sánchez et al., 2023; Naito et al., 2022). Holocene sea-level rise shaped the coastal morphology and influenced the settlement patterns of human groups in both Mesolithic and Early Neolithic times (Val-Peón et al., 2021). Changes in continental

and marine ecosystems, including variations in upwelling intensity, sea-level changes, increased aridity and temperature decrease between 8.2 and 7.3 ka BP, may have triggered a Mesolithic subsistence crisis that negatively impacted populations in the Maghreb and along the Iberian coast (Cortés Sánchez et al., 2012; Val-Peón et al., 2021). These changes affected the terrestrial and marine faunas available for Mesolithic hunter gatherers and led to a replacement of coastal economies by agricultural and pastoralist cultures. This transition set the scenario for the rapid development and dispersion of the Neolithic culture in southern Iberia at ~7.3±0.2 ka BP (Cortés Sánchez et al., 2012).

In spite of some earlier evidences and small differences in time and space, the natural evolution of landscapes, especially the vegetative landscapes, has been overprinted by human activities since the Middle-Late Holocene transition (Aranbarri et al., 2020, 2015; Brisset et al., 2020; Carrión et al., 2022; Carrión et al., 2010; González Sampériz et al., 2019; González-Sampériz et al., 2017; López-Sáez et al., 2017, 2014a, 2014b; Morales-Molino and García-Antón, 2014; Moreno et al., 2011). This agrees with the establishment of "cultural landscapes" during the expansion of the Chalcolithic culture (López-Sáez et al., 2014a). While quantifying the real human impact on vegetation throughout the Holocene is challenging, the enhanced Late Holocene forest retraction and open vegetation expansion contrasted with the absence of noticeable changes in the vegetative cover in the last part of the previous interglacial period, under no anthropogenic influence (MIS 5e, Eemian; Camuera et al., 2019; González-Sampériz et al., 2020).

Another significant human impact on natural environments since the metal ages is evidenced by the heavy metal pollution in aquatic environments, delivered by either runoff and/or atmospheric deposition, as a consequence of mining (firstly) and industrial (recently) activities in the IP, especially since Roman times (Corella et al., 2021; García-Alix et al., 2017, 2013; Griffore et al., 2023; Hillman et al., 2017; Martínez Cortizas et al., 2016; Martín-Puertas et al., 2010; Sánchez et al., 2021; Silva-Sánchez and Armada, 2023). These mining activities along with forests clearance, changes in land use, development of cultivated fields for farming and pasturing, or human-induced fires, have led to enhanced landscape erosion, more sediment delivery towards aquatic systems and, in some cases, lake eutrophication (Aranbarri et al., 2020, 2015; Barreiro-Lostres et al., 2014; Brisset et al., 2020; Corella et al., 2012, 2011; García-Alix et al., 2013; Gardoki et al., 2023; González Sampériz et al., 2019; González-Sampériz et al., 2017; López-Sáez et al., 2017, 2014a, 2014b; Martín-Puertas et al., 2010; Morales-Molino and García-Antón, 2014; Moreno et al., 2011; Ortiz et al., 2024, 2016; Vicente de Vera García et al., 2023).

In general, past human interventions in the environment were frequently designed to deal with climatic-related crises, with droughts being one the most important concerns in preindustrial Iberian societies. Iberian palaeobotanical records show a combination of weakening anthropogenic pressure and aridification dynamics around the 4.2 ka event, in the transition between the Chalcolithic and Bronze ages, with no visible stabilisation and recovery until the Late Bronze Age. However, the impact of the climatic changes around the 4.2 ka event varies across Iberia (Blanco-González et al., 2018; Brisset et al., 2020; Lillios et al., 2016). In southern Iberian societies, for example, changes in winter precipitation and seasonality could have played a major role in the development of agricultural activities. These changes likely triggered a demographic decline in

southwestern Iberia after 4.8 ka BP (Schirrmacher et al., 2020) and a population migration from southwestern to the southeastern Iberia, in agreement with the rise of the Millares culture in southeastern Iberia (Lillios et al., 2016). Despite harsh environmental conditions associated with the 4.2 ka event, characterised by decreasing winter precipitation and severe summer droughts, the Argaric culture boomed in southeastern IP Iberian during the Early Bronze Age (Lillios et al., 2016; Schirrmacher et al., 2020). This overall dry scenario in the IP also promoted the development of the Motillas culture in La Mancha (Meseta area, Central Iberia; Blanco-González et al., 2018). These communities were already settled at ~4.3 ka BP and the 4.2 ka event probably led to the appearance of the Motillas, fortified wells designed to extract and protect groundwater from shallow aquifers. These systems rapidly expanded across this region in response to the water needs during this climatic and environmental crisis (Blanco-González et al., 2018; López-Sáez et al., 2014b; Mejías Moreno et al., 2020). However, wetter conditions recovered after ~3.8 ka BP, with maximum humidity between 3.6-3.4 ka BP, promoting the elevation of phreatic levels and the recovery of rivers and humid zones. Consequently, these settlements with fortified wells were abandoned at ~3.4 ka BP (Blanco-González et al., 2018; López-Sáez et al., 2014b; Mejías Moreno et al., 2020).

The expansion of the Roman Empire in the IP coincided with a period of overall prosperity and humid conditions, but its final stages were coeval with natural disasters, such as plagues (i.e. the Plague of Cyprian, 249–262 CE), increased climate variability with periods of severe droughts, and extreme weather events that could have adversely affected crops and the agricultural system in southern Iberia (Gázquez et al., 2020). Droughts may have also contributed to Visigothic and Islamic civil wars between the mid-5th and mid-10th centuries and to the Visigothic crisis and Islamic expansion in the IP during the 8th century (Camuera et al., 2023). Many of these droughts, and other extreme climatic events, have been registered in written documents such as chronicles, diaries, or administrative sources (Camuffo et al., 2010; Domínguez-Castro et al., 2014, 2012, 2010; Fernández-Fernández et al., 2017, 2015). In addition, there are records of "propluvia" rogation ceremonies in the IP since the 14th century, but specially from the 16th–17th centuries to the first half of the 19th century, when people from different regions of the IP sought divine intervention for rain in periods of extreme dryness impacting on agriculture and livestock (Bravo-Paredes et al., 2020; Domínguez-Castro et al., 2021; Tejedor et al., 2019). In most cases, these precipitation-related archives were related to the NAO impact on the IP (Bravo-Paredes et al., 2020; Camuera et al., 2023; Domínguez-Castro et al., 2021; Gázquez et al., 2020; Tejedor et al., 2019). The palaeoenvironmental record of the IP also provides examples of ecosystem recovery when human impact on the environment decreased as a consequence of societal pandemics crises, such as the Justinian Plague (541–543 CE) or the Black Death (1348–1351 CE). These pandemics had a negative impact on demography, and caused a slowdown in agriculture, tree cultivation and livestock, while forested areas recovered (Luelmo Lautenschlaeger et al., 2021a, 2021b).

Iberian agriculture also evolved to improve crop yields, probably due to spatial variations in rainfall and socio-economic development, changing from climate-driven to human-driven cultivation between the 17th century and the first half of the 18th century (Santisteban et al., 2021), but with some exceptions. For example, after expansion of olive cultivation in the High Middle Ages, its subsequent variability depended on climate conditions, and thus,

it may have been affected by the present aridification tendency in Mediterranean areas (Ramos-Román et al., 2019).

4. Conclusions and future perspectives

This chapter has summarised the main results on past climate variability in the IP produced over the last decade by research groups of the Peninsula. The last ten years represent a major advance in the generation of new palaeoclimate knowledge in the Iberian region, thanks both to developments in proxy data and improvements in model simulations. An important novelty in the Iberian palaeoclimate community has been the stabilisation of the research line on speleothems as archives of Iberian climate variations. New speleothem records, generally with high-resolution isotopic profiles and robust chronologies, have covered interesting time intervals (e.g., the last deglaciation), providing evidence of rapid changes in the terrestrial environment (e.g., Bernal-Wormull et al., 2021). Moreover, the good overlap of some stalagmites with the instrumental record, thus linking past and present climates, has paved the way to quantify past temperature changes (Bartolomé et al., 2024; Martín-Chivelet et al., 2013). In the marine realm, the improvement of sediment core chronostratigraphies (e.g., Waelbroeck et al., 2019) has represented a significant advance in our ability to reconstruct past climate variability at unprecedented resolution (e.g., Martrat et al., 2014). For all types of archives, the increasing common use of a Bayesian approach to construct age models, together with the increased number of dates and dating methods, has led to a significant improvement in chronologies and a better definition of age uncertainties.

Another major improvement relies on the presentation and application of new proxies, the implementation of statistically robust calibration procedures, and the development of innovative transfer functions that facilitate the quantitative estimation of climate variables throughout the past. This is particularly innovative in the terrestrial environment (García-Alix et al., 2020; Gázquez et al., 2018; Jiménez-Moreno et al., 2023a; Rodrigo-Gámiz et al., 2022), where the extraction of absolute temperature values from geochemical data is not as common as in the marine domain. Although Significant improvements have been conducted in the continental palaeoclimate community to improve the interpretation of proxies by monitoring and modelling (e.g., Domínguez-Villar et al., 2021; Krklec and Domínguez-Villar, 2014), it is clear that more effort is required to untangle the complex controls of many proxies. Yet, the marine realm has witnessed the rapid implementation and application of relatively new palaeothermometers (e.g., Morcillo-Montalbá et al., 2021). The latter, along with the refinement of the existing knowledge of well-established palaeothermometers in terms of the habitat of the precursor organisms (season and depth) and the potential impact on derived temperatures of overlooked influencing factors like pre-depositional hydrodynamic transport (e.g., Ausín et al., 2022, 2019; Català et al., 2019; Morcillo-Montalbá et al., 2021), has allowed the production of more accurate temperature reconstructions from marine sediment cores.

Regional diversity is an intrinsic feature of the IP, with different responses to climate change from north to south, from the Atlantic to the Mediterranean. However, there is also a common pattern between different regions during some climatic periods and general synchrony during many rapid climate changes with other areas in the Northern Hemisphere. Thus, the rapid climate changes of the last deglaciation have been better identified in the IP with new high-resolution marine and terrestrial records, and it has even been possible to characterise the intra-event variability, i.e. YD

(Bartolomé et al., 2015) or HS1 (Camuera et al., 2021; Sierro et al., 2020), and connect it with global mechanisms of climate change (e.g., Alvarez-Solas et al., 2013). The latter recently allowed the possibility of zooming in on rapid climate changes, opening the door to identifying the role of different mechanisms that have caused important reorganisations in our climate system. The spatial and temporal diversity of the Holocene interglacial has been addressed by the increase in available records covering most of the IP and surrounding seas. Indeed, in the last decade, many new records have demonstrated the regional differences in timing and response along the Holocene sub-stages (e.g. Holocene onset, Morellón et al., 2018). Moreover, the complex interpretation of many proxies regarding the recorded season or their regional representativeness has been brought to the table, both in marine (Català et al., 2019) and terrestrial systems (Moreno et al., 2017). It is worth highlighting the complexity of the Iberian climate reconstruction, related to the characteristics of the Atlantic and Mediterranean zones, both in terms of temperature and precipitation changes, together with notable differences in the impact on vegetation or fire frequency. The last 2000 years are an important period to link the observed changes in the Iberian climate to their forcing mechanisms, such as particular atmospheric patterns explained by NAO (Hernández et al., 2015) or volcanism (Tejedor et al., 2016). Only the combination of both proxies, especially when calibrated with the instrumental record, and climate simulations for the CE will allow to further contextualise the current warming already recorded in many palaeoclimate archives (e.g., glaciers, Vidaller et al., 2023).

Finally, future efforts should be aimed at improving our ties and joint work between the two palaeoclimate communities that have historically evolved in parallel using distinct approaches: proxy data and climate models. Undoubtedly, comparing measured proxy data and simulations is an extraordinary exercise to deepen our knowledge of the drivers and impacts of the climate system. For example, the comparison of the two types of data for the past 2000 years showed important differences, probably due to the high variability of proxy data due to local forcing and internal regional variability not captured in the simulations. In addition, proxy data are often seasonally biassed and usually do not represent annual averages, making their interpretation and comparison with model simulations even more difficult. Improving chronologies, in particular, through exploring dating methods that take advantage of new methodologies (e.g. tephrochronology), is a correct way to synchronise and correlate records from different regions and will undoubtedly facilitate the comparison of data and models framed by the same age scale. Despite new quantitative reconstructions appearing in the IP, they are still scarce and truly needed to complete the remaining gaps and challenges above mentioned, in order to reduce uncertainty in future climate projections.

References

Abrantes, F., Rodrigues, T., Montanari, B., Santos, C., Witt, L., Lopes, C., Voelker, A.H.L., 2011. Climate of the last millennium at the southern pole of the North Atlantic Oscillation: an inner-shelf sediment record of flooding and upwelling. Clim. Res. 48, 261–280.

Abrantes, F., Rodrigues, T., Rufino, M., Salgueiro, E., Oliveira, D., Gomes, S., Oliveira, P., Costa, A., Mil-Homens, M., Drago, T., Naughton, F., 2017. The climate of the Common Era off the Iberian Peninsula. Clim Past 13, 1901–1918. https://doi.org/10.5194/cp-13-1901-2017

Alba-Sánchez, F., Abel-Schaad, D., López-Sáez, J.A., Sabariego-Ruiz, S., Pérez-Díaz, S., Luelmo-Lautenschlaeger, R., Garrido-García, J.A., 2021. Early anthropogenic change in western Mediterranean mountains (Sierra Nevada, SE Spain). Anthropocene 33, 100278. https://doi.org/10.1016/j.ancene.2021.100278

Alba-Sánchez, F., López-Sáez, J.A., Abel-Schaad, D., Sabariego Ruiz, S., Pérez-Díaz, S., González-Hernández, A., Linares, J.C., 2019. The impact of climate and land-use changes on the most southerly fir forests (Abies pinsapo) in Europe. The Holocene 29, 1176–1188. https://doi.org/10.1177/0959683619838043

Alcaraz-Castaño, M., Alcolea-González, J.J., de Andrés-Herrero, M., Castillo-Jiménez, S., Cuartero, F., Cuenca-Bescós, G., Kehl, M., López-Sáez, J.A., Luque, L., Pérez-Díaz, S., Piqué, R., Ruiz-Alonso, M., Weniger, G.-C., Yravedra, J., 2021. First modern human settlement recorded in the Iberian hinterland occurred during Heinrich Stadial 2 within harsh environmental conditions. Sci. Rep. 11, 15161. https://doi.org/10.1038/s41598-021-94408-w

Alday, A., Domingo, R., Sebastián, M., Soto, A., Aranbarri, J., González-Sampériz, P., Sampietro-Vattuone, M.M., Utrilla, P., Montes, L., Peña-Monné, J.L., 2018. The silence of the layers: Archaeological site visibility in the Pleistocene-Holocene transition at the Ebro Basin. Quat. Sci. Rev. 184, 85–106. https://doi.org/10.1016/j.quascirev.2017.11.006

Alonso Millán, Á., Pagés Valcarlos, J.L., 2010. Evolución del nivel del mar durante el Holoceno en el noroeste de la Península Ibérica. Rev. Soc. Geológica Esp. 23, 157–167.

Alvarez-Solas, J., Banderas, R., Robinson, A., Montoya, M., 2019. Ocean-driven millennial-scale variability of the Eurasian ice sheet during the last glacial period simulated with a hybrid ice-sheet–shelf model. Clim. Past 15, 957–979. https://doi.org/10.5194/cp-15-957-2019

Álvarez-Solas, J., Montoya, M., Ritz, C., Ramstein, G., Charbit, S., Dumas, C., Nisancioglu, K., Dokken, T., Ganopolski, A., 2011. Heinrich event 1: an example of dynamical ice-sheet reaction to oceanic changes. Clim. Past 7, 1297–1306. https://doi.org/10.5194/cp-7-1297-2011

Alvarez-Solas, J., Robinson, A., Montoya, M., Ritz, C., 2013. Iceberg discharges of the last glacial period driven by oceanic circulation changes. Proc. Natl. Acad. Sci. 110, 16350–16354. https://doi.org/10.1073/pnas.1306622110

Anderson, R.S., Jiménez-Moreno, G., Carrión, J.S., Pérez-Martínez, C., 2011. Postglacial history of alpine vegetation, fire, and climate from Laguna de Río Seco, Sierra Nevada, southern Spain. Quat. Sci. Rev. 30, 1615–1629. https://doi.org/10.1016/j.quascirev.2011.03.005

Aranbarri, J., Alcolea, M., Badal, E., Vila, S., Allué, E., Iriarte-Chiapusso, M.J., Sebastián, M., Magri, D., González-Sampériz, P., 2020. Holocene history of Aleppo pine (Pinus halepensis Mill.) woodlands in the Ebro Basin (NE Spain): Climate-biased or human-induced? Rev. Palaeobot. Palynol. 279, 104240. https://doi.org/10.1016/j.revpalbo.2020.104240

Aranbarri, J., González-Sampériz, P., Valero-Garcés, B., Moreno, A., Gil-Romera, G., Sevilla-Callejo, M., García-Prieto, E., Di Rita, F., Mata, M.P., MorellÃ³n, M., Magri, D., Rodríguez-Lázaro, J., CarriÃ³n, J.S., 2014. Rapid climatic changes and resilient vegetation during the Lateglacial and Holocene in a continental region of south-western Europe. Glob. Planet. Change 114, 50–65.

Aranbarri, J., González-Sampériz, P., Iriarte, E., Moreno, A., Rojo-Guerra, M., Peña-Chocarro, L., Valero-Garcés, B., Leunda, M., García-Prieto, E., Sevilla-Callejo, M., Gil-Romera, G., Magri, D., Rodríguez-Lázaro, J., 2015. Human–landscape interactions in the Conquezuela–Ambrona Valley (Soria, continental Iberia): From the early Neolithic land use to the origin of the current oak woodland. Palaeogeogr. Palaeoclimatol. Palaeoecol. 436, 41–57. https://doi.org/10.1016/j.palaeo.2015.06.030

Ausín, B., Flores, J.A., Sierro, F.J., Bárcena, M.A., Hernández-Almeida, I., Francés, G., Gutiérrez-Arnillas, E., Martrat, B., Grimalt, J.O., Cacho, I., 2015. Coccolithophore productivity and surface water dynamics in the Alboran Sea during the last 25kyr. Palaeogeogr. Palaeoclimatol. Palaeoecol. 418, 126–140. https://doi.org/10.1016/j.palaeo.2014.11.011

Ausín, Blanca, Flores, J.A., Sierro, F.J., Cacho, I., Hernández-Almeida, I., Martrat, B., Grimalt, J.O., 2015. Atmospheric patterns driving Holocene productivity in the Alboran Sea (Western Mediterranean): A multiproxy approach. Holocene 25, 583–595. https://doi.org/10.1177/0959683614565952

Ausín, B., Haghipour, N., Bruni, E., Eglinton, T., 2022. The influence of lateral transport on sedimentary alkenone paleoproxy signals. Biogeosciences 19, 613–627. https://doi.org/10.5194/bg-19-613-2022

Ausín, B., Hodell, D.A., Cutmore, A., Eglinton, T.I., 2020. The impact of abrupt deglacial climate variability on productivity and upwelling on the southwestern Iberian margin. Quat. Sci. Rev. 230, 106139–106139. https://doi.org/10.1016/j.quascirev.2019.106139

Ausín, B., Magill, C., Haghipour, N., Fernández, Á., Wacker, L., Hodell, D., Baumann, K.-H., Eglinton, T.I., 2019. (In)coherent multiproxy signals in marine sediments: Implications for high-resolution paleoclimate reconstruction. Earth Planet. Sci. Lett. 515, 38–46. https://doi.org/10.1016/j.epsl.2019.03.003

Ausín, B., Sarnthein, M., Haghipour, N., 2021. Glacial-to-deglacial reservoir and ventilation ages on the southwest Iberian continental margin. Quat. Sci. Rev. 255, 106818–106818. https://doi.org/10.1016/j.quascirev.2021.106818

Bahr, A., Kaboth, S., Jiménez-Espejo, F.J., Sierro, F.J., Voelker, A.H.L., Lourens, L., Röhl, U., Reichart, G.J., Escutia, C., Hernández-Molina, F.J., Pross, J., Friedrich, O., 2015. Persistent monsoonal forcing of Mediterranean Outflow Water dynamics during the late Pleistocene. Geol. Boulder 43, 951–951.

Baldini, L.M., Baldini, J.U.L., McDermott, F., Arias, P., Cueto, M., Fairchild, I.J., Hoffmann, D.L., Mattey, D.P., Müller, W., Nita, D.C., Ontañón, R., Garciá-Moncó, C., Richards, D.A., 2019. North Iberian temperature and rainfall seasonality over the Younger Dryas and Holocene. Quat. Sci. Rev. 226. https://doi.org/10.1016/j.quascirev.2019.105998

Banderas, R., Á, Ivarez-Solas, J., Montoya, M., 2012. Role of CO_2 and Southern Ocean winds in glacial abrupt climate change. Clim. Past 8, 1011–1021. https://doi.org/10.5194/cp-8-1011-2012

Banderas, R., Alvarez-Solas, J., Robinson, A., Montoya, M., 2018. A new approach for simulating the paleo-evolution of the Northern Hemisphere ice sheets. Geosci. Model Dev. 11, 2299–2314. https://doi.org/10.5194/gmd-11-2299-2018

Banderas, R., Alvarez-Solas, J., Robinson, A., Montoya, M., 2015. An interhemispheric mechanism for glacial abrupt climate change. Clim. Dyn. 44, 2897–2908. https://doi.org/10.1007/s00382-014-2211-8

Barker, S., Knorr, G., 2021. Millennial scale feedbacks determine the shape and rapidity of glacial termination. Nat. Commun. 14. https://doi.org/10.1038/s41467-021-22388-6

Barreiro-Lostres, F., Moreno, A., Giralt, S., Caballero, M., Valero-Garcés, B., 2014. Climate, palaeohydrology and land use change in the Central Iberian Range over the last 1.6 kyr: The La Parra Lake record. The Holocene.

Barreiro-Lostres, F., Moreno, A., González-Sampériz, P., Giralt, S., Nadal-Romero, E., Valero-Garcés, B., 2017. Erosion in Mediterranean mountain landscapes during the last millennium: a quantitative approach based on lake sediment sequences (Iberian Range, Spain). CATENA 149, 782–798. https://doi.org/10.1016/j.catena.2016.05.024

Barriendos, M., Gil-Guirado, S., Pino, D., Tuset, J., Pérez-Morales, A., Alberola, A., Costa, J., Balasch, J.C., Castelltort, X., Mazón, J., Ruiz-Bellet, J.L., 2019. Climatic and social factors behind the Spanish Mediterranean flood event chronologies from documentary sources (14th–20th centuries). Glob. Planet. Change 182. https://doi.org/10.1016/j.gloplacha.2019.102997

Bartels-Jónsdóttir, H.B., Voelker, A.H.L., Abrantes, F.G., Salgueiro, E., Rodrigues, T., Knudsen, K.L., 2015. High-frequency surface water changes in the Tagus prodelta off Lisbon, eastern North Atlantic, during the last two millennia. Mar. Micropaleontol. 117, 13–24. https://doi.org/10.1016/j.marmicro.2015.03.001

Bartolomé, M., Moreno, A., Sancho, C., Cacho, I., Stoll, H., Haghipour, N., Belmonte, Á., Spötl, C., Hellstrom, J., Edwards, R.L., Cheng, H., 2024. Reconstructing hydroclimate changes over the past 2500 years using speleothems from Pyrenean caves (NE Spain). Clim. Past 20, 467–494. https://doi.org/10.5194/cp-20-467-2024

Bartolomé, M., Moreno, A., Sancho, C., Stoll, H.M., Cacho, I., Spötl, C., Belmonte, Á., Edwards, R.L., Cheng, H., Hellstrom, J.C., 2015. Hydrological change in Southern Europe responding to increasing North Atlantic overturning during Greenland Stadial 1. Proc. Natl. Acad. Sci. U. S. A. 112, 6568–6572. https://doi.org/10.1073/pnas.1503990112

Bauer, E., Ganopolski, A., Montoya, M., 2004. Simulation of the cold climate event 8200 years ago by meltwater outburst from Lake Agassiz. Paleoceanography 19. https://doi.org/10.1029/2004PA001030

Bellard, C., Bertelsmeier, C., Leadley, P., Thuiller, W., Courchamp, F., 2012. Impacts of climate change on the future of biodiversity. Ecol. Lett. 15, 365–377. https://doi.org/10.1111/j.1461-0248.2011.01736.x

Benito, G., Greenbaum, N., Medialdea, A., Calle, M., Sanchez-Moya, Y., Machado, M., Ballesteros-Cánovas, J.A., Corella, J.P., 2023. Late Pleistocene–Holocene multi-decadal patterns of extreme floods in NW Iberia: The Duero River palaeoflood record. Quat. Sci. Rev. 321. https://doi.org/10.1016/j.quascirev.2023.108356

Benito, G., Macklin, M.G., Panin, A., Rossato, S., Fontana, A., Jones, A.F., Machado, M.J., Matlakhova, E., Mozzi, P., Zielhofer, C., 2015. Recurring flood distribution patterns related to short-term Holocene climatic variability. Sci. Rep. 5. https://doi.org/10.1038/srep16398

Bernal-Wormull, J.L., Moreno, A., Bartolomé, M., Arriolabengoa, M., Pérez-Mejías, C., Iriarte, E., Osácar, C., Spötl, C., Stoll, H., Cacho, I., Edwards, R.L., Cheng, H., 2023. New insights into the climate of northern Iberia during the Younger Dryas and Holocene: The Mendukilo multi-speleothem record. Quat. Sci. Rev. 305, 108006. https://doi.org/10.1016/j.quascirev.2023.108006

Bernal-Wormull, J.L., Moreno, A., Pérez-Mejías, C., Bartolomé, M., Aranburu, A., Arriolabengoa, M., Iriarte, E., Cacho, I., Spötl, C., Edwards, R.L., Cheng, H., 2021. Immediate temperature response in northern Iberia to last deglacial changes in the North Atlantic. Geology 49, 999–1003. https://doi.org/10.1130/G48660.1

Bernárdez, P., González-Álvarez, R., Francés, G., Prego, R., Bárcena, M.A., Romero, O.E., 2008. Late Holocene history of the rainfall in the NW Iberian peninsula - Evidence from a marine record. J. Mar. Syst. 72, 366–382.

Bini, M., Zanchetta, G., Perşoiu, A., Cartier, R., Català, A., Cacho, I., Dean, J.R., Di Rita, F., Drysdale, R.N., Finnè, M., Isola, I., Jalali, B., Lirer, F., Magri, D., Masi, A., Marks, L., Mercuri, A.M., Peyron, O., Sadori, L., Sicre, M.-A., Welc, F., Zielhofer, C., Brisset, E., 2019. The 4.2 ka BP Event in the Mediterranean region: an overview. Clim. Past 15, 555–577. https://doi.org/10.5194/cp-15-555-2019

Blanco-González, A., Lillios, K.T., López-Sáez, J.A., Drake, B.L., 2018. Cultural, Demographic and Environmental Dynamics of the Copper and Early Bronze Age in Iberia (3300–1500 BC): Towards an Interregional Multiproxy Comparison at the Time of the 4.2 ky BP Event. J. World Prehistory 31, 1–79. https://doi.org/10.1007/s10963-018-9113-3

Blasco, J., Tabone, I., Alvarez-Solas, J., Robinson, A., Montoya, M., 2019. The Antarctic Ice Sheet response to glacial millennial-scale \hack\break variability. Clim. Past 15, 121–133. https://doi.org/10.5194/cp-15-121-2019

Blöschl, G., Kiss, A., Viglione, A., Barriendos, M., Böhm, O., Brázdil, R., Coeur, D., Demarée, G., Llasat, M.C., Macdonald, N., Retsö, D., Roald, L., Schmocker-Fackel, P., Amorim, I., Bělínová, M., Benito, G., Bertolin, C., Camuffo, D., Cornel, D., Doktor, R., Elleder, L., Enzi, S., Garcia, J.C., Glaser, R., Hall, J., Haslinger, K., Hofstätter, M., Komma, J., Limanówka, D., Lun, D., Panin, A., Parajka, J., Petrić, H., Rodrigo, F.S., Rohr, C., Schönbein, J., Schulte, L., Silva, L.P., Toonen, W.H.J., Valent, P., Waser, J., Wetter, O., 2020. Current European flood-rich period exceptional compared with past 500 years. Nature 583, 560–566. https://doi.org/10.1038/s41586-020-2478-3

Bradley, R.S., Bakke, J., 2019. Is there evidence for a 4.2 ka BP event in the northern North Atlantic region? Clim. Past 15, 1665–1676. https://doi.org/10.5194/cp-15-1665-2019

Bravo-Paredes, N., Gallego, M.C., Domínguez-Castro, F., García, J.A., Vaquero, J.M., 2020. Pro-Pluvia Rogation Ceremonies in Extremadura (Spain): Are They a Good Proxy of Winter NAO? Atmosphere 11. https://doi.org/10.3390/atmos11030282

Brisset, E., Revelles, J., Expósito, I., Bernabeu Aubán, J., Burjachs, F., 2020. Socio-Ecological Contingencies with Climate Changes over the Prehistory in the Mediterranean Iberia. Quaternary 3. https://doi.org/10.3390/quat3030019

Brovkin, V., Brook, E., Williams, J.W., Bathiany, S., Lenton, T.M., Barton, M., DeConto, R.M., Donges, J.F., Ganopolski, A., McManus, J., Praetorius, S., de Vernal, A., Abe-Ouchi, A., Cheng, H., Claussen, M., Crucifix, M., Gallopín, G., Iglesias, V., Kaufman, D.S., Kleinen, T., Lambert, F., van der Leeuw, S., Liddy, H., Loutre, M.-F., McGee, D., Rehfeld, K., Rhodes, R., Seddon, A.W.R., Trauth, M.H., Vanderveken, L., Yu, Z., 2021. Past abrupt changes, tipping points and cascading impacts in the Earth system. Nat. Geosci. 14, 550–558. https://doi.org/10.1038/s41561-021-00790-5

Bullón, T., 2011. Relationships between precipitation and floods in the fluvial basins of Central Spain based on documentary sources from the end of the 16th century. Nat. Hazards Earth Syst. Sci. 11, 2215–2225. https://doi.org/10.5194/nhess-11-2215-2011

Burjachs, F., Expósito, I., 2015. Charcoal and pollen analysis: Examples of Holocene fire dynamics in Mediterranean Iberian Peninsula. CATENA 135, 340–349. https://doi.org/10.1016/j.catena.2014.10.006

Camuera, J., Jiménez-Espejo, F.J., Soto-Chica, J., Jiménez-Moreno, G., García-Alix, A., Ramos-Román, M.J., Ruha, L., Castro-Priego, M., 2023. Drought as a possible contributor to the Visigothic Kingdom crisis and Islamic expansion in the Iberian Peninsula. Nat. Commun. 14, 5733. https://doi.org/10.1038/s41467-023-41367-7

Camuera, J., Jiménez-Moreno, G., Ramos-Román, M.J., García-Alix, A., Jiménez-Espejo, F.J., Toney, J.L., Anderson, R.S., 2021. Chronological control and centennial-scale climatic subdivisions of the Last Glacial Termination in the western Mediterranean region. Quat. Sci. Rev. 255. https://doi.org/10.1016/j.quascirev.2021.106814

Camuera, J., Jiménez-Moreno, G., Ramos-Román, M.J., García-Alix, A., Toney, J.L., Anderson, R.S., Jiménez-Espejo, F., Bright, J., Webster, C., Yanes, Y., Carrión, J.S., 2019. Vegetation and climate changes during the last two glacial-interglacial cycles in the western Mediterranean: A new long pollen record from Padul (southern Iberian Peninsula). Quat. Sci. Rev. 205, 86–105. https://doi.org/10.1016/j.quascirev.2018.12.013

Camuera, J., Jiménez-Moreno, G., Ramos-Román, M.J., García-Alix, A., Toney, J.L., Anderson, R.S.S., Jiménez-Espejo, F., Kaufman, D., Bright, J., Webster, C., Yanes, Y., Carrión, J.S., Ohkouchi, N., Suga, H., Yamame, M., Yokoyama, Y., Martínez-Ruiz, F., 2018. Orbital-scale environmental and climatic changes recorded in a new ~200,000-year-long multiproxy sedimentary record from Padul, southern Iberian Peninsula. Quat. Sci. Rev. 198, 91–114. https://doi.org/10.1016/j.quascirev.2018.08.014

Camuera, J., Ramos-Román, M.J., Jiménez-Moreno, G., García-Alix, A., Ilvonen, L., Ruha, L., Gil-Romera, G., González-Sampériz, P., Seppä, H., 2022. Past 200 kyr hydroclimate variability in the western Mediterranean and its connection to the African Humid Periods. Sci. Rep. 12, 9050. https://doi.org/10.1038/s41598-022-12047-1

Camuffo, D., Bertolin, C., Barriendos, M., Dominguez-Castro, F., Cocheo, C., Enzi, S., Sghedoni, M., della Valle, A., Garnier, E., Alcoforado, M.-J., Xoplaki, E., Luterbacher, J., Diodato, N., Maugeri, M., Nunes, M.F., Rodriguez, R., 2010. 500-year temperature reconstruction in the Mediterranean Basin by means of documentary data and instrumental observations. Clim. Change 101, 169–199. https://doi.org/10.1007/s10584-010-9815-8

Carlson, A.E., Clark, P.U., 2012. Ice sheet sources of sea level rise and freshwater discharge during the last deglaciation. Rev. Geophys. 50. https://doi.org/10.1029/2011RG000371

Carrasco, R.M., Pedraza, J., Domínguez-Villar, D., Willenbring, J.K., Villa, J., 2015. Sequence and chronology of the Cuerpo de Hombre paleoglacier (Iberian Central System) during the last glacial cycle. Quat. Sci. Rev. 129, 163–177. https://doi.org/10.1016/j.quascirev.2015.09.021

Carrión, J,S., Munuera M, Ochando J, López-Sáez JA, Casas-Gallego M, González Sampériz P, Badal E, Pérez-Díaz S, Carrión-Marco Y, Jiménez-Moreno G, López-Merino L, Burjachs F, Abel-Schaad D, Fernández S, Morales-Molino C, Alba Sánchez F, Peña-Chocarro L, Barrón E, Postigo-Mijarra JM, Gil-García MJ, Rubiales JM, Vidal-Matutano P, Arambarri J, Ramos-Román MJ, Camuera J, Magri D, Revelles J, Altolaguirre Y, Ruiz-Zapata B, Luelmo R, Uzquiano P, Allué E, Anderson S, Dupré M, Gil-Romera G, Piqué R, García-Antón M, Amorós G, Yll R, Pérez-Jordá G, Scott L, Figueiral I, Rodríguez-Ariza MO, Morla-Jauristi C, García-Amorena I, Montoya E, Val Peón C, Ejarque A, Riera S, Peñalba C, Fierro E, Expósito I, Pérez-Obiol R, Vieira M, Gómez-Manzaneque F, Maldonado J, Leunda M, Franco F, Albert RM, Díez MJ, Marín-Arroyo AB, Manzano S, DiRita F, Andrade A, Parra I, Zapata L, Pérez A, Grau E, Alcolea M, Mesa-Fernández JM, Miras Y, Ruiz-Alonso M, Génova M, García-Alvarez S, Moreno E, Olmedo Cobo JA, Gómez Zotano J, Pardo Martínez R, Mas B, Monteiro P, Antolín F, Obea L, Martín-Seijo M, Alonso N, Amorós A, Fernández-Díaz M, Reyes PP, SánchezGiner V, Gómez-Rodríguez M, Rull V, Vegas-Villarrúbia T, López-Bultó O, Bianco S, Trapote MC, Picornell-Gelabert L, Sureda P, Brisset E, Servera Vives G, Girona A, Celant A., 2022. Paleoiberica I. URL https://www.paleofloraiberica.org/ (accessed 7.4.24).

Carrión, J.S., Fernández, S., González-Sampériz, P., Gil-Romera, G., Badal, E., Carrión-Marco, Y., López-Merino, L., López-Sáez, J.A., Fierro, E., Burjachs, F., 2010. Expected trends and surprises in the Lateglacial and Holocene vegetation history of the Iberian Peninsula and Balearic Islands. Rev. Palaeobot. Palynol. 162, 458–475. https://doi.org/10.1016/j.revpalbo.2009.12.007

Castillo Martín, A., 2016. Lagunas de Sierra Nevada. Granada.

Castro, D., Souto, M., Fraga, M.I., García-Rodeja, E., Pérez-Díaz, S., López Sáez, J.A., Pontevedra-Pombal, X., 2020. High-resolution patterns of palaeoenvironmental changes during the Little Ice Age and the Medieval Climate Anomaly in the northwestern Iberian Peninsula. Geosci. Front. 11, 1461–1475. https://doi.org/10.1016/j.gsf.2020.05.015

Castro, D., Souto, M., Garcia-Rodeja, E., Pontevedra-Pombal, X., Fraga, M.I., 2015. Climate change records between the mid- and late Holocene in a peat bog from Serra do Xistral (SW Europe) using plant macrofossils and peat humification analyses. Palaeogeogr. Palaeoclimatol. Palaeoecol. 420, 82–95. https://doi.org/10.1016/j.palaeo.2014.12.005

Català, A., Cacho, I., Frigola, J., Pena, L.D., Lirer, F., 2019. Holocene hydrography evolution in the Alboran Sea: A multi-record and multi-proxy comparison. Clim. Past 15, 927–942. https://doi.org/10.5194/cp-15-927-2019

Catalan, J., Ninot, J.M., Aniz, M.M., 2017. The High Mountain Conservation in a Changing World BT - High Mountain Conservation in a Changing World, in: Catalan, J., Ninot, J.M., Aniz, M.M., Catalan, J., Ninot, J.M., Aniz, M.M. (Eds.), Cham, pp. 3–36.

Catalan, J., Pla-Rabés, S., Wolfe, A.P., Smol, J.P., Rühland, K.M., Anderson, N.J., Kopáček, J., Stuchlík, E., Schmidt, R., Koinig, K.A., Camarero, L., Flower, R.J., Heiri, O., Kamenik, C., Korhola, A., Leavitt, P.R., Psenner, R., Renberg, I., 2013. Global change revealed by palaeolimnological records from remote lakes: a review. J. Paleolimnol. 49, 513–535. https://doi.org/10.1007/s10933-013-9681-2

Cearreta, A., Benito, X., Ibáñez, C., Trobajo, R., Giosan, L., 2016. Holocene palaeoenvironmental evolution of the Ebro Delta (Western Mediterranean Sea): Evidence for an early construction based on the benthic foraminiferal record. The Holocene 26, 1438–1456. https://doi.org/10.1177/0959683616640048

Checa, H., Margaritelli, G., Pena, L.D., Frigola, J., Cacho, I., Rettori, R., Lirer, F., 2020. High resolution paleoenvironmental changes during the Sapropel 1 in the North Ionian Sea, central Mediterranean. The Holocene 30, 1504–1515. https://doi.org/10.1177/0959683620941095

Cisneros, M., Cacho, I., Frigola, J., Canals, M., Masqué, P., Martrat, B., Casado, M., Grimalt, J.O., Pena, L.D., Margaritelli, G., Lirer, F., 2016. Sea surface temperature variability in the central-western Mediterranean Sea during the last 2700 years: a multi-proxy and multi-record approach. Clim. Past 12, 849–869. https://doi.org/10.5194/cp-12-849-2016

Cisneros, M., Cacho, I., Frigola, J., Sanchez-Vidal, A., Calafat, A., Pedrosa-Pàmies, R., Rumín-Caparrós, A., Canals, M., 2019. Deep-water formation variability in the north-western Mediterranean Sea during the last 2500 yr: A proxy validation with present-day data. Glob. Planet. Change 177, 56–68. https://doi.org/10.1016/j.gloplacha.2019.03.012

Cisneros, M., Cacho, I., Moreno, A., Stoll, H., Torner, J., Català, A., Edwards, R.L., Cheng, H., Fornós, J.J., 2021. Hydroclimate variability during the last 2700 years based on stalagmite multi-proxy records in the central-western Mediterranean. Quat. Sci. Rev. 269. https://doi.org/10.1016/j.quascirev.2021.107137

Clark, P.U., Shakun, J.D., Baker, P.A., Bartlein, P.J., Brewer, S., Brook, E., Carlson, A.E., Cheng, H., Kaufman, D.S., Liu, Z., Marchitto, T.M., Mix, A.C., Morrill, C., Otto-Bliesner, B.L., Pahnke, K., Russell, J.M., Whitlock, C., Adkins, J.F., Blois, J.L., Clark, J., Colman, S.M., Curry, W.B., Flower, B.P., He, F., Johnson, T.C., Lynch-Stieglitz, J., Markgraf, V., McManus, J., Mitrovica, J.X., Moreno, P.I., Williams, J.W., 2012. Global climate evolution during the last deglaciation. Proc. Natl. Acad. Sci. 109, E1134–E1142. https://doi.org/10.1073/pnas.1116619109

Corella, J.P., Brauer, A., Mangili, C., Rull, V., Vegas-Vilarrúbia, T., Morellón, M., Valero-Garcés, B.L., 2012. The 1.5-ka varved record of Lake Montcortès (southern Pyrenees, NE Spain). Quat. Res. 78, 323–332. https://doi.org/10.1016/j.yqres.2012.06.002

Corella, J.P., Moreno, A., Morellón, M., Rull, V., Giralt, S., Rico, M.T., Pérez-Sanz, A., Valero-Garcés, B.L., 2011. Climate and human impact on a meromictic lake during the last 6,000 years (Montcortès Lake, Central Pyrenees, Spain). J. Paleolimnol. 46, 351–367. https://doi.org/10.1007/s10933-010-9443-3

Corella, J.P., Sierra, M.J., Garralón, A., Millán, R., Rodríguez-Alonso, J., Mata, M.P., de Vera, A.V., Moreno, A., González-Sampériz, P., Duval, B., Amouroux, D., Vivez, P., Cuevas, C.A., Adame, J.A., Wilhelm, B., Saiz-Lopez, A., Valero-Garcés, B.L., 2021. Recent and historical pollution legacy in high altitude Lake Marboré (Central Pyrenees): A record of mining and smelting since pre-Roman times in the Iberian Peninsula. Sci. Total Environ. 751, 141557. https://doi.org/10.1016/j.scitotenv.2020.141557

Corella, J.P., Stefanova, V., El Anjoumi, A., Rico, E., Giralt, S., Moreno, A., Plata-Montero, A., Valero-Garcés, B.L., 2013. A 2500-year multi-proxy reconstruction of climate change and human activities in northern Spain: The Lake Arreo record. Palaeogeogr. Palaeoclimatol. Palaeoecol. 386, 555–568. https://doi.org/10.1016/j.palaeo.2013.06.022

Cortés Sánchez, M., Jiménez Espejo, F.J., Simón Vallejo, M.D., Gibaja Bao, J.F., Carvalho, A.F., Martinez-Ruiz, F., Gamiz, M.R., Flores, J.-A., Paytan, A., López Sáez, J.A., Peña-Chocarro, L., Carrión, J.S., Morales Muñiz, A., Roselló Izquierdo, E., Riquelme Cantal, J.A., Dean, R.M., Salgueiro, E., Martínez Sánchez, R.M., De la Rubia de Gracia, J.J., Lozano Francisco, M.C., Vera Peláez, J.L., Rodríguez, L.L., Bicho, N.F., 2012. The Mesolithic-Neolithic transition in southern Iberia. Quat. Res. 77, 221–234.

Cortés-Sánchez, M., Lozano-Francisco, M.C., Simón-Vallejo, M.D., Jiménez-Espejo, F., Lloret, C.O., Tejada, S.M., Muñiz, A.M., 2023. Giant limpets in southern Iberian coastal and continental archaeological sites, from Neanderthals to Copper Age. Quat. Sci. Rev. 317, 108238. https://doi.org/10.1016/j.quascirev.2023.108238

Costas, S., Ferreira, Ó., Plomaritis, T.A., Leorri, E., 2016. Coastal barrier stratigraphy for Holocene high-resolution sea-level reconstruction. Sci. Rep. 6, 38726. https://doi.org/10.1038/srep38726

Cresswell-Clay, N., Ummenhofer, C.C., Thatcher, D.L., Wanamaker, A.D., Denniston, R.F., Asmerom, Y., Polyak, V.J., 2022. Twentieth-century Azores High expansion unprecedented in the past 1,200 years. Nat. Geosci. 15, 548–553. https://doi.org/10.1038/s41561-022-00971-w

Cruz, J.A., Turrero, M.J., Cáceres, J.O., Marín-Roldán, A., Ortega, A.I., Garralón, A., Sánchez, L., Gómez, P., Muñoz-García, M.B., Edwards, R.L., Martín-Chivelet, J., 2015. Long-term hydrological changes in northern Iberia (4.9–0.9 ky BP) from speleothem Mg/Ca ratios and cave monitoring (Ojo Guareña Karst Complex, Spain). Environ. Earth Sci. 74, 7741–7753. https://doi.org/10.1007/s12665-015-4687-x

Currás, A., Zamora, L., Reed, J.M., García-Soto, E., Ferrero, S., Armengol, X., Mezquita-Joanes, F., Marqués, M.A., Riera, S., Julià, R., 2012. Climate change and human impact in central Spain during Roman times: High-resolution multi-proxy analysis of a tufa lake record (Somolinos, 1280m asl). Catena 89, 31–53. https://doi.org/10.1016/j.catena.2011.09.009

Dawson, T.P., Jackson, S.T., House, J.I., Prentice, I.C., Mace, G.M., 2011. Beyond Predictions: Biodiversity Conservation in a Changing Climate. Science 332, 53–58. https://doi.org/10.1126/science.1200303

de Andrés, E., Colangelo, M., Luelmo-Lautenschlaeger, R., López-Sáez, J.A., Camarero, J.J., 2023. Sensitivity of Eurasian Rear-Edge Birch Populations to Regional Climate and Local Hydrological Conditions. Forests 14. https://doi.org/10.3390/f14071360

deMenocal, P.B., 2011. Climate and Human Evolution. Science 331, 540–542. https://doi.org/10.1126/science.1190683

Dessandier, P.A., Bonnin, J., Malaizé, B., Lambert, C., Tjallingii, R., Warden, L., Sinninghe Damsté, J.S., Kim, J.H., 2018. Variations in benthic foraminiferal assemblages in the Tagus mud belt during the last 5700 years: Implications for Tagus River discharge. Palaeogeogr. Palaeoclimatol. Palaeoecol. 496, 225–237. https://doi.org/10.1016/j.palaeo.2018.01.040

Di Rita, F., Fletcher, W.J., Aranbarri, J., Margaritelli, G., Lirer, F., Magri, D., 2018. Holocene forest dynamics in central and western Mediterranean: periodicity, spatio-temporal patterns and climate influence. Sci. Rep. 8, 8929. https://doi.org/10.1038/s41598-018-27056-2

Diz, P., Francés, G., Pelejero, C., Grimalt, J.O., Vilas, F., 2002. The last 3000 years in the Ría de Vigo (NW Iberian Margin): climatic and hydrographic signals. The Holocene 12, 459–468. https://doi.org/10.1191/0959683602hl550rp

Domínguez-Castro, F., Alcoforado, M.J., Bravo-Paredes, N., Fernández-Fernández, M.I., Fragoso, M., Gallego, M.C., García Herrera, R., Garnier, E., Garza-Merodio, G., El Kenawy, A.M., Latorre, B., Noguera, I., Peña-Angulo, D., Reig-Gracia, F., Silva, L.P., Vaquero, J.M., Vicente Serrano, S.M., 2021. Dating historical droughts from religious ceremonies, the international pro pluvia rogation database. Sci. Data 8, 186. https://doi.org/10.1038/s41597-021-00952-5

Domínguez-Castro, F., de Miguel, J.C., Vaquero, J.M., Gallego, M.C., García-Herrera, R., 2014. Climatic potential of Islamic chronicles in Iberia: Extreme droughts (ad 711–1010). The Holocene 24, 370–374. https://doi.org/10.1177/0959683613518591

Domínguez-Castro, F., García-Herrera, R., Ribera, P., Barriendos, M., 2010. A shift in the spatial pattern of Iberian droughts during the 17th century. Clim. Past 6, 553–563. https://doi.org/10.5194/cp-6-553-2010

Domínguez-Castro, F., Ribera, P., García-Herrera, R., Vaquero, J.M., Barriendos, M., Cuadrat, J.M., Moreno, J.M., 2012. Assessing extreme droughts in Spain during 1750-1850 from rogation ceremonies. Clim. Past 8, 705–722. https://doi.org/10.5194/cp-8-705-2012

Domínguez-Villar, D., 2013. Comment on "Land surface temperature changes in Northern Iberia since 4000 yr BP, based on δ13C of speleothems." Glob. Planet. Change 100, 291–294. https://doi.org/10.1016/j.gloplacha.2012.11.005

Domínguez-Villar, D., Carrasco, R.M., Pedraza, J., Cheng, H., Edwards, R.L., Willenbring, J.K., 2013. Early maximum extent of paleoglaciers from Mediterranean mountains during the last glaciation. Sci. Rep. 3, 2034. https://doi.org/10.1038/srep02034

Domínguez-Villar, D., Fairchild, I.J., Baker, A., Wang, X., Edwards, R.L., Cheng, H., 2009. Oxygen isotope precipitation anomaly in the North Atlantic region during the 8.2 ka event. Geology 37, 1095–1098. https://doi.org/10.1130/G30393A.1

Domínguez-Villar, D., Krklec, K., Boomer, I., Fairchild, I.J., 2021. ISODRIP, a model to transfer the δ18O signal of precipitation to drip water — Implementation of the model for Eagle Cave (central Spain). Sci. Total Environ. 797, 149188. https://doi.org/10.1016/j.scitotenv.2021.149188

Domínguez-Villar, D., Wang, X., Krklec, K., Cheng, H., Edwards, R.L., 2017. The control of the tropical North Atlantic on Holocene millennial climate oscillations. Geology 45, 303–306. https://doi.org/10.1130/G38573.1

Dorado Liñán, I., Büntgen, U., González-Rouco, F., Zorita, E., Montávez, J.P., Gómez-Navarro, J.J., Brunet, M., Heinrich, I., Helle, G., Gutiérrez, E., 2012. Estimating 750 years of temperature variations and uncertainties in the Pyrenees by tree-ring reconstructions and climate simulations. Clim. Past 8, 919–933. https://doi.org/10.5194/cp-8-919-2012

Dorado Liñán, I., Zorita, E., González-Rouco, J.F., Heinrich, I., Campello, F., Muntán, E., Andreu-Hayles, L., Gutiérrez, E., 2015. Eight-hundred years of summer temperature variations in the southeast of the Iberian Peninsula reconstructed from tree rings. Clim. Dyn. 44, 75–93. https://doi.org/10.1007/s00382-014-2348-5

Ejarque, A., Julià, R., Reed, J.M., Mesquita-Joanes, F., Barba, J.M., Riera, S., 2016. Coastal evolution in a mediterranean microtidal zone: Mid to late holocene natural dynamics and human management of the castelló lagoon, NE Spain. PLoS ONE 11, 1–28. https://doi.org/10.1371/journal.pone.0155446

Esper, J., Großjean, J., Camarero, J.J., García-Cervigón, A.I., Olano, J.M., González-Rouco, J.F., Domínguez-Castro, F., Büntgen, U., 2015. Atlantic and Mediterranean synoptic drivers of central Spanish juniper growth. Theor. Appl. Climatol. 121, 571–579. https://doi.org/10.1007/s00704-014-1254-4

Esper, J., Hartl, C., Tejedor, E., de Luis, M., Günther, B., Büntgen, U., 2020. High-Resolution Temperature Variability Reconstructed from Black Pine Tree Ring Densities in Southern Spain. Atmosphere 11. https://doi.org/10.3390/atmos11070748

Eynaud, F., de Abreu, L., Voelker, A., Schönfeld, J., Salgueiro, E., Turon, J.-L., Penaud, A., Toucanne, S., Naughton, F., Sánchez Goñi, M.F., Malaizé, B., Cacho, I., 2009. Position of the Polar Front along the western Iberian margin during key cold episodes of the last 45 ka. Geochem. Geophys. Geosystems 10, n/a-n/a. https://doi.org/10.1029/2009GC002398

Eyring, V., Bony, S., Meehl, G.A., Senior, C.A., Stevens, B., Stouffer, R.J., Taylor, K.E., 2016. Overview of the Coupled Model Intercomparison Project Phase 6 (CMIP6) experimental design and organization. Geosci. Model Dev. 9, 1937–1958. https://doi.org/10.5194/gmd-9-1937-2016

Fernández-Fernández, M.I., Gallego, M.C., Domínguez-Castro, F., Trigo, R.M., Vaquero, J.M., 2017. The climate in Zafra from 1750 to 1840: temperature indexes from documentary sources. Clim. Change 141, 671–684. https://doi.org/10.1007/s10584-017-1910-7

Fernández-Fernández, M.I., Gallego, M.C., Domínguez-Castro, F., Trigo, R.M., Vaquero, J.M., 2015. The climate in Zafra from 1750 to 1840: precipitation. Clim. Change 129, 267–280. https://doi.org/10.1007/s10584-014-1315-9

Fernández-Montes, S., Gómez-Navarro, J.J., Rodrigo, F.S., García-Valero, J.A., Montávez, J.P., 2017. Covariability of seasonal temperature and precipitation over the Iberian Peninsula in high-resolution regional climate simulations (1001–2099). Glob. Planet. Change 151, 122–133. https://doi.org/10.1016/j.gloplacha.2016.09.007

Finné, M., Woodbridge, J., Labuhn, I., Roberts, C.N., 2019. Holocene hydro-climatic variability in the Mediterranean: A synthetic multi-proxy reconstruction. Holocene 29, 847–863. https://doi.org/10.1177/0959683619826634

Fletcher, W.J., Debret, M., Goñi, M.F.S., 2013. Mid-Holocene emergence of a low-frequency millennial oscillation in western Mediterranean climate: Implications for past dynamics of the North Atlantic atmospheric westerlies. Holocene 23, 153–166. https://doi.org/10.1177/0959683612460783

Fletcher, William J, Sánchez Goñi, M.F., Allen, J.R.M., Cheddadi, R., Combourieu-Nebout, N., Huntley, B., Lawson, I., Londeix, L., Magri, D., Margari, V., Müller, U.C., Naughton, F., Novenko, E., Roucoux, K., Tzedakis, P.C., 2010. Millennial-scale variability during the last glacial in vegetation records from Europe. Quat. Sci. Rev. 29, 2839–2864. https://doi.org/10.1016/j.quascirev.2009.11.015

Fletcher, W J, Sánchez Goñi, M.F., Peyron, O., Dormoy, I., 2010. Abrupt climate changes of the last deglaciation detected in a Western Mediterranean forest record. Clim. Past 6, 245–264.

Garcés-Pastor, S., Gutiérrez-Merino, E., Martínez-Sancho, E., Dorado-Liñán, I., Julio Camarero, J., Cañellas-Boltà, N., Vegas-Vilarrúbia, T., 2018. Subalpine forest dynamics reconstructed throughout the last 700 years in the Central Pyrenees by means of tree rings and pollen. The Holocene 29, 300–312. https://doi.org/10.1177/0959683618810402

García-Alix, A., Camuera, J., Ramos-Román, M.J., Toney, J.L., Sachse, D., Schefuß, E., Jiménez-Moreno, G., Jiménez-Espejo, F.J., López-Avilés, A., Anderson, R.S., Yanes, Y., 2021. Paleohydrological dynamics in the Western Mediterranean during the last glacial cycle. Glob. Planet. Change 202. https://doi.org/10.1016/j.gloplacha.2021.103527

García-Alix, A., Jimenez-Espejo, F.J., Lozano, J.A., Jiménez-Moreno, G., Martinez-Ruiz, F., García Sanjuán, L., Aranda Jiménez, G., García Alfonso, E., Ruiz-Puertas, G., Anderson, R.S., 2013. Anthropogenic impact and lead pollution throughout the Holocene in Southern Iberia. Sci. Total Environ. 449, 451–460. https://doi.org/10.1016/j.scitotenv.2013.01.081

García-Alix, A., Jiménez-Espejo, F.J., Toney, J.L., Jiménez-Moreno, G., Ramos-Román, M.J., Anderson, R.S., Ruano, P., Queralt, I., Delgado Huertas, A., Kuroda, J., 2017. Alpine bogs of southern Spain show human-induced environmental change superimposed on long-term natural variations. Sci. Rep. 7. https://doi.org/10.1038/s41598-017-07854-w

García-Alix, A., Jiménez-Moreno, G., Gázquez, F., Monedero-Contreras, R., López-Avilés, A., Jiménez-Espejo, F.J., Rodríguez-Rodríguez, M., Camuera, J., José Ramos-Román, M., Scott Anderson, R., 2022. Climatic control on the Holocene hydrology of a playa-lake system in the western Mediterranean. CATENA 214, 106292. https://doi.org/10.1016/j.catena.2022.106292

García-Alix, A., Jiménez-Moreno, G., Jiménez-Espejo, F.J., García-García, F., Delgado Huertas, A., 2014. An environmental snapshot of the Bølling interstadial in Southern Iberia. Quat. Res. 81, 284–294. https://doi.org/10.1016/j.yqres.2014.01.009

García-Alix, A., Toney, J.L., Jiménez-Moreno, G., Pérez-Martínez, C., Jiménez, L., Rodrigo-Gámiz, M., Anderson, R.S., Camuera, J., Jiménez-Espejo, F.J., Peña-Angulo, D., Ramos-Román, M.J., 2020. Algal lipids reveal unprecedented warming rates in alpine areas of SW Europe during the industrial period. Clim. Past 16, 245–263. https://doi.org/10.5194/cp-16-245-2020

García-Artola, A., Stéphan, P., Cearreta, A., Kopp, R.E., Khan, N.S., Horton, B.P., 2018. Holocene sea-level database from the Atlantic coast of Europe. Quat. Sci. Rev. 196, 177–192. https://doi.org/10.1016/j.quascirev.2018.07.031

García-Ruiz, J.M., Palacios, D., González-Sampériz, P., de Andrés, N., Moreno, A., Valero-Garcés, B., Gómez-Villar, A., 2016. Mountain glacier evolution in the Iberian Peninsula during the Younger Dryas. Quat. Sci. Rev. 138, 16–30. https://doi.org/10.1016/j.quascirev.2016.02.022

Gardoki, J., Morellón, M., Leira, M., Ezquerra, F.J., Remondo, J., Tinner, W., Canales, M.L., van der Horst, A., Morales-Molino, C., 2023. Abrupt diatom responses to recent climate and land use changes in the Cantabrian Mountains (NW Spain). J. Paleolimnol. 69, 213–230. https://doi.org/10.1007/s10933-022-00269-2

Gázquez, F., Bauska, T.K., Comas-Bru, L., Ghaleb, B., Calaforra, J.-M., Hodell, D.A., 2020. The potential of gypsum speleothems for paleoclimatology: application to the Iberian Roman Humid Period. Sci. Rep. 10, 14705. https://doi.org/10.1038/s41598-020-71679-3

Gázquez, F., Morellón, M., Bauska, T., Herwartz, D., Surma, J., Moreno, A., Staubwasser, M., Valero-Garcés, B., Delgado-Huertas, A., Hodell, D.A., 2018. Triple oxygen and hydrogen isotopes of gypsum hydration water for quantitative paleo-humidity reconstruction. Earth Planet. Sci. Lett. 481, 177–188. https://doi.org/10.1016/j.epsl.2017.10.020

Genet, M., Daniau, A.-L., Mouillot, F., Hanquiez, V., Schmidt, S., David, V., Georget, M., Abrantes, F., Anschutz, P., Bassinot, F., Bonnin, J., Dennielou, B., Eynaud, F., Hodell, D.A., Mulder, T., Naughton, F., Rossignol, L., Tzedakis, P., Sánchez-Goñi, M.F., 2021. Modern relationships between microscopic charcoal in marine sediments and fire regimes on adjacent landmasses to refine the interpretation of marine paleofire records: An Iberian case study. Quat. Sci. Rev. 270, 107148. https://doi.org/10.1016/j.quascirev.2021.107148

Gil-Guirado, S., José Gómez-Navarro, J., Pedro Montávez, J., 2019. The weather behind words-new methodologies for integrated hydrometeorological reconstruction through documentary sources. Clim. Past 15, 1303–1325. https://doi.org/10.5194/cp-15-1303-2019

Gil-Romera, G., Carrión, J.S., Pausas, J.G., Sevilla-Callejo, M., Lamb, H.F., Fernández, S., Burjachs, F., 2010. Holocene fire activity and vegetation response in South-Eastern Iberia. Quat. Sci. Rev. 29, 1082–1092. https://doi.org/10.1016/j.quascirev.2010.01.006

Gil-Romera, G., González-Sampériz, P., Lasheras-Álvarez, L., Sevilla-Callejo, M., Moreno, A., Valero-Garcés, B., López-Merino, L., Carrión, J.S., Pérez Sanz, A., Aranbarri, J., García-Prieto Fronce, E., 2014. Biomass-modulated fire dynamics during the Last Glacial–Interglacial Transition at the Central Pyrenees (Spain). Palaeogeogr. Palaeoclimatol. Palaeoecol. 402, 113–124. https://doi.org/10.1016/j.palaeo.2014.03.015

Gomes, S.D., Fletcher, W.J., Rodrigues, T., Stone, A., Abrantes, F., Naughton, F., 2020. Time-transgressive Holocene maximum of temperate and Mediterranean forest development across the Iberian Peninsula reflects orbital forcing. Palaeogeogr. Palaeoclimatol. Palaeoecol. 550, 109739. https://doi.org/10.1016/j.palaeo.2020.109739

Gómez-Navarro, J.J., Montávez, J.P., Jiménez-Guerrero, P., Jerez, S., Lorente-Plazas, R., González-Rouco, J.F., Zorita, E., 2012. Internal and external variability in regional simulations of the Iberian Peninsula climate over the last millennium. Clim. Past 8, 25–36. https://doi.org/10.5194/cp-8-25-2012

González Sampériz, P., Montes, L., Aranbarri, J., Leunda, M., Domingo, R., Laborda, R., Sanjuan, Y., Gil-Romera, G., Lasanta, T., García-Ruiz, J.M., 2019. Scenarios, timing and paleo-environmental indicators for the identification of Anthropocene in the vegetal landscape of the Central Pyrenees (NE Iberia). Cuad. Investig. Geográfica 45, 167–193. https://doi.org/10.18172/cig.3691

González-Rouco, J.F., Beltrami, H., Zorita, E., Stevens, M.B., 2009. Borehole climatology: a discussion based on contributions from climate modeling. Clim Past 5, 97–127. https://doi.org/10.5194/cp-5-97-2009

González-Sampériz, P., Aranbarri, J., Pérez-Sanz, A., Gil-Romera, G., Moreno, A., Leunda, M., Sevilla-Callejo, M., Corella, J.P., Morellón, M., Oliva, B., Valero-Garcés, B., 2017. Environmental and climate change in the southern Central Pyrenees since the Last Glacial Maximum: A view from the lake records. CATENA 149, 668–688. https://doi.org/10.1016/j.catena.2016.07.041

González-Sampériz, P., Gil-Romera, G., García-Prieto, E., Aranbarri, J., Moreno, A., Morellón, M., Sevilla-Callejo, M., Leunda, M., Santos, L., Franco-Múgica, F., Andrade, A., Carrión, J.S., Valero-Garcés, B.L., 2020. Strong continentality and effective moisture drove unforeseen vegetation dynamics since the last interglacial at inland Mediterranean areas: The Villarquemado sequence in NE Iberia. Quat. Sci. Rev. 242, 106425. https://doi.org/10.1016/j.quascirev.2020.106425

González-Sampériz, P., Leroy, S.A.G., Carrión, J.S., Fernández, S., García-Antón, M., Gil-García, M.J., Uzquiano, P., Valero-Garcés, B., Figueiral, I., 2010. Steppes, savannahs, forests and phytodiversity reservoirs

during the Pleistocene in the Iberian Peninsula. Rev. Palaeobot. Palynol. 162, 427–457. https://doi.org/10.1016/j.revpalbo.2010.03.009

González-Sampériz, P., Utrilla, P., Mazo, C., Valero-Garcés, B., Sopena, M.C., Morellón, M., Sebastián, M., Moreno, A., Martínez-Bea, M., 2009. Patterns of human occupation during the Early Holocene in the Central Ebro Basin (NE Spain) in response to the 8.2 ka climatic event. Quat. Res. 71, 121–132.

González-Sampériz, P., Valero-Garcés, B.L., Moreno, A., Jalut, G., García-Ruiz, J.M., Martí-Bono, C., Delgado-Huertas, A., Navas, A., Otto, T., Dedoubat, J.J., 2006. Climate variability in the Spanish Pyrenees during the last 30,000 yr revealed by the El Portalet sequence. Quat. Res. 66, 38–52. https://doi.org/10.1016/j.yqres.2006.02.004

Goslin, J., Fruergaard, M., Sander, L., Gałka, M., Menviel, L., Monkenbusch, J., Thibault, N., Clemmensen, L.B., 2018. Holocene centennial to millennial shifts in North-Atlantic storminess and ocean dynamics. Sci. Rep. 8, 12778. https://doi.org/10.1038/s41598-018-29949-8

Gosling, W.D., Scerri, E.M.L., Kaboth-Bahr, S., 2022. The climate and vegetation backdrop to hominin evolution in Africa. Philos. Trans. R. Soc. B Biol. Sci. 377, 20200483. https://doi.org/10.1098/rstb.2020.0483

Griffore, M.P., Shiel, A.E., Rutila, E.C., Hillman, A.L., Barreiro-Lostres, F., Valero-Garcés, B.L., Morellón, M., Abbott, M.B., 2023. Lead isotope fingerprinting techniques help identify and quantify 3000 years of atmospheric lead pollution from Laguna Roya, northwestern Iberia. Anthropocene 42, 100375. https://doi.org/10.1016/j.ancene.2023.100375

Grunert, P., Skinner, L., Hodell, D.A., Piller, W.E., 2015. A micropalaeontological perspective on export productivity, oxygenation and temperature in NE Atlantic deep-waters across Terminations I and II. Glob. Planet. Change 131, 174–191. https://doi.org/10.1016/j.gloplacha.2015.06.002

Harrison, S.P., Bartlein, P., 2012. Chapter 14 - Records from the Past, Lessons for the Future: What the Palaeorecord Implies about Mechanisms of Global Change, in: Henderson-Sellers, A., McGuffie, K.B.T.-T.F. of the W.C. (Second E., Henderson-Sellers, A., McGuffie, K.B.T.-T.F. of the W.C. (Second E. (Eds.), . Boston, pp. 403–436.

Hernández, A., Cachão, M., Sousa, P., Trigo, R.M., Luterbacher, J., Vaquero, J.M., Freitas, M.C., 2021. External forcing mechanisms controlling the North Atlantic coastal upwelling regime during the mid-Holocene. Geology 49, 433–437. https://doi.org/10.1130/G48112.1

Hernández, A., Cachão, M., Sousa, P., Trigo, R.M., Luterbacher, J., Vaquero, J.M., Freitas, M.C., 2020a. External forcing mechanisms controlling the North Atlantic coastal upwelling regime during the mid-Holocene. Geology 49, 433–437. https://doi.org/10.1130/G48112.1

Hernández, A., Sáez, A., Santos, R.N., Rodrigues, T., Martin-Puertas, C., Gil-Romera, G., Abbott, M., Carballeira, R., Costa, P., Giralt, S., Gomes, S.D., Griffore, M., Ibañez-Insa, J., Leira, M., Moreno, J., Naughton, F., Oliveira, D., Raposeiro, P.M., Trigo, R.M., Vieira, G., Ramos, A.M., 2023. The timing of the deglaciation in the Atlantic Iberian mountains: Insights from the stratigraphic analysis of a lake sequence in Serra da Estrela (Portugal). Earth Surf. Process. Landf. 48, 233–242. https://doi.org/10.1002/esp.5536

Hernández, A., Sánchez-López, G., Pla-Rabes, S., Comas-Bru, L., Parnell, A., Cahill, N., Geyer, A., Trigo, R.M., Giralt, S., 2020b. A 2,000-year Bayesian NAO reconstruction from the Iberian Peninsula. Sci. Rep. 10, 14961. https://doi.org/10.1038/s41598-020-71372-5

Hernández, A., Trigo, R.M., Pla-Rabes, S., Valero-Garcés, B.L., Jerez, S., Rico-Herrero, M., Vega, J.C., Jambrina-Enríquez, M., Giralt, S., 2015. Sensitivity of two Iberian lakes to North Atlantic atmospheric circulation modes. Clim. Dyn. 45, 3403–3417. https://doi.org/10.1007/s00382-015-2547-8

Hillman, A.L., Abbott, M.B., Valero-Garcés, B.L., Morellon, M., Barreiro-Lostres, F., Bain, D.J., 2017. Lead pollution resulting from Roman gold extraction in northwestern Spain. The Holocene 27, 1465–1474. https://doi.org/10.1177/0959683617693903

Hodell, D.A., 2016. The smoking gun of the ice ages. Science 354, 1235–1236. https://doi.org/10.1126/science.aal4111

Hodell, D.A., Nicholl, J.A., Bontognali, T.R.R., Danino, S., Dorador, J., Dowdeswell, J.A., Einsle, J., Kuhlmann, H., Martrat, B., Mleneck-Vautravers, M.J., Rodríguez-Tovar, F.J., Röhl, U., 2017. Anatomy of Heinrich Layer 1 and its role in the last deglaciation. Paleoceanography 32, 284–303. https://doi.org/10.1002/2016PA003028

Hopcroft, P.O., Valdes, P.J., Shuman, B.N., Toohey, M., Sigl, M., 2023. Relative importance of forcings and feedbacks in the Holocene temperature conundrum. Quat. Sci. Rev. 319, 108322. https://doi.org/10.1016/j.quascirev.2023.108322

Hu, H.M., Trouet, V., Spötl, C., Tsai, H.C., Chien, W.Y., Sung, W.H., Michel, V., Yu, J.Y., Valensi, P., Jiang, X., Duan, F., Wang, Y., Mii, H.S., Chou, Y.M., Lone, M.A., Wu, C.C., Starnini, E., Zunino, M., Watanabe, T.K., Watanabe, T., Hsu, H.H., Moore, G.W.K., Zanchetta, G., Pérez-Mejías, C., Lee, S.Y., Shen, C.C., 2022. Tracking westerly wind directions over Europe since the middle Holocene. Nat. Commun. 13. https://doi.org/10.1038/s41467-022-34952-9

Ilvonen, L., López-Sáez, J.A., Holmström, L., Alba-Sánchez, F., Pérez-Díaz, S., Carrión, J.S., Ramos-Román, M.J., Camuera, J., Jiménez-Moreno, G., Ruha, L., Seppä, H., 2022. Spatial and temporal patterns of Holocene precipitation change in the Iberian Peninsula. Boreas 51, 776–792. https://doi.org/10.1111/bor.12586

IPCC, 2023. Climate Change 2023: Synthesis Report. Contribution of Working Groups I, II and III to the Sixth Assessment Report of the Intergovernmental Panel on Climate Change. Geneva.

IPCC, 2022. Climate Change 2022: Impacts, Adaptation and Vulnerability, Summary for Policymakers. Cambridge, UK and New York, USA.

Jambrina-Enríquez, M., Rico, M., Moreno, A., Leira, M., Bernárdez, P., Prego, R., Recio, C., Valero-Garcés, B.L., 2014. Timing of deglaciation and postglacial environmental dynamics in NW Iberia: the Sanabria Lake record. Quat. Sci. Rev. 94, 136–158. https://doi.org/10.1016/j.quascirev.2014.04.018

Jiménez-Amat, P., Zahn, R., 2015. Offset timing of climate oscillations during the last two glacial-interglacial transitions connected with large-scale freshwater perturbation. Paleoceanography 30, 768–788. https://doi.org/10.1002/2014PA002710

Jiménez-Espejo, F.J., García-Alix, A., Jiménez-Moreno, G., Rodrigo-Gámiz, M., Anderson, R.S., Rodríguez-Tovar, F.J., Martínez-Ruiz, F., Giralt, S., Delgado Huertas, A., Pardo-Igúzquiza, E., 2014. Saharan aeolian input and effective humidity variations over western Europe during the Holocene from a high altitude record. Chem. Geol. 374–375, 1–12. https://doi.org/10.1016/j.chemgeo.2014.03.001

Jiménez-Moreno, G., García-Alix, A., Anderson, R.S., Ramos-Román, M.J., Camuera, J., Mesa-Fernández, J.M., Toney, J.L., Jiménez-Espejo, F.J., Carrión, J.S., López-Avilés, A., Rodrigo-Gámiz, M., Webster,

C.E., 2022. Reconstruction of Past Environment and Climate Using Wetland Sediment Records from the Sierra Nevada - The Landscape of the Sierra Nevada: A Unique Laboratory of Global Processes in Spain, in: Zamora, R., Oliva, M., Zamora, R., Oliva, M. (Eds.), Cham, pp. 95–114.

Jiménez-Moreno, G., García-Alix, A., Hernández-Corbalán, M.D., Anderson, R.S., Delgado-Huertas, A., 2013. Vegetation, fire, climate and human disturbance history in the southwestern Mediterranean area during the late Holocene. Quat. Res. U. S. 79, 110–122. https://doi.org/10.1016/j.yqres.2012.11.008

Jiménez-Moreno, G., Heiri, O., García-Alix, A., Anderson, R.S., Jiménez-Espejo, F.J., López-Blanco, C., Jiménez, L., Pérez-Martínez, C., Rodrigo-Gámiz, M., López-Avilés, A., Camuera, J., 2023a. Holocene summer temperature reconstruction based on a chironomid record from Sierra Nevada, southern Spain. Quat. Sci. Rev. 319, 108343. https://doi.org/10.1016/j.quascirev.2023.108343

Jiménez-Moreno, G., López-Avilés, A., García-Alix, A., Ramos-Román, M.J., Camuera, J., Mesa-Fernández, J.M., Jiménez-Espejo, F.J., López-Blanco, C., Carrión, J.S., Anderson, R.S., 2023b. Laguna Seca sediments reveal environmental and climate change during the latest Pleistocene and Holocene in Sierra Nevada, southern Iberian Peninsula. Palaeogeogr. Palaeoclimatol. Palaeoecol. 631, 111834. https://doi.org/10.1016/j.palaeo.2023.111834

Jungclaus, J.H., Bard, E., Baroni, M., Braconnot, P., Cao, J., Chini, L.P., Egorova, T., Evans, M., González-Rouco, J.F., Goosse, H., Hurtt, G.C., Joos, F., Kaplan, J.O., Khodri, M., Klein Goldewijk, K., Krivova, N., LeGrande, A.N., Lorenz, S.J., Luterbacher, J., Man, W., Maycock, A.C., Meinshausen, M., Moberg, A., Muscheler, R., Nehrbass-Ahles, C., Otto-Bliesner, B.I., Phipps, S.J., Pongratz, J., Rozanov, E., Schmidt, G.A., Schmidt, H., Schmutz, W., Schurer, A., Shapiro, A.I., Sigl, M., Smerdon, J.E., Solanki, S.K., Timmreck, C., Toohey, M., Usoskin, I.G., Wagner, S., Wu, C.-J., Yeo, K.L., Zanchettin, D., Zhang, Q., Zorita, E., 2017. The PMIP4 contribution to CMIP6 – Part 3: The last millennium, scientific objective, and experimental design for the PMIP4 past1000 simulations. Geosci. Model Dev. 10, 4005–4033. https://doi.org/10.5194/gmd-10-4005-2017

Kaufman, D., McKay, N., Routson, C., Erb, M., Dätwyler, C., Sommer, P.S., Heiri, O., Davis, B., 2020. Holocene global mean surface temperature, a multi-method reconstruction approach. Sci. Data 7, 201. https://doi.org/10.1038/s41597-020-0530-7

Krklec, K., Domínguez-Villar, D., 2014. Quantification of the impact of moisture source regions on the oxygen isotope composition of precipitation over Eagle Cave, central Spain. Geochim. Cosmochim. Acta 134, 39–54. https://doi.org/10.1016/j.gca.2014.03.011

Lambeck, K., Rouby, H., Purcell, A., Sun, Y., Sambridge, M., 2014. Sea level and global ice volumes from the Last Glacial Maximum to the Holocene. Proc. Natl. Acad. Sci. U. S. A. 111, 15296–15303. https://doi.org/10.1073/pnas.1411762111

Lambeck, K., Yokoyama, Y., Purcell, T., 2002. Into and out of the Last Glacial Maximum: sea-level change during Oxygen Isotope Stages 3 and 2. Quat. Sci. Rev. 21, 343–360. https://doi.org/10.1016/S0277-3791(01)00071-3

Lear, C.H., Anand, P., Blenkinsop, T., Foster, G.L., Gagen, M., Hoogakker, B., Larter, R.D., Lunt, D.J., McCave, I.N., McClymont, E., Pancost, R.D., Rickaby, R.E.M., Schultz, D.M., Summerhayes, C., Williams, C.J.R., Zalasiewicz, J., 2021. Geological Society of London Scientific Statement: what the geological record tells us about our present and future climate. J. Geol. Soc. 178, jgs2020-239. https://doi.org/10.1144/jgs2020-239

Lebreiro, S.M., Antón, L., Reguera, M.I., Marzocchi, A., 2018. Paleoceanographic and climatic implications of a new Mediterranean Outflow branch in the southern Gulf of Cadiz. Quat. Sci. Rev. 197, 92–111. https://doi.org/10.1016/J.QUASCIREV.2018.07.036

Lenton, T.M., Rockström, J., Gaffney, O., Rahmstorf, S., Richardson, K., Steffen, W., Schellnhuber, H.J., 2019. Climate tipping points — too risky to bet against. Nature 575, 592–595.

Leunda, M., Gil-Romera, G., Daniau, A.-L., Benito, B.M., González-Sampériz, P., 2020. Holocene fire and vegetation dynamics in the Central Pyrenees (Spain). CATENA 188, 104411. https://doi.org/10.1016/j.catena.2019.104411

Leunda, M., González-Sampériz, P., Gil-Romera, G., Bartolomé, M., Belmonte-Ribas, Á., Gómez-García, D., Kaltenrieder, P., Rubiales, J.M., Schwörer, C., Tinner, W., Morales-Molino, C., Sancho, C., 2019. Ice cave reveals environmental forcing of long-term Pyrenean tree line dynamics. J. Ecol. 107, 814–828. https://doi.org/10.1111/1365-2745.13077

Lillios, K.T., Blanco-González, A., Drake, B.L., López-Sáez, J.A., 2016. Mid-late Holocene climate, demography, and cultural dynamics in Iberia: A multi-proxy approach. Quat. Sci. Rev. 135, 138–153. https://doi.org/10.1016/j.quascirev.2016.01.011

Liu, M., Shen, Y., González-Sampériz, P., Gil-Romera, G., Ter Braak, C.J.F., Prentice, I.C., Harrison, S.P., 2023. Holocene climates of the Iberian Peninsula: pollen-based reconstructions of changes in the west-east gradient of temperature and moisture. Clim. Past 19, 803–834. https://doi.org/10.5194/cp-19-803-2023

López-Avilés, A., Jiménez-Moreno, G., García-Alix, A., García-García, F., Camuera, J., Scott Anderson, R., Sanjurjo-Sánchez, J., Arce Chamorro, C., Carrión, J.S., 2022. Post-glacial evolution of alpine environments in the western Mediterranean region: The Laguna Seca record. CATENA 211, 106033. https://doi.org/10.1016/j.catena.2022.106033

López-Belzunce, M., Blázquez, A.M., Sánchez-Palencia, Y., Torres, T., Ortiz, J.E., 2022. Environmental evidence of Valencia lagoon coastal barrier stabilization from 8500 BP to Present. Climate and eustatic variations. Sci. Total Environ. 807, 151230. https://doi.org/10.1016/j.scitotenv.2021.151230

López-Blanco, C., Romero-Viana, L., 2019. Dry and wet periods over the last millennium in central-eastern Spain a paleolimnological perspective. Limnetica 38. https://doi.org/10.23818/limn.38.03

López-Martínez, C., Grimalt, J.O., Hoogakker, B., Gruetzner, J., Vautravers, M.J., McCave, I.N., 2006. Abrupt wind regime changes in the North Atlantic Ocean during the past 30,000–60,000 years. Paleoceanography 21. https://doi.org/10.1029/2006PA001275

López-Sáez, J.A., Abel Schaad, D., Iriarte Avilés, E., Alba-Sánchez, F., Pérez Díaz, S., Guerra Doce, E., Delibes de Castro, G., Abarquero Moras, F.J., 2017. Una perspectiva paleoambiental de la explotación de la sal en las Lagunas de Villafáfila (Tierra de Campos, Zamora). Cuaternario Geomorfol. Rev. Soc. Esp. Geomorfol. Asoc. Esp. Para El Estud. Cuaternario 31, 73–103.

López-Sáez, J.A., Abel-Schaad, D., Pérez-Díaz, S., Blanco-González, A., Alba-Sánchez, F., Dorado, M., Ruiz-Zapata, B., Gil-García, M.J., Gómez-González, C., Franco-Múgica, F., 2014a. Vegetation history, climate and human impact in the Spanish Central System over the last 9000 years. Quat. Int. 353, 98–122.

López-Sáez, J.A., Alba-Sánchez, F., Nájera, T., Molina González, F.R., Pérez Díaz, S., Sabariego Ruiz, S., 2014b. Paleoambiente y Ssciedad en la Edad del Bronce de La Mancha: La Motilla del Azuer. Cuad. Prehist. Arqueol. Univ. Granada 391–422.

López-Sáez, J.A., Carrasco, R.M., Turu, V., Ruiz-Zapata, B., Gil-García, M.J., Luelmo-Lautenschlaeger, R., Pérez-Díaz, S., Alba-Sánchez, F., Abel-Schaad, D., Ros, X., Pedraza, J., 2020. Late Glacial-early holocene vegetation and environmental changes in the western Iberian Central System inferred from a key site: The Navamuño record, Béjar range (Spain). Quat. Sci. Rev. 230, 106167. https://doi.org/10.1016/j.quascirev.2020.106167

Ludwig, P., Gómez-Navarro, J.J., Pinto, J.G., Raible, C.C., Wagner, S., Zorita, E., 2019. Perspectives of regional paleoclimate modeling. Ann. N. Y. Acad. Sci. 1436, 54–69. https://doi.org/10.1111/nyas.13865

Luelmo Lautenschlaeger, M. de los R., Izdebski, A., Blanco González, A., Pérez Díaz, S., López Sáez, J.A., 2021a. La peste negra bajomedieval (1348-1351 AD) en el valle del Tiétar (sierra de Gredos, Ávila): aspectos económicos y paleoambientales. Bol. Asoc. Geógrafos Esp.

Luelmo Lautenschlaeger, M. de los R., Izdebski, A., Blanco González, A., Pérez Díaz, S., López Sáez, J.A., 2021b. Historia paleoambiental de la sierra de Gredos (Sistema Central español, Ávila) en época visigoda: incidencia de la plaga de Justiniano (541-543 a. D.). Arqueol. Iberoam. 13, 78–90.

Luelmo-Lautenschlaeger, R., Blarquez, O., Pérez-Díaz, S., Morales-Molino, C., López-Sáez, J.A., 2019. The Iberian Peninsula's Burning Heart—Long-Term Fire History in the Toledo Mountains (Central Spain). Fire 2. https://doi.org/10.3390/fire2040054

Luetscher, M., Boch, R., Sodemann, H., Spötl, C., Cheng, H., Edwards, R.L., Frisia, S., Hof, F., Müller, W., 2015. North Atlantic storm track changes during the Last Glacial Maximum recorded by Alpine speleothems. Nat. Commun. 6. https://doi.org/10.1038/ncomms7344

Machado, M.J., Benito, G., Barriendos, M., Rodrigo, F.S., 2011. 500 Years of rainfall variability and extreme hydrological events in southeastern Spain drylands. J. Arid Environ. 75, 1244–1253. https://doi.org/10.1016/j.jaridenv.2011.02.002

Maiorano, P., Flores, J.A., Marino, M., Ducassou, E., Trotta, S., Balestra, B., 2023. Surface water dynamics of the last 20 kyr documented by coccolithophores in the Gulf of Cadiz. Palaeogeogr. Palaeoclimatol. Palaeoecol. 617, 111498–111498. https://doi.org/10.1016/J.PALAEO.2023.111498

Manzano, S., Carrión, J.S., López-Merino, L., Jiménez-Moreno, G., Toney, J.L., Amstrong, H., Anderson, R.S., García-Alix, A., Pérez, J.L.G., Sánchez-Mata, D., 2019. A palaeoecological approach to understanding the past and present of Sierra Nevada, a Southwestern European biodiversity hotspot. Glob. Planet. Change 175, 238–250. https://doi.org/10.1016/j.gloplacha.2019.02.006

Marco-Barba, J., Holmes, J.A., Mesquita-Joanes, F., Miracle, M.R., 2013. The influence of climate and sea-level change on the Holocene evolution of a Mediterranean coastal lagoon: Evidence from ostracod palaeoecology and geochemistry. Geobios 46, 409–421. https://doi.org/10.1016/j.geobios.2013.05.003

Margari, V., Hodell, D.A., Parfitt, S.A., Ashton, N.M., Grimalt, J.O., Kim, H., Yun, K.-S., Gibbard, P.L., Stringer, C.B., Timmermann, A., Tzedakis, P.C., 2023. Extreme glacial cooling likely led to hominin depopulation of Europe in the Early Pleistocene. Science 381, 693–699. https://doi.org/10.1126/science.adf4445

Marsicek, J., Shuman, B.N., Bartlein, P.J., Shafer, S.L., Brewer, S., 2018. Reconciling divergent trends and millennial variations in Holocene temperatures. Nature 554, 92–96. https://doi.org/10.1038/nature25464

Martín-Chivelet, J., Muñoz-García, M.B., Edwards, R.L., Turrero, M.J., Ortega, A.I., 2011. Land surface temperature changes in Northern Iberia since 4000 yr BP, based on d13C of speleothems. Glob. Planet. Change 77, 1–12.

Martín-Chivelet, J., Muñoz-García, M.B., Edwards, R.L., Turrero, M.J., Ortega, A.I., 2013. Reply to Comment by Domínguez-Villar on "Land surface temperature changes in Northern Iberia since 4000 yr BP, based in δ13C of speleothems" (Martín-Chivelet et al., 2011). Glob. Planet. Change 101, 129–130. https://doi.org/10.1016/j.gloplacha.2012.12.005

Martínez Cortizas, A., López-Merino, L., Bindler, R., Mighall, T., Kylander, M.E., 2016. Early atmospheric metal pollution provides evidence for Chalcolithic/Bronze Age mining and metallurgy in Southwestern Europe. Sci. Total Environ. 545–546, 398–406. https://doi.org/10.1016/j.scitotenv.2015.12.078

Martínez-García, B., Rodríguez-Lázaro, J., Pascual, A., Mendicoa, J., 2015. The "Northern guests" and other palaeoclimatic ostracod proxies in the late Quaternary of the Basque Basin (S Bay of Biscay). Palaeogeogr. Palaeoclimatol. Palaeoecol. 419, 100–114. https://doi.org/10.1016/J.PALAEO.2014.06.032

Martinez-Ruiz, F., Kastner, M., Gallego-Torres, D., Rodrigo-Gámiz, M., Nieto-Moreno, V., and Ortega-Huertas, M. 2015. Paleoclimate and paleoceanography over the past 20,000 yr in the Mediterranean Sea Basins as indicated by sediment elemental proxies, Quat. Sci. Rev., 107, 25–46, https://doi.org/10.1016/j.quascirev.2014.09.018.

Martin-Puertas, C., Hernandez, A., Pardo-Igúzquiza, E., Boyall, L., Brierley, C., Jiang, Z., Tjallingii, R., Blockley, S.P.E., Rodríguez-Tovar, F.J., 2023. Dampened predictable decadal North Atlantic climate fluctuations due to ice melting. Nat. Geosci. 16, 357–362. https://doi.org/10.1038/s41561-023-01145-y

Martín-Puertas, C., Jiménez-Espejo, F., Martínez-Ruiz, F., Nieto-Moreno, V., Rodrigo, M., Mata, M.P., Valero-Garcés, B.L., 2010. Late Holocene climate variability in the southwestern Mediterranean region: an integrated marine and terrestrial geochemical approach. Clim. Past 6, 807–816. https://doi.org/10.5194/cp-6-807-2010

Martín-Puertas, C., Valero-Garcés, B.L., Mata, M.P., Moreno, A., Giralt, S., Martínez-Ruiz, F., Jiménez-Espejo, F., 2011. Geochemical processes in a Mediterranean Lake: a high-resolution study of the last 4,000 years in Zoñar Lake, southern Spain. J. Paleolimnol. 46, 405–421. https://doi.org/10.1007/s10933-009-9373-0

Martín-Puertas, C., Valero-Garcés, B.L., Pilar Mata, M., González-Sampériz, P., Bao, R., Moreno, A., Stefanova, V., 2008. Arid and humid phases in southern Spain during the last 4000 years: the Zoñar Lake record, Córdoba. The Holocene 18, 907–921. https://doi.org/10.1177/0959683608093533

Martins, M.V.A., Perretti, A.R., Salgueiro, E., Frontalini, F., Moreno, J., Soares, A.M., Mahiques, M., Silva, S., de Azevedo, C.A., Dias, J.A., 2015. Atlantic sea surface temperatures estimated from planktonic foraminifera off the Iberian Margin over the last 40Ka BP. Mar. Geol. 367, 191–201. https://doi.org/10.1016/j.margeo.2015.06.001

Martrat, B., Jimenez-Amat, P., Zahn, R., Grimalt, J.O., 2014. Similarities and dissimilarities between the last two deglaciations and interglaciations in the North Atlantic region. Quat. Sci. Rev. 99, 122–134. https://doi.org/10.1016/j.quascirev.2014.06.016

Mejías Moreno, M., Benítez de Lugo Enrich, L., López Sáez, J.A., Lillios, K.T., 2020. La Cultura de Las Motillas de La Mancha: testigos del evento climático 4.2 ka cal BP. Bol. Geológico Min. 131, 89–108.

Mellado-Cano, J., Barriopedro, D., García-Herrera, R., Trigo, R.M., Hernández, A., 2019. Examining the North Atlantic Oscillation, East Atlantic Pattern, and Jet Variability since 1685. J. Clim. 32, 6285–6298. https://doi.org/10.1175/JCLI-D-19-0135.1

Mesa-Fernández, J.M., Jiménez-Moreno, G., Rodrigo-Gámiz, M., García-Alix, A., Jiménez-Espejo, F.J., Martínez-Ruiz, F., Anderson, R.S., Camuera, J., Ramos-Román, M.J., 2018. Vegetation and geochemical responses to Holocene rapid climate change in the Sierra Nevada (southeastern Iberia): the Laguna Hondera record. Clim. Past 14, 1687–1706. https://doi.org/10.5194/cp-14-1687-2018

Mesa-Fernández, J.M., Martínez-Ruiz, F., Rodrigo-Gámiz, M., Jiménez-Espejo, F.J., García, M., Sierro, F.J., 2022. Paleocirculation and paleoclimate conditions in the western Mediterranean basins over the last deglaciation: New insights from sediment composition variations. Glob. Planet. Change 209. https://doi.org/10.1016/j.gloplacha.2021.103732

Mighall, T.M., Martínez Cortizas, A., Silva-Sánchez, N., López-Costas, O., López-Merino, L., 2023. Climate Change, Fire and Human Activity Drive Vegetation Change during the Last Eight Millennia in the Xistral Mountains of NW Iberia. Quaternary 6. https://doi.org/10.3390/quat6010005

Moffa-Sánchez, P., Born, A., Hall, I.R., Thornalley, D.J.R., Barker, S., 2014. Solar forcing of North Atlantic surface temperature and salinity over the past millennium. Nat. Geosci. 7, 275–278. https://doi.org/10.1038/ngeo2094

Montes, L., Domingo, R., González-Sampériz, P., Sebastián, M., Aranbarri, J., Castaños, P., García-Simón, L.M., Alcolea, M., Laborda, R., 2016. Landscape, resources and people during the Mesolithic and Neolithic times in NE Iberia: The Arba de Biel Basin. Quat. Int. 403, 133–150. https://doi.org/10.1016/j.quaint.2015.05.041

Montoya, M., Levermann, A., 2008. Surface wind-stress threshold for glacial Atlantic overturning. Geophys. Res. Lett. 35. https://doi.org/10.1029/2007GL032560

Morales-Molino, C., Colombaroli, D., Tinner, W., Perea, R., Valbuena-Carabaña, M., Carrión, J.S., Gil, L., 2018. Vegetation and fire dynamics during the last 4000years in the Cabañeros National Park (central Spain). Rev. Palaeobot. Palynol. 253, 110–122. https://doi.org/10.1016/j.revpalbo.2018.04.001

Morales-Molino, C., García-Antón, M., 2014. Vegetation and fire history since the last glacial maximum in an inland area of the western Mediterranean Basin (Northern Iberian Plateau, NW Spain). Quat. Res. 81, 63–77. https://doi.org/10.1016/j.yqres.2013.10.010

Morcillo-Montalbá, L., Rodrigo-Gámiz, M., Martínez-Ruiz, F., Ortega-Huertas, M., Schouten, S., Sinninghe Damsté, J.S., 2021. Rapid Climate Changes in the Westernmost Mediterranean (Alboran Sea) Over the Last 35 kyr: New Insights From Four Lipid Paleothermometers (UK'37, TEXH86, RI-OH', and LDI). Paleoceanogr. Paleoclimatology 36. https://doi.org/10.1029/2020PA004171

Morellón, M., Aranbarri, J., Moreno, A., González-Sampériz, P., Valero-Garcés, B.L., 2018. Early Holocene humidity patterns in the Iberian Peninsula reconstructed from lake, pollen and speleothem records. Quat. Sci. Rev. 181, 1–18. https://doi.org/10.1016/j.quascirev.2017.11.016

Morellón, M., Pérez-Sanz, A., Corella, J.P., Büntgen, U., Catalán, J., González-Sampériz, P., González-Trueba, J.J., López-Sáez, J.A., Moreno, A., Pla-Rabes, S., Saz-Sánchez, M.A., Scussolini, P., Serrano, E., Steinhilber, F., Stefanova, V., Vegas-Vilarrúbia, T., Valero-Garcés, B., 2012. A multi-proxy perspective on millennium-long climate variability in the Southern Pyrenees. Clim. Past 8, 683–700. https://doi.org/10.5194/cp-8-683-2012

Morellón, M., Valero-Garcés, B., Anselmetti, F., Ariztegui, D., Schnellmann, M., Moreno, A., Mata, P., Rico, M., Corella, J.P., 2009a. Late Quaternary deposition and facies model for karstic Lake Estanya (North-eastern Spain). Sedimentology 56, 1505–1534. https://doi.org/10.1111/j.1365-3091.2008.01044.x

Morellón, M., Valero-Garcés, B., González-Sampériz, P., Vegas-Vilarrúbia, T., Rubio, E., Rieradevall, M., Delgado-Huertas, A., Mata, P., Romero, Ó., Engstrom, D.R., López-Vicente, M., Navas, A., Soto, J., 2011. Climate changes and human activities recorded in the sediments of Lake Estanya (NE Spain) during the Medieval Warm Period and Little Ice Age. J. Paleolimnol. 46, 423–452. https://doi.org/10.1007/s10933-009-9346-3

Morellón, M., Valero-Garcés, B., Vegas-Vilarrúbia, T., González-Sampériz, P., Romero, Ó., Delgado-Huertas, A., Mata, P., Moreno, A., Rico, M., Corella, J.P., 2009b. Lateglacial and Holocene palaeohydrology in the western Mediterranean region: The Lake Estanya record (NE Spain). Quat. Sci. Rev. 28, 2582–2599. https://doi.org/10.1016/j.quascirev.2009.05.014

Moreno, A., González-Sampériz, P., Morellón, M., Valero-Garcés, B.L., Fletcher, W.J., 2012a. Northern Iberian abrupt climate change dynamics during the last glacial cycle: A view from lacustrine sediments. Quat. Sci. Rev. 36, 139–153. https://doi.org/10.1016/j.quascirev.2010.06.031

Moreno, A., López-Merino, L., Leira, M., Marco-Barba, J., González-Sampériz, P., Valero-Garcés, B.L., López-Sáez, J.A., Santos, L., Mata, P., Ito, E., 2011. Revealing the last 13,500 years of environmental history from the multiproxy record of a mountain lake (Lago Enol, northern Iberian Peninsula). J. Paleolimnol. 46, 327–349. https://doi.org/10.1007/s10933-009-9387-7

Moreno, A., Pérez, A., Frigola, J., Nieto-Moreno, V., Rodrigo-Gámiz, M., Martrat, B., González-Sampériz, P., Morellón, M., Martín-Puertas, C., Corella, J.P., Belmonte, Á., Sancho, C., Cacho, I., Herrera, G., Canals, M., Grimalt, J.O., Jiménez-Espejo, F., Martínez-Ruiz, F., Vegas-Vilarrúbia, T., Valero-Garcés, B.L., 2012b. The Medieval Climate Anomaly in the Iberian Peninsula reconstructed from marine and lake records. Quat. Sci. Rev. 43, 16–32. https://doi.org/10.1016/j.quascirev.2012.04.007

Moreno, A., Pérez-Mejías, C., Bartolomé, M., Sancho, C., Cacho, I., Stoll, H., Delgado-Huertas, A., Hellstrom, J., Edwards, R.L., Cheng, H., 2017. New speleothem data from molinos and ejulve caves reveal holocene hydrological variability in northeast iberia. Quat. Res. U. S. 88, 223–233. https://doi.org/10.1017/qua.2017.39

Moreno, A., Stoll, H., Jiménez-Sánchez, M., Cacho, I., Valero-Garcés, B., Ito, E., Edwards, R.L., 2010. A speleothem record of glacial (25–11.6 kyr BP) rapid climatic changes from northern Iberian Peninsula. Glob. Planet. Change, Oxygen isotopes as tracers of Mediterranean variability: linking past, present and future 71, 218–231. https://doi.org/10.1016/j.gloplacha.2009.10.002

Moreno, J., Ramos, A.M., Raposeiro, P.M., Santos, R.N., Rodrigues, T., Naughton, F., Moreno, F., Trigo, R.M., Ibañez-Insa, J., Ludwig, P., Shi, X., Hernández, A., 2023. Identifying imprints of externally derived dust and halogens in the sedimentary record of an Iberian alpine lake for the past ~13,500 years – Lake Peixão, Serra da Estrela (Central Portugal). Sci. Total Environ. 903. https://doi.org/10.1016/j.scitotenv.2023.166179

Muñoz Sobrino, C., García-Gil, S., Iglesias, J., Martínez Carreño, N., Ferreiro Da Costa, J., Díaz Varela, R.A., Judd, A., 2012. Environmental change in the Ría de Vigo, NW Iberia, since the mid-Holocene: new palaeoecological and seismic evidence. Boreas 41, 578–601. https://doi.org/10.1111/j.1502-3885.2012.00255.x

Muñoz Sobrino, C., García-Moreiras, I., Castro, Y., Martínez Carreño, N., de Blas, E., Fernandez Rodríguez, C., Judd, A., García-Gil, S., 2014. Climate and anthropogenic factors influencing an estuarine ecosystem from NW Iberia: new high resolution multiproxy analyses from San Simón Bay (Ría de Vigo). Quat. Sci. Rev. 93, 11–33. https://doi.org/10.1016/j.quascirev.2014.03.021

Muñoz Sobrino, C., Heiri, O., Hazekamp, M., van der Velden, D., Kirilova, E.P., García-Moreiras, I., Lotter, A.F., 2013. New data on the Lateglacial period of SW Europe: a high resolution multiproxy record from Laguna de la Roya (NW Iberia). Quat. Sci. Rev. 80, 58–77. https://doi.org/10.1016/j.quascirev.2013.08.016

Naito, Y.I., Belmaker, M., Jiménez-Espejo, F.J., Simón-Vallejo, M.D., Riquelme Cantal, J.A., Parrilla-Giráldez, R., Cortés-Sánchez, M., 2022. Evidence for Marine Consumption During the Upper Palaeolithic at "El Pirulejo" Inland Rock- Shelter (Southern Iberia Peninsula, Spain). Open Quat. https://doi.org/10.5334/oq.109

Naughton, F., Costas, S., Gomes, S.D., Desprat, S., Rodrigues, T., Sanchez Goñi, M.F., Renssen, H., Trigo, R., Bronk-Ramsey, C., Oliveira, D., Salgueiro, E., Voelker, A.H.L., Abrantes, F., 2019. Coupled ocean and atmospheric changes during Greenland stadial 1 in southwestern Europe. Quat. Sci. Rev. 212, 108–120. https://doi.org/10.1016/j.quascirev.2019.03.033

Naughton, F., Sanchez Goñi, M.F., Rodrigues, T., Salgueiro, E., Costas, S., Desprat, S., Duprat, J., Michel, E., Rossignol, L., Zaragosi, S., Voelker, A.H.L., Abrantes, F., 2016. Climate variability across the last deglaciation in NW Iberia and its margin. Quat. Int. 414, 9–22. https://doi.org/10.1016/j.quaint.2015.08.073

Nieto-Moreno, V., Martínez-Ruiz, F., Giralt, S., Jiménez-Espejo, F., Gallego-Torres, D., Rodrigo-Gámiz, M., García-Orellana, J., Ortega-Huertas, M., De Lange, G.J., 2011. Tracking climate variability in the western Mediterranean during the Late Holocene: A multiproxy approach. Clim. Past 7, 1395–1414. https://doi.org/10.5194/cp-7-1395-2011

Oliva, M., Palacios, D., Fernández-Fernández, J.M., Rodríguez-Rodríguez, L., García-Ruiz, J.M., Andrés, N., Carrasco, R.M., Pedraza, J., Pérez-Alberti, A., Valcárcel, M., Hughes, P.D., 2019. Late Quaternary glacial phases in the Iberian Peninsula. Earth-Sci. Rev. 192, 564–600. https://doi.org/10.1016/j.earscirev.2019.03.015

Oliva, M., Ruiz-Fernández, J., Barriendos, M., Benito, G., Cuadrat, J.M., Domínguez-Castro, F., García-Ruiz, J.M., Giralt, S., Gómez-Ortiz, A., Hernández, A., López-Costas, O., López-Moreno, J.I., López-Sáez, J.A., Martínez-Cortizas, A., Moreno, A., Prohom, M., Saz, M.A., Serrano, E., Tejedor, E., Trigo, R., Valero-Garcés, B., Vicente-Serrano, S.M., 2018. The Little Ice Age in Iberian mountains. Earth-Sci. Rev. 177, 175–208. https://doi.org/10.1016/j.earscirev.2017.11.010

Ortega, P., Lehner, F., Swingedouw, D., Masson-Delmotte, V., Raible, C.C., Casado, M., Yiou, P., 2015. A model-tested North Atlantic Oscillation reconstruction for the past millennium. Nature 523, 71–74. https://doi.org/10.1038/nature14518

Ortiz, J.E., Gallego, J.L.R., Torres, T., Díaz-Bautista, A., Sierra, C., 2010. Palaeoenvironmental reconstruction of Northern Spain during the last 8000 cal yr BP based on the biomarker content of the Roñanzas peat bog (Asturias). Org. Geochem. 41, 454–466. https://doi.org/10.1016/j.orggeochem.2010.02.003

Ortiz, J.E., Sánchez-Palencia, Y., López-Cilla, I., Morales-Molino, C., Gardoki, J., Torres, T., Morellón, M., 2024. Lipid biomarkers in high mountain lakes from the Cantabrian range (Northern Spain): Coupling the interplay between natural and anthropogenic drivers. Anthropocene 46, 100431. https://doi.org/10.1016/j.ancene.2024.100431

Ortiz, J.E., Sánchez-Palencia, Y., Torres, T., Domingo, L., Mata, M.P., Vegas, J., Sánchez España, J., Morellón, M., Blanco, L., 2016. Lipid biomarkers in Lake Enol (Asturias, Northern Spain): Coupled natural and human induced environmental history. Org. Geochem. 92, 70–83. https://doi.org/10.1016/j.orggeochem.2015.12.005

Palumbo, E., Flores, J.A., Perugia, C., Emanuele, D., Petrillo, Z., Rodrigues, T., Voelker, A.H.L., Amore, F.O., 2013. Abrupt variability of the last 24ka BP recorded by coccolithophore assemblages off the Iberian Margin (core MD03-2699). J. Quat. Sci. 28, 320–328. https://doi.org/10.1002/jqs.2623

Paniagua, L.L., García-Martín, A., Moral, F.J., Rebollo, F.J., 2019. Aridity in the Iberian Peninsula (1960–2017): distribution, tendencies, and changes. Theor. Appl. Climatol. 138, 811–830. https://doi.org/10.1007/s00704-019-02866-0

Pascual, A., Rodríguez-Lázaro, J., Martínez-García, B., Varela, Z., 2020. Palaeoceanographic and palaeoclimatic changes during the last 37,000 years detected in the SE Bay of Biscay based on benthic foraminifera. Quat. Int. 566–567, 323–336. https://doi.org/10.1016/J.QUAINT.2020.03.043

Pellicer, X.M., Corella, J.P., Gutiérrez, F., Roqué, C., Linares, R., Carbonel, D., Zarroca, M., Guerrero, J., Comas, X., 2016. Sedimentological and palaeohydrological characterization of Late Pleistocene and Holocene tufa mound palaeolakes using trenching methods in the Spanish Pyrenees. Sedimentology 63, 1786–1819. https://doi.org/10.1111/sed.12290

Pena, L.D., Francés, G., Diz, P., Esparza, M., Grimalt, J.O., Nombela, M.A., Alejo, I., 2010. Climate fluctuations during the Holocene in NW Iberia: High and low latitude linkages. Cont. Shelf Res. 30, 1487–1496. https://doi.org/10.1016/j.csr.2010.05.009

Pérez Díaz, S., López-Sáez, J.A., 2019. The Western Pyrenean (Northern Iberian Peninsula) during the upper paleolithic: a palaeoenvironmental approach, in: Human Adaptations to the Last Glacial Maximum: The Solutrean and Its Neighbors. pp. 416–432.

Pérez-Asensio, J.N., Frigola, J., Pena, L.D., Sierro, F.J., Reguera, M.I., Rodríguez-Tovar, F.J., Dorador, J., Asioli, A., Kuhlmann, J., Huhn, K., Cacho, I., 2020a. Changes in western Mediterranean thermohaline circulation in association with a deglacial Organic Rich Layer formation in the Alboran Sea. Quat. Sci. Rev. 228. https://doi.org/10.1016/j.quascirev.2019.106075

Pérez-Asensio, J.N., Frigola, J., Pena, L.D., Sierro, F.J., Reguera, M.I., Rodríguez-Tovar, F.J., Dorador, J., Asioli, A., Kuhlmann, J., Huhn, K., Cacho, I., 2020b. Changes in western Mediterranean thermohaline

circulation in association with a deglacial Organic Rich Layer formation in the Alboran Sea. Quat. Sci. Rev. 228. https://doi.org/10.1016/j.quascirev.2019.106075

Pérez-Lambán, F., Peña-Monné, J.L., Badía-Villas, D., Picazo Millán, J.V., Sampietro-Vattuone, M.M., Alcolea Gracia, M., Aranbarri, J., González-Sampériz, P., Fanlo Loras, J., 2018. Holocene environmental variability in the Central Ebro Basin (NE Spain) from geoarchaeological and pedological records. CATENA 163, 147–164. https://doi.org/10.1016/j.catena.2017.12.017

Pérez-Obiol, R., Bal, M.-C., Pèlachs, A., Cunill, R., Soriano, J.M., 2012. Vegetation dynamics and anthropogenically forced changes in the Estanilles peat bog (southern Pyrenees) during the last seven millennia. Veg. Hist. Archaeobotany 21, 385–396. https://doi.org/10.1007/s00334-012-0351-5

Pérez-Obiol, R., Jalut, G., Julià, R., Pèlachs, A., Iriarte, M.J., Otto, T., Hernández-Beloqui, B., 2011. Mid-Holocene vegetation and climatic history of the Iberian Peninsula. The Holocene 21, 75–93. https://doi.org/10.1177/0959683610384161

Pérez-Sanz, A., González-Sampériz, P., Moreno, A., Valero-Garcés, B., Gil-Romera, G., Rieradevall, M., Tarrats, P., Lasheras-Álvarez, L., Morellón, M., Belmonte, A., Sancho, C., Sevilla-Callejo, M., Navas, A., 2013. Holocene climate variability, vegetation dynamics and fire regime in the central Pyrenees: the Basa de la Mora sequence (NE Spain). Quat. Sci. Rev. 73, 149–169. https://doi.org/10.1016/j.quascirev.2013.05.010

Plaza-Morlote, M., Rey, D., Santos, J.F., Ribeiro, S., Heslop, D., Bernabeu, A., Mohamed, K.J., Rubio, B., Martíns, V., 2017. Southernmost evidence of large European Ice Sheet-derived freshwater discharges during the Heinrich Stadials of the Last Glacial Period (Galician Interior Basin, Northwest Iberian Continental Margin). Earth Planet. Sci. Lett. 457, 213–226. https://doi.org/10.1016/j.epsl.2016.10.020

Ramos-Román, M.J., Jiménez-Moreno, G., Anderson, R.S., García-Alix, A., Camuera, J., Mesa-Fernández, J.M., Manzano, S., 2019. Climate controlled historic olive tree occurrences and olive oil production in southern Spain. Glob. Planet. Change 182. https://doi.org/10.1016/j.gloplacha.2019.102996

Ramos-Román, M.J., Jiménez-Moreno, G., Anderson, R.S., García-Alix, A., Toney, J.L., Jiménez-Espejo, F.J., Carrión, J.S., 2016. Centennial-scale vegetation and North Atlantic Oscillation changes during the Late Holocene in the southern Iberia. Quat. Sci. Rev. 143, 84–95. https://doi.org/10.1016/j.quascirev.2016.05.007

Ramos-Román, María J, Jiménez-Moreno, G., Camuera, J., García-Alix, A., Anderson, R.S., Jiménez-Espejo, F.J., Carrión, J.S., 2018. Holocene climate aridification trend and human impact interrupted by millennial- and centennial-scale climate fluctuations from a new sedimentary record from Padul (Sierra Nevada, southern Iberian Peninsula). Clim. Past 14, 117–137. https://doi.org/10.5194/cp-14-117-2018

Ramos-Román, María J., Jiménez-Moreno, G., Camuera, J., García-Alix, A., Scott Anderson, R., Jiménez-Espejo, F.J., Sachse, D., Toney, J.L., Carrión, J.S., Webster, C., Yanes, Y., 2018. Millennial-scale cyclical environment and climate variability during the Holocene in the western Mediterranean region deduced from a new multi-proxy analysis from the Padul record (Sierra Nevada, Spain). Glob. Planet. Change 168, 35–53. https://doi.org/10.1016/j.gloplacha.2018.06.003

Rasmussen, S.O., Bigler, M., Blockley, S.P., Blunier, T., Buchardt, S.L., Clausen, H.B., Cvijanovic, I., Dahl-Jensen, D., Johnsen, S.J., Fischer, H., Gkinis, V., Guillevic, M., Hoek, W.Z., Lowe, J.J., Pedro, J.B., Popp, T., Seierstad, I.K., Steffensen, J.P., Svensson, A.M., Vallelonga, P., Vinther, B.M., Walker,

M.J.C., Wheatley, J.J., Winstrup, M., 2014. A stratigraphic framework for abrupt climatic changes during the Last Glacial period based on three synchronized Greenland ice-core records: refining and extending the INTIMATE event stratigraphy. Quat. Sci. Rev., Dating, Synthesis, and Interpretation of Palaeoclimatic Records and Model-data Integration: Advances of the INTIMATE project(INTegration of Ice core, Marine and TErrestrial records, COST Action ES0907) 106, 14–28. https://doi.org/10.1016/j.quascirev.2014.09.007

Rea, B.R., Pellitero, R., Spagnolo, M., Hughes, P., Ivy-Ochs, S., Renssen, H., Ribolini, A., Bakke, J., Lukas, S., Braithwaite, R.J., 2020. Atmospheric circulation over Europe during the Younger Dryas, Sci. Adv.

Repschläger, J., Garbe-Schönberg, D., Weinelt, M., Schneider, R., 2017. Holocene evolution of the North Atlantic subsurface transport. Clim. Past 13, 333–344. https://doi.org/10.5194/cp-13-333-2017

Ribeiro, S., Amorim, A., Abrantes, F., Ellegaard, M., 2016. Environmental change in the Western Iberia Upwelling Ecosystem since the preindustrial period revealed by dinoflagellate cyst records. The Holocene 26, 874–889. https://doi.org/10.1177/0959683615622548

Ribeiro, S., Amorim, A., Andersen, T.J., Abrantes, F., Ellegaard, M., 2012. Reconstructing the history of an invasion: the toxic phytoplankton species Gymnodinium catenatum in the Northeast Atlantic. Biol. Invasions 14, 969–985. https://doi.org/10.1007/s10530-011-0132-6

Roberts, N., Moreno, A., Valero-Garcés, B.L., Corella, J.P., Jones, M., Allcock, S., Woodbridge, J., Morellón, M., Luterbacher, J., Xoplaki, E., Türkeş, M., 2012. Palaeolimnological evidence for an east-west climate see-saw in the Mediterranean since AD 900. Glob. Planet. Change 84–85, 23–34. https://doi.org/10.1016/j.gloplacha.2011.11.002

Rodrigo, F.S., 2019. Coherent variability between seasonal temperatures and rainfalls in the Iberian Peninsula, 1951–2016. Theor. Appl. Climatol. 135, 473–490. https://doi.org/10.1007/s00704-018-2400-1

Rodrigo, F.S., 2018. A review of the Little Ice Age in Andalusia (Southern Spain): results and research challenges. Cuad. Investig. Geográfica 44, 245–265. https://doi.org/10.18172/cig.3316

Rodrigo, F.S., 2012. Completing the early instrumental weather record from Cádiz (Southern Spain): new data from 1799 to 1803. Clim. Change 111, 697–704. https://doi.org/10.1007/s10584-011-0174-x

Rodrigo, F.S., Gómez-Navarro, J.J., Montávez Gómez, J.P., 2012. Climate variability in Andalusia (southern Spain) during the period 1701-1850 based on documentary sources: Evaluation and comparison with climate model simulations. Clim. Past 8, 117–133. https://doi.org/10.5194/cp-8-117-2012

Rodrigo-Gámiz, M., García-Alix, A., Jiménez-Moreno, G., Ramos-Román, M.J., Camuera, J., Toney, J.L., Sachse, D., Anderson, R.S., Sinninghe Damsté, J.S., 2022. Paleoclimate reconstruction of the last 36 kyr based on branched glycerol dialkyl glycerol tetraethers in the Padul palaeolake record (Sierra Nevada, southern Iberian Peninsula). Quat. Sci. Rev. 281. https://doi.org/10.1016/j.quascirev.2022.107434

Rodrigo-Gámiz, M., Martínez-Ruiz, F., Jiménez-Espejo, F.J., Gallego-Torres, D., Nieto-Moreno, V., Romero, O., Ariztegui, D., 2011. Impact of climate variability in the western Mediterranean during the last 20,000 years: Oceanic and atmospheric responses. Quat. Sci. Rev. 30, 2018–2034. https://doi.org/10.1016/j.quascirev.2011.05.011

Rodrigo-Gámiz, M., Martínez-Ruiz, F., Rampen, S.W., Schouten, S., Sinninghe Damsté, J.S., 2014. Sea surface temperature variations in the western Mediterranean Sea over the last 20 kyr: A dual-organic proxy (UK'37 and LDI) approach. Paleoceanography 29, 87–98. https://doi.org/10.1002/2013PA002466

Rodrigo-Gámiz, Marta, Martínez-Ruiz, F., Rodríguez-Tovar, F.J., Jiménez-Espejo, F.J., Pardo-Igúzquiza, E., 2014. Millennial- to centennial-scale climate periodicities and forcing mechanisms in the westernmost Mediterranean for the past 20,000 yr. Quat. Res. U. S. 81, 78–93. https://doi.org/10.1016/j.yqres.2013.10.009

Rodrigues, T., Grimalt, J.O., Abrantes, F., Naughton, F., Flores, J.A., 2010. The last glacial-interglacial transition (LGIT) in the western mid-latitudes of the North Atlantic: Abrupt sea surface temperature change and sea level implications. Quat. Sci. Rev. 29, 1853–1862. https://doi.org/10.1016/j.quascirev.2010.04.004

Rodriguez-Lazaro, J., Pascual, A., Cacho, I., Varela, Z., Pena, L.D., 2017. Deep-sea benthic response to rapid climatic oscillations of the last glacial cycle in the SE Bay of Biscay. J. Sea Res. 130, 49–72. https://doi.org/10.1016/j.seares.2017.06.002

Roldán-Gómez, P.J., González-Rouco, J.F., Melo-Aguilar, C., Smerdon, J.E., 2020. Dynamical and hydrological changes in climate simulations of the last millennium. Clim. Past 16, 1285–1307. https://doi.org/10.5194/cp-16-1285-2020

Roldán-Gómez, P.J., González-Rouco, J.F., Smerdon, J.E., García-Pereira, F., 2023. Model and proxy evidence for coordinated changes in the hydroclimate of distant regions over the Last Millennium. Clim. Past 19, 2361–2387. https://doi.org/10.5194/cp-19-2361-2023

Romero-Viana, L., Julià, R., Schimmel, M., Camacho, A., Vicente, E., Miracle, M.R., 2011. Reconstruction of annual winter rainfall since A.D.1579 in central-eastern Spain based on calcite laminated sediment from Lake La Cruz. Clim. Change 107, 343–361. https://doi.org/10.1007/s10584-010-9966-7

Ruiz, A., Onea, F., Rusu, E., 2020. Study Concerning the Expected Dynamics of the Wind Energy Resources in the Iberian Nearshore. Energies 13, 4832. https://doi.org/10.3390/en13184832

Ruiz-Pérez, J.-M., Carmona, P., 2019. Turia river delta and coastal barrier-lagoon of Valencia (Mediterranean coast of Spain): Geomorphological processes and global climate fluctuations since Iberian-Roman times. Quat. Sci. Rev. 219, 84–101. https://doi.org/10.1016/j.quascirev.2019.07.005

Sáez, A., Carballeira, R., Pueyo, J.J., Vázquez-Loureiro, D., Leira, M., Hernández, A., Valero-Garcés, B.L., Bao, R., 2018. Formation and evolution of back-barrier perched lakes in rocky coasts: An example of a Holocene system in north-west Spain. Sedimentology 65, 1891–1917. https://doi.org/10.1111/sed.12451

Salgueiro, E., Naughton, F., Voelker, A.H.L., de Abreu, L., Alberto, A., Rossignol, L., Duprat, J., Magalhães, V.H., Vaqueiro, S., Turon, J.L., Abrantes, F., 2014. Past circulation along the western Iberian margin: A time slice vision from the Last Glacial to the Holocene. Quat. Sci. Rev. 106, 316–329. https://doi.org/10.1016/j.quascirev.2014.09.001

Sánchez Goñi, M.F., Llave, E., Oliveira, D., Naughton, F., Desprat, S., Ducassou, E., Hodell, D.A., Hernández-Molina, F.J., 2016. Climate changes in south western Iberia and Mediterranean Outflow variations during two contrasting cycles of the last 1 Myrs: MIS 31–MIS 30 and MIS 12–MIS 11. Glob. Planet. Change 136, 18–29. https://doi.org/10.1016/j.gloplacha.2015.11.006

Sánchez, N.S., Merino, L.L., Armada, X.-L., Cortizas, A.M., 2021. Medieval mining and its impact on peat records: a case study from Cruz do Bocelo Mire (nw iberia).

Sánchez-García, C., Schulte, L., 2023. Historical floods in the southeastern Iberian Peninsula since the 16th century: Trends and regional analysis of extreme flood events. Glob. Planet. Change 231. https://doi.org/10.1016/j.gloplacha.2023.104317

Sánchez-Goñi, M.F., Bard, E., Landais, A., Rossignol, L., d'Errico, F., 2013. Air-sea temperature decoupling in western Europe during the last interglacial-glacial transition. Nat. Geosci. advance online publication. https://doi.org/10.1038/ngeo1924

Sánchez-López, G., Hernández, A., Pla-Rabes, S., Trigo, R.M., Toro, M., Granados, I., Sáez, A., Masqué, P., Pueyo, J.J., Rubio-Inglés, M.J., Giralt, S., 2016. Climate reconstruction for the last two millennia in central Iberia: The role of East Atlantic (EA), North Atlantic Oscillation (NAO) and their interplay over the Iberian Peninsula. Quat. Sci. Rev. 149, 135–150. https://doi.org/10.1016/j.quascirev.2016.07.021

Sancho, C., Belmonte, Á., Bartolomé, M., Moreno, A., Leunda, M., López-Martínez, J., 2018. Middle-to-late Holocene palaeoenvironmental reconstruction from the A294 ice-cave record (Central Pyrenees, northern Spain). Earth Planet. Sci. Lett. 484, 135–144. https://doi.org/10.1016/j.epsl.2017.12.027

Santisteban, J.I., Celis, A., Mediavilla, R., Gil-García, M.J., Ruiz-Zapata, B., Castaño, S., 2021. The transition from climate-driven to human-driven agriculture during the Little Ice Age in Central Spain: Documentary and fluvial records evidence. Palaeogeogr. Palaeoclimatol. Palaeoecol. 562, 110153. https://doi.org/10.1016/j.palaeo.2020.110153

Santisteban, J.I., Mediavilla, R., Galán de Frutos, L., López Cilla, I., 2019. Holocene floods in a complex fluvial wetland in central Spain: Environmental variability, climate and time. Glob. Planet. Change 181, 102986. https://doi.org/10.1016/j.gloplacha.2019.102986

Schirrmacher, J., Andersen, N., Schneider, R.R., Weinelt, M., 2020. Fossil leaf wax hydrogen isotopes reveal variability of Atlantic and Mediterranean climate forcing on the southeast Iberian Peninsula between 6000 to 3000 cal. BP. PLoS ONE 15. https://doi.org/10.1371/journal.pone.0243662

Schirrmacher, J., Weinelt, M., Blanz, T., Andersen, N., Salgueiro, E., Schneider, R.R., 2019. Multi-decadal atmospheric and marine climate variability in southern Iberia during the mid-to late-Holocene. Clim. Past 15, 617–634. https://doi.org/10.5194/cp-15-617-2019

Schmidt, G.A., Jungclaus, J.H., Ammann, C.M., Bard, E., Braconnot, P., Crowley, T.J., Delaygue, G., Joos, F., Krivova, N.A., Muscheler, R., Otto-Bliesner, B.L., Pongratz, J., Shindell, D.T., Solanki, S.K., Steinhilber, F., Vieira, L.E.A., 2011. Climate forcing reconstructions for use in PMIP simulations of the last millennium (v1.0). Geosci. Model Dev. 4, 33–45. https://doi.org/10.5194/gmd-4-33-2011

Schröder, T., López-Sáez, J.A., van't Hoff, J., Reicherter, K., 2020. Unravelling the Holocene environmental history of south-western Iberia through a palynological study of Lake Medina sediments. Holocene 30, 13–22. https://doi.org/10.1177/0959683619865590

Schröder, T., van't Hoff, J., López-Sáez, J.A., Viehberg, F., Melles, M., Reicherter, K., 2018. Holocene climatic and environmental evolution on the southwestern Iberian Peninsula: A high-resolution multi-

proxy study from Lake Medina (Cádiz, SW Spain). Quat. Sci. Rev. 198, 208–225. https://doi.org/10.1016/j.quascirev.2018.08.030

Sicre, M.A., Jalali, B., Martrat, B., Schmidt, S., Bassetti, M.A., Kallel, N., 2016. Sea surface temperature variability in the North Western Mediterranean Sea (Gulf of Lion) during the Common Era. Earth Planet. Sci. Lett. 456, 124–133. https://doi.org/10.1016/j.epsl.2016.09.032

Sierro, F.J., Hodell, D.A., Andersen, N., Azibeiro, L.A., Jimenez-Espejo, F.J., Bahr, A., Flores, J.A., Ausin, B., Rogerson, M., Lozano-Luz, R., Lebreiro, S.M., Hernandez-Molina, F.J., 2020. Mediterranean Overflow Over the Last 250 kyr: Freshwater Forcing From the Tropics to the Ice Sheets. Paleoceanogr. Paleoclimatology 35. https://doi.org/10.1029/2020PA003931

Silva-Sánchez, N., Armada, X.-L., 2023. Environmental Impact of Roman Mining and Metallurgy and Its Correlation with the Archaeological Evidence: A European Perspective. Environ. Archaeol. 1–25. https://doi.org/10.1080/14614103.2023.2181295

Singh, H., Singh, A.D., Tripathi, R., Singh, P., Verma, K., Voelker, A.H.L., Hodell, D.A., 2023. Centennial-millennial scale ocean-climate variability in the northeastern Atlantic across the last three terminations. Glob. Planet. Change 223. https://doi.org/10.1016/j.gloplacha.2023.104100

Smith, A.C., Wynn, P.M., Barker, P.A., Leng, M.J., Noble, S.R., Tych, W., 2016. North Atlantic forcing of moisture delivery to Europe throughout the Holocene. Sci. Rep. 6. https://doi.org/10.1038/srep24745

Stewart, J.R., Stringer, C.B., 2012. Human Evolution Out of Africa: The Role of Refugia and Climate Change. Science 335, 1317–1321. https://doi.org/10.1126/science.1215627

Tabone, I., Blasco, J., Robinson, A., Alvarez-Solas, J., Montoya, M., 2018. The sensitivity of the Greenland Ice Sheet to glacial–interglacial oceanic forcing. Clim. Past 14, 455–472. https://doi.org/10.5194/cp-14-455-2018

Tarrats, P., Heiri, O., Valero-Garcés, B., Cañedo-Argüelles, M., Prat, N., Rieradevall, M., González-Sampériz, P., 2018. Chironomid-inferred Holocene temperature reconstruction in Basa de la Mora Lake (Central Pyrenees). Holocene 28, 1685–1696. https://doi.org/10.1177/0959683618788662

Tejedor, E., De Luis, M., Barriendos, M., Cuadrat, J.M., Luterbacher, J., Saz, M.Á., 2019. Rogation ceremonies: A key to understanding past drought variability in northeastern Spain since 1650. Clim. Past 15, 1647–1664. https://doi.org/10.5194/cp-15-1647-2019

Tejedor, E., de Luis, M., Cuadrat, J.M., Esper, J., Saz, M.Á., 2016. Tree-ring-based drought reconstruction in the Iberian Range (east of Spain) since 1694. Int. J. Biometeorol. 60, 361–372. https://doi.org/10.1007/s00484-015-1033-7

Tejedor, E., Saz, M.A., Esper, J., Cuadrat, J.M., de Luis, M., 2017. Summer drought reconstruction in northeastern Spain inferred from a tree ring latewood network since 1734. Geophys. Res. Lett. 44, 8492–8500. https://doi.org/10.1002/2017GL074748

Thatcher, D.L., Wanamaker, A.D., Denniston, R.F., Asmerom, Y., Polyak, V.J., Fullick, D., Ummenhofer, C.C., Gillikin, D.P., Haws, J.A., 2020. Hydroclimate variability from western Iberia (Portugal) during the Holocene: Insights from a composite stalagmite isotope record. Holocene 30, 966–981. https://doi.org/10.1177/0959683620908648

Timmermann, A., Yun, K.-S., Raia, P., Ruan, J., Mondanaro, A., Zeller, E., Zollikofer, C., Ponce de León, M., Lemmon, D., Willeit, M., Ganopolski, A., 2022. Climate effects on archaic human habitats and species successions. Nature 604, 495–501. https://doi.org/10.1038/s41586-022-04600-9

Toney, J.L., García-Alix, A., Jiménez-Moreno, G., Anderson, R.S., Moossen, H., Seki, O., 2020. New insights into Holocene hydrology and temperature from lipid biomarkers in western Mediterranean alpine wetlands. Quat. Sci. Rev. 240. https://doi.org/10.1016/j.quascirev.2020.106395

Trias-Navarro, S., Pena, L.D., de la Fuente, M., Paredes, E., Garcia-Solsona, E., Frigola, J., Català, A., Caruso, A., Lirer, F., Haghipour, N., Pérez-Asensio, J.N., Cacho, I., 2023. Eastern Mediterranean water outflow during the Younger Dryas was twice that of the present day. Commun. Earth Environ. 4. https://doi.org/10.1038/s43247-023-00812-7

Trigo, R.M., Vaquero, J.M., Alcoforado, M.-J., Barriendos, M., Taborda, J., García-Herrera, R., Luterbacher, J., 2009. Iberia in 1816, the year without a summer. Int. J. Climatol. 29, 99–115. https://doi.org/10.1002/joc.1693

Turu, V., Carrasco, R.M., López-Sáez, J.A., Pontevedra-Pombal, X., Pedraza, J., Luelmo-Lautenschlaeger, R., Pérez-Díaz, S., Echeverria-Moreno, A., Frigola, J., Alba-Sánchez, F., Sánchez-Vizcaíno, J., Pèlachs-Mañosa, A., Cunill-Artigas, R., Nadal-Tersa, J., Mur-Cacuho, E., Soriano-López, J.M., 2021. Palaeoenvironmental changes in the Iberian central system during the Late-glacial and Holocene as inferred from geochemical data: A case study of the Navamuño depression in western Spain. Catena 207. https://doi.org/10.1016/j.catena.2021.105689

Turu, V., Carrasco, R.M., Pedraza, J., Ros, X., Ruiz-Zapata, B., Soriano-López, J.M., Mur-Cacuho, E., Pélachs-Mañosa, A., Muñoz-Martín, A., Sánchez, J., Echeverria-Moreno, A., 2018. Late glacial and post-glacial deposits of the Navamuño peatbog (Iberian Central System): Chronology and paleoenvironmental implications. Quat. Int. 470, 82–95. https://doi.org/10.1016/j.quaint.2017.08.018

Val-Peón, C., Santisteban, J.I., López-Sáez, J.A., Weniger, G.-C., Reicherter, K., 2021. Environmental Changes and Cultural Transitions in SW Iberia during the Early-Mid Holocene. Appl. Sci. 11. https://doi.org/10.3390/app11083580

van Westen, R.M., Kliphuis, M., Dijkstra, H.A., 2024. Physics-based early warning signal shows that AMOC is on tipping course. Sci. Adv. 10, eadk1189. https://doi.org/10.1126/sciadv.adk1189

Vegas, J., Ruiz-Zapata, B., Ortiz, J.E., Galán, L., Torres, T., García-Cortés, Á., Gil-García, M.J., Pérez-González, A., Gallardo-Millán, J.L., 2010. Identification of arid phases during the last 50 cal. ka BP from the Fuentillejo maar-lacustrine record (Campo de Calatrava Volcanic Field, Spain). J. Quat. Sci. 25, 1051–1062. https://doi.org/10.1002/jqs.1262

Vegas-Vilarrúbia, T., Corella, J.P., Sigró, J., Rull, V., Dorado-Liñan, I., Valero-Garcés, B., Gutiérrez-Merino, E., 2022. Regional precipitation trends since 1500 CE reconstructed from calcite sublayers of a varved Mediterranean lake record (Central Pyrenees). Sci. Total Environ. 826. https://doi.org/10.1016/j.scitotenv.2022.153773

Vicente de Vera García, A., Mata-Campo, M.P., Pla, S., Vicente, E., Prego, R., Frugone-Álvarez, M., Polanco-Martínez, J., Galofré, M., Valero-Garcés, B.L., 2023. Unprecedented recent regional increase in organic carbon and lithogenic fluxes in high altitude Pyrenean lakes. Sci. Rep. 13, 8586. https://doi.org/10.1038/s41598-023-35233-1

Vidaller, I., Izagirre, E., Del Rio, L.M., Alonso-González, E., Rojas-Heredia, F., Serrano, E., Moreno, A., López-Moreno, J.I., Revuelto, J., 2023. The Aneto glacier's (Central Pyrenees) evolution from 1981 to 2022: ice loss observed from historic aerial image photogrammetry and remote sensing techniques. The Cryosphere 17, 3177–3192. https://doi.org/10.5194/tc-17-3177-2023

Voelker, A.H.L., De Abreu, L., 2011. A Review of Abrupt Climate Change Events in the Northeastern Atlantic Ocean (Iberian Margin): Latitudinal, Longitudinal, and Vertical Gradients, in: Abrupt Climate Change: Mechanisms, Patterns, and Impacts. Wiley, pp. 15–37.

Waelbroeck, C., Lougheed, B.C., Vazquez Riveiros, N., Missiaen, L., Pedro, J., Dokken, T., Hajdas, I., Wacker, L., Abbott, P., Dumoulin, J.P., Thil, F., Eynaud, F., Rossignol, L., Fersi, W., Albuquerque, A.L., Arz, H., Austin, W.E.N., Came, R., Carlson, A.E., Collins, J.A., Dennielou, B., Desprat, S., Dickson, A., Elliot, M., Farmer, C., Giraudeau, J., Gottschalk, J., Henderiks, J., Hughen, K., Jung, S., Knutz, P., Lebreiro, S., Lund, D.C., Lynch-Stieglitz, J., Malaizé, B., Marchitto, T., Martínez-Méndez, G., Mollenhauer, G., Naughton, F., Nave, S., Nürnberg, D., Oppo, D., Peck, V., Peeters, F.J.C., Penaud, A., Portilho-Ramos, R. da C., Repschläger, J., Roberts, J., Rühlemann, C., Salgueiro, E., Sanchez Goni, M.F., Schönfeld, J., Scussolini, P., Skinner, L.C., Skonieczny, C., Thornalley, D., Toucanne, S., Rooij, D.V., Vidal, L., Voelker, A.H.L., Wary, M., Weldeab, S., Ziegler, M., 2019. Consistently dated Atlantic sediment cores over the last 40 thousand years. Sci. Data 6. https://doi.org/10.1038/s41597-019-0173-8

Wagner, B., Vogel, H., Francke, A., Friedrich, T., Donders, T., Lacey, J.H., Leng, M.J., Regattieri, E., Sadori, L., Wilke, T., Zanchetta, G., Albrecht, C., Bertini, A., Combourieu-Nebout, N., Cvetkoska, A., Giaccio, B., Grazhdani, A., Hauffe, T., Holtvoeth, J., Joannin, S., Jovanovska, E., Just, J., Kouli, K., Kousis, I., Koutsodendris, A., Krastel, S., Lagos, M., Leicher, N., Levkov, Z., Lindhorst, K., Masi, A., Melles, M., Mercuri, A.M., Nomade, S., Nowaczyk, N., Panagiotopoulos, K., Peyron, O., Reed, J.M., Sagnotti, L., Sinopoli, G., Stelbrink, B., Sulpizio, R., Timmermann, A., Tofilovska, S., Torri, P., Wagner-Cremer, F., Wonik, T., Zhang, X., 2019. Mediterranean winter rainfall in phase with African monsoons during the past 1.36 million years. Nature 573, 256–260. https://doi.org/10.1038/s41586-019-1529-0

Walczak, I.W., Baldini, J.U.L., Baldini, L.M., McDermott, F., Marsden, S., Standish, C.D., Richards, D.A., Andreo, B., Slater, J., 2015. Reconstructing high-resolution climate using CT scanning of unsectioned stalagmites: A case study identifying the mid-Holocene onset of the Mediterranean climate in southern Iberia. Quat. Sci. Rev. 127, 117–128. https://doi.org/10.1016/j.quascirev.2015.06.013

Wanner, H., Beer, J., Bütikofer, J., Crowley, T.J., Cubasch, U., Flückiger, J., Goosse, H., Grosjean, M., Joos, F., Kaplan, J.O., Küttel, M., Müller, S.A., Prentice, I.C., Solomina, O., Stocker, T.F., Tarasov, P., Wagner, M., Widmann, M., 2008. Mid- to Late Holocene climate change: an overview. Quat. Sci. Rev. 27, 1791–1828.

Wanner, H., Solomina, O., Grosjean, M., Ritz, S.P., Jetel, M., 2011. Structure and origin of Holocene cold events. Quat. Sci. Rev. 30, 3109–3123. https://doi.org/10.1016/j.quascirev.2011.07.010

Zamora, R., Oliva, M., 2022. The Landscape of the Sierra Nevada.

Zielhofer, C., Fletcher, W.J., Mischke, S., De Batist, M., Campbell, J.F.E., Joannin, S., Tjallingii, R., El Hamouti, N., Junginger, A., Stele, A., Bussmann, J., Schneider, B., Lauer, T., Spitzer, K., Strupler, M., Brachert, T., Mikdad, A., 2017. Atlantic forcing of Western Mediterranean winter rain minima during the last 12,000 years. Quat. Sci. Rev. 157, 29–51. https://doi.org/10.1016/j.quascirev.2016.11.037

CHAPTER 2
THE STUDY OF THE CRYOSPHERE IN THE IBERIAN PENINSULA

Leading Authors: Jesús Revuelto[1], Marc Oliva[2], Enrique Serrano[3], Miguel Bartolomé[4, 5, 6], Ana Moreno[1], Juan Ignacio López-Moreno[1]

[1] Pyrenean Institute of Ecology, CSIC, Zaragoza, Spain

[2] Department of Geography, Universitat de Barcelona, Barcelona, Catalonia, Spain

[3] Department of Geography, University of Valladolid, Valladolid, Spain

[4] Department of Geology, Museo Nacional de Ciencias Naturales (CSIC), Madrid, Spain

[5] Swiss Institute for Speleology and Karst Studies (SISKA), La Chaux-de-Fonds, Switzerland

[6] Department of Earth Sciences, Geological Institute, ETH, Zurich, Switzerland

1. Introduction

The term "cryosphere" comes from the Greek word "kryo" meaning cold. It is therefore a concept that includes the elements of the Earth system where low temperatures favour the presence of water in its solid state. It comprises glaciers, snow, frozen ground, sea ice and frozen lakes and rivers (Figure 2.1). As a result, it is found in regions where the temperature and humidity regimes vary throughout the year, with some areas having permanent negative temperatures (the interior of the polar ice caps, the summits of the highest mountains) and others with contrasting climates, very cold in winter and warm in summer (such as continental areas: Siberia, Tibet, etc.). Some cryospheric elements extend over large areas for millions or hundreds of thousands of years (continental glaciers), others cover large areas for tens of thousands to hundreds of years (mountain glaciers and permafrost), and others have a seasonal component, and can affect large continental areas during the cold annual period (seasonal snow or frozen ground).

This high spatial and temporal variability makes the cryosphere one of the components of the natural system that responds most visibly to climate fluctuations and, in turn, has the greatest impact on the climate dynamics of the planet as a whole (Intergovernmental Panel On Climate Change (Ipcc), 2022). Thus, the climatic oscillations that have characterized the Quaternary have led to periods of significant expansion of the cryosphere and its various components, and others in which the cold world has shrunk and retreated towards higher latitudes and mountains.

This chapter presents the research carried out in the last decade to better understand the spatio-temporal variability of the different elements of the cryosphere (glaciers, permafrost, snow and ice caves) in the Iberian Peninsula (IP). Thus, each section begins with a review of the progress made in the study of the Quaternary up to the end of the Little Ice Age, and continues with the analysis of trends, projections into the future and the analysis of extreme events.

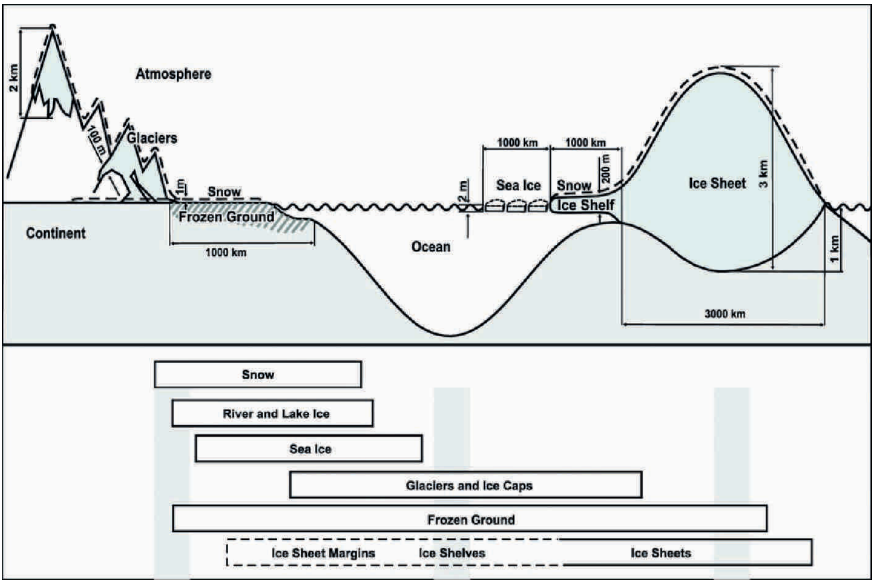

Figure 2.1. Components of the cryosphere and their scales (modified from IPCC, 2013).

2. Glaciers

In the IP, the alternation between glacial and interglacial periods has favoured the expansion and contraction (and disappearance) of ice masses in mountainous areas. In general, these were glaciers of modest size, which remained at high elevation areas and at the headwaters of the valleys, without reaching the surrounding plains (Figure 2.2). Glaciers have shaped the current Alpine landscape and their impact on the relief is one of the main tourist attractions of the natural heritage of our mountains; the imposing the U-shaped valley of Pineta, the "jous" of the Picos de Europa or the "corrales" of the Sierra Nevada are landforms carved out by Quaternary cold-climate processes. Of these frozen masses, only small traces remain in the highest massifs of the Pyrenees, all of them in accelerated retreat (Vidaller et al., 2021).

The distribution of sediments left by the glaciers (mainly moraines and erratic boulders) and the derived erosive landforms (such as the "roche moutonnée" and striated rock surfaces) has made possible to reconstruct the extent of the main glacial phases that have occurred in the Iberian mountains. The great erosive capacity of glacial masses during periods of advance eliminates the traces left in the landscape by previous glaciations, so that few sectors include evidence of glacial phases prior to the last Pleistocene glacial cycle (MIS 4-2; ca. 80-20 ka) (Oliva et al., 2019, 2022a).

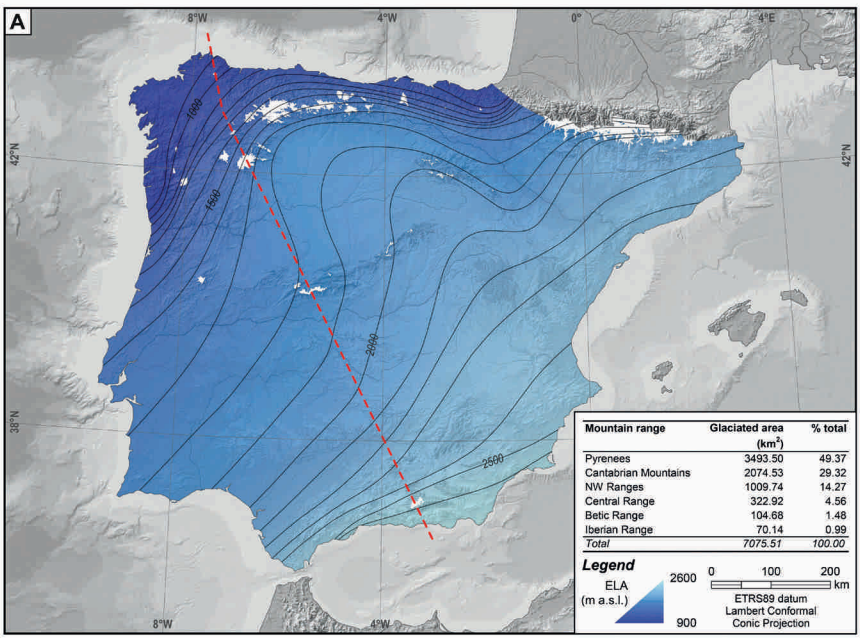

Figure 2.2. Maximum ice extent in the Iberian mountains during the last glacial maximum (modified from Oliva et al., 2021).

The oldest evidence of glacial activity in the Iberian Mountains dates back to ca. 130-170 ka (MIS 6) (Oliva et al., 2022a), although the existence of other older glacial phases cannot be excluded. The last Pleistocene glacial cycle was generally associated with an expansion of glaciers in the Iberian mountains, although the maximum ice volume was not reached synchronously: while some mountain ranges such as the Cantabrian and the Pyrenees recorded the maximum ice accumulation before the global Last Glacial Maximum (LGM) between 30 and 60 ka, this pattern occurred around 30 ka in the Sierra Nevada and in the Galician-Leonese massif, and was (almost) synchronous with the LGM in the Central and Iberian systems (Oliva et al., 2019, 2022c).

The change in global radiative balance that began between 19 and 20 ka favoured the retreat of glacier masses in polar and mountain regions (Clark et al., 2009). In the Iberian mountains, all glaciated mountains experienced a rapid retreat during the last glacial cycle, with smaller glaciers remaining around 17-18 ka as a consequence of higher temperatures. The transition to the current interglacial, the Holocene, was not gradual as a result of continuous progressive warming, but was interrupted by colder and warmer phases. After the initial phase of retreat during

the Oldest Dryas (OD; 17.5-14.7 ka, stadial GS-2.1a), climatic conditions characterised by milder summers favoured glacial advance in all mountains above 2,000 m between 17 and 15.5 ka, with glaciers having between 40 and 75% of the area occupied during the LGM and their fronts located within 0.1-1 km of the moraines of that phase (Oliva et al., 2023). A strong warming of 3-5 ºC then occurs around 15.5-15 ka, just before the onset of the warm phase known as the Bølling-Allerød (B-A; 14.7-12.9 ka, interstadial GI-1), which accelerated the retreat of the frozen masses: glaciers disappeared from most Iberian mountains and may have only persisted in the highest massifs of the Pyrenees (Oliva et al., 2022d). Warmer conditions led to the transformation of debris-free glaciers into debris-covered glaciers or even developed to rock glaciers, although high temperatures favoured the rapid thawing of permafrost and many of them become relict (Santos-González et al., 2022). The 2-3 °C cooling recorded during the transition to the short, but intense cold event known as the Younger Dryas (YD; 12.9-11.7 ka, stadial GS1) promoted glacial expansion between 13.5-12.5 ka (Fernandes et al., 2022); it is the last widespread phase with the formation of small glaciers up to 0.5-4 km long descending from the highest peaks (García-Ruiz et al., 2016). After the YD, the gradual disappearance of these glaciers was facilitated by the temperature increase, many of which drifted towards debris-covered glaciers and rock glaciers (Andrés et al., 2018).

The climate of the present interglacial, the Holocene (last 11,700 years), has been outside the range favourable for the development of extensive glaciers and only during the coldest phases did small ice masses form and expand within the highest cirques of the Pyrenees, Sierra Nevada and Picos de Europa (García-Ruiz et al., 2014; González Trueba et al., 2008; Oliva and Gómez-Ortiz, 2012). A moderate cooling of 1-2 ºC and slight increases in precipitation in the form of snow favoured the ephemeral formation of glaciers during the so-called Neoglacial period around 6 and 3 ka, during the Dark Ages around 0.4-0.9 ka (García-Ruiz et al., 2020), as well as during the Little Ice Age (LIA, 1300-1850 CE; Oliva et al., 2018). In fact, in the highest massifs of the Pyrenees such as Monte Perdido, the ice is estimated to be at least 2000 years old, which means that the highest glaciers have survived warmer phases, such as the Medieval Climate Anomaly (900-1300 CE; Moreno et al., 2021).

The LIA was the coldest and longest period of the last millennia in the Iberian mountains, with geomorphological evidence and historical documents attesting to the expansion of glaciers in the Pyrenees (Serrano Cañadas, 2023), as well as the formation of small glaciers in the highest northern glacial cirques in Sierra Nevada (Gómez-Ortiz et al., 2018) and Picos de Europa (González Trueba, 2005). In the case of Pyrenees, since the end of the LIA the number of glaciers has decreased from 52 in 1850, to 39 in 1984 and 21 in 2016, and their extent has been reduced by almost 90% during this period: from 2,066 ha to 242 in 2016 (Rico et al., 2017). The most recent studies published in the Pyrenees show how this reduction in surface area has accelerated, and the surface area of the Pyrenees is estimated to be less than 230 ha in 2020 (Vidaller et al., 2021). In addition, estimates of the evolution of ice thickness in recent decades indicate an average decrease of 6.4 m in the Pyrenees over the period 2011-2020, with an average thickness of 30.4 m in the case of the Aneto Glacier between 1981 and 2022 (Figure 2.3 (Martínez-Fernández et al., 2023; Vidaller et al., 2023).

3. Permafrost

Ground ice and frozen rocks are an essential feature of today's high mountain environments in mid-latitude regions. The existence of frozen ground is mainly determined by altitude, which is key because the temperature decreases with altitude; by the aspect, which determines the radiation received; and by the thickness and evolution of the snow cover, which partially protects the ground from atmospheric temperatures. Ground ice is formed in different ways; as occasional ice, of daily or diurnal-nightly character, driven by the atmospheric thermal regime and the snow cover; as seasonal frozen ground, also dependent on the atmospheric thermal regime and to a lesser extent on the snow cover; and finally, as permanently frozen ground, permafrost, associated with mean annual ground temperatures (TMAS) below 0 ºC for at least two years. All of them are sensitive to atmospheric warming so that the increase in atmospheric temperature determines the thermal regime of the ground and the presence or degradation of mountain permafrost.

During the Quaternary, the extent of permafrost in the mountains of the Mediterranean basin expanded or contracted depending on the intensity of the prevailing cold (Oliva et al., 2018b). However, its spatial reconstruction is complex due to the multiple factors that condition its distribution: climate, lithology, geomorphological setting, interaction with glaciers, vegetation, etc. For example, past permafrost conditions have only been inferred from the geomorphological evidence that exist in our mountains, and even in areas of the Castilian Meseta in the form of relict sand wedges (Serrano et al., 2010). The rock glaciers, block streams or stone circles of metric dimensions found in most of the Iberian mountains are geoindicators of permafrost conditions that developed during the cold phases of the last glacial cycle, as well as during the cold events of the last deglaciation (OD, YD) (Oliva et al., 2016b). Although the distribution of relict rock glaciers has been used to reconstruct the paleotemperature regime in the Iberian mountains (Palma et al., 2017), the absolute dating of these landforms shows that their origin is more related to the readjustment of the relief to postglacial conditions rather than to a regional climate control (Fernandes et al., 2024; Santos-González et al., 2022).

In the IP, seasonal frozen soils and mountain permafrost are currently important components of the high mountains, particularly in the Pyrenees. Seasonally frozen soils are the most widespread, while the presence of permafrost has only been detected in the highest mountains of the Sierra Nevada, the Picos de Europa and the Pyrenees. Ice melting, freezing, frost heave, and solifluction are the main processes that organise in altitude and space the complex geoecological dynamics of the high mountains with decametric variations in the distribution of frozen soils. Changes in atmospheric temperature affect the thickness and distribution of the snowpack (López-Moreno et al., 2020), the thermal regimes of the ground and thus the presence and dynamics of on the ground ice and the permanence or degradation of permafrost, which is showing a rapid trend towards degradation in Europe (Etzelmüller et al., 2020).

In the Sierra Nevada and the Picos de Europa soil sensors have shown that permafrost is located in marginal areas in relation to topoclimatic conditions. Frozen soils in Sierra Nevada have been detected in culminating areas of flat topography (Collado de los Machos, Allanada del Mulhacén, etc.) and in north-facing glacial cirques (Gómez et al., 2001; Gómez-Ortiz et al., 2014; Oliva et al., 2016a; Salvador Franch et al., 2013; Tanarro et al., 2001), always at elevations above 2,900 m, although not on summits and somite walls (Oliva et al., 2016b). In the Picos de Europa, icy soils

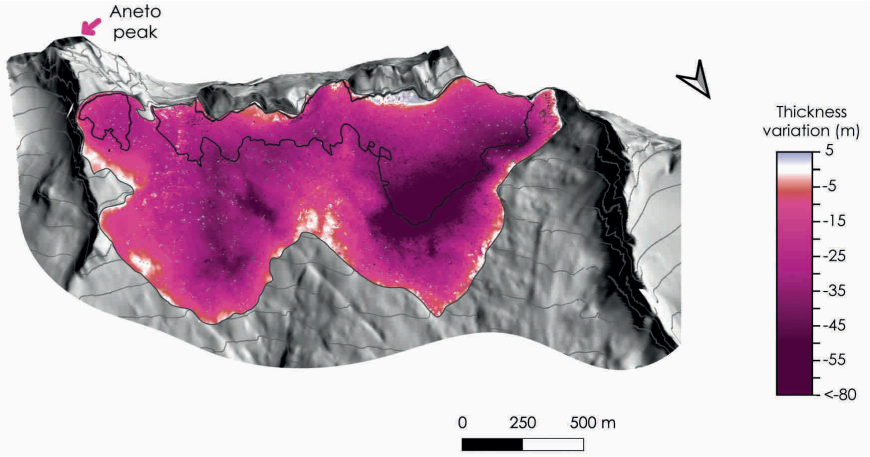

Figure 2.3. Thickness loss of the Aneto glacier from 1981 to 2022. The black line delineates the glacier in 2022, while the grey line represents the glacier in 1981. The arrow indicates the north direction (modified from Vidaller et al., 2023).

are sporadic and are located at moderate altitudes, around 2,200 m, but not in the summit areas (Pisabarro et al., 2017; Serrano et al., 2011).

In the Pyrenees, the distribution of frozen and unfrozen ground indicates an irregular pattern throughout the periglacial belt, but the lower limit of potential existence of frozen ground is at ~2,650 m altitude, with the presence of permafrost possible and probable on both north- and south-facing slopes (Oliva et al., 2022b, 2018a; Serrano et al., 2020, 2019). Below this altitude, down to 2,590 m and even lower, local factors such as topography, slope morphology, orientation, hydrology, or the thickness and duration of the snowpack may create conditions for the presence of sporadic permafrost and seasonally frozen soils (Julián and Chueca, 2007).

Potential environments with mountain permafrost in the Pyrenees are very small and represent recent transitions from glacial and permafrost environments to environments with seasonal frozen soils (Rico et al., 2021; Serrano et al., 2020, 2019). The permafrost indicator features that are located at lower elevations are rock glaciers. There are currently more than 80 active rock glaciers and protalud lobes in the Pyrenees, with a wide altitudinal distribution (Serrano et al., 1999; Ventura Roca, 2016). All of them show cm/year displacement velocities, and in some cases surface morphologies such as subsidence or velocity reduction are detected, indicating the evolution from active to transitional rock glaciers (Martínez-Fernández et al., 2022; Serrano et al., 2010, 2006). The distribution of rock glaciers indicates that the lower limit of permafrost is around 2,630-2,700 m altitude (Oliva et al., 2016a; Serrano et al., 2019, 2012, 2010, 1999). Above 2,650 m altitude

there is the possibility of permafrost environments, characterised by temperate conditions in a very sensitive environment. Probable permafrost - when there is a high probability of the existence of permafrost - is located above 2,700 m altitude on north-facing slopes, and above 2,900 m altitude on south-facing slopes,where topoclimatic conditions (umbria, frost, scree accumulations or rocky escarpments) favour the development of permafrost (García et al., 2017; González García et al., 2013; Lugon et al., 2004; Serrano et al., 2020, 2019, 2012, 2006, 2001). Above 2,900 m altitude probable permafrost prevails on both north- and south-facing slopes, although it alternates with unfrozen soils.

The cold permafrost environment (TMAS < - 2 ºC) is typical of flat thresholds, flat summits and walls above 3,000-3,100 m altitude, where atmospheric thermal conditions are favourable, although at these altitudes there are very few surfaces or walls capable of maintaining this icy environment (Serrano et al., 2020, 2019). On the northern walls at altitudes above 2,800 m the thermal record indicates temperate permafrost (TMAS between 0 ºC and -2 ºC), while around 3,200 m the presence of cold permafrost is possible, and again it is temperate or absent on the upper ridges, where it is significantly affected by the incoming heat flow from the southern walls (Rico et al., 2021). It can be noted that ideal conditions for the existence of cold mountain permafrost may exist from 2,750 m, which are only generalised from 3,000 m.

Thermal data show that the most widespread frozen soils in the high temperate Pyrenees are seasonal frozen soils, alternating with unfrozen soils at lower altitudes, where the snow cover is the most important element in determining the soil thermal regime (Serrano et al., 2018b, 2019). Seasonal frozen ground is locally present from 2,500 m altitude, but are more representative above 2,650 m, in an elevation range above 800 m where they alternate with non-frozen soils and in the highest portions with permafrost. Both non-frozen soils and seasonally frozen soils are distributed up to the summits, as seen on the walls of Vignemale, where permafrost is absent or patchy at 2600 m, and on the northern slopes of Monte Perdido, where 89% of the temperatures > 2°C extend above 2780 m (Rico et al., 2021; Serrano et al., 2020). The ground thermal regimes controlled by the snow cover are not related to ground ice, although snow is part of the cryosphere and any modification of the snow cover (precipitation, melting rates, permanence of the snow cover) has consequences and potential changes on ground frost. In the Pyrenees, unfrozen ground with geomorphological processes associated with cold reaches an altitude of 2,900 m.

In the Pyrenees, areas close to the 0 °C mean annual mean air temperature isotherm, located at 2,950-3,000 m altitude (López-Moreno et al., 2020; OPCC-CTP, 2018), are the most sensitive to climate warming and permafrost degradation. Cold permafrost (< -2 ºC) can currently exist above 2,750 m altitude in preferred orientations, but has its niche above 3,100-3,200 m altitude (Rico et al., 2021; Serrano et al., 2020, 2019). This means a small spatial representation, as there are only eleven massifs with altitudes above 3,000 m. The presence of permafrost environments from 2,750 m, two hundred metres below the 0 °C isotherm altitude, implies the transformation of temperate permafrost environments to permafrost-free environments or from cold to temperate permafrost in the 2,750-3,100 m range. In cold permafrost environments, the rock remains consolidated by the presence of ice, so that at the transition between cold and temperate permafrost, above 3,100 m, the changes are not significant. However, where there is temperate permafrost, between this altitude and 2,750 m, and in some cases at lower altitudes, an increase in the average ground

temperature of less than 1 ºC means that the permafrost is deteriorating or disappearing and that new processes are taking place. In the walls and ridges, the dilation of the rock due to the increase in temperature, the deconsolidation of the walls due to the absence of ice and the presence of periglacial processes associated with thermal changes, such as frost shattering, cause instability and an increase in the intensity of gravitational processes, in particular rockfall. In slope deposits, the transition from cold to warm permafrost causes an increase in slope flow and displacement velocities of cm/year due to cryoreptation and ice deformation as the ice temperature approaches freezing point. In the transition to non-frozen ground, the presence of meltwater, ice/thaw cycles and surface frost causes an increase in mass movements by creep or sliding and debris flows. Although the hazard is low, it represents important geo-ecological changes. All these changes occur in the Pyrenees, mainly between 2,700 and 3,100 m, in a 400-m zone where there is no infrastructure but a high summer population. On the northern face of the Vignemale (Rico et al., 2021), the simulated substrate temperature for the period 1961-1990 shows that warm permafrost (> -2 °C) could have existed between 2,600 and 3,100 m and cold permafrost (< -2 °C) above 3,100 m.

In the last thirty years, temperatures have increased by 1.2 °C (Cuadrat et al., 2016; OPCC-CTP, 2018) and the rise of the permafrost environment has been 6.5 m/year, so at this rate it can be estimated that permafrost will disappear before 2080, with the corresponding increase in instability during this period. These results confirm the gradual degradation of permafrost over the last thirty years as a result of the rise in temperature and the persistence of the processes associated with instability - rockfall, landslides, creep, debris flows, subsidence - as long as atmospheric warming continues. It is also possible to foresee changes at lower elevations related to variations in the duration and thickness of snow cover, leading to increased activity of periglacial processes in the lower and higher parts of the periglacial belt in the near future. This is a narrow altitudinal margin of moderate extension, but very frequented in the most attractive massifs (Maladeta-Aneto, Posets, Monte Perdido, Vignemale, Balaitous, Bachimala, Aigues Tortes or Pica d'Estats massifs), which increases the risk for mountaineering activities.

4. Snow

Snow is a seasonal component of great socio-economic and environmental importance in the Iberian mountains (Alonso González, 2020). Its distribution, thickness and duration are crucially determined by temperature and precipitation conditions, which, in the IP are subject to a high interannual and intraannual variability (López-Moreno et al., 2017; Revuelto et al., 2017). Logically, snow is a key element for glacial evolution; although there are no reconstructions of its past extent before the satellite epoch, its presence and persistence must have shown a direct correlation with the winter/spring temperature and precipitation regime. Already in historical times, for the last centuries of the LIA, there are documentary sources (writings, engravings, photographs, etc.) that describe and graphically attest to the greater persistence of late melting snowpacks in the highest Iberian massifs, such as the Sierra Nevada (Gómez-Ortiz et al., 2018) or the Pyrenees (Serrano Cañadas, 2023). In other massifs, an increase in geomorphological activity related to the increased presence and duration of snow on the ground during these centuries has been also inferred (Palacios et al., 2003). Since then, variations in snow accumulation and melting patterns, as well as changes in land use in the Iberian highlands

(increased depopulation, ski resorts, construction of reservoirs, etc.), have led to significant changes in the prevailing geoecological and hydrological dynamics, both in the highlands and in the adjacent valleys (García-Ruiz et al., 2015).

The study of the temporal variability of snowfall days, snow accumulation and the duration of the snow cover on the ground in recent decades and its prediction for the future have benefited from important methodological advances in the field of observations and numerical simulations (Alonso-González et al., 2017; López-Moreno et al., 2013; Revuelto et al., 2014a).

Monitoring precipitation and temperature is particularly complex in areas with heavy snowfall, but clear guidelines have been provided to improve precipitation measurement to reduce the effect of the undercatch phenomenon - the loss of precipitation in solid form due to wind action (Buisán et al., 2017), and which sensors and in what arrangement should be installed to measure temperature in high mountain areas (Navarro-Serrano et al., 2019). Thermal gradients have also been measured to determine how temperature varies as a function of altitude for different mountain areas of the IP (Navarro-Serrano et al., 2018) and at a detailed scale in relation to topography and dominant synoptic situations (Navarro-Serrano et al., 2020). New methodological proposals have also been made for the use of satellite imagery to track snow cover at spatial resolutions below 30 m (Pimentel et al., 2017; Revuelto et al., 2021a), or even cm resolutions with the use of drones or terrestrial laser scanners (Revuelto et al., 2021b, 2014b). In the last decade, significant progress has also been made in the numerical simulation of the snowpack using the WRF (Weather Research and Forecasting) model, either by searching for optimal parameterisations (Melón-Nava et al., 2023) or by refining the spatial resolution of the simulations initially obtained to high resolutions to generate time series of high temporal length for the entire IP (Alonso-González et al., 2017). Similarly, it has been possible to determine the control exerted by topography on the spatial distribution of snow cover at different scales and its interannual variability (López-Moreno et al., 2013; Revuelto et al., 2014a) and how snow accumulation and melting processes are also influenced by climate variability (Sanmiguel-Vallelado et al., 2020).

Studies of recent trends observed in snowfall days, snow accumulation and snow cover duration reveal that the selection of the study period largely determines the magnitude and statistical significance of the changes obtained, although there is a generalized trend towards a lower presence of snow in the Spanish mountains. Thus, in the Pyrenees a significant decrease in snowfall days has been found for the period 1970-2000, but this trend disappears if the periods 1961-2013 and 1980-2010 are considered (Buisan et al., 2015). Similarly, for snow accumulation, no significant trend is observed for the period 1981-2010, and even if the series start in 1985, most of the series show a positive evolution (Buisan et al., 2016). However, using series obtained by numerical simulation enhanced by assimilation of observations (SAFRAN-CROCUS) for the period 1958-2017, a statistically significant decrease in both mean annual accumulation and snowpack duration can be observed (Figure 2.4), with the decreases being more pronounced at the highest elevations of the mountain range (López-Moreno et al., 2020). The frequency of arrival of air masses of Atlantic origin, synthesized by the fluctuations of the North Atlantic Oscillation (NAO) is the main control of snow fluctuations in the western and central sector of the southern slope of the Pyrenees (Buisan et al., 2016), while flows of Mediterranean origin gain importance in the eastern sector of the mountain range (Bonsoms et al., 2021).

In the Central System, a significant decrease in snow cover duration has been detected for the period 2000-2021 (-0.5 days/year), while winter precipitation has shown no changes, evidencing

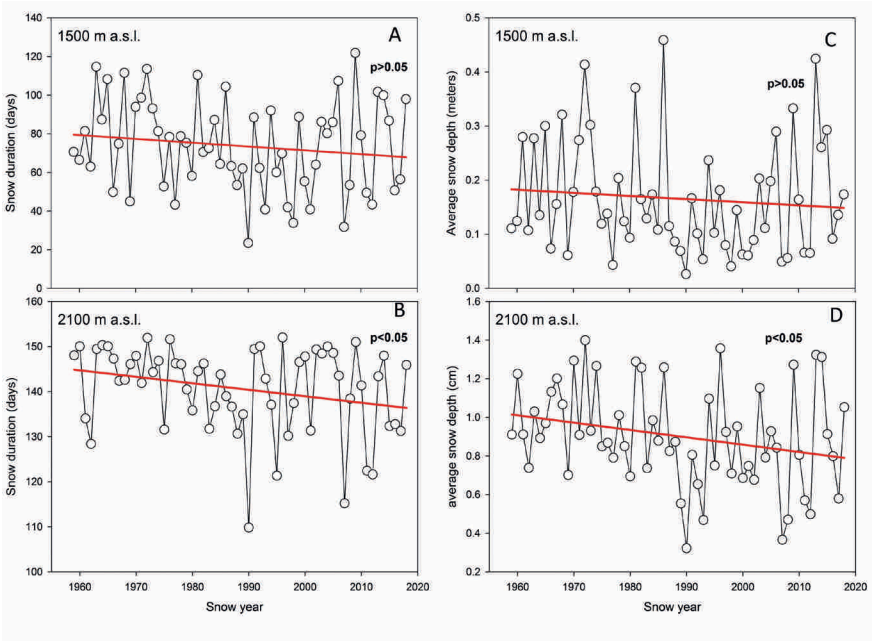

Figure 2.4: Evolution of annual snow cover duration (a, b) and average snow depth from December to April (c, d) at 1,500 and 2,100 m,. respectively (López-Moreno et al., 2020a).

that the thermal increase has been the main cause of this decrease (González-Flórez et al., 2022). In Sierra Nevada, there is a statistically significant decrease in snow cover extent and persistence during the period 1960-2000, being in this case precipitation the main cause of these changes, followed by thermal increase (Pérez-Palazón et al., 2018, 2015). For northern Spain, mainly in the Cantabrian Mountains, and based on a set of General Circulation Atmospheric Models (GCMs), a decrease in snow cover (1960-2000) ranging from -8.5 to 0.2 days per decade has been detected, with a mean value of the set of models of -1.5 days per decade (Pons et al., 2016). For the Cantabrian Mountains, a greater intensity of snowfall has been associated with situations from the north or northeast (De Pablo Dávila et al., 2021); while for the Central System the greatest snow accumulations are recorded in cyclonic synoptic situations or those that favor the arrival of westerly easterlies, abundant in phases of negative NAO (González-Flórez et al., 2022). In the Valencian Community, the presence of snow has been associated with a higher frequency of easterly flows (Mora et al., 2016).

All works presenting projections for the coming decades of snowpack accumulation and duration indicate a generalized decrease in both parameters regardless of the models considered; in fact, the Spanish mountains have been identified as one of the areas of the world where snowpack responds most rapidly to atmospheric warming, even if this is moderate (López-Moreno et al.,

2020; López-Moreno et al., 2020). For the mountains of northern Spain, models forced with moderate gas emission scenarios (A1B) project a reduction in snowpack duration of between -3.7 and -0.5 days per decade (period 2011-2050), with a model ensemble mean of -2 days per decade (Pons et al., 2016). In Sierra Nevada, Pérez-Palazón et al., 2018 project for the end of the 21st century a decrease in snowfall of -0.068 and -0.11 mm/day per year for the RCP 4.5 and 8.5 scenarios respectively. Also for Sierra Nevada, a stochastic time generator has been used to project a decrease in snow cover for the 2071-2100 horizon ranging from 42 to 66% between December and February, being higher if the spring and autumn months are included. Such changes are equivalent to increasing the snow line by approximately 400 meters (Collados-Lara et al., 2021). In the Central Pyrenees, using a high emissions scenario (RCP .5), it was estimated that snow accumulation at 1800 m could be reduced by half by 2050 (OPCC-CTP, 2018).

Finally, in the last decade, a number of studies have been carried out to quantify the magnitude and spatial extent, as well as the prevailing atmospheric conditions that triggered extreme events related to snowpack, such as the avalanches that affected the Cantabrian Mountains in 1888 (García-Hernández et al., 2018), the snowfall that affected Catalonia in March 2010 (Bech et al., 2013; Llasat et al., 2014), the Filomena storm in January 2021 (Tapiador et al., 2021), or the exceptional snowfall in the western Pyrenees during 2013 (Añel et al., 2014).

5. Ice caves

Ice caves, one of the less studied cryopheric systems, are rock cavities that host perennial ice resulting from the diagenesis of snow (firn) and/or the freezing of infiltrating water reaching the cave (Perşoiu and Lauritzen, 2018). In many ice caves, the arrival of cold and dense air in winter effectively cools the cave (open phase), whereas in warmer seasons the cave acts as a cold trap (closed phase), with the effect of higher temperatures being almost negligible (Luetscher et al., 2008). The currently observed ice retreat is primarily regulated by the decrease in winter precipitation and the increase in winter temperatures (Luetscher et al., 2008, 2005). In addition, the increase in precipitation and the occurrence of extreme precipitation events in warm seasons (closed phase within the ice caves) lead to melting of ice due to heat transfer from dripping water to the cave environment (Luetscher et al., 2008; Perşoiu et al., 2021). Ice caves provide data for the study of past climatic conditions inferred from geochemical and biological proxies (Bartolomé et al., 2023; Feurdean et al., 2011; Leunda et al., 2019; Luetscher et al., 2005; Perșoiu et al., 2017; Racine et al., 2022; Ruiz-Blas et al., 2023; Sancho et al., 2018; Stoffel et al., 2009; Žák et al., 2012). Numerous ice caves are located in regions where the mean annual air temperature (MAAT) outside the cave exceeds 0 ºC (Perşoiu and Lauritzen, 2018), making them particularly vulnerable to potential future climate warming (Kern and Perşoiu, 2013). These ice caves are local thermal anomalies (T mean ≤ 0 ºC), which are controlled by the cave geometry and the associated ventilation pattern. Thus, the number of cave entrances and their relative elevation and dimensions (Gómez Lende et al., 2016; Gómez-Lende and Sánchez-Fernández, 2018; Lende et al., 2014) play an important role in firn/ice preservation. Although these caves represent sporadic permafrost occurrences, they do not provide information on the wider thermal environment. The presence of permafrost in these subsurface environments has been observed to extend to depths between 200 and 400 m (Bartolomé et al., 2023; Gómez Lende, 2016; Gómez-Lende and Serrano Cañadas, 2021).

More than 100 ice caves have been reported in the limestone massifs of the highest peaks of the Pyrenees and the Cantabrian Mountains. Ice caves have been recognised in all the calcareous massifs from the west to the east of the central Pyrenees (from Aspe to the Maladeta massif), between ~2,000 and 3,000 m, while in the case of the Cantabrian Mountains, and more specifically in the Picos de Europa, ice caves are found from 1,300 m and are more common above 2,000 m (Serrano et al., 2018a). In the Pyrenees and Picos de Europa, ice caves are located in areas with/without permafrost (Bartolomé et al., 2023; *Comprendiendo el relieve del pasado al futuro*, 2016; Gómez-Lende and Serrano Cañadas, 2021; Serrano et al., 2018a). For those located in non-permafrost areas, ice formation and preservation is controlled by cave geomorphology, ventilation patterns and current climatic conditions (Belmonte et al., 2014; Gómez Lende et al., 2016; Gómez-Lende and Sánchez-Fernández, 2018; Lende et al., 2014). On the contrary, in permafrost areas above ~2,800 m, where mountain permafrost can reach ~200 m in thickness (Bartolomé et al., 2023; Serrano et al., 2020, 2019), the ice bodies are maintained by a combination of rock undercooling facilitated by cave air ventilation and the specific climatic conditions of the area, leading to the formation of permafrost or the preservation of the permafrost inherited from colder periods in the past (e.g. Bartolomé et al., 2023).

In both mountain ranges, ice caves host perennial ice bodies that provide highly valuable palaeoenvironmental information based on the study of geochemical and biological proxies (Bartolomé et al., 2015; Gómez Lende, 2016; Leunda et al., 2019; Ruiz-Blas et al., 2023; Sancho et al., 2018). For example, the oldest ice accumulation based on radiocarbon dating of terrestrial plant macroremains (6.1-1.8 ka, A294 ice cave, Cotiella massif, Pyrenees) provided information on favourable ice accumulation during the Neoglacial (Sancho et al., 2018). In addition, the identification of plant macroremains and pollen provided long-term tree-line fluctuations during this period (Leunda et al., 2019). In the Picos de Europa, the dating of organic remains preserved in ice bodies reported ages related to the coldest phases of the LIA, around 1660-1680 AD during the Maunder Minimum event (Gómez Lende, 2015), although most ice bodies cover the last millennium and were mainly formed during the LIA (Serrano et al., 2018a). In relation to past permafrost evolution in the Pyrenees, the presence and chronology of cryogenic cave carbonates (CCC) in some caves in the Pyrenees (Bartolomé et al., 2023, 2015) provide information on permafrost thawing (e.g. during the Medieval Climate Anomaly, Bartolomé et al., 2015) and ice phase formation under permafrost conditions (Bartolomé et al., 2023).

In 2013, the scientific community recognised the need for significant efforts to recover the untapped physical, chemical and biological information contained in ice bodies before their complete disappearance (Kern and Perşoiu, 2013). Monitoring of caves in the Pyrenees and Picos de Europa shows large losses of ice masses (ranging from 20 to 400 cm^{a-1} in fossil and seasonal ice, e.g. Veronica, Altaiz, Castil ice caves in the Picos and A294 and Casteret in the Pyrenees) (Belmonte et al., 2014). These caves follow the observed loss of underground ice bodies on a global scale (Kern and Perşoiu, 2013). Thus, the increase in temperatures, especially winter temperatures, which play an important role in cave cooling, as well as the increase in the number of rainfall events (or extreme rainfall events) during the warmer seasons and the decrease in snow, which feeds the ice caves, seem to be behind the observed high loss of ice in the ice caves. On the contrary, ice caves located in permafrost areas, where ice loss ranges between 0-3 mm^{t-1} (Bartolomé et al., 2023), seem to be still protected from the ongoing global warming.

Ice caves in the Picos de Europa are always located below the permafrost belt. In the Pyrenees, their distribution extends from 1,900 m and includes both environments with permafrost, especially in the Monte Perdido massif, and without (Serrano et al., 2018a). In both cases, the endoclimatic characteristics indicate the presence of environments with permafrost that are completely independent of current climatic conditions, making them very sensitive to future climate warming (Kern and Perşoiu, 2013). Air circulation is the basic thermal element for maintaining average temperatures below freezing, and snow and water circulation are the basic hydrological elements for ice nourishment and persistence. These characteristics allow ice caves to be defined as indicators of permafrost environments, independent of surface environmental conditions, although temperatures around 0 and -1°C in the chambers and gallery mean that any atmospheric thermal change will result in summer temperature increases and melting of the ice masses.

6. Conclusion and future perspectives

The study of the cryosphere in the IP has progressed considerably in recent years. Research on current trends has also been complemented by new investigations into the extent and timing of past changes in the cryosphere, particularly those affecting glaciers and permafrost. Indeed, there has been considerable progress in our understanding of the Quaternary glacier oscillations in the Iberian mountains, which are among the best studied in terms of their glacial and periglacial evolution.

The study of the present-day cryosphere in the Iberian mountains confirms that the accelerated increase in air temperatures affects all the mountain areas studied, as well as all the cryospheric components. The coldest conditions in the IP have shifted in altitude and are increasingly concentrated on the highest surfaces. The increase in the equilibrium line in all the massifs has led to a critical situation for the Pyrenean glaciers, with predictions of their imminent disappearance. Only the longest records show a statistically significant decrease in snow cover, due to the high interannual variability of snow phenomena, which is strongly influenced by the frequency of weather types during the winter and spring months.

Permafrost is probably the most uncertain element of the cryosphere, both in terms of its spatial extent and temporal changes. Ongoing research in this area is expected to provide more accurate results in the Pyrenees in the coming years, confirming the definitive disappearance of the last remaining permafrost areas in the Sierra Nevada. The ice caves in the Picos de Europa and the Pyrenees have also seen a reduction in the ice masses they contain.

In summary, and in line with international reports predicting warmer temperatures in the IP, the cryosphere in our mountains is expected to shrink in space and time. Glaciers are expected to decrease in number and disappear in the coming decades, the snow season will be shorter and the spatio-temporal patterns of snow cover will also change, permafrost will degrade, increasing the risk of natural hazards in the highest areas of the Pyrenees, and ice caves will continue to lose ice. The unique natural heritage that the different cryospheric components of the Iberian mountains still represent today will thus be affected, and we will see significant changes in the alpine landscape of the highest massifs.

References

Alonso González, E., 2020. El manto de nieve en la península ibérica: climatología y sensibilidad a la variabilidad climática. Universidad de Valladolid. https://doi.org/10.35376/10324/45329

Alonso-González, E., López-Moreno, J. ¬Ignacio, Gascoin, S., García-Valdecasas Ojeda, M., Sanmiguel-Vallelado, A., Navarro-Serrano, F., Revuelto, J., Ceballos, A., Esteban-Parra, M.J., Essery, R., 2017. Daily gridded datasets of snow depth and snow water equivalent for the Iberian Peninsula from 1980 to 2014. https://doi.org/10.5194/essd-2017-106

Andrés, N., Gómez-Ortiz, A., Fernández-Fernández, J.M., Tanarro, L.M., Salvador-Franch, F., Oliva, M., Palacios, D., 2018. Timing of deglaciation and rock glacier origin in the southeastern Pyrenees: a review and new data. Boreas 47, 1050–1071. https://doi.org/10.1111/bor.12324

Añel, J.A., López-Moreno, J.I., Otto, F.E.L., Vicente Serrano, S.M., Schaller, N., Massey, N., Buisán, S.T., Allen, M.R., 2014. The extreme snow accumulation in the western Spanish Pyrenees during winter and spring 2013.

Bartolomé, M., Cazenave, G., Luetscher, M., Spötl, C., Gázquez, F., Belmonte, Á., Turchyn, A.V., López-Moreno, J.I., Moreno, A., 2023. Mountain permafrost in the Central Pyrenees: insights from the Devaux ice cave. The Cryosphere 17, 477–497. https://doi.org/10.5194/tc-17-477-2023

Bartolomé, M., Sancho Marcén, C., Osácar Soriano, M.C., Moreno, A., Leunda Esnaola, M., Spötl, C., Luetscher, M., López Martínez, J., Belmonte Ribas, Á., 2015. Characteristics of cryogenic carbonates in a Pyrenean ice cave (northern Spain). Geogaceta 107–110.

Bech, J., Pineda, N., Rigo, T., Aran, M., 2013. Remote sensing analysis of a Mediterranean thundersnow and low-altitude heavy snowfall event. Atmospheric Res. 123, 305–322. https://doi.org/10.1016/j.atmosres.2012.06.021

Belmonte, Á., Sancho, C., Moreno, A., López-Martínez, J. & Bartolomé, M., 2014. Present-day environmental dynamics in ice cave a294, Central Pyrenees, Spain. Geogr. Fis. E Din. Quat. 131--140. http://dx.doi.org/10.4461/GFDQ.2014.37.12

Bonsoms, J., Gonzalez, S., Prohom, M., Esteban, P., Salvador-Franch, F., López-Moreno, J.I., Oliva, M., 2021. Spatio-temporal patterns of snow in the Catalan Pyrenees (NE Iberia). Int. J. Climatol. 41, 5676–5697. https://doi.org/10.1002/joc.7147

Buisán, S.T., Earle, M.E., Collado, J.L., Kochendorfer, J., Alastrué, J., Wolff, M., Smith, C.D., López-Moreno, J.I., 2017. Assessment of snowfall accumulation underestimation by tipping bucket gauges in the Spanish operational network. Atmospheric Meas. Tech. 10, 1079–1091. https://doi.org/10.5194/amt-10-1079-2017

Buisan, S.T., López-Moreno, J.I., Saz, M.A., Kochendorfer, J., 2016. Impact of weather type variability on winter precipitation, temperature and annual snowpack in the Spanish Pyrenees. Clim. Res. 69, 79–92. https://doi.org/10.3354/cr01391

Buisan, S.T., Saz, M.A., López-Moreno, J.I., 2015. Spatial and temporal variability of winter snow and precipitation days in the western and central Spanish Pyrenees. Int. J. Climatol. 35, 259–274. https://doi.org/10.1002/joc.3978

Clark, P.U., Dyke, A.S., Shakun, J.D., Carlson, A.E., Clark, J., Wohlfarth, B., Mitrovica, J.X., Hostetler, S.W., McCabe, A.M., 2009. The Last Glacial Maximum. Science 325, 710–714. https://doi.org/10.1126/science.1172873

Collados-Lara, A.-J., Pardo-Igúzquiza, E., Pulido-Velazquez, D., 2021. Assessing the impact of climate change – and its uncertainty – on snow cover areas by using cellular automata models and stochastic weather generators. Sci. Total Environ. 788, 147776. https://doi.org/10.1016/j.scitotenv.2021.147776

Comprendiendo el relieve del pasado al futuro: actas de la XIV Reunión Nacional de Geomorfología Málaga, 22-25 de Junio de 2016, 2016. Instituto Geológico y Minero de España, Madrid.

Cuadrat, J., Serrano-Notivoli, R., Saz, M. & Tejedor, E., 2016. Trends in temperature and precipitation in the Pyrenees range over the period 1950–2010. Presented at the International Geographical Union (IGU), Beijing. https://doi.org/10.13140/RG.2.2.33451.23843.

De Pablo Dávila, F., Rivas Soriano, L.J., Mora García, M., González-Zamora, Á., 2021. Characterization of snowfall events in the northern Iberian Peninsula and the synoptic classification of heavy episodes (1988–2018). Int. J. Climatol. 41, 699–713. https://doi.org/10.1002/joc.6646

Etzelmüller, B., Guglielmin, M., Hauck, C., Hilbich, C., Hoelzle, M., Isaksen, K., Noetzli, J., Oliva, M., Ramos, M., 2020. Twenty years of European mountain permafrost dynamics—the PACE legacy. Environ. Res. Lett. 15, 104070. https://doi.org/10.1088/1748-9326/abae9d

Fernandes, M., Oliva, M., Fernández-Fernández, J.M., Vieira, G., Palacios, D., Garcia-Oteyza, J., Ventura, J., Schimmelpfennig, I., ASTER Team, 2024. Geomorphological record of the glacial to periglacial transition from the Bølling–Allerød to the Holocene in the Central Pyrenees: the Lòcampo cirque in the regional context. Boreas 53, 71–87. https://doi.org/10.1111/bor.12633

Fernandes, M., Oliva, M., Vieira, G., Palacios, D., Fernández-Fernández, J.M., Garcia-oteyza, J., Schimmelpfennig, I., Team, A., Antoniades, D., 2022. Glacial oscillations during the Bølling–Allerød Interstadial–Younger Dryas transition in the Ruda Valley, Central Pyrenees. J. Quat. Sci. 37, 42–58. https://doi.org/10.1002/jqs.3379

Feurdean, A., Perşoiu, A., Pazdur, A., Onac, B.P., 2011. Evaluating the palaeoecological potential of pollen recovered from ice in caves: A case study from Scărişoara Ice Cave, Romania. Rev. Palaeobot. Palynol. 165, 1–10. https://doi.org/10.1016/j.revpalbo.2011.01.007

García, M.G., Cañadas, E.S., Blasco, J.J.S., Trueba, J.J.G., 2017. Surface dynamic of a protalus lobe in the temperate high mountain. Western Maladeta, Pyrenees. CATENA 149, 689–700. https://doi.org/10.1016/j.catena.2016.08.011

García-Hernández, C., Ruiz-Fernández, J., Sánchez-Posada, C., Pereira, S., Oliva, M., 2018. An extreme event between The Little Ice Age and the 20th century: the snow avalanche cycle of 1888 in the Asturian Massif (Northern Spain). Cuad. Investig. Geográfica 44, 187–212. https://doi.org/10.18172/cig.3386

García-Ruiz, J.M., López-Moreno, J.I., Lasanta, T., Vicente-Serrano, S.M., González-Sampériz, P., Valero-Garcés, B.L., Sanjuán, Y., Beguería, S., Nadal-Romero, E., Lana-Renault, N., Gómez-Villar, A., 2015. Los efectos geoecológicos del cambio global en el Pirineo Central español: una revisión a distintas escalas espaciales y temporales. Pirineos 170, e012. https://doi.org/10.3989/Pirineos.2015.170005

García-Ruiz, J.M., Palacios, D., Andrés, N., López-Moreno, J.I., 2020. Neoglaciation in the Spanish Pyrenees: a multiproxy challenge. Mediterr. Geosci. Rev. 2, 21–36. https://doi.org/10.1007/s42990-020-00022-9

García-Ruiz, J.M., Palacios, D., De Andrés, N., Valero-Garcés, B.L., López-Moreno, J.I., Sanjuán, Y., 2014. Holocene and 'Little Ice Age' glacial activity in the Marboré Cirque, Monte Perdido Massif, Central Spanish Pyrenees. The Holocene 24, 1439–1452. https://doi.org/10.1177/0959683614544053

García-Ruiz, J.M., Palacios, D., González-Sampériz, P., de Andrés, N., Moreno, A., Valero-Garcés, B., Gómez-Villar, A., 2016. Mountain glacier evolution in the Iberian Peninsula during the Younger Dryas. Quat. Sci. Rev. 138, 16–30. https://doi.org/10.1016/j.quascirev.2016.02.022

Gómez, A., Palacios, D., Ramos, M., Tanarro, L.M., Schulte, L., Salvador, F., 2001. Location of permafrost in marginal regions: Corral del Veleta, Sierra Nevada, Spain. Permafr. Periglac. Process. 12, 93–110. https://doi.org/10.1002/ppp.375

Gómez Lende, M., 2016. Cuevas heladas en el Parque Nacional Picos de Europa. Fronteras subterráneas del hielo en el Macizo Central. Ed. Organismo Autónomo Parques Nacionales, Madrid, pp 254. ISBN:9788480148917

Gómez Lende, M., 2015. Cuevas heladas en Picos de Europa: clima, morfologías y dinámicas. Tesis doctoral, Univ. de Valladolid. https://doi.org/10.35376/10324/16520

Gómez Lende, M., Serrano, E., Bordehore, L.J., Sandoval, S., 2016. The role of GPR techniques in determining ice cave properties: Peña Castil ice cave, Picos de Europa. Earth Surf. Process. Landf. 41, 2177–2190. https://doi.org/10.1002/esp.3976

Gómez-Lende, M., Sánchez-Fernández, M., 2018. Cryomorphological Topographies in the Study of Ice Caves. Geosciences 8, 274. https://doi.org/10.3390/geosciences8080274

Gómez-Lende, M., Serrano Cañadas, E., 2021. Cave mountain permafrost environments in Picos de Europa and their implications. Cuaternario Geomorfol. 35, 55–76. https://doi.org/10.17735/cyg.v35i3-4.89377

Gómez-Ortiz, A., Oliva, M., Salvador-Franch, F., Salvà-Catarineu, M., Palacios, D., De Sanjosé-Blasco, J.J., Tanarro-García, L.M., Galindo-Zaldívar, J., Sanz De Galdeano, C., 2014. Degradation of buried ice and permafrost in the Veleta cirque (Sierra Nevada, Spain) from 2006 to 2013 as a response to recent climate trends. Solid Earth 5, 979–993. https://doi.org/10.5194/se-5-979-2014

Gómez-Ortiz, A., Oliva, M., Salvador-Franch, F., Salvà-Catarineu, M., Plana-Castellví, J., 2018. The geographical interest of historical documents to interpret the scientific evolution of the glacier existing in the Veleta cirque (Sierra Nevada, Spain) during the Little Ice Age. Cuad. Investig. Geográfica 44, 267–292. https://doi.org/10.18172/cig.3415

González García, M., Serrano, E., Sanjosé Blasco, J.J., González Trueba, J.J., 2013. Dinámica superficial y estado actual del glaciar rocoso de la Madaleta Occidental (Pirineos). Cuad. Investig. Geográfica 37, 81–94. https://doi.org/10.18172/cig.1257

González Trueba, J.J., 2005. La Pequeña Edad del Hielo en los Picos de Europa (Cordillera Cantábrica, NO de España). Análisis morfológico y reconstrucción del avance glaciar histórico. Cuaternario Geomorfol.-479-94.

González Trueba, J.J., Moreno, R.M., Martínez De Pisón, E., Serrano, E., 2008. `Little Ice Age' glaciation and current glaciers in the Iberian Peninsula. The Holocene 18, 551–568. https://doi.org/10.1177/0959683608089209

González-Flórez, C., González-Cervera, Á., Durán, L., 2022. Characterising Large-Scale Meteorological Patterns Associated with Winter Precipitation and Snow Accumulation in a Mountain Range in the Iberian Peninsula (Sierra de Guadarrama). Atmosphere 13, 1600. https://doi.org/10.3390/atmos13101600

Intergovernmental Panel On Climate Change (Ipcc), 2022. The Ocean and Cryosphere in a Changing Climate: Special Report of the Intergovernmental Panel on Climate Change, 1st ed. Cambridge University Press. https://doi.org/10.1017/9781009157964

Julián, A., Chueca, J., 2007. Permafrost distribution from BTS measurements (Sierra de Telera, Central Pyrenees, Spain): assessing the importance of solar radiation in a mid-elevation shaded mountainous area. Permafr. Periglac. Process. 18, 137–149. https://doi.org/10.1002/ppp.576

Kern, Z., Perşoiu, A., 2013. Cave ice—the imminent loss of untapped mid-latitude cryospheric palaeoenvironmental archives. Quat. Sci. Rev. 67, 1–7. https://doi.org/10.1016/j.quascirev.2013.01.008

Lende, M.G., Berenguer, F., Serrano, E., 2014. Morphology, ice types and thermal regime in a high mountain ice cave. First studies applying Terrestrial Laser Scanner in the Peña Castil ice cave (Picos de Europa, Northern Spain). Geogr. Fis. E Din. Quat. 37, 141–150. https://doi.org/10.4461/GFDQ.2014.37.13

Leunda, M., González-Sampériz, P., Gil-Romera, G., Bartolomé, M., Belmonte-Ribas, Á., Gómez-García, D., Kaltenrieder, P., Rubiales, J.M., Schwörer, C., Tinner, W., Morales-Molino, C., Sancho, C., 2019. Ice cave reveals environmental forcing of long-term Pyrenean tree line dynamics. J. Ecol. 107, 814–828. https://doi.org/10.1111/1365-2745.13077

Llasat, M.C., Turco, M., Quintana-Seguí, P., Llasat-Botija, M., 2014. The snow storm of 8 March 2010 in Catalonia (Spain): a paradigmatic wet-snow event with a high societal impact. Nat. Hazards Earth Syst. Sci. 14, 427–441. https://doi.org/10.5194/nhess-14-427-2014

López-Moreno, J.I., Fassnacht, S.R., Heath, J.T., Musselman, K.N., Revuelto, J., Latron, J., Morán-Tejeda, E., Jonas, T., 2013. Small scale spatial variability of snow density and depth over complex alpine terrain: Implications for estimating snow water equivalent. Adv. Water Resour. 55, 40–52. https://doi.org/10.1016/j.advwatres.2012.08.010

López-Moreno, J.I., Gascoin, S., Herrero, J., Sproles, E.A., Pons, M., Alonso-González, E., Hanich, L., Boudhar, A., Musselman, K.N., Molotch, N.P., Sickman, J., Pomeroy, J., 2017. Different sensitivities of snowpacks to warming in Mediterranean climate mountain areas. Environ. Res. Lett. 12, 074006. https://doi.org/10.1088/1748-9326/aa70cb

López-Moreno, J.I., Pomeroy, J.W., Alonso-González, E., Morán-Tejeda, E., Revuelto, J., 2020. Decoupling of warming mountain snowpacks from hydrological regimes. Environ. Res. Lett. 15, 114006. https://doi.org/10.1088/1748-9326/abb55f

López-Moreno, J.I., Soubeyroux, J.M., Gascoin, S., Alonso-Gonzalez, E., Durán-Gómez, N., Lafaysse, M., Vernay, M., Carmagnola, C., Morin, S., 2020. Long-term trends (1958–2017) in snow cover duration and depth in the Pyrenees. Int. J. Climatol. 40, 6122–6136. https://doi.org/10.1002/joc.6571

Luetscher, M., Jeannin, P.-Y., Haeberli, W., 2005. Ice caves as an indicator of winter climate evolution: a case study from the Jura Mountains. The Holocene 15, 982–993. https://doi.org/10.1191/0959683605hl872ra

Luetscher, M., Lismonde, B., Jeannin, P., 2008. Heat exchanges in the heterothermic zone of a karst system: Monlesi cave, Swiss Jura Mountains. J. Geophys. Res. Earth Surf. 113, 2007JF000892. https://doi.org/10.1029/2007JF000892

Lugon, R., Delaloye, R., Serrano, E., Reynard, E., Lambiel, C., González-Trueba, J.J., 2004. Permafrost and Little Ice Age glacier relationships, Posets Massif, Central Pyrenees, Spain. Permafr. Periglac. Process. 15, 207–220. https://doi.org/10.1002/ppp.494

Martínez-Fernández, A., Serrano, E., De Sanjosé, J.J., Gómez-Lende, M., Sánchez-Fernández, M., López-Moreno, J.I., Rico, I., Pisabarro, A., 2023. The final countdown? Monitoring the rapid shrinkage of the Maladeta glacier (2010–2020), Southern Pyrenees. Land Degrad. Dev. 34, 5905–5922. https://doi.org/10.1002/ldr.4886

Martínez-Fernández, A., Serrano, E., Pisabarro, A., Sánchez-Fernández, M., De Sanjosé, J.J., Gómez-Lende, M., Rangel-de Lázaro, G., Benito-Calvo, A., 2022. The Influence of Image Properties on High-Detail SfM Photogrammetric Surveys of Complex Geometric Landforms: The Application of a Consumer-Grade UAV Camera in a Rock Glacier Survey. Remote Sens. 14, 3528. https://doi.org/10.3390/rs14153528

Melón-Nava, A., Merino, A., Sánchez, J.L., Santos-González, J., Gómez-Villar, A., García-Ortega, E., 2023. Snowfall events in the Cantabrian Mountains of northwestern Spain: WRF multiphysics ensemble assessment based on ground and multi-satellite observations. Atmospheric Res. 288, 106719. https://doi.org/10.1016/j.atmosres.2023.106719

Mora, J.Á.N., Martín, J.R., García, M.M., De Pablo Davila, F., Rivas Soriano, L., 2016. Climatological characteristics and synoptic patterns of snowfall episodes in the central Spanish Mediterranean area. Int. J. Climatol. 36, 4488–4496. https://doi.org/10.1002/joc.4645

Moreno, A., Bartolomé, M., López-Moreno, J.I., Pey, J., Corella, J.P., García-Orellana, J., Sancho, C., Leunda, M., Gil-Romera, G., González-Sampériz, P., Pérez-Mejías, C., Navarro, F., Otero-García, J., Lapazaran, J., Alonso-González, E., Cid, C., López-Martínez, J., Oliva-Urcia, B., Faria, S.H., Sierra, M.J., Millán, R., Querol, X., Alastuey, A., García-Ruíz, J.M., 2021. The case of a southern European glacier which survived Roman and medieval warm periods but is disappearing under recent warming. The Cryosphere 15, 1157–1172. https://doi.org/10.5194/tc-15-1157-2021

Navarro-Serrano, F., López-Moreno, J.I., Azorin-Molina, C., Alonso-González, E., Aznarez-Balta, M., Buisán, S.T., Revuelto, J., 2020. Elevation Effects on Air Temperature in a Topographically Complex Mountain Valley in the Spanish Pyrenees. Atmosphere 11, 656. https://doi.org/10.3390/atmos11060656

Navarro-Serrano, F., López-Moreno, J.I., Azorin-Molina, C., Alonso-González, E., Tomás-Burguera, M., Sanmiguel-Vallelado, A., Revuelto, J., Vicente-Serrano, S.M., 2018. Estimation of near-surface air temperature lapse rates over continental Spain and its mountain areas. Int. J. Climatol. 38, 3233–3249. https://doi.org/10.1002/joc.5497

Navarro-Serrano, F., López-Moreno, J.I., Azorin-Molina, C., Buisán, S., Domínguez-Castro, F., Sanmiguel-Vallelado, A., Alonso-González, E., Khorchani, M., 2019. Air temperature measurements using autonomous self-recording dataloggers in mountainous and snow covered areas. Atmospheric Res. 224, 168–179. https://doi.org/10.1016/j.atmosres.2019.03.034

Oliva, M., Andrés, N., Fernández-Fernández, J.M., Palacios, D., 2023. The evolution of glacial landforms in the Iberian Mountains during the Bølling–Allerød Interstadial, in: European Glacial Landscapes. Elsevier, pp. 369–377. https://doi.org/10.1016/B978-0-323-91899-2.00013-9

Oliva, M., Fernández-Fernández, J.M., Palacios, D., 2022a. The Iberian Mountains: glacial landforms prior to the Last Glacial Maximum, in: European Glacial Landscapes. Elsevier, pp. 309–316. https://doi.org/10.1016/B978-0-12-823498-3.00041-8

Oliva, M., Gómez-Ortiz, A., 2012. Late-Holocene environmental dynamics and climate variability in a Mediterranean high mountain environment (Sierra Nevada, Spain) inferred from lake sediments and historical sources. The Holocene 22, 915–927. https://doi.org/10.1177/0959683611434235

Oliva, M., Gómez-Ortiz, A., Salvador-Franch, F., Salvà-Catarineu, M., Palacios, D., Tanarro, L., Ramos, M., Pereira, P., Ruiz-Fernández, J., 2016a. Inexistence of permafrost at the top of the Veleta peak (Sierra Nevada, Spain). Sci. Total Environ. 550, 484–494. https://doi.org/10.1016/j.scitotenv.2016.01.150

Oliva, M., Nývlt, D., Fernández-Fernández, J.M. (Eds.), 2022b. Periglacial Landscapes of Europe. Springer International Publishing, Cham. https://doi.org/10.1007/978-3-031-14895-8

Oliva, M., Palacios, D., Fernández-Fernández, J.M., 2022c. The Iberian Peninsula, in: Iberia, Land of Glaciers. Elsevier, pp. 55–60. https://doi.org/10.1016/B978-0-12-821941-6.00004-9

Oliva, M., Palacios, D., Fernández-Fernández, J.M., 2022d. Iberia, in: Iberia, Land of Glaciers. Elsevier, pp. 555–588. https://doi.org/10.1016/B978-0-12-821941-6.00026-8

Oliva, M., Palacios, D., Fernández-Fernández, J.M., Rodríguez-Rodríguez, L., García-Ruiz, J.M., Andrés, N., Carrasco, R.M., Pedraza, J., Pérez-Alberti, A., Valcárcel, M., Hughes, P.D., 2019. Late Quaternary glacial phases in the Iberian Peninsula. Earth-Sci. Rev. 192, 564–600. https://doi.org/10.1016/j.earscirev.2019.03.015

Oliva, M., Ruiz-Fernández, J., Barriendos, M., Benito, G., Cuadrat, J.M., Domínguez-Castro, F., García-Ruiz, J.M., Giralt, S., Gómez-Ortiz, A., Hernández, A., López-Costas, O., López-Moreno, J.I., López-Sáez, J.A., Martínez-Cortizas, A., Moreno, A., Prohom, M., Saz, M.A., Serrano, E., Tejedor, E., Trigo, R., Valero-Garcés, B., Vicente-Serrano, S.M., 2018a. The Little Ice Age in Iberian mountains. Earth-Sci. Rev. 177, 175–208. https://doi.org/10.1016/j.earscirev.2017.11.010

Oliva, M., Serrano, E., Gómez-Ortiz, A., González-Amuchastegui, M.J., Nieuwendam, A., Palacios, D., Pérez-Alberti, A., Pellitero-Ondicol, R., Ruiz-Fernández, J., Valcárcel, M., Vieira, G., Antoniades, D., 2016b. Spatial and temporal variability of periglaciation of the Iberian Peninsula. Quat. Sci. Rev. 137, 176–199. https://doi.org/10.1016/j.quascirev.2016.02.017

Oliva, M., Žebre, M., Guglielmin, M., Hughes, P.D., Çiner, A., Vieira, G., Bodin, X., Andrés, N., Colucci, R.R., García-Hernández, C., Mora, C., Nofre, J., Palacios, D., Pérez-Alberti, A., Ribolini, A., Ruiz-Fernández, J., Sarıkaya, M.A., Serrano, E., Urdea, P., Valcárcel, M., Woodward, J.C., Yıldırım, C., 2018b. Permafrost conditions in the Mediterranean region since the Last Glaciation. Earth-Sci. Rev. 185, 397–436. https://doi.org/10.1016/j.earscirev.2018.06.018

OPCC-CTP, 2018. Climate change in the Pyrenees: Impacts, vulnerabilities and adaptation. Bases of knowledge for the future climate change adaptation strategy in the Pyrenees.

Palacios, D., De Andrés, N., Luengo, E., 2003. Distribution and effectiveness of nivation in Mediterranean mountains: Peñalara (Spain). Geomorphology 54, 157–178. https://doi.org/10.1016/S0169-555X(02)00340-9

Palma, P., Oliva, M., García-Hernández, C., Gómez Ortiz, A., Ruiz-Fernández, J., Salvador-Franch, F., Catarineu, M., 2017. Spatial characterization of glacial and periglacial landforms in the highlands of Sierra Nevada (Spain). Sci. Total Environ. 584–585, 1256–1267. https://doi.org/10.1016/j.scitotenv.2017.01.196

Pérez-Palazón, M., Pimentel, R., Polo, M., 2018. Climate Trends Impact on the Snowfall Regime in Mediterranean Mountain Areas: Future Scenario Assessment in Sierra Nevada (Spain). Water 10, 720. https://doi.org/10.3390/w10060720

Pérez-Palazón, M.J., Pimentel, R., Herrero, J., Aguilar, C., Perales, J.M., Polo, M.J., 2015. Extreme values of snow-related variables in Mediterranean regions: trends and long-term forecasting in Sierra Nevada (Spain). Proc. Int. Assoc. Hydrol. Sci. 369, 157–162. https://doi.org/10.5194/piahs-369-157-2015

Perşoiu, A., Buzjak, N., Onaca, A., Pennos, C., Sotiriadis, Y., Ionita, M., Zachariadis, S., Styllas, M., Kosutnik, J., Hegyi, A., Butorac, V., 2021. Record summer rains in 2019 led to massive loss of surface and cave ice in SE Europe. The Cryosphere 15, 2383–2399. https://doi.org/10.5194/tc-15-2383-2021

Perşoiu, A., Lauritzen, S.-E. (Eds.), 2018. Ice caves. Elsevier, Amsterdam, Netherlands.

Perșoiu, A., Onac, B.P., Wynn, J.G., Blaauw, M., Ionita, M., Hansson, M., 2017. Holocene winter climate variability in Central and Eastern Europe. Sci. Rep. 7, 1196. https://doi.org/10.1038/s41598-017-01397-w

Pimentel, R., Herrero, J., Polo, M., 2017. Quantifying Snow Cover Distribution in Semiarid Regions Combining Satellite and Terrestrial Imagery. Remote Sens. 9, 995. https://doi.org/10.3390/rs9100995

Pisabarro, A., Pellitero, R., Serrano, E., Gómez-Lende, M., González-Trueba, J.J., 2017. Ground temperatures, landforms and processes in an Atlantic mountain. Cantabrian Mountains (Northern Spain). CATENA 149, 623–636. https://doi.org/10.1016/j.catena.2016.07.051

Pons, M.R., Herrera, S., Gutiérrez, J.M., 2016. Future trends of snowfall days in northern Spain from ENSEMBLES regional climate projections. Clim. Dyn. 46, 3645–3655. https://doi.org/10.1007/s00382-015-2793-9

Racine, T.M.F., Spötl, C., Reimer, P.J., Čarga, J., 2022. RADIOCARBON CONSTRAINTS ON PERIODS OF POSITIVE CAVE ICE MASS BALANCE DURING THE LAST MILLENNIUM, JULIAN ALPS (NW SLOVENIA). Radiocarbon 64, 333–356. https://doi.org/10.1017/RDC.2022.26

Revuelto, J., Alonso-González, E., Gascoin, S., Rodríguez-López, G., López-Moreno, J.I., 2021a. Spatial Downscaling of MODIS Snow Cover Observations Using Sentinel-2 Snow Products. Remote Sens. 13, 4513. https://doi.org/10.3390/rs13224513

Revuelto, J., Azorin-Molina, C., Alonso-González, E., Sanmiguel-Vallelado, A., Navarro-Serrano, F., Rico, I., López-Moreno, J.I., 2017. Meteorological and snow distribution data in the Izas Experimental Catchment (Spanish Pyrenees) from 2011 to 2017. Earth Syst. Sci. Data 9, 993–1005. https://doi.org/10.5194/essd-9-993-2017

Revuelto, J., López-Moreno, J.I., Alonso-González, E., 2021b. Light and Shadow in Mapping Alpine Snowpack With Unmanned Aerial Vehicles in the Absence of Ground Control Points. Water Resour. Res. 57, e2020WR028980. https://doi.org/10.1029/2020WR028980

Revuelto, J., López-Moreno, J.I., Azorin-Molina, C., Vicente-Serrano, S.M., 2014a. Topographic control of snowpack distribution in a small catchment in the central Spanish Pyrenees: intra- and inter-annual persistence. The Cryosphere 8, 1989–2006. https://doi.org/10.5194/tc-8-1989-2014

Revuelto, J., López-Moreno, J.I., Azorin-Molina, C., Zabalza, J., Arguedas, G., Vicente-Serrano, S.M., 2014b. Mapping the annual evolution of snow depth in a small catchment in the Pyrenees using the long-range terrestrial laser scanning. J. Maps 10, 379–393. https://doi.org/10.1080/17445647.2013.869268

Rico, I., Izagirre, E., Serrano, E., López-Moreno, J.I., 2017. Superficie glaciar actual en los Pirineos: Una actualización para 2016. Pirineos 172, 029. https://doi.org/10.3989/Pirineos.2017.172004

Rico, I., Magnin, F., López Moreno, J.I., Serrano, E., Alonso-González, E., Revuelto, J., Hughes-Allen, L., Gómez-Lende, M., 2021. First evidence of rock wall permafrost in the Pyrenees (Vignemale peak, 3,298 m a.s.l., 42°46′16″N/0°08′33″W). Permafr. Periglac. Process. 32, 673–680. https://doi.org/10.1002/ppp.2130

Ruiz-Blas, F., Muñoz-Hisado, V., Garcia-Lopez, E., Moreno, A., Bartolomé, M., Leunda, M., Martinez-Alonso, E., Alcázar, A., Cid, C., 2023. The hidden microbial ecosystem in the perennial ice from a Pyrenean ice cave. Front. Microbiol. 14, 1110091. https://doi.org/10.3389/fmicb.2023.1110091

Salvador Franch, F., Gómez Ortiz, A., Salvà Catarineu, M., Palacios Estremera, D., 2013. Caracterización térmica de la capa activa de un glaciar rocoso en medio periglaciar de alta montaña mediterránea : El ejemplo del Corral del Veleta (Sierra Nevada, España). Cuad. Investig. Geográfica 37, 25–48. https://doi.org/10.18172/cig.1255

Sancho, C., Belmonte, Á., Bartolomé, M., Moreno, A., Leunda, M., López-Martínez, J., 2018. Middle-to-late Holocene palaeoenvironmental reconstruction from the A294 ice-cave record (Central Pyrenees, northern Spain). Earth Planet. Sci. Lett. 484, 135–144. https://doi.org/10.1016/j.epsl.2017.12.027

Sanmiguel-Vallelado, A., López-Moreno, J.I., Morán-Tejeda, E., Alonso-González, E., Navarro-Serrano, F.M., Rico, I., Camarero, J.J., 2020. Variable effects of forest canopies on snow processes in a valley of the central Spanish Pyrenees. Hydrol. Process. 34, 2247–2262. https://doi.org/10.1002/hyp.13721

Santos-González, J., González-Gutiérrez, R.B., Redondo-Vega, J.M., Gómez-Villar, A., Jomelli, V., Fernández-Fernández, J.M., Andrés, N., García-Ruiz, J.M., Peña-Pérez, S.A., Melón-Nava, A., Oliva, M., Álvarez-Martínez, J., Charton, J., Palacios, D., 2022. The origin and collapse of rock glaciers during the Bølling-Allerød interstadial: A new study case from the Cantabrian Mountains (Spain). Geomorphology 401, 108112. https://doi.org/10.1016/j.geomorph.2022.108112

Serrano Cañadas, E., 2023. Glaciares, cultura y patrimonio: la huella cultural de los glaciares pirenaicos. Universidad de Valladolid.

Serrano, E., Agudo, C., Delaloyé, R., González-Trueba, J.J., 2001. Permafrost distribution in the Posets massif, Central Pyrenees. Nor. Geogr. Tidsskr. - Nor. J. Geogr. 55, 245–252. https://doi.org/10.1080/00291950152746603

Serrano, E., Agudo, C., Martinez De Pisón, E., 1999. Rock glaciers in the Pyrenees. Permafr. Periglac. Process. 10, 101–106. https://doi.org/10.1002/(SICI)1099-1530(199901/03)10:1<101::AID-PPP308>3.0.CO;2-U

Serrano, E., De Sanjosé, J.J., González-Trueba, J.J., 2010. Rock glacier dynamics in marginal periglacial environments. Earth Surf. Process. Landf. 35, 1302–1314. https://doi.org/10.1002/esp.1972

Serrano, E., De Sanjosé-Blasco, J.J., Gómez-Lende, M., López-Moreno, J.I., Pisabarro, A., Martínez-Fernández, A., 2019. Periglacial environments and frozen ground in the central Pyrenean high mountain area: Ground thermal regime and distribution of landforms and processes. Permafr. Periglac. Process. 30, 292–309. https://doi.org/10.1002/ppp.2032

Serrano, E., Gómez-Lende, M., Belmonte, Á., Sancho, C., Sánchez-Benítez, J., Bartolomé, M., Leunda, M., Moreno, A., Hivert, B., 2018a. Ice Caves in Spain, in: Ice Caves. Elsevier, pp. 625–655. https://doi.org/10.1016/B978-0-12-811739-2.00028-0

Serrano, E., González-trueba, J.J., Sanjosé, J.J., Del Río, L.M., 2011. Ice patch origin, evolution and dynamics in a temperate high mountain environment: the jou negro, picos de europa (nw spain). Geogr. Ann. Ser. Phys. Geogr. 93, 57–70. https://doi.org/10.1111/j.1468-0459.2011.00006.x

Serrano, E., López-Moreno, J.I., Gómez-Lende, M., Pisabarro, A., Martín-Moreno, R., Rico, I., Alonso-González, E., 2020. Frozen ground and periglacial processes relationship in temperate high mountains: a case study at Monte Perdido-Tucarroya area (The Pyrenees, Spain). J. Mt. Sci. 17, 1013–1031. https://doi.org/10.1007/s11629-019-5614-5

Serrano, E., Morales, C., González-Trueba, J., Martín, R., 2012. Cartografía del permafrost de montaña en los Pirineos españoles. Finisterra vol. 44 n.o 87 (2009). https://doi.org/10.18055/FINIS1376

Serrano, E., Oliva, M., González-García, M., López-Moreno, J.I., González-Trueba, J., Martín-Moreno, R., Gómez-Lende, M., Martín-Díaz, J., Nofre, J., Palma, P., 2018b. Post-little ice age paraglacial processes and landforms in the high Iberian mountains: A review. Land Degrad. Dev. 29, 4186–4208. https://doi.org/10.1002/ldr.3171

Serrano, E., San José, J.J., Agudo, C., 2006. Rock glacier dynamics in a marginal periglacial high mountain environment: Flow, movement (1991–2000) and structure of the Argualas rock glacier, the Pyrenees. Geomorphology 74, 285–296. https://doi.org/10.1016/j.geomorph.2005.08.014

Stoffel, M., Luetscher, M., Bollschweiler, M., Schlatter, F., 2009. Evidence of NAO control on subsurface ice accumulation in a 1200 yr old cave-ice sequence, St. Livres ice cave, Switzerland. Quat. Res. 72, 16–26. https://doi.org/10.1016/j.yqres.2009.03.002

Tanarro, L.M., Hoelzle, M., García, A., Ramos, M., Gruber, S., Gómez, A., Piquer, M., Palacios, D., 2001. Permafrost distribution modelling in the mountains of the Mediterranean: Corral del Veleta, Sierra Nevada, Spain. Nor. Geogr. Tidsskr. - Nor. J. Geogr. 55, 253–260. https://doi.org/10.1080/00291950152746612

Tapiador, F.J., Villalba-Pradas, A., Navarro, A., Martín, R., Merino, A., García-Ortega, E., Sánchez, J.L., Kim, K., Lee, G., 2021. A Satellite View of an Intense Snowfall in Madrid (Spain): The Storm 'Filomena' in January 2021. Remote Sens. 13, 2702. https://doi.org/10.3390/rs13142702

Ventura Roca, J., 2016. IDENTIFICACIÓN E INVENTARIO DE POTENCIALES GLACIARES ROCOSOS ACTIVOS EN LOS PIRINEOS MEDIANTE FOTOINTEPRETACIÓN EN VISORES CARTOGRÁFICOS

2D Y 3D: PRIMEROS RESULTADOS. Polígonos Rev. Geogr. 95. https://doi.org/10.18002/pol.v0i28.4289

Vidaller, I., Izagirre, E., Del Rio, L.M., Alonso-González, E., Rojas-Heredia, F., Serrano, E., Moreno, A., López-Moreno, J.I., Revuelto, J., 2023. The Aneto glacier's (Central Pyrenees) evolution from 1981 to 2022: ice loss observed from historic aerial image photogrammetry and remote sensing techniques. The Cryosphere 17, 3177–3192. https://doi.org/10.5194/tc-17-3177-2023

Vidaller, I., Revuelto, J., Izagirre, E., Rojas-Heredia, F., Alonso-González, E., Gascoin, S., René, P., Berthier, E., Rico, I., Moreno, A., Serrano, E., Serreta, A., López-Moreno, J.I., 2021. Toward an Ice-Free Mountain Range: Demise of Pyrenean Glaciers During 2011–2020. Geophys. Res. Lett. 48, e2021GL094339. https://doi.org/10.1029/2021GL094339

Žák, K., Richter, D.K., Filippi, M., Živor, R., Deininger, M., Mangini, A., Scholz, D., 2012. Coarsely crystalline cryogenic cave carbonate – a new archive to estimate the Last Glacial minimum permafrost depth in Central Europe. Clim. Past 8, 1821–1837. https://doi.org/10.5194/cp-8-1821-2012.

CHAPTER 3

REVISITING THE ATMOSPHERIC VARIABLES IN SPAIN DURING THE OBSERVATIONAL PERIOD: VARIABILITY, TRENDS AND DRIVERS

Coordinators: Roberto Serrano-Notivoli[1], Cristina Peña[2], Raquel Nieto[3]

Leading Authors: Carmen Álvarez-Castro[2], Shalenys Bedoya-Valestt[4], David Corell[5], Pedro Dorta-Antequera[6], Luis Durán[7], José Carlos Fernández-Álvarez[8,3], Santos J. González-Rojí[9,10,11], Sixto Herrera[12], Agustí Jansà[13], Belén Rodríguez-Fonseca[7,14], Paloma Trascasa-Castro[15], Eduardo Utrabo-Carazo[4]

Collaborators: Arnau Amengual[13], Blanca Ayarzagüena[7], César Azorín-Molina[4], Samuel Barrao[1], Jorge Castillo-Mateo[16], Ana C. Cebrián[16], Jordan Correa González[6], Ahmed El Kenawy[17], María José Estrela[5], David Gallego[2], Iñigo Gómara[18], Amelia Gómez-Villar[19], Álvaro González[7], José A. Guijarro[20], Javier Herrero[21], Samira Khodayar[22], Aleksander Lacima-Nadolnik[15], Abel López-Díez[6], Teresa Losada[14], María C. Llasat[23], Maialen Martija-Diez[11,24], José L. Martín Esquivel[25], Adrián Melón-Nava[19], Javier Miró[5], Alfonso Pisabarro[19], Miguel A. Saz[1], Margarida Samso-Cabre[15], Javier Santos-González[19]

[1] Departmento de Geografía y Ordenación del Territorio, Instituto Universitario de Ciencias Ambientales (IUCA), Universidad de Zaragoza, Zaragoza, España.

[2] Departamento de Sistemas Físicos, Químicos y Naturales. Universidad Pablo de Olavide, Sevilla, España.

[3] Centro de Investigación Mariña, Environmental Physics Laboratory (EPhysLab), Universidade de Vigo, Ourense, España.

[4] Centro de Investigaciones sobre Desertificación, Consejo Superior de Investigaciones Científicas (CIDE, CSIC-UV-Generalitat Valenciana), Climate, Atmosphere and Ocean Laboratory (Climatoc-Lab), Moncada, Valencia, España.

[5] Departamento de Geografía, Universidad de Valencia, Valencia, España.

[6] Cátedra Universitaria de Reducción del Riesgo de Desastres y Ciudades Resilientes de la Universidad de La Laguna, San Cristóbal de La Laguna, España.

[7] Departamento de Física de la Tierra y Astrofísica, Universidad Complutense de Madrid, Madrid, España.

[8] Galicia Supercomputing Center (CESGA), Santiago de Compostela, Spain

[9] Climate and Environmental Physics, University of Bern, Bern, Switzerland

[10] Oeschger Centre for Climate Change Research, University of Bern, Bern, Switzerland

[11] Departamento de Física, Universidad del País Vasco, Leioa, España.

[12] Departamento de Matemática aplicada y Ciencias de la Computación, Universidad de Cantabria, Santander, España.

[13] Grupo de Meteorología, Dtp. De Física, Univ. de les Illes Balears (UIB), Palma de Mallorca, España.

[14] Instituto de Geociencias (IGEO), UCM-CSIC, Madrid, España.

[15] Barcelona Supercomputing Center-Centro Nacional de Supercomputación, Barcelona, España.

[16] Departamento de Métodos Estadísticos, Universidad de Zaragoza, Zaragoza, España.

[17] Instituto Pirenaico de Ecología, Consejo Superior de Investigaciones Científicas (IPE-CSIC), Zaragoza, España.

[18] Departamento de Matemática Aplicada, Escuela de Ingeniería Informática, Universidad de Valladolid, Segovia, España.

[18] Departamento de Geografía y Geología, Universidad de León, León, España.

[20] Retirado de la Agencia Estatal de Meteorología (AEMET), Palma de Mallorca, España.

[21] Modeling Nature (MNAT), Facultad de Ciencias, Universidad de Granada, Granada, Spain

[22] Área de Meteorología y Climatología, Centro de Estudios Ambientales del Mediterráneo (CEAM), Valencia, España.

[23] GAMA, Departamento de Física Aplicada, Universitat de Barcelona, Barcelona, España.

[24] EUSKALMET, Agencia Vasca de Meteorología, Vitoria-Gasteiz, España.

[25] Parque Nacional del Teide, La Orotava, Tenerife, Islas Canarias, España.

1. Introduction

Natural climate variability refers to variations in climate caused by processes other than human influence. It includes variability generated internally within the climate system and variability driven by natural external factors. In Spain, the climate shows a very marked natural variability, with important changes at different timescales from interannual to multidecadal, which is most pronounced in precipitation and especially in the areas of the Mediterranean basin. In this region, the annual coefficient of variation of precipitation exceeds 20 % and can reach 40 % in the southeastern part of the IP, with a frequent occurrence of wet and dry years. Different studies have shown that the weather systems affecting the IP are controlled by a small number of large-scale patterns (e.g., Rodriguez-Puebla et al., 1998; Sánchez-López, 2016; Trigo et al., 2002). Among these patterns, the one that shows the greatest influence is the North Atlantic Oscillation (NAO), which is the most prominent and recurrent pattern of atmospheric variability over the middle and high latitudes of the Northern Hemisphere (Hurrell et al., 2003). The NAO exerts a significant influence on temperature and precipitation patterns over the IP and even on precipitation over the Canary Islands (Sánchez-Benítez et al., 2017; Trigo et al., 2002). During the positive phase of the NAO the IP tends to experience milder and drier conditions. Conversely, during the negative phase of the NAO, colder air masses can penetrate further southward into the IP, leading to cooler temperatures. Additionally, the negative phase of the NAO is associated with enhanced storm track activity across the North Atlantic, which can result in increased precipitation over most of the IP (Castro-Díez et al., 2002; Trigo et al., 2002). In addition to the NAO, other North Atlantic-European modes of climate variability, such as the East Atlantic and Scandinavian patterns, are also known to play a significant role in modulating climate variables in the IP (Comas-Bru and McDermott, 2014; Jerez and Trigo, 2013; Sánchez-López, 2016). Despite its weaker influence, the Southern Oscillation (SO, El Niño/La Niña) can also affect

the precipitation over the IP and the Canary Islands (Brönnimann, 2007; Rodriguez-Puebla et al., 1998; Vicente-Serrano, 2005). Furthermore, precipitation over the eastern coast of the IP is influenced by low frequency regional patterns such as the Mediterranean Oscillation and the Western Mediterranean Oscillation (WeMO, Dünkeloh and Jacobeit, 2003; Martin-Vide and López-Bustins, 2006).

Another important aspect of climate variability in Spain is the occurrence of temperature and precipitation extremes. Although recently, in January 2021, Spain was affected by two extreme events, a long cold spell and a heavy snowfall event associated with the extratropical cyclone Filomena, winter extremes of such intensity are very unusual (Buisán et al., 2022). On the other hand, torrential rainfall events are frequent at the end of summer and in autumn along a coastal and pre-coastal fringe on the eastern, Mediterranean side of the IP, including the Balearic Islands, usually linked to convective "cold drops" or cut-off low (COL) type phenomena (isolated low level pressure systems at atmospheric high levels) (Ferreira, 2021; Nieto et al., 2007). However, the extremes that pose the greatest risk to the health and well-being of the population as well as to ecosystems and the economy are heat waves and droughts, which frequently affect large areas of the country (García-Herrera et al., 2010; Salvador et al, 2020; IPCC, 2023; Serrano-Notivoli et al., 2023). Although the occurrence of these extremes is common in the Mediterranean climate (Domínguez-Castro et al., 2019; IPCC, 2023; Serrano-Notivoli et al., 2022), climate change is intensifying the frequency and intensity of heat waves and droughts, making Spain, along with the entire Mediterranean basin, particularly sensitive to rising concentrations of greenhouse gases (IPCC, 2023).

Due to its location on the border between the arid subtropics and the temperate midlatitudes, Spain is highly vulnerable to the effects of climate change. Large parts of its territory, especially the southeastern IP and the Canary Islands, are characterised by warm and dry summers, low annual precipitation totals and high interannual variability, leading to a state of semi permanent water stress. The subtropical location under the descending air extending from the North Atlantic subtropical high controls the low summer precipitation, while the high precipitation in the cold season is mainly controlled by midlatitude westerly wind regimes. Consequently, winter precipitation is key to the region's agriculture and economy, and understanding how climate change is affecting them or how precipitation will evolve with rising global temperatures is critical. However, the pronounced decadal variability over the IP, coupled with the fact that observations show a strong spatial and seasonal variability in precipitation trends, determines a large uncertainty that makes difficult to identify long-term links between precipitation in the IP and global temperature (Lionello and Scarascia, 2018; Vicente-Serrano et al., 2017). Models project, across all scenarios, a large reduction in cold season precipitation that could be in the range between 10-20 % for a 4 ºC global warming (IPCC, 2023), which could be even stronger in summer, when it could reach a reduction of 40 % at 4 ºC global warming relative to 1995-2014. This would exacerbate the increased trend observed over the last decades in the severity of summer droughts, related to precipitation variations (Liu et al., 2022).

In terms of air temperature, observations indicate that Spain, together with the entire Mediterranean basin, has indeed been warming since the 1980's at a higher rate than the global average (IPCC, 2023; Lionello and Scarascia, 2018). The observed air temperature has increased in all seasons, but in a particularly pronounced way during summer. Furthermore, the frequency and intensity of

hot extremes have increased in recent decades and are projected to keep increasing regardless of the greenhouse gas emissions scenario (IPCC, 2023).

This context, in which we are observing how the climatic conditions in Spain are becoming increasingly severe, in terms of an increase in the frequency and intensity of droughts and heat extremes, while projections indicate that this situation will worsen in the future, makes it essential to rigorously monitor the evolution of the climate behaviour in our territory. Instrumental data, obtained from direct measurements using various climate-monitoring instruments and techniques, provide a comprehensive record of climate variables such as temperature, precipitation, wind, etc. Analysing these data allows the detection of long-term trends indicative of climate change. They are also crucial for understanding natural variability, which in turn is essential for distinguishing between natural climate fluctuations and those induced by external factors, particularly human-induced climate change.

This chapter offers a review of the changes in climate variability over the instrumental period in Spain. The first section describes the observational gridded datasets available for precipitation and temperature in Spain, at different temporal and spatial resolutions. Sections 2, 3 and 4 describe the most recent results on observed changes in air temperature, precipitation, wind and atmosphere moisture. In section 5, the main circulation modes affecting Spain are analysed and section 6 describes the specific conditions of some particular regions such as the Canary and Balearic Islands, as well as those of mountain systems and cities.

2. Data

Changes in climate variability over the instrumental period are assessed through the available observations recorded at meteorological stations. However, they do not cover the whole spatial domain and they are especially scarce in remote and complex topography areas. Gridded datasets provide a continuous representation of climatic variables that, depending on the spatial and temporal resolution as well as the number of observations used to create them (Merino et al., 2021), provide reliable and representative climatic information for any spatial domain. Over the last decade, the number of available gridded datasets have greatly increased, mainly influenced by the higher reproducibility of the methods, the computational power, and the availability of the data, which have promoted the current and unprecedented ease of data access (Serrano-Notivoli and Tejedor, 2021). The datasets developed for almost all countries included similar methodologies but different spatial and temporal resolutions.

In Spain, the National Climatic Data Bank (BNDC) of the State Meteorological Agency (AEMET), together with other databases of regional and national official organizations, comprise discontinuous information on climatic data from more than 10,000 observatories, of which <0.2 % have more than 99 % of the data available for the period from the mid-20th century to the present. In addition, the Ministry of Agriculture, Fisheries and Food and the Automatic Hydrological Information Systems from Hydrological Confederations also maintain their own meteorological networks with several hundred stations. While all of this information can be accessed and used to study climate variability in Spain, a lot of work must be done in filtering the data, removing abnormal values, and reconstructing time series where necessary, to obtain reliable long-term information. Since the mid-2000's, great efforts have been made to develop a number of gridded datasets in Spain. As a result, different gridded databases are now available

Name	Variable(s)	Temporal range [resolution] Spatial domain [resolution]	Source
Iberia01	pr, tas, tasmax, tasmin	1971-2015 [daily] IP/BI [0.1ºx0.1º regular]	https://doi.org/10.5194/essd-11-1947-2019
SPREAD	pr	1950-2012 [daily] (IP) 1971-2012 [daily] (BI/CI) IP/BI/CI [5x5 km regular]	https://doi.org/10.5194/essd-9-721-2017
STEAD	tasmax, tasmin	1901-2014 [daily] (IP) 1971-2014 [daily] (BI/CI) IP/BI/CI [5x5 km regular]	https://doi.org/10.5194/essd-11-1171-2019
SPAIN-AEMET	pr, tasmax, tasmin	1951-2022 [daily] IP/BI [5x5 km rotated]	https://www.AEMET.es/documentos/es/conocermas/recursos_en_linea/publicaciones_y_estudios/publicaciones/NT_24_AEMET/NT_24_AEMET.pdf
MOTEDAS century	tasman, tasmin	1916-2015 [monthly] IP/BI [10x10 km regular]	https://doi.org/10.1002/joc.6520
MOPREDAS century	pr	1916-2020 [monthly] IP [10x10 km regular]	https://doi.org/10.1002/joc.8060
CLIMPY	pr, tasmax, tasmin	1981-2020 [daily] Pyrenees [1x1 km regular]	https://doi.org/10.1016/j.scitotenv.2024.173052
Climatic atlas of Aragón	pr, tasmax, tasmin	1950-2020 [daily] Aragón [1x1 km regular]	https://idearagon.aragon.es/atlas/Clima/info/atlas-climatico-aragon
Climatic Scenarios of Euskadi and observations (viewfinder/thredds)	pr, tas, tasmax, tasmin	1971-2016 [monthly] País Vasco [1x1 km regular]	http://escenariosklima.ihobe.eus/ http://escenariosklima.ihobe.eus/thredds/catalog.html

Table 3.1. Observational datasets available for Spain. pr: precipitation; tas: mean temperature; tasmax: maximum temperature; tasmin: minimum temperature; IP: Iberian Peninsula; BI: Balearic Islands; CI: Canary Islands; SPREAD: Spanish Precipitation At Daily Scale; STEAD: Spanish Temperature At Daily Scale; MOTEDAS: MOnthly Temperature Dataset of Spain; MOPREDAS: MOnthly PREcipitation Dataset of Spain; CLIMPY: CLImate of the PYrenees.

(Table 3.1) based on the use of all or part of the observations over time. Although they span different periods at different spatial and temporal resolutions, their reliability has been proven and endorsed by scientific publications. Some of them can be accessed through web map services, but all are available as open-access download or by request.

3. Temperature

The present report builds on the scientific results published since the previous effort by Vicente-Serrano et al., 2017 to describe the recent evolution and trends of different surface variables, and their extremes, based on observational networks. In their review, Vicente-Serrano et al., 2017 found a strong increase in temperature since the 1960's, which was more pronounced during summer months (0.3 ºC/decade). However, a slowdown of the mean temperature increase was recorded from the end of the 1990's, mainly driven by the evolution of the maximum temperature. Nevertheless, the frequency of extreme warm temperature events (heat waves) noticeably increased from 2000. As a result, the observed warming has impacts on the definition of the warm season in Spain, with an increment in the length of the summer season ranging between 5 and 12 days/decade for the period 1979-2012 (Peña-Ortiz et al., 2015). The increase in the frequency of warm temperature extremes was continuous during the past two decades in the whole country. Since 2017 some of these results have been ratified and/or extended/complemented in the literature, as reflected in this report. In addition, new datasets (see Table 3.1), indices and methodologies have been published and made accessible for the scientific community, allowing a deeper analysis of the trends observed during the observational period.

Although the BNDC-AEMET is the main source of data for climate analysis, it does not contain all the historical records from the observatory network, as a large amount of data has not been digitised. In recent years, several authors have made great efforts to rescue and digitise historical datasets, such as the Annual Climate Summaries books published by the meteorological services from 1860 to 1950, scientific annals, newspapers and monographs (Beguería et al., 2023; González-Hidalgo et al., 2020; Vaquero et al., 2022). In addition, the European Climate Assessment and Dataset project (ECA&D, Klein Tank et al., 2002) has progressively incorporated new observational datasets (e.g. Meteorological Service of Catalonia and synoptical messages from the Global Telecommunications System (GTS) network) and stations over Spain, increasing both the temporal and the spatial coverage.

Despite the overall warming signal observed in the last century, this rise has not been homogeneous in time nor space. Moreover, recent studies have highlighted the need to analyse independently, for the same variable, the evolution of the central part and the tails of the distribution (Castillo-Mateo et al., 2023; Schliep et al., 2021), to consider the heat- and cold-waves as interrelated events (Serrano-Notivoli et al., 2022), and to analyse the different sources of uncertainty that could affect the historical trend analysis (Padial-Iglesias et al., 2022).

3.1 Changes in annual and seasonal mean temperature

Sandonis et al., 2021, using the MOTEDAS gridded dataset (see Table 3.1, González-Hidalgo et al., 2020), reveals an increase in the mean annual temperature of 0.10 ºC/decade in continental Spain for the period 1916-2015. These results are similar to those obtained by Brunet et al., 2007, who, using the 22 longest temperature series of all those available for the Iberian Peninsula, found a significant increase in the mean annual temperature of 0.10 ºC/decade in the period 1850-2005 and 0.13 ºC/decade for the period 1901-2005. Their analysis through 50-year moving windows revealed that the highest positive (and significant) trends occurred between 1950 and 2012 (Figure 3.1).

According to Sandonis et al., 2021, the mean annual temperature in continental Spain has had several fluctuations from the beginning of the 20th century to the present day, and different

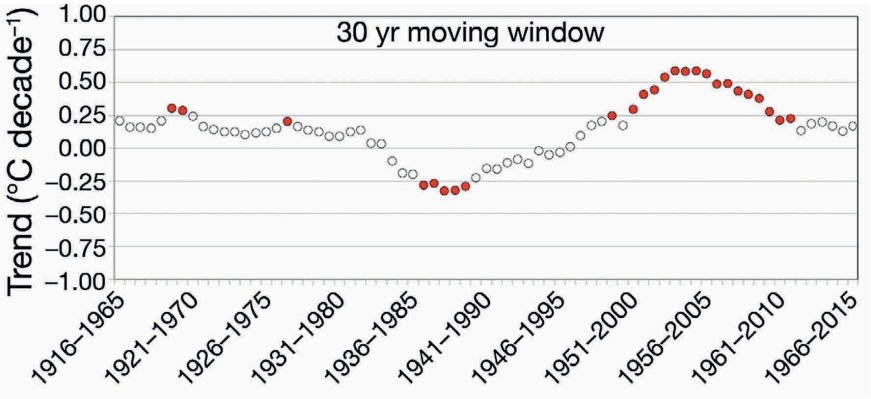

Figure 3.1. Annual mean value rate trend (°C/decade) over 30 years. Filled red circles: $p < 0.05$; empty circles: not significant. Source: Sandonis et al., 2021.

phases can be distinguished. In the first phase, a slight increase in air temperature was observed from the beginning of the series until the 1950's. In the second phase, no clear trend was observed in the early years, while a cooling was observed between the 1960's and 1970's. In the third phase, a sharp warming was detected from the 1970's to the present day. Note that these two overall sub-periods have also been reflected by other authors using different data sources (AEMET, 2023, 2022; Paniagua et al., 2019). During the last phase, the increase has not been monotonous either, with the authors describing a period of pause or hiatus between 1990 and 2015, where the values, despite being high, did not show a clear upward trend. However, other studies using gridded and high-quality observational data for peninsular Spain, Ceuta, Melilla and the Balearic Islands, and for the period 1961-2018, calculated a warming trend in the mean annual temperature of 0.21 ºC/decade, showing the same pattern of temperature increase in the last annual records of the series (AEMET, 2023, 2022).

Some studies have analysed the seasonal behaviour of the mean temperature and differences between seasons have been observed. According to AEMET, 2023, 2022, summer has been the season that has contributed most to the temperature increase in Spain (including peninsular Spain, Ceuta, Melilla and the Balearic Islands) during the period 1961-2018. The results show a statistically significant trend towards temperature increase of 0.27 ºC/decade in this season and 0.24 ºC/decade in spring, both seasons having a greater weight in the warming effect than autumn and winter, whose trend has been in both cases of 0.16 ºC/decade. The greater weight of summer and spring in the annual warming has also been observed by other authors (Espín-Sánchez et al., 2023; Rodrigo, 2019; Sandonis et al., 2021) considering different data sources.

3.2 Changes in annual and seasonal maximum (Tmax) and minimum (Tmin) temperatures

González-Hidalgo et al., 2020, using gridded data obtained from the observations of 5,259 thermometric stations, analysed the evolution of Tmax and Tmin temperature over

continental Spain. This study revealed an increasing temperature trend of 0.12 ºC/decade for Tmax and 0.10 ºC/decade for Tmin in the 1916-2015 period. The results are similar to those obtained by Brunet et al., 2007, who, using the longest data series available, estimated an increase of 0.11 ºC/decade for Tmax and 0.08 ºC/decade for Tmin during the period 1850-2005, as well as 0.17 ºC/decade for Tmax and 0.09 ºC/decade for Tmin during the period 1901-2005.

The evolution of maximum and minimum temperatures over the last 100 years has not been homogeneous, with a behaviour similar to that of the mean temperature. There was a first phase of slight temperature increase observed until the 1950's. Then, there was a second phase without a clear trend, followed by a cooling phase between the 1960's and 1970's. And, finally, there was a phase of greater increase in temperature from the 1970's to the present. As with the mean temperature, the authors speak of a pause or hiatus period from the late 1980's to 2015. Likewise, the AEMET study (AEMET, 2023, 2022), which uses more recent data from Peninsular Spain, Ceuta, Melilla and the Balearic Islands, estimated, for the period 1961-2018, an increase of 0.20 ºC/decade for maximum temperatures and 0.21 ºC/decade for minimum temperatures, observing a temperature increase in both variables in recent years.

The seasonal behaviour of maximum and minimum temperatures has also been analysed by several authors. According to Peña-Angulo et al., 2021, the highest trend rates for the period 1916-2015 correspond to Tmax in spring (0.16 °C/decade) and summer (0.13 °C/decade), while for Tmin, the highest rates occur in summer (0.13 °C/decade) and autumn (0.11 °C/decade). Statistically significant warming trends were found in all the seasons analysed. The study also indicates the presence of two rising periods, and also intermediate and a final pause. In turn, it points out that the trend observed in Tmax depends mainly on spring, summer and autumn during the first rising period; and winter, spring and summer during the second. As for Tmin, spring, summer and autumn define the two periods of increase. On the other hand, for the period 1961-2018 and peninsular Spain, Ceuta, Melilla and the Balearic Islands, summer and spring have been the seasons that have shown the greatest warming trend in Tmax (0.26 ºC/decade), while winter has been the season with the lowest trend (0.05 ºC/decade). In the case of Tmin, summer was the season that contributed the most to warming (0.28 ºC/decade) (AEMET, 2023, 2022).

González-Hidalgo et al., 2022 analysed the monthly evolution of Tmax and Tmin, using the same database and the same study period as Peña-Angulo et al., 2021 and Sandonis et al., 2021. The main conclusions of this study can be summarised as follows: 1) Temperature increases have not occurred uniformly in all months, but have been specific to certain months, in particular March and December, as well as June and July in a lesser extent, for Tmax; and August and October for Tmin; 2) The warming trend has not followed a monotonic trajectory and two different periods of temperature increase have been identified, affecting specific months; 3) A period of temperature stagnation in both Tmax and Tmin has been observed in all months during the last decades; 4) Tmax and Tmin presented an asynchronous behaviour, showing independent evolution from each other; 5) Large spatial variability and differences between months, with two predominating gradients of expansion–contraction: east–west for Tmax and west–east for Tmin.

3.3 Changes in extreme temperature events

As has been reflected by the Intergovernmental Panel On Climate Change, 2023, many changes in the climate system become larger in direct relation to increasing global warming, including increases in the frequency and intensity of hot extremes. In the previous sections, an overall positive trend for the historical period in mean, maximum and minimum temperatures has been described based on observational and gridded datasets. However, other studies have emphasised that extreme temperature events should be analysed from a multi-dimensional perspective (Díaz-Poso et al., 2023a, 2023b; Sánchez-Benítez et al., 2020) or considering both cold and heat extremes (Paredes-Fortuny and Khodayar, 2023; Serrano-Notivoli et al., 2022) to properly assess the impact of extreme events. To achieve this goal, various indices for both cold and heat extremes, and/or methods, have been proposed in the literature to characterise the intensity, duration, frequency, and spatial extension of extreme events during the historical period (Cebrián et al., 2022; Schliep et al., 2021). In this context, Castillo-Mateo et al., 2023 found that the effect of an increasing trend in the occurrence of record events in daily maximum temperature is statistically significant throughout Spain, except in the North and the Cantabrian Coast areas.

In relation with heat-waves, regardless the index analysed, an increment in frequency (+0.3 events/decade), intensity (+0.1 ºC/decade), duration (+0.9 days/decade for the yearly maximum duration) and spatial extent (+1.3 % of the IP/decade) has been observed during the period 1951-2019 (Paredes-Fortuny and Khodayar, 2023, Figure 3.2) using the gridded dataset produced by AEMET (see Table 3.1). In addition, the onset of the heat-wave season occurs earlier in time (4 days/decade) leading to a larger warm season. In terms of spatial impacts, the most affected region in terms of frequency is the centre of the Iberian Peninsula, while the northern and south-eastern Mediterranean are the most affected regions in terms of intensity, and the southern and north-eastern regions of the Peninsula suffer the longest duration. Similar results were obtained by (Díaz-Poso et al., 2023b) considering the period 1950-2020 and the European gridded dataset E-OBS (Cornes et al., 2018). As could be expected based on the previous sections, these frequencies increase when a shorter and more recent period is considered, reaching a trend for the frequency of +1.0 to +2.6 heat-wave events per decade during the period 1979-2017 (Sánchez-Benítez et al., 2020). As has been previously reflected this evolution is not constant or linear during the historical period with a change in the 1980's from colder to warmer conditions, from more intense cold-waves to more intense heat-waves (Serrano-Notivoli et al., 2022).

The overall warming affects also to the cold extreme events, mainly over the mountain ranges of Spain (Díaz-Poso et al., 2023b; García-Martín et al., 2021), which tend to decrease during the observational period. García-Martín et al., 2021 concludes that the number of frost days per year decrease for 68 weather stations over the IP during the period 1975-2018, leading to an increment of the frost-free period due to a delay of the autumn frost (0.4-1.06 days/year) and an a decrease of early spring frosts ((-0.43)-(-1.29) days/year). This reduction in the number of frosts was more pronounced in the higher-elevation stations as well as the increment of the frost-free period. Díaz-Poso et al., 2023b shows that there is no increase in the number of cold wave days at any point of the Iberian Peninsula for the period 1971–2000, being the negative trend more accentuated in the east of the Peninsula and in the main mountain systems, where there is a significant trend of –2 days/decade.

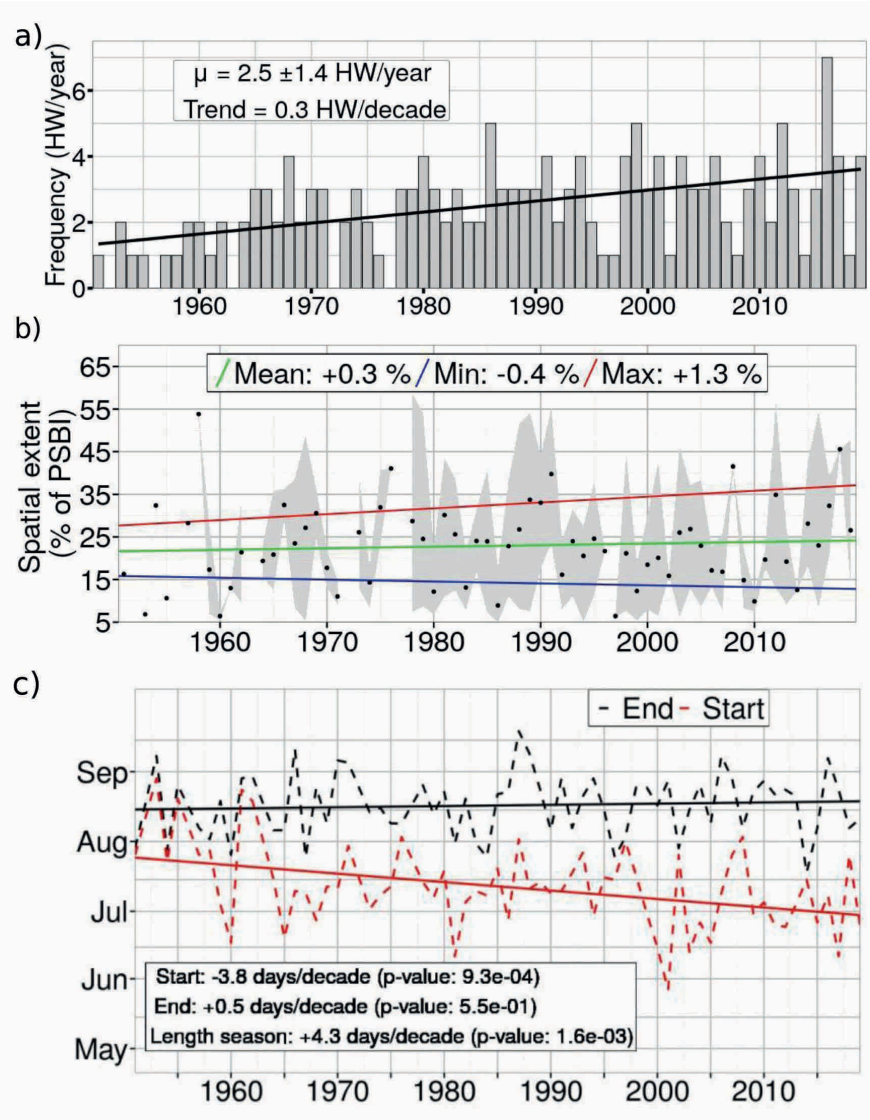

Figure 3.2. Frequency of heatwaves in 1951–2019 period in IP and Balearic Islands. a) Temporal evolution of the extended summer (May to September) frequency of the heatwaves in grey bars and its corresponding trend. b) Temporal evolution of the spatial extent, where black dots represent the yearly mean, the shaded grey area represents the range between the yearly maximum and minimum values. Straight lines represent the trend of the yearly maximum value (red), minimum value (blue), and mean value (green). c) Temporal evolution of the heatwave season (HWS) starting day (red), ending day (black) in dashed lines and its corresponding trends in continuous lines. **Source:** Paredes-Fortuny and Khodayar, 2023.

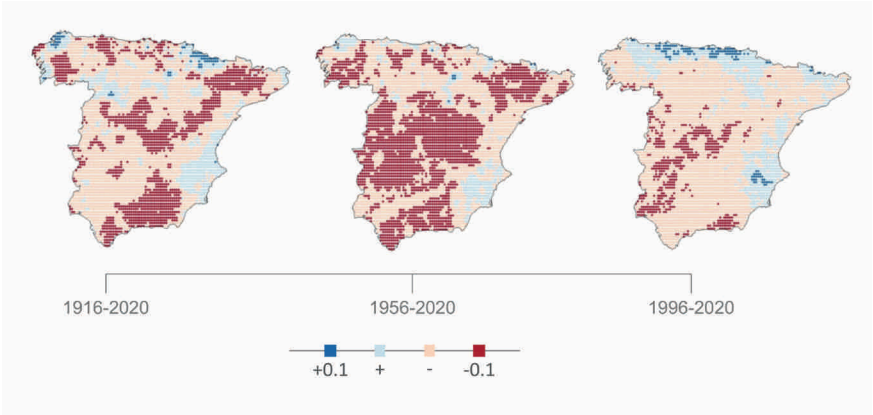

Figure 3.3. Annual precipitation trends in three temporal windows from 1916–2020 (105 years) 1956–2020 (65 years) and 1996–2020 (25 years). Blue (red) colours indicate positive (negative) trends, while dark (pale) colour shades indicate significance (nonsignificance), according to Mann–Kendall test and significance level $\alpha = 0.10$. Source: Adapted from González-Hidalgo et al., 2023.

At regional scale, some studies have focused on the temporal evolution of the minimum temperature over the eastern and south-eastern region of the IP (Olcina Cantos et al., 2019; Sánchez-Benítez et al., 2020), reflecting an increment of the intensity (~0.2 ºC/decade), frequency (11 days and 2-3 3-day spell events) and length of the season (13-19 days) of tropical nights, more significant over the coast than inland, and a reduction of cold-nights, cold-spell duration and frost days.

4. Precipitation

4.1 Changes in annual and seasonal mean precipitation

Most of the annual precipitation trends in Spain are not significant (Caloiero et al., 2018; Coll et al., 2017; González-Hidalgo et al., 2023; Paniagua et al., 2019; Philandras et al., 2011). Although, in general, there is no clear and homogeneous trend in the sign of precipitation, most studies (e.g., Camuffo et al., 2013; Serrano-Notivoli, 2017; Peña-Angulo et al., 2020; Senent-Aparicio et al., 2023) point to a slight decrease (not significant in all areas) in annual totals since the second half of the 20th century, which masks potential heterogeneous behaviours at a seasonal and monthly scale. As stated in Bladé, I. et al., 2010, "*when studies on precipitation trends in the Iberian Peninsula are compared, it is common to find discrepancies and contradictions in the results, even when they are trends relative to the same period*". In this regard, González-Hidalgo et al., 2024, 2023 showed that precipitation trends greatly change their spatial variability when temporal period is changed (Figure 3.3). However, spatial patterns in the similar period as previous research (mid-1950's to 2020), also showed large variability with a general decrease.

The general decline shown in Peninsular Spain is conditioned by a marked interannual variation and with important spatial contrasts. Two well-differentiated areas are highlighted: the Mediterranean coast that shows positive trends (although previous studies (e.g. Valdés-Abellán et al., 2017) found specific areas and temporal periods with inverse behaviour), and the rest of the Peninsular Spain in which trends are negative, of greater magnitude and significance especially in the south of Galicia, southeastern and central Peninsula, and also in the eastern Pyrenees. However, these patterns experimented great changes over the 20th century and in different regions, for example, northern area experimented positive significant changes since the 1980's decade and the Ebro basin have shown negative trends with great differences from lowlands to the Pyrenees (López-Moreno et al., 2011; Lutz et al., 2016). Regional-oriented studies of eastern IP for the period 1955-2016, using a dense network of rainfall stations, showed a general negative trend in the area covering the basins of the Tagus and Segura rivers (Miró et al., 2018). The general loss of precipitation is due to the decrease in rainfall recorded in winter (December, January and February) and, mainly, in summer (June, July and August). Miró et al., 2023 detected a notable loss of moderate precipitation in the headwaters of several of the rivers that have their origin in this region in the east of the Iberian Peninsula, such as the Tajo, Guadiana, Júcar and Segura. According to Miró et al., 2018 differences in the eastern Iberian Peninsula precipitation can be detected depending on the origin: 1) Precipitation of Atlantic origin has been significantly reduced, which may explain the loss of rainfall detected in the headwaters of several rivers, since this is their main source; 2) Precipitation of Mediterranean genesis, which may result in torrential rains, has increased in areas more susceptible to this type of rain; 3) The temporal distribution of convective rains is undergoing changes, with a decreasing frequency observed in summer (resulting in a decline in summer storms) and an increased frequency in the remaining months of the year.

Even with differences depending on the period and regions studied, there is a consensus in the confirmation of a decrease of precipitation in March and June and a slight increase in October (del Río et al., 2011; González-Hidalgo et al., 2011), potentially due to a temporary shift in the spring and autumn maximums, respectively, due to the increasingly warm conditions of the atmosphere and ocean masses. García-Barrón et al., 2018 reported a multidecadal shift in the seasonal cycle of precipitation from the 1970's, towards an increase of frequency of rain in spring.

Seasonal precipitation shows a significant negative trend in winter, spring and summer in very specific sectors of the northeast of the peninsula in the first two cases and the eastern Pyrenees in the third, with some geographical areas of lesser spatial importance in the southern half of the peninsula (De Luis et al., 2010; Serrano-Notivoli, 2017). Negative trends were also significant in inland areas of southeastern Andalusia and in Balearic Islands until the first decade of the 21st century (Homar et al., 2010; Ruiz Sinoga et al., 2011). These negative trends are especially related to the 1960's and 1970's and linked to decreases in precipitation at the end of winter (February and March) and to a lesser extent in June (Bladé, I. et al., 2010). Autumn depicts a general positive trend that is only significantly evident in some sectors of the southern third of the Peninsula, the westernmost Atlantic provinces and specific areas of the middle section of the Ebro River. These positive trends are associated with an increase in October rainfall and less in November, with a high regional differentiation.

The spatial distribution of trends indicates a general decrease in precipitation in winter (with increases on the Mediterranean coast), which is only significant in very specific areas of the territory. The negative trend in the northern third has been explained in previous works (Pérez et al., 2010) by its relationship with the NAO. In the winter months, when the strength of the westerly winds is greater and the latitudinal pressure contrasts are more intense, changes in the NAO contribute, in the long term, to producing changes in the expected precipitation regime. Declines are also observed throughout the peninsula in summer (Serrano-Notivoli, 2017), especially in the eastern Pyrenees, the headwaters of the Tagus River, the northeastern foothills of the central system and some isolated points in the northern third of the peninsula. A somewhat different behaviour in spring shows, on the one hand, negative trends in the western half that, generalised in the interior of Galicia, respond to a significant reduction in totals in March, as indicated in the majority of the studies. Intense decreases are also observed in the southeast of the peninsula, in Cabo de Gata. The eastern half shows positive trends in the southern half of Aragon and the interior of the Valencian Community. In autumn the increase is generalised, with special intensity and significance in the southern half of the peninsula, covering the Guadalquivir valley, Extremadura and Castilla-La Mancha.

4.2 Changes in extreme precipitation and droughts

Regarding the changes observed as a function of rainfall intensity, Miró et al., 2018, pointed to a decrease in moderate rainfall, and a simultaneous increase in torrential rainfall. According to this, the regions traditionally susceptible to frequent torrential rainfall events, in particular the coastal area between the south of the province of Valencia and the north of the province of Alicante, have shown a clear upward trend in this type of precipitation. As a result, an increase of extreme torrential rainfall events (≥ 200 mm/day), both in terms of magnitude and frequency is confirmed. A significant number of the torrential rainfall events are related to COL configurations (Miró et al., 2018), atmospheric situations with an interannual variability of 20 % in 1960-2017 period (Muñoz et al., 2020) and is changing in terms of temporal distribution (Meseguer-Ruiz et al., 2021). An increase in this type of precipitation has been detected in November and a decrease in October. The progressive warming of the Mediterranean sea temperatures in November, combined with easterly circulation in the lower troposphere and advection of polar air in the mid and high troposphere, might explain this change. These conditions can transport more energy and water vapour, leading to extreme torrential events (Meseguer-Ruiz et al., 2021).

The analysis of the temporal evolution of convective precipitation in the Júcar Hydrographic Confederation (CHJ) and the Internal Basins of Catalonia (CIC), showed a significant increase in convective precipitation in the CHJ and a significant increase in convective episodes in both regions (Llasat et al., 2021). Convective precipitation has been defined as this one that overpasses the average 5-min intensity threshold of 35 mm/hour (Llasat, 2001) and has been calculated for 129 rain gauges covering both regions. Although it can contribute to total annual precipitation by up to 16 % on average, it is generated by a very small percentage of annual rainfall events (between 3 % and 6 % across all the stations). Highly convective events are usually responsible for flash-floods in the region that show a significant slight positive trend (Llasat et al., 2016).

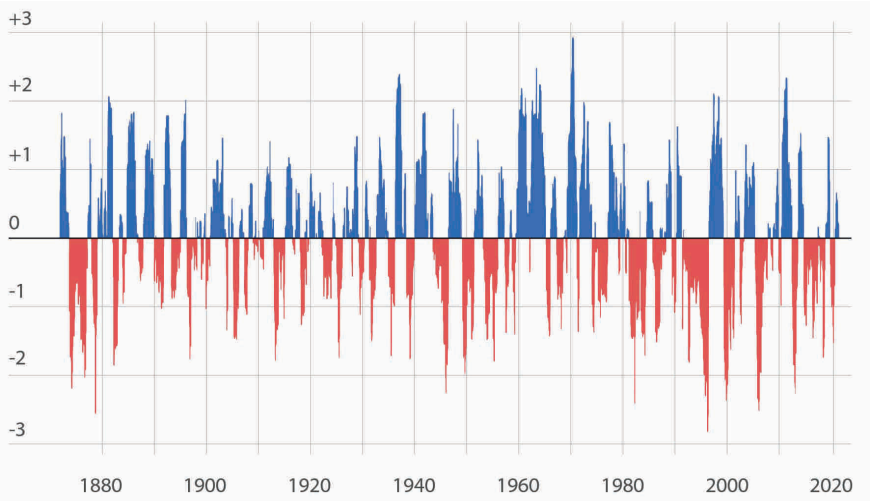

Figure 3.4. Evolution of the average standardised precipitation index (SPI) in Spain in the 1870-2020 period. Source: Adapted from Vicente-Serrano et al., 2023.

The droughts of the 20th century in Spain have been widely studied (Vicente-Serrano, 2021) since instrumental records have allowed the detailed evaluation of hydroclimatic conditions in a broad temporal context. Most of the studies have used two widely recognised drought indices: the Standardised Precipitation Index (SPI) and the Standardised Precipitation-Evapotranspiration Index (SPEI). The high spatial variability in the occurrence of droughts is, like other climatic variables, recurrent in Spain. Some of the most important episodes have not affected the country completely, not even within the IP. Previous studies (Vicente-Serrano, 2013) indicate an increase in droughts in the northeast, south and centre of the peninsula, showing a severity that has increased since the last third of the 20th century. Domínguez-Castro et al., 2019 found a higher frequency of drought events in the northern than in the southern regions of IP in 1951-2014 period. However, non-significant tendency toward higher drought duration and magnitude was observed over the majority of IP. Conversely, Páscoa et al., 2021 found positive duration trends for most of the territory in the 1971-2015 period. Noguera et al., 2020 found that flash droughts (droughts characterised by rapid development and intensification) during a period of 58 years (1961–2018) were the 40 % of all droughts in mainland Spain and Balearic Islands, and that such droughts have a negative trend in the northern regions of the IP, while in the southern regions the trend was generally positive.

At a local scale, trends observed in the east of the Iberian Peninsula, particularly in the basins of the Tagus and Segura rivers between 1955 and 2016, indicate an increase in aridity and temporal concentration of precipitation (Miró et al., 2018). The increase in the length of dry periods in recent decades could have been one of the causes of an increase in the values of drought indices, such as the SPEI. According to a study in the Sierra de Albarracín, a high rainfall area in the east of the Iberian Peninsula, where the headwaters of several river basins

(Júcar, Tajo, Ebro and Guadiana rivers) converge, it has been in a period of severe drought since the 1980's (Miró et al., 2023). The Tajo river basin has been the most affected basin and, in the last 4 decades, it has barely had any period without drought. In northwestern Spain, Lorenzo et al., 2022 showed an increase in drought conditions from 1960 to 2020. The events tended to become longer over time, with a clear increase in the worst drought conditions.

Among the drivers of droughts in the IP (see Vicente-Serrano, 2021), several authors found that the variability of the Arctic Oscillation (AO) and NAO showed significant impacts mainly in winter, while the WeMO pattern showed the largest influence on hydrological behaviour over the southeastern region (Manzano et al., 2019). The study of humidity sources and its moisture transport for the IP showed that they have a heavy influence on drought events genesis (Gimeno-Sotelo et al., 2024; see moisture variable section in this chapter).

Overall, the 21st century has experienced the greatest frequency of severe droughts of the last 150 years (Figure 3.4). However, the 1991–1995 drought was the greatest experienced in the observational period, and it was especially intense in the southwestern part of the IP. Previous events such as those in the decades of 1980 and 1940 were also highly impacting on the socioeconomic system of the country (Vicente-Serrano et al., 2023).

4.3 New water resources

In the current context, with some regions of Spain facing significant losses of precipitation, it is important to explore new sources of water supply to reduce the impact of this situation. One of these sources could be water from fog, which has already been collected and used in other countries in the world, such as Morocco, Chile or South Africa. According to Estrela et al., 2019, in a study carried out along the Mediterranean coast, from Girona to Almería, in some mountainous locations, collection rates higher than 5 $l*m^{-2}$/day have been registered, such as the Montseny Mountains or in the Sierra de Mariola. Additionally, important collection rates (> 2 $l*m^{-2}$/day) have been documented in southeastern Spain, particularly in the provinces of Alicante, Murcia and Almería, which represents the most arid region of the peninsula. According to Corell et al., 2020, the most favourable synoptic situations for the presence of advection fogs on the Mediterranean coast are those of anticyclonic type, although those of maritime and cyclonic origin are the ones that provide greater volumes of this kind of water. Likewise, this study highlights a robust correlation between negative values of the WeMO index (WeMOi) and fog collection. Chemical analyses of the collected fog water, as reported by Corell et al., 2021, confirm compliance with national regulations for human consumption. This positions fog water as a viable alternative to be considered for future water supply strategies.

4.4 Relationships between precipitation-temperature, multidecadal variability and trends

Rodrigo, 2023 found a weakening in the negative relationship between temperature and precipitation, which means a shift towards warm-wet (cold-dry) conditions from the 1970's decade. The study related the trends with NAO, WeMO, East Atlantic (EAP) and Scandinavian (SCAN) teleconnection patterns, which modulate the thermodynamic relationship between temperature and precipitation. A low WeMOi was also related to more extreme events in Catalonia by (López-Bustins et al., 2020).

Finally, some studies related the trends of precipitation and temperature to those of aridity and droughts (Coll et al., 2017; Paniagua et al., 2019). The main conclusion was that, even though precipitation trends were not clear, due to the increase of evaporation produced by the positive air temperature trend, aridity in the Iberian Peninsula showed a positive trend from the 1980's decade.

5. Wind

5.1 Changes in winds

Global warming has not only altered air temperature and precipitation patterns, but has also induced changes in planetary winds (McVicar et al., 2012), though little attention has been paid to changes of this essential climate variable. Several studies have shown how reanalyses are not able to reproduce the observed variability in near-surface winds (e.g., Ramon et al., 2019); therefore, observations are the backbone of wind research. Efforts to compile historical wind observations, such as the one carried out by Rojas-Labanda et al., 2023 for Europe and Engström et al., 2023 for Sweden, play a crucial role in characterising surface winds.

5.2 Wind speed changes

Over the IP, the wind weakening (a phenomenon known as *wind stilling*) was reported for the first time in Azorín-Molina et al., 2014 for 1961-2011, and updated by Utrabo-Carazo et al., 2022 till 2019 (Figure 3.5), in an attempt to find the onset of the *"wind reversal"* reported in other regions of the globe (Zeng et al., 2019). Both studies agree that the near-surface wind speed in Spain and Portugal has declined until 2010, at an annual rate of about -0.15 $m*s^{-1}$/decade ($p < 0.05$), being followed by a cessation of the stilling or a weak and non-significant wind strengthening period of +0.04 $m*s^{-1}$/decade. The starting year of this cessation varies between 1999 and 2018 depending on the variable and the season of the year under consideration (Utrabo-Carazo et al., 2022). Furthermore, despite the 1961-2019 climatology did not show seasonal differences, the marked seasonality found by Azorín-Molina et al., 2014 is still worth mentioning, since the slight decrease in winter-spring and weak increase in summer-autumn dominated around 50 % of the weather stations (76 wind series). Such observed changes might be explained by changes in regional and local winds, although the state-of-the-art of changes according to the types of winds is still incipient.

To give an instance, Azorín-Molina et al., 2018 found decoupled wind trends between coastal and mountain stations (high altitude winds) over the Canary Islands, but also distinct seasonal trend patterns of trade-winds with increases in summer and decreases throughout the rest of seasons. In addition, Ortega et al., 2023 showed the great capability of the high-resolution reanalysis COSMO-REA6 (Consortium of small scale modelling – Reanalysis – 6 km) in capturing regional winds variability in Spain, finding weak negative trends for *Levante* and *Poniente* regimes in Gibraltar for 2000-2018. They also found the European Blocking and Atlantic ridge weather patterns driving *Levante* and *Cierzo* frequency of occurrence, respectively. Finally, Bedoya-Valestt et al., 2023 reported weakened sea-breeze speeds (-0.08 $m*s^{-1}$/decade, $p < 0.05$) for Eastern Iberian Peninsula for 1961-2019, increased

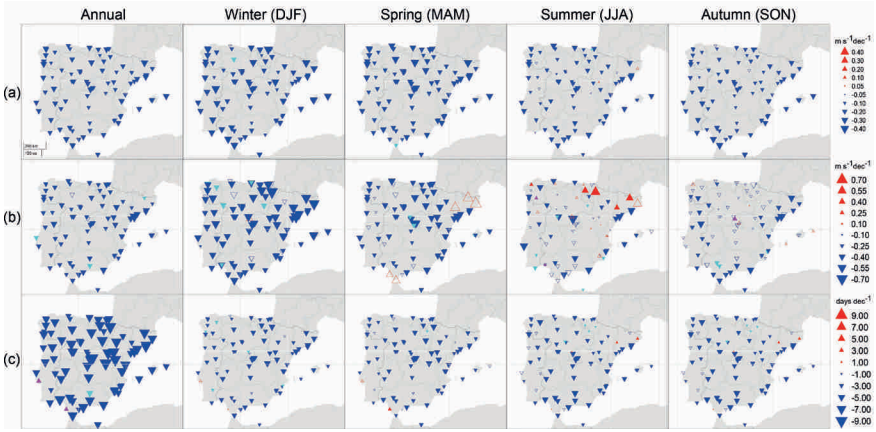

Figure 3.5. Annual and seasonal spatial trends of (a) monthly mean near-surface wind speed anomaly (in ms^{-1} $decade^{-1}$), (b) monthly mean daily peak wind gust anomaly (in $m*s^{-1}$/decade) and (c) 90th percentile of daily peak wind gust (in days/decade) for 87 homogenised wind series for 1961–2019. Blue and red filled triangles are significant at $p < 0.05$; cyan and magenta filled triangles are significant at $p < 0.10$; and non-filled triangles are non-significant at $p < 0.10$. Different scales have been used for each variable in order to highlight trends. Source: Utrabo-Carazo et al., 2022.

occurrence in winter (+1.70 days/decade, $p<0.05$), probably influenced by higher anticyclonic activity related to NAO+; and decreased sea-breeze days in summer (-0.58 days/decade, $p<0.05$). The latter may have an important influence on the wind speeds observed at coastal stations in summer, especially in locations where the sea-breeze is blowing most of the year as the the eastern coast of the IP (Azorín-Molina et al., 2011).

5.3 Changes in wind extremes

Trends of wind gusts and storminess over the IP have been even less addressed than near-surface wind speed, although in recent decades has gained greater interest within the scientific community due to the potential effect of air temperature rise on the frequency and magnitude of extreme winds and associated disasters. In fact, for the period 1961-2001 storm events in north-western Spain have decreased from 5 to 4 events per year with shorter durations and non-trending change in wind gusts. A more recent work of Azorín-Molina et al., 2016 covering the entire region for 1961-2014 has evidenced annual decreasing trends in the occurrence of gusty winds of around -1.49 days/decade ($p <$ 0.05), which also exhibits a marked winter-summer seasonality: significant downward trends in winter in magnitude (-0.168 $m*s^{-1}$/decade, $p < 0.10$) and frequency (-0.73 days/decade), and upward trends in summer, being only significant in magnitude (+0.148 $m*s^{-1}$/decade, $p < 0.05$). Nevertheless, such seasonal (and spatial) differences were not clearly shown in Utrabo-Carazo et al., 2022 for 1961-2019, despite trends of lesser magnitude

and significance being observed in summer and autumn, particularly over north-eastern Spain with positive trends. Overall, the magnitude of the trends are slightly higher for the daily peak wind gusts than for the daily mean wind speed. Conversely, Laurila et al. (2020) found more extreme high wind events in winter than in summer after analysing 40 years (1979-2018) of near-surface wind speed from the Fifth Generation ECMWF reanalysis (ERA5). The last may be explained by the increased wind events producing cyclones reported over the western IP until 1990's (Nissen et al., 2010), since most windstorms events occurring in winter are associated with cyclogenesis. In fact, the northern part of the IP is greatly affected by extreme winds associated with Atlantic and extratropical cyclones, whose frequency and intensity are expected to rise in a changing climate (Ramos et al., 2016), while the southeastern part is mostly influenced by strong winds coming from Mediterranean cyclones (Hénin et al., 2021; Raveh-Rubin and Wernli, 2015), which enhance regional winds such as Mistral, Tramontana or Sirocco (Flaounas et al., 2022). Lastly, Bedoya-Valestt et al., 2023 found a strengthening of the sea-breeze gusts at annual scale and during the cold months for 1961-2019, being only significant in autumn (+0.07 $m*s^{-1}$/decade, $p < 0.01$); and a non-significant weakening in summertime.

5.4 Causes of wind changes

Among the causes proposed in Utrabo-Carazo et al., 2022 for the IP wind *stilling*, we found an increase in atmospheric thermal stability and a northward shift of the jet stream. No other cause was found for the cessation of ***stilling*** than a change in the trend of the western Mediterranean oscillation. In fact, the high interannual variability of wind speed in this region makes the results not statistically significant in such short periods, so more data would be needed to elucidate the intricacies of the cessation of stilling. Furthermore, all these results are seasonally dependent indicating a possible difference in the mechanisms. For example, the winter trends could have been enhanced by ocean-atmosphere oscillations. Thus, the observed strengthening of the NAO between 1960 and 1990 (Scaife et al., 2005) would explain why in the IP the trends are greater in magnitude in winter than in summer, which is the opposite to what is observed in Sweden, since wind speed is negatively correlated with NAO in the IP (Utrabo-Carazo et al., 2022) and positively in Sweden (Minola et al., 2016). In fact, Utrabo-Carazo et al., 2023 have shown that there is a clear influence of the stratospheric polar vortex on the surface wind over the IP, such that a sudden stratospheric warming event would correspond to stronger winds over the IP up to two months later. The possible influence of other atmospheric oscillations, such as WeMO and the Mediterranean Oscillation (MO), has been widely discussed in literature. These two patterns are, together with the NAO, ones of the major drivers in the observed surface wind changes during the last half century across the IP (Azorín-Molina et al., 2014; Bedoya-Valestt et al., 2023; Utrabo-Carazo et al., 2022). In particular, the WeMO has shown a stronger correlation with wind speeds and gusts than MO at all time scales, being positive and highly significant at $\boldsymbol{p} < 0.05$ (Utrabo-Carazo et al., 2022). In fact, the WeMOi shows statistically significant negative trends for 1961-2010 and positive ones for 2010-2019, in agreement with the observed wind speed trends. In the case of other wind regimes forced by thermal differences such as sea breezes, WeMOi also appears to have a positive influence on mean velocity changes, but other physical-local factors such as changes in land use appear to play a greater role in driving wind gusts. More attention must be given to the influence of changes in land

use, which is a poorly quantified issue with respect to its influence on wind speed in the IP. In fact, Azorín-Molina et al., 2014 detected changes between observed winds at urban and rural locations, highlighting the potential contribution of urbanisation growth to global wind ***stilling*** (Vautard et al., 2010). Finally, other factors such as anemometer changes and ageing can lead to significant biases in wind series (Azorín-Molina et al., 2018), or even the time intervals in measuring wind speed (Azorín-Molina et al., 2017) and wind gusts (Minola et al., 2021).

5.5 Wind impacts in the environment and society

Advances in the knowledge of wind changes and their associated causes is essential due to their direct implications in wide range of areas, among which the following stand out: (i) wind industry; (ii) agriculture and hydrology; (iii) risks and natural disasters; (iv) air quality and health; (v) airport operations and road traffic; (vi) forest fire spread; (vii) tourism and wind sports, among many other fields.

High winds are responsible for large economic losses and loss of human lives every year. In Spain, regions such as the northern Spain, the Mediterranean coast or the islands are affected by extratropical wind storms reaching gusts of around 200 km/h, severely affecting the agricultural industry and the fishing industry to give an instance. In fact, the report prepared by the Consorcio de Compensación de Seguros, 2022, the only official source available in Spain, estimates total economic losses of 12.3 million € in 2022 due to the "atypical cyclonic storm" (>120 km/hour and tornado) in national territory. In addition, in 2022, extreme winds were the second cause of accident rate (after floods) with 20,292 claims. In this regard, the number of fatalities in Spain due to windstorms amounted to 110 people between 2000 and 2019.

On the other hand, one of the main interests when studying wind is its application to energy production. Numerous studies have tried to estimate the wind resource in the region both onshore and offshore, generally through data from reanalysis. As the IP is located south of Europe, wind power is highly negatively correlated with the NAO in winter, so it will be considerably influenced by the multidecadal variability of this mode of variability (Neubacher et al., 2021). In particular, an increase in the number of high-impact storms with associated strong winds would have a positive effect on wind energy production in winter according to Gonçalves et al., 2021. Carreno-Madinabeitia et al., 2021 showed an increase in offshore wind power density (WPD) and capacity factor (CF in the IP waters during 1900-2010 of around 174 W*m² for WPD and 8.8 % for CF. This increase is consistent with the increase in the wind over ocean surfaces (Young and Ribal, 2019), which contrasts with the *stilling* observed over land, leading to a decrease in the wind resource over continental surfaces. Moreover, both Carreno-Madinabeitia et al., 2021 and de Castro et al., 2019 agree that the Gulf of Lyon and the Strait of Gibraltar correspond to optimal locations for installing and maintaining offshore wind farms. Nevertheless, Onea et al., 2020 highlighted the northern Spanish coast as the location with the best characteristics for the possible development of offshore wind farms, while Salvador et al., 2018 studied the suitability of certain locations on the western part of this coast taking into account the legal restrictions in terms of environmental impact.

Closing up, in 2023, the wind represented the main source of clean energy in Spain. Under a warming climate scenario, wind is key to decarbonizing the production system and achieving a low-carbon economy. This is particularly pertinent in the context of the ongoing energy transition aimed at mitigating the increasing pace of global change. Understanding better the wind changes and decadal variability is crucial to improve the great uncertainties in future climate projections.

6. Atmospheric Moisture

Moisture, or humidity, measures the amount of water in the atmosphere or soil. Its implications for meteorological processes such as cloud formation and precipitation are well-known. In the hydrological cycle, moisture is essential for triggering precipitation, along with a mechanism to force the moist air to rise. Various observational studies and numerical modelling have shown a strong dependence between saturated vapour pressure and temperature, resulting in increased evaporation and, consequently, precipitation (Gimeno et al., 2015).

Generally, precipitation dynamics over a specific region depend on three atmospheric moisture sources: moisture already present in the atmosphere, moisture advected by atmospheric transports, and moisture originating from local evapotranspiration or moisture recycling (Eltahir and Bras, 1996; Gómez-Hernández et al., 2013; Trenberth, 1999). However, moisture recycling and advection are the two main moisture sources (Gimeno et al., 2010). In this context, the so-called atmospheric rivers are of great importance. They are elongated and narrow regions where large amounts of moisture are transported towards mid-latitudes, causing extreme precipitation (and floods) over western Europe.

Additionally, atmospheric moisture plays a key role in a positive feedback loop that significantly influences the soil's water balance, alongside solar radiation. A decrease in atmospheric moisture reduces cloud formation, allowing more radiation to reach the surface, enhancing soil warming and further decreasing humidity (Rowell and Jones, 2006). Current investigations have determined a direct relationship between increases in various atmospheric moisture sources on a global scale and extreme precipitation events in different regions (Nieto et al., 2014), which may become more frequent and severe during the 21st century (Giorgi et al., 2019). Therefore, analysing moisture is essential for understanding the complex internal processes of the hydrological cycle and the origin of continental precipitation (Gimeno et al., 2020).

Moreover, human health is also affected by humidity. When core body temperature exceeds 37 °C, internal heat must be released through sweat evaporation. In extremely humid environments, this process is less effective, and the body can reach dangerous temperature levels (Kjellstrom et al., 2016).

Several studies have been developed to determine the moisture sources that contribute to precipitation over the Iberian Peninsula (Gimeno et al., 2012). Gimeno et al., 2010, which used the FLEXible PARTicle dispersion (FLEXPART) model forced with ECMWF (European Centre for Medium-Range Weather Forecasts) operational analyses every 6 h on 60 vertical levels, confirms that the most important moisture source regions are the entire tropical–subtropical North Atlantic corridor (TSNA), stretching from the Gulf of Mexico to the IP, the local source, including the IP itself, and the surrounding western Mediterranean basin. Moisture contribution from the TSNA increases during winter and decreases strongly during summer. In contrast, the contribution of the western

Mediterranean basin increases during summer, but it is relatively minor during autumn and winter. These results show the dominance of long-distance moisture transport relative to recycling during winter, but the importance of recycling during summer. Moreover, Ciric et al., 2018, using the Multi-Source Weighted-Ensemble Precipitation (MSWEP) database and the same FLEXPART model and reanalysis ERA-Interim (ECMWF Re-Analysis) in the period 1980–2016, showed that the contribution of the Mediterranean Sea to extreme precipitation events during January and July is more pronounced in the IP and regions around. (Batibeniz et al., 2020) confirms both oceanic sources of moisture for the period 1980–2013 using data from ERA-Interim, MERRA2 (Modern-Era Retrospective analysis for Research and Applications), CFSR (Climate Forecast System Reanalysis), and JRA25 (Japanese 25-year Re-Analysis) reanalyses and the DRM (Dynamical Recycling Model) Lagrangian approach for particle tracking, and their important role on daily precipitation extremes in the Mediterranean region. Additionally, the importance of NAO as a large-scale forcing over the Mediterranean region, in contrast to the relatively weak and less robust El Niño - Southern Oscillation (ENSO) influence, was also highlighted. The three main source regions contributing moisture to the IP (the North Atlantic, the Mediterranean Sea and the owner IP) are confirmed and well represented with the new ERA5 reanalysis using the latest version of FLEXPARTv10.3 model and FLEXPART-WRF fed with new dynamical downscaled data from Weather Research and Forecasting (WRF) simulations at different horizontal resolutions (Fernández-Álvarez et al., 2023).

On the other hand, monthly WRF model simulations forced with ERA-Interim for a domain over the IP for the period 2010–2014 (González-Rojí et al., 2019) showed that the lowest values for moisture recycling processes (~3 %) are observed from November to February limited to the southeast region, while the maximum values (16 %) are observed in spring, for the period 1990-2007. Rios-Entenza et al., 2014 also determined that the local recycling ratios peaked at the highest values in spring and early summer. This behaviour is the key to explain the spring precipitation, particularly over the eastern and northeastern areas of the IP; during spring and summer a gradient towards the northeast region of the IP is observed (González-Rojí et al., 2019). It should be noticed that the availability of sufficient soil moisture is necessary to achieve high ratios of recycling in coexistence with the occurrence of synoptic patterns that favour convective movements to result in precipitation. The linkage between summer moisture recycling and precipitation over the IP is confirmed through the comparison of precipitation from 1980 to 1997 and 1998 to 2019 using the Eulerian Water Accounting Model-2 layers (WAM-2 layers) with ERA5 data (Liu et al., 2022). The remarkable decrease in recent summer precipitation can be attributed to the simultaneous and large reduction in evaporation over the eastern and western parts of the North Atlantic, with a decrease of 57 % and 17 % reduction, respectively, after and before 1997. The local IP contribution suffered a 26 % reduction (Liu et al., 2022).

Over the IP, there is a strong relationship between moisture transport and hydrometeorological extremes, such as extreme precipitation or meteorological drought (Gimeno-Sotelo et al., 2024; Gimeno-Sotelo and Gimeno, 2023). Over the western half of the IP, moisture transport controls extreme precipitation at least as much as the water column or atmospheric instability (Gimeno-Sotelo et al., 2023), mainly due to atmospheric rivers, and the probability of droughts occurring when moisture from the North Atlantic is extremely low (Gimeno-Sotelo et al., 2024).

The study of the moisture sources associated with extreme events is essential for a greater understanding of these meteorological phenomena and impacts (Gimeno et al., 2010), and several

investigations have focused on such events. Specifically, the individual analysis of moisture sources for case-studies have increased during the last years, focusing them in the autumn season when the extreme precipitation usually affects the IP. Using the FLEXPART-WRF set-up forced with ERA5 Álvarez-Socorro et al., 2023 investigated two extreme precipitation events that affected the IP: an extratropical cyclone occurred on 18 September 1999 and a cutoff low system occurred on 7 September 1989. Both events were in the top ranking of extreme precipitation on IP in the period 1950–2007 (Ramos et al., 2018). For the first case, the main contribution of moisture comes from the central and eastern North Atlantic (32%), due to an intense atmospheric river. In contrast, for the second event, the origin of the moisture was mainly the Western Mediterranean Sea (40%). Using the regional atmospheric WRF model with a moisture tagging tool, Insua-Costa et al., 2019 also analysed the main moisture sources for two catastrophic flood events in 1982 in the Western Mediterranean area. The case of 20 October, known as the Tous event, was associated with a cold-core COL over the Spanish Levante, and the long distance moisture sources for precipitation from the tropical and subtropical North Atlantic ocean played a similar role to near and local sources from the western and central Mediterranean Sea (46 % versus 40 %). Whereas in the November case under a deep low-pressure system located off the coast of Galicia with a strong atmospheric river the dominant moisture source for precipitation was associated with remote sources (about 70 %). Using the same model Eiras-Barca et al., 2017 analysed the so-called Great Storm of 1987, which is also associated with an intense atmospheric river in the North Atlantic. They found that the percentage of tropical origin precipitation is about 60 %. Moreover, focusing on the general moisture transport associated with the atmospheric rivers developed in the North Atlantic Ocean and make landfall towards the northern coasts of the West Atlantic basin (including the IP), the so-called Western Hemisphere Warm Pool was found the large moisture reservoir (Algarra et al., 2020).

Measures of precipitable water vapour for the period 2002-2008 at 18 sites on the IP, calculated from MODIS (Moderate-Resolution Imaging Spectroradiometer) satellite data, showed an annual cycle with low values in winter (minimum ~1 cm) and high values in summer (maximum ~3 cm), a smaller cycle amplitude at continental sites than at coastal sites, and the existence of a clear north-south gradient, with higher values in the north of the IP (Bennouna et al., 2013). Similar results were found on the Atlantic coast of Spain by Perdiguer-López et al., 2023 using Global Navigation Satellite System (GNSS) observations. This seasonal variability is also observed in the multi-year diurnal anomalies, being higher in summer and lower in winter. Although the sites have different behaviour in their diurnal variation, a similar pattern is detected with a minimum in the late evening to reach a maximum in the afternoon, corroborating results from Ortiz de Galisteo et al., 2011. A review of this methodology and global station measures (including the IP) was done by Vaquero-Martínez and Antón, 2021. Vaquero-Martínez et al., 2017 validated integrated water vapour (IWV) measurements from the Ozone Monitoring Instrument (OMI) with ground-based GPS (Global Positioning System) stations and cautioned that the origin of the measurements must be taken into account, as they found differences in IWV estimates, with OMI significantly overestimating the lowest GPS-recorded IWV data (~40 %) and underestimating the highest IWV reference values (~20 %). In the same line Román et al., 2015 compared total water vapour column from GOME-2 (Global Ozone Monitoring Experiment 2) to GPS, finding an overestimation (10 %) of GOME-2 being the highest over the southwestern IP (17 %). Measures of IWV were used to study heavy precipitating systems in the northwestern Mediterranean (including northern IP) during the Intense Observation Period for the Hydrological Cycle in the Mediterranean Experiment (HyMeX IOP12) using instrumental observations and high-resolution numerical simulation with the

COSMO regional model (Khodayar et al., 2018; Khodayar and Caldas-Alvarez, 2022). The results showed that all heavy precipitating systems form in periods and/or areas of maximum integrated water vapour (IWV; 35-45 kg/m2) after an increase of ~10-20 kg/m2.

7. Atmospheric Circulation

The IP, a geographically diverse region, is significantly influenced by atmospheric circulation patterns in the North Atlantic that play a pivotal role in shaping its climate (Trigo et al., 2002). Not only the well-known NAO plays a role in the climate of the IP, also patterns as the Mediterranean oscillation (Martín-Vide and López-Bustins, 2006; Redolat et al., 2019) and teleconnections with remote modes, like ENSO (García-Serrano et al., 2011; López-Parages et al., 2016; Martija-Díez et al., 2023, 2021; Rodríguez-Fonseca et al., 2016), or the stratospheric polar vortex variability, among others, exert a noticeable influence in southwestern Europe. Thus, the understanding of the dynamics of North Atlantic atmospheric patterns, local regimes and the teleconnections is essential for comprehending the variability in the weather and climate experienced by the region. The associated changes in circulation systems can have cascading effects on the frequency and intensity of extreme weather events (Casanueva et al., 2014; Gómara et al., 2016, 2014; González-Alemán et al., 2023), sea-level rise, and ecosystem dynamics (Capa-Morocho et al., 2016, 2014; Gómara et al., 2020; López-Parages et al., 2022).

7.1 The case of the North Atlantic Oscillation

The NAO, as the dominant variability mode of the atmosphere in the North Atlantic (Hurrell et al., 2003; Pinto and Raible, 2012), drives the strength and the latitude of the westerly winds (Woollings et al., 2010) and the North Atlantic storm track (Gómara et al., 2016; Pinto et al., 2009). As a consequence, it affects the Mediterranean and North Atlantic area (MedNA) and has a significant influence on the occurrence of meteorological and climate events that affect society, such as explosive cyclones (Gómara et al., 2014), COLss (Nieto et al., 2007), etc. Extreme precipitation in the western Mediterranean and northwestern Europe (Krichak et al., 2014), water availability for intensive agriculture and hydropower in the Iberian Peninsula (Trigo et al., 2004), wind energy and solar potential over Iberia (Jerez et al., 2013) or crop yields in Europe and North Africa (Capa-Morocho et al., 2016, 2014; Gómara et al., 2020) constitute, among many others, good examples of the NAO influence on socio-economic activity.

In general, a positive phase of the NAO is associated with cooler and drier conditions throughout the MedNA region (Rodríguez-Fonseca et al., 2016) but there is strong evidence that the impacts of the NAO in the MedNA area could be unstable at multidecadal and longer timescales (Gómara et al., 2016; Pinto and Raible, 2012; Raible et al., 2014), making it relevant to perform analysis for periods as long as possible. Quantifying the NAO using instrumental measurements prior to the early 19th century is a challenge. However, during the last decade it has been possible to compute instrumental series of NAO-like indices for several centuries by relying on early wind direction observations made at, for example, inland stations, lighthouses, or by ships at sea or in ports (Allan et al., 2011; Freeman et al., 2019; García-Herrera et al., 2005).

Using these early data, Barriopedro et al., 2014 approached the problem by designing the so-called Westerly Index (WI), as a direct measurement of the persistence of the

westerly winds at monthly scale in the English Channel. By using mostly wind directions from the ICOADS (International Comprehensive Ocean-Atmosphere Data Set) database (Freeman et al., 2019), these authors were able to compute the WI between 1685 and 2008 (subsequently updated to 2014) demonstrating that their index not only represented NAO-like temperature and precipitation anomalies in the MedNa region, but it provided complementary information, as the WI did not only represented the relative strength of the NAO centres of action, but the shifts in their relative position. In fact, Vicente-Serrano et al., 2016 found that the NAO and the WI were complementary at the time of explaining the variability of drought severity over most of Europe. Subsequently, the method developed for the WI was applied to other areas of the world (Gallego et al., 2019; Gómez-Delgado et al., 2019) and to other wind components in the North Atlantic by Mellado-Cano et al., 2020. In particular, Mellado-Cano et al., 2020 built "Directional Indices", by relying only on wind direction data as in WI, but considering the entire compass rose. With the directional indices they were able to explain a considerable amount of European climate variability, in most cases larger than the explained by the NAO alone, further suggesting that the geographical changes in the North Atlantic surface pressure patterns are relevant to investigate variability in atmospheric circulation and their impacts in the Mediterranean climate through the instrumental period. In other words, it is evident that the particular phase of the NAO is not enough to fully characterise the MedNA climate (Barriopedro et al., 2011), being important to take into account other possible patterns. Recent studies put forward how the EAP pattern has increased its influence through its teleconnection with ENSO in recent years (King et al., 2023).

7.2 Weather Regimes

Apart from the dipole structure characteristic of the NAO, the climatic situation on the Iberian Peninsula is largely influenced by consistent patterns of large-scale atmospheric circulation that repeatedly occur over the Mediterranean and the North Atlantic area, often referred to as "weather regimes" (Corti et al., 1999; Michelangeli et al., 1995). These regimes serve as crucial tools for simplifying the continuum of atmospheric circulation into a relatively small number of clusters, typically ranging from 4 to 10, on a seasonal or yearly basis (Cortesi et al., 2019; Michelangeli et al., 1995).

Weather regimes (WR) are generally defined by grouping similar atmospheric circulation anomalies at daily resolution, such as geopotential height (Sánchez-Benítez et al., 2020), sea-level pressure (Álvarez-Castro et al., 2018), or wind speed direction (Hannachi et al., 2017). WR classifications in the Northern Hemisphere are often conducted for the boreal winter (December to February) or the extended winter (November to April), as winter anomalies have proved to be more effective predictors of the local climate (Vrac et al., 2014; Thornton et al., 2017; Ruggieri et al., 2020). However, WR can also be derived for summer (Álvarez-Castro et al., 2018; Cassou et al., 2005; Guemas et al., 2010; Martija-Díez et al., 2023; Quesada et al., 2012), spring, or autumn, although these two seasons have been less explored. Annual classifications that analyze all days of the year together (Grams et al., 2017), or separately for each month of the year (Cortesi et al., 2021, 2019), have also proven useful for various applications (Torralba et al., 2019). Although names can vary, the weather regimes in reanalysis such as NCEP (National Centers for Environmental Prediction), ERA-interim or ERA5, are usually described as positive phase of NAO (NAO+),

negative phase of NAO (NAO-), Scandinavian Blocking (BLO) and Atlantic Ridge (ARG) for winter/annual (Cortesi et al., 2021) and NAO-, ARG, BLO and Atlantic Low (AL) in summer (Álvarez-Castro et al., 2018; Cassou et al., 2005; Martija-Díez et al., 2023). Cold spells are usually characterised in winter by either the negative North Atlantic oscillation (NAO-) regime, as was the case for the winter of 2009–2010 (Cattiaux et al., 2010) and the late winter and spring of 2018 (García-Burgos et al., 2023; González-Alemán et al., 2023), or by the BLO regime (Vautard et al, 2018). Mild winters with persistent rainfalls over Western Europe are characterised by NAO+ (Gómara et al., 2014; Pinto and Raible, 2012). Heat waves are usually associated with the BLO regime, as for instance the summer of 2003, 2010 or 2022 (Barriopedro et al., 2023), and AL (Barriopedro et al., 2023; Sánchez-Benítez et al., 2020). However, the use of longer reanalysis such as the 20th Century Reanalysis by the NOAA (20CR, Compo et al., 2011) or the ECMWF twentieth century reanalysis ((ERA20C, Poli et al., 2016) have shown that heat waves have not always been linked to BLO and/or AL regimes and that, during the first part of the 20th century, other regimes were involved in these events (Álvarez-Castro et al., 2018; Coumou et al., 2018).

The concept of weather regimes is based on dynamical systems theory analysis of atmospheric variability (Vautard et al., 2019). Using dynamical systems theory to understand the predictability of the atmospheric circulation in the North Atlantic region, Faranda et al., 2017 found that NAO+/- regimes were associated with higher predictability whereas BLO/ ARG were associated with lower predictability. In the case of some extreme events such as the Filomena (January 2021) storm, this technique showed that the atmospheric pattern when the event started was not associated with any regimes and in fact was very rare and unpredictable.

7.3 Remote Teleconnections patterns and forcings

The oceans are getting warmer and it is unequivocal that human influence, through greenhouse gas (GHG) emissions, has a substantial contribution in this process (IPCC, 2023), accelerating warming more rapidly in the last century than since the end of the last deglacial transition. We know the state of the oceans thanks to monitoring programs such as Marine Copernicus (Von Schuckmann et al., 2021), which has been responsible for reporting, among other changes, a warming trend, an increase in the frequency of marine heat waves, acidification and regional changes in primary production. Future climate scenarios indicate that, during the remainder of the 21st century, ocean warming is likely to range from 2-4 (SSP1-2.6) to 4-8 times (SSP5-8.5) the 1971-2018 change (IPCC, 2023).

Focusing on the MedNA, the above future scenarios have predicted a drastic warming of the Mediterranean Sea and an increase in the hydrological cycle, whereby subtropical areas, such as our target area, are destined to become less and less productive land (IPCC, 2023), with significant environmental consequences, from more frequent fires to food insecurity. The global oceans exhibit interannual to decadal variability that is reflected in sea surface temperature (SST) patterns that affect atmospheric circulation leading to both regional air-sea coupled processes and climate teleconnections (Von Schuckmann et al., 2021).

On interannual time scales, ENSO is the dominant mode of tropical variability in the boreal winter and its effects are felt worldwide (McPhaden et al., 2006). El Niño is characterised

by anomalous SSTs in the central-eastern tropical Pacific. In the tropical Atlantic, the Meridional Mode (MM) and Atlantic El Niño (AN) control the interannual variability of the boreal spring and summer, respectively (Polo et al., 2008). The MM shows a trans-equatorial SST gradient and the AN is the Atlantic counterpart of El Niño. The low-frequency variability of the oceans is reflected in prominent large-scale SST patterns in the Atlantic and Pacific oceans, namely the Atlantic Multidecadal Variability (AMV; Knight et al., 2005) and Pacific Decadal Variability (PDV; Dong and Dai, 2015) patterns. On the one hand, the AMV shows SST anomalies of the same sign in the North Atlantic basin, with maximum values over the subpolar gyre and the positive phase of the PDV pattern is characterised by pronounced positive SST anomalies along the western coasts of North and South America and along the equatorial band (Cassou et al., 2018). Although AMV and PDV are usually considered internal modes, external forcings such as greenhouse gases, solar variability, or volcanic eruptions can also influence their decadal variability (Dong et al., 2014; Otterå et al., 2010).

The atmospheric variability of MedNA is not only driven by the NAO, as we have seen above, it is also associated with atmospheric teleconnections forced by the SST, not only from the surrounding oceans, such as the Mediterranean Sea and the northern tropical Atlantic (Losada et al., 2010; Polo et al., 2005; Rodríguez-Fonseca et al., 2006) but also from remote regions such as the Pacific Ocean. ENSO has been noted as a mode of variability with a modest but significant impact on the MedNA region (García-Serrano et al., 2011). This ENSO influence has been related to an atmospheric dipolar pattern that resembles the NAO, identifying a link between the positive phase of ENSO and a negative NAO-like pattern, mainly during the boreal winter (García-Serrano et al., 2011; López-Parages and Rodríguez-Fonseca, 2012; Mezzina et al., 2020). In the rest of the seasons the ENSO impact on the North Atlantic is not stationary (López-Parages and Rodríguez-Fonseca, 2012; Martija-Díez et al., 2023, 2021; Rodríguez-Fonseca et al., 2016). Thus, different impacts on the MedNA have been found to be associated with different spatial configurations of ENSO or relative phase shifts (López-Parages and Rodríguez-Fonseca, 2012; Martija-Díez et al., 2023, 2021). Notably, the ENSO teleconnection has been found to be non-stationary in time modulated by ocean decadal modes of variability (López-Parages et al., 2016, 2015).

Tropical Atlantic modes of variability can also exert an influence on the Mediterranean region. SST anomalies in the Tropical North Atlantic (TNA), as part of the meridional mode (MM), can excite a Rossby wave train in the boreal spring that extends from the western tropical Atlantic to the extratropics becoming a NAO-like structure during the following autumn-winter season (García-Serrano et al., 2011, 2008; Losada et al., 2007). However, the TNA-NAO relationship undergoes variations during the observational record, depending on the ENSO forcing and the intensity of North Atlantic atmospheric variability (Chen et al., 2015). Interestingly, the northwest African upwelling appears to be a key factor in the SST pattern of the TNA that drives winter precipitation over the MedNA (Yang et al., 2018). During the boreal summer, the Atlantic Niño (AN) is able to excite atmospheric Rossby waves that travel trapped in the North African-Asiatic jet, triggering a circumglobal response (García-Serrano et al., 2008; Haarsma and Hazeleger, 2007). These waves ultimately translate into patterns of atmospheric variability over the North Atlantic that modify the precipitation regime of the MedNA region. However, this atmospheric teleconnection pattern also changes with the spatial configuration of the AN (Chen et al., 2024) and its coexistence with ENSO (Losada et al., 2012). At multidecadal and longer timescales, the AMV and

Atlantic Meridional Overturning Circulation have been shown to affect the large-scale north Atlantic circulation, including the storm track (Dong et al., 2013; Gómara et al., 2016; Woollings et al., 2012) and weather regimes (Zampieri et al., 2017).

Given the evidence that the modes of variability and their teleconnections change according to the mean ocean state and given the effect of anthropogenic climate change on ocean heat content, the characteristics of the modes of variability along with their impacts could also change in future scenarios (Rodríguez-Fonseca et al., 2005). Several studies, in fact, suggest that the modes have changed as a function of a modification of ocean climatology (Fedorov and Philander, 2000; Martín-Rey et al., 2018). Wang et al., 2019, showed that, since the 1970's, there has been an increased occurrence of extreme ENSO events, to which the increase in greenhouse gases could have contributed (Zhang et al., 2008). In addition, the ratio of central Pacific (CP) ENSO to eastern Pacific ENSO has increased since 1901 (Wang et al., 2019) and is consistent with a similar increase in climate change projections (Yeh et al., 2009), possibly due to a warmer ocean state and a deeper thermocline (Choi et al., 2011). Although uncertainty remains regarding the robustness of the ENSO response to global warming (Chen et al., 2017), CMIP (Coupled Model Intercomparison Project) models tend to show a greater degree of consensus (Cai et al., 2021). Several studies have suggested a stronger link between ENSO and the NAO in the future (Michel et al., 2020; Müller and Roeckner, 2008), and (Drouard and Cassou, 2019) and stronger wave guidance between the North Pacific and Atlantic during La Niña episodes as the reason for this stronger link.

As for the tropical Atlantic modes of variability, they have also undergone changes during the 20th century, some of them associated with the AMV (Martín-Rey et al., 2019; Martín-Rey et al., 2018). The future warmer climate is expected to modify the mean ocean state and, therefore, the mechanisms responsible for generating the different configurations of the AN and MM modes (Mechoso, 2020). Future climate scenarios have revealed a weakening of the MM pattern (Breugem et al., 2007). The projected warmer mean state could modify the position of the Hadley cell and the jet stream, which could affect the teleconnection with the MedNA region (Studholme et al., 2021). Under a warmer scenario, deep convection associated with the AN is expected to cover a large extent in the tropical Atlantic basin, resulting in an eastward shift of its atmospheric teleconnections. This suggests a possible shift in the atmospheric Rossby wave response, which may modify the impact of AN on European summer heat waves (Mohino and Losada, 2015). When the impacts of SST patterns and teleconnections affect climate variables directly related to socioeconomic sectors (e.g., energy and food production, health, water management), this information can be translated into customised tools, products, and services to support decision making (also known as climate services).

Apart from the ocean, there are other remote sources of variability of the Southwestern European region. One of those is the variability of the polar stratospheric vortex in winter. The polar stratospheric vortex is a strong cyclonic circulation that encircles the polar region in high latitudes. It forms in fall as a result of the negative meridional temperature gradient between midlatitudes and the polar, and decays in spring as the sunlight comes back to high latitudes (Waugh et al., 2017). In the last decades many studies have shown that extreme polar vortex events can influence wintertime European surface weather as their

signal projects on the NAO (Baldwin et al., 2021 and references herein). In particular, Sudden Stratospheric Warmings (SSWs) (i.e. extreme weak polar vortex events) have been related to a negative phase of the NAO and consequently, mild weather and wet conditions in the Iberian Peninsula. A good example is the extraordinary event of heavy precipitation in March 2018 that put an end to the strong European drought of 2016/17 and was strongly influenced by the SSW of February 2018 (Ayarzagüena et al., 2018).

However, the influence of the polar vortex on the weather conditions in the Iberian Peninsula is not only restricted to the winter season. Springtime conditions in the Iberian Peninsula can also be modulated by the polar vortex state and more strictly, the timing of the final breakup of the polar vortex. In the Northern Hemisphere, the vortex breakup ranges from March and May and atmospheric conditions in the Euro-Atlantic sector are different depending if the vortex breakup happens very early or very late (Ayarzagüena and Serrano, 2009; Gimeno et al., 2007; Hardiman et al., 2011).

8. Regions of special interest

8.1 Canary Islands

The Canary Islands, located in the southeastern North Atlantic facing the west coast of Africa, have an area of about 7,500 km², divided into eight major populated islands and several smaller islets. Only Tenerife has an area slightly larger than 2,000 km², being La Graciosa the smallest one, with only 29 km². In addition, the central and western islands have a very complex orography, with mountain ranges of considerable heights and full of ravines. In five of the islands the maximum altitude is above 1,500 m, being around 2,400 in La Palma and 3,700 in Tenerife. This complex orography favours the creation of microclimates and it is one of the main factors that define the distribution of precipitation. The uniqueness of their location and geographical and climatic characteristics, conditioned by the subtropical latitude at which they are situated (27º–29º N), their high population density and their considerable dependence on the external environment and, specifically, on tourist activity, justify the need to individualise their analysis with respect to the rest of the Spanish national territory. Despite the complexity inherent to the climate analysis of small island territories, in recent years there have been numerous efforts aimed at studying, in greater detail, the impacts of climate change in Macaronesian latitudes (Carrillo et al., 2023; Cropper, 2013; Dorta-Antequera et al., 2018; Martín et al., 2012; Máyer et al., 2017). Hence, this chapter is largely based on the main conclusions of research that has attempted to adapt the major global analyses to a local and, undoubtedly, peculiar scale.

8.1.1 Changes in temperature

Thus, a review of the scientific literature published in recent years provides solid evidence of the temperature increase that the region is experiencing (Dorta Antequera et al., 2018). Virtually all studies on the issue agree that temperature increase is the climate parameter with the greatest statistical certainty (Cropper and Hanna, 2014), particularly from the 1970's and 1980's onwards (Cropper, 2013; Cropper and Hanna, 2014; Hernández Barrera et al., 2012; Luque et al.,

2014; Martín et al., 2012; Sperling et al., 2004). Specifically, the increase is higher in minimum temperatures (Luque et al., 2014; Martín et al., 2012), which causes an increase in the already high number of tropical and equatorial nights and also tends to cause a decrease in the daily thermal amplitude. Another issue pointed out by research is the confirmation that the temperature rise is higher in the high mountains (Martín et al., 2012; Sperling et al., 2004), a fact also observed in other island territories with similar features (Díaz et al., 2011). Furthermore, it is worth noting that, according to several of the aforementioned studies, the increase is particularly accentuated during the summer season and, moreover, in the province of Las Palmas, which is more easterly and closer to the African continent. All in all, the rise in temperatures in the Canary Islands is higher than the global average in recent decades (+0.27 °C between 1981 and 2010) and similar to the archipelagos that are experiencing the greatest temperature increase worldwide (Cropper and Hanna, 2014).

Heat waves deserve special mention, whose frequency has significantly increased in the 21st century; according to data from the AEMET, the number of heat waves in the Canary Islands has increased from 17 in the period between 1975 and 2000 to 40 between the latter date and 2023 (AEMET, 2022). It is also worth mentioning the record temperatures that have been observed in recent years; in several stations located in the archipelago, the absolute maximum temperature has recently been exceeded: for example, at El Hierro Airport, whose data series began in 1973, 35.4 °C were reached on October 10, 2023. On August 16, 2021, the highest absolute temperature recorded at Tenerife South Airport (44.3 °C) was reached, with exceptional episodes such as the one that occurred in May 2015 in Lanzarote, when 42.6 °C was exceeded.

8.1.2 Changes in precipitation

On another note, the pluviometric analysis of any territory always implies greater complexity given the statistical difficulty involved in the high irregularity of precipitation, as well as its high temporal variability and considerable temporal and spatial concentration. These circumstances, combined with the absence of quality records, prevent the identification of clear patterns with high statistical significance. Moreover, the Canary Islands have traditionally presented the most prominent coefficients of variation in the whole country (Dorta Antequera et al., 2018), making it highly adventurous to identify temporal or spatial trends with complete certainty.

In any case, most published studies point to a general decrease in rainfall (De Luque, A. & Martín-Esquivel, J.L., 2011; García-Herrera et al., 2003; Máyer et al., 2017; Máyer Suárez et al., 2015), although the trends are not completely significant (Cropper, 2013; Sánchez-Benítez et al., 2017), and can be slightly more clearly identified on the northern facades of Tenerife and, above all, Gran Canaria (Máyer et al., 2017). The most acute pluviometric reduction tends to be quantified at about 40 mm per decade in specific enclaves of the islands (De Luque, A. & Martín-Esquivel, J.L., 2011; Máyer Suárez et al., 2015), reaching 60 mm of

decrease per decade in the high mountains since 1970 (Hernández Barrera et al., 2012). Small sectors of the islands, such as the northeastern region of La Palma or the island of El Hierro, show increases in rainfall that are not statistically relevant (Hernández Barrera et al., 2012). On the other hand, it is possible to appreciate an increase in rainfall intensity, although only in some observatories, so it cannot be stated that this is a generalised trend (Máyer et al., 2017).

In the pluviometric context of the last decades, the frequency of very dry winters has increased (Dorta Antequera et al., 2018), evidencing, in addition, a considerable increase in the intensity of droughts, particularly in the meridional sectors of the region (Amador González and Marzol Jaén, 2021). Obviously, this situation has negative consequences in terms of ecosystems, the risk of forest fires, agricultural and livestock activity and the islands' water supply.

On the other hand, records from recent decades suggest a possible alteration of the annual rainfall regime in the region. Thus, the Canary Islands, with a clear Mediterranean rainfall pattern, has traditionally shown an almost total absence of rainfall during the summer; however, according to the data for the last century, this pattern seems to have undergone an incipient and still insignificant variation. In the last twenty-five years, there have been important rainfall events during the month of August that have broken, among others, the monthly precipitation record for that month at the centennial Izaña Observatory, Tenerife (Dorta Antequera et al., 2018). Similarly, tropical phenomena such as storm Hermine, which reached the Canary Islands in September 2022, leaving in its wake abundant and unprecedented rainfall for that month (AEMET, 2022), are events that, even considering the reservations expressed about the statistical significance of rainfall, invite us to think about a tropicalization of rainfall in the region. In this context, increasingly frequent -although, for now, isolated- episodes of convective nature and purely tropical origin may play a very important role in this eventual change in the seasonal distribution of precipitation. In this sense, a consistent trend seems to be identified in the extension towards the southeastern North Atlantic, in the vicinity of the Canary Islands and the Gulf of Cadiz (Dorta Antequera et al., 2023). These low pressure centres, formed around the Cape Verde archipelago, generally tend to head westward, moving towards the Caribbean and the Gulf of Mexico following warm waters (Dorta Antequera et al., 2018). However, anomalously and punctually their trajectory has been modified to turn eastward and approach the Azores, Madeira and the Canary Islands. This is the case of storms Delta (2005), which caused severe damage in the region, Hermine (2022) and Hurricane Vince (2005). However, despite the reported increase in the number of disturbances of this type in the southeastern North Atlantic (Dorta Antequera et al., 2023), it should be noted that there are written records that report the occurrence of extreme events in the area -in 1724 and 1842, for example-, so that the occurrence of these phenomena in the Canary Islands is not unprecedented and should not be attributed, at least directly and completely, to climate change. A different matter is that global warming encourages the increasingly evident odds of the appearance of unstable phenomena of tropical origin or, in any case, of a convective nature, considering

the thermal rise of the ocean surface near the Canary Islands estimated for the coming decades -surpassing 2 °C by the end of the century- (Guijarro et al., 2014).

8.1.3 Other variables

Although the impacts and trends described above reflect the consensus of most published research on climate change in the Canary Islands, the treatment of other climatic variables of interest, such as pressure, relative humidity and insolation, should not be overlooked. Regarding pressure, experts such as Cropper and Hanna, 2014 point to an increase in the barometric gradient between the Azores and Cape Verde, which could imply an increase in the intensity of trade winds also reported by other authors (Guijarro et al., 2014). However, studies with NCEP/NCAR such as those of Marrero-Betancort et al., 2020 show a net decrease of 1 m/s in the intensity of the trade winds. Using the upwelling to the east of the Canary Islands as a proxy, Gallego et al., 2022 do not find a clear relationship with the winds according to the NAO index analysis, but they do with the summer NAO, which is increasingly positioned more towards the northeast of Europe in its positive phase, causing a decrease in the northeast winds favourable to the upwelling.

Notwithstanding, it has also been pointed out that, as a consequence of the extension of the Azores Anticyclone towards the Sahara, a change in wind conditions is to be expected -in the cold months, the area of high pressure occupies increasingly zonal positions, producing more frequent easterly winds with a zonal component that could be intensifying Saharan intrusions in the region- (Alonso-Pérez et al., 2011). Note, however, that no significant trends in these suspended dust episodes are observed in other investigations (García et al., 2016).

In relation to relative humidity, the obtained results are not conclusive; some studies identify increases in coastal sectors of 1.1%/decade (Sperling et al., 2004), while others report a decrease that could be behind the 18.2 mm/decade increase in evapotranspiration, especially during the summer season (Vicente-Serrano et al., 2016). Insolation is a variable for which no significant trends have yet been identified (Sanroma et al., 2010).

In short, variations in various climatic parameters are evident in this region of the southeastern North Atlantic. Thermal increase, especially at night, is very significant, and precipitation shows a trend, still very incipient, towards a decrease and extreme phenomena of tropical origin are becoming a growing threat in a warmer context and, above all, with warming sea surface temperatures.

8.2 Balearic Islands

8.2.1 Changes in temperature

The most complete analysis on temperature trends in the Balearic Islands is from Homar et al., 2010, who examined trends in maximum and minimum temperatures using information collected from three temperature stations, with daily records spanning from 1976 to 2006. These stations were located at the head of the

runways of the airports of the three main islands, where urbanisation did not have a relevant impact on the recorded values. In addition, the annual mean temperature in the middle troposphere and lower stratosphere was evaluated using data from specific radiosondes from the Balearic Islands for the period from 1981 to 2006. The analysis of temperature records showed that minimum temperatures increased by 0.58 ºC/decade during the 31-year period, while maximum temperatures exhibited an increase of 0.50 ºC/decade. Both trends showed a statistical confidence greater than 99%. At the same time, temperatures in the middle troposphere showed a decrease at a rate of -0.54 ºC/decade, while the lower stratosphere showed a trend of -0.78 ºC/decade. Despite considerable interannual variability in both series, the statistical confidence for the sign of linear trends in the troposphere and stratosphere exceeded 98 %.

Later, Guijarro, 2013 estimated temperature trends in all Spanish regions –including the Balearic Islands– covering a longer period starting in 1951, with homogenised series, although very low trends resulted for the region. The information of trends is also included in the quarterly and annual reports of the state of the climate in the Balearic Islands, published by the Interdisciplinary Climate Change Laboratory of the University of the Balearic Islands (LINCC-UIB), since 2017 (Jansà et al., 2017).

A recent work on climatic trends in the Balearic Islands obtained from instrumental observations is that of (Guijarro and Jansà, 2022). It refers only to temperature trends and reviews previous literature on the issue, including Homar et al., 2010. In addition, trends were recalculated with recent data (up to 2020) and homogenised. Their results showed that temperature trends varied depending on whether homogenization procedures were applied or not, and they were extremely sensitive to sample characteristics (length and date). Although the trends were always positive when sufficiently long and recent samples were taken (at least 30 years long, starting around 1995 or later), the variations between one sample or another were very strong, from just over 0.1 ºC/decade to almost 0.7 ºC/decade, which shows that the high natural variability precludes more robust thermometric trends.

Finally, data obtained from the meteo-oceanographic buoy sensors from *Puertos del Estado* were used to analyse interannual variations in parameters such as air temperature over the sea. Some results can be seen in Barrientos et al., 2022.

8.2.2 Changes in precipitation

Homar et al., 2010 also examined precipitation variations in the Balearic Islands by analysing data from 18 rain gauges with complete daily records between 1951 and 2006. This study found a notable negative trend in annual rainfall, showing a decrease of 163 mm per century, with a confidence level of 85 %. An algorithm for the detection of significant changes in the trend, based on the optimization of the explained variance by segments of the complete series (Oosterbaan, 1994), resulted in a consistent detection of a breakpoint between years 1979–1983. The breakpoint detection algorithm identified abrupt decreases in annual precipitation of 65 mm in average between the two distinct periods (1951-1980 and 1981-

Reference	Period	Number of series	Maximum temp.	Mean temp.	Minimum temp.
Guijarro, 2001	1978-2000	4		0.77	
Homar et al., 2010	1976-2006	3	0.58	0.54	0.50
Jansà, 2012	1973-2009	1		0.54	
Guijarro, 2013	1951-2012	48	0.14	0.11	0.07
Jansà et al., 2017	1973-2012	48		0.41	
Jansà, 2018	1973-2017	3		0.35	
Jansà et al., 2019	1973-2017	4		0.28	
Guijarro and Jansà, 2022	1961-2020	22	0.19	0.21	
Guijarro and Jansà, 2022	1991-2020	22	0.37	0.28	

Table 3.2. Compilation of published temperature trends (°C/decade) of the Balearic Islands. (Adapted from Guijarro and Jansà, 2022; homogenised series in bold)

2006). The analysis also highlighted a change in the composition of the total annual precipitation: low rainfall (up to 4 mm) and very heavy rainfall (more than 64 mm) showed a greater contribution, while the contribution of moderate to heavy rainfall (i.e. between 16 and 32 mm) decreased.

Mixing hydrological and instrumental precipitation data, García et al., 2017 conducted a comprehensive analysis focusing on annual and seasonal trends in daily flow data observed at 14 gauging stations located along temporary streams throughout Mallorca. Using a Mann-Kendall test, trends in data spanning 1977 to 2009 were examined for discharge, number of water days, accumulated precipitation, potential evapotranspiration and land cover changes. Their findings revealed a general decreasing trend in flow during the spring and summer, with reductions between 4 and 17 % in particular basins. Seasonal changes especially affected the headwaters of the basins located in the mountains of Mallorca. Consequently, a regional Kendall test was performed in 12 basins within the Tramuntana mountain range, revealing a significant decrease in the number of days with flow of -0.44 days/year. Despite substantial interannual variability, the decrease in the number of days with running water was attributed to a confluence of factors: i) decreased annual precipitation, ii) increased temperatures, and iii) the influence of forest colonisation and the growth of agricultural abandoned fields.

In relation to the observed trends of precipitation in the Balearic Islands, the

variability, the dependence on the period or the considered sample is even more important than that of the temperature trend. Jansà et al., 2019 showed that, depending on the chosen sample or period, the trend can even change its sign, from negative to positive. The negative trend in precipitation estimated by Homar et al., 2010 cannot, therefore, be taken as stable and permanent, as evidenced by the lengthening of the data series. When looking at 30-year running trends for the average precipitation at the three airports of the Balearic Islands, great differences in signs were observed, from decreasing trends of up to -4.5 mm/year (1971-2000) to increasing ones of +4.5 mm/year (1981-2010).

8.2.3 Temperature and precipitation trends in Menorca

With reference, not to the Balearic Islands as a whole but to the island of Menorca in particular, Jansà et al., 2019 calculated temperature and precipitation trends based on AEMET data from the airport. These highlighted the notable changes in sign in the precipitation trend, depending on the period taken into account. It is also mentioned that few changes were observed in Menorca, associated with climate change, in other variables such as sunshine, wind, etc. Some of these results were obtained within the framework of the BIOCLIMA 2017 project, directed by the OBSAM-IME (Menorca) and financed by the Biodiversity Foundation (Madrid). A brief summary of the obtained results were published in Catalan and Spanish in OBSAM-IME (2018).

Jansà et al., 2019 also highlighted the high seasonality of trends, especially of temperatures, in Menorca. Something similar was revealed for Mallorca (Jansà, A., 2012). This marked seasonality of the temperature trend, with a marked maximum in late spring, resulted into a specific study referring to the Balearic Islands as a whole, with extension to the entire Iberian-Mediterranean and south-western European region, in which the frequency and intensity of an upper air anticyclonic ridge increase, particularly in late spring (Jansa et al., 2017).

8.3 Mountains

Mountains play a crucial role in the climate system at different temporal and spatial scales. They affect the flow of air masses through dynamical and thermodynamic effects, which influence the climate of large areas of the Earth (Buzzi and Tibaldi, 1978; Frei and Schär, 1998; Yasunari et al., 2006). At a regional scale, mountains create distinct and recurring meteorological conditions in their immediate surroundings and areas of influence, resulting in what is commonly referred to as an alpine or mountain climate (James, 1922).

Although mountains only cover 27 % of the Earth's surface, they receive significantly more precipitation than lower lands and contain 70 % of the world's freshwater (Casassa et al., 2007). Mountains play a crucial role in the water cycle, acting as giant 'water towers' that collect, store, and gradually release freshwater to surrounding areas (Viviroli et al., 2007).

The Sixth Assessment Report (AR6) of the IPCC (IPCC, 2023) states that spring snow cover across the Northern Hemisphere has significantly reduced since the 1950's. Additionally, high mountain regions have experienced significant warming since the early 20th century,

resulting in reduced snowpack on average (Marty et al., 2017). The shift from snow to rain as the primary form of precipitation has been found to cause a decline in both streamflow and groundwater storage in regions where snowmelt is the primary source of recharge (Berghuijs et al., 2014; Earman and Dettinger, 2011). This change is associated with a greater reduction of snow water equivalent (SWE) at lower elevations.

Central System

The region experiences frequent droughts, and the intensity of precipitation is expected to change. A lower ratio of snow water equivalent is expected, and faster snowmelt is anticipated due to rising temperatures (Durán et al., 2023). Planners will need to adapt to this new scenario, which may result in a redistribution of the seasonal runoff cycle and changes in intensities. Also, a significant tendency of decreasing days with snow cover above 3 cm since 2000 has been found (González-Flórez et al., 2022). This is attributed to higher ground temperatures resulting from climate change and the elevation of the zero degrees Celsius isotherm. This hypothesis, which is consistent with other works in the area (Rubio-Romero, A.; Granados, I., 2008), requires further investigation in the future.

Unfortunately, there is a lack of regional climate variability studies and links between climate and hydrology at these mountains due to the complexity of the phenomena. There are some exceptions like Durán et al., 2013 and the following publications for Sierra de Guadarrama or Azorín-Molina et al. (2021) for Gredos, but further research is encouraged.

Sierra Nevada

The spatial and temporal variability of Sierra Nevada is primarily influenced by the NAO in the western part, while the eastern part is more affected by Mediterranean depressions, especially the WeMO (Esteban-Parra et al., 2022). Sierra Nevada experiences marked inter and intra-annual variability in precipitation, which is typical of the Mediterranean climate (Castillo, et al., 1996). Precipitation is concentrated mainly between October and April. There is a clear decrease in precipitation from West to East, and a trend of increasing precipitation with altitude. The mean annual precipitation on the north-western face, which faces the prevailing direction of incoming storms, is 550 mm at 1,000 m and 750 mm at 2,000 m. Moving towards the East, the rain shadow effect reduces the mean annual precipitation to 300 mm at 1,000 m and 465 mm at 2000 m. The mean gradient of precipitation with elevation along the entire Sierra Nevada is about 150 mm/km above 1,300 m. The fraction of snow is highly variable and unpredictable. Snow processes are dominant above 2300 m in the north-west and 2,500 m in the rest of the Sierra. Sublimation from snow is an important factor, with local values reaching up to 30 % over time (Herrero and Polo, 2016). At the massif scale, it accounts for around 15-20 % of the total snow accumulated on the surface. Rain-on-snow phenomena are frequent and significant from a hydrological perspective due to marked temperature variations, even during the winter season.

Historical analysis by Pérez Palazón, 2019 shows an overall decreasing trend of 2.3 and 0.3 mm/year for annual precipitation and snowfall, respectively, in Sierra Nevada over a 55-year period. Although there are local differences in values and significance, this trend does not necessarily result in an increase in drought episodes characterised by SPI. Enhanced drought conditions are instead related to increased atmospheric demand (Esteban-Parra et

al., 2022). Significant temperature trends have been detected. Globally, annual increased rates are slightly higher for maximum temperatures than for minimum temperatures. The greatest increases are observed during the summer, with very significant trends above 0.3 °C/decade for both maximum and minimum temperatures. Positive significant trends are also found during spring and autumn.

This behaviour is reinforced in future scenarios. Climate change projections depict a clear warming trend and a reduction in precipitation over Sierra Nevada (Esteban-Parra et al., 2022). This trend is more intense for the far future under the RCP8.5 scenario. Drought events are likely to become slightly longer and more frequent in the near future, with a marked increase in duration and intensity for the far future. The northwestern face experiences greater annual snowfall losses in millimetres. However, in relative terms, the eastern area (Andarax river), which is less snowy, is the most affected (Polo et al., 2022). Additionally, the apparent shift towards torrential events may result in negligible changes or even slight local increases in annual snowfall in the southern areas.

Pyrenees

Several studies in the last decade have focused their efforts on understanding the behaviour of precipitation regimes in the Pyrenees. López-Moreno et al., 2011 showed a general decrease (1955-2006) in annual precipitation, in the number of rainy days and in precipitation intensity, while an increase in the duration of dry spells. This decrease was especially significant at headwaters during winter and spring. Lemus-Canovas et al., 2019 increased the detail of these results by obtaining a classification of 8 regions exhibiting differentiated precipitation characteristics. Two of them, located in the southern slope, showed a significant decrease. However, Buisan et al., 2015 did not find significant trends in the number of precipitation or snow days for the 1981–2010 period.

In terms of extreme events, Lemus-Canovas et al., 2021 found a clear dependence on the maritime influences and teleconnections, with the WeMO the most important, especially for the eastern side of the range. Under return periods of 5 years, magnitudes of 150 mm per day are highly expected in this area. For temperatures, an increase in dry–hot compound events in the 1981-2015 period was noted (Lemus-Canovas and López-Bustins, 2021), which is of paramount importance for snow cover (Bonsoms et al., 2023). But not only in extremes, the rate temperature increase in the Pyrenees has been pointed out as higher than global warming (Deaux, et al., 2014; El Kenawy et al., 2013; Espejo F, Ferraz J, Palomo M., 2008; Spagnoli et al., 2002). Significant increases, especially in spring (Pérez-Zanon et al., 2017), foster a notable decrease of snow cover and an accelerated retreat of ice masses and glaciers (Albalat et al., 2022; López-Moreno et al., 2020, 2016; Martínez-Fernández et al., 2022; Vidaller et al., 2023). While meteorological information is sparse and intermittent in time, a recent dataset from a joint international effort is available from the mid 20th century (Cuadrat et al., 2024).

Cantabrian Mountains

The Cantabrian Mountains extends longitudinally (from west to east) for about 300 km, separating the Cantabrian Sea from the Northern Plateau. It is a mountainous area with a marked asymmetry between slopes, exhibiting significant structural and geomorphological differences.

Its climate is distinctive, displaying a wide range of nuances, resulting in significant landscape richness. The northern slope has an oceanic character with a steep altitude gradient, while the southern slope has a lower altitude gradient, transitioning towards sub-Mediterranean and sub-Atlantic taxa (Ortega Villazán and Morales Rodríguez, 2015), in addition to greater continentality and insolation. The highest sectors include Picos de Europa, Fuentes Carrionas Massif, Peña Ubiña Massif, Sierra de Híjar, Mampodre Massif, or Sierra de Gistredo, where peak elevations surpass 2,000 m, reaching 2,650 m at Torre Cerredo (Picos de Europa).

On the one hand, the northern slope is characterised by cool temperatures throughout the year, with low annual thermal amplitude, moderate precipitation, and no summer aridity. On the southern slope, at higher altitudes, summers are cool and short, while winters are long and harsh. There is a high annual thermal oscillation, and in the more southern sectors, summer aridity occurs. Winters are especially cold when retrograde circulations are present and snowfall is frequent (Ortega Villazán and Morales Rodríguez, 2015). Low temperatures in the higher massifs cause permafrost to be preserved in frozen caves (Gómez Lende, 2016; Gómez-Lende and Serrano Cañadas, 2021) and very small ice patches (remnants from small glaciers formed during Little Ice Age) persist (González Trueba, 2005; Serrano et al., 2018).

There are no specific scientific studies for the entire Cantabrian Mountains regarding observed trends and medium-term predictions in the context of Climate Change. However, some studies conducted for the entire Iberian Peninsula allow distinguishing trends in the Cantabrian Mountains compared to other mountain systems and adjacent areas (del Río et al., 2011; Díaz-Poso et al., 2023a, 2023b; Ferreiro Lera et al., 2022; Lastrada et al., 2021). Some studies partially cover aspects of climate trends in parts of the range or local studies that also show different responses to Climate Change (Álvarez-Martínez et al., 2014; del Río González, S, 2005; Gallinar Cañedo et al., 2022; Ortega Villazán and Morales Rodríguez, 2015; Pisabarro et al., 2019).

An analysis of meteorological stations on the southern slope since the mid-20th century shows an increase in average annual temperatures, especially due to the thermal behaviour of spring and summer, estimated at 0.05 °C per year (Ortega Villazán and Morales Rodríguez, 2015). Increasing trends have been observed in the values of anomalies in maximum, minimum, and mean temperatures, both annually and seasonally (Álvarez-Martínez et al., 2014; Morales et al., 2005). An increase (both in daily maximums and minimums) in the annual frequency of higher extreme values is observed, and also a decrease in the annual frequency of lower extreme values (Morales et al., 2005). Locally, a trend of 1.5 ºC in the mean annual temperature of the period 1961 to 2014 has been observed in one of the headwater catchments of the central sector of the Cordillera, the Alto Pisuerga (Pisabarro et al., 2019). Recent studies confirm this trend, with an increase in the intensity, frequency, and duration of heat waves (Díaz-Poso et al., 2023b) and, to a greater extent, a decrease in cold spells (Díaz-Poso et al., 2023a) for the near future period (2021-2050), with a greater impact on the Cantabrian Mountains environment compared to other mountain systems and adjacent areas.

At the seasonal level, an analysis of temperatures in the period 1961-2006 showed significant positive trends in spring and summer temperature values in the Cantabrian Mountains area, with increases of 0.1 °C or 0.2 °C in average temperature per decade (del Río et al., 2011). Through the study of flow peaks due to snowmelt, a greater and recurrent impact of high winter and spring temperatures has been detected, which has caused the

flow peaks of the rivers analysed on the southern slope to be two months earlier (Morán-Tejeda et al., 2021, 2010; Pisabarro et al., 2019).

Other studies have analysed the importance of snow cover at the local level in high-altitude areas (González Trueba and Serrano Cañadas, 2010), in some cases using data loggers to study the insulation effect of snow on ground temperatures and its geomorphological implications. These studies highlight interannual variability in days with annual snow cover (Gallinar Cañedo et al., 2022) and a regressive trend since the mid-20th century in the western sector of the range (Santos González et al., 2013), in the northern slope (Beato Bergua et al., 2019) or on the southern slope of the Cantabrian Mountains (Merino et al., 2014; Pisabarro, 2020). However, temperature trends recorded at high-altitude locations (short series) show more stable trends, as local topography has a significant impact on the thermal regime at higher altitudes (Melón-Nava et al., 2022; Pisabarro et al., 2017; Ruíz-Fernández et al., 2023). Therefore, these areas become of great interest for future monitoring of climatic conditions at the local scale, and the maintenance of time series data should be promoted to assess the response to climate change based on longer series.

In recent years, multidisciplinary projects have been developed to highlight the biophysical peculiarities of the Cantabrian Mountains and its interest to try to create an observatory to monitor the effects of Global Change in this area, despite the administrative division of this space (Barquín Ortiz et al., 2018). They highlight a profound transformation in land use in recent decades, a consequence of depopulation and changes in livestock models towards the loss of extensive models and concentration, favouring the abandonment and reforestation of large areas (Álvarez-Martínez et al., 2014; Beato Bergua et al., 2019; García-Hernández et al., 2017; García-Llamas et al., 2019) and environmental problems due to overgrazing. The decrease in runoff has also been analysed, a possible consequence of this profound transformation in the context of changes in thermo-pluviometric regimes (Pisabarro et al., 2019).

The negative effect of increased forest and shrub vegetation, coupled with changing rainfall patterns (greater irregularity) and rising temperatures, favours conditions conducive to more virulent and extensive wildfires, given the greater difficulty of extinguishing them with a higher volume of fuel exposed to increasingly prolonged drought periods.

8.4 Cities

The characterisation and analysis of regional climate changes due to urbanisation pose an additional challenge in urban environments for the development of climate change adaptation policies. Global warming and its local impacts present significant challenges for the sustainability, quality of life and health of urban populations. Anthropogenic emissions of greenhouse gases have led to an increase of the global mean surface temperature by 1.15 ºC (IPCC, 2023b). This is particularly relevant considering that the Mediterranean region is warming at a faster rate than the global average, and an increase of 2 °C relative to preindustrial times is expected within the next 20 years (Zittis et al., 2019).

Spain is especially sensitive to the Urban Heat Island (UHI) effect, given that a high percentage of its population resides in urban areas (approximately 81 %). The UHI further exacerbates the heat exposure to cities already evident under climate change conditions, especially in

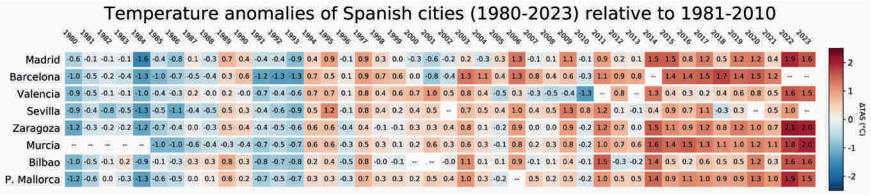

Figure 3.6. Surface temperature anomalies from 1980 to 2023 (relative to 1981-2010) for the most populated Spanish cities. Missing data from specific stations/years appears in white. Data source: AEMET OpenData.

summer (Cuadrat, et al., 2022). This phenomenon is mainly caused by the concentration of buildings and pavements in urban cores, as well as artificial surfaces capable of absorbing and retaining incoming solar radiation, and re-emitting it as heat. The lack of vegetation and water bodies, the heat release from human activities and the urban morphology (with the formation of urban canyons), significantly contribute to temperature increases in urban areas, relative to their surrounding environments. The temperature difference is especially significant in summer, when nighttime temperatures in urban areas can be 2 °C higher than outside the cities (Martín-Vide and Moreno-García, 2020), reaching up to 8 °C under high atmospheric stability conditions. This combination of factors expose large percentages of the country's population to health-related risks driven by heat (Heaviside et al., 2017; Hsu et al., 2021).

In the last decade, the most populated cities in Spain have experienced unprecedented temperature records. Figure 3.6 shows annual temperature anomalies in 8 of the most populated Spanish cities from 1980 to 2023. Despite interannual variability, there is a clear trend in surface temperatures driven by climate change and exacerbated by urban factors such as the UHI effect. Annual temperature values have risen by up to 2.1 °C (Zaragoza) above the climatological period (1981-2010). In all cities displayed in Figure 3.6, the hottest year on record occurred in the last 5 years, except for the case of Seville. The extreme heat conditions experienced in several Spanish cities in the last years have shown to increase the risk of acute cardiovascular events (Salvador et al., 2023), and mortality (Royé et al., 2020). For example, the summer of 2022 was the hottest on record since 1961, and led to an excess mortality of more than 5,000 people due to extreme heat conditions in the Spanish province capitals (Tobías et al., 2023).

The observed climate trends along with the accelerated urban growth emphasise the need for specific research that allows us to understand and address the complex interactions between urbanisation and climate dynamics in Spain. These studies should not only contribute to sustainable urban planning, but are also essential for mitigating the adverse impacts of climate on societal wellbeing.

Research efforts were made to understand urban climate in Spain in the 1980's in some Spanish cities, with the aim of characterise and quantify the UHI in the form of centre-periphery anomalies. However, these works did not take into account the spatial perspective

of the factors contributing to the anomalies (López Gómez, 1993; López Gómez, A., 1988; Torrecilla et al., 1998. It is important to highlight the difficulties in obtaining data with adequate temporal and spatial resolution due to the lack of observation networks with sufficient density to robustly assess the characteristics of urban climate dynamics. This limitation hinders the replicability and comparison of studies between cities, as each has its own protocols for network design, installation and sensor specification, not to mention the heterogeneous length of data available for each location.

Nevertheless, current research continues to focus on characterising UHI (Acero et al., 2013), as well as on the different impacts of heatwaves (Tejedor et al., 2016), and even on refining information and detailed mapping of urban temperatures (Barrao et al., 2022). In the last decade, modelling studies aimed to represent the thermal structure of cities (Banks et al., 2015; Núñez-Peiró et al., 2021; Salamanca et al., 2012), also using climate projections (José et al., 2018).

The difficulty in obtaining climate information from urban environments paves the way for the search of new methodologies, including the rising use of satellite and remote sensing information. However, it is important to note that these studies focus on the temperature of materials, not on air temperature, leading to the concept of the Surface Urban Heat Island (SUHI), which is different from the UHI, which refers to air temperature. While these studies allow for detailed and continuous spatial resolution, this scale often does not match the dimensions of medium or small-sized cities, as it depends entirely on the satellite image resolution, making detailed intra-urban studies challenging.

Despite the limitations of satellite imagery, including a lack of continuous time information, the absence of hourly data and challenges derived by cloud cover or other atmospheric phenomena, the integration of satellite data in urban climate studies enables comparisons between different cities (Hidalgo García et al., 2022; Rodríguez-Gómez et al., 2022). There has even been an exploration of the use of drones and their applications through thermal sensors in urban spaces (Rodríguez et al., 2022).

Recent studies highlight the need of integrating urban climate studies in multidisciplinary analyses. One notable interaction is between urban climate and health, exploring how climatic conditions affect human health based on data from hospital admissions and mortality rates (Carmona et al., 2016; Iñiguez et al., 2021; Kim et al., 2019; Tobías et al., 2023). There is also a growing interest in understanding how the urban climate is linked to tourism (Díaz-Poso et al., 2023c; Millán López and Fernández García, 2018), including future trends under climate change conditions (Martínez-Ibarra, 2015; Millán López, 2019).

Another crucial research focus is on mitigation and adaptation to climate change in urban environments (Gandini et al., 2021; Hidalgo-García and Rezapouraghdam, 2023; Martínez-Juárez et al., 2019; Pietrapertosa et al., 2023; Salvia et al., 2021). This goes beyond proposing solutions, encompassing the future evaluation of these measures and the identification of urban areas most vulnerable to adverse climate impacts. An emerging perspective, strongly linked to architecture and urban planning, involves incorporating climatic variables and concepts into issues related to energy efficiency and thermal comfort in buildings and urban spaces (Álvarez et al., 2021; Aram et al., 2020; Lomba-Fernández et al., 2019; Rodríguez Algeciras and Matzarakis, 2016). This approach reflects the growing

awareness of the importance of designing sustainable and resilient urban environments, considering local climatic conditions.

This multidisciplinary approach allows for a broader understanding of the impacts of urban climate on society and the environment. However, this does not exempt us from the need for specific research that addresses urban climatology with detail. Understanding meteorological and geographical variables, as well as physical processes in the urban context will allow to better understand the interaction between regional climate and urban dynamics, and ultimately be useful for adaptation and mitigation policies.

9. Conclusions

This chapter is a review of current knowledge on climate variability over the instrumental period in Spain. Spain has a solid and well-distributed observation network for all atmospheric variables which, together with a number of reliably built gridded datasets, allow for a comprehensive analysis of past climate variability (Serrano-Notivoli and Tejedor, 2021). In relation to temperature, different studies have found a positive trend during the instrumental period (in different periods during the last 100 years), although this shows a noticeable temporal and spatial variability. For annual mean temperatures, this trend reaches a value of 0.21 ºC/decade over the period 1961-2018 (AEMET, 2023, 2022). However, temperature increase is higher for the summer or spring, when it can reach 0.27 ºC/decade and 0.24 ºC/decade, respectively (AEMET, 2023, 2022). Furthermore, extreme temperature events, such as the occurrence of heat waves, have increased in frequency (+0.3/decade), intensity (+0.1 ºC/decade), duration (+0.9 days/decade for the yearly maximum duration) and spatial extent (+1.3% of the IP by decade) over the period 1951-2019 (Paredes-Fortuny and Khodayar, 2023).

Yet, in general, there is no clear and homogeneous trend in the sign of precipitation. Most of the studies (e.g., Camuffo et al., 2013; Serrano-Notivoli, 2017; Peña-Angulo et al., 2020; Senent-Aparicio et al., 2023) point to a slight decrease (not significant in all areas) in annual totals since the second half of the 20th century. The general decline shown in Peninsular Spain is conditioned by a marked interannual variation and with important spatial contrasts. However, there is a consensus in the confirmation of a decrease of precipitation in March and June and a slight increase in October (del Río et al., 2011; González-Hidalgo et al., 2024; González-Hidalgo et al., 2011), potentially due to a temporary shift in the spring and autumn maximums, respectively, due to the increasingly warm conditions of the atmosphere and ocean masses.

Extreme precipitation trends are variable for the whole territory or temporal period, but an increase of convective events has been observed, leading to an increase of high precipitation events, especially in the end of autumn, probably related to a warmer Mediterranean sea (Meseguer-Ruíz et al., 2021; Miró et al., 2018; Muñoz et al., 2020). On the other hand, the 21st century has experienced the greatest frequency of severe droughts of the last 150 years (Vicente-Serrano et al., 2023). While precipitation amounts have been around average values, higher temperatures pushed a higher atmospheric evaporative demand, leading to longer and more intense droughts (Coll et al., 2017; Paniagua et al., 2019).

The IP shows a strong relationship between moisture transport from its dominant moisture sources (the tropical–subtropical North Atlantic, the IP itself (recycling), and the surrounding western Mediterranean basin) and hydrometeorological extremes, such as extreme precipitation

or meteorological drought . The extreme precipitation shows a high dependence on the moisture contribution from these moisture sources, as well as from the water column or atmospheric instability. Meteorological droughts are due to a low moisture contribution (Gimeno-Sotelo et al., 2024; Gimeno-Sotelo and Gimeno, 2023). The atmospheric moisture contribution from the dominant sources has a clear seasonal behaviour, with the tropical–subtropical North Atlantic contribution dominating during the cold season and the Mediterranean and recycling contribution increasing during the warm season (Gimeno et al., 2010). The remarkable decrease in recent summer precipitation over the Iberian Peninsula can be attributed to reductions in moisture contributions from the IP itself (26%) and from the east of the North Atlantic (57%), compared to before and after 1997 (Liu et al., 2022).

Concerning the wind variability, it has been pointed out that near-surface wind speed over the IP has declined (i.e., "stilling" phenomenon) from the early 1960's to 2010 at an annual rate of about -0.15 $m*s^{-1}$/decade ($p < 0.05$), being followed by a cessation of the stilling or a weak and non-significant wind strengthening period. The stilling may have been caused by an increase in atmospheric thermal stability and a northward shift of the jet stream. No other cause was found for the cessation of the stilling than a change in the trend of the Western Mediterranean Oscillation (Azorín-Molina et al., 2014; Utrabo-Carazo et al., 2022).

Beyond the IP the Canary Islands and the Balearic Islands deserve special attention due to the particularities of their location and geographical and climatic characteristics. The Canary Islands are experiencing higher temperatures especially in summer, leading to a higher frequency of heatwaves (Dorta Antequera et al., 2018). Precipitation trends are not homogeneous, but a general decrease in total amounts have been observed (Dorta Antequera et al., 2018). On the other hand, Balearic Islands temperature records showed that both minimum and maximum temperatures have increased above 0.50 ºC per decade over the period 1976-2006 (Homar et al., 2010). They also experienced a notable negative trend in annual rainfall of 1,63 mm per year over the period 1951-2006, although it was not stable along the entire period (Homar et al., 2010).

Other territories that present special climatic conditions and specific vulnerabilities to climate change are the mountain systems. The Spanish mountain systems suffer from the same impacts as the rest of the territory (droughts, heat waves, etc.), triggered by a subtle decrease in annual precipitation and a clear increase in temperatures. However, these are accelerating snowmelt processes that will make the glaciers disappear in the next decades. Water resources have been already affected, with a significant impact on mountain ecosystems.

Finally, given that a high percentage of its population resides in urban areas (approximately 81 %), Spain is especially sensitive to the Urban Heat Island (UHI) effect. In the last decade, the most populated cities in Spain have experienced unprecedented temperature records driven by climate change and exacerbated by urban factors such as the UHI effect, giving rise to a growing awareness of the importance of designing sustainable and resilient urban environments, considering local climatic conditions (Cuadrat, et al., 2022; Heaviside et al., 2017; Hsu et al., 2021).

Lastly, there is still room for improvement in the analysis of the recent past variability of atmospheric variables in Spain. The solid observation network, centennial in some cases for temperature and precipitation, is useful for certain purposes like averaging climate variables or extracting trends for specific regions. However, there are several areas in the country, such as high-elevation mountains or relatively remote non-populated areas, with no observational information and for which the

models do not accurately reproduce the behaviour of some variables. This is due to uneven locations and the inaccessibility of weather stations, and also the use of all-purpose models that do not reflect the local conditions of such high-scattered variables. The observational coverage is non-homogeneous at all spatial and temporal scales making difficult, for example, comparative trends analyses. For recent periods, several researches have explored and implemented the inclusion of different sources of observations based on remote sensing technologies such as satellite information, radar-based data, and even UAVs (Unmanned Aerial Vehicles) to improve the knowledge of climate behaviour from regional to local scales. While this could be valid for the last decades, the problem grows as we extend back in time the period of study and no information is available. Before the mid-20th century, the challenge of completing observations in Spain involved greater efforts on digitising old documents with meteorological information and precious metadata. All of these new sources of information can be used to improve the already existing gridded datasets, which necessarily need to be regularly updated and, preferably, with increased spatial resolution.

References

Acero, J.A., Arrizabalaga, J., Kupski, S., Katzschner, L., 2013. Urban heat island in a coastal urban area in northern Spain. Theor. Appl. Climatol. 113, 137–154. https://doi.org/10.1007/s00704-012-0774-z

AEMET, 2023. Olas de calor en España desde 1975, Área de Climatología y Aplicaciones Operativas. Agencia Española de Meteorología.

AEMET, 2022. Avance climatológico de Canarias. Septiembre de 2022.

Albalat, A., Trapero, L., Lemus, M., Pons, M., 2022. Indicadores para el análisis de la evolución del espesor del manto de nieve en las estaciones de esquí: el caso de Andorra. Asociación Española de Climatología.

Algarra, I., Nieto, R., Ramos, A.M., Eiras-Barca, J., Trigo, R.M., Gimeno, L., 2020. Significant increase of global anomalous moisture uptake feeding landfalling Atmospheric Rivers. Nat. Commun. 11, 5082. https://doi.org/10.1038/s41467-020-18876-w

Allan, R., Brohan, P., Compo, G.P., Stone, R., Luterbacher, J., Brönnimann, S., 2011. The International Atmospheric Circulation Reconstructions over the Earth (ACRE) Initiative. Bull. Am. Meteorol. Soc. 92, 1421–1425. https://doi.org/10.1175/2011BAMS3218.1

Alonso-Pérez, S., Cuevas, E., Pérez, C., Querol, X., Baldasano, J.M., Draxler, R., De Bustos, J.J., 2011. Trend changes of African airmass intrusions in the marine boundary layer over the subtropical Eastern North Atlantic region in winter: TREND CHANGES OF AFRICAN AIRMASS INTRUSIONS. Tellus B 63, 255–265. https://doi.org/10.1111/j.1600-0889.2010.00524.x

Álvarez, I., Quesada-Ganuza, L., Briz, E., Garmendia, L., 2021. Urban Heat Islands and Thermal Comfort: A Case Study of Zorrotzaurre Island in Bilbao. Sustainability 13, 6106. https://doi.org/10.3390/su13116106

Álvarez-Castro, M.C., Faranda, D., Yiou, P., 2018. Atmospheric Dynamics Leading to West European Summer Hot Temperatures Since 1851. Complexity 2018, 1–10. https://doi.org/10.1155/2018/2494509

Álvarez-Martínez, J.M., Suárez-Seoane, S., Stoorvogel, J.J., De Luis Calabuig, E., 2014. Influence of land use and climate on recent forest expansion: a case study in the E urosiberian– M editerranean limit of north-west S pain. J. Ecol. 102, 905–919. https://doi.org/10.1111/1365-2745.12257

Álvarez-Socorro, G., Fernández-Álvarez, J.C., Nieto, R., 2023. Moisture Source Analysis of Two Case Studies of Major Extreme Precipitation Events in Summer in the Iberian Peninsula. Atmosphere 14, 1213. https://doi.org/10.3390/atmos14081213

Amador González, A., Marzol Jaén, M.V., 2021. La frecuencia e intensidad de las sequías en las vertientes meridionales de las islas Canarias (1970 – 2018). Investig. Geográficas 78. https://doi.org/10.5354/0719-5370.2021.64047

Aram, F., Solgi, E., García, E.H., Mosavi, A., 2020. Urban heat resilience at the time of global warming: evaluating the impact of the urban parks on outdoor thermal comfort. Environ. Sci. Eur. 32, 117. https://doi.org/10.1186/s12302-020-00393-8

Ayarzagüena, B., Barriopedro, D., Garrido-Perez, J.M., Abalos, M., De La Cámara, A., García-Herrera, R., Calvo, N., Ordóñez, C., 2018. Stratospheric Connection to the Abrupt End of the 2016/2017 Iberian Drought. Geophys. Res. Lett. 45. https://doi.org/10.1029/2018GL079802

Ayarzagüena, B., Serrano, E., 2009. Monthly Characterization of the Tropospheric Circulation over the Euro-Atlantic Area in Relation with the Timing of Stratospheric Final Warmings. J. Clim. 22, 6313–6324. https://doi.org/10.1175/2009JCLI2913.1

Azorín-Molina, C., Asín, J., McVicar, T.R., Minola, L., López-Moreno, J.I., Vicente-Serrano, S.M., Chen, D., 2018. Evaluating anemometer drift: A statistical approach to correct biases in wind speed measurement. Atmospheric Res. 203, 175–188. https://doi.org/10.1016/j.atmosres.2017.12.010

Azorín-Molina, C., Chen, D., Tijm, S., Baldi, M., 2011. A multi-year study of sea breezes in a Mediterranean coastal site: Alicante (Spain). Int. J. Climatol. 31, 468–486. https://doi.org/10.1002/joc.2064

Azorín-Molina, C., Guijarro, J., McVicar, T.R., Vicente-Serrano, S.M., Chen, D., Jerez, S., Espírito-Santo, F., 2016. Trends of daily peak wind gusts in Spain and Portugal, 1961–2014. J. Geophys. Res. Atmospheres 121, 1059–1078. https://doi.org/10.1002/2015JD024485

Azorín-Molina, C., Vicente-Serrano, S.M., McVicar, T.R., Jerez, S., Sánchez-Lorenzo, A., López-Moreno, J.-I., Revuelto, J., Trigo, R.M., López-Bustins, J.A., Espírito-Santo, F., 2014. Homogenization and Assessment of Observed Near-Surface Wind Speed Trends over Spain and Portugal, 1961–2011*. J. Clim. 27, 3692–3712. https://doi.org/10.1175/JCLI-D-13-00652.1

Azorín-Molina, C., Vicente-Serrano, S.M., McVicar, T.R., Revuelto, J., Jerez, S., López-Moreno, J.-I., 2017. Assessing the impact of measurement time interval when calculating wind speed means and trends under the stilling phenomenon: IMPACT OF MEASUREMENT TIME INTERVAL ON WIND SPEED MEANS AND TRENDS. Int. J. Climatol. 37, 480–492. https://doi.org/10.1002/joc.4720

Baldwin, M.P., Ayarzagüena, B., Birner, T., Butchart, N., Butler, A.H., Charlton-Pérez, A.J., Domeisen, D.I.V., Garfinkel, C.I., Garny, H., Gerber, E.P., Hegglin, M.I., Langematz, U., Pedatella, N.M., 2021. Sudden Stratospheric Warmings. Rev. Geophys. 59, e2020RG000708. https://doi.org/10.1029/2020RG000708

Banks, R.F., Tiana-Alsina, J., Rocadenbosch, F., Baldasano, J.M., 2015. Performance Evaluation of the Boundary-Layer Height from Lidar and the Weather Research and Forecasting Model at an Urban Coastal Site in the North-East Iberian Peninsula. Bound.-Layer Meteorol. 157, 265–292. https://doi.org/10.1007/s10546-015-0056-2

Barquín Ortiz, J., Álvarez-Martínez, J.M., Jiménez-Alfaro, B., García, Daniel, García, David, Serrano, E., González-Díez, A., Tejón, S., De Luis Calabuig, E., Taboada, Á., Purroy, F.J., Del Jesús, M., Naves, J., Fernández-Gil, A., Serdio, Á., Lucio, A., Suárez, R., Araujo, J., 2018. The Integration of knowledge about the Cantabrian Cordillera: towards an inter-regional observatory of global change. Ecosistemas 27, 96–104. https://doi.org/10.7818/ECOS.1422

Barrao, S., Serrano-Notivoli, R., Cuadrat, J.M., Tejedor, E., Saz Sánchez, M.A., 2022. Characterization of the UHI in Zaragoza (Spain) using a quality-controlled hourly sensor-based urban climate network. Urban Clim. 44, 101207. https://doi.org/10.1016/j.uclim.2022.101207

Barrientos, N., R. Vaquer-Sunyer,, A. Jansà, 2022. Temperatura del aire sobre el mar (Informe Mar Balear 2024).

Barriopedro, D., Fischer, E.M., Luterbacher, J., Trigo, R.M., García-Herrera, R., 2011. The Hot Summer of 2010: Redrawing the Temperature Record Map of Europe. Science 332, 220–224. https://doi.org/10.1126/science.1201224

Barriopedro, D., Gallego, D., Álvarez-Castro, M.C., García-Herrera, R., Wheeler, D., Peña-Ortiz, C., Barbosa, S.M., 2014. Witnessing North Atlantic westerlies variability from ships' logbooks (1685–2008). Clim. Dyn. 43, 939–955. https://doi.org/10.1007/s00382-013-1957-8

Barriopedro, D., García-Herrera, R., Ordóñez, C., Miralles, D.G., Salcedo-Sanz, S., 2023. Heat Waves: Physical Understanding and Scientific Challenges. Rev. Geophys. 61, e2022RG000780. https://doi.org/10.1029/2022RG000780

Batibeniz, F., Ashfaq, M., Önol, B., Turuncoglu, U.U., Mehmood, S., Evans, K.J., 2020. Identification of major moisture sources across the Mediterranean Basin. Clim. Dyn. 54, 4109–4127. https://doi.org/10.1007/s00382-020-05224-3

Beato Bergua, S., Poblete Piedrabuena, M.Á., Marino Alfonso, J.L., 2019. Snow avalanches, land use changes, and atmospheric warming in landscape dynamics of the Atlantic mid-mountains (Cantabrian Range, NW Spain). Appl. Geogr. 107, 38–50. https://doi.org/10.1016/j.apgeog.2019.04.007

Bedoya-Valestt, S., Azorín-Molina, C., Gimeno, L., Guijarro, J.A., Sánchez-Morcillo, V.J., Aguilar, E., Brunet, M., 2023. Opposite trends of sea-breeze speeds and gusts in Eastern Spain, 1961–2019. Clim. Dyn. 60, 2847–2869. https://doi.org/10.1007/s00382-022-06473-0

Beguería, S., Peña-Angulo, D., Trullenque-Blanco, V., González-Hidalgo, C., 2023. MOPREDAScentury: a long-term monthly precipitation grid for the Spanish mainland. Earth Syst. Sci. Data 15, 2547–2575. https://doi.org/10.5194/essd-15-2547-2023

Bennouna, Y.S., Torres, B., Cachorro, V.E., Ortiz De Galisteo, J.P., Toledano, C., 2013. The evaluation of the integrated water vapour annual cycle over the Iberian Peninsula from EOS-MODIS against different ground-based techniques. Q. J. R. Meteorol. Soc. 139, 1935–1956. https://doi.org/10.1002/qj.2080

Berghuijs, W.R., Woods, R.A., Hrachowitz, M., 2014. A precipitation shift from snow towards rain leads to a decrease in streamflow. Nat. Clim. Change 4, 583–586. https://doi.org/10.1038/nclimate2246

Bladé, I., Castro-Díez, Y., Gutiérrez, J.M., Herrera, S., López Moreno, J.I., Vicente Serrano, S.M., 2010. Tendencias atmosféricas en la Península Ibérica en período instrumental en el contexto de la variabilidad natural | DIGITAL.CSIC [WWW Document]. URL https://digital.csic.es/handle/10261/46752 (accessed 3.8.24).

Bonsoms, J., López-Moreno, J.I., Alonso-González, E., 2023. Snow sensitivity to temperature and precipitation change during compound cold–hot and wet–dry seasons in the Pyrenees. The Cryosphere 17, 1307–1326. https://doi.org/10.5194/tc-17-1307-2023

Brönnimann, S., 2007. Impact of El Niño–Southern Oscillation on European climate. Rev. Geophys. 45, 2006RG000199. https://doi.org/10.1029/2006RG000199

Brunet, M., Jones, P.D., Sigro, J., Saladie, O., Aguilar, E., Moberg, A., Della-Marta, P.M., Lister, D., Walther, A., López, D., 2007. Temporal and spatial temperature variability and change over Spain during 1850-2005. J. Geophys. Res.-Atmospheres 112.

Buisan, S.T., Saz, M.A., López-Moreno, J.I., 2015. Spatial and temporal variability of winter snow and precipitation days in the western and central Spanish Pyrenees. Int. J. Climatol. 35, 259–274. https://doi.org/10.1002/joc.3978

Buisán, S.T., Serrano-Notivoli, R., Kochendorfer, J., Bello-Millán, F.J., 2022. Adjustment of Solid Precipitation during the Filomena Extreme Snowfall Event in Spain: From Observations to "True Precipitation." Bull. Am. Meteorol. Soc. 103, E2570–E2578. https://doi.org/10.1175/BAMS-D-22-0012.1

Buzzi, A., Tibaldi, S., 1978. Cyclogenesis in the lee of the Alps: A case study. Q. J. R. Meteorol. Soc. 104, 271–287. https://doi.org/10.1002/qj.49710444004

Cai, W., Santoso, A., Collins, M., Dewitte, B., Karamperidou, C., Kug, J.-S., Lengaigne, M., McPhaden, M.J., Stuecker, M.F., Taschetto, A.S., Timmermann, A., Wu, L., Yeh, S.-W., Wang, G., Ng, B., Jia, F., Yang, Y., Ying, J., Zheng, X.-T., Bayr, T., Brown, J.R., Capotondi, A., Cobb, K.M., Gan, B., Geng, T., Ham, Y.-G., Jin, F.-F., Jo, H.-S., Li, X., Lin, X., McGregor, S., Park, J.-H., Stein, K., Yang, K., Zhang, L., Zhong, W., 2021. Changing El Niño–Southern Oscillation in a warming climate. Nat. Rev. Earth Environ. 2, 628–644. https://doi.org/10.1038/s43017-021-00199-z

Caloiero, T., Caloiero, P., Frustaci, F., 2018. Long-term precipitation trend analysis in Europe and in the Mediterranean basin. Water Environ. J. 32, 433–445. https://doi.org/10.1111/wej.12346

Camuffo, D., Bertolin, C., Diodato, N., Cocheo, C., Barriendos, M., Domínguez-Castro, F., Garnier, E., Alcoforado, M.J., Nunes, M.F., 2013. Western Mediterranean precipitation over the last 300 years from instrumental observations. Clim. Change 117, 85–101. https://doi.org/10.1007/s10584-012-0539-9

Capa-Morocho, M., Rodríguez-Fonseca, B., Ruiz-Ramos, M., 2016. Sea surface temperature impacts on winter cropping systems in the Iberian Peninsula. Agric. For. Meteorol. 226–227, 213–228. https://doi.org/10.1016/j.agrformet.2016.06.007

Capa-Morocho, M., Rodríguez-Fonseca, B., Ruiz-Ramos, M., 2014. Crop yield as a bioclimatic index of El Niño impact in Europe: Crop forecast implications. Agric. For. Meteorol. 198–199, 42–52. https://doi.org/10.1016/j.agrformet.2014.07.012

Carmona, R., Díaz, J., Mirón, I.J., Ortiz, C., Luna, M.Y., Linares, C., 2016. Mortality attributable to extreme temperatures in Spain: A comparative analysis by city. Environ. Int. 91, 22–28. https://doi.org/10.1016/j.envint.2016.02.018

Carreno-Madinabeitia, S., Ibarra-Berastegi, G., Sáenz, J., Ulazia, A., 2021. Long-term changes in offshore wind power density and wind turbine capacity factor in the Iberian Peninsula (1900–2010). Energy 226, 120364. https://doi.org/10.1016/j.energy.2021.120364

Carrillo, J., Hernández-Barrera, S., Expósito, F.J., Díaz, J.P., González, A., Pérez, J.C., 2023. The uneven impact of climate change on drought with elevation in the Canary Islands. Npj Clim. Atmospheric Sci. 6, 31. https://doi.org/10.1038/s41612-023-00358-7

Casanueva, A., Rodríguez-Puebla, C., Frías, M.D., González-Reviriego, N., 2014. Variability of extreme precipitation over Europe and its relationships with teleconnection patterns. Hydrol Earth Syst Sci 18, 709–725. https://doi.org/10.5194/hess-18-709-2014

Casassa, G., Haeberli, W., Jones, G., Kaser, G., Ribstein, P., Rivera, A., Schneider, C., 2007. Current status of Andean glaciers. Glob. Planet. Change 59, 1–9. https://doi.org/10.1016/j.gloplacha.2006.11.013

Cassou, C., Kushnir, Y., Hawkins, E., Pirani, A., Kucharski, F., Kang, I.-S., Caltabiano, N., 2018. Decadal Climate Variability and Predictability: Challenges and Opportunities. Bull. Am. Meteorol. Soc. 99, 479–490. https://doi.org/10.1175/BAMS-D-16-0286.1

Cassou, C., Terray, L., Phillips, A.S., 2005. Tropical Atlantic Influence on European Heat Waves. J. Clim. 18, 2805–2811. https://doi.org/10.1175/JCLI3506.1

Castillo, A., Del-Valle, M., Rubio-Campos, J. C., Fernández-Rubio, R., 1996. Síntesis hidrológica del macizo de Sierra Nevada (Granada y Almería). Presented at the 1ª Conferencia Internacional Sierra Nevada: Conservación y Desarrollo Sostenible, pp. 389–417.

Castillo-Mateo, J., Cebrián, A.C., Asín, J., 2023. Statistical analysis of extreme and record-breaking daily maximum temperatures in peninsular Spain during 1960–2021. Atmospheric Res. 293, 106934. https://doi.org/10.1016/j.atmosres.2023.106934

Castro-Díez, Y., Pozo-Vázquez, D., Rodrigo, F.S., Esteban-Parra, M.J., 2002. NAO and winter temperature variability in southern Europe. Geophys. Res. Lett. 29. https://doi.org/10.1029/2001GL014042

Cebrián, A.C., Asín, J., Gelfand, A.E., Schliep, E.M., Castillo-Mateo, J., Beamonte, M.A., Abaurrea, J., 2022. Spatio-temporal analysis of the extent of an extreme heat event. Stoch. Environ. Res. Risk Assess. 36, 2737–2751. https://doi.org/10.1007/s00477-021-02157-z

Chen, B., Zhang, L., Wang, C., 2024. Distinct Impacts of the Central and Eastern Atlantic Niño on the European Climate. Geophys. Res. Lett. 51, e2023GL107012. https://doi.org/10.1029/2023GL107012

Chen, C., Cane, M.A., Wittenberg, A.T., Chen, D., 2017. ENSO in the CMIP5 Simulations: Life Cycles, Diversity, and Responses to Climate Change. J. Clim. 30, 775–801. https://doi.org/10.1175/JCLI-D-15-0901.1

Chen, J., Chen, F., Feng, S., Huang, W., Liu, J., Zhou, A., 2015. Hydroclimatic changes in China and surroundings during the Medieval Climate Anomaly and Little Ice Age: spatial patterns and possible mechanisms. Quat. Sci. Rev. 107, 98–111. https://doi.org/10.1016/j.quascirev.2014.10.012

Choi, J., An, S.-I., Kug, J.-S., Yeh, S.-W., 2011. The role of mean state on changes in El Niño's flavor. Clim. Dyn. 37, 1205–1215. https://doi.org/10.1007/s00382-010-0912-1

Ciric, D., Nieto, R., Losada, L., Drumond, A., Gimeno, L., 2018. The Mediterranean Moisture Contribution to Climatological and Extreme Monthly Continental Precipitation. Water 10, 519. https://doi.org/10.3390/w10040519

Coll, J.R., Aguilar, E., Ashcroft, L., 2017. Drought variability and change across the Iberian Peninsula. Theor. Appl. Climatol. 130, 901–916. https://doi.org/10.1007/s00704-016-1926-3

Comas-Bru, L., McDermott, F., 2014. Impacts of the EA and SCA patterns on the European twentieth century NAO–winter climate relationship. Q. J. R. Meteorol. Soc. 140, 354–363. https://doi.org/10.1002/qj.2158

Compo, G.P., Whitaker, J.S., Sardeshmukh, P.D., Matsui, N., Allan, R.J., Yin, X., Gleason, B.E., Vose, R.S., Rutledge, G., Bessemoulin, P., Brönnimann, S., Brunet, M., Crouthamel, R.I., Grant, A.N., Groisman, P.Y., Jones, P.D., Kruk, M.C., Kruger, A.C., Marshall, G.J., Maugeri, M., Mok, H.Y., Nordli, Ø., Ross, T.F., Trigo, R.M., Wang, X.L., Woodruff, S.D., Worley, S.J., 2011. The Twentieth Century Reanalysis Project. Q. J. R. Meteorol. Soc. 137, 1–28. https://doi.org/10.1002/qj.776

Consorcio de Compensación de Seguros, 2022. Informe Anual 2022, Catálogo de Publicaciones de la Administración General del Estado (http://publicacionesoficiales.boe.es).

Corell, D., Estrela, M.J., Valiente, J.A., 2021. Chemical characterization in coastal fog and rain at Mount Monduver fog-collection station, Mediterranean Iberian Peninsula. Atmospheric Res. 258, 105636. https://doi.org/10.1016/j.atmosres.2021.105636

Corell, D., Estrela, M.J., Valiente, J.A., Azorín-Molina, C., Chen, D., 2020. Influences of synoptic situation and teleconnections on fog-water collection in the Mediterranean Iberian Peninsula, 2003–2012. Int. J. Climatol. 40, 3297–3317. https://doi.org/10.1002/joc.6398

Cornes, R.C., Van Der Schrier, G., Van Den Besselaar, E.J.M., Jones, P.D., 2018. An Ensemble Version of the E-OBS Temperature and Precipitation Data Sets. J. Geophys. Res. Atmospheres 123, 9391–9409. https://doi.org/10.1029/2017JD028200

Cortesi, N., Torralba, V., González-Reviriego, N., Soret, A., Doblas-Reyes, F.J., 2019. Characterization of European wind speed variability using weather regimes. Clim. Dyn. 53, 4961–4976. https://doi.org/10.1007/s00382-019-04839-5

Cortesi, N., Torralba, V., Lledó, L., Manrique-Suñén, A., González-Reviriego, N., Soret, A., Doblas-Reyes, F.J., 2021. Yearly evolution of Euro-Atlantic weather regimes and of their sub-seasonal predictability. Clim. Dyn. 56, 3933–3964. https://doi.org/10.1007/s00382-021-05679-y

Corti, S., Molteni, F., Palmer, T.N., 1999. Signature of recent climate change in frequencies of natural atmospheric circulation regimes. Nature 398, 799–802. https://doi.org/10.1038/19745

Coumou, D., Di Capua, G., Vavrus, S., Wang, L., Wang, S., 2018. The influence of Arctic amplification on mid-latitude summer circulation. Nat. Commun. 9, 2959. https://doi.org/10.1038/s41467-018-05256-8

Cropper, T., 2013. The weather and climate of Macaronesia: past, present and future. Weather 68, 300–307. https://doi.org/10.1002/wea.2155

Cropper, T.E., Hanna, E., 2014. An analysis of the climate of Macaronesia, 1865–2012. Int. J. Climatol. 34, 604–622.

Cuadrat, J. M., Serrano-Notivoli, R., Barrao, S., Saz, M. Á., and Tejedor, E., 2022. Variabilidad temporal de la isla de calor urbana de la ciudad de Zaragoza (España). Cuad. Investig. Geográfica 48, 97–110.

Cuadrat, J.M., Serrano-Notivoli, R., Prohom, M., Cunillera, J., Tejedor, E., Saz, M.Á., De Luis, M., Llabrés-Brustenga, A., Soubeyroux, J.-M., 2024. Climate of the Pyrenees: Extremes indices and long-term trends. Sci. Total Environ. 933, 173052. https://doi.org/10.1016/j.scitotenv.2024.173052

De Luis, M., Brunetti, M., González-Hidalgo, J.C., Longares, L.A., Martín-Vide, J., 2010. Changes in seasonal precipitation in the Iberian Peninsula during 1946–2005. Glob. Planet. Change 74, 27–33. https://doi.org/10.1016/j.gloplacha.2010.06.006

De Luque, A. & Martín-Esquivel, J.L., 2011. Cualificación y homogeneización de las series climáticas mensuales de precipitación de Canarias. Estimación de Tendencias de la Precipitación. Memoria explicativa de resultados. Agencia Canaria de Desarrollo Sostenible y Cambio Climático, Gobierno de Canarias.

Deaux, N., Soubayroux, J. M., Cuadrat, J. M., Cunillera, J., Esteban, P., Prohom, M., Serrano-Notivoli, R., 2014. Homogénéisation transfrontalière des températures sur le massif des Pyrénées. Presented at the XXVII Colloque de l'Association Internationale de Climatologie, Dijon, France, pp. 344–350.

de Castro, M., Costoya, X., Salvador, S., Carvalho, D., Gómez-Gesteira, M., Sanz-Larruga, F.J., Gimeno, L., 2019. An overview of offshore wind energy resources in Europe under present and future climate. Ann. N. Y. Acad. Sci. 1436, 70–97. https://doi.org/10.1111/nyas.13924

del Río González, S, 2005. El cambio climático y su influencia en la vegetación de Castilla y León (España), Itinera Geobotanica.

del Río, S., Herrero, L., Pinto-Gomes, C., Penas, A., 2011. Spatial analysis of mean temperature trends in Spain over the period 1961-2006. Glob. Planet. Change 78, 65–75.

Díaz, H.F., Giambelluca, T.W., Eischeid, J.K., 2011. Changes in the vertical profiles of mean temperature and humidity in the Hawaiian Islands. Glob. Planet. Change 77, 21–25. https://doi.org/10.1016/j.gloplacha.2011.02.007

Díaz-Poso, A., Lorenzo, N., Martí, A., Royé, D., 2023a. Cold wave intensity on the Iberian Peninsula: Future climate projections. Atmospheric Res. 295, 107011. https://doi.org/10.1016/j.atmosres.2023.107011

Díaz-Poso, A., Lorenzo, N., Royé, D., 2023b. Spatio-temporal evolution of heat waves severity and expansion across the Iberian Peninsula and Balearic islands. Environ. Res. 217, 114864. https://doi.org/10.1016/j.envres.2022.114864

Díaz-Poso, A., Royé, D., Martínez-Ibarra, E., 2023c. Turismo y Cambio Climático: Aplicación del Holiday Climate Index (HCI:Urban) en España en los meses de verano para mediados y finales de siglo. Investig. Tur. 274–296. https://doi.org/10.14198/INTURI.23493

Domínguez-Castro, F., Vicente-Serrano, S.M., Tomás-Burguera, M., Peña-Gallardo, M., Beguería, S., El Kenawy, A., Luna, Y., Morata, A., 2019. High spatial resolution climatology of drought events for Spain: 1961–2014. Int. J. Climatol. 39, 5046–5062. https://doi.org/10.1002/joc.6126

Dong, B., Dai, A., 2015. The influence of the Interdecadal Pacific Oscillation on Temperature and Precipitation over the Globe. Clim. Dyn. 45, 2667–2681. https://doi.org/10.1007/s00382-015-2500-x

Dong, B., Sutton, R.T., Woollings, T., Hodges, K., 2013. Variability of the North Atlantic summer storm track: mechanisms and impacts on European climate. Environ. Res. Lett. 8, 034037. https://doi.org/10.1088/1748-9326/8/3/034037

Dong, L., Zhou, T., Chen, X., 2014. Changes of Pacific decadal variability in the twentieth century driven by internal variability, greenhouse gases, and aerosols. Geophys. Res. Lett. 41, 8570–8577. https://doi.org/10.1002/2014GL062269

Dorta Antequera, P., Domínguez Hernández, A., Díaz Pacheco, J., López Díez, A., Martín Raya, N., 2023. Tropical disturbances in the southeastern North Atlantic. State of the art and future prospects. Investig. Geográficas 33. https://doi.org/10.14198/INGEO.22559

Dorta Antequera, P., López Díez, A., Díaz Pacheco, J.S., 2018. El calentamiento global en el Atlántico Norte Suroriental. El caso de Canarias. Estado de la cuestión y perspectivas de futuro. Cuad. Geográficos 57, 27–52. https://doi.org/10.30827/cuadgeo.v57i2.5934

Drouard, M., Cassou, C., 2019. A Modeling- and Process-Oriented Study to Investigate the Projected Change of ENSO-Forced Wintertime Teleconnectivity in a Warmer World. J. Clim. 32, 8047–8068. https://doi.org/10.1175/JCLI-D-18-0803.1

Dünkeloh, A., Jacobeit, J., 2003. Circulation dynamics of Mediterranean precipitation variability 1948–98. Int. J. Climatol. 23, 1843–1866. https://doi.org/10.1002/joc.973

Durán L., González-Florez & Rodrígez-Fonseca B., 2023. Climate Variability, Teleconnections and Climate Change in a Mountainous Region of Central Spain (Sierra de Guadarrama). Presented at the CLIVAR 2023: TOWARDS AN INTEGRATED VIEW OF CLIMATE, Madrid.

Durán, L., Sánchez, E., Yagüe, C., 2013. Climatology of precipitation over the Iberian Central System mountain range. Int. J. Climatol. 33, 2260–2273.

Earman, S., Dettinger, M., 2011. Potential impacts of climate change on groundwater resources – a global review. J. Water Clim. Change 2, 213–229. https://doi.org/10.2166/wcc.2011.034

Eiras-Barca, J., Domínguez, F., Hu, H., Garaboa-Paz, D., Míguez-Macho, G., 2017. Evaluation of the moisture sources in two extreme landfalling atmospheric river events using an Eulerian WRF tracers tool. Earth Syst. Dyn. 8, 1247–1261. https://doi.org/10.5194/esd-8-1247-2017

El Kenawy, A., López-Moreno, J.I., Vicente-Serrano, S.M., 2013. Summer temperature extremes in northeastern Spain: spatial regionalization and links to atmospheric circulation (1960–2006). Theor. Appl. Climatol. 113, 387–405. https://doi.org/10.1007/s00704-012-0797-5

Eltahir, E.A.B., Bras, R.L., 1996. Precipitation recycling. Rev. Geophys. 34, 367–378. https://doi.org/10.1029/96RG01927

Engström, J.E., Wern, L., Hellström, S., Kjellström, E., Zhou, C., Chen, D., Azorín-Molina, C., 2023. Data rescue of historical wind observations in Sweden since the 1920s. Earth Syst. Sci. Data 15, 2259–2277. https://doi.org/10.5194/essd-15-2259-2023

Espejo F, Ferraz J, Palomo M., 2008. Tendencias recientes en las series de temperatura del Pirineo Central y Occidental (No. 6). Asociación Española de Climatología.

Espín-Sánchez, D., Olcina-Cantos, J., Conesa-García, C., 2023. Temporal Changes in Tourists' Climate-Based Comfort in the Southeastern Coastal Region of Spain. Climate 11, 230. https://doi.org/10.3390/cli11110230

Esteban-Parra, M.J., García-Valdecasas Ojeda, M., Peinó-Calero, E., Romero-Jiménez, E., Yeste, P., Rosa-Cánovas, J.J., Rodríguez-Brito, A., Gámiz-Fortis, S.R., Castro-Díez, Y., 2022. Climate Variability and Trends, in: Zamora, R., Oliva, M. (Eds.), The Landscape of the Sierra Nevada. Springer International Publishing, Cham, pp. 129–148. https://doi.org/10.1007/978-3-030-94219-9_9

Estrela, M.J., Corell, D., Valiente, J.A., Azorín-Molina, C., Chen, D., 2019. Spatio-temporal variability of fog-water collection in the eastern Iberian Peninsula: 2003–2012. Atmospheric Res. 226, 87–101. https://doi.org/10.1016/j.atmosres.2019.04.016

Faranda, D., Messori, G., Yiou, P., 2017. Dynamical proxies of North Atlantic predictability and extremes. Sci. Rep. 7, 41278. https://doi.org/10.1038/srep41278

Fedorov, A.V., Philander, S.G., 2000. Is El Niño Changing? Science 288, 1997–2002. https://doi.org/10.1126/science.288.5473.1997

Fernández-Álvarez, J.C., Vázquez, M., Pérez-Alarcón, A., Nieto, R., Gimeno, L., 2023. Comparison of Moisture Sources and Sinks Estimated with Different Versions of FLEXPART and FLEXPART-WRF Models Forced with ECMWF Reanalysis Data. J. Hydrometeorol. 24, 221–239. https://doi.org/10.1175/JHM-D-22-0018.1

Ferreira, R.N., 2021. Cut-Off Lows and Extreme Precipitation in Eastern Spain: Current and Future Climate. Atmosphere 12, 835. https://doi.org/10.3390/atmos12070835

Ferreiro Lera, G.B., Álvarez Santacoloma, A., González Pérez, A., Penas Merino, Á., Río González, S. del, 2022. Presente y futuro de la sequía en la Península Ibérica: un análisis comparado. Asociación Española de Climatología.

Flaounas, E., Davolio, S., Raveh-Rubin, S., Pantillon, F., Miglietta, M.M., Gaertner, M.A., Hatzaki, M., Homar, V., Khodayar, S., Korres, G., Kotroni, V., Kushta, J., Reale, M., Ricard, D., 2022. Mediterranean cyclones: current knowledge and open questions on dynamics, prediction, climatology and impacts. Weather Clim. Dyn. 3, 173–208. https://doi.org/10.5194/wcd-3-173-2022

Freeman, E., Kent, E.C., Brohan, P., Cram, T., Gates, L., Huang, B., Liu, C., Smith, S.R., Worley, S.J., Zhang, H.-M., 2019. The International Comprehensive Ocean-Atmosphere Data Set – Meeting Users Needs and Future Priorities. Front. Mar. Sci. 6, 435. https://doi.org/10.3389/fmars.2019.00435

Frei, C., Schär, C., 1998. A precipitation climatology of the Alps from high-resolution rain-gauge observations. Int. J. Climatol. 18, 873–900. https://doi.org/10.1002/(SICI)1097-0088(19980630)18:8<873::AID-JOC255>3.0.CO;2-9

Gallego, D., García-Herrera, R., Gómez-Delgado, F.D.P., Ordoñez-Pérez, P., Ribera, P., 2019. Tracking the moisture transport from the Pacific towards Central and northern South America since the late 19th century. Earth Syst. Dyn. 10, 319–331. https://doi.org/10.5194/esd-10-319-2019

Gallego, D., García-Herrera, R., Mohino, E., Losada, T., Rodríguez-Fonseca, B., 2022. Secular Variability of the Upwelling at the Canaries Latitude: An Instrumental Approach. J. Geophys. Res. Oceans 127, e2021JC018039. https://doi.org/10.1029/2021JC018039

Gallinar Cañedo, D., Ruíz-Fernández, J., García-Hernández, C., 2022. La nieve en el Macizo de las Ubiñas (Montañas Cantábricas) y sus implicaciones geomorfológicas. Bol. Asoc. Geógrafos Esp. https://doi.org/10.21138/bage.3224

Gandini, A., Quesada, L., Prieto, I., Garmendia, L., 2021. Climate change risk assessment: A holistic multi-stakeholder methodology for the sustainable development of cities. Sustain. Cities Soc. 65, 102641. https://doi.org/10.1016/j.scs.2020.102641

García, M.G., Cañadas, E.S., Blasco, J.J.S., Trueba, J.J.G., 2017. Surface dynamic of a protalus lobe in the temperate high mountain. Western Maladeta, Pyrenees. CATENA 149, 689–700. https://doi.org/10.1016/j.catena.2016.08.011

García, R.D., García, O.E., Cuevas, E., Cachorro, V.E., Barreto, A., Guirado-Fuentes, C., Kouremeti, N., Bustos, J.J., Romero-Campos, P.M., De Frutos, A.M., 2016. Aerosol optical depth retrievals at the Izaña Atmospheric Observatory from 1941 to 2013 by using artificial neural networks. Atmospheric Meas. Tech. 9, 53–62. https://doi.org/10.5194/amt-9-53-2016

García-Barrón, L., Aguilar-Alba, M., Morales, J., Sousa, A., 2018. Intra-annual rainfall variability in the Spanish hydrographic basins. Int. J. Climatol. 38, 2215–2229. https://doi.org/10.1002/joc.5328

García-Burgos, M., Gómara, I., Rodríguez-Fonseca, B., González-Alemán, J.J., Zurita-Gotor, P., Ayarzagüena, B., 2023. Abrupt and persistent atmospheric circulation changes in the North Atlantic under La Niña conditions. Weather Clim. Extrem. 42, 100609. https://doi.org/10.1016/j.wace.2023.100609

García-Hernández, C., Ruíz-Fernández, J., Sánchez-Posada, C., Pereira, S., Oliva, M., Vieira, G., 2017. Reforestation and land use change as drivers for a decrease of avalanche damage in mid-latitude mountains (NW Spain). Glob. Planet. Change 153, 35–50. https://doi.org/10.1016/j.gloplacha.2017.05.001

García-Herrera, R., Díaz, J., Trigo, R.M., Luterbacher, J., Fischer, E.M., 2010. A Review of the European Summer Heat Wave of 2003. Crit. Rev. Environ. Sci. Technol. 40, 267–306. https://doi.org/10.1080/10643380802238137

García-Herrera, R., Gallego, D., Hernández, E., Gimeno, L., Ribera, P., Calvo, N., 2003. Precipitation trends in the Canary Islands. Int. J. Climatol. 23, 235–241.

García-Herrera, R., Können, G.P., Wheeler, D.A., Prieto, M.R., Jones, P.D., Koek, F.B., 2005. CLIWOC: A Climatological Database for the World's Oceans 1750–1854. Clim. Change 73, 1–12. https://doi.org/10.1007/s10584-005-6952-6

García-Llamas, P., Geijzendorffer, I.R., García-Nieto, A.P., Calvo, L., Suárez-Seoane, S., Cramer, W., 2019. Impact of land cover change on ecosystem service supply in mountain systems: a case study in the Cantabrian Mountains (NW of Spain). Reg. Environ. Change 19, 529–542. https://doi.org/10.1007/s10113-018-1419-2

García-Martín, A., Paniagua, L.L., Moral, F.J., Rebollo, F.J., Rozas, M.A., 2021. Spatiotemporal Analysis of the Frost Regime in the Iberian Peninsula in the Context of Climate Change (1975–2018). Sustainability 13, 8491. https://doi.org/10.3390/su13158491

García-Romero, L., Carreira-Galbán, T., Rodríguez-Báez, J.Á., Máyer-Suárez, P., Hernández-Calvento, L., Yánes-Luque, A., 2023. Mapping Environmental Impacts on Coastal Tourist Areas of Oceanic Islands (Gran Canaria, Canary Islands): A Current and Future Scenarios Assessment. Remote Sens. 15, 1586. https://doi.org/10.3390/rs15061586

García-Serrano, J., Losada, T., Rodríguez-Fonseca, B., Polo, I., 2008. Tropical Atlantic Variability Modes (1979–2002). Part II: Time-Evolving Atmospheric Circulation Related to SST-Forced Tropical Convection. J. Clim. 21, 6476–6497. https://doi.org/10.1175/2008JCLI2191.1

García-Serrano, J., Rodríguez-Fonseca, B., Bladé, I., Zurita-Gotor, P., De La Cámara, A., 2011. Rotational atmospheric circulation during North Atlantic-European winter: the influence of ENSO. Clim. Dyn. 37, 1727–1743. https://doi.org/10.1007/s00382-010-0968-y

Gimeno, L., Nieto, R., Trigo, R.M., 2007. Decay of the Northern Hemisphere stratospheric polar vortex and the occurrence of cut-off low systems: An exploratory study. Meteorol. Atmospheric Phys. 96, 21–28. https://doi.org/10.1007/s00703-006-0218-3

Gimeno, L., Nieto, R., Trigo, R.M., Vicente-Serrano, S.M., López-Moreno, J.I., 2010. Where Does the Iberian Peninsula Moisture Come From? An Answer Based on a Lagrangian Approach. J. Hydrometeorol. 11, 421–436. https://doi.org/10.1175/2009JHM1182.1

Gimeno, L., Stohl, A., Trigo, R.M., Domínguez, F., Yoshimura, K., Yu, L., Drumond, A., Durán-Quesada, A.M., Nieto, R., 2012. Oceanic and terrestrial sources of continental precipitation. Rev. Geophys. 50, 2012RG000389. https://doi.org/10.1029/2012RG000389

Gimeno, L., Vázquez, M., Eiras-Barca, J., Sorí, R., Stojanovic, M., Algarra, I., Nieto, R., Ramos, A.M., Durán-Quesada, A.M., Domínguez, F., 2020. Recent progress on the sources of continental precipitation as

revealed by moisture transport analysis. Earth-Sci. Rev. 201, 103070. https://doi.org/10.1016/j.earscirev.2019.103070

Gimeno, L., Vázquez, M., Nieto, R., Trigo, R.M., 2015. Atmospheric moisture transport: the bridge between ocean evaporation and Arctic ice melting. Earth Syst. Dyn. 6, 583–589. https://doi.org/10.5194/esd-6-583-2015

Gimeno-Sotelo, L., Bevacqua, E., Gimeno, L., 2023. Combinations of drivers that most favor the occurrence of daily precipitation extremes. Atmospheric Res. 294, 106959. https://doi.org/10.1016/j.atmosres.2023.106959

Gimeno-Sotelo, L., Gimeno, L., 2023. Where does the link between atmospheric moisture transport and extreme precipitation matter? Weather Clim. Extrem. 39, 100536. https://doi.org/10.1016/j.wace.2022.100536

Gimeno-Sotelo, L., Sorí, R., Nieto, R., Vicente-Serrano, S.M., Gimeno, L., 2024. Unravelling the origin of the atmospheric moisture deficit that leads to droughts. Nat. Water. https://doi.org/10.1038/s44221-023-00192-4

Giorgi, F., Raffaele, F., Coppola, E., 2019. The response of precipitation characteristics to global warming from climate projections. Earth Syst. Dyn. 10, 73–89. https://doi.org/10.5194/esd-10-73-2019

Gómara, I., Bellocchi, G., Martín, R., Rodríguez-Fonseca, B., Ruiz-Ramos, M., 2020. Influence of climate variability on the potential forage production of a mown permanent grassland in the French Massif Central. Agric. For. Meteorol. 280, 107768. https://doi.org/10.1016/j.agrformet.2019.107768

Gómara, I., Rodríguez-Fonseca, B., Zurita-Gotor, P., Pinto, J.G., 2014. On the relation between explosive cyclones affecting Europe and the North Atlantic Oscillation: Gomara et al.: Cyclones affecting Europe and the NAO. Geophys. Res. Lett. 41, 2182–2190. https://doi.org/10.1002/2014GL059647

Gómara, I., Rodríguez-Fonseca, B., Zurita-Gotor, P., Ulbrich, S., Pinto, J.G., 2016. Abrupt transitions in the NAO control of explosive North Atlantic cyclone development. Clim. Dyn. 47, 3091–3111. https://doi.org/10.1007/s00382-016-3015-9

Gómez-Delgado, F.D.P., Gallego, D., Peña-Ortiz, C., Vega, I., Ribera, P., García-Herrera, R., 2019. Long term variability of the northerly winds over the Eastern Mediterranean as seen from historical wind observations. Glob. Planet. Change 172, 355–364. https://doi.org/10.1016/j.gloplacha.2018.10.008

Gómez-Hernández, M., Drumond, A., Gimeno, L., García-Herrera, R., 2013. Variability of moisture sources in the Mediterranean region during the period 1980-2000: Variability of Mediterranean Moisture Sources. Water Resour. Res. 49, 6781–6794. https://doi.org/10.1002/wrcr.20538

Gómez-Lende, M., 2016. Cuevas heladas en el Parque Nacional Picos de Europa fronteras subterráneas del hielo en el Macizo Central. Organismo Autónomo Parques Nacionales, Madrid.

Gómez-Lende, M., Serrano Cañadas, E., 2021. Cave mountain permafrost environments in Picos de Europa and their implications. Cuaternario Geomorfol. 35, 55–76. https://doi.org/10.17735/cyg.v35i3-4.89377

Gonçalves, A., Liberato, M.L.R., Nieto, R., 2021. Wind Energy Assessment during High-Impact Winter Storms in Southwestern Europe. Atmosphere 12, 509. https://doi.org/10.3390/atmos12040509

González Trueba, J.J., 2005. La Pequeña Edad del Hielo en los Picos de Europa (Cordillera Cantábrica, NO de España). Análisis morfológico y reconstrucción del avance glaciar histórico. Cuaternario Geomorfol.-479-94.

González Trueba, J.J., Serrano Cañadas, E., 2010. La nieve en los Picos de Europa: implicaciones geomorfológicas y ambientales. Cuad. Investig. Geográfica Geogr. Res. Lett. 36, 61–84.

González-Alemán, J.J., Insua-Costa, D., Bazile, E., González-Herrero, S., Marcello Miglietta, M., Groenemeijer, P., Donat, M.G., 2023. Anthropogenic Warming Had a Crucial Role in Triggering the Historic and Destructive Mediterranean Derecho in Summer 2022. Bull. Am. Meteorol. Soc. 104, E1526–E1532. https://doi.org/10.1175/BAMS-D-23-0119.1

González-Flórez, C., González-Cervera, Á., Durán, L., 2022. Characterising Large-Scale Meteorological Patterns Associated with Winter Precipitation and Snow Accumulation in a Mountain Range in the Iberian Peninsula (Sierra de Guadarrama). Atmosphere 13, 1600. https://doi.org/10.3390/atmos13101600

González-Hidalgo, J.C., Beguería, S., Peña-Angulo, D., Sandonis, L., 2022. Variability of maximum and minimum monthly mean air temperatures over mainland Spain and their relationship with low-variability atmospheric patterns for period 1916–2015. Int. J. Climatol. 42, 1723–1741. https://doi.org/10.1002/joc.7331

González-Hidalgo, J.C., Beguería, S., Peña-Angulo, D., Trullenque-Blanco, V., 2023. MOPREDAS_century database and precipitation trends in mainland Spain, 1916–2020. Int. J. Climatol. 43, 3828–3840. https://doi.org/10.1002/joc.8060

González-Hidalgo, J.C., Brunetti, M., De Luis, M., 2011. A new tool for monthly precipitation analysis in Spain: MOPREDAS database (monthly precipitation trends December 1945–November 2005). Int. J. Climatol. 31, 715–731. https://doi.org/10.1002/joc.2115

González-Hidalgo, J.C., Peña-Angulo, D., Beguería, S., Brunetti, M., 2020. MOTEDAS century: A new high-resolution secular monthly maximum and minimum temperature grid for the Spanish mainland (1916–2015). Int. J. Climatol. 40, 5308–5328. https://doi.org/10.1002/joc.6520

González-Hidalgo, J.C., Trullenque-Blanco, V., Beguería, S., Peña-Angulo, D., 2024. Seasonal precipitation changes in the western Mediterranean Basin: The case of the Spanish mainland, 1916–2015. Int. J. Climatol. 44, 1800–1815. https://doi.org/10.1002/joc.8412

González-Rojí, S.J., Sáenz, J., Díaz De Argandoña, J., Ibarra-Berastegi, G., 2019. Moisture Recycling over the Iberian Peninsula: The Impact of 3DVAR Data Assimilation. Atmosphere 11, 19. https://doi.org/10.3390/atmos11010019

Grams, C.M., Beerli, R., Pfenninger, S., Staffell, I., Wernli, H., 2017. Balancing Europe's wind-power output through spatial deployment informed by weather regimes. Nat. Clim. Change 7, 557–562. https://doi.org/10.1038/nclimate3338

Guemas, V., Salas-Mélia, D., Kageyama, M., Giordani, H., Voldoire, A., Sánchez-Gómez, E., 2010. Summer interactions between weather regimes and surface ocean in the North-Atlantic region. Clim. Dyn. 34, 527–546. https://doi.org/10.1007/s00382-008-0491-6

Guijarro, J.A., 2013. Tendencias de la temperatura., in: Fenómenos Meteorológicos Adversos En España. pp. 313–323.

Guijarro, J.A., Conde, J., Campins, J., Picornell, M.A., Orro, M.L., 2014. Tendencias de viento, oleaje y temperatura superficial Mediterráneo y Atlántico próximos a partir de datos de reanálisis., in: Cambio Climático y Cambio Global. Asociación Española de Climatología, Serie A. pp. 315–324.

Guijarro, J.A., Jansà, A., 2022. Variabilidad de las tendencias de las temperaturas e impacto en su comunicación al público: ejemplo en las Islas Baleares. Asociación Española de Climatología.

Haarsma, R.J., Hazeleger, W., 2007. Extratropical Atmospheric Response to Equatorial Atlantic Cold Tongue Anomalies. J. Clim. 20, 2076–2091. https://doi.org/10.1175/JCLI4130.1

Hannachi, Abdel., Straus, D.M., Franzke, C.L.E., Corti, S., Woollings, T., 2017. Low-frequency nonlinearity and regime behavior in the Northern Hemisphere extratropical atmosphere. Rev. Geophys. 55, 199–234. https://doi.org/10.1002/2015RG000509

Hardiman, S.C., Butchart, N., Charlton-Pérez, A.J., Shaw, T.A., Akiyoshi, H., Baumgaertner, A., Bekki, S., Braesicke, P., Chipperfield, M., Dameris, M., García, R.R., Michou, M., Pawson, S., Rozanov, E., Shibata, K., 2011. Improved predictability of the troposphere using stratospheric final warmings. J. Geophys. Res. 116, D18113. https://doi.org/10.1029/2011JD015914

Heaviside, C., Macintyre, H., Vardoulakis, S., 2017. The Urban Heat Island: Implications for Health in a Changing Environment. Curr. Environ. Health Rep. 4, 296–305. https://doi.org/10.1007/s40572-017-0150-3

Hénin, R., Ramos, A.M., Pinto, J.G., Liberato, M.L.R., 2021. A ranking of concurrent precipitation and wind events for the Iberian Peninsula. Int. J. Climatol. 41, 1421–1437. https://doi.org/10.1002/joc.6829

Hernández Barrera, S., Tarife Méndez, R., Gámiz Fortis, S.R., Castro Díez, Y., Esteban Parra, M.J., 2012. Estudio de las sequías en las Islas Canarias mediante el análisis de índices multiescalares. Asociación Española de Climatología.

Herrero, J., Polo, M.J., 2016. Evaposublimation from the snow in the Mediterranean mountains of Sierra Nevada (Spain). The Cryosphere 10, 2981–2998. https://doi.org/10.5194/tc-10-2981-2016

Hidalgo-García, D., Arco Díaz, J., Martín Martín, A., Gómez Cobos, E., 2022. Spatiotemporal Analysis of Urban Thermal Effects Caused by Heat Waves through Remote Sensing. Sustainability 14, 12262. https://doi.org/10.3390/su141912262

Hidalgo-García, D., Rezapouraghdam, H., 2023. Variability of heat stress using the UrbClim climate model in the city of Seville (Spain): mitigation proposal. Environ. Monit. Assess. 195, 1164. https://doi.org/10.1007/s10661-023-11768-8

Homar, V., Ramis, C., Romero, R., Alonso, S., 2010. Recent trends in temperature and precipitation over the Balearic Islands (Spain). Clim. Change 98, 199–211. https://doi.org/10.1007/s10584-009-9664-5

Hsu, A., Sheriff, G., Chakraborty, T., Manya, D., 2021. Disproportionate exposure to urban heat island intensity across major US cities. Nat. Commun. 12, 2721. https://doi.org/10.1038/s41467-021-22799-5

Hurrell, J.W., Kushnir, Y., Ottersen, G., Visbeck, M., 2003. An Overview of the North Atlantic Oscillation, in: W, H.J., Y, K., G, O., M, V. (Eds.), The North Atlantic Oscillation: Climatic Significance and Environmental Impact. American Geophysical Union (AGU), Washington, US, pp. 1–35.

Íñiguez, C., Royé, D., Tobías, A., 2021. Contrasting patterns of temperature related mortality and hospitalization by cardiovascular and respiratory diseases in 52 Spanish cities. Environ. Res. 192, 110191. https://doi.org/10.1016/j.envres.2020.110191

Insua-Costa, D., Míguez-Macho, G., Llasat, M.C., 2019. Local and remote moisture sources for extreme precipitation: a study of the two catastrophic 1982 western Mediterranean episodes. Hydrol. Earth Syst. Sci. 23, 3885–3900. https://doi.org/10.5194/hess-23-3885-2019

Intergovernmental Panel On Climate Change, 2023. Climate Change 2021 – The Physical Science Basis: Working Group I Contribution to the Sixth Assessment Report of the Intergovernmental Panel on Climate Change, 1st ed. Cambridge University Press. https://doi.org/10.1017/9781009157896

Intergovernmental Panel On Climate Change (Ipcc), 2023. Climate Change 2022 – Impacts, Adaptation and Vulnerability: Working Group II Contribution to the Sixth Assessment Report of the Intergovernmental Panel on Climate Change, 1st ed. Cambridge University Press. https://doi.org/10.1017/9781009325844

James, P.E., 1922. KÖPPEN'S CLASSIFICATION OF CLIMATES: A REVIEW. Mon. Weather Rev. 50, 69–72. https://doi.org/10.1175/1520-0493(1922)50<69:KCOCAR>2.0.CO;2

Jansà, A., 2012. Primavera i canvi climàtic (Territoris No. 8). Universitat de les Illes Balears.

Jansà, A., Guijarro, J.A., Maimó, A., 2019. Time and spatial differences on climate tendencies in the Balearics, in: 7th International Conference on Meteorology and Climatology of the Mediterranean (MetMed). Palma, Spain,.

Jansà, A., Homar, V., Romero, R., Alonso, S., Guijarro, J.A., Ramis, C., 2017. Extension of summer climatic conditions into spring in the Western Mediterranean area. Int. J. Climatol. 37, 1938–1950. https://doi.org/10.1002/joc.4824

Jerez, S., Trigo, R.M., 2013. Time-scale and extent at which large-scale circulation modes determine the wind and solar potential in the Iberian Peninsula. Environ. Res. Lett. 8, 044035. https://doi.org/10.1088/1748-9326/8/4/044035

Jerez, S., Trigo, R.M., Vicente-Serrano, S.M., Pozo-Vázquez, D., Lorente-Plazas, R., Lorenzo-Lacruz, J., Santos-Alamillos, F., Montávez, J.P., 2013. The Impact of the North Atlantic Oscillation on Renewable Energy Resources in Southwestern Europe. J. Appl. Meteorol. Climatol. 52, 2204–2225. https://doi.org/10.1175/JAMC-D-12-0257.1

José, R.S., Pérez, J.L., Pérez, L., Barras, R.M.G., 2018. Impacts of global climate scenarios over three European cities using mesoscale and CFD simulations with very high horizontal resolution. Int. J. Environ. Pollut. 64, 341. https://doi.org/10.1504/IJEP.2018.099467

Khodayar, S., Caldas-Álvarez, A., 2022. Seasonal heavy precipitation sensitivity to moisture corrections in the western Mediterranean across resolutions. Atmospheric Res. 280, 106429. https://doi.org/10.1016/j.atmosres.2022.106429

Khodayar, S., Czajka, B., Caldas-Álvarez, A., Helgert, S., Flamant, C., Di Girolamo, P., Bock, O., Chazette, P., 2018. Multi-scale observations of atmospheric moisture variability in relation to heavy precipitating systems in the northwestern Mediterranean during HyMeX IOP12. Q. J. R. Meteorol. Soc. 144, 2761–2780. https://doi.org/10.1002/qj.3402

Kim, Y., Kim, H., Gasparrini, A., Armstrong, B., Honda, Y., Chung, Y., Ng, C.F.S., Tobias, A., Íñiguez, C., Lavigne, E., Sera, F., Vicedo-Cabrera, A.M., Ragettli, M.S., Scovronick, N., Acquaotta, F., Chen, B.-Y., Guo, Y.-L.L., Seposo, X., Dang, T.N., De Sousa Zanotti Stagliorio Coelho, M., Saldiva, P.H.N., Kosheleva, A., Zanobetti, A., Schwartz, J., Bell, M.L., Hashizume, M., 2019. Suicide and Ambient Temperature: A Multi-Country Multi-City Study. Environ. Health Perspect. 127, 117007. https://doi.org/10.1289/EHP4898

King, M.P., Keenlyside, N., Li, C., 2023. ENSO teleconnections in terms of non-NAO and NAO atmospheric variability. Clim. Dyn. 61, 2717–2733. https://doi.org/10.1007/s00382-023-06697-8

Kjellstrom, T., Briggs, D., Freyberg, C., Lemke, B., Otto, M., Hyatt, O., 2016. Heat, Human Performance, and Occupational Health: A Key Issue for the Assessment of Global Climate Change Impacts. Annu. Rev. Public Health 37, 97–112. https://doi.org/10.1146/annurev-publhealth-032315-021740

Klein Tank, A.M.G., Wijngaard, J.B., Können, G.P., Böhm, R., Demarée, G., Gocheva, A., Mileta, M., Pashiardis, S., Hejkrlik, L., Kern-Hansen, C., Heino, R., Bessemoulin, P., Müller-Westermeier, G., Tzanakou, M., Szalai, S., Pálsdóttir, T., Fitzgerald, D., Rubin, S., Capaldo, M., Maugeri, M., Leitass, A., Bukantis, A., Aberfeld, R., Van Engelen, A.F.V., Forland, E., Mietus, M., Coelho, F., Mares, C., Razuvaev, V., Nieplova, E., Cegnar, T., Antonio López, J., Dahlström, B., Moberg, A., Kirchhofer, W., Ceylan, A., Pachaliuk, O., Alexander, L.V., Petrovic, P., 2002. Daily dataset of 20th-century surface air temperature and precipitation series for the European Climate Assessment. Int. J. Climatol. 22, 1441–1453. https://doi.org/10.1002/joc.773

Knight, J.R., Allan, R.J., Folland, C.K., Vellinga, M., Mann, M.E., 2005. A signature of persistent natural thermohaline circulation cycles in observed climate. Geophys. Res. Lett. 32, 1–4. https://doi.org/10.1029/2005GL024233

Krichak, S., Breitgand, J., Gualdi, S., Feldstein, S., 2014. Teleconnection-extreme precipitation relationships over the Mediterranean region. Theor. Appl. Climatol. 117, 679–692.

Lastrada, E., Garzón-Roca, J., Cobos, G., Torrijo, F.J., 2021. A Decrease in the Regulatory Effect of Snow-Related Phenomena in Spanish Mountain Areas Due to Climate Change. Water 13, 1550. https://doi.org/10.3390/w13111550

Lemus-Canovas, M., López-Bustins, J.A., 2021. Assessing internal changes in the future structure of dry–hot compound events: the case of the Pyrenees. Nat. Hazards Earth Syst. Sci. 21, 1721–1738. https://doi.org/10.5194/nhess-21-1721-2021

Lemus-Canovas, M., López-Bustins, J.A., Martín-Vide, J., Halifa-Marín, A., Insua-Costa, D., Martínez-Artigas, J., Trapero, L., Serrano-Notivoli, R., Cuadrat, J.M., 2021. Characterisation of Extreme Precipitation Events in the Pyrenees: From the Local to the Synoptic Scale. Atmosphere 12, 665. https://doi.org/10.3390/atmos12060665

Lemus-Canovas, M., López-Bustins, J.A., Trapero, L., Martín-Vide, J., 2019. Combining circulation weather types and daily precipitation modelling to derive climatic precipitation regions in the Pyrenees. Atmospheric Res. 220, 181–193. https://doi.org/10.1016/j.atmosres.2019.01.018

Lionello, P., Scarascia, L., 2018. The relation between climate change in the Mediterranean region and global warming. Reg. Environ. Change 18, 1481–1493. https://doi.org/10.1007/s10113-018-1290-1

Liu, Y., García, M., Zhang, C., Tang, Q., 2022. Recent decrease in summer precipitation over the Iberian Peninsula closely links to reduction in local moisture recycling. Hydrol. Earth Syst. Sci. 26, 1925–1936. https://doi.org/10.5194/hess-26-1925-2022

Llasat, M., 2001. An objective classification of rainfall events on the basis of their convective features: application to rainfall intensity in the northeast of spain. Int. J. Climatol. 21, 1385–1400. https://doi.org/10.1002/joc.692

Llasat, M.C., Del Moral, A., Cortès, M., Rigo, T., 2021. Convective precipitation trends in the Spanish Mediterranean region. Atmospheric Res. 257, 105581. https://doi.org/10.1016/j.atmosres.2021.105581

Llasat, M.C., Marcos, R., Turco, M., Gilabert, J., Llasat-Botija, M., 2016. Trends in flash flood events versus convective precipitation in the Mediterranean region: The case of Catalonia. J. Hydrol. 541, 24–37. https://doi.org/10.1016/j.jhydrol.2016.05.040

Lomba-Fernández, C., Hernantes, J., Labaka, L., 2019. Guide for Climate-Resilient Cities: An Urban Critical Infrastructures Approach. Sustainability 11, 4727. https://doi.org/10.3390/su11174727

López Gómez, A., 1993. El clima de la ciudades españolas, Geografía menor. Cátedra, Madrid.

López Gómez, A., C.S. de I.C. (España) I. de E. y G., 1988. El clima urbano de Madrid: la isla de calor. CSIC, Instituto de Economía y Geografía Aplicadas.

López-Bustins, J.A., Arbiol-Roca, L., Martín-Vide, J., Barrera-Escoda, A., Prohom, M., 2020. Intra-annual variability of the Western Mediterranean Oscillation (WeMO) and occurrence of extreme torrential precipitation in Catalonia (NE Iberia). Nat. Hazards Earth Syst. Sci. 20, 2483–2501. https://doi.org/10.5194/nhess-20-2483-2020

López-Moreno, J.I., Pomeroy, J.W., Alonso-González, E., Morán-Tejeda, E., Revuelto, J., 2020. Decoupling of warming mountain snowpacks from hydrological regimes. Environ. Res. Lett. 15, 114006. https://doi.org/10.1088/1748-9326/abb55f

López-Moreno, J.I., Revuelto, J., Rico, I., Chueca-Cía, J., Julián, A., Serreta, A., Serrano, E., Vicente-Serrano, S.M., Azorín-Molina, C., Alonso-González, E., García-Ruiz, J.M., 2016. Thinning of the Monte Perdido Glacier in the Spanish Pyrenees since 1981. The Cryosphere 10, 681–694. https://doi.org/10.5194/tc-10-681-2016

López-Moreno, J.I., Vicente-Serrano, S.M., Morán-Tejeda, E., Zabalza, J., Lorenzo-Lacruz, J., García-Ruiz, J.M., 2011. Impact of climate evolution and land use changes on water yield in the ebro basin. Hydrol. Earth Syst. Sci. 15, 311–322. https://doi.org/10.5194/hess-15-311-2011

López-Parages, J., Gómara, I., Rodríguez-Fonseca, B., García-Lafuente, J., 2022. Potential SST drivers for Chlorophyll-a variability in the Alboran Sea: A source for seasonal predictability? Front. Mar. Sci. 9, 931832. https://doi.org/10.3389/fmars.2022.931832

López-Parages, J., Rodríguez-Fonseca, B., 2012. Multidecadal modulation of El Niño influence on the Euro-Mediterranean rainfall. Geophys. Res. Lett. 39, 2011GL050049. https://doi.org/10.1029/2011GL050049

López-Parages, J., Rodríguez-Fonseca, B., Dommenget, D., Frauen, C., 2016. ENSO influence on the North Atlantic European climate: a non-linear and non-stationary approach. Clim. Dyn. 47, 2071–2084. https://doi.org/10.1007/s00382-015-2951-0

López-Parages, J., Rodríguez-Fonseca, B., Terray, L., 2015. A mechanism for the multidecadal modulation of ENSO teleconnection with Europe. Clim. Dyn. 45, 867–880. https://doi.org/10.1007/s00382-014-2319-x

Lorenzo, M.N., Álvarez, I., Taboada, J.J., 2022. Drought evolution in the NW Iberian Peninsula over a 60 year period (1960–2020). J. Hydrol. 610, 127923. https://doi.org/10.1016/j.jhydrol.2022.127923

Losada, T., Rodríguez-Fonseca, B., Janicot, S., Gervois, S., Chauvin, F., Ruti, P., 2010. A multi-model approach to the Atlantic Equatorial mode: impact on the West African monsoon. Clim. Dyn. 35, 29–43. https://doi.org/10.1007/s00382-009-0625-5

Losada, T., Rodríguez-Fonseca, B., Kucharski, F., 2012. Tropical influence on the summer Mediterranean climate. Atmospheric Sci. Lett. 13, 36–42. https://doi.org/10.1002/asl.359

Losada, T., Rodríguez-Fonseca, B., Mechoso, C.R., Ma, H.-Y., 2007. Impacts of SST anomalies on the North Atlantic atmospheric circulation: a case study for the northern winter 1995/1996. Clim. Dyn. 29, 807–819. https://doi.org/10.1007/s00382-007-0261-x

Luque, A., Martín, J.L., Dorta, P., Mayer, P., 2014. Temperature Trends on Gran Canaria (Canary Islands). An Example of Global Warming over the Subtropical Northeastern Atlantic. Atmospheric Clim. Sci. 04, 20–28. https://doi.org/10.4236/acs.2014.41003

Lutz, S.R., Mallucci, S., Diamantini, E., Majone, B., Bellin, A., Merz, R., 2016. Hydroclimatic and water quality trends across three Mediterranean river basins. Sci. Total Environ. 571, 1392–1406. https://doi.org/10.1016/j.scitotenv.2016.07.102

Manzano, A., Clemente, M.A., Morata, A., Luna, M.Y., Beguería, S., Vicente-Serrano, S.M., Martín, M.L., 2019. Analysis of the atmospheric circulation pattern effects over SPEI drought index in Spain. Atmospheric Res. 230, 104630. https://doi.org/10.1016/j.atmosres.2019.104630

Marrero-Betancort, N., Marcello, J., Rodríguez Esparragón, D., Hernández-León, S., 2020. Wind variability in the Canary Current during the last 70 years. Ocean Sci. 16, 951–963. https://doi.org/10.5194/os-16-951-2020

Marrero-Betancort, N., Marcello, J., Rodríguez-Esparragón, D., Hernández-León, S., 2022. Sea Level Change in the Canary Current System during the Satellite Era. J. Mar. Sci. Eng. 10, 936. https://doi.org/10.3390/jmse10070936

Martija-Díez, M., López-Parages, J., Rodríguez-Fonseca, B., Losada, T., 2023. The stationarity of the ENSO teleconnection in European summer rainfall. Clim. Dyn. 61, 489–506. https://doi.org/10.1007/s00382-022-06596-4

Martija-Díez, M., Rodríguez-Fonseca, B., López-Parages, J., 2021. "ENSO Influence on Western European summer and fall Temperatures." J. Clim. 1–51. https://doi.org/10.1175/JCLI-D-20-0808.1

Martín, J.L., Bethencourt, J., Cuevas-Agulló, E., 2012. Assessment of global warming on the island of Tenerife, Canary Islands (Spain). Trends in minimum, maximum and mean temperatures since 1944. Clim. Change 114, 343–355. https://doi.org/10.1007/s10584-012-0407-7

Martínez-Fernández, A., Serrano, E., Pisabarro, A., Sánchez-Fernández, M., De Sanjosé, J.J., Gómez-Lende, M., Rangel-de Lázaro, G., Benito-Calvo, A., 2022. The Influence of Image Properties on High-Detail SfM Photogrammetric Surveys of Complex Geometric Landforms: The Application of a Consumer-

Grade UAV Camera in a Rock Glacier Survey. Remote Sens. 14, 3528. https://doi.org/10.3390/rs14153528

Martínez-Ibarra, E., 2015. Climate, water and tourism: causes and effects of droughts associated with urban development and tourism in Benidorm (Spain). Int. J. Biometeorol. 59, 487–501. https://doi.org/10.1007/s00484-014-0851-3

Martínez-Juárez, P., Chiabai, A., Suárez, C., Quiroga, S., 2019. Insights on Urban and Periurban Adaptation Strategies Based on Stakeholders' Perceptions on Hard and Soft Responses to Climate Change. Sustainability 11, 647. https://doi.org/10.3390/su11030647

Martín-Rey, M., Polo, I., Rodríguez-Fonseca, B., Lazar, A., Losada, T., 2019. Ocean Dynamics Shapes the Structure and Timing of Atlantic Equatorial Modes. J. Geophys. Res. Oceans 124, 7529–7544. https://doi.org/10.1029/2019JC015030

Martín-Rey, M., Polo, I., Rodríguez-Fonseca, B., Losada, T., Lazar, A., 2018. Is There Evidence of Changes in Tropical Atlantic Variability Modes under AMO Phases in the Observational Record? J. Clim. 31, 515–536. https://doi.org/10.1175/JCLI-D-16-0459.1

Martín-Vide, J., López-Bustins, J.A., 2006. The Western Mediterranean Oscillation and rainfall in the Iberian Peninsula. Int. J. Climatol. 26, 1455–1475. https://doi.org/10.1002/joc.1388

Martín-Vide, J., Moreno-García, M.C., 2020. Probability values for the intensity of Barcelona's urban heat island (Spain). Atmospheric Res. 240, 104877. https://doi.org/10.1016/j.atmosres.2020.104877

Marty, C., Tilg, A.-M., Jonas, T., 2017. Recent Evidence of Large-Scale Receding Snow Water Equivalents in the European Alps. J. Hydrometeorol. 18, 1021–1031. https://doi.org/10.1175/JHM-D-16-0188.1

Máyer, P., Marzol, M.V., Parreño, J.M., 2017. Precipitation trends and a daily precipitation concentration index for the mid-Eastern Atlantic (Canary Islands, Spain). Cuad. Investig. Geográfica 43, 255–268. https://doi.org/10.18172/cig.3095

Máyer Suárez, P., Marzol Jaén, M.V., Parreño Castellano, J.M., 2015. Tendencias de la precipitación en Canarias. Instituto Geológico y Minero de España.

McPhaden, M.J., Zebiak, S.E., Glantz, M.H., 2006. ENSO as an Integrating Concept in Earth Science. Science 314, 1740–1745. https://doi.org/10.1126/science.1132588

McVicar, T.R., Roderick, M.L., Donohue, R.J., Li, L.T., Van Niel, T.G., Thomas, A., Grieser, J., Jhajharia, D., Himri, Y., Mahowald, N.M., Mescherskaya, A.V., Kruger, A.C., Rehman, S., Dinpashoh, Y., 2012. Global review and synthesis of trends in observed terrestrial near-surface wind speeds: Implications for evaporation. J. Hydrol. 416–417, 182–205. https://doi.org/10.1016/j.jhydrol.2011.10.024

Mechoso, C.R. (Ed.), 2020. Interacting Climates of Ocean Basins: Observations, Mechanisms, Predictability, and Impacts, 1st ed. Cambridge University Press. https://doi.org/10.1017/9781108610995

Mellado-Cano, J., Barriopedro, D., García-Herrera, R., Trigo, R.M., 2020. New observational insights into the atmospheric circulation over the Euro-Atlantic sector since 1685. Clim. Dyn. 54, 823–841. https://doi.org/10.1007/s00382-019-05029-z

Melón-Nava, A., Santos-González, J., M., Redondo-Vega, J., B., González-Gutiérrez, R., Gómez-Villar, A., 2022. Factors influencing the ground thermal regime in a mid-latitude glacial cirque (Hoyo Empedrado, Cantabrian Mountains, 2006–2020). CATENA 212, 106110. https://doi.org/10.1016/j.catena.2022.106110

Merino, A., Fernández, S., Hermida, L., López, L., Sánchez, J.L., García-Ortega, E., Gascón, E., 2014. Snowfall in the Northwest Iberian Peninsula: Synoptic Circulation Patterns and Their Influence on Snow Day Trends. Sci. World J. 2014, 1–14. https://doi.org/10.1155/2014/480275

Merino, A., García-Ortega, E., Navarro, A., Fernández-González, S., Tapiador, F.J., Sánchez, J.L., 2021. Evaluation of gridded rain-gauge-based precipitation datasets: Impact of station density, spatial resolution, altitude gradient and climate. Int. J. Climatol. 41, 3027–3043. https://doi.org/10.1002/joc.7003

Meseguer-Ruíz, O., López-Bustins, J.A., Arbiol-Roca, L., Martín-Vide, J., Miró, J., Estrela, M.J., 2021. Temporal changes in extreme precipitation and exposure of tourism in Eastern and South-Eastern Spain. Theor. Appl. Climatol. 144, 379–390. https://doi.org/10.1007/s00704-021-03548-6

Mezzina, B., García-Serrano, J., Bladé, I., Kucharski, F., 2020. Dynamics of the ENSO Teleconnection and NAO Variability in the North Atlantic–European Late Winter. J. Clim. 33, 907–923. https://doi.org/10.1175/JCLI-D-19-0192.1

Michel, S., Swingedouw, D., Chavent, M., Ortega, P., Mignot, J., Khodri, M., 2020. Reconstructing climatic modes of variability from proxy records using ClimIndRec version 1.0. Geosci. Model Dev. 13, 841–858. https://doi.org/10.5194/gmd-13-841-2020

Michelangeli, P.-A., Vautard, R., Legras, B., 1995. Weather Regimes: Recurrence and Quasi Stationarity. J. Atmospheric Sci. 52, 1237–1256. https://doi.org/10.1175/1520-0469(1995)052<1237:WRRAQS>2.0.CO;2

Millán López, A., 2019. Cambio climático y actividad turística en los espacios urbanos del interior de España: impactos sobre el modelo de aptitud climático-turística de León, Granada y Madrid. Investig. Geográficas 53. https://doi.org/10.14198/INGEO2019.72.03

Millán López, A., Fernández García, F., 2018. Propuesta de un índice climático-turístico adaptado al turismo de interior en la Península Ibérica: aplicación a la ciudad de Madrid. Investig. Geográficas 31. https://doi.org/10.14198/INGEO2018.70.02

Minola, L., Azorín-Molina, C., Chen, D., 2016. Homogenization and Assessment of Observed Near-Surface Wind Speed Trends across Sweden, 1956–2013. J. Clim. 29, 7397–7415. https://doi.org/10.1175/JCLI-D-15-0636.1

Minola, L., Azorín-Molina, C., Guijarro, J.A., Zhang, G., Son, S., Chen, D., 2021. Climatology of Near-Surface Daily Peak Wind Gusts Across Scandinavia: Observations and Model Simulations. J. Geophys. Res. Atmospheres 126, e2020JD033534. https://doi.org/10.1029/2020JD033534

Miró, J.J., Estrela, M.J., Caselles, V., Gómez, I., 2018. Spatial and temporal rainfall changes in the Júcar and Segura basins (1955–2016): Fine-scale trends. Int. J. Climatol. 38, 4699–4722. https://doi.org/10.1002/joc.5689

Miró, J.J., Estrela, M.J., Corell, D., Gómez, I., Luna, M.Y., 2023. Precipitation and drought trends (1952–2021) in a key hydrological recharge area of the eastern Iberian Peninsula. Atmospheric Res. 286, 106695. https://doi.org/10.1016/j.atmosres.2023.106695

Mohino, E., Losada, T., 2015. Impacts of the Atlantic Equatorial Mode in a warmer climate. Clim. Dyn. 45, 2255–2271. https://doi.org/10.1007/s00382-015-2471-y

Morales, C.G., Ortega, M.T., Labajo, J.L., Piorno, A., 2005. Recent trends and temporal behavior of thermal variables in the region of Castilla-León (Spain). Atmósfera 18, 71–90.

Morán-Tejeda, E., Ceballos-Barbancho, A., Llorente-Pinto, J.M., 2010. Hydrological response of Mediterranean headwaters to climate oscillations and land-cover changes: The mountains of Duero River basin (Central Spain). Glob. Planet. Change 72, 39–49. https://doi.org/10.1016/j.gloplacha.2010.03.003

Morán-Tejeda, E., Llorente-Pinto, J.M., Ceballos-Barbancho, A., Tomás-Burguera, M., Azorín-Molina, C., Alonso-González, E., Revuelto, J., Herrero, J., López-Moreno, J.I., 2021. The significance of monitoring high mountain environments to detect heavy precipitation hotspots: a case study in Gredos, Central Spain. Theor. Appl. Climatol. 146, 1175–1188. https://doi.org/10.1007/s00704-021-03791-x

Müller, W.A., Roeckner, E., 2008. ENSO teleconnections in projections of future climate in ECHAM5/MPI-OM. Clim. Dyn. 31, 533–549. https://doi.org/10.1007/s00382-007-0357-3

Muñoz, C., Schultz, D., Vaughan, G., 2020. A Midlatitude Climatology and Interannual Variability of 200- and 500-hPa Cut-Off Lows. J. Clim. 33, 2201–2222. https://doi.org/10.1175/JCLI-D-19-0497.1

Neubacher, C., Witthaut, D., Wohland, J., 2021. Multi-decadal offshore wind power variability can be mitigated through optimized European allocation. Adv. Geosci. 54, 205–215. https://doi.org/10.5194/adgeo-54-205-2021

Nieto, R., Castillo, R., Drumond, A., Gimeno, L., 2014. A catalog of moisture sources for continental climatic regions. Water Resour. Res. 50, 5322–5328. https://doi.org/10.1002/2013WR013901

Nieto, R., Gimeno, L., Añel, J.A., De La Torre, L., Gallego, D., Barriopedro, D., Gallego, M., Gordillo, A., Redaño, A., Delgado, G., 2007. Analysis of the precipitation and cloudiness associated with COLs occurrence in the Iberian Peninsula. Meteorol. Atmospheric Phys. 96, 103–119. https://doi.org/10.1007/s00703-006-0223-6

Nissen, K.M., Leckebusch, G.C., Pinto, J.G., Renggli, D., Ulbrich, S., Ulbrich, U., 2010. Cyclones causing wind storms in the Mediterranean: characteristics, trends and links to large-scale patterns. Nat. Hazards Earth Syst. Sci. 10, 1379–1391. https://doi.org/10.5194/nhess-10-1379-2010

Noguera, I., Domínguez-Castro, F., Vicente-Serrano, S.M., 2020. Characteristics and trends of flash droughts in Spain, 1961–2018. Ann. N. Y. Acad. Sci. 1472, 155–172. https://doi.org/10.1111/nyas.14365

Núñez-Peiró, M., Mavrogianni, A., Symonds, P., Sánchez-Guevara Sánchez, C., Neila González, F.J., 2021. Modelling Long-Term Urban Temperatures with Less Training Data: A Comparative Study Using Neural Networks in the City of Madrid. Sustainability 13, 8143. https://doi.org/10.3390/su13158143

Olcina Cantos, J., Serrano-Notivoli, R., Miró, J., Meseguer-Ruiz, O., 2019. Tropical nights on the Spanish Mediterranean coast, 1950-2014. Clim. Res. 78, 225–236. https://doi.org/10.3354/cr01569

Onea, F., Ruíz, A., Rusu, E., 2020. An Evaluation of the Wind Energy Resources along the Spanish Continental Nearshore. Energies 13, 3986. https://doi.org/10.3390/en13153986

Ortega, M., Sánchez, E., Gutiérrez, C., Molina, M.O., López-Franca, N., 2023. Regional winds over the Iberian Peninsula (Cierzo, Levante and Poniente) from high-resolution COSMO-REA6 reanalysis. Int. J. Climatol. 43, 1016–1033. https://doi.org/10.1002/joc.7860

Ortega Villazán, M.T., Morales Rodríguez, C.G., 2015. El clima de la Cordillera Cantábrica castellano-leonesa: diversidad, contrastes y cambios. Investig. Geográficas 45. https://doi.org/10.14198/INGEO2015.63.04

Ortíz De Galisteo, J.P., Cachorro, V., Toledano, C., Torres, B., Laulainen, N., Bennouna, Y., De Frutos, A., 2011. Diurnal cycle of precipitable water vapor over Spain. Q. J. R. Meteorol. Soc. 137, 948–958. https://doi.org/10.1002/qj.811

Otterå, O.H., Bentsen, M., Drange, H., Suo, L., 2010. External forcing as a metronome for Atlantic multidecadal variability. Nat. Geosci. 3, 688–694. https://doi.org/10.1038/ngeo955

Padial-Iglesias, M., Pons, X., Serra, P., Ninyerola, M., 2022. Does the gap-filling method influence long-term (1950–2019) temperature and precipitation trend analyses? GeoFocus Rev. Int. Cienc. Tecnol. Inf. Geográfica 5–33. https://doi.org/10.21138/GF.773

Paniagua, L.L., García-Martín, A., Moral, F.J., Rebollo, F.J., 2019. Aridity in the Iberian Peninsula (1960–2017): distribution, tendencies, and changes. Theor. Appl. Climatol. 138, 811–830. https://doi.org/10.1007/s00704-019-02866-0

Paredes-Fortuny, L., Khodayar, S., 2023. Understanding the Magnification of Heatwaves over Spain: Relevant changes in the most extreme events. Weather Clim. Extrem. 42, 100631. https://doi.org/10.1016/j.wace.2023.100631

Páscoa, P., Russo, A., Gouveia, C.M., Soares, P.M.M., Cardoso, R.M., Careto, J.A.M., Ribeiro, A.F.S., 2021. A high-resolution view of the recent drought trends over the Iberian Peninsula. Weather Clim. Extrem. 32, 100320. https://doi.org/10.1016/j.wace.2021.100320

Peña-Angulo, D., González-Hidalgo, J.C., Sandonís, L., Beguería, S., Tomás-Burguera, M., López-Bustins, J.A., Lemus-Canovas, M., Martín-Vide, J., 2021. Seasonal temperature trends on the Spanish mainland: A secular study (1916–2015). Int. J. Climatol. 41, 3071–3084. https://doi.org/10.1002/joc.7006

Peña-Angulo, D., Vicente-Serrano, S.M., Domínguez-Castro, F., Murphy, C., Reig, F., Tramblay, Y., Trigo, R.M., Luna, M.Y., Turco, M., Noguera, I., Aznárez-Balta, M., García-Herrera, R., Tomás-Burguera, M., El Kenawy, A., 2020. Long-term precipitation in Southwestern Europe reveals no clear trend attributable to anthropogenic forcing. Environ. Res. Lett. 15, 094070. https://doi.org/10.1088/1748-9326/ab9c4f

Peña-Ortiz, C., Barriopedro, D., García-Herrera, R., 2015. Multidecadal Variability of the Summer Length in Europe. J. Clim. 28, 5375–5388. https://doi.org/10.1175/JCLI-D-14-00429.1

Perdiguer-Lopez, R., Berne Valero, J.L., Garrido-Villen, N., 2023. GNSS-retrieved precipitable water vapour in the Atlantic coast of France and Spain with GPT3 model. Acta Geod. Geophys. 58, 575–600. https://doi.org/10.1007/s40328-023-00427-6

Pérez, F.F., Boscolo, R., Bladé, I., Cacho, I., Castro-Díez, Y., Gomis, D., González-Sampériz, P., Míguez-Macho, G., Rodríguez-Fonseca, B., Rodríguez-Puebla, C., Sánchez, E., Sotillo, M.G., Valero-Garcés, B.L., Vargas-Yáñez, M., 2010. Clima en España: pasado, presente y futuro. Informe de Evaluación del Cambio Climático Regional. Climate in Spain: past, present and future. Regional climate change assessment report.

Pérez Palazón, M.J., 2019. Análisis de tendencias en los flujos de agua y energía de la capa de nieve a diversas escalas en Sierra Nevada. Trend analysis of water and energy fluxes in snowpacks on different scales in Sierra Nevada.

Philandras, C.M., Nastos, P.T., Kapsomenakis, J., Douvis, K.C., Tselioudis, G., Zerefos, C.S., 2011. Long term precipitation trends and variability within the Mediterranean region. Nat Hazards Earth Syst Sci 11, 3235–3250.

Pietrapertosa, F., Olazabal, M., Simoes, S.G., Salvia, M., Fokaides, P.A., Ioannou, B.I., Viguié, V., Spyridaki, N.-A., De Gregorio Hurtado, S., Geneletti, D., Heidrich, O., Tardieu, L., Feliu, E., Rižnar, K., Matosović, M., Balzan, M.V., Flamos, A., Šel, N.B., Reckien, D., 2023. Adaptation to climate change in cities of Mediterranean Europe. Cities 140, 104452. https://doi.org/10.1016/j.cities.2023.104452

Pinto, J.G., Raible, C.C., 2012. Past and recent changes in the North Atlantic oscillation. Wiley Interdiscip. Rev. Clim. Change 3, 79–90. https://doi.org/10.1002/wcc.150

Pinto, J.G., Zacharias, S., Fink, A.H., Leckebusch, G.C., Ulbrich, U., 2009. Factors contributing to the development of extreme North Atlantic cyclones and their relationship with the NAO. Clim. Dyn. 32, 711–737. https://doi.org/10.1007/s00382-008-0396-4

Pisabarro, A., 2020. Snow cover as a morphogenic agent determining ground climate, landforms and runoff in the Valdecebollas massif, Cantabrian Mountains. Cuad. Investig. Geográfica 46, 81–102. https://doi.org/10.18172/cig.3823

Pisabarro, A., Pellitero, R., Serrano, E., Gómez-Lende, M., González-Trueba, J.J., 2017. Ground temperatures, landforms and processes in an Atlantic mountain. Cantabrian Mountains (Northern Spain). CATENA 149, 623–636. https://doi.org/10.1016/j.catena.2016.07.051

Pisabarro, A., Pellitero, R., Serrano, E., López-Moreno, J.I., 2019. Impacts of land abandonment and climate variability on runoff generation and sediment transport in the Pisuerga headwaters (Cantabrian Mountains, Spain). Geogr. Ann. Ser. Phys. Geogr. 101, 211–224. https://doi.org/10.1080/04353676.2019.1591042

Poli, P., Hersbach, H., Dee, D.P., Berrisford, P., Simmons, A.J., Vitart, F., Laloyaux, P., Tan, D.G.H., Peubey, C., Thépaut, J.-N., Trémolet, Y., Hólm, E.V., Bonavita, M., Isaksen, L., Fisher, M., 2016. ERA-20C: An Atmospheric Reanalysis of the Twentieth Century. J. Clim. 29, 4083–4097. https://doi.org/10.1175/JCLI-D-15-0556.1

Polo, I., De Fonseca, B.R., Sheinbaum, J., 2005. Northwest Africa upwelling and the Atlantic climate variability. Geophys. Res. Lett. 32, 2005GL023883. https://doi.org/10.1029/2005GL023883

Polo, I., Rodríguez-Fonseca, B., Losada, T., García-Serrano, J., 2008. Tropical Atlantic Variability Modes (1979–2002). Part I: Time-Evolving SST Modes Related to West African Rainfall. J. Clim. 21, 6457–6475. https://doi.org/10.1175/2008JCLI2607.1

Polo, M.J., Herrero, J., Millares, A., Pimentel, R., Moñino, A., Pérez-Palazón, M.-J., Aguilar, C., Losada, M.A., 2022. Snow Dynamics, Hydrology, and Erosion, in: Zamora, R., Oliva, M. (Eds.), The Landscape of the Sierra Nevada. Springer International Publishing, Cham, pp. 149–164. https://doi.org/10.1007/978-3-030-94219-9_10

Quesada, B., Vautard, R., Yiou, P., Hirschi, M., Seneviratne, S.I., 2012. Asymmetric European summer heat predictability from wet and dry southern winters and springs. Nat. Clim. Change 2, 736–741. https://doi.org/10.1038/nclimate1536

Raible, C.C., Lehner, F., González-Rouco, J.F., Fernández-Donado, L., 2014. Changing correlation structures of the Northern Hemisphere atmospheric circulation from 1000 to 2100 AD. Clim. Past 10, 537–550. https://doi.org/10.5194/cp-10-537-2014

Ramon, J., Lledó, L., Torralba, V., Soret, A., Doblas-Reyes, F.J., 2019. What global reanalysis best represents near-surface winds? Q. J. R. Meteorol. Soc. 145, 3236–3251. https://doi.org/10.1002/qj.3616

Ramos, A.M., Martins, M.J., Tomé, R., Trigo, R.M., 2018. Extreme Precipitation Events in Summer in the Iberian Peninsula and Its Relationship With Atmospheric Rivers. Front. Earth Sci. 6, 110. https://doi.org/10.3389/feart.2018.00110

Ramos, A.M., Tomé, R., Trigo, R.M., Liberato, M.L.R., Pinto, J.G., 2016. Projected changes in atmospheric rivers affecting Europe in CMIP5 models. Geophys. Res. Lett. 43, 9315–9323. https://doi.org/10.1002/2016GL070634

Raveh-Rubin, S., Wernli, H., 2015. Large-scale wind and precipitation extremes in the Mediterranean: a climatological analysis for 1979–2012. Q. J. R. Meteorol. Soc. 141, 2404–2417. https://doi.org/10.1002/qj.2531

Redolat, D., Monjo, R., López-Bustins, J.A., Martín-Vide, J., 2019. Upper-Level Mediterranean Oscillation index and seasonal variability of rainfall and temperature. Theor. Appl. Climatol. 135, 1059–1077. https://doi.org/10.1007/s00704-018-2424-6

Ríos-Entenza, A., Soares, P.M.M., Trigo, R.M., Cardoso, R.M., Míguez-Macho, G., 2014. Moisture recycling in the Iberian Peninsula from a regional climate simulation: Spatiotemporal analysis and impact on the precipitation regime. J. Geophys. Res. Atmospheres 119, 5895–5912. https://doi.org/10.1002/2013JD021274

Rodrigo, F.S., 2023. Spatiotemporal variability of the relationship between seasonal temperatures and precipitation in Spain, 1951–2019. Theor. Appl. Climatol. 153, 1371–1391. https://doi.org/10.1007/s00704-023-04550-w

Rodrigo, F.S., 2019. Coherent variability between seasonal temperatures and rainfalls in the Iberian Peninsula, 1951–2016. Theor. Appl. Climatol. 135, 473–490. https://doi.org/10.1007/s00704-018-2400-1

Rodríguez Algeciras, J.A., Matzarakis, A., 2016. Quantification of thermal bioclimate for the management of urban design in Mediterranean climate of Barcelona, Spain. Int. J. Biometeorol. 60, 1261–1270. https://doi.org/10.1007/s00484-015-1121-8

Rodríguez, M.V., Melgar, S.G., Márquez, J.M.A., 2022. Assessment of aerial thermography as a method of in situ measurement of radiant heat transfer in urban public spaces. Sustain. Cities Soc. 87, 104228. https://doi.org/10.1016/j.scs.2022.104228

Rodríguez-Fonseca, B., Polo, I., Serrano, E., Castro, M., 2006. Evaluation of the North Atlantic SST forcing on the European and Northern African winter climate. Int. J. Climatol. 26, 179–191. https://doi.org/10.1002/joc.1234

Rodríguez-Fonseca, B., Sánchez, E., Arribas, A., 2005. Winter climate variability changes over Europe and the Mediterranean region under increased greenhouse conditions. Geophys. Res. Lett. 32, 2005GL022800. https://doi.org/10.1029/2005GL022800

Rodríguez-Fonseca, B., Suárez-Moreno, R., Ayarzagüena, B., López-Parages, J., Gómara, I., Villamayor, J., Mohino, E., Losada, T., Castaño-Tierno, A., 2016. A Review of ENSO Influence on the North Atlantic. A Non-Stationary Signal. Atmosphere 7, 87. https://doi.org/10.3390/atmos7070087

Rodríguez-Gómez, F., Fernández-Cañero, R., Pérez, G., Del Campo-Ávila, J., López-Rodríguez, D., Pérez-Urrestarazu, L., 2022. Detection of unfavourable urban areas with higher temperatures and lack of green spaces using satellite imagery in sixteen Spanish cities. Urban For. Urban Green. 78, 127783. https://doi.org/10.1016/j.ufug.2022.127783

Rodríguez-Puebla, C., Encinas, A.H., Nieto, S., Garmendia, J., 1998. Spatial and temporal patterns of annual precipitation variability over the Iberian Peninsula. Int. J. Climatol. 18, 299–316. https://doi.org/10.1002/(SICI)1097-0088(19980315)18:3<299::AID-JOC247>3.0.CO;2-L

Rojas-Labanda, C., González-Rouco, F., García-Bustamante, E., Navarro, J., Lucio-Eceiza, E.E., Van Der Schrier, G., Kaspar, F., 2023. Surface wind over Europe: Data and variability. Int. J. Climatol. 43, 134–156. https://doi.org/10.1002/joc.7739

Román, R., Antón, M., Cachorro, V.E., Loyola, D., Ortiz De Galisteo, J.P., De Frutos, A., Romero-Campos, P.M., 2015. Comparison of total water vapor column from GOME-2 on MetOp-A against ground-based GPS measurements at the Iberian Peninsula. Sci. Total Environ. 533, 317–328. https://doi.org/10.1016/j.scitotenv.2015.06.124

Rowell, D.P., Jones, R.G., 2006. Causes and uncertainty of future summer drying over Europe. Clim. Dyn. 27, 281–299. https://doi.org/10.1007/s00382-006-0125-9

Royé, D., Codesido, R., Tobías, A., Taracido, M., 2020. Heat wave intensity and daily mortality in four of the largest cities of Spain. Environ. Res. 182, 109027. https://doi.org/10.1016/j.envres.2019.109027

Rubio-Romero, A.; Granados, I., 2008. Efectos del cambio climático sobre los macroinvertebrados fluviales del Alto Lozoya. Presented at the XIV Congreso de la Asociación Ibérica de Limnologá, Huelva - Spain.

Ruíz Sinoga, J.D., García Marín, R., Martínez Murillo, J.F., Gabarrón Galeote, M.A., 2011. Precipitation dynamics in southern Spain: trends and cycles. Int. J. Climatol. 31, 2281–2289. https://doi.org/10.1002/joc.2235

Ruíz-Fernández, J., García-Hernández, C., Ochoa-Álvarez, M., Van Den Bergh, M., Gallinar Cañedo, D., González-Díaz, B., 2023. Ground and Near-Rock Surface Air Thermal Regimes in the High Mountain of the Picos De Europa (Cantabrian Mountains, NW Spain). Air Soil Water Res. 16, 117862212311766. https://doi.org/10.1177/11786221231176676

Salamanca, F., Martilli, A., Yagüe, C., 2012. A numerical study of the Urban Heat Island over Madrid during the DESIREX (2008) campaign with WRF and an evaluation of simple mitigation strategies. Int. J. Climatol. 32, 2372–2386. https://doi.org/10.1002/joc.3398

Salvador, C., Gullón, P., Franco, M., Vicedo-Cabrera, A.M., 2023. Heat-related first cardiovascular event incidence in the city of Madrid (Spain): Vulnerability assessment by demographic, socioeconomic, and health indicators. Environ. Res. 226, 115698. https://doi.org/10.1016/j.envres.2023.115698

Salvador, C., Nieto, R., Linares, C., Díaz, J., Gimeno, L., 2020. Short-term effects of drought on daily mortality in Spain from 2000 to 2009, Environmental Research, 183, 109200. https://doi.org/10.1016/j.envres.2020.109200

Salvador, S., Costoya, X., Sanz-Larruga, F., Gimeno, L., 2018. Development of Offshore Wind Power: Contrasting Optimal Wind Sites with Legal Restrictions in Galicia, Spain. Energies 11, 731. https://doi.org/10.3390/en11040731

Salvia, M., Olazabal, M., Fokaides, P.A., Tardieu, L., Simoes, S.G., Geneletti, D., De Gregorio Hurtado, S., Viguié, V., Spyridaki, N.-A., Pietrapertosa, F., Ioannou, B.I., Matosović, M., Flamos, A., Balzan, M.V., Feliu, E., Rižnar, K., Šel, N.B., Heidrich, O., Reckien, D., 2021. Climate mitigation in the Mediterranean Europe: An assessment of regional and city-level plans. J. Environ. Manage. 295, 113146. https://doi.org/10.1016/j.jenvman.2021.113146

Sánchez-Benítez, A., Barriopedro, D., García-Herrera, R., 2020. Tracking Iberian heatwaves from a new perspective. Weather Clim. Extrem. 28, 100238. https://doi.org/10.1016/j.wace.2019.100238

Sánchez-Benítez, A., García-Herrera, R., Vicente-Serrano, S.M., 2017. Revisiting precipitation variability, trends and drivers in the Canary Islands. Int. J. Climatol. 37, 3565–3576. https://doi.org/10.1002/joc.4937

Sánchez-López, G., 2016. North Atlantic Oscillation imprints in the Central Iberian Peninsula for the last two millennia: from ordination analyses to the Bayesian approach. University of Barcelona, Barcelona.

Sandonis, L., González-Hidalgo, J., Peña-Angulo, D., Beguería, S., 2021. Mean temperature evolution on the Spanish mainland 1916-2015. Clim. Res. 82, 177–189. https://doi.org/10.3354/cr01627

Santos-González, J., Redondo Vega, J.M., Gómez Villar, A., González-Gutiérrez, R.B., 2013. Dinámica actual de los nichos de nivación del Alto Sil (Cordillera Cantábrica). Cuad. Investig. Geográfica 36, 87–106. https://doi.org/10.18172/cig.1229

Scaife, A.A., Knight, J.R., Vallis, G.K., Folland, C.K., 2005. A stratospheric influence on the winter NAO and North Atlantic surface climate. Geophys. Res. Lett. 32. https://doi.org/10.1029/2005GL023226

Schliep, E.M., Gelfand, A.E., Abaurrea, J., Asín, J., Beamonte, M.A., Cebrián, A.C., 2021. Long-Term Spatial Modelling for Characteristics of Extreme Heat Events. J. R. Stat. Soc. Ser. A Stat. Soc. 184, 1070–1092. https://doi.org/10.1111/rssa.12710

Senent-Aparicio, J., López-Ballesteros, A., Jimeno-Sáez, P., Pérez-Sánchez, J., 2023. Recent precipitation trends in Peninsular Spain and implications for water infrastructure design. J. Hydrol. Reg. Stud. 45, 101308. https://doi.org/10.1016/j.ejrh.2022.101308

Serrano, E., Oliva, M., González-García, M., López-Moreno, J.I., González-Trueba, J., Martín-Moreno, R., Gómez-Lende, M., Martín-Díaz, J., Nofre, J., Palma, P., 2018. Post-little ice age paraglacial processes and landforms in the high Iberian mountains: A review. Land Degrad. Dev. 29, 4186–4208. https://doi.org/10.1002/ldr.3171

Serrano, V., M, S., 2013. Spatial and temporal evolution of precipitation droughts in Spain in the last century.

Serrano-Notivoli, R.S., 2017. Reconstrucción climática instrumental de la precipitación diaria en España: ensayo metodológico y aplicaciones.

Serrano-Notivoli, R., Lemus-Canovas, M., Barrao, S., Sarricolea, P., Meseguer-Ruíz, O., Tejedor, E., 2022. Heat and cold waves in mainland Spain: Origins, characteristics, and trends. Weather Clim. Extrem. 37, 100471. https://doi.org/10.1016/j.wace.2022.100471

Serrano-Notivoli, R., Tejedor, E., 2021. From rain to data: A review of the creation of monthly and daily station-based gridded precipitation datasets. WIREs Water 8, e1555. https://doi.org/10.1002/wat2.1555

Serrano-Notivoli, R., Tejedor, E., Sarricolea, P., Meseguer-Ruíz, O., De Luis, M., Saz, M.Á., Longares, L.A., Olcina, J., 2023. Unprecedented warmth: A look at Spain's exceptional summer of 2022. Atmospheric Res. 293, 106931. https://doi.org/10.1016/j.atmosres.2023.106931

Spagnoli, B., Planton, S., Déqué, M., Mestre, O., Moisselin, J. -M., 2002. Detecting climate change at a regional scale: the case of France. Geophys. Res. Lett. 29. https://doi.org/10.1029/2001GL014619

Sperling, F.N., Washington, R., Whittaker, R.J., 2004. Future Climate Change of the Subtropical North Atlantic: Implications for the Cloud Forests of Tenerife. Clim. Change 65, 103–123. https://doi.org/10.1023/B:CLIM.0000037488.33377.bf

Tejedor, E., Cuadrat, J.M., Saz, M.Á., Serrano-Notivoli, R., López, N., Aladrén, M., 2016. Islas de calor y confort térmico en Zaragoza durante la ola de calor de julio de 2015, in: Clima, Sociedad, Riesgos y Ordenación Del Territorio. Servicio de Publicaciones de la UA, pp. 141–151. https://doi.org/10.14198/XCongresoAECAlicante2016-13

Tobías, A., Royé, D., Íñiguez, C., 2023. Heat-attributable Mortality in the Summer of 2022 in Spain. Epidemiology 34, e5–e6. https://doi.org/10.1097/EDE.0000000000001583

Torrecilla, R.C., Gallego, E.G., García, F.F., 1998. Clima y ambiente urbano en ciudades ibéricas e iberoamericanas. Parteluz.

Trenberth, K.E., 1999. Atmospheric Moisture Recycling: Role of Advection and Local Evaporation. J. Clim. 12, 1368–1381.

Trigo, R., Osborn, T., Corte-Real, J., 2002. The North Atlantic Oscillation influence on Europe: climate impacts and associated physical mechanisms. Clim. Res. 20, 9–17. https://doi.org/10.3354/cr020009

Trigo, R.M., Pozo-Vázquez, D., Osborn, T.J., Castro-Díez, Y., Gámiz-Fortis, S., Esteban-Parra, M.J., 2004. North Atlantic oscillation influence on precipitation, river flow and water resources in the Iberian Peninsula. Int. J. Climatol. 24, 925–944.

Utrabo-Carazo, E., Azorin-Molina, C., Aguilar, E., Brunet, M., 2023. A Spectral Analysis of Near-Surface Mean Wind Speed and Gusts Over the Iberian Peninsula. Geophys. Res. Lett. 50, e2023GL103323. https://doi.org/10.1029/2023GL103323

Utrabo-Carazo, E., Azorin-Molina, C., Serrano, E., Aguilar, E., Brunet, M., Guijarro, J.A., 2022. Wind stilling ceased in the Iberian Peninsula since the 2000s. Atmospheric Res. 272, 106153. https://doi.org/10.1016/j.atmosres.2022.106153

Valdes-Abellan, J., Pardo, M.A., Tenza-Abril, A.J., 2017. Observed precipitation trend changes in the western Mediterranean region. Int. J. Climatol. 37, 1285–1296. https://doi.org/10.1002/joc.4984

Vaquero, J.M., Bravo-Paredes, N., Obregón, M.A., Carrasco, V.M.S., Valente, M.A., Trigo, R.M., Domínguez-Castro, F., Montero-Martín, J., Vaquero-Martínez, J., Antón, M., García, J.A., Gallego, M.C., 2022. Recovery of early meteorological records from Extremadura region (SW Iberia): The 'CliPastExtrem' (v1.0) database. Geosci. Data J. 9, 207–220. https://doi.org/10.1002/gdj3.131

Vaquero-Martínez, J., Antón, M., 2021. Review on the Role of GNSS Meteorology in Monitoring Water Vapor for Atmospheric Physics. Remote Sens. 13, 2287. https://doi.org/10.3390/rs13122287

Vaquero-Martínez, J., Antón, M., Ortíz De Galisteo, J.P., Cachorro, V.E., Wang, H., González Abad, G., Román, R., Costa, M.J., 2017. Validation of integrated water vapor from OMI satellite instrument against reference GPS data at the Iberian Peninsula. Sci. Total Environ. 580, 857–864. https://doi.org/10.1016/j.scitotenv.2016.12.032

Vargas-Yáñez, M., Tel, E., Marcos, M., Moya, F., Ballesteros, E., Alonso, C., García-Martínez, M.C., 2023. Factors Contributing to the Long-Term Sea Level Trends in the Iberian Peninsula and the Balearic and Canary Islands. Geosciences 13, 160. https://doi.org/10.3390/geosciences13060160

Vautard, R., Cattiaux, J., Yiou, P., Thépaut, J.-N., Ciais, P., 2010. Northern Hemisphere atmospheric stilling partly attributed to an increase in surface roughness. Nat. Geosci. 3, 756–761. https://doi.org/10.1038/ngeo979

Vicente-Serrano, S., 2021. The evolution of climatic drought studies in Spain over the last few decades. Geographicalia 7–34. https://doi.org/10.26754/ojs_geoph/geoph.2021734640

Vicente-Serrano, S.M., Beguería, S., Hernández-Santana, V., Durán, J.J., Rosales, M.A., Camarero, J.J., 2023. Sequías. Informe de transferencia de conocimiento. https://doi.org/10.20350/digitalCSIC/15371

Vicente-Serrano, S.M., 2005. El Niño and La Niña influence on droughts at different timescales in the Iberian Peninsula. Water Resour. Res. 41, 2004WR003908. https://doi.org/10.1029/2004WR003908

Vicente-Serrano, S.M., Azorín-Molina, C., Sánchez-Lorenzo, A., El Kenawy, A., Martín-Hernández, N., Peña-Gallardo, M., Beguería, S., Tomás-Burguera, M., 2016. Recent changes and drivers of the atmospheric evaporative demand in the Canary Islands. Hydrol. Earth Syst. Sci. 20, 3393–3410. https://doi.org/10.5194/hess-20-3393-2016

Vicente-Serrano, S.M., Rodríguez-Camino, E., Domínguez-Castro, F., El Kenawy, A., Azorín-Molina, C., 2017. An updated review on recent trends in observational surface atmospheric variables and their extremes over Spain. Cuad. Investig. Geográfica 43, 209–232. https://doi.org/10.18172/cig.3134

Vidaller, I., Izagirre, E., del Río, L.M., Alonso-González, E., Rojas-Heredia, F., Serrano, E., Moreno, A., López-Moreno, J.I., Revuelto, J., 2023. The Aneto glacier's (Central Pyrenees) evolution from 1981 to 2022: ice loss observed from historic aerial image photogrammetry and remote sensing techniques. The Cryosphere 17, 3177–3192. https://doi.org/10.5194/tc-17-3177-2023

Viviroli, D., Dürr, H.H., Messerli, B., Meybeck, M., Weingartner, R., 2007. Mountains of the world, water towers for humanity: Typology, mapping, and global significance. Water Resour. Res. 43, 2006WR005653. https://doi.org/10.1029/2006WR005653

Von Schuckmann, K., Le Traon, P.-Y., Smith, N., Pascual, A., Djavidnia, S., Gattuso, J.-P., Grégoire, M., Aaboe, S., Alari, V., Alexander, B.E., Alonso-Martirena, A., Aydogdu, A., Azzopardi, J., Bajo, M., Barbariol, F., Batistić, M., Behrens, A., Ismail, S.B., Benetazzo, A., Bitetto, I., Borghini, M., Bray, L., Capet, A., Carlucci, R., Chatterjee, S., Chiggiato, J., Ciliberti, S., Cipriano, G., Clementi, E., Cochrane, P., Cossarini, G., D'Andrea, L., Davison, S., Down, E., Drago, A., Druon, J.-N., Engelhard, G., Federico, I., Garić, R., Gauci, A., Gerin, R., Geyer, G., Giesen, R., Good, S., Graham, R., Grégoire, M., Greiner, E., Gundersen, K., Hélaouët, P., Hendricks, S., Heymans, J.J., Holt, J., Hure, M., Juza, M., Kassis, D., Kellett, P., Knol-Kauffman, M., Kountouris, P., Kõuts, M., Lagemaa, P., Lavergne, T., Legeais, J.-F., Traon, P.-Y.L., Libralato, S., Lien, V.S., Lima, L., Lind, S., Liu, Y., Macías, D., Maljutenko, I., Mangin, A., Männik, A., Marinova, V., Martellucci, R., Masnadi, F., Mauri, E., Mayer, M., Menna, M., Meulders, C., Møgster, J.S., Monier, M., Mork, K.A., Müller, M., Nilsen, J.E.Ø., Notarstefano, G., Oviedo, J.L., Palerme, C., Palialexis, A., Panzeri, D., Pardo, S., Peneva, E., Pezzutto, P., Pirro, A., Platt, T., Poulain, P.-M., Prieto, L., Querin, S., Rabenstein, L., Raj, R.P., Raudsepp, U., Reale, M., Renshaw, R., Ricchi, A., Ricker, R., Rikka, S., Ruiz, J., Russo, T., Sanchez, J., Santoleri, R., Sathyendranath, S., Scarcella, G., Schroeder, K., Sparnocchia, S., Spedicato, M.T., Stanev, E., Staneva, J., Stocker,

A., Stoffelen, A., Teruzzi, A., Townhill, B., Uiboupin, R., Valcheva, N., Vandenbulcke, L., Vindenes, H., Schuckmann, K.V., Vrgoč, N., Wakelin, S., Zupa, W., 2021. Copernicus Marine Service Ocean State Report, Issue 5. J. Oper. Oceanogr. 14, 1–185. https://doi.org/10.1080/1755876X.2021.1946240

Wang, B., Luo, X., Yang, Y.-M., Sun, W., Cane, M.A., Cai, W., Yeh, S.-W., Liu, J., 2019. Historical change of El Niño properties sheds light on future changes of extreme El Niño. Proc. Natl. Acad. Sci. 116, 22512–22517. https://doi.org/10.1073/pnas.1911130116

Waugh, D.W., Sobel, A.H., Polvani, L.M., 2017. What Is the Polar Vortex and How Does It Influence Weather? Bull. Am. Meteorol. Soc. 98, 37–44. https://doi.org/10.1175/BAMS-D-15-00212.1

Woollings, T., Gregory, J.M., Pinto, J.G., Reyers, M., Brayshaw, D.J., 2012. Response of the North Atlantic storm track to climate change shaped by ocean–atmosphere coupling. Nat. Geosci. 5, 313–317. https://doi.org/10.1038/ngeo1438

Woollings, T., Hannachi, A., Hoskins, B., Turner, A., 2010. A Regime View of the North Atlantic Oscillation and Its Response to Anthropogenic Forcing. J. Clim. 23, 1291–1307. https://doi.org/10.1175/2009JCLI3087.1

Yanes Luque, A., Rodríguez-Báez, J.A., Máyer Suárez, P., Dorta Antequera, P., López-Díez, A., Díaz-Pacheco, J., Pérez-Chacón, E., 2021. Marine storms in coastal tourist areas of the Canary Islands. Nat. Hazards 109, 1297–1325. https://doi.org/10.1007/s11069-021-04879-3

Yasunari, T., Saito, K., Takata, K., 2006. Relative Roles of Large-Scale Orography and Land Surface Processes in the Global Hydroclimate. Part I: Impacts on Monsoon Systems and the Tropics. J. Hydrometeorol. 7, 626–641. https://doi.org/10.1175/JHM515.1

Yeh, S.-W., Kug, J.-S., Dewitte, B., Kwon, M.-H., Kirtman, B.P., Jin, F.-F., 2009. El Nino in a changing climate. Nature 461, 511–514.

Young, I.R., Ribal, A., 2019. Multiplatform evaluation of global trends in wind speed and wave height. Science 364, 548–552. https://doi.org/10.1126/science.aav9527

Zeng, Z., Ziegler, A.D., Searchinger, T., Yang, L., Chen, A., Ju, K., Piao, S., Li, L.Z.X., Ciais, P., Chen, D., Liu, J., Azorín-Molina, C., Chappell, A., Medvigy, D., Wood, E.F., 2019. A reversal in global terrestrial stilling and its implications for wind energy production. Nat. Clim. Change 9, 979–985. https://doi.org/10.1038/s41558-019-0622-6

Zhang, X., Sorteberg, A., Zhang, J., Gerdes, R., Comiso, J.C., 2008. Recent radical shifts of atmospheric circulations and rapid changes in Arctic climate system. Geophys. Res. Lett. 35. https://doi.org/10.1029/2008GL035607

Zittis, G., Hadjinicolaou, P., Klangidou, M., Proestos, Y., Lelieveld, J., 2019. A multi-model, multi-scenario, and multi-domain analysis of regional climate projections for the Mediterranean. Reg. Environ. Change 19, 2621–2635. https://doi.org/10.1007/s10113-019-01565-w

CHAPTER 4

PHYSICAL AND BIOGEOCHEMICAL CHANGES IN THE OCEAN AROUND SPAIN DURING THE OBSERVATIONAL PERIOD: VARIABILITY, TRENDS AND DRIVERS

Coordinators/Main Authors: Manuel Vargas-Yáñez[(1)], Marta Marcos[(2)], Marcos Fontela[(3)] y Raquel Somavilla [(1)]

Collaborators: Ángel Amores[2], Miguel Agulles[2], Mélanie Juza[4] ,Iván Parra-Berrocal[5], Jordi Salat[6], Josep Pascual[6], Alonso Hernández-Guerra[7], Almudena Fontán[8], Marina Chiffet[8], Moncho Gómez-Gesteira[9]

[1] Instituto Español de Oceanografía (IEO-CSIC).Málaga, España

[2] Institut Mediterrani d'Estudis Avançats (IMEDEA, Universidad de las Islas Baleares) Palma, España

[3] Instituto de Investigaciones Marinas (IIM-CSIC). Vigo, España

[4] Sistema de Observación y Predicción Costero de las Islas Baleares (SOCIB), Palma, España

[5] Centre National de Recherhes Météorologiques, Toulouse, Francia

[6] Institut de Ciencies del Mar (CSIC), Barcelona, España.

[7] Instituto de Oceanografía y Cambio Global (IOCAG), Universidad de Las Palmas de Gran Canaria, España.

[8] AZTI, Centro de Investigación Marina y Alimentaria, Pasaia (Gipuzkoa) España

[9] Universidad de Vigo, Vigo, España

1. Introduction

The oceans cover more than seventy percent of the Earth surface and, due to its large volume and its thermal inertia -about 4000 times greater than that of the air-, they accumulate 93% of the energy in the Earth Climate System, being the main driver of climate regulation and acting as a heat buffer for climate warming (Intergovernmental Panel On Climate Change (IPCC), 2023). Besides, the global ocean not only absorbs, stores, and redistributes vast amounts of heat, but also of carbon. The ocean contains 50 times more carbon than the atmosphere and it is actively absorbing about 30% of the emitted anthropogenic carbon dioxide (Le Quéré et al., 2015). Half of the net primary production on Earth is produced in the upper layers of the ocean by phytoplankton with the consequent liberation of oxygen (Keeling et al., 2010). The regulation of atmospheric and marine carbon dioxide (CO_2) concentrations and the provision of oxygen are just some of the services that marine ecosystems and marine biodiversity provide for human well-being.

As greenhouse gas concentrations increase the Earth's radiative imbalance (the energy received from the Sun exceeds the energy that leaves the atmosphere back to the space), the oceans sequester up to 93% of the extra heat in the climate system (IPCC, 2023), and as a result, the ocean is warming (Balmaseda et al., 2013; Cheng et al., 2019, 2022; Roemmich et al., 2015). The air-sea interface is a key gateway in the Earth system. It is where the atmosphere sets the ocean in motion, climate/weather relevant air-sea processes occur and pollutants (i.e. plastic, anthropogenic CO_2, radioactive/chemical waste) enter the sea. It is so clear that precise knowledge of the exchanges across this interface are fundamental both to the evolution of the

ocean and to our climate as a whole that, in fact, turbulent and radiative heat fluxes between the ocean and the atmosphere are found among both the Essential Ocean Variables (EOV) and the Essential Climate Variables (ECV). The in-situ observations for these variables come mostly from fixed buoys and ships. This means that despite the importance of these measurements, there are currently only about 300 in situ observation sites of the exchange of heat, water and momentum over the immensity of the entire ocean and with a non-homogeneous distribution. As a result, our ability to resolve the wide range of ocean-atmosphere interaction processes with adequate spatial and temporal resolution is still limited. This means, that heat flux estimates where exchanges between the atmosphere and the ocean take place enabling the ocean to accumulate more than 90% of the energy in the climate system are still far from being able to close the heat budget to +1 Wm^{-2} -as current estimates based on the increase in ocean heat content (+0.6 ± 0.3 Wm^{-2}), showing an uncertainty (±17 Wm^{-2}) even greater than estimates from TOA (Top Of the Atmosphere) heat fluxes. A global average net heat gain from the atmosphere to the ocean of +1 Wm^{-2}, if mixed with the upper 700 m of the ocean, leads to an increase in the average temperature in that layer of 0.11 °C/decade, enough to explain current warming trends. Thus, ocean heat content estimates provide the most precise estimation of the warming of our climate system.

Not only is the ocean warming, tide gauge and altimetry data also yield conclusive results: sea level is rising at increasing rates and accelerating (IPCC, 2023). Besides, in response to the intensification of the hydrological cycle because a warmer atmosphere is able to maintain and redistribute more moisture, saltier areas are getting saltier and fresher areas are getting fresher. In other words, drier areas are getting drier and fresher areas are getting fresher. Here again, for the understanding and monitoring of this pattern with global consequences also at land, oceanographic data are crucial. The measurement of the geographic distribution of latent heat flux is particularly important as it involves changes in evaporation and the hydrological cycle, but it is difficult to determine these air-sea fluxes with precision. Thus, given the dominance of the ocean in the hydrological cycle, one of the better evidences of the intensification of the hydrological cycle comes in fact from hydrography: from the trends observed in oceanic salinities.

The drastic surge in anthropogenic CO_2 emissions since the industrialisation not only results in ocean warming, sea level rise,a dn the intensification of the hydrological cycle, but is also the cause of ocean acidification (a set of changes in the chemistry of seawater due the progressive increase in ocean inorganic carbon concentrations that leads to decreased water pH and calcium carbonate saturation, among others) and a significant decrease in the dissolved oxygen content (Keeling et al., 2010).

Other fundamental factors shaping this pivotal role of the ocean in climate by taking up, storing and redistributing vast amounts of heat, carbon and other tracers is the ocean circulation, ocean's stratification, and mixed layer depth.

Based on ocean observations, this chapter aims to provide an update of these physical and biogeochemical properties and processes underlying regional observed changes and trends during the historical record in the oceanic waters surrounding the Iberian Peninsula and the Canary and Balearic archipelagos.

2. Observed changes in the ocean.

2.1. Upper Ocean Changes. Temperature, salinity, stratification and mixed layer depth variability and trends.

2.1.1. Sea surface temperature.

The last IPCC Sixth Assessment Report (AR6) (IPCC, 2023) assessed that it is virtually certain that global sea surface temperature (SST) has increased since the beginning of the 20th century. Globally sea surface temperature (SST) has increased by 0.88 [0.68 to 1.01] °C from 1850–1900 to 2011–2020 and of 0.60 [0.44 to 0.74] °C from 1980 to 2020, which results in an average rate of 0.15 ºC/decade. Rates of SST warming are geographically heterogeneous, with some regions warming faster than others. The same is true for waters surrounding the Iberian Peninsula and the Canary Islands, that encompass very different oceanic regimes, with transition from subpolar to subtropical regions in the Bay of Biscay and North Eastern Atlantic, to more subtropicals waters within the Gulf of Cadiz, eastern boundary currents in the Canary Islands, and finally the Mediterranean Sea.

The North Eastern Atlantic, east of the two main currents in the basin, the North Atlantic Current and Azores Current, and towards the European Margin in the Bay of Biscay shows a gradient in SST warming similar to SST averages climatological values, with faster warming rates towards the south-eastern corner of the Bay of Biscay where warmer summer SST values are found. Thus, SST trends towards the inner corner of the Bay of Biscay reach 0.35 ºC/decade. As one moves westwards this warming rate decreases, and in oceanic waters north and west off Cape Finisterre SST trend is 0.25 ºC/decade. Similar warming trends are found further south towards the Gulf of Cadiz. Although smaller than those in the inner waters of the Bay of Biscay or in the Mediterranean Sea as described below, these rates are still significantly higher than the global average of 0.15 ºC/decade. Upwelling regions in the west and north coast of the Iberian Peninsula seem to be a 'reducto' of global warming, and depending on the area even cooling trends are observed as also reported for the Canary Current Upwelling System (see Fig. 4.1). Changes in coastal upwelling strength have been widely studied since 1990 when Bakun proposed that global warming can induce cooling in coastal areas via the intensification of upwelling-favorable winds. The required intensification of wind stress in these regions seems to occur in some upwelling regions (Seabra et al., 2019; Sydeman et al., 2014; R. Varela et al., 2015; Rubén Varela et al., 2018). However, intensifying winds not necessarily must completely support an increase in the mean flow and Ekman transport (upwelling). The additional energy imparted from intensifying winds is partially cascaded to the oceanic mesoscale activity of boundary currents instead of supporting an acceleration of their mean flow, an effect known as eddy compensation (Beal & Elipot, 2016; Marshall & Speer, 2012). Additionally, other processes can slow down global warming rates temporarily in oceanic waters too. Thus, the Bay of Biscay seemed to pause its warming for the decade from the mid-2000s to the mid-2010s (Somavilla et al., 2017). As

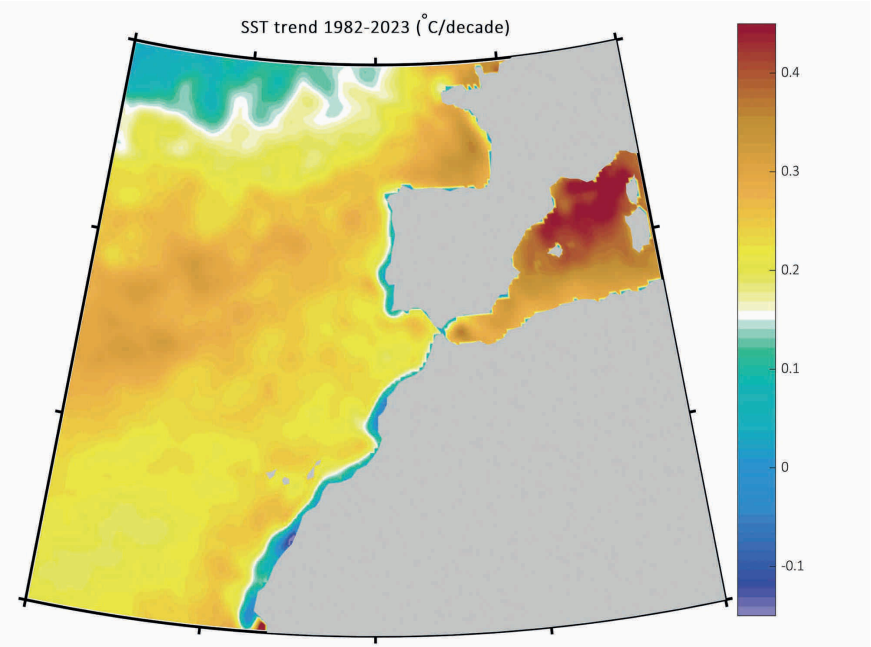

Figure 4.1. SST trends from NOAA OI SST V2 High Resolution Dataset (https://psl.noaa.gov/data/gridded/data.noaa.oisst.v2.highres.html) or the satellite-derived SST period 1982-2023. SST trends are indicated by the color scale. White color marks the averaged global SST warming trend (0.15 ºC/decade) for the period 1980-2020 as reference. As observed, with the only exception of some coastal waters, all oceanic waters surrounding the Iberian Peninsula and archipelagos are warming faster than the global average.

a result, warming trends have varied significantly in the last decades in the area with averages values of 0.35 ºC/decade when calculated from the beginning of the 1980s up to mid-2000s (Costoya et al., 2014; Goikoetxea et al., 2009), decreasing to less than 0.20 ºC/decade when including the colder decade of the mid-2010s for the area (Fontán et al., 2008; Somavilla et al., 2017; Taboada & Anadón, 2012). This slowing of warming trends was also observable in oceanic waters west of the Iberian Peninsula from the northwestern corner of Galicia to the south of Portugal (Taboada & Anadón, 2012). This warming halt seems to have ceased, and warming rates are accelerating again.

The Mediterranean Sea is usually considered a hot spot for climate change and, because of its reduced dimensions and semi-closed character, it has been referred to as a sea under siege. The increase of SST in this region of the world's ocean presents an example of this situation. According to Juza & Tintoré, 2021 the warming of the Mediterranean surface, estimated from satellite data since the beginning of the 1980s, could be two or three times larger than that observed for

the global ocean (see Fig. 4.1). These trends are not spatially homogeneous with a larger warming in the Eastern Mediterranean over the last four decades. There are also important differences within the Western Mediterranean, and more specifically within the Spanish Mediterranean waters where a south-north gradient is clearly observed. The lowest trends over the period 1982-2022 for the mean annual SST would be observed in the northern sector of the Alboran Sea (2.4 ± 0.5 ºC/century), increasing northwards and reaching 3.9 ± 0.6 ºC/century to the northern Catalan Sea (Manuel Vargas-Yáñez et al., 2023). This intense warming estimated from satellite data is confirmed by those obtained from in situ measurements. Vargas-Yáñez et al., 2023 estimated a warming of 1.78 ± 0.01 ºC/century from a daily time series of water temperature in the Fuengirola beach (northwestern Alboran Sea), and Salat et al., 2019 have obtained a warming of the surface water in L'Estartit oceanographic station (Girona coast, northern Catalan Sea) of 2.8 ± 0.4 ºC/century. It is worth noting that the intense warming in L'Estartit coast does not only affect the surface waters, but the whole depth range of the continental shelf as warming trends at the bottom of L'Estartit station (80 m) also showed a positive trend of 2.0 ± 0.3 ºC/century.

This increase of SST also affects the waters surrounding the Canary Islands. These waters form part of the known as Canary Current Upwelling System (CCUS) which extends from the northern tip of Galicia (Northwestern Iberian Peninsula) to the south of Senegal, and is one of the four Eastern Boundary Upwelling Systems in the world. According to Siemer et al., 2021, SST in this region increased at a rate of 0.16 ºC/decade. However, as in the case of the Mediterranean Sea, this warming is not homogeneous. Trends increase seawards. In the area of Canary Islands, Vélez-Belchí et al., 2015 found that SST had increased at a rate of 0.27 ± 0.21 ºC/decade as depicted in Figure 4.1. On the contrary, temperature trends are lower or even negative in some parts of the coast where the upwelling caused by trade winds is more intense and permanent (Siemer et al., 2021). These authors point out that this would be caused by an intensification of upwelling favorable winds. This is an effect of climate change that had already been hypothesized by Bakun, 1990. However, Siemer et al., 2021 found that the results were somehow contradictory as the negative SST trends and the increase of upwelling intensity was also associated with a decrease in chlorophyll concentration and primary production.

This warming of the sea surface is not only revealed by the long-term temperature increase, but also by the number and intensity of extreme events. Although there is not one single definition of Marine Heat Waves (MHW), it is frequently accepted as an episode in which SST overcomes a certain threshold during more than five days. This threshold is usually considered as the 90th percentile calculated from a long-term climatology (at least 30 years; see for instance Hobday et al., 2016). Juza et al., 2022 have studied the MHWs in the Mediterranean Sea for the period 1982-2020, analyzing the mean intensity, the maximum intensity, the duration and the frequency of these extreme events. These authors found that all these properties had increased along the analyzed period. These trends were updated in Vargas-Yáñez et al., 2023 over the period 1982-2022 and showed maximum values of 0.18 ºC/decade for the mean intensity, 0.65 ºC/decade for the maximum intensity,

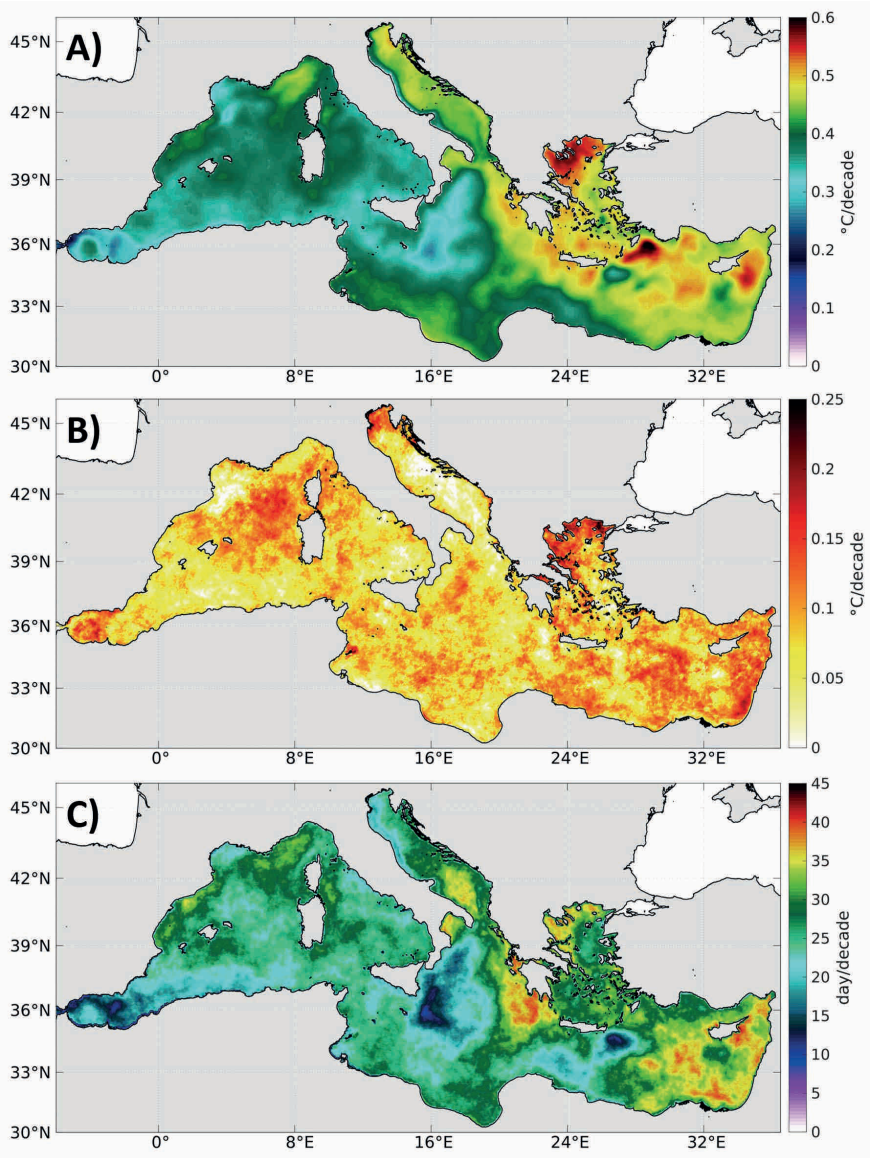

Figure 4.2 A) Linear trends in ºC/decade for the SST in the Mediterranean Sea. B) Intensity of MHWs in ºC/deacade, C) linear trends for the annual number of days with MHWs in the Mediterranean Sea

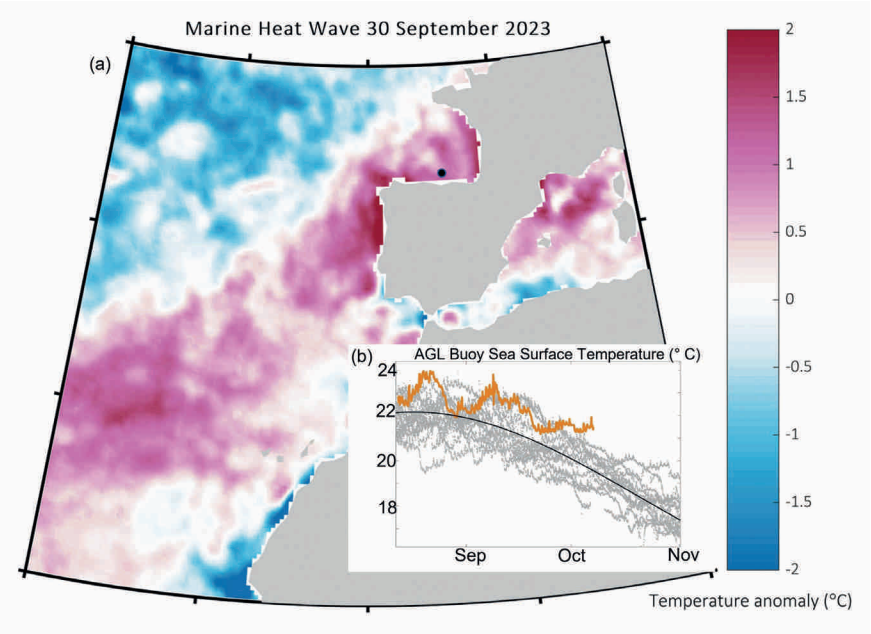

Figure 4.3. (a) Marine heat wave in the eastern North Atlantic and Western Mediterranean detected from satellite-derived sea surface temperature data (NOAA OI SST V2 High Resolution Dataset, https://psl.noaa.gov/data/gridded/data.noaa.oisst.v2.highres.html) following Hobday et al., 2016 at the end of September 2023, where after the summer temperatures were between 1.5 and 2°C above the 90th percentile of sea surface temperature. The black dot in (a) marks the location of the AGL buoy in the Bay of Biscay. (b) Sea surface temperature recorded by the buoy from mid-August to mid-October (orange line) in comparison with remaining data recorded by AGL buoy for the same days of the year since its deployment in 2007 (gray dots) and its annual climatological cycle (black line).

12.4 days /decade for the mean duration and 2.4 events/decade for the frequency of MHWs. This information is continuously updated in the web application (https://apps.socib.es/subregmed-marine-heatwaves/, Juza & Tintoré, 2021). Figure 4.2 shows the linear trends for the surface temperature (A),for the intensity of heat waves (B), and for the total days of MHWs for the period 1982-2022 in the Mediterranean Sea (C).

In the North East Atlantic, MHWs have received less attention, but the onset of El Niño in summer 2023 has been associated with the development of the major registered marine heat wave in the North East Atlantic during summer 2023 (GOOS Observation Coordination Group, 2023) (Fig. 4.3). Satellite and in-situ data show how sea surface remained above its climatological value for the whole summer 2023, accumulating a value of 2 °C above the climatological value and 1 ºC above the highest value recorded previously at the beginning of the autumn (Fig. 4.3b). As

for SST trends, upwelling regions seem to be a 'reducto' for ocean warming being less affected by MHW (Rubén Varela et al., 2018).

2.1.2. Upper-ocean Stratification and Surface Mixed Layers

Ocean surface warming is commonly associated with a more stratified, less productive, and less oxygenated ocean. Such an assertion is mainly based on consistent projections of increased near surface stratification and shallower mixed layers under global warming scenarios (Cabré et al., 2015; Capotondi et al., 2012). However, recent studies have shown that a generalized stratification increase of 1-9%/dec (G. Li et al., 2020; Sallée et al., 2021; Yamaguchi & Suga, 2019) and mixed layer deepening of several meters per decade (Sallée et al., 2021; Somavilla et al., 2017) have occurred in the last 60 years. Such finding is at odds with the expectation – realized across climate model projections (Cabré et al., 2015; Capotondi et al., 2012; Fu et al., 2016; Moore et al., 2018) – of concurrent stratification strengthening and mixed layer shoaling brought about by anthropogenic global warming, as recognized in the last IPCC report (IPCC, 2023).

This pattern was firstly observed from long-term monthly oceanographic time-series in the Bay of Biscay and extended to other long-term oceanographic time-series and Argo floats (Somavilla et al., 2017). It was found that while the SST is rising as reported in the previous section, the concurrent ocean record shows using different stratification and MLD indexes that stratification is not unequivocally increasing nor is MLD shoaling. Conversely, in the Bay of Biscay concurrent with surface warming trends previously reported, MLD deepens with enhanced deepening of winter MLDs at rates over 10 m/decade. As the aforementioned changes in surface temperature, this trend persisted until the mid-2010s due to the occurrence in that decade of exceptionally intense mixing events in the years 2005, 2006, 2009, and 2010 that reached 350 m while the climatological value in oceanic waters of the Gulf of Vizcaya is around 200 m (Charria et al., 2017; Chust et al., 2022; Costoya et al., 2014; Somavilla et al., 2017; Valencia et al., 2019). These extreme mixing events strongly eroded the stratification of the water column to levels of the permanent pycnocline throughout the decade of the mid-2000s and 2010s, generating effects on the redistribution of heat and circulation at the basin scale of the North Atlantic as described in the next section. Since 2010, only one episode of abnormally deep mixing has occurred in 2018, making deepening trends appear to have stopped so far (Chust et al., 2022; Valencia et al., 2019). Consequently, unlike other basins, MLD trends in the Eastern North Atlantic are linked to the occurrence of extreme cooling and mixing events associated with the occurrence of atmospheric blocking anomalies whose frequency may increase under global warming (Somavilla et al., 2016). It must be noted that these conspicuous effects on ocean conditions are due to specific regional configuration of atmospheric forcing (blocking anomalies associated to the presence of a persistent anticyclone West to the British Isles) that is not captured by the large-scale atmospheric indices. Moreover, the occurrence of such anomalous high-pressure center and its prevailing location during winter appears to be a key factor determining similar atmospheric forcing (very cold and dry winds inducing strong heat losses from the ocean to the atmosphere) and the

synchronicity of oceanic processes in the Bay of Biscay and NW mediterranean. The resulting oceanographic processes are extreme deepening of the MLD in the Bay of Biscay and the occurrence of deep convection in the NW Mediterranean (Chust et al., 2022; Font et al., 2007; López-Jurado et al., 2005; Schroeder et al., 2016; Somavilla et al., 2017; Valencia et al., 2019). The major modes of atmospheric variability over the North Atlantic/Europe region have been discussed in several works (e.g. Cassou et al., 2011; Josey & Marsh, 2005; Rogers, 1990; Tréguer et al., 2014), being the North Atlantic Oscillation (NAO) and the East Atlantic Pattern (EAP) the principal modes of atmospheric variability in the North Eastern Atlantic and North Western Mediterranean.

Different indexes are used to estimate ocean stratification based on the ocean interior vertical structure in three vertical layers: the mixed layer, the seasonal pycnocline, and the permanent pycnocline. Because it is assumed that beyond the deepest depth reached historically by winter mixed layer ocean stratification remains constant, most of the research efforts in both observing and understanding ocean stratification have been concentrated in the surface stratification (Chu & Fan, 2019; G. Li et al., 2020; Sallée et al., 2021; Somavilla et al., 2017; Yamaguchi & Suga, 2019). Thus, ocean stratification indexes typically try to estimate surface stratification. The most frequently employed surface stratification index is the density difference between the sea surface and 200 m, $\Delta D200$. Although relatively easy to obtain, surface stratification calculated on a fixed depth range as $\Delta D200$ estimates stratification within the mixed layer in regions with MLDs deeper than 200 m depending on locations and seasons. It stresses the drawback of using stratification indexes on fixed depth ranges differences as universal stratification indexes, and the need of a specific comparison of this quantity with other surface stratification estimates such as maximum stratification in the water column, Brunt–Väisälä frequency or potential energy deficit (Chu & Fan, 2019; Sallée et al., 2021; Somavilla et al., 2017).

The Mediterranean is usually considered as a three-layer sea. The upper layer would extend from the surface to 150 m and is occupied by the Atlantic Water (AW) that flows into the Mediterranean through the Strait of Gibraltar. The intermediate layer is formed by waters originated mainly in the Levantine Basin (Levantine Intermediate Water, LIW and Cretan Intermediate Water, CIW) and also by intermediate waters originated in the Western Mediterranean (Western Mediterranean Water, WIW). Finally, the deep waters are originated by deep convection in the Adriatic and Aegean Seas (in the Eastern Mediterranean) and in the Gulf of Lions in the Western Mediterranean. The water mass formed in the latter region is the Western Mediterranean Deep Water (WMDW).

Rixen et al., 2005 was one of the first works that analyzed the temperature and salinity changes in the Mediterranean Sea for these three layers. Regarding the upper one, these authors found that the upper layer had cooled since 1950 to the beginning of the 1980s and warmed since then, with an overall warming trend for the period 1950-2000. Vargas-Yáñez et al., 2010; Vargas-Yáñez et al., 2017 have shown that the available in situ temperature and salinity data in the Western

Mediterranean are very scarce and this situation worsens with increasing depth. As a result of this scarcity, the calculation of trends is very sensitive to the data processing methods, increasing the uncertainty of the estimations. This uncertainty is also enhanced by the high natural variability of these waters which are subject to the interaction with the atmosphere. Vargas-Yáñez et al., 2023 estimated the temperature and salinity trends in the upper 150 m of the water column in the Spanish Mediterranean waters for the periods 1900-2020 and 1945-2020 taking into account the uncertainty imposed by the natural variability of the time series and that caused by the processing method and the data scarcity. These works found that these trends were positive and had intensified for the second period analyzed (since the mid-20th century). However, such trends were not statistically different from zero in the case of the temperature and ranged between -0.22 and 1.22 ºC/century. The salinity increase was statistically significant and was between 0.08 and 0.39 century^{-1}. The lack of statistical significance must be associated with the data scarcity as SST and in situ time series in the upper 80 m of L'Estartit station have shown a significant and very intense warming of the upper layer. This hypothesis is supported by Llasses et al., 2015, who found that the time and space frequency of the available data in the Mediterranean Sea were not appropriate for the detection of long-term trends.

This warming of the upper layer could produce an increase of the stratification that would decrease the efficiency of wind mixing. Vargas-Yáñez et al., 2022 analyzed the evolution of the mixed layer depth from CTD time series extending from 1992 to 2021 in some cases and from 2007 to 2021 in others and found no significant changes. The analysis of mixed layer depth from Argo profiles (mixedlayer.ucsd.edu; Holte et al., 2017) neither showed any significant trend. As the increase of the stratification could potentially reduce the productivity of the surface waters, these authors checked the evolution of surface chlorophyll concentration from 1997 to 2021 and found no significant changes, in agreement with results from in situ chlorophyll measurements obtained by García-Martínez et al., 2019. However, Gómez-Jakobsen et al., 2022 found a decrease of Surface chlorophyll concentration over the Spanish Mediterranean waters. It should be noted that this variable has a very large variance and the discrepancy in the results could be due to the lack of time series long enough for the calculation of long-term trends (Boyce & Worm, 2015).

2.2. Ocean heat and fresh water content.

As previously explained, ocean warming – that is, increasing ocean heat content (OHC) – is a crucial aspect of energy on Earth dominating the increase in the Earth's energy inventory with more than 90% of the increasing radiative forcing imbalance reflected as ocean warming and increase of the OHC (IPCC, 2023). Over the period from 1971 to 2019, the ocean warmed at average rates of 0.015 °C/decade in the first 2000 m (Cheng et al., 2019). Although these temperature increases may seem small, they should be seen in relation to the large body of water that has been heated. If the same amount of heat that had been buried in the upper 2000m of the ocean would have been accumulated in the atmosphere, the surface of the Earth would have warmed more than 30 °C instead of 0.85 °C for the past 50 years (IPCC, 2022).

Prior to the 2000s, the North Atlantic was the basin showing the greatest warming. However, since the mid-2000s during the so-called global warming hiatus, large amounts of heat were transferred in this basin from upper to deeper levels while the dominance in terms of atmospheric heat capture moved into the Indo-Pacific. A large transformation of modal waters in the eastern North Atlantic (ENA) played a crucial role in such contrasting behavior (Somavilla et al., 2016; Sullivan, 2016). In the mid-2000s, extraordinary convective mixing events transformed ENA modal waters into a much saltier, warmer, and denser variety, transferring upper ocean heat and salt gained slowly over time to deeper layers. The induced deep convective mixing resulted in homogenization of properties of the water column from the surface to density levels at depth ranges of 350-500 m. This mixing of (warmer and saltier) upper water and (colder and fresher) modal waters made the upper waters colder (−0.4 ºC), creating a denser (+0.1 kgm^{-3}), warmer (+0.23 ºC), and more saline (+0.015) type of Eastern North Atlantic Central Water (ENACW). Most of the enhanced warming observed at intermediate depths (+0.33 ºC gained between 1997 and 2012) was explained by the increase in the modal waters during the winter of 2005 (+0.23 ºC). The estimated overall heat content increase in the region accounted for 44% of the total heat content increase at intermediate depths in the North Atlantic (36º to 65ºN) from 1997 to 2012. Since the mid-2010s, saltening trends reversed and accelerated freshening in the upper ocean has been observed first in the subpolar North Atlantic, but now it is widespread and has reached the mid-latitudes of the ENA, the Gulf of Cadiz and the Canary region (Gonzalez-Pola et al., 2023). Annually averaged, the freshening is accompanied by above average temperatures.

In the Mediterranean, the intermediate and deep layers have a much lower variability than the upper one and therefore the changes of temperature and salinity have been estimated in a significant way. Intermediate and deep layers increased their temperature at rates ranging between 0.10 and 0.36 ºC/century and between 0.16 and 0.35 ºC/century respectively. The trends for the salinity were between 0.04 and 0.14 $century^{-1}$ for the intermediate layer, and between 0.09 and 0.13 $century^{-1}$ for the deep layer. The warming of the whole water column yielded an equivalent heat absorption of 0.22 to 0.72 W/m^2, which is in accordance with the heat content increase at a global scale (Von Schuckmann et al., 2023).

In the Canary Islands, the central waters are found below the Surface water. This water mass is the Eastern North Atlantic Central Water (ENACW) that extends from 100 to 700 m forming the main thermocline. Intermediate waters extend below this water mass until 1500 m approximately. This layer is made of Mediterranean Water (MW) and Antarctic Intermediate Water (AAIW). Finally, deep waters (Eastern North Atlantic Deep Water, NADW) extend below the intermediate waters. Vélez-Belchí et al., 2010 analyzed the changes of temperature and salinity in the Atlantic Ocean along the 24.5 ºN, using repeated hydrographic sections and Argo data. According to these authors the waters above 2000 m depth warmed and increased their salinity from 1957 to 2004. However, two different periods could be distinguished. There is a warming and salting of central and intermediate waters from 1957 to 1998, and a cooling and freshening since then until 2004. Vélez-Belchí et al., 2015) analyzed SST dta and CTD data and found that SST increased at a rate of 0.28 ºC/decade in the Canary Islands waters. The temperature trend for central waters was 0.27 ± 0.21 ºC/decade, but the salinity trend was not significant. These authors distinguished two different strata for the deep waters: the upper one, from 1700 to 2600 dbar where

no significant changes were detected, and the lower one from 2600 to 3600 dbar where cooling and freshening trends were observed.

2.3. Ocean circulation.

The circulation patterns in the Eastern Atlantic where the Iberian Peninsula and Canary Islands are located are weak in comparison with the main North Atlantic currents. The western boundary current of the North Atlantic, the Gulf Stream, continues its pathway following the eastern coastlines of the United States before turning to the east within 40°N feeding the North Atlantic current (NAC) crossing the Atlantic Ocean. In the vicinity of the Mid-Atlantic Ridge at about 30°W a bifurcation of the flow of subtropical water occurs. The NAC continues its path towards the north-east and the Azores Current (AC) rises toward the south-east. The main circulation in the waters surrounding the Iberian Peninsula and Canary Islands is the residue of these main currents west of the Iberian Peninsula. The Iberian Peninsula and Canary Islands are also located at the Eastern Boundary Current (EBC) system of the North Atlantic spreading from the African upwelling system to Ireland. The area is influenced by a geostrophically balanced poleward flow, trapped within 50 Km of the shelf edge and due to a cross slope density gradient to the Iberian Peninsula coast known as Iberian Poleward Current (IPC), also sometimes Navidad Current due to it tending to reach the Cantabrian slope around Christmas.

Besides these currents, the North Atlantic basin is a unique basin in terms of circulation and climate due to the existence several places of deep water formation in the northern North Atlantic, a vital component of the Atlantic Meridional Overturning Circulation (AMOC) that transports a substantial amount of heat northward across the equator in the Atlantic. In this respect, it differs radically from the Indian and Pacific Oceans, where the heat transport is away from the equator and towards poles (Trenberth et al., 2019). Thus, the AMOC is the name given to the circulation pattern in the North Atlantic that controls heat exchange between the tropics and polar latitudes and includes the northward surface flow of warm, saline waters from the tropics in the Gulf Stream (North Atlantic Western Boundary Current) and the deep southward flow of cold waters from polar regions. The intensity of the AMOC is assumed to be closely linked to the deep convection process that connects the surface and depth water flows of this circulation. There are only a few places on the planet where this convection process, generating waters dense enough to mix with those at the bottom, ventilates the deep ocean from its surface. In the North Atlantic, the Labrador and Irminger seas in the subpolar North Atlantic and the Greenland Sea in the Nordic seas are examples of deep convection sites. Hydrographic sections and tracer data support the conclusion that from these locations, in the Labrador and Irminger Seas in the North Atlantic, the AMOC transports recently formed deep waters southward (M. Susan Lozier, 2012). However, there is no evidence from in-situ data of the existence of a relationship between variations in the intensity of deep convection and the formation of deep water masses with variations in the intensity of the AMOC (M. S. Lozier et al., 2019; Rhein, 2019; University of Southampton et al., 2016; Zou & Lozier, 2016). The absence of this evidence clashes irremediably with the model results that agree on the existence of this relationship. All of this highlights not only that there is plenty room for improvement of climate models but also that our knowledge of the mechanisms that control AMOC and deep-water ventilation is still limited. Prior to the establishment of RAPID and OSNAP arrays, the accepted picture of the overturning

circulation was of a large-scale 'conveyor belt'-like flow as proposed by Broeker. Discoveries from in-situ oceanographic observations from RAPID, OSNAP, SAMBA and other mooring arrays in North Atlantic have challenged these previous AMOC paradigms. It is now known that the AMOC is highly variable on all time scales not only from years to millennia but from days upwards with wind forcing dominating shorter time-scale variability and thermohaline forcing increasing importance for longer time scales (Srokosz et al., 2023). AMOC deep return flow is not confined to the Deep Western Boundary Current (DWBC) and interior pathways exist in both the North and South Atlantic, away from the western boundary. AMOC and deep water ventilation may not be controlled by the formation and injection of dense water at great depths, but by the upwelling mechanisms that 'pull' these waters upward and their incorporation into boundary currents (M. S. Lozier et al., 2019; Somavilla et al., 2017; Straneo, 2006; Visbeck, 2007).

Despite many open questions regarding the AMOC variability, forcing and pathways exit, its relation with the western boundary current system in the North Atlantic, the Gulf Stream forming the surface limb of the AMOC, is permanently studied and revised. However, the effects and potential contribution of the AMOC on circulation changes in the lower energetic mid-latitude eastern North Atlantic is very much unknown (Frazão et al., 2022). Periods of intensification (1950s, 1980-2000) and weakening (1960s and 2000s) of the Gulf Stream and Azores Currents occur concurrently in both regions (Frazao et al., 2022) and coincide with conspicuous changes in the Eastern North Atlantic Central Water region (Somavilla et al., 2016), but the potential relation between these changes remained unexplored.

The large transformation of modal waters in the eastern North Atlantic described in the previous section also had large implications for ocean circulation at ocean basin scales. Increasing densities altered the zonal dynamic height gradient reversing the southward regional flow and enhancing the access of saltier ENACW to higher latitudes. These intrusions of salty North Atlantic water during the late 2000s and early 2010s obscured the freshening signal expected from increasing melting from Greenland and elsewhere in the Arctic, becoming relevant for dense water formation (Dukhovskoy et al., 2016). This reversal lasted for one decade. Since the mid-2010s, saltening trends reversed and accelerated freshening in the upper ocean has been observed first in the subpolar North Atlantic, but now it is widespread and has reached the mid-latitudes of the Eastern North Atlantic. Annually averaged, the freshening is accompanied by above average temperatures and the restoration of northern (southwards) flow. Changes in circulation at intermediate water levels seem to be associated with changes in the strength of upwelling in southern Biscay. Thus, during the circulation reversal (northwards) between the mid-200s and mid-2010s upwelling weakened in the area, starting a process of restoration of upwelling conditions previously known from 2014 onwards (Gonzalez-Pola, C., et al., 2024, under review). The decade-long reversal flow stage meant a temporal boost of ongoing meridionalization trends attributed to climate change affecting ecosystems, while subsequent recovery to traditional circulation brought the region back to a classical more boreal character (Gonzalez-Pola, C., et al., 2024, under review). The possible recurrence and, if so, timescales of shift reversals in the region and possible relation or implication with concurrent larger scale circulation patterns are yet unknown. Moreover, these may be affected now and in the future by climate change, with any of the two possible regimes potentially being favored.

In the Western Mediterranean, and more specifically in the Spanish waters, no changes in the circulation of the upper layer have been reported. However, important changes have been observed for the LIW and WMDW both in the Eastern and Western Mediterranean. The formation of WMDW in the open sea waters of the Gulf of Lions is a process with a high inter-annual variability as shown by Herrmann et al., 2010, with years when the deep convection reaches the sea bottom, as the winter 1986/87, and others when mild conditions prevail and the convection is much shallower, as for instance the 1990s decade. In winter 2004/05 and 2005/06 very cold conditions occurred in the Gulf of Lions and an exceptionally large volume of WMDW was formed. This WMDW was saltier, warmer and denser than the deep water formed in previous years, changing the shape of the typical WMED TS diagrams (López-Jurado et al., 2005; Schroeder et al., 2016). This change in the thermohaline structure of the WMED was named as the Western Mediterranean Transition (WMT). One of the causes proposed for this transition is the arrival of saltier and warmer LIW from the EMED under the influence of the Eastern Mediterranean Transient (EMT: an extreme event that changed the properties and formation site of deep waters in the EMED). The other cause could be the accumulation of salt and heat in the intermediate layer of the WMED during the 1990s and beginning of the 2000s because of the absence of deep convection during several mild winters. It is very likely that the origin of the WMT is a combination of both causes. According to Margirier et al., 2020, there was no formation of deep waters during winter 2007/08, but new episodes of deep convection were observed from 2009 to 2013 (Houpert et al., 2016) and then this process was absent from 2014 to 2017.

The changes in the properties of the water masses and their rates of formation that have been briefly described above do not only affect to the WMED and EMED, but also to the Mediterranean outflow through the Strait of Gibraltar, and therefore, to the Atlantic Ocean and its meridional overturning circulation. García-Lafuente et al., 2021 have shown that the outflow of Mediterranean waters increased during the period 2004-2012, being these outflowing waters cooler and fresher. On the contrary, the outflow decreased and became saltier and hotter during the following period 2013-2020. During the first period, the outflow was made in a larger percentage of WMDW that was being drained after the large volumes of deep water formed since 2004/05. On the contrary, deep convection did not occur after 2013 and the outflow decreased at the same time that LIW (saltier and warmer than WMDW) became the main component of the Mediterranean outflow.

2.4. Sea level

Global mean sea level (GMSL) has been rising at 1.73 [1.28-2.17] mm/yr since the early 20th century (IPCC, 2023), a rate that is faster than in the last three millennia (Kopp et al., 2014). Almost 40% of this increase is attributed to thermal expansion of the oceans due to ocean heat uptake, another 40% to glacier ice melting and 25% to Greenland ice melting, with small contributions from the Antarctic ice sheet and from (negative) changes in land water reservoirs (IPCC, 2023). The observed rate of GMSL has furthermore been accelerating since the 1960s (Dangendorf et al., 2019), reaching a value of 3.7 mm/yr during the period 2006-2018. The most recent acceleration, since the 1990s, has been primarily driven by an enhanced rate of ice sheet mass loss. It is now well established that these increasing rates of GMSL respond to anthropogenic forcing, at least since the 1970s when acceleration began (Marcos et al., 2017; Marcos & Amores, 2014; Slangen et al., 2016).

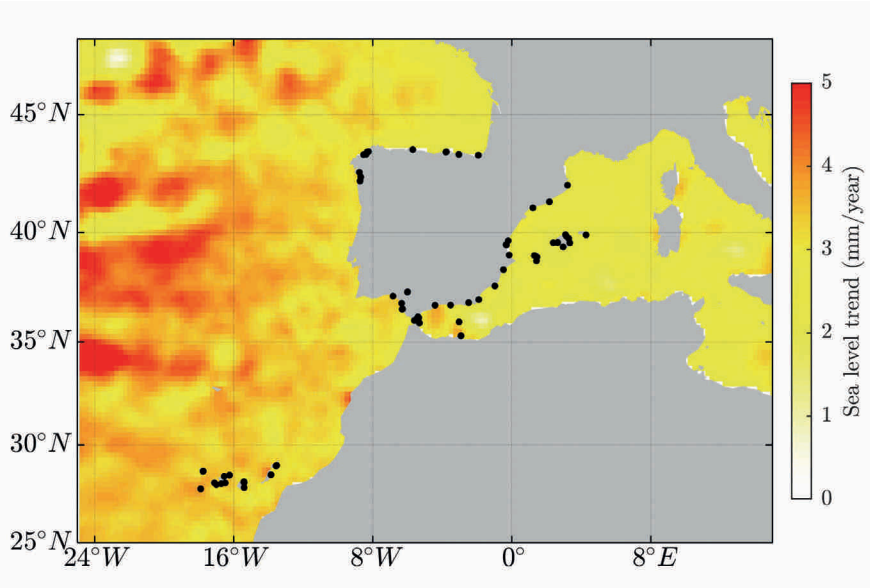

Figure 4.4. Absolute sea level trends from altimetry observations (1993-2023) and location of tide gauge stations along the Spanish coasts.

At a regional scale, mean sea level rise may differ from the global mean. Altimeters on board of satellites have been measuring absolute (i.e., referenced to an ellipsoid) sea level since the early 1990s with increasing accuracy, and have revealed regionally varying changes. The regional patterns, which are also temporally variable due to climate internal modes, are dominated by the non-uniform thermal expansion of the oceans linked to changes in both wind-forced ocean circulation and atmosphere-ocean heat fluxes (Meyssignac et al., 2017). Other factors, such as surface redistribution of ice mass grounded on land and hydrologic reservoirs, the so-called changes in gravity, rotation and deformation (GRD), also impact regional mean sea level changes. Along the Spanish coasts, altimetric measurements display overall rates of mean sea level rise above 3 mm/yr since 1993, similar to those of GMSL for the same period (Figure 4.4).

In terms of coastal impacts, what matters is the relative sea level change with respect to land. Relative sea level changes are the combination of absolute sea level (the ocean component) and vertical land motions that can be caused by a variety of mechanisms both natural and of anthropogenic origin (Wöppelmann & Marcos, 2016). These include glacial isostatic adjustment, tectonics and volcanism, but also subsidence due to groundwater extraction and other human activities. Currently, vertical land motions are monitored by GNSS networks that provide accurate point-wise records of ground motion. However, many areas still have very scarce information either because GNSS records are too short or

because they do not exist. A recent product combines GNSS, tide gauges and altimetric data to produce land motion rates along coastal regions for the period 1995-2020 (Oelsmann et al., 2023). The obtained linear trends along mainland Spain reveal a small but spatially variable vertical land movement contribution of -0.4+/-0.3 mm/yr, with higher values (in absolute terms) reaching -0.7 mm/yr in northwestern Spain.

Tide gauges provide pointwise, direct observations of relative sea level change with respect to the land upon which they are grounded. The Spanish coasts are well covered by tide gauge stations (Figure 4.3), operated by different agencies (see Pérez Gómez et al., 2022 for a comprehensive list along Mediterranean coasts, that include all tide gauge operators in Spain). Tide gauges record sea level changes at hourly or higher frequency sampling rates; thus, they measure not only mean sea level, but also high-frequency sea level changes linked to storminess, seiches and tsunamis or meteotsunamis (these will be further discussed below). The temporal coverage of tide gauges differs among locations, with stations longer than 100 years (e.g., in Alicante) and the majority spanning 30 years or less (Marcos & Tsimplis, 2008). Yearly time series of a set of selected stations is represented in Figure 4.5, together with linear trends. The differences among linear trends reflect the different time spans of the observational records and also the spatial variations in vertical land movements.

Although the impacts of mean sea level changes are local, its drivers are, to a large extent, global. These include, as already stated above, ocean thermal expansion and land-based ice melting. The spatial patterns derived from gravitational effects of Greenland and Antarctic ice melt cancel each other out along the Spanish coasts (Bamber & Riva, 2010). Regional sterodynamic sea level trends (i.e., associated to ocean circulation and density changes) are mapped in Figure 4.4 as measured by satellite altimetry, with rates of around 3 mm/yr since 1993. At decadal and multi-decadal time scales, the sea level variability along the Spanish coasts (up to 15 cm) is coherent with that from the nearby North Atlantic (Calafat et al., 2012). These slow changes are driven by longshore winds propagating northwards along the European continental shelves (Calafat et al., 2012; Hughes et al., 2019). On top of these, the atmospheric contribution to sea level changes (which is absent in altimetric products), acting through the mechanical forcing of atmospheric pressure and surface winds, also accounts for a significant part of the observed sea level variability at these long time scales (Calafat et al., 2012; Gomis et al., 2008; Marcos & Tsimplis, 2008). At interannual time scales, nearby records show very coherent variability (Figure 2), which is to a large extent controlled by large-scale atmospheric circulation patterns (Martínez-Asensio et al., 2014; Volkov & Landerer, 2015). The most important of these climate patterns in the region is the NAO that accounts for up to 40% of the yearly winter variance of sea level at some tide gauge sites (Martínez-Asensio et al., 2014). Overall, the atmospheric contribution to sea level changes has been shown to be responsible for 20-40% of the yearly variance observed at tide gauge sites on the basis of hydrodynamic ocean simulations (Marcos & Tsimplis, 2008).

Coastal extreme sea levels arise from the combination of mean sea level changes, storm surges, tides and wind-waves (Pugh & Woodworth, 2014). Extreme sea level episodes are triggered by atmospheric perturbations, which in the Iberian region are caused by extra-tropical cyclones and also by medicanes (Mediterranean hurricanes) in its Mediterranean

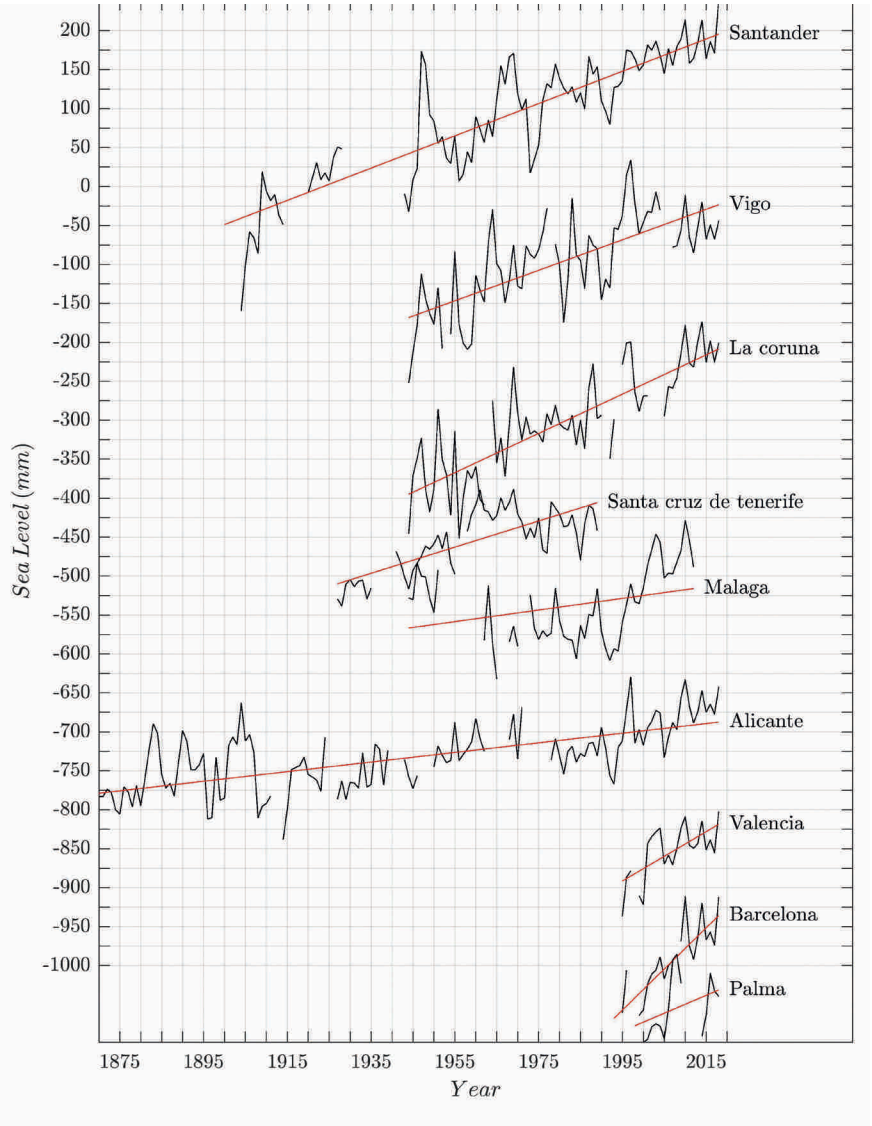

Figure 4.5. Yearly mean sea level changes at selected tide gauges along the Spanish coasts. Red lines indicate the linear trends for the observational periods.

side (Emanuel, 2005). The occurrence and intensity of these coastal extreme sea levels are, in the long term, modulated by mean sea level changes, as these modify the water levels upon which extremes reach the coastlines (Woodworth et al., 2019). Along the Atlantic coasts of the Iberian Peninsula and the Canary Islands, astronomical tides are also an important contributor to coastal extreme sea levels, unlike in the Mediterranean coasts. Although in some regions tides and storm surges may interact with each other and modify coastal extreme sea levels, this is not the case along the Spanish coasts, due to the presence of narrow continental shelves (Marcos et al., 2009). At some coastal locations, very high-frequency (with periods of the order of minutes) sea level oscillations, generated by tsunamis, meteotsunamis or seiches, can also contribute to coastal extreme sea levels (Monserrat et al., 2006). These are particularly common in the Mediterranean Sea (Vilibić et al., 2021) and can reach amplitudes of several tens of cm.

Observations of coastal extreme sea levels rely on high-frequency tide gauge measurements. Currently, there are 70 tide gauge stations along the Spanish coasts operated by four institutions, with different temporal coverage (Figure 4.6). Instruments sample sea level at high frequencies to record all processes contributing to extreme events, as those mentioned above. Despite the relatively good spatial coverage of the Spanish coasts, coastal extreme sea levels can vary spatially due to the local coastal topography.

Hydrodynamic models, forced by mean sea level pressure and surface wind fields, are a common tool used to provide a complete picture of the likelihood and intensity of coastal extreme sea levels. Their accuracy depends on the spatio-temporal resolution of the forcing fields and on the resolution of coastal bathymetries. In general, hydrodynamic models display a good correspondence with coastal observations, even with coastal resolutions of the order of kilometers. For example, linear correlations between tide gauge records and the output of a global hydrodynamic model are above 0.5 in the Atlantic Iberian coasts and around 0.4 in the Mediterranean basin (Muis et al., 2020). The 50-year return level of the storm surge contribution to coastal extreme sea levels is, on average, 0.5 m along the Spanish Atlantic coasts and the Canary Islands, as obtained from both pointwise tide gauge observations (Marcos & Woodworth, 2017) and regional ocean models (Chaigneau et al., 2022). These values increase from around 20 cm in the southernmost locations up to 60 cm in the northern coast of Spain. Along the Spanish Mediterranean coasts, 50-year return levels of storm surges are between 40 and 50 cm, according to a high-resolution regional numerical model (Toomey et al., 2022). These values from regionalized models are consistent with other works that provide global-scale assessments (Muis et al., 2020).

2.5. Biogeochemical changes

In the framework of anthropogenic climate change the ocean faces several biogeochemical challenges. Mainly, three acute and global stressors are concurrently acting together: warming, acidification and deoxygenation. The described alterations in physical processes of the ocean are deeply intertwined with these forcing drivers, causing deep-rooted shifts in biogeochemical cycles. Their impact is far-reaching, with some biogeochemical changes already evident and others expected in the mid-term. While some changes are a direct consequence of the anthropogenic carbon dioxide and heat uptake, like ocean acidification (Raven et al., 2005), warming (Z. Li et al., 2023) or the intensifying vertical

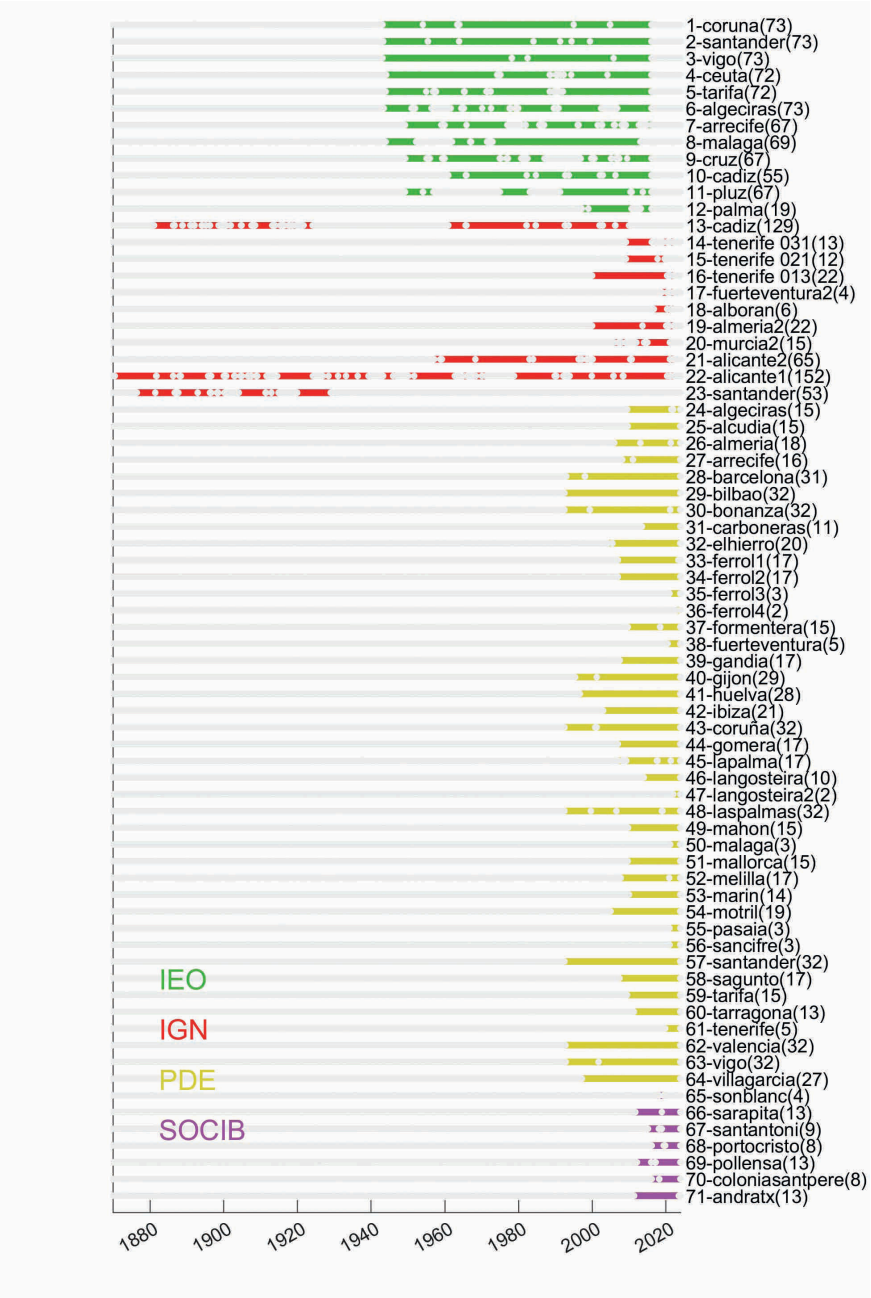

Figure 4.6. Spatio-temporal distribution of tide gauge observations along the Spanish coasts.

stratification (Sallée et al., 2021), there are also changes mediated by more complex and interconnected responses.

As heat uptake and increasing temperatures around Iberian Peninsula and Canarias have been previously described in this chapter, we are going to focus on two main stressors of climate change in the ocean: ocean acidification and oxygen loss or deoxygenation. The end-of-the century projections from Coupled Model Intercomparison Project Phase 6 (CMIP6) models show ocean acidification and deoxygenation concurrent with warming, decline in upper-ocean nitrate levels and primary production directly proportional to the emissions trajectories of Shared Socioeconomic Pathways (SSP) scenarios (Kwiatkowski et al., 2020). Although ocean acidification and deoxygenation are global processes, there exists large regional variability. Furthermore, a large fraction of the ocean waters surrounding Iberian Peninsula and Canary Islands belong to the eastern boundary upwelling system of Canary Current Large Marine Ecosystem (Arístegui et al., 2009), and upwelling zones are hotspots for affection of the main biogeochemical stressors (Gruber, 2011). It is worth noting that inorganic nutrient content available in seawater, while being important biogeochemical tracers, are out of the scope of current changes description as the baseline for their changes are still not well resolved. The same holds for a wide range of processes, like for example wind regimes, storm tracks, vertical mixing and turbulence that ultimately dictate the limits of primary production, changes in redox states of trace elements, alterations in riverine influx of allochthonous nutrients and/or contaminants… All the processes in this non-extensive list exhibit regional nuances that result in a diverse spectrum of trends and consequences hard to predict. The scarcity of long-term, sustained observations highlights the need for comprehensive monitoring to unravel the intricacies of these biogeochemical shifts, which are critical for our understanding of the evolving oceanic ecosystem.

2.5.1. Ocean acidification

Ocean acidification (OA) is a multifaceted consequence of the ocean's absorption of excess CO_2 from the atmosphere. This process alters the inorganic carbon balance of the ocean, leading to a multitude of chemical changes in seawater: from decreasing pH and carbonate ion content to increasing partial pressure of CO_2. Is *virtually certain*, the maximum likelihood term in the IPCC level of confidence scale, that ocean pH is declining at a rate of 0.0017-0.0027 pH units yr^{-1} (IPCC, 2022). These deviations from the natural state supposes a thermodynamic challenge for the formation and maintenance of calcium carbonate ($CaCO_3$) structures like shells and skeletons in marine organisms. The progress of OA is not globally homogenous and is greatly influenced by its geographical context (Bates et al., 2014): there are susceptible areas by its inherent physicochemical properties like for example the high latitudes due to their lower buffer capacity. The current progression towards carbonate undersaturation due to OA could compromise the sustainability of habitats and ecosystem services developed by ecosystem engineers like cold-water corals communities that are currently living in deep waters close to or in their way to carbonate undersaturation (Guinotte et al., 2006).

Upper waters show seasonal changes in their carbon chemistry due to several processes: some are led by biology, like primary production (that consumes CO_2

from the water), and organic matter remineralization (that releases inorganic carbon from the organic pool) but also $CaCO_3$ formation and dissolution (Zeebe, 2012). Besides, there are inorganic processes in the ocean-atmosphere interface like the dissolution of atmospheric CO_2 in surface waters or the release of dissolved CO_2 to the atmosphere (Takahashi et al., 2009). In subsurface waters the seasonal variability in carbon system properties is buffered (Vázquez-Rodríguez, Padin, et al., 2012) and related to episodic ventilation events in water mass formation areas (Pérez et al., 2021), while in deeper waters the acidification signal is strongly modulated by water mass dynamics (Fontela et al., 2020; García-Ibáñez et al., 2016; Lauvset et al., 2020).

Here, it should be taken into account that while we are going to include and summarize OA trends around the Iberian Peninsula and Canary islands based on observations, some of the study sites have a strong coastal component. Coastal and shallower areas, usually more productive and prone to land discharges, are affected by different complex and dynamic processes than oceanic areas. Consequently, the annual rates of change in surface pH in coastal areas can be an order of magnitude larger than in the surface ocean (Bates et al., 2014; Flecha et al., 2022).

A summary of known pH rates of change along the water column (0 - 2000 m depth) in the different geographical locations based exclusively on measurements is included in Figure 4.7. This graphical representation offers a comprehensive insight into the different pH trend magnitudes published around Iberian Peninsula and Canary islands along with the time periods considered. At a global scale, mean surface open ocean pH decreased at a rate of 0.0018 pH units yr^{-1} (Lauvset et al., 2015, Figure 4.7). Although anthropogenic carbon uptake is the main forcing driver, the increase in sea temperature reinforces OA (Lauvset et al., 2015; Pérez et al., 2021). The longest available time-series of OA around the Iberian Peninsula is in the northern limit of the Iberian upwelling system in Galician waters (Padin et al., 2020). There, the progress of OA in coastal and shelf waters has been assessed since 1976 and the interannual acidification trends range from –0.0012 to –0.0039 pH units yr^{-1} (Padin et al., 2020, Figure 4.7). Also in the North Atlantic but from an in-depth oceanic perspective, there is an unequivocal pH decrease in the Eastern North Atlantic (ENA, Figure 4.7) in the water mass North Atlantic Central Water (NACW) (Vázquez-Rodríguez, Pérez, et al., 2012). As NACW in the study zone is located below the seasonal mixed layer until 500 m depth approx, the observed declining rate of -0.0009 ± 0.0001 pH units yr^{-1} is represented at 250 m depth in Figure 4.7. This acidification signal within the upper layer of the Eastern North Atlantic in the period 1981-2008 undergoes a partial compensation due to amplified ventilation processes (Vázquez-Rodríguez, Pérez, et al., 2012). Th*f* is high ventilation period due to deep convective mixing events previously described in section 2.1.2, associated with predominantly positive NAO years, results in lower-than-anticipated rates of acidification. Notably, the last year of the evaluated time period (2008) coincides with the start date for a period of significant low ventilation in the Eastern North Atlantic, a phenomenon that has persisted since at least 2014 (Fröb et al., 2016). Following in the ENA, the acidification rate was also significant for the layer affected by mediterranean influence, and the reported

pH decrease trend for the Mediterranean Water (MW) was -0.00058 ± 0.0001 pH units yr^{-1} (Vázquez-Rodríguez, Padin, et al., 2012). The deeper water mass where a statistically significant pH decrease was observed in the Labrador Sea Water layer (LSW) at around 2000 m depth, with a pH decrease trend of -0.00083±0.0001 pH units yr^{-1} (Vázquez-Rodríguez, Padin, et al., 2012). Note that the OA progress in LSW was faster than in MW. As OA is a complex process that affects several biogeochemical variables, some of the alterations due climate change have been reported in other carbon-related variables, like for example the saturation state of aragonite or the decrease in carbonate ions. In the Northeast Atlantic ocean close to the Iberian Upwelling System the carbonate content is decreasing in the upper and intermediate water masses. Specifically, there is a decrease in carbonate of -0.57 ± 0.12 $\mu molkg^{-1}yr^{-1}$ in NACW (Fontela et al., 2020). This decline affects also MW at a rate of -0.39 ± 0.05 $\mu molkg^{-1}yr^{-1}$ and reaches even to the LSW at -0.21 ± 0.03 $\mu molkg^{-1}yr^{-1}$ (Fontela et al., 2020). The progress toward carbonate undersaturation is related to the increase in anthropogenic carbon content and its convey toward deeper depths mediated by meridional overturning in deep-water mass formation zones (Perez et al., 2018), but an in-depth analysis of ocean acidification forcing drivers in the Northeast Atlantic is still absent. Finally, the deeper water wass of the Northeast Atlantic, the North Atlantic Deep Water (NADW) does not exhibit any statistically significant decrease in carbon variables (Fontela et al., 2020; Vázquez-Rodríguez, Pérez, et al., 2012) and is therefore not included in Figure 4.7.

Further south, within the Eastern North Atlantic subtropical region, comprehensive long-time series of high-quality measurements have been extensively documented around the Canary Islands (M. González-Dávila et al., 2010; Melchor González-Dávila & Santana-Casiano, 2023; Santana-Casiano et al., 2007). The ESTOC site (*European Station for Time series in the Ocean at the Canary Islands*), in particular, stands out as a remarkable dataset spanning 25 years (1995-2019), establishing itself as one of the lengthiest carbon-focused reference station in the North Atlantic (Lange et al., 2023). On the surface, the decrease in seawater pH of around 0.0017 ± 0.0004 pH units yr^{-1} is also evident in the positive rate of increase in surface seawater pCO_2 (Santana-Casiano et al., 2007). There, the seawater pCO_2 increased at a similar rate that atmospheric pCO_2 observed at the Izaña station (~1.6 $\mu atmyr^{-1}$), pointing towards the direct control of the increased atmospheric CO_2 concentration as a result of anthropogenic emissions over the surface ocean carbon variables (Santana-Casiano et al., 2007). The NACW acidification rate for the period 1995–2004 in ESTOC closely aligns with the rate determined at ENA for the period 1981-2008 (Figure 4.7). Here, the central waters at 250 m depth had a decreasing trend of -0.0013 ± 0.0004 pH units yr−1 and a carbonate decrease of -0.5 ± 0.1 $\mu molkg^{-1}yr^{-1}$ (M. González-Dávila et al., 2010). Moreover, the most recent data on ocean rates at ESTOC, extending the previously published trends from the 1995-2010 period by almost a decade (1995-2019), indicates a ~20% acceleration of OA (Fig.4). This gradual decline, totaling 0.051 pH units since the onset of the measurements, represents a substantial +13% increase in acidity. Taking into account that usual seasonal

ranges in pH in subtropical latitudes are less than 0.4 pH units (Carstensen & Duarte, 2019), the observed magnitude of change is already above the natural seasonal variability. The pH decrease trend at 1000 m depth has changed from –0.0005 pH units yr^{-1} when the time period 1995-2004 is analyzed until –0.0011 pH units yr^{-1} when the period covers 1995-2019 (González-Dávila & Santana-Casiano, 2023, Figure 4.7). This trend acceleration accentuates the much faster progress of OA at 1000 m depth. This recent reinvigoration is in line with the increase in the CO_2 flux into the ocean in the mid-latitude North Atlantic during the period 2002–2016 (Macovei et al., 2020). Furthermore, interannual changes in the NAO index affects North Atlantic sink variability (Schuster & Watson, 2007) and anthropogenic carbon dioxide uptake (Pérez et al., 2013). The trend at 2000 m depth for the period 1995-2019 remains almost equally as it was for 1995-2004 (Figure 4.7). The observed carbonate system changes at ESTOC unequivocally point to anthropogenic influence, further emphasizing the need for continued monitoring and understanding of these evolving dynamics in the Canary waters.

The Gulf of Cadiz, located in the eastern sector of the North Atlantic Ocean, between the Iberian Peninsula and the African Continent, is an oceanographic gateway connecting the Atlantic Ocean and the Mediterranean Sea through the Strait of Gibraltar (Sánchez-Leal et al., 2017). There, the first insights into acidification trends were acquired with high-frequency autonomous observational data (Flecha et al., 2015). A quite large decreasing trend of -0.0044±0.00006 pH units yr^{-1}, in the Mediterranean Outflow Water (MOW) was determined based on a continuous autonomous observational period of around three years (Flecha et al., 2015). This short-time trend was also supported by a concomitant change in pCO_2 registered with an independent equipment (Flecha et al., 2015). Subsequent measurements have extended this period until March 2017, confirming a continued acidification trend (~4.5 years) at a rate of -0.00462±0.0006 yr^{-1} (García-Lafuente et al., 2021) along with a warming trend of 0.339±0.008 ºC $decade^{-1}$ in the deepest layer of the outflow. Note that the rate of pH decrease found at ~300 m depth in the Strait of Gibraltar is notably higher (2-3 times) than acidification rates recorded in multiple ocean surface time series. In the same zone, using ship-based cruises and discrete analytical measurements instead of autonomous equipment, the acidification trends were backed at decadal scale from 2005 until 2015 (Flecha et al., 2019) and 2021 (Amaya-Vías et al., 2023). Supported by spectrophotometric seawater pH measurements, a large decrease trend of -0.0036 ±0.0003 pH units yr^{-1} was found for the NACW and -0.0009 ±0.0005 pH units yr^{-1} in the West Mediterranean Deep Water (WMDW, around 360 m) (Flecha et al., 2019). The different rates between these water masses is attributed to the geographical distance from their respective source regions and the age of the water masses: WDMW has been recently in contact with the atmosphere, leading to a lower pH due recent formation. Decadal acidification in the Strait of Gibraltar was reinforced for natural processes in the upper and intermediate water masses, representing the 60% and 40% of the overall pH decrease in the NACW and the WMDW respectively. The pH measurements

show a steep decline in winter 2016 that points towards a replacement in the prevalence of Levantine Intermediate Water (LIW) fraction with respect to WMDW in the outflow. The time-series has been recently extended up to 2021, spanning 17 years (2005-2021, Amaya-Vías et al., 2023). The most recent observations confirm the previously published trends in NACW, increase twofold the acidification trend in WMDW (-0.0019 ±0.0003 pH units yr^{-1}), and for the first time, detect a significant pH decay trend in LIW (Amaya-Vías et al., 2023).

The Atlantic Water that flows through the Strait of Gibraltar supposes a net transport of anthropogenic carbon into the Mediterranean (Huertas et al., 2009). Coupled with the relatively short overturning time-scale of the Mediterranean Sea the circulation conveys a strong acidification signal to deep waters (Álvarez et al., 2014). Even so, the Mediterranean Sea is a semi enclosed basin where no problem of aragonite undersaturation is expected in the mid-long term (Hassoun et al., 2015). At a basin-scale and from a modeling approach, Palmiéri et al., 2015 reported a surface pH decrease trend of 0.0004 pH units yr^{-1}, a total magnitude of -0.084 pH units since the preindustrial era. In the western Mediterranean, machine learning approaches reconstructed a time series of 9 years (2012-2021) in the coastal Balearic Sea (Palma) with a decreasing trend of 0.002±0.00054 pH units yr^{-1}, (Flecha et al., 2022, Figure 4.7). There, recurrent neural networks techniques have proven to be effective in addressing gaps within acidification time series, particularly when there are doubts about sensor malfunctions or a lack of confidence in autonomous measurements (i.e., drift). Presently, commercial pH sensors are less trusted compared to temperature, salinity, or oxygen sensors, and it was precisely those three parameters which made the basis of a Bidirectional Long-Short Term Memory neural network (Flecha et al., 2022). While the main forcing agent of pH decrease in Palma bay was the increase in atmospheric CO_2, it is noteworthy that they also found a statistically significant trend in total alkalinity ($-$ 4.0 ± 0.4 µmol kg^{-1} $year^{-1}$), closely associated with a significant surface freshening (-0.059 ± 0.002 yr^{-1}) (Flecha et al., 2022). At the end date of this chapter, there are no available trends for intermediate and deeper layers of the northwest Mediterranean Sea close to the Iberian Peninsula.

Despite the considerable advancement in both geographical diversity and volume of published trends on ocean acidification surrounding the Iberian Peninsula and Canary Islands, as outlined above, there remains an opportunity to further enrich our understanding through the utilization of emerging data-synthesis products. These innovative approaches, based on reanalysis and machine learning, offer the opportunity for a more cohesive and comprehensive insight. For ocean acidification, we are going to leverage the OceanSODA-ETHZ dataset (Gregor & Gruber, 2021). OceanSODA provides global gridded monthly fields of surface carbon-related variables in the ocean. It is based on a combination of observations and machine learning approaches and uninterruptedly covers the period since 1982. Therefore, this dataset is valuable for studying the ocean carbon cycle and its evolution over the past few decades. In Figure 4.8, five zones have been selected as representatives of the Iberian Peninsula and Canary Island

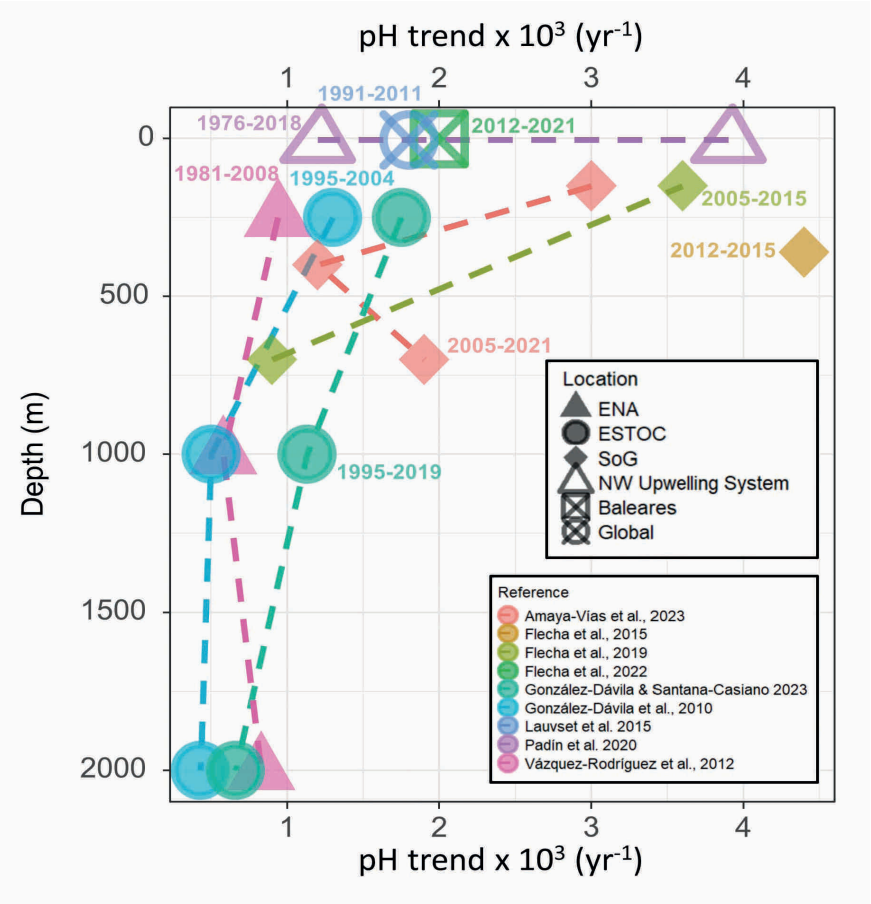

Figure 4.7. Published trends showing the annual pH rate of change (pH units x 10^3 yr^{-1}) in relation to the depth (from surface to 2000 m) for the waters surrounding the Iberian Peninsula and Canary Islands. The data points are color-coded by references and connected by dashed lines to visualize the vertical patterns. Shape of each data point corresponds to its geographical location. The label includes the temporal period of observations that support the trend (in years).

sea waters. For the sake of consistency, we have intentionally avoided coastal zones when possible, as acidification trends are likely not well resolved by data synthesis or modeling products in coastal areas (OSPAR OA report, McGovern et al., 2023). Across all zones, the pH shows an unequivocally net decrease of almost 0.1 pH units during those 40 years, from surface values of 8.15 pH units to 8.05 nowadays (Figure 4.8).

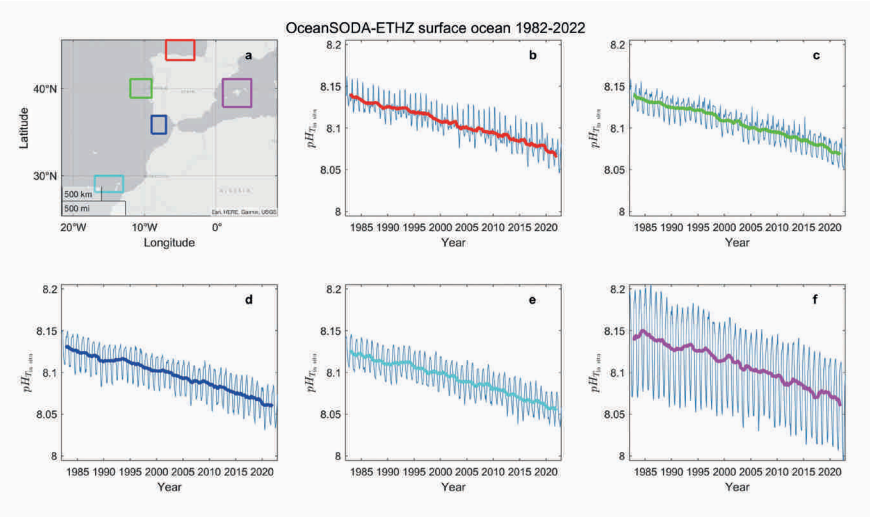

Figure 4.8. Temporal evolution of surface pH for the period 1982-2022 at different zones around Iberian Peninsula and Canary Islands. The zones are represented as squares in subplot (a) and the color code is shared with the time-series subplots (b-f). Data from OceanSODA-ETHZ (Gregor & Gruber, 2021).

2.5.2. Ocean deoxygenation

Ocean deoxygenation is the long-term decline in the concentration of dissolved oxygen in the ocean pool due to climate change (Keeling et al., 2010). The observed decrease in ocean oxygen content (Schmidtko et al., 2017; Stendardo & Gruber, 2012) aligns with the prediction that a warmer ocean will lose oxygen (Laurent Bopp et al., 2002; Sarmiento et al., 1998). In fact, ocean deoxygenation is an ongoing process that will continue for several centuries even after net zero CO_2 emissions are reached (Oschlies, 2021). The observation and attribution of oxygen decrease in seawater is not straightforward since the amount of oxygen is closely related to several interconnected factors. On one hand, warming directly affects solubility, while dynamical changes in circulation, stratification, mixing, and ventilation also influence the oxygen exported to depth (Oschlies et al., 2018). Furthermore, there are also biological effects since photosynthesis generates oxygen in the upper layer of the ocean, and respiration consumes it through the whole water column. Therefore, below the photosynthetic layer of the ocean, the amount of oxygen at depth is an interplay between respiration (that consumes) and vertical mixing (that replenishes oxygen). In fact, the proportion of deoxygenation currently explained by

ocean heat excess in the upper layer is around 15%, with the bulk of the decrease driven by increased stratification (Helm et al., 2011) and consequent less transport of dissolved oxygen from surface to subsurface waters (Frölicher et al., 2009).

Observation-based estimates show that the global oceanic oxygen content has already decreased more than 2% (Schmidtko et al., 2017). This global average decline encompasses large regional heterogeneity. The ocean oxygen pool is projected to decrease at the end of the century, with independence of climate scenario (an additional –1.81% in RCP2.6 until –3.45% in RCP8.5) (L. Bopp et al., 2013; Kwiatkowski et al., 2020), and the largest losses are going to be in the subsurface waters of mid-latitude regions (Gattuso et al., 2015). Even if the modeled rate of decline in Earth System Models is small, 0.05 $mmolm^{-3}yr^{-1}$ (Oschlies, 2021), it is projected that significant deoxygenation will occur in the global benthic ocean, even at depths exceeding 2000 meters, under all the climate scenarios (Kwiatkowski et al., 2020). Furthermore, current models underestimate the oceanic oxygen loss compared with observations by a factor of two (Oschlies et al., 2018) emphasizing the need for continued efforts in this subject. The time of emergence of interior oxygen content decreases, i.e., the moment when the signals of ocean deoxygenation become persistently detectable from its internal variability, is much longer than for climate change-driven pH trends (Henson et al., 2017). An ensemble analysis of CMIP5 models determined that trends in deoxygenation will become apparent around mid-century (Henson et al., 2017). Therefore, unequivocally detection of ocean deoxygenation will not be possible in many regions unless there is a sufficient availability of internally consistent long-term observations.

The North Atlantic shows susceptibility to compound stressors of deoxygenation, acidification and nutrient stress (Kwiatkowski et al., 2020). The upper layers of the subpolar and eastern North Atlantic have been found as hotspots of oxygen decrease (Stendardo & Gruber, 2012; Tanhua & Keeling, 2012). Time series (1965-2005) of oxygen content for the west european basin shows a decline of -0.3 ± 0.12 $\mu molkg^{-1}yr^{-1}$ and -0.2 ± 0.34 $\mu molkg^{-1}yr^{-1}$ in the density horizon of mode-water masses and Labrador Sea Water respectively (Stendardo & Gruber, 2012). The long-term decrease points to a possible acceleration since the early 1990s (Stendardo & Gruber, 2012), but the large natural North Atlantic oxygen variability constrains the detection and attribution of ocean deoxygenation to specific drivers (Frölicher et al., 2009).

Within a coastal perspective, the largest up-to-date database for the long-term trends of biogeochemical properties in the Iberian upwelling system (1976-2018) detected a deoxygenation rate of -0.7 ± 0.2 $\mu molkg^{-1}yr^{-1}$ in the surface waters of the inner Ría de Vigo (Padin et al., 2020). The magnitude coincides with the observed deoxygenation rate of ~0.8 $\mu molkg^{-1}yr^{-1}$ at 100 m depth in the Bay of Biscay during the period 2002-2019 (Chust et al., 2022). In contrast, also in the Bay of Biscay, observations in coastal waters show evidence of dissolved oxygen increase in surface waters at a rate of +0.3 $\mu molkg^{-1}yr^{-1}$ during the period 1995-2019 (Chust et al., 2022). The authors relate the oxygen increase in surface waters

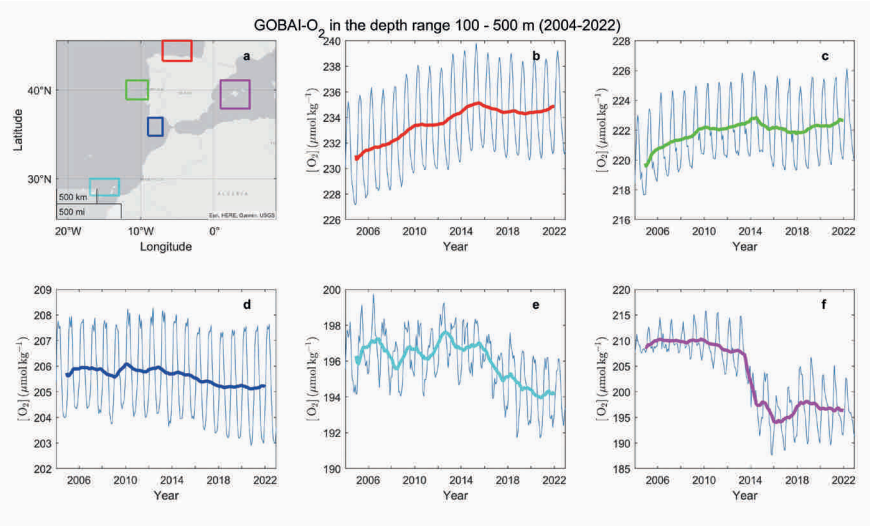

Figure 4.9. Mean concentration of dissolved oxygen [O_2] (μmolkg^{-1}) in the depth layer 100-500 m for the period 2004-2022 at different zones around Iberian Peninsula and Canary Islands. The zones are represented as squares in subplot (a) and the color code is shared with time-series subplot (b-f). Note that the y-axis is not the same for each subplot. Data from GOBAI-O_2 (Sharp et al., 2023).

to an increase in primary production motivated by increased availability of inorganic nutrients in the studied period (Chust et al., 2022). The oxygen decrease at 100 m depth could be related to i) the parallel sea temperature increase in the water column (0-100 m depth) from 1986 to 2019 (Chust et al., 2022), ii) an increase in remineralization of organic matter at subsurface depths due to enhanced primary production, or iii) both processes mutually reinforcing each other.

At global scale, mid and low latitudes have lower surface oxygen concentrations. In the ESTOC site at the Canary Islands there is a non-significant oxygen decrease in the upper thousand meters associated with higher temperatures (Melchor González-Dávila & Santana-Casiano, 2023). Although the oxygen content has decreased in ENACW, it has increased at a rate of +0.25±0.08 μmolkg^{-1}yr^{-1} at depths below 2000 m, in the NADW (Melchor González-Dávila & Santana-Casiano, 2023). The authors relate the NADW oxygen increase with recent events of deep Atlantic ventilation in the LSW layer (Koelling et al., 2022) and with a increasing influence of Antarctic Bottom Water (AABW) in the subtropical North Atlantic in recent times (Krasheninnikova et al., 2021).

Echoing our methodology for surface ocean acidification trends, here we leverage a different four-dimensional gridded product that offers a systematic and scalable approach to explore interior ocean dissolved oxygen content. The GOBAI-O_2 (Gridded Ocean Biogeochemistry from Artificial Intelligence – Oxygen) product provides a gridded dataset that offers monthly fields of interior dissolved oxygen in the global

ocean from 2004 until 2000 m depth (Sharp et al., 2023). The data is derived using machine learning algorithms trained on observed dissolved oxygen data from multiple observing platforms, including ship-based surveys and ARGO profiles. The algorithms used to produce GOBAI-O_2 have been validated using real observations and synthetic data from model output, and the data product itself has been compared against the World Ocean Atlas and selected discrete measurements, reproducing with an independent approach the observed declining trend in the oxygen inventory in the upper 2000 m of the global ocean (Sharp et al., 2023).

As oceanic waters representatives of the Iberian Peninsula and the Canary Islands five zones have been selected, and the analysis is centered in the depth band 100-500 m (Figure 4.9). The chosen depth layer targets central-modal waters while avoiding biological variability and seasonal changes typically occurring in surface waters (here defined as 0-100 m). As expected, the oxygen content and the seasonal variability in the North Atlantic is larger at North than at South zones. The time-series does not show any significant interannual trend for the period 2004-2022 around the Iberian Peninsula and Canary Islands within the North Atlantic Ocean. There is a quite modest increase in oxygen concentration in the NW Iberian Peninsula (40ºN), rising from 230 $\mu molkg^{-1}$ in 2004 until 235 $\mu molkg^{-1}$ in 2016-2022, that could be related with annually recurrent ventilation events that had its peak at the year 2016. The Gulf of Cádiz shows the most stable of the time-series, centered around 205-206 $\mu molkg^{-1}$. Around Canary Islands the first part of the timeseries (2004-2015) is stable at 196 $\mu molkg^{-1}$, while there is a very small decline of 2 $\mu molkg^{-1}$ since 2016 until the end of the time series. In the Mediterranean Sea there is a sharp steep decline in oxygen concentration happening in 2013-2014 in the Balearic Sea (Figure 4.9f). This change coincides with the end of deep convection events observed annually in the Gulf of Lion until 2013 (Houpert et al., 2016) and their absence from 2014 onwards. It should be noted that these results are not confirmed from an observational perspective and its meaning should be taken very cautiously.

Certainly, to detect the pace of ocean deoxygenation, as for almost every environmental driver of climate change, long-term sustained observational networks are mandatory to describe future changes in the anthropogenic ocean.

References

Álvarez, M., Sanleón-Bartolomé, H., Tanhua, T., Mintrop, L., Luchetta, A., Cantoni, C., et al. (2014). The CO₂ system in the Mediterranean Sea: a basin wide perspective. *Ocean Science*, *10*(1), 69–92. https://doi.org/10.5194/os-10-69-2014

Amaya-Vías, S., Flecha, S., Pérez, F. F., Navarro, G., García-Lafuente, J., Makaoui, A., & Huertas, I. E. (2023). The time series at the Strait of Gibraltar as a baseline for long-term assessment of vulnerability of calcifiers to ocean acidification. *Frontiers in Marine Science*, *10*. https://doi.org/10.3389/fmars.2023.1196938

Arístegui, J., Barton, E. D., Álvarez-Salgado, X. A., Santos, A. M. P., Figueiras, F. G., Kifani, S., et al. (2009). Sub-regional ecosystem variability in the Canary Current upwelling. *Progress in Oceanography*, *83*(1–4), 33–48. https://doi.org/10.1016/j.pocean.2009.07.031

Bakun, A. (1990). Global Climate Change and Intensification of Coastal Ocean Upwelling. *Science*, *247*(4939), 198–201. https://doi.org/10.1126/science.247.4939.198

Balmaseda, M. A., Trenberth, K. E., & Källén, E. (2013). Distinctive climate signals in reanalysis of global ocean heat content. *Geophysical Research Letters*, *40*(9), 1754–1759. https://doi.org/10.1002/grl.50382

Bamber, J., & Riva, R. (2010). The sea level fingerprint of recent ice mass fluxes. *The Cryosphere*, *4*(4), 621–627. https://doi.org/10.5194/tc-4-621-2010

Bates, N., Astor, Y., Church, M., Currie, K., Dore, J., Gonaález-Dávila, M., et al. (2014). A Time-Series View of Changing Ocean Chemistry Due to Ocean Uptake of Anthropogenic CO_2 and Ocean Acidification. *Oceanography*, *27*(1), 126–141. https://doi.org/10.5670/oceanog.2014.16

Beal, L. M., & Elipot, S. (2016). Broadening not strengthening of the Agulhas Current since the early 1990s. *Nature*, *540*(7634), 570–573. https://doi.org/10.1038/nature19853

Bopp, L., Resplandy, L., Orr, J. C., Doney, S. C., Dunne, J. P., Gehlen, M., et al. (2013). Multiple stressors of ocean ecosystems in the 21st century: projections with CMIP5 models. *Biogeosciences*, *10*(10), 6225–6245. https://doi.org/10.5194/bg-10-6225-2013

Bopp, Laurent, Le Quéré, C., Heimann, M., Manning, A. C., & Monfray, P. (2002). Climate-induced oceanic oxygen fluxes: Implications for the contemporary carbon budget. *Global Biogeochemical Cycles*, *16*(2). https://doi.org/10.1029/2001GB001445

Boyce, D., & Worm, B. (2015). Patterns and ecological implications of historical marine phytoplankton change. *Marine Ecology Progress Series*, *534*, 251–272. https://doi.org/10.3354/meps11411

Cabré, A., Marinov, I., & Leung, S. (2015). Consistent global responses of marine ecosystems to future climate change across the IPCC AR5 earth system models. *Climate Dynamics*, *45*(5–6), 1253–1280. https://doi.org/10.1007/s00382-014-2374-3

Calafat, F. M., Chambers, D. P., & Tsimplis, M. N. (2012). Mechanisms of decadal sea level variability in the eastern North Atlantic and the Mediterranean Sea. *Journal of Geophysical Research: Oceans*, *117*(C9), 2012JC008285. https://doi.org/10.1029/2012JC008285

Capotondi, A., Alexander, M. A., Bond, N. A., Curchitser, E. N., & Scott, J. D. (2012). Enhanced upper ocean stratification with climate change in the CMIP3 models. *Journal of Geophysical Research: Oceans*, *117*(C4), 2011JC007409. https://doi.org/10.1029/2011JC007409

Carstensen, J., & Duarte, C. M. (2019). Drivers of pH Variability in Coastal Ecosystems. *Environmental Science & Technology*, *53*(8), 4020–4029. https://doi.org/10.1021/acs.est.8b03655

Cassou, C., Minvielle, M., Terray, L., & Périgaud, C. (2011). A statistical–dynamical scheme for reconstructing ocean forcing in the Atlantic. Part I: weather regimes as predictors for ocean surface variables. *Climate Dynamics*, *36*(1), 19–39. https://doi.org/10.1007/s00382-010-0781-7

Chaigneau, A. A., Reffray, G., Voldoire, A., & Melet, A. (2022). IBI-CCS: a regional high-resolution model to simulate sea level in western Europe. *Geoscientific Model Development*, *15*(5), 2035–2062. https://doi.org/10.5194/gmd-15-2035-2022

Charria, G., Theetten, S., Vandermeirsch, F., Yelekçi, Ö., & Audiffren, N. (2017). Interannual evolution of (sub)mesoscale dynamics in the Bay of Biscay. *Ocean Science*, *13*(5), 777–797. https://doi.org/10.5194/os-13-777-2017

Cheng, L., Abraham, J., Hausfather, Z., & Trenberth, K. E. (2019). How fast are the oceans warming? *Science*, *363*(6423), 128–129. https://doi.org/10.1126/science.aav7619

Cheng, L., Foster, G., Hausfather, Z., Trenberth, K. E., & Abraham, J. (2022). Improved Quantification of the Rate of Ocean Warming. *Journal of Climate*, *35*(14), 4827–4840. https://doi.org/10.1175/JCLI-D-21-0895.1

Chu, P. C., & Fan, C. (2019). Global ocean synoptic thermocline gradient, isothermal-layer depth, and other upper ocean parameters. *Scientific Data*, *6*(1), 119. https://doi.org/10.1038/s41597-019-0125-3

Chust, G., González, M., Fontán, A., Revilla, M., Alvarez, P., Santos, M., et al. (2022). Climate regime shifts and biodiversity redistribution in the Bay of Biscay. *Science of The Total Environment*, *803*, 149622. https://doi.org/10.1016/j.scitotenv.2021.149622

Costoya, X., deCastro, M., Gómez-Gesteira, M., & Santos, F. (2014). Mixed Layer Depth Trends in the Bay of Biscay over the Period 1975–2010. *PLoS ONE*, *9*(6), e99321. https://doi.org/10.1371/journal.pone.0099321

Dangendorf, S., Hay, C., Calafat, F. M., Marcos, M., Piecuch, C. G., Berk, K., & Jensen, J. (2019). Persistent acceleration in global sea-level rise since the 1960s. *Nature Climate Change*, *9*(9), 705–710. https://doi.org/10.1038/s41558-019-0531-8

Dukhovskoy, D. S., Myers, P. G., Platov, G., Timmermans, M., Curry, B., Proshutinsky, A., et al. (2016). Greenland freshwater pathways in the sub- A rctic S eas from model experiments with passive tracers. *Journal of Geophysical Research: Oceans*, *121*(1), 877–907. https://doi.org/10.1002/2015JC011290

Emanuel, K. (2005). Genesis and maintenance of "Mediterranean hurricanes" *Advances in Geosciences*, *2*, 217–220. https://doi.org/10.5194/adgeo-2-217-2005

Flecha, S., Pérez, F. F., García-Lafuente, J., Sammartino, S., Ríos, Aida. F., & Huertas, I. E. (2015). Trends of pH decrease in the Mediterranean Sea through high frequency observational data: indication of ocean acidification in the basin. *Scientific Reports*, *5*(1), 16770. https://doi.org/10.1038/srep16770

Flecha, S., Pérez, F. F., Murata, A., Makaoui, A., & Huertas, I. E. (2019). Decadal acidification in Atlantic and Mediterranean water masses exchanging at the Strait of Gibraltar. *Scientific Reports*, *9*(1), 15533. https://doi.org/10.1038/s41598-019-52084-x

Flecha, S., Giménez-Romero, À., Tintoré, J., Pérez, F. F., Alou-Font, E., Matías, M. A., & Hendriks, I. E. (2022). pH trends and seasonal cycle in the coastal Balearic Sea reconstructed through machine learning. *Scientific Reports*, *12*(1), 12956. https://doi.org/10.1038/s41598-022-17253-5

Font, J., Palanques, A., Puig, P., Salat, J., & Emelianov, M. (2007). Sequence of hydrographic changes in NW Mediterranean deep water due to the exceptional winter of 2005. *Scientia Marina*, *71*, 339–346.

Fontán, A., Valencia, V., Borja, Á., & Goikoetxea, N. (2008). Oceano-meteorological conditions and coupling in the southeastern Bay of Biscay, for the period 2001–2005: A comparison with the past two decades. *Journal of Marine Systems*, *72*(1–4), 167–177. https://doi.org/10.1016/j.jmarsys.2007.08.003

Fontela, M., Pérez, F. F., Carracedo, L. I., Padín, X. A., Velo, A., García-Ibañez, M. I., & Lherminier, P. (2020). The Northeast Atlantic is running out of excess carbonate in the horizon of cold-water corals communities. *Scientific Reports*, *10*(1), 14714. https://doi.org/10.1038/s41598-020-71793-2

Frazão, H. C., Prien, R. D., Schulz-Bull, D. E., Seidov, D., & Waniek, J. J. (2022). The Forgotten Azores Current: A Long-Term Perspective. *Frontiers in Marine Science*, *9*, 842251. https://doi.org/10.3389/fmars.2022.842251

Fröb, F., Olsen, A., Våge, K., Moore, G. W. K., Yashayaev, I., Jeansson, E., & Rajasakaren, B. (2016). Irminger Sea deep convection injects oxygen and anthropogenic carbon to the ocean interior. *Nature Communications*, *7*(1), 13244. https://doi.org/10.1038/ncomms13244

Frölicher, T. L., Joos, F., Plattner, G. -K., Steinacher, M., & Doney, S. C. (2009). Natural variability and anthropogenic trends in oceanic oxygen in a coupled carbon cycle–climate model ensemble. *Global Biogeochemical Cycles*, *23*(1), 2008GB003316. https://doi.org/10.1029/2008GB003316

Fu, W., Randerson, J. T., & Moore, J. K. (2016). Climate change impacts on net primary production (NPP) and export production (EP) regulated by increasing stratification and phytoplankton community structure in the CMIP5 models. *Biogeosciences*, *13*(18), 5151–5170. https://doi.org/10.5194/bg-13-5151-2016

García-Ibáñez, M. I., Zunino, P., Fröb, F., Carracedo, L. I., Ríos, A. F., Mercier, H., et al. (2016). Ocean acidification in the subpolar North Atlantic: rates and mechanisms controlling pH changes. *Biogeosciences*, *13*(12), 3701–3715. https://doi.org/10.5194/bg-13-3701-2016

García-Lafuente, J., Sammartino, S., Huertas, I. E., Flecha, S., Sánchez-Leal, R. F., Naranjo, C., et al. (2021). Hotter and Weaker Mediterranean Outflow as a Response to Basin-Wide Alterations. *Frontiers in Marine Science*, *8*. https://doi.org/10.3389/fmars.2021.613444

García-Martínez, M. D. C., Vargas-Yáñez, M., Moya, F., Santiago, R., Muñoz, M., Reul, A., et al. (2019). Average nutrient and chlorophyll distributions in the western Mediterranean: RADMED project. *Oceanologia*, *61*(1), 143–169. https://doi.org/10.1016/j.oceano.2018.08.003

Gattuso, J.-P., Magnan, A., Billé, R., Cheung, W. W. L., Howes, E. L., Joos, F., et al. (2015). Contrasting futures for ocean and society from different anthropogenic CO_2 emissions scenarios. *Science*, *349*(6243), aac4722. https://doi.org/10.1126/science.aac4722

Goikoetxea, N., Borja, Á., Fontán, A., González, M., & Valencia, V. (2009). Trends and anomalies in sea-surface temperature, observed over the last 60 years, within the southeastern Bay of Biscay. *Continental Shelf Research*, *29*(8), 1060–1069. https://doi.org/10.1016/j.csr.2008.11.014

Gómez-Jakobsen, F., Ferrera, I., Yebra, L., & Mercado, J. M. (2022). Two decades of satellite surface chlorophyll a concentration (1998–2019) in the Spanish Mediterranean marine waters (Western Mediterranean Sea): Trends, phenology and eutrophication assessment. *Remote Sensing Applications: Society and Environment, 28*, 100855. https://doi.org/10.1016/j.rsase.2022.100855

Gomis, D., Ruiz, S., Sotillo, M. G., Álvarez-Fanjul, E., & Terradas, J. (2008). Low frequency Mediterranean sea level variability: The contribution of atmospheric pressure and wind. *Global and Planetary Change, 63*(2–3), 215–229. https://doi.org/10.1016/j.gloplacha.2008.06.005

González-Dávila, M., Santana-Casiano, J. M., Rueda, M. J., & Llinás, O. (2010). The water column distribution of carbonate system variables at the ESTOC site from 1995 to 2004. *Biogeosciences*, *7*(10), 3067–3081. https://doi.org/10.5194/bg-7-3067-2010

González-Dávila, Melchor, & Santana-Casiano, J. M. (2023). Long-term trends of pH and inorganic carbon in the Eastern North Atlantic: the ESTOC site. *Frontiers in Marine Science, 10*, 1236214. https://doi.org/10.3389/fmars.2023.1236214

Gonzalez-Pola, C., Larsen, K. M. H., Fratantoni, P., & Beszczynska-Möller, A. (2023). *ICES Report on ocean climate 2020* (p. 29037302 Bytes). [object Object]. https://doi.org/10.17895/ICES.PUB.19248602.V3

Gonzalez-Pola, C., Somavilla, R., Graña, R., & Viloria, A., I., L. (2024). A decade-long flow reversal in the intergyre region of the Eastern North Atlantic. *Progress in Oceanography*.

GOOS. (2023). OceanOPS Report Card 2023. Retrieved March 5, 2024, from https://www.ocean-ops.org/reportcard/

Gregor, L., & Gruber, N. (2021). OceanSODA-ETHZ: a global gridded data set of the surface ocean carbonate system for seasonal to decadal studies of ocean acidification. *Earth System Science Data*, *13*(2), 777–808. https://doi.org/10.5194/essd-13-777-2021

Gruber, N. (2011). Warming up, turning sour, losing breath: ocean biogeochemistry under global change. *Philosophical Transactions of the Royal Society A: Mathematical, Physical and Engineering Sciences*, *369*(1943), 1980–1996. https://doi.org/10.1098/rsta.2011.0003

Guinotte, J. M., Orr, J., Cairns, S., Freiwald, A., Morgan, L., & George, R. (2006). Will human-induced changes in seawater chemistry alter the distribution of deep-sea scleractinian corals? *Frontiers in Ecology and the Environment*, *4*(3), 141–146. https://doi.org/10.1890/1540-9295(2006)004[0141:WHCISC]2.0.CO;2

Hassoun, A. E. R., Gemayel, E., Krasakopoulou, E., Goyet, C., Abboud-Abi Saab, M., Guglielmi, V., et al. (2015). Acidification of the Mediterranean Sea from anthropogenic carbon penetration. *Deep Sea Research Part I: Oceanographic Research Papers*, *102*, 1–15. https://doi.org/10.1016/j.dsr.2015.04.005

Helm, K. P., Bindoff, N. L., & Church, J. A. (2011). Observed decreases in oxygen content of the global ocean: GLOBAL DECREASES IN OCEAN OXYGEN LEVELS. *Geophysical Research Letters*, *38*(23), n/a-n/a. https://doi.org/10.1029/2011GL049513

Henson, S. A., Beaulieu, C., Ilyina, T., John, J. G., Long, M., Séférian, R., et al. (2017). Rapid emergence of climate change in environmental drivers of marine ecosystems. *Nature Communications*, *8*(1), 14682. https://doi.org/10.1038/ncomms14682

Herrmann, M., Sevault, F., Beuvier, J., & Somot, S. (2010). What induced the exceptional 2005 convection event in the northwestern Mediterranean basin? Answers from a modeling study. *Journal of Geophysical Research: Oceans*, *115*(C12), 2010JC006162. https://doi.org/10.1029/2010JC006162

Hobday, A. J., Alexander, L. V., Perkins, S. E., Smale, D. A., Straub, S. C., Oliver, E. C. J., et al. (2016). A hierarchical approach to defining marine heatwaves. *Progress in Oceanography*, *141*, 227–238. https://doi.org/10.1016/j.pocean.2015.12.014

Holte, J., Talley, L. D., Gilson, J., & Roemmich, D. (2017). An Argo mixed layer climatology and database. *Geophysical Research Letters*, *44*(11), 5618–5626. https://doi.org/10.1002/2017GL073426

Houpert, L., Durrieu De Madron, X., Testor, P., Bosse, A., D'Ortenzio, F., Bouin, M. N., et al. (2016). Observations of open-ocean deep convection in the northwestern Mediterranean Sea: Seasonal and interannual variability of mixing and deep water masses for the 2007-2013 Period: DEEP CONVECTION OBS. NWMED 2007-2013. *Journal of Geophysical Research: Oceans*, *121*(11), 8139–8171. https://doi.org/10.1002/2016JC011857

Huertas, I. E., Ríos, A. F., García-Lafuente, J., Makaoui, A., Rodríguez-Gálvez, S., Sánchez-Román, A., et al. (2009). Anthropogenic and natural CO_2 exchange through the Strait of Gibraltar. *Biogeosciences*, *6*(4), 647–662. https://doi.org/10.5194/bg-6-647-2009

Hughes, C. W., Fukumori, I., Griffies, S. M., Huthnance, J. M., Minobe, S., Spence, P., et al. (2019). Sea Level and the Role of Coastal Trapped Waves in Mediating the Influence of the Open Ocean on the Coast. *Surveys in Geophysics*, *40*(6), 1467–1492. https://doi.org/10.1007/s10712-019-09535-x

Intergovernmental Panel On Climate Change. (2023). *Climate Change 2021 – The Physical Science Basis: Working Group I Contribution to the Sixth Assessment Report of the Intergovernmental Panel on Climate Change* (1st ed.). Cambridge University Press. https://doi.org/10.1017/9781009157896

Ipcc. (2022). *Global Warming of 1.5°C: IPCC Special Report on Impacts of Global Warming of 1.5°C above Pre-industrial Levels in Context of Strengthening Response to Climate Change, Sustainable Development, and Efforts to Eradicate Poverty* (1st ed.). Cambridge University Press. https://doi.org/10.1017/9781009157940

Josey, S. A., & Marsh, R. (2005). Surface freshwater flux variability and recent freshening of the North Atlantic in the eastern subpolar gyre. *Journal of Geophysical Research: Oceans*, *110*(C5), 2004JC002521. https://doi.org/10.1029/2004JC002521

Juza, M., & Tintoré, J. (2021). Multivariate Sub-Regional Ocean Indicators in the Mediterranean Sea: From Event Detection to Climate Change Estimations. *Frontiers in Marine Science*, *8*, 610589. https://doi.org/10.3389/fmars.2021.610589

Juza, M., Fernández-Mora, À., & Tintoré, J. (2022). Sub-Regional Marine Heat Waves in the Mediterranean Sea From Observations: Long-Term Surface Changes, Sub-Surface and Coastal Responses. *Frontiers in Marine Science*, *9*, 785771. https://doi.org/10.3389/fmars.2022.785771

Keeling, R. F., Körtzinger, A., & Gruber, N. (2010). Ocean Deoxygenation in a Warming World. *Annual Review of Marine Science*, *2*(1), 199–229. https://doi.org/10.1146/annurev.marine.010908.163855

Koelling, J., Atamanchuk, D., Karstensen, J., Handmann, P., & Wallace, D. W. R. (2022). Oxygen export to the deep ocean following Labrador Sea Water formation. *Biogeosciences*, *19*(2), 437–454. https://doi.org/10.5194/bg-19-437-2022

Kopp, R. E., Horton, R. M., Little, C. M., Mitrovica, J. X., Oppenheimer, M., Rasmussen, D. J., et al. (2014). Probabilistic 21st and 22nd century sea-level projections at a global network of tide-gauge sites. *Earth's Future*, *2*(8), 383–406. https://doi.org/10.1002/2014EF000239

Krasheninnikova, S. B., Demidov, A. N., & Ivanov, A. A. (2021). Variability of the Characteristics of the Antarctic Bottom Water in the Subtropical North Atlantic. *Oceanology*, *61*(2), 151–158. https://doi.org/10.1134/S0001437021020090

Kwiatkowski, L., Torres, O., Bopp, L., Aumont, O., Chamberlain, M., Christian, J. R., et al. (2020). Twenty-first century ocean warming, acidification, deoxygenation, and upper-ocean nutrient and primary production decline from CMIP6 model projections. *Biogeosciences*, *17*(13), 3439–3470. https://doi.org/10.5194/bg-17-3439-2020

Lange, N., Fiedler, B., Álvarez, M., Benoit-Cattin, A., Benway, H., Buttigieg, P. L., et al. (2023, July 31). Synthesis Product for Ocean Time-Series (SPOTS) – A ship-based biogeochemical pilot. https://doi.org/10.5194/essd-2023-238

Lauvset, S. K., Gruber, N., Landschützer, P., Olsen, A., & Tjiputra, J. (2015). Trends and drivers in global surface ocean pH over the past 3 decades. *Biogeosciences*, *12*(5), 1285–1298. https://doi.org/10.5194/bg-12-1285-2015

Lauvset, S. K., Carter, B. R., Pèrez, F. F., Jiang, L. -Q., Feely, R. A., Velo, A., & Olsen, A. (2020). Processes Driving Global Interior Ocean pH Distribution. *Global Biogeochemical Cycles*, *34*(1), e2019GB006229. https://doi.org/10.1029/2019GB006229

Le Quéré, C., Moriarty, R., Andrew, R. M., Canadell, J. G., Sitch, S., Korsbakken, J. I., et al. (2015). Global Carbon Budget 2015. *Earth System Science Data*, *7*(2), 349–396. https://doi.org/10.5194/essd-7-349-2015

Li, G., Cheng, L., Zhu, J., Trenberth, K. E., Mann, M. E., & Abraham, J. P. (2020). Increasing ocean stratification over the past half-century. *Nature Climate Change, 10*(12), 1116–1123. https://doi.org/10.1038/s41558-020-00918-2

Li, Z., England, M. H., & Groeskamp, S. (2023). Recent acceleration in global ocean heat accumulation by mode and intermediate waters. *Nature Communications*, *14*(1), 6888. https://doi.org/10.1038/s41467-023-42468-z

Llasses, J., Jordà, G., & Gomis, D. (2015). Skills of different hydrographic networks in capturing changes in the Mediterranean Sea at climate scales. *Climate Research*, *63*(1), 1–18. https://doi.org/10.3354/cr01270

López-Jurado, J. -L., González-Pola, C., & Vélez-Belchí, P. (2005). Observation of an abrupt disruption of the long-term warming trend at the Balearic Sea, western Mediterranean Sea, in summer 2005. *Geophysical Research Letters, 32*(24), 2005GL024430. https://doi.org/10.1029/2005GL024430

Lozier, M. S., Li, F., Bacon, S., Bahr, F., Bower, A. S., Cunningham, S. A., et al. (2019). A sea change in our view of overturning in the subpolar North Atlantic. *Science*, *363*(6426), 516–521. https://doi.org/10.1126/science.aau6592

Lozier, M. Susan. (2012). Overturning in the North Atlantic. *Annual Review of Marine Science*, *4*(1), 291–315. https://doi.org/10.1146/annurev-marine-120710-100740

Macovei, V. A., Hartman, S. E., Schuster, U., Torres-Valdés, S., Moore, C. M., & Sanders, R. J. (2020). Impact of physical and biological processes on temporal variations of the ocean carbon sink in the mid-latitude North Atlantic (2002–2016). *Progress in Oceanography*, *180*, 102223. https://doi.org/10.1016/j.pocean.2019.102223

Marcos, M., & Amores, A. (2014). Quantifying anthropogenic and natural contributions to thermosteric sea level rise: Marcos and Amores: Anthropogenic ocean warming. *Geophysical Research Letters*, *41*(7), 2502–2507. https://doi.org/10.1002/2014GL059766

Marcos, M., & Tsimplis, M. N. (2008). Coastal sea level trends in Southern Europe. *Geophysical Journal International*, *175*(1), 70–82. https://doi.org/10.1111/j.1365-246X.2008.03892.x

Marcos, M., & Woodworth, P. L. (2017). Spatiotemporal changes in extreme sea levels along the coasts of the N orth A tlantic and the G ulf of M exico. *Journal of Geophysical Research: Oceans*, *122*(9), 7031–7048. https://doi.org/10.1002/2017JC013065

Marcos, M., Tsimplis, M. N., & Shaw, A. G. P. (2009). Sea level extremes in southern Europe. *Journal of Geophysical Research: Oceans*, *114*(C1), 2008JC004912. https://doi.org/10.1029/2008JC004912

Marcos, M., Marzeion, B., Dangendorf, S., Slangen, A. B. A., Palanisamy, H., & Fenoglio-Marc, L. (2017). Internal Variability Versus Anthropogenic Forcing on Sea Level and Its Components. *Surveys in Geophysics*, *38*(1), 329–348. https://doi.org/10.1007/s10712-016-9373-3

Margirier, F., Testor, P., Heslop, E., Mallil, K., Bosse, A., Houpert, L., et al. (2020). Abrupt warming and salinification of intermediate waters interplays with decline of deep convection in the Northwestern Mediterranean Sea. *Scientific Reports*, *10*(1), 20923. https://doi.org/10.1038/s41598-020-77859-5

Marshall, J., & Speer, K. (2012). Closure of the meridional overturning circulation through Southern Ocean upwelling. *Nature Geoscience*, *5*(3), 171–180. https://doi.org/10.1038/ngeo1391

Martínez-Asensio, A., Marcos, M., Tsimplis, M. N., Gomis, D., Josey, S., & Jordà, G. (2014). Impact of the atmospheric climate modes on Mediterranean sea level variability. *Global and Planetary Change*, *118*, 1–15. https://doi.org/10.1016/j.gloplacha.2014.03.007

McGovern, E., Schilder, J., Artioli, Y., Birchenough, S., Dupont, S., Findlay, H., Skjelvan, I., Skogen, M.D., Álvarez, M., Büsher, J.V., Chierici, M., Aagaard Christensen, J.P., Diaz, P.L., Grage, A., Gregor, L., Humphreys, M., Järnegren, J., Knockaert, M., Krakau, M., Nogueira, M., Ólafsdóttir, S.R., von Schuckmann, K., Carreiro-Silva, M., Stiasny, M., Walsham, P., Widdicombe, S., Gehlen, M., Chau, T.T.T., Chevallier, F., Savoye, N., Clark, J., Galli, G., Hordoir, R. and Moffat. C. (2023). The 2023 Quality Status Report for the North-East Atlantic. Retrieved July 5, 2024, from https://unesdoc.unesco.org/ark:/48223/pf0000387263

Meyssignac, B., Piecuch, C. G., Merchant, C. J., Racault, M.-F., Palanisamy, H., MacIntosh, C., et al. (2017). Causes of the Regional Variability in Observed Sea Level, Sea Surface Temperature and Ocean Colour Over the Period 1993–2011. *Surveys in Geophysics*, *38*(1), 187–215. https://doi.org/10.1007/s10712-016-9383-1

Monserrat, S., Vilibić, I., & Rabinovich, A. B. (2006). Meteotsunamis: atmospherically induced destructive ocean waves in the tsunami frequency band. *Natural Hazards and Earth System Sciences*, *6*(6), 1035–1051. https://doi.org/10.5194/nhess-6-1035-2006

Moore, J. K., Fu, W., Primeau, F., Britten, G. L., Lindsay, K., Long, M., et al. (2018). Sustained climate warming drives declining marine biological productivity. *Science*, *359*(6380), 1139–1143. https://doi.org/10.1126/science.aao6379

Muis, S., Apecechea, M. I., Dullaart, J., De Lima Rego, J., Madsen, K. S., Su, J., et al. (2020). A High-Resolution Global Dataset of Extreme Sea Levels, Tides, and Storm Surges, Including Future Projections. *Frontiers in Marine Science*, *7*, 263. https://doi.org/10.3389/fmars.2020.00263

Oelsmann, J., Marcos, M., Passaro, M., Sanchez, L., Dettmering, D., Dangendorf, S., & Seitz, F. (2023). *Vertical land motion reconstruction unveils non-linear effects on relative sea level* (preprint). In Review. https://doi.org/10.21203/rs.3.rs-1714816/v1

Oschlies, A. (2021). A committed fourfold increase in ocean oxygen loss. *Nature Communications*, *12*(1), 2307. https://doi.org/10.1038/s41467-021-22584-4

Oschlies, A., Brandt, P., Stramma, L., & Schmidtko, S. (2018). Drivers and mechanisms of ocean deoxygenation. *Nature Geoscience*, *11*(7), 467–473. https://doi.org/10.1038/s41561-018-0152-2

Padin, X. A., Velo, A., & Pérez, F. F. (2020). ARIOS: a database for ocean acidification assessment in the Iberian upwelling system (1976–2018). *Earth System Science Data*, *12*(4), 2647–2663. https://doi.org/10.5194/essd-12-2647-2020

Palmiéri, J., Orr, J. C., Dutay, J.-C., Béranger, K., Schneider, A., Beuvier, J., & Somot, S. (2015). Simulated anthropogenic CO₂ storage and acidification of the Mediterranean Sea. *Biogeosciences*, *12*(3), 781–802. https://doi.org/10.5194/bg-12-781-2015

Pérez, F. F., Mercier, H., Vázquez-Rodríguez, M., Lherminier, P., Velo, A., Pardo, P. C., et al. (2013). Atlantic Ocean CO_2 uptake reduced by weakening of the meridional overturning circulation. *Nature Geoscience*, *6*(2), 146–152. https://doi.org/10.1038/ngeo1680

Perez, F. F., Fontela, M., García-Ibáñez, M. I., Mercier, H., Velo, A., Lherminier, P., et al. (2018). Meridional overturning circulation conveys fast acidification to the deep Atlantic Ocean. *Nature*, *554*(7693), 515–518. https://doi.org/10.1038/nature25493

Pérez, F. F., Olafsson, J., Ólafsdóttir, S. R., Fontela, M., & Takahashi, T. (2021). Contrasting drivers and trends of ocean acidification in the subarctic Atlantic. *Scientific Reports*, *11*(1), 13991. https://doi.org/10.1038/s41598-021-93324-3

Pérez Gómez, B., Vilibić, I., Šepić, J., Međugorac, I., Ličer, M., Testut, L., et al. (2022). Coastal sea level monitoring in the Mediterranean and Black seas. *Ocean Science*, *18*(4), 997–1053. https://doi.org/10.5194/os-18-997-2022

Pugh, D., & Woodworth, P. (2014). *Sea-Level Science: Understanding Tides, Surges, Tsunamis and Mean Sea-Level Changes* (1st ed.). Cambridge University Press. https://doi.org/10.1017/CBO9781139235778

Raven, J, K Caldeira, H Elderfield, O Hoegh-Guldberg, P Liss, U Riebesell, J Shepherd, C Turley, and A Watson. (2005). Ocean acidification due to increasing atmospheric carbon dioxide. London Document No. 12/05. The Royal Society. Retrieved from https://royalsociety.org/-/media/policy/publications/2005/9634.pdf

Rhein, M. (2019). Taking a close look at ocean circulation. *Science*, *363*(6426), 456–457. https://doi.org/10.1126/science.aaw3111

Rixen, M., Beckers, J. -M., Levitus, S., Antonov, J., Boyer, T., Maillard, C., et al. (2005). The Western Mediterranean Deep Water: A proxy for climate change. *Geophysical Research Letters*, *32*(12), 2005GL022702. https://doi.org/10.1029/2005GL022702

Roemmich, D., Church, J., Gilson, J., Monselesan, D., Sutton, P., & Wijffels, S. (2015). Unabated planetary warming and its ocean structure since 2006. *Nature Climate Change*, *5*(3), 240–245. https://doi.org/10.1038/nclimate2513

Rogers, J. C. (1990). Patterns of Low-Frequency Monthly Sea Level Pressure Variability (1899–1986) and Associated Wave Cyclone Frequencies. *Journal of Climate*, *3*(12), 1364–1379. https://doi.org/10.1175/1520-0442(1990)003<1364:POLFMS>2.0.CO;2

Salat, J., Pascual, J., Flexas, M., Chin, T. M., & Vazquez-Cuervo, J. (2019). Forty-five years of oceanographic and meteorological observations at a coastal station in the NW Mediterranean: a ground truth for satellite observations. *Ocean Dynamics*, *69*(9), 1067–1084. https://doi.org/10.1007/s10236-019-01285-z

Sallée, J.-B., Pellichero, V., Akhoudas, C., Pauthenet, E., Vignes, L., Schmidtko, S., et al. (2021). Summertime increases in upper-ocean stratification and mixed-layer depth. *Nature*, *591*(7851), 592–598. https://doi.org/10.1038/s41586-021-03303-x

Sánchez-Leal, R. F., Bellanco, M. J., Fernández-Salas, L. M., García-Lafuente, J., Gasser-Rubinat, M., González-Pola, C., et al. (2017). The Mediterranean Overflow in the Gulf of Cadiz: A rugged journey. *Science Advances*, *3*(11), eaao0609. https://doi.org/10.1126/sciadv.aao0609

Santana-Casiano, J. M., González-Dávila, M., Rueda, M., Llinás, O., & González-Dávila, E. (2007). The interannual variability of oceanic CO_2 parameters in the northeast Atlantic subtropical gyre at the ESTOC site. *Global Biogeochemical Cycles*, *21*(1), 2006GB002788. https://doi.org/10.1029/2006GB002788

Sarmiento, J. L., Hughes, T. M. C., Stouffer, R. J., & Manabe, S. (1998). Simulated response of the ocean carbon cycle to anthropogenic climate warming. *Nature*, *393*(6682), 245–249. https://doi.org/10.1038/30455

Schmidtko, S., Stramma, L., & Visbeck, M. (2017). Decline in global oceanic oxygen content during the past five decades. *Nature*, *542*(7641), 335–339. https://doi.org/10.1038/nature21399

Schroeder, K., Chiggiato, J., Bryden, H. L., Borghini, M., & Ben Ismail, S. (2016). Abrupt climate shift in the Western Mediterranean Sea. *Scientific Reports*, *6*(1), 23009. https://doi.org/10.1038/srep23009

Schuster, U., & Watson, A. J. (2007). A variable and decreasing sink for atmospheric CO_2 in the North Atlantic. *Journal of Geophysical Research: Oceans*, *112*(C11), 2006JC003941. https://doi.org/10.1029/2006JC003941

Seabra, R., Varela, R., Santos, A. M., Gómez-Gesteira, M., Meneghesso, C., Wethey, D. S., & Lima, F. P. (2019). Reduced Nearshore Warming Associated With Eastern Boundary Upwelling Systems. *Frontiers in Marine Science*, *6*, 104. https://doi.org/10.3389/fmars.2019.00104

Sharp, J. D., Fassbender, A. J., Carter, B. R., Johnson, G. C., Schultz, C., & Dunne, J. P. (2023). GOBAI-O_2: temporally and spatially resolved fields of ocean interior dissolved oxygen over nearly 2 decades. *Earth System Science Data*, *15*(10), 4481–4518. https://doi.org/10.5194/essd-15-4481-2023

Siemer, J. P., Machín, F., González-Vega, A., Arrieta, J. M., Gutiérrez-Guerra, M. A., Pérez-Hernández, M. D., et al. (2021). Recent Trends in SST, Chl- *a* , Productivity and Wind Stress in Upwelling and Open Ocean Areas in the Upper Eastern North Atlantic Subtropical Gyre. *Journal of Geophysical Research: Oceans*, *126*(8), e2021JC017268. https://doi.org/10.1029/2021JC017268

Slangen, A. B. A., Church, J. A., Agosta, C., Fettweis, X., Marzeion, B., & Richter, K. (2016). Anthropogenic forcing dominates global mean sea-level rise since 1970. *Nature Climate Change*, *6*(7), 701–705. https://doi.org/10.1038/nclimate2991

Somavilla, R., González-Pola, C., Schauer, U., & Budéus, G. (2016). Mid-2000s North Atlantic shift: Heat budget and circulation changes. *Geophysical Research Letters*, *43*(5), 2059–2068. https://doi.org/10.1002/2015GL067254

Somavilla, R., González-Pola, C., & Fernández-Diaz, J. (2017). The warmer the ocean surface, the shallower the mixed layer. H ow much of this is true? *Journal of Geophysical Research: Oceans*, *122*(9), 7698–7716. https://doi.org/10.1002/2017JC013125

Srokosz, M. A., Holliday, N. P., & Bryden, H. L. (2023). Atlantic overturning: new observations and challenges. *Philosophical Transactions of the Royal Society A: Mathematical, Physical and Engineering Sciences*, *381*(2262), 20220196. https://doi.org/10.1098/rsta.2022.0196

Stendardo, I., & Gruber, N. (2012). Oxygen trends over five decades in the North Atlantic. *Journal of Geophysical Research: Oceans*, *117*(C11), 2012JC007909. https://doi.org/10.1029/2012JC007909

Straneo, F. (2006). Heat and Freshwater Transport through the Central Labrador Sea*. *Journal of Physical Oceanography*, *36*(4), 606–628. https://doi.org/10.1175/JPO2875.1

Sullivan, C. (2016). The North Atlantic Ocean's Missing Heat Is Found in Its Depths. *Eos*, *97*. https://doi.org/10.1029/2016EO047009

Sydeman, W. J., García-Reyes, M., Schoeman, D. S., Rykaczewski, R. R., Thompson, S. A., Black, B. A., & Bograd, S. J. (2014). Climate change and wind intensification in coastal upwelling ecosystems. *Science*, *345*(6192), 77–80. https://doi.org/10.1126/science.1251635

Taboada, F. G., & Anadón, R. (2012). Patterns of change in sea surface temperature in the North Atlantic during the last three decades: beyond mean trends. *Climatic Change*, *115*(2), 419–431. https://doi.org/10.1007/s10584-012-0485-6

Takahashi, T., Sutherland, S. C., Wanninkhof, R., Sweeney, C., Feely, R. A., Chipman, D. W., et al. (2009). Climatological mean and decadal change in surface ocean pCO_2, and net sea–air CO_2 flux over the global oceans. *Deep Sea Research Part II: Topical Studies in Oceanography*, *56*(8–10), 554–577. https://doi.org/10.1016/j.dsr2.2008.12.009

Tanhua, T., & Keeling, R. F. (2012). Changes in column inventories of carbon and oxygen in the Atlantic Ocean. *Biogeosciences*, *9*(11), 4819–4833. https://doi.org/10.5194/bg-9-4819-2012

Toomey, T., Amores, A., Marcos, M., & Orfila, A. (2022). Coastal sea levels and wind-waves in the Mediterranean Sea since 1950 from a high-resolution ocean reanalysis. *Frontiers in Marine Science*, *9*, 991504. https://doi.org/10.3389/fmars.2022.991504

Tréguer, P., Goberville, E., Barrier, N., L'Helguen, S., Morin, P., Bozec, Y., et al. (2014). Large and local-scale influences on physical and chemical characteristics of coastal waters of Western Europe during winter. *Journal of Marine Systems*, *139*, 79–90. https://doi.org/10.1016/j.jmarsys.2014.05.019

Trenberth, K. E., Zhang, Y., Fasullo, J. T., & Cheng, L. (2019). Observation-Based Estimates of Global and Basin Ocean Meridional Heat Transport Time Series. *Journal of Climate*, *32*(14), 4567–4583. https://doi.org/10.1175/JCLI-D-18-0872.1

University of Southampton, Frajka-Williams, E., Bamber, J., & Våge, K. (2016). Greenland Melt and the Atlantic Meridional Overturning Circulation. *Oceanography*, *29*(4), 22–33. https://doi.org/10.5670/oceanog.2016.96

Valencia, V., Fontán, A., Goikoetxea, N., Chifflet, M., González, M., & López, A. (2019). Long-term evolution of the stratification, winter mixing and θ-S signature of upper water masses in the southeastern Bay of Biscay. *Continental Shelf Research*, *181*, 124–134. https://doi.org/10.1016/j.csr.2019.05.010

Varela, R., Álvarez, I., Santos, F., deCastro, M., & Gómez-Gesteira, M. (2015). Has upwelling strengthened along worldwide coasts over 1982-2010? *Scientific Reports*, *5*(1), 10016. https://doi.org/10.1038/srep10016

Varela, Rubén, Lima, F. P., Seabra, R., Meneghesso, C., & Gómez-Gesteira, M. (2018). Coastal warming and wind-driven upwelling: A global analysis. *Science of The Total Environment*, *639*, 1501–1511. https://doi.org/10.1016/j.scitotenv.2018.05.273

Vargas-Yáñez, M., Zunino, P., Benali, A., Delpy, M., Pastre, F., Moya, F., et al. (2010). How much is the western Mediterranean really warming and salting? *Journal of Geophysical Research: Oceans*, *115*(C4), 2009JC005816. https://doi.org/10.1029/2009JC005816

Vargas-Yáñez, M., García-Martínez, M. C., Moya, F., Balbín, R., López-Jurado, J. L., Serra, M., et al. (2017). Updating temperature and salinity mean values and trends in the Western Mediterranean: The RADMED project. *Progress in Oceanography*, *157*, 27–46. https://doi.org/10.1016/j.pocean.2017.09.004

Vargas-Yáñez, Manuel, Moya, F., Balbín, R., Santiago, R., Ballesteros, E., Sánchez-Leal, R. F., et al. (2022). Seasonal and Long-Term Variability of the Mixed Layer Depth and its Influence on Ocean Productivity in the Spanish Gulf of Cádiz and Mediterranean Sea. *Frontiers in Marine Science*, *9*, 901893. https://doi.org/10.3389/fmars.2022.901893

Vargas-Yáñez, Manuel, Moya, F., Serra, M., Juza, M., Jordà, G., Ballesteros, E., et al. (2023). Observations in the Spanish Mediterranean Waters: A Review and Update of Results of 30-Year Monitoring. *Journal of Marine Science and Engineering*, *11*(7), 1284. https://doi.org/10.3390/jmse11071284

Vázquez-Rodríguez, M., Pérez, F. F., Velo, A., Ríos, A. F., & Mercier, H. (2012). Observed acidification trends in North Atlantic water masses. *Biogeosciences*, *9*(12), 5217–5230. https://doi.org/10.5194/bg-9-5217-2012

Vázquez-Rodríguez, M., Padin, X. A., Pardo, P. C., Ríos, A. F., & Pérez, F. F. (2012). The subsurface layer reference to calculate preformed alkalinity and air–sea CO_2 disequilibrium in the Atlantic Ocean. *Journal of Marine Systems*, *94*, 52–63. https://doi.org/10.1016/j.jmarsys.2011.10.008

Vélez-Belchí, P., Hernández-Guerra, A., Fraile-Nuez, E., & Benítez-Barrios, V. (2010). Changes in Temperature and Salinity Tendencies of the Upper Subtropical North Atlantic Ocean at 24.5°N. *Journal of Physical Oceanography*, *40*(11), 2546–2555. https://doi.org/10.1175/2010JPO4410.1

Vélez-Belchí, P., González-Carballo, M., Pérez-Hernández, M. D., Hernández-Guerra. (2015). *Oceanographic and biological features in the Canary Current Large Marine Ecosystem.* Paris, France: IOC-UNESCO. Retrieved from http://hdl.handle.net/1834/9135

Vilibić, I., Denamiel, C., Zemunik, P., & Monserrat, S. (2021). The Mediterranean and Black Sea meteotsunamis: an overview. *Natural Hazards*, *106*(2), 1223–1267. https://doi.org/10.1007/s11069-020-04306-z

Visbeck, M. (2007). Power of pull. *Nature*, *447*(7143), 383–383. https://doi.org/10.1038/447383a

Volkov, D. L., & Landerer, F. W. (2015). Internal and external forcing of sea level variability in the Black Sea. *Climate Dynamics*, *45*(9–10), 2633–2646. https://doi.org/10.1007/s00382-015-2498-0

Von Schuckmann, K., Minière, A., Gues, F., Cuesta-Valero, F. J., Kirchengast, G., Adusumilli, S., et al. (2023). Heat stored in the Earth system 1960–2020: where does the energy go? *Earth System Science Data*, *15*(4), 1675–1709. https://doi.org/10.5194/essd-15-1675-2023

Woodworth, P. L., Melet, A., Marcos, M., Ray, R. D., Wöppelmann, G., Sasaki, Y. N., et al. (2019). Forcing Factors Affecting Sea Level Changes at the Coast. *Surveys in Geophysics*, *40*(6), 1351–1397. https://doi.org/10.1007/s10712-019-09531-1

Wöppelmann, G., & Marcos, M. (2016). Vertical land motion as a key to understanding sea level change and variability. *Reviews of Geophysics*, *54*(1), 64–92. https://doi.org/10.1002/2015RG000502

Yamaguchi, R., & Suga, T. (2019). Trend and Variability in Global Upper-Ocean Stratification Since the 1960s. *Journal of Geophysical Research: Oceans*, *124*(12), 8933–8948. https://doi.org/10.1029/2019JC015439

Zeebe, R. E. (2012). History of Seawater Carbonate Chemistry, Atmospheric CO_2, and Ocean Acidification. *Annual Review of Earth and Planetary Sciences*, *40*(1), 141–165. https://doi.org/10.1146/annurev-earth-042711-105521

Zou, S., & Lozier, M. S. (2016). Breaking the Linkage Between Labrador Sea Water Production and Its Advective Export to the Subtropical Gyre. *Journal of Physical Oceanography*, *46*(7), 2169–2182. https://doi.org/10.1175/JPO-D-15-0210.1

CHAPTER 5

AN UPDATED REVIEW OF REGIONAL ATMOSPHERIC CLIMATE CHANGE OVER SPAIN: MODEL EVALUATION AND PROJECTIONS

Coordinators: Marta Domínguez-Alonso (Tragsatec - AEMET, Sist. Inf. Gest. Doc. y Consult., Madrid, España), Jesús Fernández (Instituto de Física de Cantabria (IFCA), CSIC-Universidad de Cantabria, Santander, España), Sixto Herrera (Departamento de Matemática Aplicada y Ciencias de la Computación, Universidad de Cantabria, Santander, España)

Main authors: Miguel Andrés-Martín[1], Jesús Asín[2], Joaquín Bedia[3,4], Swen Brands[5], Ana Casanueva[3,4], Matilde García-Valdecasas Ojeda[6,7], Albano González[8], Santos J. González-Rojí[9,10,14], Claudia Gutiérrez[11], Alfonso Hernanz[12], Maialen Martija-Díez[13,14], Ángel G. Muñoz[15], Matias Olmo[15], Rubén Vázquez[11], Daniel Argüeso[16], César Azorín-Molina[1], William Cabos[11], Alba de la Vara[17], Javier Díez-Sierra[5], José Carlos Fernández-Álvarez[18,19], Sonia R. Gámiz-Fortis[6,7], Maddalen Iza[13], Juan Carlos Pérez Darias[8], Enrique Sánchez[20]

[1] Centro de Investigaciones sobre Desertificación, Consejo Superior de Investigaciones Científicas (CIDE, CSIC-UV-Generalitat Valenciana), Moncada, Spain

[2] Universidad de Zaragoza, Zaragoza, Spain

[3] Dept. Matemática Aplicada y Ciencias de la Computación, Universidad de Cantabria, Santander, Spain

[4] Grupo de Meteorología y Computación (unidad asociada al CSIC), Universidad de Cantabria, Santander, Spain

[5] Instituto de Física de Cantabria (IFCA), CSIC-Universidad de Cantabria, Santander, Spain

[6] Departamento de Física Aplicada, Universidad de Granada, Granada, Spain

[7] Instituto Interuniversitario de Investigación del Sistema Tierra en Andalucía (IISTA-CEAMA), Granada, Spain

[8] Departamento de Física, Universidad de La Laguna, San Cristóbal de La Laguna, Spain

[9] Climate and Environmental Physics, University of Bern, Bern, Switzerland

[10] Oeschger Centre for Climate Change Research, University of Bern, Bern, Switzerland

[11] Departamento de Física y Matemáticas, Universidad de Alcalá, Madrid, Spain

[12] State Meteorological Agency (AEMET), Madrid, Spain

[13] EUSKALMET, Agencia Vasca de Meteorología, Vitoria-Gasteiz, Spain

[14] Departamento de Física, Universidad del País Vasco (UPV/EHU), Leioa, Spain

[15] Barcelona Supercomputing Center, Barcelona, Spain

[16] Departamento de Física, Universidad de las Islas Baleares, Palma, Spain

[17] Kveloce (Senior Europa S.L.), Valencia, Spain

[18] Galicia Supercomputing Center (CESGA), Santiago de Compostela, Spain

[19] Centro de Investigación Mariña, Environmental Physics Laboratory (EPhysLab), Universidade de Vigo, Ourense, Spain

[20] Facultad de Ciencias Ambientales y Bioquímica, Universidad de Castilla-La Mancha (UCLM), Toledo, Spain

1. Introduction

The impacts of changes in the Earth's climate under the observed global warming have become of critical importance for multiple different socio-economic and environmental sectors around the world. As unprecedented climate hazards have been registered over Spain in recent decades, with severe consequences on societal activities, infrastructure, and human health, there has been increasing research focused on the study of the past and future climate of the Iberian Peninsula (IP) and its surrounding seas (Soares et al., 2023a; Ventura et al., 2023).

Anthropogenic emissions can modify the frequency and intensity of extreme events, such as heavy precipitation, dry spells and Heat Waves (HWs), although natural variability is also a major source of changes in climate (Intergovernmental Panel On Climate Change (IPCC), 2023). The latter is an inherent component of the climate system, whereas human-induced changes are mostly related to emissions of greenhouse gases (GHGs), industrialization, urbanisation, and land-use modifications. Although both natural variability and anthropogenic climate change interact with each other to produce the observed climate, it is important to identify whether the main drivers of the changes in climate are due to natural or human-made causes, as adaptation and mitigation policies are -generally speaking- different depending on the drivers. It is also important to bear in mind that the impact of anthropogenic climate change is different for different climate variables.

For example, a 120-year-long timescale decomposition analysis (Greene et al., 2011) conducted considering the period 1901-2020 over the IP for the winter season helps assess how much of the total variance is explained by the observed long-term anthropogenic climate change signal, the natural inter-decadal variability and the natural inter-annual variability (Figure 5.1). Other seasons exhibit a similar decomposition. While roughly one third of the total variance in surface temperature over the IP is explained by the anthropogenic climate change signal (Figure 5.1c), it explains very little of the precipitation signal (Figure 5.1d). As in many other regions of the world (e.g. Muñoz et al., 2016; Thomson et al., 2018), most of the observed variance in temperature (Figure 5.1g) and precipitation (Figure 5.1h) over the IP is dominated by the natural inter-annual variability signal. This analysis implies that natural variability must always be considered when studying climate impacts, in addition to the anthropogenic (or greenhouse-forced) climate change signal. Furthermore, the timescale decomposition analysis can be conducted to diagnose how well climate models represent the observed explained variance for each timescale, and identify biases in related physical processes; to the best of the authors' knowledge– this model diagnostic approach has not been explored in the literature yet.

The use of climate simulations is key to understanding the complexity of the climate system and its variability throughout the past and future periods. For example, Fernández-Montes et al., 2017 studied the covariability of precipitation and temperature for the long period of 1001-2099 using model simulations, finding that a positive phase of the Atlantic Multidecadal Variability (AMV) was related with a negative correlation between precipitation and temperature, meaning a warm-dry regime. In this sense, Global climate models (GCMs) are essential tools that numerically model the climate system and provide outputs globally for different scenarios. Individual GCMs are developed and improved over decades to replicate global climate processes with as much accuracy as possible. However, the GCMs computational grid resolution is often not enough to describe some regional phenomena that are parametrized and often misrepresented, including sub-grid processes and extreme events (Meehl et al., 2020).

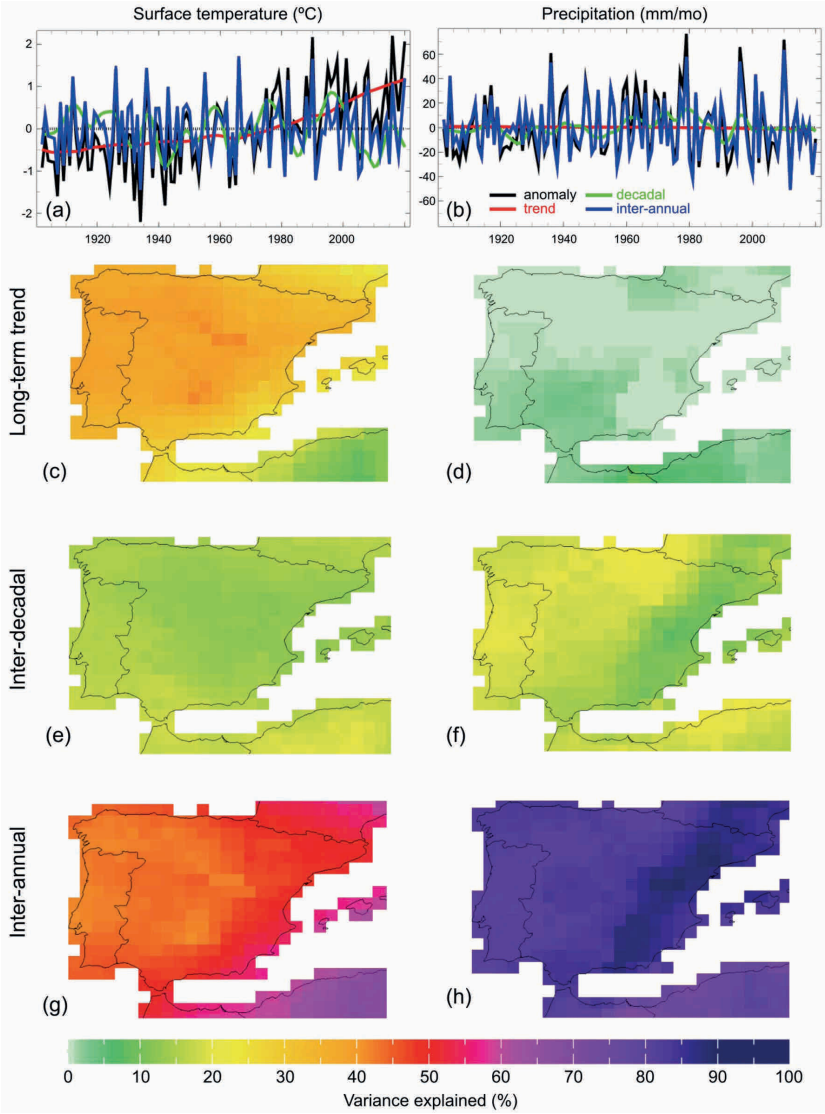

Figure 5.1: Timescale decomposition of observed time series for surface temperature (a) and precipitation (b), averaged over the IP. The original (observed) time series (black) are decomposed in terms of a superposition of the long-term non-linear trend (red), the inter-decadal signal (green) and the inter-annual one (blue). Spatial maps exhibiting the variance explained by the long-term trend (c,d), the inter-decadal signal (e,f) and the inter-annual signal (g,h) are also included. Source: International Research Institute for Climate and Society (IRI) Timescale Decomposition Maproom[1].

[1] https://iridl.ldeo.columbia.edu/maproom/Global/Time_Scales/index.html

In this sense, the Coupled Model Intercomparison Project (CMIP) encompasses a large ensemble of global simulations for a variety of past and future scenarios (Eyring et al., 2016). For the 21st century, the latest CMIP6 ensemble provides multiple shared socio-economic pathways (SSPs), that describe plausible storylines of global societal developments in the context of climate change, reflecting the difficulty and challenges of implementing mitigation or adaptation responses based on societal features such as demographic changes and technical developments (IPCC, 2023).

There is a need to gain insight into the sensitivity of the regional and local features of climate variability and change, which enables us to better describe the processes and forcing mechanisms responsible for regional climate conditions. In this sense, the scientific community has made significant efforts to obtain higher-resolution information, which is needed for impact modelling and decision-making. This is done by means of dynamical or statistical downscaling strategies, using regional climate models (RCMs) and empirical statistical downscaling (ESD) methods. Although both have their different skills and limitations, they have demonstrated capabilities to simulate the main regional climatic features (Casanueva et al., 2016; Gutiérrez et al., 2019; Hernanz et al., 2022; Vautard et al., 2021).

Other techniques to reduce the gap between GCMs and local information include bias adjustment (BA) procedures, which typically consist of scaling climate model outputs to account for their systematic errors (Maraun, 2016). Furthermore, the importance of process-based understanding and model evaluation can ascertain our confidence in future climate projections. This issue can be addressed by a variety of constraints, weighting methods and storyline approaches to be applied into large model ensembles (Palmer et al., 2023; Shepherd et al., 2018). All of these are essential tools employed in multiple research studies —that were considered for this report– devoted to understanding the registered and expected projections of different climate hazards.

The last CLIVAR-Spain review of regional atmospheric evaluation (Montávez et al., 2017) and future projections (Fernández et al., 2017) consisted of brief overviews of existing studies, which were published in a Special Issue of CLIVAR Exchanges (Sánchez et al., 2017). They were mostly based on information from the ENSEMBLES (Déqué et al., 2012), ESCENA (Domínguez et al., 2013), esTcena (Gutiérrez et al., 2013), VALUE (Maraun et al., 2015) and EURO-CORDEX (European branch of COordinated Regional Climate Downscaling EXperiment, Jacob et al., 2020a) initiatives. Quantitative future projections were mostly restricted to seasonal mean precipitation and temperature, where a comprehensive set of uncertainties could be covered for dynamical downscaling (DD, Fernández et al., 2019) using EURO-CORDEX data, which were matched by four different statistical downscaling methods. Amblar Francés et al., 2017 provide a detailed and consistent guideline for future climate change scenarios over Spain exploiting these data.

This chapter describes the state-of-the-art literature on future projections of different atmospheric variables covering Spain based mostly on global simulations from the CMIP5 and CMIP6 initiatives, and regional assessments considering RCMs from the CORDEX (COordinated Regional Climate Downscaling EXperiment) initiative (Carvalho et al., 2022; Coppola et al., 2021a; Cos et al., 2022; Vautard et al., 2021) and ESD models, including brand-new deep-learning methods (Baño-Medina et al., 2020, 2021, 2022; Hernanz et al., 2024; Soares et al., 2023a). In parallel to this literature review, the *Escenarios-PNACC 2023* initiative, led by State Meteorological Agency (AEMET), collects and harmonises data to provide a new set of comprehensive regional climate change scenarios to feed the different sectors, systems and resources covered by the Spanish *Plan Nacional de Adaptación al Cambio Climático (PNACC)*.

The chapter is structured with an initial section gathering the common methodological framework followed in most of the studies considered, along with common data sources. The rest of the chapter is devoted to sections focused on the future projection of different variables, followed by a section dedicated to multi-variable indices. The final section is devoted to regions of special interest, which deserve a separate treatment due to their peculiarities: the Canary Islands and mountain regions. At the end of each section, we gather knowledge gaps identified during the review and areas where more research is needed.

2. Methodology and data sources

In the following sections, the key advances in regional climate projections for Spain are summarised by variable, and also focusing on regions of special interest, such as mountain areas or islands. Many of these advances rely on new climate datasets that have become available in recent years. A brief summary is provided next by source.

The main source of future climate information are GCMs, which can simulate the response of the climate system to different forcings. GCM simulations from virtually all existing models are organised internationally in the CMIP, which feeds the Intergovernmental Panel for Climate Change (IPCC) assessment reports. The last cycle, CMIP6, includes the newest GCM generation, mostly composed of Earth system Models (ESMs), which simulate a broad range of processes and capture the complex dynamics of the entire Earth system, including the carbon cycle, biogeochemical cycles, and interactions between different components (Bonan and Doney, 2018).

CMIP6 provides simulation outputs for a wealth of activities (Eyring et al., 2016). The most relevant activity to project the future climate is ScenarioMIP, which considers transient global simulations forced by the main SSPs (Riahi et al., 2017). In combination with concentrations of long-lived GHG from the Representative Concentration Pathways (RCPs), these new sets of scenarios provide model forcings representing alternative socio-economic developments, ranging from sustainable development to fossil-fueled development. Historical simulations in the CMIP experiment, driven by observed natural and anthropogenic forcings, are also crucial for establishing a reference for future projections. ScenarioMIP simulations branch off the historical simulation from 2015 on. Thus, CMIP6 scenarioMIP simulations provide all climate variables for the present century and beyond, with global coverage, and for a set of about 60 different models. This allows us to explore model uncertainty in the projections. Moreover, each model, forced by the historical forcing and a given SSP, is run under different initial conditions to generate different ensemble members that account for internal model variability, resulting from unforced natural variability in the coupled system.

CMIP6 GCMs have spatial resolutions of about 100 km, insufficient to resolve many local and regional features (coastlines, small orographic barriers, lakes, islands, etc.) which modulate regional climate. The process of downscaling refines the coarse output of GCMs to account for these regional features. DD is usually based on RCMs, which reach grid spacings of ~10-50 km over a limited area. RCMs are nested, generally one-way, within the GCM, which provides boundary conditions for the simulation. In CMIP6, alongside scenarioMIP simulations, the High Resolution Model Intercomparison Project (HighResMIP) experiment produced global high-resolution (~25-50 km grid spacing) simulations (Haarsma et al., 2016a), to assess the impact of enhanced horizontal-resolution in global simulations. This experiment has reached the resolution of DD approaches, and could therefore be used in combination with them to produce regional climate scenarios (Demory et al., 2020a). Other forms of DD use GCMs with unstructured or stretched computational grids,

which have variable resolution, increasing over a target region. Such grid-refinement techniques have not been applied recently over Europe, though.

ESD consists of training statistical models to exploit the relationships between large-scale climate features, well represented by GCMs, and the regional climate. ESD models are trained from reanalysis data and local observations, and applied to the large-scale climate produced by a GCM. Classical ESD methods can be based on regression-type models, analog procedures, weather generators (WG) or combinations of them. There are comprehensive comparisons of these methods over Europe (Gutiérrez et al., 2019) and also specifically over Spain (Hernanz et al., 2022c, b, a). Machine learning techniques are also used for ESD (Baño-Medina et al., 2020, 2021, 2022; Hernanz et al., 2023a; Soares et al., 2023a) and to build emulators of RCMs (Doury et al., 2023), which can potentially be used to alleviate the burden of DD, although their transferability to downscale different GCMs is a matter of debate (Baño-Medina et al., 2023; Hernanz et al., 2024).

Downscaling provides climate data at fine scales, but also introduces additional uncertainties as a result of the different approaches available and the different models within each approach. Thus, individual research efforts can hardly cover all uncertainties involved in the generation of regional climate information. CORDEX aims at providing historical and future climate projections at high resolution for a set of 14 domains worldwide (Gutowski et al., 2016). Downscaling activity is thus coordinated within and across regional communities in the different domains. The EURO-CORDEX community (Jacob et al., 2020b) provided simulations based on DD from CMIP5 at two resolutions: EUR-44 with a standard resolution of 0.44º (~50 km) and EUR-11 with a higher-resolution, at 0.11º grid spacing (~12.5 km). The upcoming CORDEX experiments for the DD of CMIP6 (CORDEX-CMIP6) are targeted to provide a grid spacing of 12.5 km (0.11º) over Europe (Katragkou et al., 2024) with a balanced scenario-GCM-RCM combination matrix (Sobolowski et al., 2023).

A key uncertainty source in dynamical models (GCMs and RCMs) is the parameterization of unresolved processes, which occur at spatial scales smaller than their computational grid cells. Parameterizations model the effect of these subgrid processes (radiation, turbulence, cloud microphysics, etc.) on the model resolved variables. Parameterizations have a sound physical background, but can only represent statistically these subgrid processes. A particularly uncertain subgrid process is deep convection, which strongly modifies the vertical moisture and heat profiles, and can produce large precipitation amounts, which are key for impact assessments. As model resolution increases beyond a few kilometres, convective cells can be explicitly resolved and the deep convection parameterization can be switched off. Such convection-permitting RCMs (CP-RCMs) operate at grid spacings below 4 km and are particularly useful for impact studies, as local precipitation triggering and amounts are improved with respect to standard RCMs (Lucas-Picher et al., 2021). CP-RCM simulations cannot be extensively afforded yet at continental scale, but have been carried out as part of more focused CORDEX Flagship Pilot Studies (Coppola et al., 2020). None of the CORDEX Flagship Pilot Studies (CORDEX-FPS) to date cover the Spanish territory, though. Alternatively, there are several individual CP-RCM efforts (see Table 5.1), especially over the Canary Islands.

The Earth System Grid Federation (ESGF) is an international collaboration to develop and maintain the software infrastructure that allows for the management and open access of large-scale climate science data such as reanalysis products, model simulations and satellite observations. ESGF supports, among other projects, the data services of CMIP and CORDEX. CORDEX data are also available through other services, such as impact portals (https://climate4impact.eu) and other visualisation portals (Table 5.2), that can combine CORDEX data with other downscaling efforts, such as ESD.

Data set	Type	Period	Region (res.)	Reference	Availability
CMIP6 (BCCAQ)	Scen(3)-GCM(18)-BA	2015-2100	Global (0.25º)	Gebrechorkos et al. (2023)	Open CEDA
HighResMIP CMIP6	Tiers (3)-GCM(19-Tier 1)	2015-2050(2100)	Global (25-50 km)	Haarsma et al., 2016	Open CEDA
EURO-CORDEX	Scen(3)-GCM(8)-RCM(14) ensemble	1950-2100	Continental Europe (12.5 km)	Jacob et al. (2020)	Open ESGF
	Scen(2)-GCM(3)-RCM(1) ensemble		Canary Islands (3 km)	González et al. (2023a, 2023b, 2023c)	Open ULL repository
EUCP CAN-1	PGW	2006-2015 2106-2115	Canary Islands (1.1 km)	Gao et al. (2023)	On request (to appear on ESGF)
	Scen(3)-GCM(1)-RCM(1) ensemble	2010-2014 2049-2053 2093-2010	North Atlantic and Europe (20 km)	Fernández-Álvarez et al. (2023a,b)	On request
DeepESD-EE	Scen(1)-GCM(8)-ESD(1) ensemble	1975-2100	Europe (50 km)	Baño-Medina et al. (2022)	Open ESGF
ESGCM-DL	Scen(4)-GCM(7)-MME(1)	1981-2010 2015-2040 2041-2070 2071-2100	Iberian Peninsula (0.1º)	Soares et al. (2023a)	The DL configuration is available upon request
	Scen(1)-GCM(1)-RCM(1)	1995-2014 2046-2065 2081-2100	Portugal (6 km)	Claro et al. (2023)	On request
WorldCLIM	Scen (4) - GCM (23) - Delta Method	1971-20002021-2040 2041-2060 2061-20802081-2100	Global Land Areas (1 km)	Fick and Hijmans, (2017)	Worldclim (https://www.worldclim.org/)
AEMET-rejilla	Scen (3) - GCM (24) - ESD (3)	1961-2100	Iberian Peninsula and Balearic Islands (0.05º)	Amblar-Francés et al. (2017)	Open AEMET repository
AEMET-estaciones	Scen (3) - GCM (24) - ESD (3)	1961-2100	Spain (stations)	Amblar-Francés et al. (2017)	Open AEMET repository

Table 5.1: Data sources considered in this chapter. For each data set, the data type and uncertainties considered, the time span, regional coverage and resolution, main references and availability are displayed in columns.

Data viewer	Data Source	Type	Period	Region (res.)	Availability
AdapteCCa – Visor de Escenarios de Cambio Climático	EURO-CORDEX / AEMET (ESD)	Scen(2)-GCM(6)-RCM(7) / Scen (3) - GCM (24) - ESD (2)	1971-2000 2011-2040 2041-2071 2071-2100	Peninsular Spain, Balearic Island (10 km) / Spain stations	Open (THREDDS catalog)
Geoportal Observatorio Pirenaico de Cambio Climático (OPCC)	EURO-CORDEX	Scen(2)	2030 2050 2070 2090	Pyrenees (10 km)	Open
Escenarios climáticos de Euskadi y series de datos	EURO-CORDEX	Scen(2)-GCM(5)-RCM(4)	1971-2000 2011-2040 2041-2071 2071-2100	Basque Country (1 km)	Open (THREDDS catalog)
Aplicación de descarga y visualización de escenarios climáticos regionalizados para Andalucía	CMIP5	Scen(2)-GCM(4)	1961-2000 2011-2040 2041-2070 2071-2099	Andalucia (200 m)	Open
Sistema de Información para la Gobernanza Climática en Canarias	CMIP5	RCM	1980-2009 2030-2059 2070-2099	Canary Islands (3 km)	Open
Copernicus Interactive Climate Atlas	CORDEX, CMIP5, CMIP6	GCM, RCM	1850-2100	Global	Open

Table 5.2: Web portals providing visualisations of climate data for future projections over Spain.

Models have biases, that is, deviations from the observed climate. They are useful tools trying to represent as many relevant processes as possible but, still, they cannot perfectly represent the climate system. In particular, GCMs have biases that can also propagate through the downscaling process. In order to separate the biases of the GCM from those of the downscaling step, it is customary to perform evaluation simulations, nested into reanalysis, as a surrogate for the observed large scale conditions. With these perfect boundary conditions for RCMs, or input fields for ESD, the resulting biases can be ascribed to the downscaling method. Historical GCM simulations allow us to assess the combined biases of the GCM and downscaling model.

Biases can be quite large, and need to be adjusted before future regional climate projections can be interpreted, especially for climate indices derived from absolute thresholds (Dosio, 2016). The simplest adjustment consists of considering only future changes (delta method or delta changes) with respect to a given reference climate period. This assumes that models that tend to be e.g. too warm or too rainy will keep that behaviour in the future, and these biases will cancel out in the delta. However, potential changes in the temporal structure that might be simulated by the models are disregarded by delta change (e.g. possible changes in the overall interannual variability or in extremes) since the simulated time series mimics the temporal structure of the observations. The alternative is BA, which typically adjusts some features of the model distribution towards the observed counterparts. As a result, systematic model errors are partly removed. There is a large variety of BA methods (Gutiérrez et al., 2019), either empirical or parametric, either adjusting the mean, some percentiles or all quantiles. Empirical Quantile Mapping (EQM) is one of the most widely used and best-performing BA and ESD methods in evaluation experiments (Gutiérrez et al., 2019; Hertig et al., 2019). EQM consists of matching the simulated and observed distributions by establishing a quantile-dependent transfer function in the control period, which is applied to the modelled distribution in a target period. By construction, it is able to correct for intensity-dependent biases (i.e. biases that change throughout the distribution) and as a consequence, it can modify the raw model climate change signal, which is debatable (Casanueva et al., 2018). More advanced BA methods try to preserve other properties, such as trends, extremes or multivariable relationships. As BA methods become more complex by adjusting more features, they become also more sensitive to the observational dataset used to calibrate the correction function (Casanueva et al., 2020b).

Downscaling and impact models can be costly to run. In principle, uncertainties are assessed by means of ensembles with members exploring different GHG concentration pathways, GCMs, GCM initializations, etc. An alternative to the downscaling of historical plus scenario simulations with different GCMs is the pseudo-global warming (PGW) approach (Brogli et al., 2023). PGW takes advantage of the evaluation simulation nested into reanalysis and considers it also as historical reference simulation. This is done by performing the future run nested into boundary conditions consisting of the daily variability of the reanalysis and adding a monthly-varying delta-change signal. This signal can come from a single or from several GCMs together. This approach is more appropriate for annual or seasonal changes, but less adequate for the study of certain extreme phenomena.

Another way to alleviate the cost of internal variability and scenario uncertainty is to use average global surface air temperature (GSAT) as an analysis dimension instead of time, taking advantage of the monotonic relation of these variables under global warming (Díez-Sierra, et al., 2024; Seneviratne and Hauser, 2020). Different models and model realisations reach different global

warming levels (GWLs) at different times, also depending on the scenario. The GWL approach focuses on particular GSAT increase targets (e.g. +1.5 ºC or +2 ºC) regardless of when these targets are reached by different model realisations or scenarios. These GWLs can then be translated to other variables or to particular regions. Moreover, since the changes with respect to this variable are relatively linear, rates of change are also meaningful (e.g. a summer decrease of precipitation of -7% per ºC of global warming).

As a final remark before proceeding to the literature review in the next sections, we would like to have a word of caution regarding specific figures provided next, e.g. referring to a particular increase of a variable in the future. These figures are highly dependent on the future period we are considering (oftentimes we will just refer to the near-, mid- or far-future) and also to the period used as baseline climate reference to compute the delta change. The scientific community is far from adopting a standard set of periods for the assessment of future climate change. As an illustrative example, benefiting from the extensive literature database collected for this chapter, Figure 5.2 shows the variety of periods considered in the studies of this database. Therefore, we encourage the interested reader to refer to the original sources cited for detailed information behind the actual figures and also to resort to the ever-increasing set of web portals exploiting the existing projections (see Table 5.2) to obtain particular estimates of future changes. Some of these portals (e.g. the Copernicus Interactive Climate Atlas) provide a choice of reference baselines, to adapt to the user needs.

3. Climate variables evaluation and projections

3.1. Temperature

Systematic biases in the direct temperature output of climate models hamper their direct use in impact studies at local or regional scale, in particular when extreme events are the focus. That situation was identified in CMIP5 GCMs (Brands et al., 2013), holds valid in CMIP6 and, at some point, it is inherited by the RCMs of CORDEX (Coppola et al., 2021a). CMIP6 GCMs capture the observed changes in extreme indices and HWs over the second half of the 20th century, although with some tendency to overestimate the magnitude of trends in hot days (Barriopedro et al., 2023). The skill of GCMs in representing temperature extremes varies with the season, region, reference data set and extreme index, yielding lower spatial pattern skill scores for duration and percentile indices. In general, there is a better representation of absolute and threshold indices in the tropics, and of percentile indices in the extratropics (Barriopedro et al., 2023).

The IP has been identified as a hotspot of projected temperature extremes (Cos et al., 2022; Lionello and Scarascia, 2018). The Mediterranean region (10º W, 40º E, 30º N, 45º N; Iturbide et al., 2020) shows a higher annual temperature increase than the global mean, with highest amplifications obtained over the IP in summer (1.6 times higher than the global-mean warming, Cos et al., 2022). Vautard et al., 2023 estimated summer daily maximum temperature trends for 1950-2022, and found that warming trends for “the 20° × 10° western Europe region has the highest TXx (Maximum Annual Temperature) trend of all regions of the same size around the globe between 75°S and 75°N shifted by steps of 5° (including sea points).” The work also found that historical simulations of 32 GCMs do

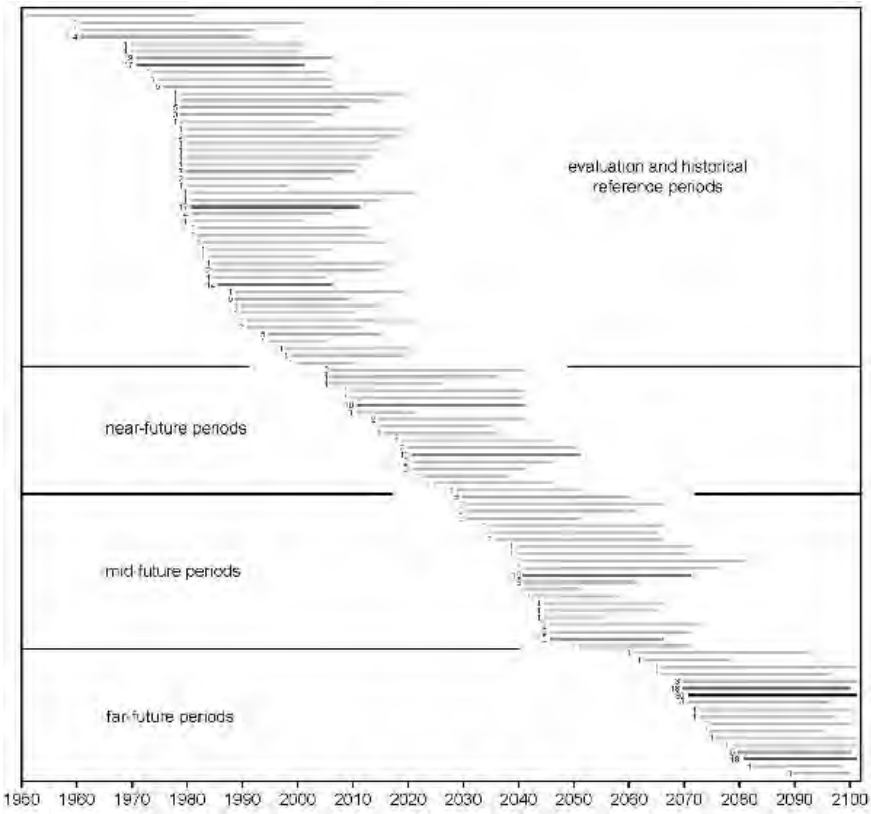

Figure 5.2: Time periods used as baseline climate reference and future targets in the studies considered in the chapter. Only periods with lengths between 10 and 40 years are included in the Figure. They are sorted by start year and then by decreasing period length. The number of studies using a given period are indicated on the left of the line corresponding to the period. Darker shades of grey identify the periods most commonly used.

not show circulation-induced heat trends as large as observed, explaining that "over the last 70 years, extreme heat has been increasing at a disproportionate rate in Western Europe, compared to climate model simulations". Then the future summer heat in GCM projections for IP could be conservative.

GCMs have a coarse spatial resolution (~100s of km) that limits their application on regional analysis, and higher-resolution information is obtained by downscaling the GCMs with RCMs – typically ~12 – 50 km resolution, but over a limited area of the Earth (e.g. Europe), and/or ESD. In the framework of CMIP6, a new experiment HighResMIP (Haarsma et al., 2016b) was defined to improve, compared to existing lower-resolution models, the process

representation in all components of the climate system, considering global simulations, but at spatial resolutions typically considered by RCMs (~ 25-50 km), and improving the different model's components to better represent processes and high-impact extreme events. Using these simulations Squintu et al., 2021 found that low resolution (LR) models present similar patterns in the trend biases than the high resolution (HR) models over Iberia, and that the reproduction of trends of warm extremes with HR has not considerably improved the LW over Europe for most of the models.

DD methods are able to generate, considering the GCM as boundary conditions, regional physically-consistent projections for a suite of climate variables; particularly for those less affected by model parametrization. Different uncertainties affecting numerical simulations have been considered in the last decade: the spatial resolution has been continuously increasing, from the 0.12º of CORDEX to the current convection-permitting (~3 km) resolution (e.g. Pérez et al., 2022; Solano-Farias et al., 2024); the integration domain can also change as the IP is located in the intersection of the European, African, Mediterranean and the middle east North Africa CORDEX domains (Driouech et al., 2020; Legasa et al., 2020); as a Peninsula surrounded by two very different water masses, it could be relevant the air-sea coupling considered for the simulation (De La Vara et al., 2021; Falquina et al., 2022); the observational uncertainty of the models' evaluation has been also considered (Herrera et al., 2020).

Despite the spatial resolution, DD may still suffer from relevant biases (Careto et al., 2022; Casanueva et al., 2020b; Coppola et al., 2021a) which require statistical post-processing before they can be used in impact applications (Gutiérrez et al., 2019). The European COST Action VALUE (http://www.value-cost.eu/, Maraun et al., 2019; Rössler et al., 2019), in which several Spanish research groups were involved, considered the state-of-the-art methods of ESD, that can be classified according to the nature of predictors in the training phase (PP: Perfect Prognosis; MOS: Model Output Statistics, including BA and WG: weather generators), and made a systematic validation of their properties assessing the temporal and spatial variability, the extreme events, spatial coherence and variability, and inter-variable consistency. In particular, the open software R packages climate4R (Iturbide et al., 2019) and downscaleR (Bedia et al., 2020) have been developed by CSIC-Universidad de Cantabria group, following the FAIR (Findability, Accessibility, Interoperability and Reusability) principles (Iturbide et al., 2022a), to facilitate the procedure of statistical downscaling to local or regional scales. As a result of the effort of this scientific community, statistical methods have been discussed in the Working Group I contribution to the Sixth Assessment Report of the Intergovernmental Panel on Climate Change (IPCC-AR6-WGI, IPCC 2023, Section 10.3.3.7), concluding that there is a high confidence on that "statistical downscaling methods with carefully chosen predictors and an appropriate model structure for a given application realistically represent many statistical aspects of present-day daily temperature and precipitation" and "BA has proven beneficial as an interface between climate model projections and impact modelling in many different contexts", although these last methods, their relevance and limitations are extensively discussed in the Cross-Chapter Box 10.2. In addition, the ESD methods have been included as another "domain" of CORDEX (Gutowski Jr. et al., 2016, https://cordex.org) to contribute to the climate change projections obtained with those methods.

Model evaluation

Although the representation of the HWs has improved from CMIP5 to CMIP6, capturing, with some tendency to overestimate the magnitude of trends in hot days, the observed changes in extreme indices and HWs over the second half of the 20th century, there have been limited additional improvements in mean biases or model spread (Barriopedro et al., 2023). Ossó et al., 2023 also found a warm bias in southern Europe in summer, that could be related with differences over the North Atlantic, whilst in winter, the bias seems to be related with the continentality. Also the trend for both observations and GCMs, reflect that the IP and Balearic Islands have experienced unusual temperatures during the last decade in comparison with the 20th Century. This warming has also affected the seasons' length (Wang et al., 2021), with the summer/winter length extended/shortened at an average rate of 4.2/2.1 days every 10 years, strengthening the seasonality near the Mediterranean region since the 1950s.

On the other hand, considering the multi-model ensemble (MME) of the multi-decadal experiment of CMIP6, De Luca et al., 2023, conclude that constraining decadal variability in climate projections can improve the prediction of temperature extremes for the next 20 years.

Most of the studies considering RCMs have considered the European domain of CORDEX. As the IP is included in several CORDEX domains, Legasa et al., 2020 analysed, for some precipitation indices, this uncertainty source, reflecting that, although the contribution of the domain alone is nearly negligible (below 5% in all cases), for some cases (index and region) the combined domain/model effect reach up to 40% of the total variance, opening the window of to enlarge the ensemble of a particular domain using as proxies additional GCM-RCM runs from an overlapping domain. Driouech et al., 2020 considered the middle east and north Africa, finding some cold biases over the IP but capturing reasonably well several climate extreme indices. Several authors (Cabos et al., 2020; De La Vara et al., 2021; Falquina et al., 2022) analysed the effect on the regional climate of the ocean-atmosphere coupling, finding, for the period 1976-2005, some shifts of regional climate to hotter and drier conditions in summer. Changes in winter were lower than in summer, mainly associated with the orographic pattern and mostly affecting the minimum temperature, but also with a positive bias, excepting the area surrounding Sierra Nevada with a slight cold bias. Herrera et al., 2020 considered different types of observations over the IP to evaluate an ensemble of RCMs of EURO-CORDEX and analyse the observational uncertainty of the results obtained for several indices reflecting the mean and extreme regimes. RCMs are able to reproduce the spatial pattern and the variability observed in the IP. The observational uncertainty increases when extremes are considered with the main contribution of the observations found for the lower (MAE01 - Mean Absolute Error of the 1st percentile) and upper (MAE99 - Mean Absolute Error of the 99st percentile) percentiles. Considering a large ensemble of EURO-CORDEX, Vautard et al., 2021 made an extensive evaluation of the RCMs. A strong dependence of the bias from the RCM was obtained for minimum temperature. Mean and maximum temperatures present a similar behaviour with biases ranging between -3.4 ºC and 1.2 ºC in winter and between -4 ºC and 1.5 ºC in summer. For TXx, as well as for mean summer temperature, a general cold bias has been found over the IP. The number of days with maximum temperature exceeding 35°C (TX35) has a low median bias over

the IP. For TNn (Minimum Annual Temperature), median biases are moderate and do not follow the mean winter temperature bias patterns, while extreme biases reach more than 5°C in absolute values. Cold extremes were decreasing, being more relevant the decrease in the main mountain systems of the IP. Regarding the number of cold wave days, the reduction found was larger in the east of the Peninsula and also over the mountain systems where the trend (-2 days/decade) was almost twice the trend for the whole domain (-1.3 days/decade). In order to increase the spatial resolution over Canarias, Pérez et al., 2022 considered a WRF-based ensemble of convection-permitting simulations. Despite the high spatial and temporal resolution of the models, a bias, even when the simulations are driven by reanalysis data, is obtained for maximum (2.6 ºC) and minimum (2.1 ºC) temperatures, which increases for the 20-year return value (2 ºC on average) reaching 2.9 ºC and 4.2 ºC for the highest stations (Izaña and Tenerife Norte). From the ensembles, the one driven by MIROC was the one fitting best the observations.

Gutiérrez et al., 2019 summarised the results of an ensemble of over 50 ESD methods produced within the VALUE framework, which covers the three common downscaling approaches (PP, MOS including BA and WGs). For temperatures, most of the downscaling methods greatly improve model biases and no downscaling approach or technique seems to be superior in general. Recently, Baño-Medina et al., 2020 extended the VALUE approach to deep learning techniques. They used deep convolutional neural networks (CNNs) and, although the added value is limited for temperature extremes, these techniques outperform classic techniques, mainly for precipitation, and they could be applied to large regions (e.g., continents), fostering their use in international initiatives such as CORDEX (Baño-Medina et al., 2022). Moreover, recent explainable artificial intelligence (XAI) techniques provide insights into the physical consistency of these deep learning models (González-Abad et al., 2023) and allow to discern plausible models by studying the predictor selection (Baño-Medina et al., 2023). Hard physical constraints can also be applied to deep learning techniques to guarantee physical consistency in cross-variable relationships (González-Abad et al., 2023).

Focusing on the IP, Casanueva et al., 2020 analysed the uncertainty linked with ESD, using daily precipitation and temperature data. The sensitivity to the observational reference used to calibrate the method and the effect of the resolution mismatch between model and observations were assessed on the climate change signal of temperature and precipitation considering marginal, temporal and extreme aspects. Observational gridded datasets were used, the E-OBS v19e (Cornes et al., 2018) and the Iberia01 (Herrera et al., 2019) covering the IP, and the GCM EC-EARTH (r12i1p1) from CMIP5. The R package climate4R was applied to use different ESDs methods, quantile mapping, empirical, parametric, Generalized Pareto parametric, and others with trend-preserving features. For temperature, two extreme indices are considered, maximum number of consecutive days with maximum daily temperature (Tx) >90th percentile and Tropical nights (days with minimum temperature (Tn) >20°C). Standard quantile mapping methods yield warmer future conditions, but with no physical mechanisms justifying the signal increase. All methods tend to increase the raw model signals, and to a larger extent when Iberia01 is used as reference. They conclude that the choice of trend-preserving methods is recommended in general applications of BA to postprocess model outputs since they are conservative methods.

Regarding the projections of extremes, some efforts have been developed by Spanish groups in the VALUE project. Hertig et al., 2019 focused particularly in evaluation of ESD methods to downscaling of extremes, and they found that methods using parametric distributions require non-standard distributions to correctly represent marginal aspects of extremes, because a Gaussian distribution for temperature tend to misrepresent extreme values. There is no optimum downscaling method for all aspects of extreme events; depending on the specific phenomenon of interest an appropriate method needs to be chosen.

The research activities of AEMET includes evaluation of statistical downscaling methods. Hernanz et al., 2022c compared 5 ESDs for maximum and minimum daily temperatures: analog, Multiple Linear Regression, Artificial Neural Networks, Support Vector Machines and Kernel Ridge Regression. Tx and Tn came from the ROCIO_IBEB high-resolution 5 km grid (Peral García et al., 2017) consisting of 16,156 points over Spain, and predictors from ERA-Interim with spatial resolution of 1.5° x 1.5°. Comparisons were based on 3 indices: mean value, 10^{th} and 90^{th} percentiles. The improvements of performing any type of downscaling are clear, due to mean values being satisfactorily represented, with biases generally below 0.5°C. Biases are, in general, lower and more spread out for regression and analog. For all methods, biases for the lower tail of the Tx distribution are generally larger than for mean values, with a strong overestimation in winter for the lower tail of Tn distribution, where all methods show biases concentrated around almost +1°C, probably related to thermal inversions. Additionally, the pyClim-SDM has been developed (Hernanz et al., 2023b), approaches based on quantile mapping, analog, weather generator, machine learning algorithms and regression models are implemented. Some restriction of this software is that selection of predictors is linked to the nearest grid point of climate models.

Efforts to analyse extreme events have appeared considering that the effects of those types of events require daily projections at a local spatial scale, such as health studies linked to heat extremes in big cities. Heatwaves occur increasingly in most regions worldwide (Perkins-Kirkpatrick and Lewis, 2020), and this fact is observed in the IP (Díaz-Poso et al., 2023a), and in Spanish cities (Abaurrea et al., 2018) for daytime, nighttime and compound (Tx and Tn) HWs that increase in frequency and in the ratio of compound type to total number of all types. In order to obtain projections, some studies have been based on direct GCM output (Barriopedro et al., 2023; Lorenzo et al., 2021; Molina et al., 2020). Also specific ESD methods for extreme temperatures, HW or similar extreme events have been developed, Abaurrea et al., 2018 used statistical models to represent daily occurrences of extreme events in Tx, Tn and compound simultaneous extremes, based on non-stationary Poisson processes, using regression-type models the rates of occurrences of excesses over threshold are estimated. as functions of time and temperature related covariates.

Predictors for ESD methods applied to temperature are selected from grids using temperature, humidity, geopotential height, zonal and meridional wind speed, at 850, 700, 500 hPa, generally using anomalies (Amblar-Francés et al., 2020; Baño-Medina et al., 2022; Soares et al., 2023a). Information about the evolution of the climate signal summarised using aggregated monthly mean for example, is also included as predictors (Abaurrea et al., 2018).

Verifications of non-extrapolation conditions must be considered in the statistical procedures. Abaurrea et al., 2018 checked both marginal and multivariate extrapolation

conditions in each future trajectory, all the predictors in a day must be lower than their corresponding maxima in the fitting data, and the Mahalanobis distance of the predictor vector must be lower than the maximum ones in the fitting sample. When the percentage of days not projected in a trajectory is greater than 25%, it is removed from the analysis, then the statistical procedure was not usable in some inner stations for RCP 8.5 and also for 2041-60 for RCP 4.5. Iturbide et al., 2022b could not use quantile mapping method to project temperature in RCP 8.5 because it is affected by extrapolation problems for the outlying values of the latest percentile.

Climate change projections

Different hot extremes indices have been used specifically over Spain, but similar results are reached about the underlying extremes. Lorenzo et al., 2021 analyse 2021–2050 heatwave projections in the IP. The median value during 1971–2000 is around 23 days of HWs, but the EURO-CORDEX ensemble median number predicts 44 days in RCP 4.5, and 50 days in RCP 8.5, i.e., an overall positive trend of 6.4 and 7.6 days/decade in the RCP 4.5 and RCP 8.5 scenarios, respectively. The spatial extent of HWs will almost double in RCP 8.5 for 2021–2050, and the average duration of HWs over 10 days appears on practically the whole peninsula, except for the Atlantic coast, where durations are between 6 and 7 days. A spatial analysis of the trend of the annual number of heatwave days shows that the highest values are located in the Pyrenees, inland and south of the IP.

Amblar-Francés et al., 2020 generated projections for 21st century for Tx and Tn over the Pyrenees region, using a 5 km × 5 km grid and 24 CMIP5 models, with historical, RCP 4.5, RCP6.0, RCP 8.5 scenarios. Results about 17th and 83rd percentiles and number of warm days (WD), warm night (WN) and warm spell duration (WSDI). An increase of WD and WN is especially noticeable at the end of the century and for the more emissive scenarios, where the increases probably will be between 10–55 days for WD, 10–40 days for WSDI and 10–55 days for WN.

Abaurrea et al., 2018 developed a joint modelling of extreme heat event occurrence in daily Tx and Tn, applied to five Spanish cities, used to generate projections for 2031-60 under RCP 4.5, 6.0, 8.5, with data from 4 CMIP5 GCMs. Projections are obtained for rates of occurrences of excesses over threshold for 3 types of events: only extreme in Tx, only in Tn, simultaneous event. Three scenarios suggest a clear increase in the intensity, but relevant differences are found between the evolution in the different scenarios, cities (climates) and type of event. In 2031-40, similar values are obtained under RCP 8.5 and RCP 4.5, and the median of ratios between 2031-40 projection and 1971-2000 is 3.5 for simultaneous events, 2.2 for only in Tx, 2.4 for only in Tn, but different spatial patterns appear with the highest intensities projected for only Tx in Zaragoza, for only Tn in Burgos, for simultaneous event in Zaragoza and Barcelona. However, in 2041-50 the projections grow faster under RCP 8.5, and from 2051 onwards much higher values than in the other scenarios are projected.

The global projected changes would be used as reference to compare those projections over Spain, Barriopedro et al., 2023 summarises that with a 2°C warming at global scale a hot day with frequency 1 of 20 years in the present-day climate would be approximately 2.5 times more likely, but a 1/50 warm day would be increased by 5 times. Carvalho et al.,

2021 agreed with these results, reflecting that all the temperature variables are projected to increase under the SSP5-8.5 scenario, mainly in summer with increments of 2-3 ºC (5-6 ºC) at the middle (end) of the century. Also the occurrence of tropical nights, hot (tas > 30 ºC) and very hot (tasmax > 40 ºC) days will increase by the end of the century on 50-80 nights/year, 40–60 days/year and 30–40 days/year, respectively. As a result of these trends, spring and summer will start earlier (~3.3 days and ~4.6 days per decade under RCP 8.5/SSP5-8.5) while autumn and winter will start later (~3.8 days and ~1.4 days per decade under RCP 8.5/SSP5-8.5) potentially leading to a 166-days summer and 31-days Winter in 2100 (Wang et al., 2021). Cos et al., 2022 extended the analysis to RCM, CMIP5 and CMIP6 simulations obtaining similar results under the RCP 8.5/SSP5-8.5 scenario but projecting a recovery of the precipitation decline under the low emission scenario, following mitigation. These trends are partially modulated by the RCMs of CORDEX under the RCP 8.5 with increments for day with maximum temperature greater than 35 ºC / 40 ºC of 30 days / 10 days in the mid-century and 50 days / 20 days for the end of the century (Coppola et al., 2021a), and an increment of the mean/maximum/minimum temperature of 2.1/2.3/1.8 (4.1/4.4/3.8) °C in the medium (long) term future (Carvalho et al., 2021b). However, much higher increases are projected for inland central areas, especially in the south, in the Cantabrian and Pyrenees Mountain ranges, leading to a decrease in the occurrence of Frost Days (FDs) and cold waves (days and intensity) as has been reflected by Díaz-Poso et al., 2023. De Luca et al., 2023 summarise projections of hot extremes 1950-2100, using 25 CMIP6 models, and they found under SSP5-8.5 that an index about Tx exceeding the 90th percentile shows largest increases in the intensity of hot extremes over central South America, central North America and Europe. Molina et al., 2020 and Herrera-Lormendez et al., 2023, considering the EURO-CORDEX RCM and the CMIP6 GCM ensemble, established that the strongest present-day HWs over the Mediterranean could become almost the norm by the end of the 21st century under a RCP 8.5 scenario.

Regarding the uncertainties between scenarios, Amblar-Francés et al., 2020 found that spatial distribution of changes in temperature extreme indexes over Pyrenees is strongly model dependent. They found that the influence of scenarios becomes noticeable from approximately 2050, and there is also an increase in uncertainties linked to both scenarios and models. However, they found that scenario-related uncertainties predominate over model-related uncertainties. Uncertainties between climate models in every scenario associated with hot extreme projections are shown using graphs (Abaurrea et al., 2018; Lorenzo et al., 2021). Abaurrea et al., 2018 analysed the sources of the uncertainty using the mean of fitted rates corresponding to the available GCM trajectories, then a decomposition of variability analogous to ANOVA (Analysis of Variance) model was used in every month-decade, considering three factors: Location, Scenario and ESM, the latter nested in the first two. The differences between locations explain around 20% of variability, between scenarios 6.9% in 2031-40 and 15.8% in 2051-60, then the most part of variability is between GCMs.

3.2. Precipitation

Precipitation is one of the variables with most uncertain future evolution worldwide, but the Mediterranean area, and the IP in particular, remains as a drought hot spot, identified in different global studies using large ensembles of either GCMs (De Luca and Donat, 2023;

Trancoso et al., 2024) or RCMs (Coppola et al., 2021b; Spinoni et al., 2020). As a means to reduce the uncertainties arising from the different models and internal decadal variability, the use of GCM projections constrained based on observations has shown some skill in 20 year drought predictions in particular regions (De Luca et al., 2023).

Most regional climate projection uncertainties are covered in different studies focused on mean and extreme precipitation indices in Europe and the IP, or Spain in particular. EURO-CORDEX projections cover most of these uncertainties, but there are also studies assessing the downscaling approach uncertainty by including BA (Cardell et al., 2019a; Casanueva et al., 2020b; Dosio, 2016) and ESD techniques (Baño-Medina et al., 2022; Hernanz et al., 2023a; Soares et al., 2023a). Also, a few studies conducted dedicated RCM simulations exploring other sources of uncertainty, such as additional coupled components like a regional ocean (Cabos et al., 2020; De La Vara et al., 2021) or interactive aerosols (López-Romero et al., 2021). Pereira et al., 2021 did a relatively recent review of studies focusing on extreme precipitation over the IP.

The discontinuous nature of precipitation makes mean precipitation a less relevant variable than e.g. mean temperature. A number of indices are commonly used to account for, on one hand, the occurrence of precipitation (frequency of wet days, number of consecutive wet or dry days, etc.) and, on the other hand, the amount of precipitation during wet days (mean precipitation on wet days, percentiles, fraction of precipitation arising from extreme precipitation events, etc.). These indices are discussed in the next sections regarding the ability of existing models to reproduce them and their future projection.

Model evaluation

Downscaling model evaluation for EURO-CORDEX RCMs over the IP (Herrera et al., 2020) shows biases very dependent on the model and synoptic situation. Although most RCMs are generally able to reproduce the spatial pattern and variability of precipitation, biases remain for both mean precipitation (up to 25%) and extreme values (e.g. 50-year return values can reach up to 50% biases). Med-CORDEX (Mediterranean branch of CORDEX) simulations also cover the IP and show a performance similar to EURO-CORDEX regarding different mean and extreme precipitation indices (Fantini et al., 2018).

Other individual RCM evaluation simulations nested into reanalysis, have also been assessed and show biases comparable to EURO-CORDEX models (e.g. Driouech et al., 2020; Tuel et al., 2021). Unlike radiation and temperature, a more realistic representation of aerosols and their interaction with radiation and clouds using the WRF model showed negligible effects on precipitation over the IP (López-Romero et al., 2021). A regional, interactive ocean component in REMO was shown to have a major effect on precipitation along the northern and eastern portions of the IP during winter, when the air-sea coupling causes a pronounced precipitation increase, while the western coast of Iberia becomes drier (Cabos et al., 2020). This was attributed to a southeastward shift of the Gulf Stream and the North Atlantic Current. Moister air transported towards the IP favours enhanced precipitation in the northwest of the IP. To the south, a weaker storm track results in drier conditions.

Another important aspect of model evaluation is the added value with respect to the driving fields. This involves comparing both the driving and downscaled fields against an

observational dataset, in order to assess whether the downscaled product outperforms the original low-resolution product. Over the IP, large added value of CORDEX EUR-11 simulations was found for precipitation intensity and less so for the wet-day frequency (Careto et al., 2022). Added value occurs especially over coastal areas and mountainous regions of the IP. Also, the added value increased when considering extreme values, especially during summer and fall. Although added value is expected to increase with resolution, Reder et al., 2022, in a CP-RCM simulation nested into ERA5 found no added value for Bilbao and Pamplona, the two Spanish cities considered in their study. This could also be due to the quality of the reference observational database (E-OBS) in the area. Convection-permitting simulation over southwestern Europe at 3 km resolution (SWE3) was shown to add value on wet-day precipitation frequency and intensity, and also in the reproduction of the heavy precipitation events for each season as compared to a 20 km simulation (Shahi et al., 2022). No added value was found in mean seasonal precipitation, which was underestimated by the SWE3 simulation.

Regarding ESD models, the EU cost action VALUE has produced a thorough evaluation of over 50 methods, including BA, for mean (Gutiérrez et al., 2019) and extreme values (Hertig et al., 2019). Most methods greatly improve model biases and no approach seems superior in general. However, the results show the inadequacy of linear regression methods for downscaling daily precipitation value. The most decisive factors explaining the variability of the results are the introduction of a seasonal component (e.g. training the methods separately each calendar season, month or moving window), which improves the results, and the deterministic or stochastic nature of the method. The IP shows one of the weakest correlations for summer precipitation. Regarding the marginal aspects of extremes, the best performance is found for MOS methods, WGs as well as PP methods using analogues. Spell-length-related extremes are best represented by MOS and PP methods using analogues. The skill of PP methods with transfer functions varies strongly across the methods and depends on the extreme index, region and season considered. In general, extreme dry spells show a larger intra-method spread compared to long wet spells, particularly on the IP.

Hernanz et al., 2023a fitted a machine learning ESD method based on extreme gradient boost (XGB) that showed better scores than the EURO-CORDEX RCMs for all precipitation metrics with only a few exceptions, mainly related to an underestimation of the variance. After BA, both the SDM and the six RCMs present similar results, with no significant differences among them.

Regarding the evaluation of the historical experiment, the CMIP6 ensemble shows no significant signal of precipitation change over the IP for either summer or winter (Ossó et al., 2023). ERA5 or E-OBS show stronger signal-to-noise ratios, although still non-significant. The very low signal in CMIP6 is due to the diversity of signal-to-noise ratios in the individual models, which exhibit different patterns and even opposite signals over the area.

For EURO-CORDEX, Vautard et al., 2021 conducted a thorough evaluation of the grand-ensemble historical simulations over Europe, considering both the RCMs and their driving GCMs. In winter, there is a widespread overestimation of precipitation over land, with relative median bias values reaching 50% in the mid-northern IP. In summer, positive biases are even larger, since rain is essentially absent in observations, while the majority of simulations produce convective (parameterised) precipitation. Biases in daily accumulated precipitation

averaged for the IP reach up to 2.4 mm/day (all positive) in winter and up to 2.6 mm/day (all but two, positive) in summer. This overestimation was also found for annual precipitation and other related indices over continental Spain for a subset of the EURO-CORDEX ensemble (Lorenzo and Álvarez, 2020), showing different individual bias patterns depending on the driving GCM. More local studies also find this overestimation (e.g. Moyano et al., 2023, over the Miño river basin). The analysis of the grand-ensemble (Vautard et al., 2021) shows that for indices depending on seasonal or long-duration, large-scale phenomena (Consecutive Dry Days - CDD, Dry spell Frequency exceeding 6 months -DF6-), the contribution of the driving GCMs to the biases is dominant, although this occurs systematically over all individual regions only for DF6. For extreme precipitation, the contribution of RCMs to the biases is dominant over all regions, probably due to the strong dependence on physical parameterizations. For heavy precipitation indices there is a general wet bias following the mean precipitation pattern. Over the IP, maximum daily precipitation is overestimated by 27% and the number of days above the 99th percentile by 23%. Some works found smaller biases for extreme precipitation (annual daily maxima) than for mean precipitation (Garijo and Mediero, 2019), though. In the Mediterranean, Requena et al., 2023 found an underestimation of daily annual maximum precipitation, attributed to the limitation of RCMs to adequately represent convective precipitation typical of these areas, which could also affect reliability of results in these regions.

In CMIP6, the spatial resolution of GCMs has reached the grid spacing of the coarser RCMs. In particular, CMIP6 HighResMIP GCMs can be compared to CORDEX EUR-44 over Europe (Demory et al., 2020b). HighResMIP and EUR-11 simulate an overall decrease in low-intensity precipitation and an increase in high-intensity precipitation compared to the CMIP5 GCMs driving EURO-CORDEX RCMs, particularly over coastal and orographic regions such as the IP. Model resolution is identified as the most important aspect to capture a realistic distribution of daily precipitation contribution to different precipitation rates. EUR-11 and EUR-44 show larger precipitation overestimation over orography than HighResMIP. Both HighResMIP and EURO-CORDEX are best in representing summer and autumn precipitation, while they suffer from large wet biases (smaller for HighResMIP) in winter and spring.

Cabos et al., 2020 evaluates the impact of the driving fields on ocean-coupled vs. uncoupled REMO RCM simulations. Precipitation biases are more sensitive to the coupling when driven by a GCM (CMIP5 MPI-ESM), than when driven by perfect boundary conditions (ERA-Interim). This was found to be consistent with the deficiencies of the driving model MPI-ESM, which exhibits a strong westerly flow entering the IP across the western coast. Results are likely very dependent on the driving and regional models used, and a multi-model experiment would be needed to reach robust conclusions regarding the regional ocean coupling.

The added value of EURO-CORDEX simulations with respect to the driving GCM can be derived from historical simulations. As for the evaluation simulations, distributional added value is stronger for precipitation intensity and extremes and less so for wet-day frequency (Careto et al., 2022). Added value is very dependent on the GCM, with strong added value, regardless of the RCM, with respect to poor performing GCMs.

RCM precipitation at sub-daily timescales has been investigated less. Berg et al., 2019 studied extreme summer sub-daily precipitation in the EURO-CORDEX ensemble. All models

perform poorly at an hourly duration, with increasing performance for longer durations. Both the GCM and RCM affect both magnitudes and spatial patterns across Europe, but the RCM is most prominent in shaping the spatial structure at short durations.

BA methods adjust model output towards observations and this may indirectly affect the trends and the resulting climate change signal. There are cases when this is justified, e.g. for climate indices defined using absolute thresholds, where the raw signal is not reliable (Dosio, 2016). However, in general, without a physical mechanism justifying a modification, preserving the trends of the basic distributional statistics is a desirable property of BA methods. In a recent assessment (Casanueva et al., 2020b), the methods which largely preserve the raw climate change signals across the different variables and indices are the quantile trend-preserving methods, although some of them exhibit problems with the adjustment of the wet-day frequency. However, for precipitation indices representing marginal aspects (SDII - Simple Daily Intensity Index), these elaborated methods show also a higher sensitivity to the choice of the observational reference, as compared to the standard ones. Standard BA methods, in turn, are more sensitive to the observational dataset for extreme indices (P98We-98th Percentile of Wet Days). Thus, a high-quality reference is desirable in any case. In general, trend-preserving methods are recommended to post process model output, since they are conservative methods well suited to alleviate biases while maintaining the raw original climate change signal.

In a series of studies, AEMET has tested 5 different ESD methods over continental Spain and the Balearic islands, before including them in the Escenarios-PNACC 2023 database. They followed the VALUE framework to evaluate them under perfect boundaries coming from reanalysis (Hernanz et al., 2022c), imperfect boundaries from GCMs (Hernanz et al., 2022b) and a pseudo-reality setting to assess the stationarity assumption (Hernanz et al., 2022a). In the pseudo-reality setting all methods revealed difficulties to represent a drier future climate. Analog and linear regression methods display a positive bias when applied to a drier future climate, and the machine learning algorithms larger precipitation biases under future drier conditions when compared with their results in the historical period. In experiments 1 and 2 (Hernanz et al., 2022b, c) analog methods were able to capture the total precipitation amount, the precipitation occurrence and intense precipitations, while transfer function methods appear only suitable for the total precipitation amount. Nevertheless, with the transferability problems revealed by all methods, it seems reasonable to use, at least, one method of each family to generate the climate projections.

CNNs have recently emerged as a promising tool for ESD, outperforming classical ESD methods (linear and generalised linear models) using large-scale perfect predictors from reanalysis (Baño-Medina et al., 2020). This continental-wide assessment was extended (Baño-Medina et al., 2021) by considering the suitability of CNNs for downscaling future climate change projections using GCM outputs as predictors. As compared to well-established GLMs, CNNs preserve better the raw GCM projections for the end of the century, resulting in more plausible downscaling results for climate change applications and provide more spatially homogeneous downscaled patterns than GLMs. GLMs based on local predictors are more sensitive to the possible inconsistencies that may arise between reanalysis and GCM predictor data, resulting in larger biases, especially for precipitation amount metrics (SDII and 98th percentile). These results have been extended to a MME and compared

to EURO-CORDEX RCMs (Baño-Medina et al., 2022). DeepESD (Empirical Statistical Downscaling with Deep Learning techniques) reduces the systematic distributional biases exhibited by GCMs and RCMs in the historical period. It produces climate change signals broadly comparable to the RCM ones. Climate change signal uncertainty, as measured by inter-model spread, is reduced for precipitation.

Climate change projections

The most recent assessment of climate change projections within the EURO-CORDEX grand ensemble (Coppola et al., 2021a) considered not only CORDEX RCMs, but also their driving CMIP5 GCMs and the newer GCM generation from CMIP6. For precipitation, they considered indices for mean (mean seasonal precipitation, mean daily intensity, mean CDD) and extreme (annual maximum precipitation, number of days above the 99th percentile, 6-month drought frequency) regimes.

CMIP6 SSP5-8.5 projects a significant decrease ~40% all over the IP in mean summer precipitation by the end of the century, strongest toward the southwest. CMIP5 and EURO-CORDEX (RCP 8.5) show smaller (30%) but still significant decreases. During winter, the 3 data sets project a significant decrease (20-30%) in the southern half of the IP, and non-significant changes to the north. This decrease of precipitation has been attributed to changes in atmospheric circulation and the poleward shift of the mid-latitude westerly zonal winds and associated storm tracks with climate change (Zappa et al., 2015). For mid-century, these figures are approximately halved. Changes in annual extremes and mean daily intensity are less significant, generally decreasing to the south, non-significant in the mid-IP and increasing to the north. Drought conditions (CDD, DF6) increase significantly with a north-south gradient.

These figures essentially agree with those of other studies using either sub-ensembles of the EURO-CORDEX RCM simulations (Lorenzo and Álvarez, 2020) or extending them with other CORDEX domains (Driouech et al., 2020; Fernández et al., 2019; Zittis et al., 2019), even though slightly different future and reference periods are considered. Individual, dedicated RCM simulations also agree (Tuel et al., 2021). The estimates provided by global CMIP projections also agree with other studies (Cos et al., 2022), that show a stronger summer drying in the new CMIP6 ensemble than in CMIP5. Actual figures can be obtained using different web portals (Table 5.2) for the different scenarios, periods and regions. As an example, Figure 5.3 shows the annual cycle for the relative precipitation change aggregated by the end of the century, as provided by the new Copernicus Interactive Climate Atlas for continental Spain.

Cardell et al., 2019 computed delta changes after BA reaching similar conclusions. No systematic assessment of the impact of BA on the delta changes was conducted. An earlier work (Dosio, 2016) evaluated the impact of BA on the delta changes for several precipitation indices. Bias-adjusted results are relatively similar to the original ones, both in winter and summer, especially for the change in mean and total precipitation and the number of wet days, despite the original RCMs largely overestimated the present climate values. Results for other indices are more heterogeneous.

Despite the decrease in mean precipitation, upper percentiles, e.g. 95th, are projected to increase above 2 mm/day along the Mediterranean coast and southern IP during JJA (June-

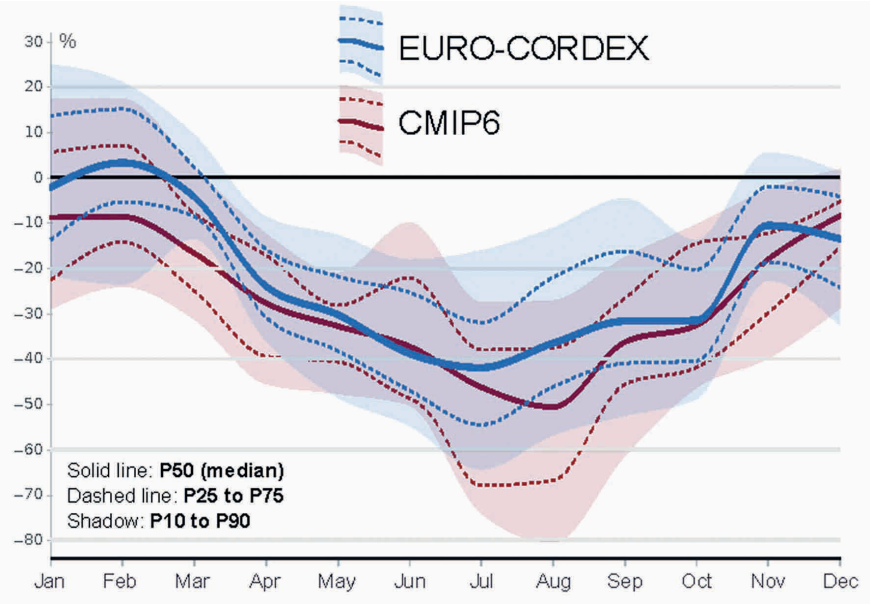

Figure 5.3: Mean precipitation relative change (%) by 2081-2100 vs 1981-2100 over continental Spain and the Balearic islands according to the EURO-CORDEX (RCP 8.5) and CMIP6 (SSP5-8.5) ensembles. Source: Adapted from the Copernicus Interactive Climate Atlas (C3S/ECMWF), https://atlas.climate.copernicus.eu

July-August) and SON (September-October-November) (Molinié et al., 2016). Decreases up to -2 mm/day are projected in the northwest, especially during SON. Return levels of 10-year 24h precipitation are projected to increase by 20-30% by the end of the century in the RCP 8.5 scenario (Schmith et al., 2021). Other studies also project increases in most areas in return levels for longer periods, although their significance is lower due to the large sampling uncertainty (Garijo and Mediero, 2019). Increases of about 25% in the 50-year precipitation are reported by Zittis et al., 2021 over most of the IP by the end of the century, despite the decline in total precipitation amounts. The 100-year precipitation extremes are also projected to increase (Del Jesús and Díez-Sierra, 2023).

The Standardised Precipitation Index (SPI; García-Valdecasas Ojeda et al., 2021; Lorenzo et al., 2024) or other variants (Andrade et al., 2021b) results are aligned with previous findings for precipitation, showing that the IP is likely to undergo longer and more severe drought episodes in the future, particularly strong by the end of the century under the higher emissions scenario (RCP 8.5), when greater duration and severity of drought events extend over most of the IP. Specific results regarding the changes in frequency, intensity and duration for the near future are less robust and depend on the scenario and the particular studies, which consider different EURO-CORDEX sub-ensembles and ad hoc simulations. See further details in the Drought and Aridity section below.

Individual precipitation systems leading to extreme events are projected to become larger and more intense as temperature increases (Matte et al., 2022). This applies for all European subregions, considering 20-year precipitation events. For the IP, the larger precipitation systems are projected to increase in number, intensity and size, while intermediate-size systems are projected to decrease in number.

An ocean-coupled RCM simulation (De La Vara et al., 2021) reduced the magnitude of future changes, while mostly agreeing on the spatial patterns. Different spatial patterns of change were only found in winter over northwestern IP due to differences in the large-scale oceanic circulation in the North Atlantic subtropical Gyre. Mean precipitation shows regionally-dependent changes in winter, whilst a drier climate is found in summer. Further research is necessary, though, especially to account for multi-model (GCM and RCM) uncertainty.

One way to overcome the uncertainty in delta changes due to the subjective selection of future and reference time periods (Figure 5.2) is the use of global warming as an independent coordinate, instead of time (Díez-Sierra, et al., 2024). Regional, and even local, future changes in most variables scale linearly with GSAT, unlike than with time. Such a linear response enables the use of the scaling slope as a measure of future change. For instance, summer precipitation shows all over the IP a decrease of 10-15% per degree of global warming. This is independent of the emissions scenario (Díez-Sierra et al., 2023), which only dictates when and at which speed a particular GWL is expected to occur. Other seasons show non-significant slopes (5-10% decreases in spring and autumn and ~3% increases or decreases in the northern or southern IP, respectively). CDD (i.e. dry spell length) show change rates with increases of about 10 days/ºC in the southern half of the IP and 4-9 days/ºC in the northern part, with the smaller increases projected along the northern coast and the Pyrenees.

Hourly precipitation changes are projected to be of greater magnitude and extension than for daily precipitation, leading to a torrentiality rise, which is also supported by the analysis of torrential rate changes (Requena et al., 2023). The areas presenting significant sub-daily precipitation positive trends and changes increase as duration decreases; showing greater intensity for the most pessimistic scenario and far future periods. So the effect of climate change may be stronger for extreme events with short precipitation durations. This may be attributed to a stronger scaling, at short time scales, between changes in extreme precipitation and mean surface temperature (Requena et al., 2023). The linear relationship between extreme precipitation changes and temperature, arising from the Clausius-Clapeyron equation, seems to be a valid approach to project changes in summer extreme precipitation (Berg et al., 2019). Over the Mediterranean and IP land regions, there is weaker temperature scaling than implied by the Clausius-Clapeyron relation, likely connected to the low summer moisture availability.

Statistical downscaling of daily into sub-daily precipitation (Del Jesús and Díez-Sierra, 2023) show also reduced average precipitation as the century progresses, with variances also increasing; i.e. pointing towards more torrential precipitation. Average precipitation will decrease in most climate types from April to October, except for the most arid climates, BWh (Tropical and subtropical desert climate) and BSh (Mid-latitude steppe and desert climate), where the reduction is greater from September to June. Changes are more robust for RCP 8.5 than for RCP 4.5. Overall, the most extreme sub-daily events are expected to intensify,

as well as increase the number of dry spells. However, most of the effects are concentrated on a few dry climate types.

DeepESD downscaling over Europe (Baño-Medina et al., 2022) presents only slight regional differences in future precipitation change with respect to GCMs and RCMs, with DeepESD presenting a weaker decrease of precipitation over the IP, especially when compared to GCMs. The spatial patterns and magnitudes of change are broadly similar to those of RCMs, with some regional differences in the climate change signals among DeepESD and the dynamical models. For the case of precipitation, these differences lead to a decrease in the multi-model uncertainty with respect to that of their driving GCMs.

Soares et al., 2023 made a thorough study of 4 different deep CNN architectures to downscale 7 CMIP6 GCMs over the IP using ERA5 and Iberia01 as observational training datasets. GCMs project a homogeneous decrease in the mean daily precipitation for all future periods and scenarios, while the deep learning downscaled ensemble shows mostly consistent decreases in the western and northern areas of Iberia. Regional increases in central and eastern Iberia, regardless of the period and scenario, are non-robust, with fewer than two-thirds of the ensemble in agreement, but may be consistent with changes in convective precipitation that are not captured by the original Earth System Global Climate Models (ESGCM). Decreasing precipitation projections are found mainly in the northern, western and southwestern portions of Iberia, increasing in area and robustness towards 2100, and with the SSP5-8.5 scenario. Deep learning projections show reductions of extreme precipitation (95th percentile) reaching more than 3 mm/day across southwestern Iberia, expanding eastward (for part of southern Iberia) throughout the 21st century, and more pronounced for SSP3-7.0 and SSP5-8.5 scenarios. Over central, southeastern and northwestern Iberia, downscaled projections show more extreme precipitation (increases above 3 mm/day) in all scenarios and time periods. Therefore, both mean and extreme precipitation showed greater discrepancies with respect to the driving GCMs.

In a study over the Júcar and Segura rivers basins, Miró et al., 2021 applied a statistical downscaling method (LARS-WG, Long Ashton Research Station Weather Generator) plus BA (ISIMIP-Inter-Sectoral Impact Model Intercomparison Project) to 4 CMIP5 CGMs. They found a trend towards greater precipitation irregularity and torrential rain in the short term, along with a loss of mean precipitation in the long term, greater towards inland headwaters where the main rivers supplying the region rise. This loss appears in the short term and is aggravated in the long term, with greater losses projected for spring and summer. However, reduced precipitation in the Júcar headwaters is found even in winter.

Knowledge gaps

Sub-daily precipitation extremes remain largely unexplored, mainly due to the lack of convection-permitting simulations over the area and the difficulty in implementing ESD approaches at these time scales. The performance of RCMs is poor for short durations and does not inspire trust in their application for future projections (Berg et al., 2019). The few available km-scale simulations from the EU-funded project EUropean Climate Prediction (EUCP, Shahi et al., 2022) provide an opportunity for further research on short duration extremes, as an initial step towards longer km-scale simulations better exploring multi-

model uncertainty. Convection-permitting simulations have shown promising results in reducing future precipitation uncertainty (Fosser et al., 2020).

EURO-CORDEX simulations are the ensemble of choice for many studies, but simulations from other CORDEX domains also cover the IP with comparable skill (Fantini et al., 2018; Legasa et al., 2020; Zittis et al., 2019) and remain underused. Some of them (e.g. Med-CORDEX) provide simulations coupled to a regional ocean and other interactive components which are poorly assessed over Spain. This kind of process understanding can be key to build confidence in the different downscaling approaches and understand their discrepancies.

3.3. Wind

In a climate change context (IPCC, 2023), historical variations in near-surface wind speed (NSWS) have been the forgotten part of the climate system compared to e.g. air temperature or precipitation changes. While scientists were skeptical to assess trends and multidecadal variability in NSWS due to low availability and quality of wind measurements, new data rescue and homogenization protocols reduced this uncertainty (Azorín-Molina et al., 2014; Azorín-Molina et al., 2019; Wan et al., 2010). During the last decades, two phenomena were discovered using observational NSWS. The term "stilling" was introduced for the first time by Roderick et al., 2007 to refer to the decline of terrestrial NSWS in Australia, a phenomenon observed across the Northern Hemisphere (McVicar et al., 2012), such as in Sweden (Minola et al., 2016) or the IP (Azorín-Molina et al., 2014), among other regions. Since ~2010, a "reversal" of NSWS has been found in many Northern Hemisphere land areas (Zeng et al., 2019), with a cessation of the "stilling" also observed in the IP (Utrabo-Carazo et al., 2022).

NSWS play a key role in the climate system with far reaching socioeconomic and environmental implications. Approximately, 25% of the total installed capacity power in the IP comes from the wind sector (Directorate-General for Energy (European Commission), 2021). Changes in NSWS directly affect the energy sector, crucial for decarbonization (Sherman et al., 2021; Wu et al., 2021). Moreover, changes in NSWS affect irrigated agriculture and desertification due to the link between wind and evapotranspiration (McVicar et al., 2012) and soil erosion (Zhang et al., 2019), but also visibility and air quality (Cai et al., 2017), ocean circulation and upwellings (Sousa et al., 2017), lake thermal responses (Woolway et al., 2019), forest fires (Schulte and Mladenoff, 2005), among others. Given the above mentioned implications, the projections of future NSWS changes under different future scenarios is an area of urgent research. GCMs from the CMIP are the main tool. However, the spatial resolution of global models is not sufficient for regional assessments. Higher resolution regional models are necessary, as they permit the simulation of regional- and local-scale processes in areas of complex topography (Molina et al., 2023), such as the IP where local regimes such as Cierzo or Levante prevail (Ortega et al., 2023). Furthermore, in addition to the regional models, the regionally coupled atmosphere-ocean models (e.g. Darmaraki et al., 2019; Sein et al., 2015; Somot et al., 2008) allow us to provide added value in representing both the wind mechanisms generated by the land-sea thermal gradient (e.g. sea breezes or alongshore upwelling winds; De León and Orfila, 2013; Vázquez et al., 2022), and in assessing the mechanisms resulting from climate change in the ocean that could affect NSWS.

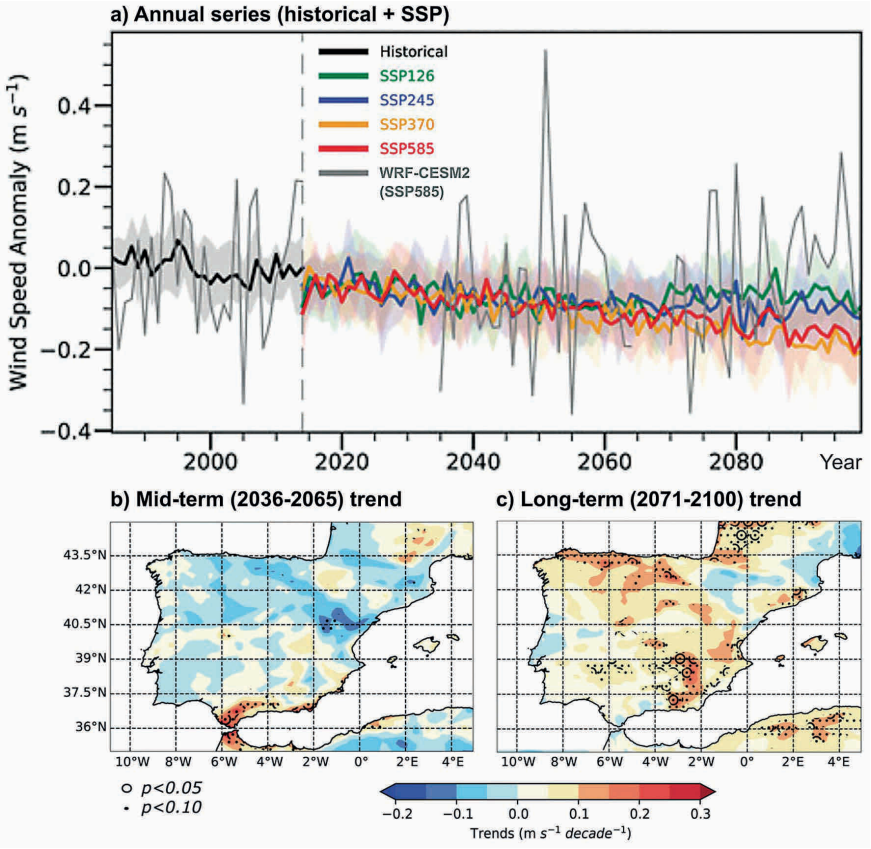

Figura 5.4: a) Anomalías anuales del NSWS (m*s^{-1}) del MME (línea gruesa), dispersión de los modelos inter-CMIP6 (sombreado del rango entre los percentiles 25th y 75th), y el WRF-CESM2 (bajo SSP5-8.5); tendencias del NSWS (m*s *dec^{-1-1}) para b) los períodos a medio plazo (2036-2065) y c) a largo plazo (2071-2100) del WRF-CESM2 bajo SSP5-8.5. Fuente: Adaptado de Andrés-Martín y otros, 2023.

Model evaluation

To trust in future projections, models must be able to reproduce past NSWS changes and multidecadal variability. Globally, most CMIP6 models fail in reproducing the observed long-term NSWS variability and trends, with CESM2 showing the best performance metrics (Shen et al., 2022). Over the IP, CMIP6 models and an RCM (WRF nested into CESM2) showed poor performance in capturing the observed NSWS (against in situ AEMET observations) and large uncertainties in future projections (Andrés-Martín et al., 2023). Reanalysis products underestimate past NSWS anomalies and fail in reproducing decadal variability (Torralba et al., 2017), with the ERA5 reanalysis being the best in simulating winds among other reanalysis datasets (Ramon et al., 2019).

Figure 5.4: a) Annual NSWS anomalies ($m*s^{-1}$) of the MME (thick line), inter-CMIP6 models spread (shading the range between the 25th and 75th percentiles), and the WRF-CESM2 (under SSP5-8.5); NSWS trends ($m*s^{-1}*dec^{-1}$) for b) mid-term (2036–2065) and c) long-term (2071–2100) periods of the WRF-CESM2 driven by SSP5-8.5. Source: Adapted from Andrés-Martín et al., 2023.

Climate change projections

In general, there is a large uncertainty regarding the evolution of NSWS over the IP at the end of the century. In fact, there are discrepancies on whether it will increase or decrease. In this context, some studies using models from CMIP5 and CMIP6 indicate a reduction in winds over Europe by the end of the century (Carvalho et al., 2021c; Karnauskas et al., 2018; Shen et al., 2022), specifically over the IP (Jung and Schindler, 2022). Furthermore, this reduction has been demonstrated in studies using regional models such as WRF (along the Iberian Atlantic coasts; Soares et al., 2017) and EURO-CORDEX (Santos et al., 2018), in RCP 4.5 and RCP 8.5 scenarios. Several drivers have been identified as the origin of these trends: changes in the surface roughness associated with modifications in the land use and vegetation cover, aerosol emissions and changes in the large-scale circulation. However, there is such difficulty in assessing changes in the wind pattern that, even though they may decrease overall, they could increase in specific regions of the Peninsula (for example, Galicia and the Strait of Gibraltar; Santos et al., 2018), or increase in terms of extreme winds, especially in the northwestern regions (Martins et al., 2020), or due to an intensification of thunderstorm straight line winds due to climate change (Prein, 2023).

Contrary to studies demonstrating a decline in the wind field, there are studies based on regional models forced by both CMIP5 and CMIP6 that show an increase in winds over the IP (Claro et al., 2023; Fernández-Álvarez et al., 2023a; Soares et al., 2017b; Vázquez Medina, 2023). These studies have indicated an increase in stronger winds during the summer months. In this regard, an intensification of the Azores High during the winter, spring, and fall at the end of the century could lead to an increase in the wind pattern (Soares et al., 2017b; Sousa et al., 2017; Sylla et al., 2019; Vázquez et al., 2023). However, using a coupled atmosphere-ocean regional model, (Vázquez Medina, 2023) found that the summer increase could be associated with an intensification of the Iberian thermal low (caused by temperature rise; Miranda et al., 2013) along with an increase in pressure in the British Islands (as a trigger for the weakening of the Atlantic Meridional Overturning Circulation (AMOC); Haarsma et al., 2015). Finally, Andrés-Martín et al., 2023 found that the CMIP6 GCMs and the WRF-CESM2 RCM poorly perform the simulation of the observed NSWS changes and multidecadal variability over the IP (1985–2014). Despite the improvement in spatial resolution, the WRF-CESM2 did not outperform its driving GCM. Under high anthropogenic forcings (i.e. SSP3-7.0 and SSP5-8.5), the CMIP6 GCMs projected a continuous decline in winds, while under SSP2-4.5 and SSP1-2.6 showed an interdecadal oscillation (Figure 5.4). Contrarily, the WRF-CESM2 projected a reinforcement on NSWS for mid- and long-term in the 21st century. Due to the large uncertainty found, projections should be taken with caution, and further efforts are strongly needed to improve the parametrizations and assimilation in GCMs and RCMs for accurately simulating NSWS.

Knowledge gaps

Assessing future changes in the frequency and severity of wind extremes to global warming is challenging. A recent study (González-Alemán et al., 2023) attributed the historic and destructive Mediterranean derecho (12 people died and 106 people were injured) in August 2022 to the (i) record-breaking marine heatwave, and (ii) the anthropogenic climate change, which contributed to the triggering of the straight-line winds by enhancing the environmental factors to develop deep convection. Without the current anthropogenic climate change forcing, the dynamical synoptic situation would have only developed ordinary convection without a derecho (González-Alemán et al., 2023). Another recent study concluded that the 2020 Midwest derecho would have covered twice as much ground if it happened in the warmer climate projected for 2100 (Lasher-Trapp et al., 2023). Moreover, new research showed how thunderstorm straight-line winds intensify with climate change in the central United States over the past 40-years (Prein, 2023). Theoretical estimations suggest that gusty winds should intensity at a rate of ~7.5% per ºC, yet the observed rates show a more pronounced increase of ~7.5% per ºC. Simulations also showed about a 5-fold increase in the geographical extent affected by straight-line winds. To conclude, future extreme winds would intensify in a warming climate across the IP, despite there is a lack of research and large uncertainty on this topic.

In general, more thorough RCM evaluation is missing, especially accounting for multi-model uncertainty and evaluating against observational data, since reanalysis products have been proved suboptimal as reference. Also, changes in dominant wind directions or in the frequency of occurrence of local winds are also much less studied than wind speed (Obermann-Hellhund et al., 2018; Ortega et al., 2023). This would be another topic to strengthen our knowledge about the future evolution of wind patterns.

3.4. Atmospheric Circulation

This section reviews progress on atmospheric circulation studies involving the IP. Large-scale or synoptic circulation indices are discussed first, followed by a review of the work related to weather regimes, also known as atmospheric circulation patterns (CPs).

Large-scale atmospheric Circulation

In the North Atlantic-European sector, and generally in the extratropics, the long-term tendencies or epoch differences along the 21st century are much more uncertain for Sea Level Pressure (SLP) than for temperature and precipitation (Deser et al., 2012).

The main uncertainty source is natural variability and a minimum of 20 to 30 ensemble members initialised from distinct initial conditions is needed to detect a significant ensemble mean (i.e. externally forced) wintertime SLP response by the end of the 21st century, with more members being necessary for mid-century climate projections and less of them for projections of the summer season (Deser et al., 2012, 2017; Maher et al., 2019; McKenna and Maycock, 2021).

For the large-scale circulation indices driving climate variability over the IP, a significant shift in the wintertime decadal mean Northern Annular Mode towards its positive phase

emerges in the 2040ies (Deser et al., 2012) and the wintertime North Atlantic Oscillation (NAO), Scandinavian (SCA), East Atlantic (EA) and East Atantic-Western Russia (EA-WR) patterns do not exhibit significant changes along the entire 21st century in any case if computed upon SLP.

However, if computed upon geopotential height values, the wintertime EA exhibits a pronounced trend towards its positive phase, associated with westerly flow and advection of mild, oceanic air masses to the IP, whose magnitude increases with height up to 100 hPa (Cusinato et al., 2021). Calculated this way, EA-WR exhibits a slight trend towards its negative phase while SCA remains stable like its SLP-derived version (Cusinato et al., 2021). Depending on the applied GCMs and methods, the NAO is projected to either remain stable during the 21st century (Cusinato et al., 2021) or to slightly thrive towards its positive phase (Deser and Phillips, 2023). The aforementioned large differences between the wintertime EA projections derived from SLP and geopotential heights might be explained by the fact that the associated tripole teleconnection pattern in the geopotential height field is modified by thermal expansion along the course of the 21st century, whereas the respective SLP pattern remains relatively stable along time. This would mean that SLP is the more robust variable to describe large-scale circulation changes.

By the end of the century, atmospheric blocking situations in and around the IP are projected to significantly decrease during the winter season, and are expected to remain largely unchanged in the summer (Davini and D'Andrea, 2020).

Since, in the extratropics, the contribution of internal variability to total uncertainty is larger than the contribution of model-related uncertainty (Deser et al., 2012), the aforementioned results have been derived from MMEs, Single Model Initial-condition Large Ensembles (SMILES) or combinations thereof (Deser et al., 2020).

Weather regimes and Circulation patterns

A variety of clustering procedures have been employed in the literature to discretize the atmospheric circulation on spatial scales ranging from entire continents or ocean basins down to the sub-continental, regional and even local scale. The thereby obtained clusters (or groups) are commonly referred to as *weather regimes, weather types* or *synoptic CPs,* whose spatial patterns can coincide with the large-scale CPs described in the former section.

Irrespective of the considered spatial scale, GCM performance in representing the observed climatological CP frequency and persistence has generally improved from CMIP5 to CMIP6 (Brands et al., 2022, 2023; Cannon, 2020; Fernández-Granja et al., 2021) and this finding holds for the IP in particular (Brands et al., 2022). However, reanalysis uncertainty may compromise the evaluation outcomes in some regions and seasons, such as the Mediterranean in summer (Fernández-Granja et al., 2023).

When the focus is put on large-scale weather regimes, four characteristic types reminiscent of the positive and negative NAO phases, a blocking pattern, and an Atlantic ridge pattern have been identified in the observational record (Delgado-Torres et al., 2022). These are associated with various climate phenomena over the IP operating on multiple spatio-temporal scales, promoting wet/dry and hot/cold spells there.

Moreover, the unique combination of the large-scale dynamic response and the independent, regional-scale thermodynamic response explain the robust regional maximisation of wintertime climate change over the Mediterranean, a global hotspot of climate change where warming and drying trends have been detected (Cos et al., 2022; Tuel and Eltahir, 2020).

At the synoptic scale, anticyclonic and easterly CPs are generally associated with higher-than-average occurrences of dry conditions. The CPs affecting the Iberian climate distinguish the position and intensity of the subtropical Azores High and the lower pressures at higher latitudes and Mediterranean cyclogenesis (Olmo, et al., 2024). Daily transitions between patterns are much faster in autumn and spring, while the summer season is dominated by a persistent high-pressure structure -the Azores High- leading to warm and dry conditions over Spain.

During winter, an intense subpolar low near Iceland and the subtropical high centered over southern Europe and the Mediterranean diminish precipitation development. Long-term changes are larger for winter structures, which have been found to be significantly linked with the NAO positive phase, showing the importance of cross time-scale interactions in the regional and local climate (Stryhal and Huth, 2019).

In addition, specific synoptic patterns modulate the occurrence of different climate hazards, such as severe precipitation events and heatwave episodes (Gil-Guirado et al., 2022; Herrera-Lormendez et al., 2023a; Materia et al., 2022; Miralles et al., 2019). Particularly, over southern Catalonia, the presence of a low-pressure system (advecting warm and wet air from the Mediterranean Sea at low atmospheric levels), a cold front, and enhanced low-level humidity promote the destabilisation of the atmosphere, needed for the development of the precipitation systems (Pérez-Zanón et al., 2018).

In addition, a set of CPs indicating mostly stationary and stable conditions or dynamic and advective structures are responsible for a large fraction of the variance in HWs in Spain (Ventura et al., 2023). Furthermore, Saharan air intrusions depict synoptic configurations that are often related to cyclonic circulation off the coast, in the Northeastern Atlantic and a strong subtropical ridge pattern, promoting the advection of anomalously warm air mass leading to HWs in the IP (Sousa et al., 2020a).

As projected climate change suggests, the already experienced drying -especially in the summer season- will strengthen over southern Europe (IPCC, 2023). Future circulation changes, based on a large ensemble of GCMs (Herrera-Lormendez et al., 2023a), are expected to further exacerbate hot and dry extremes over Europe, as changes in the frequency and intra-pattern characteristics of CPs can have direct influence on impactful events.

Projections also indicate a robust decrease in the frequency of the westerlies and an increase of easterly CPs that favour more continental, dry and warm air masses over central Europe. These atmospheric configurations enhance the projected summer drying over central and southern Europe, including Spain (Herrera-Lormendez et al., 2023b). In northern, eastern and southeastern Spain, SLP is projected to increase in all seasons except summer, whereas in the south and southwest it is expected to increase in winter and decrease in summer (Ozturk et al., 2022).

Further studies are needed focusing on the analysis of future changes in the seasonal or intraseasonal sequencing of CPs (in addition to the already available studies analysing total seasonal frequency of occurrence of CPs), and its implication in changes in physical mechanisms and related impacts (Muñoz et al., 2017).

3.5. Atmospheric Moisture

As has been reflected in Chapter3 Section 6, atmospheric moisture is one of the key variables to be investigated under climate change, not only for the evaluation of potential changes in moisture sources or transport mechanisms, but also for the evaluation of potential health risks under different climate scenarios. However, the literature available focusing only on atmospheric moisture is scarce, and most of the time, it is considered as an additional explanatory variable in temperature and/or precipitation studies.

Model evaluation

CMIP3 GCMs tend to correctly simulate relative humidity (RH) over Europe during autumn and winter, and over oceans and seas. However, during spring and summer, some differences arise compared to observational products. In spring, global models overestimated RH by 5-10% over wide areas of Europe, while in summer an underestimation of RH by 10-20% is found over eastern and southern Europe, contrasting with an overestimation of 5% over northernmost Europe (Ruosteenoja and Räisänen, 2013). However, observational datasets are also limited by the low density of weather stations and their varying temporal coverage over Europe.

More recently, CMIP5 GCMs have been evaluated against the latest observational humidity dataset (HadISDH), showing a broad agreement in large-scale and long-term changes for both relative and specific humidity (Dunn et al., 2017). However, none of these CMIP5 simulations reproduced the changes observed during the last decade, raising concerns on their ability to project reliable changes for the future. The suitability of CMIP5 GCMs for the detection of ARs was also evaluated as represented by the integrated water vapour transports (Espinoza et al., 2018). In contrast to relative and specific humidity, the multi-model mean showed a good representation of zonal and meridional water vapour transports and AR frequency compared to ERA-Interim reanalysis, with biases below ~10% in midlatitude regions. Global CMIP5 simulations also capture the spatial patterns of land precipitation and evaporation, necessary for moisture recycling analysis (Findell et al., 2019). The suitability of the latest CMIP6 simulations for the detection of AR has also been confirmed (O'Brien et al., 2022).

High-resolution climate simulations from the EURO-CORDEX initiative have also been employed to evaluate changes in humidity under different climate scenarios. The specific humidity of these simulations under present climate conditions is comparable to those provided by the Japanese JRA-55 reanalysis, which assimilates observations through a 4D-VAR assimilation scheme (Scoccimarro et al., 2017). The RH from these simulations were also bias-corrected using the Quantile-Quantile method based on weather stations. The bias-corrected simulations provide reasonable values of RH over the Basque Country (northern Spain) when compared against E-OBS dataset, but they underestimate the extremes of RH (Martija-Díez et al., 2023).

Climate change projections

Future changes in RH projected by CMIP3 global models vary across Europe under the A1B intermediate-emissions scenario. A remarkable reduction of RH is found over the IP during all seasons, but particularly during summer, when the maximum reduction (10%) is found (Ruosteenoja and Räisänen, 2013). A regional study over the Basque Country (northern Spain) using EURO-CORDEX data confirms this reduction in RH for both the intermediate and high emission scenarios (RCP 4.5 and RCP 8.5) over most of the area (Martija-Díez et al., 2023). By the end of the century, the results show a RH reduction by 2% over inland areas and a 1% increase in the coast for RCP 8.5 (0.5% decrease and increase, respectively, for RCP 4.5). This is caused mainly by the increase of oceanic evaporation in a warmer climate. This reduction of RH over the IP agrees with the slight increase in specific humidity projected by EURO-CORDEX RCMs under the warmer high-emission RCP 8.5 scenario (Boé et al., 2020; Scoccimarro et al., 2017). At the same time, precipitation recycling on the IP is projected to increase in all seasons except summer for mid-century under the SSP5-8.5 scenario, reaching an increase of 2-8% in annual terms (Fernández-Alvarez et al., 2023b). Furthermore, as detailed in Chapter 3, the Mediterranean Sea and the North Atlantic basin are fundamental to the moisture budget associated with the IP, and therefore their changes are essential in future climates. By mid- (2036-2065) and end-century (2071-2100) under the SSP5-8.5 scenario, an increase is projected for winter, spring, and autumn from the Mediterranean moisture source (>10 % compared to the present) but with a slight decrease in summer. In addition, the North Atlantic source will contribute with more moisture to the IP, with values greater than 20 % in winter, summer and autumn except spring (Fernández-Álvarez et al., 2023b).

Similar considerable reductions in RH are also found over inland areas of southern Europe. However, an increase in RH is projected for north-eastern Europe, particularly during winter. A similar geographic distribution of changes in RH are also found for the low-emission B1 and high-emission A2 scenarios. In those cases, the maximum drop in RH during summer varies from 7 to 13% respectively over Europe (Ruosteenoja and Räisänen, 2013). The increase in RH over northern Europe agrees with the projected increase in specific humidity in northern Europe by the RCP 8.5 scenario in EURO-CORDEX regional simulations (Boé et al., 2020; Scoccimarro et al., 2017). The increase in evaporation over the Mediterranean Sea is also responsible for increasing the specific humidity over the sea and the adjacent land areas, which could lead to smaller RH changes over the continent (Boé et al., 2020). The changes in humidity projected over northern and southern Europe will affect cloud cover, by reducing it over the Mediterranean region while increasing it over Scandinavian countries (Coppola et al., 2021a). Concurrently, global mean recycling rations are also expected to decrease (by 2-3% per degree of global warming according to a CMIP6 simulation), and a larger amount of oceanic evaporation will contribute to continental precipitation (Findell et al., 2019).

Thus, all projections agree on a tendency toward more arid climates over the IP and southern Europe (Ruosteenoja and Räisänen, 2013; Scoccimarro et al., 2017). The declining RH will enhance potential evapotranspiration, which together with the increasing temperatures and decreasing precipitation, will exacerbate the water scarcity over already dry areas. Therefore, wet and dry seasons will be amplified regionally, mainly due to more intense moisture fluxes

and a weakening of the tropical circulation, and the water cycle will be intensified with increased moisture fluxes triggering heavier precipitation (Allan et al., 2020).

Regarding ARs, evidence suggests that increasing global atmospheric moisture, affected by the Clausius-Clapeyron scaling, will increase the intensity of ARs and their related precipitation (Payne et al., 2020). CMIP5 climate simulations under the high-emission scenario RCP 8.5 confirm this by projecting a 50% increase in AR frequency and a 20% increase in the more extreme water vapour transports in the mid-latitudes, which include the coasts of the IP and western Europe (Espinoza et al., 2018). The same simulations also show an expansion in the size of ARs (25% longer and wider), and a decrease in the number of ARs by 10% approximately (Espinoza et al., 2018). This northward expansion is associated with a poleward shift of the storm tracks (Sousa et al., 2020b), which will cause a decrease in precipitation over Mediterranean regions. Under SSP5-8.5, an increase in the strength and moisture transport in the ARs that reach the IP is projected. In addition, moisture sources increase their progressive contribution to landfalling ARs arriving at the IP, showing a latitudinal shift and a loss of importance in the moisture contribution for regions such as the Gulf of Mexico in summer and autumn (Fernández-Álvarez et al., 2023c). Thus, the contribution to precipitation from the North Atlantic Ocean to Europe and the IP will be reduced and will have an impact on the precipitation regime and a reduction in rainfall by the end of the century (2071-2100) according to a regional WRF model simulation under the SSP5-8.5 scenario (Fernández-Álvarez et al., 2023b). This reduction in precipitation has been confirmed over southwestern IP with alternative WRF simulations for RCP 4.5 and 8.5 scenarios (Tuel and Eltahir, 2020). During days with landfalling ARs, increases in latent and sensible heat transports are also projected to increase over western Europe (Shields et al., 2019).

The Atmospheric Rivers Tracking Method Intercomparison Project (ARTMIP; O'Brien et al., 2022) has confirmed that most AR trackers and CMIP5 and CMIP6 simulations agree on the increasing AR frequency, size and number under high emission scenarios (RCP 8.5 and SSP5-8.5). However, ARTMIP also noted that the AR detector employed can restrict the degree to which the ARs penetrate inland or their total extension, highlighting that way the importance of understanding the implications of uncertainty for AR-related research.

Knowledge gaps

Despite the increasing attention that AR are receiving during recent years, alternative variables related to moisture such as relative or specific humidity are being neglected. In most of the cases, such variables are considered an addition to temperature or precipitation studies, and few studies have a real focus on them. Furthermore, the number of publications over the IP is rather scarce, which is surprising since the IP is considered a hot spot under climate change. Therefore, a clear need for further investigation on moisture is highlighted.

3.6. Radiation, clouds and aerosols

Surface solar radiation (SSR) plays a crucial role in the climate system as the primary source of energy that drives the atmospheric dynamics, ocean currents, and processes on the global biosphere. As the major component of the surface energy balance it controls many processes such as the temperature cycles, evapotranspiration processes or other biological

activities like photosynthesis. In addition, in recent decades it has become an important resource for renewable energy development, so understanding variability and evolution in SSR has major environmental and socioeconomic implications.

Solar radiation reaching the surface depends on its attenuation through the atmosphere, where it is partly absorbed and partly scattered by its constituents. Due to that, SSR is subject to significant changes due to either natural or anthropogenic activities. Natural changes are driven by astronomical factors, the increase of aerosol loads after volcanic eruptions or variability of cloud cover. Among them, cloudiness can be considered as the main cause of variability of the solar radiation at the Earth's surface (García-Díez et al., 2015; Kothe et al., 2011) but despite the efforts to determine their influence, large uncertainties remain about the climatology and trends of clouds (Hartmann et al., 2000), as well as about their response and feedbacks to the anthropogenic forcing (Dufresne and Bony, 2008; IPCC, 2014a; Randall et al., 2007).

It is, in fact, the inaccuracy of cloud representation in GCMs the main source of uncertainty in climate sensitivity estimates and climate change predictions (Bony et al., 2015; IPCC, 2014a). Although a tremendous effort to improve cloud processes representation in weather models and also in GCMs has been performed over the past decades (Randall et al., 2013), several studies still show large differences between observations and model simulations of clouds (Klein et al., 2013).

There is also evidence on the anthropogenic impact on solar radiation reaching the surface, with a decrease also in highly polluted areas (see for instance Li et al., 2017). These changes on SSR can have profound effects on the climate system due to its above mentioned important role but also economic implications.

Researchers have focused on evaluating future changes in SSR considering its implications not only for climate but also for the development of sustainable energy strategies, and due to that, the number of studies analysing SSR has increased in recent years, although its analysis of future changes is limited compared with other variables (see for instance Dutta et al., 2022; Feron et al., 2020; Gernaat et al., 2021).

Projected changes in SSR under different scenarios are not homogeneous across the world, as demonstrated by various studies, and drivers of change are also regionally dependent (see, for instance, Crook et al., 2011; Dutta et al., 2022; Wild et al., 2015), linked to its variability in related variables (cloud cover and aerosols). Thus, regional variations in SSR trends and patterns highlight the need for localised analysis and assessment.

Despite the importance of SSR for the reasons explained above, studies on its variability and future projections, as well as studies on related variables, are scarce for the IP, and most of the literature conducts analyses on a larger spatial scale. In addition, literature is based mostly on mean changes and research conducted on extremes is scarce.

Main results on SSR changes until 2017 are conducted for wider regions (global or european level) using GCMs and RCMs (Bartók et al., 2017; Crook et al., 2011; Jerez et al., 2015; Wild et al., 2015).

In a continental scale, a discrepancy for SSR projections was observed in particular for central Europe especially in spring and summer months between global and regional

models. An ensemble of EURO-CORDEX RCMs suggested a general decrease in SSR over central Europe (Bartók et al., 2017; Jerez et al., 2015) in different scenarios by the end of the century with a decreasing trend of –0.60 W/m^2 per decade found in Bartók et al., 2017, where authors attribute the discrepancy to the different behaviour of cloud cover. On the other hand, GCMs indicated a general increase (Wild et al., 2015) in SSR over Europe, and it is attributed to an increase in clear-sky radiation over the area. The discrepancy over the European sector increased uncertainty in SSR projections over the continent.

Related to that uncertainty is the evaluation of cloud cover from GCMs and RCMs. Some authors have seen an underestimation of Total Cloud Cover (TCC) in CMIP5 simulations in the Mediterranean region for present climate compared to RCMs (Enríquez-Alonso et al., 2016), especially in the spring-summer time. But despite the slight improvement in describing the TCC seasonal behaviour for the whole period, RCMs are unable to capture the observed decadal trend in TCC (Enríquez-Alonso et al., 2017).

Over the IP, projected changes are however subtle as seen in the above mentioned references. Global models from CMIP-5 projected for the mid century a slightly negative trend for clear-sky radiation (0.002 W/m^2/year), and a positive trend for all-sky radiation (0.115 W/m^2/year) (Wild et al., 2015). Regional models project for an extreme-case scenario (RCP 8.5) values around 5 W/m^2 by the end of the century in annual terms, driven mostly by the positive signal in summer changes (Jerez et al., 2015). Changes in that area seems to be driven mostly by changes in cloud cover in the mediterranean region, where a decrease is projected as a consequence of the hadley cell displacement to the north (Bartók et al., 2017; Enríquez-Alonso et al., 2017; Sánchez-Lorenzo et al., 2017) although a deeper analysis is needed to determine the causes of SSR changes over the IP.

Since 2017, several studies have been conducted on SSR, cloud cover, and aerosol changes, which contribute to the analysis of future changes over the IP. However, most of these studies do not specifically focus on this area and more specific research is still missing.

From a continental point of view, by the end of the century, projections from global models see an increase in clear-sky radiation and a reduction in cloud cover go together in SSP1-2.6 scenario, but the effect of a decrease in clear-sky radiation is outweighed by a decrease in cloud cover in SSP5-8.5, resulting in an increase in all-sky radiation over Europe (Hou et al., 2021).

The discrepancy in SSR changes during the summer months between RCMs and GCMs over Europe seen in previous studies has been attributed recently by several authors (Boé et al., 2020; Coppola et al., 2021a; Gutiérrez et al., 2020) to the absence of aerosol evolution in RCMs as reported in (Boé et al., 2020; Gutiérrez et al., 2020; Nabat et al., 2014). This inconsistency highlights the importance of considering aerosol in RCMs to better project trends in SSR and their associated climate impacts.

However, major impact of the aerosol content is projected in central Europe, and that is the area where uncertainty of SSR projections is higher. The impact of aerosols on the SSR over southern europe seems to be low for future projections, compared to cloud cover evolution, as well as it was in past trends during brightening and dimming periods, where clouds were

the key factor responsible for explaining "brightening" trends, as they explain approximately 75% of the solar radiation changes (Mateos et al., 2014).

For the IP, a future increase in solar irradiation is projected in annual terms for mid century (Gil et al., 2019) with RCMs from the ESCENA project, although not all scenarios agree on the geographical distribution of this increase. The spatial distribution of the changes shows a maximum in southwestern IP and the minimum change values over the mountainous areas of the north and in the southeast, in most simulations.

Annual mean changes for the end of the century are projected to be less than 5 W/m² with respect to 1971-2000 with an ensemble of RCMs (Bartók et al., 2019) after a bias correction methodology. Some spatial variability is found with larger changes in the northwestern part of Spain compared to other regions. In the Basque Country, for RCP 4.5 scenario, the evolution found is different in the middle and in the late future (Martija-Díez et al., 2023). In the period 2041-2070 there is spatial variability with areas in which radiation tends to decrease, while in the last decades, although less than in the RCP 8.5 scenario, the increase in SSR is homogeneous in the whole area.

On a seasonal basis, the largest relative decrease of TCC in the Mediterranean for future projections is observed in summer and, secondly, in autumn, whereas winter is the season with the smallest rate of decrease (Enríquez-Alonso et al., 2016), this is in accordance to the pattern observed for SSR in Müller and Pfeifroth, 2022.

Summer SSR mean changes for the RCP 8.5 scenario depends on the model used. In general, changes in SSR are larger in the GCMs, because the decrease of cloud cover is also larger (Boé et al., 2020). Cloud cover is reduced by 5 to 10% over the IP and SSR varies between ~5 to more than 10 W/m² depending on the model and region (Boé et al., 2020). In the mid-century, changes found in cloud cover and SSR are similar but less intense (Gutiérrez et al., 2020). Although differences between RCMs with and without aerosol evolution are found, the relative importance of clear sky changes compared to total sky changes is smaller over western Europe suggesting an important decrease of cloud cover there (Boé et al., 2020; Müller et al., 2019).

Over western Europe the projected decrease of TCC is important for the end of the century (Boé et al., 2020). Nevertheless, for the near future (2021-2050) the changes in the TCC are relatively weak for all GCMs and RCMS in summer and have a patchy spatial pattern (Gutiérrez et al., 2020). The GCM models show a decrease of around 3-4% in TTC in the centre and south of the IP, while in the north a slight increase (0-1%) is found. In Galicia, Catalonia, Aragon and Balearic Islands the models disagree. The RCM models analysed in Gutiérrez et al., 2020 present overall the same tendencies.

Despite the increase of research on SSR and its sources of variability including cloudiness and aerosols, there is still a lack of local references concerning the IP. Also, while many studies concentrate on changes in average values, few of them analyse variability or possible shifts in extreme values (Feron et al., 2020; Gil et al., 2019; Hou et al., 2021). Therefore, further investigation is necessary to deepen our understanding in this domain.

3.7. Multi-variable indices

Fire danger

The Canadian Fire Weather Index (FWI) system, developed by the Canadian Forest Service, integrates daily meteorological records (RH, wind speed, air temperature and last 24 h accumulated precipitation) and calculates fuel dryness and other intermediate parameters (van Wagner, C.E., 1987). It is the most widely used system internationally, and the reference index for the European Forest Fire Information System (EFFIS, San-Miguel-Ayanz et al., 2012), in order to assess the fire danger level in a harmonised way throughout Europe. In Spain, most future fire danger projections have been calculated building upon the FWI system.

From a global perspective, Europe emerges as one of the world regions with a robust (positive) FWI signal, that is reinforced in intensity and spatial extent for higher GWLs, according to the most recent global CMIP6 future FWI projections (Quilcaille et al., 2023). These results are in agreement with the previous global assessment undertaken with an ensemble of CMIP5 models (Bedia et al., 2015) that found that the fire-weather sensitivity of many vulnerable temperate European biomes will increase during the forthcoming decades. The study showed that the Mediterranean region has a high fire-weather sensitivity, and that this sensitivity will increase in the near future, especially under the high emission scenario (RCP 8.5), although the actual effects on burned areas may not increase accordingly once surpassed an empirically-derived mean FWI threshold, linked to an increased aridity and fuel availability limitations, as shown in future burned area statistical projections for Europe (Turco et al., 2018).

Previous early studies projected FWI changes in Mediterranean Europe (EUMED), the IP and Spain using different models, scenarios, and methods. Moriondo et al., 2006 used a single GCM-RCM coupling (HadCM3-HadRM3, 0.44ºx0.44º) and the A2 and B2 Special Report Emissions Scenarios (SRES) to show a general increase in fire danger across EUMED. Giannakopoulos et al. (2009) confirmed these results using the same GCM model (HadCM3) and a +2 ºC GWL scenario. Both studies indicated a general increase in fire danger in both future scenarios over the whole region, mainly due to three factors: (1) increase in the number of years with high fire danger; (2) increase in the length of the fire danger season; (3) increase of extreme events (e.g. total number of days with FWI > 45 and episodes with FWI > 45 for 7 consecutive days) during the fire season. These studies indicated an increase in fire danger for most of the IP, especially in the southern and eastern regions. Furthermore, the total number of days with extreme FWI values, and the persistence of extreme FWI events progressively decreases when moving from flat to mountainous areas (Moriondo et al., 2006). However, in the IP high frequencies (~90%) were also observed at high altitudes.

In the same vein, using EURO-CORDEX simulations over the Mediterranean Basin, the frequency of heat-induced fire-weather is projected to increase by 14% by the end of the century (2071-2100) under the RCP 4.5 scenario, and by 30% under the RCP 8.5, suggesting that the frequency and extent of large wildfires will increase triggered by the projected shifts in the frequency of dangerous Fire Weather Types (FWTs, Ruffault et al.,

2020). Here, FWTs are described by five variables that characterise different levels of fuel aridity (from weekly to monthly scale) and the synchronous, short-term weather conditions (i.e. daily scale) that control the occurrence and spread of wildfires. The variables include the daily mean temperature, wind speed, RH, and two cumulative fuel moisture codes of the FWI System, namely, the duff moisture code (DMC) and the drought code (DC).

Bedia et al., 2013 applied the analog method to downscale FWI projections from a single GCM (ECHAM5) under the A1B scenario for several locations in Spain and Greece. They validated their method with reanalysis data and compared it with an RCM (RACMO2), finding similar spatial patterns than the previous studies of fire danger increase in the first half of the 21st century, but diverging in the second half, attributed by the authors to limitations of the statistical method to extrapolate to the unprecedented extreme conditions of FWI projected for the latter part of the period in some areas.

Herrera et al., 2013 identified methodological problems with using daily mean values for FWI calculation, which could affect the projected climate change signals in some previous studies. To this aim, they developed their own RCM simulations (WRF coupled to ECHAM5). Their results aligned with the previous studies in terms of positive FWI anomalies, more accentuated in central parts of Spain, and paved the way for the use of the ENSEMBLES database (van der Linden, P., Mitchell, J.F.B., 2009) for FWI calculation, the state-of-the art high resolution simulations at the time. As a result, new dynamical projections of FWI changes in the Mediterranean region were produced using the simulations from ENSEMBLES from five different GCM-RCM couplings (Bedia et al., 2014). An optimal proxy variable combination was applied to overcome the limitations of the ENSEMBLES data for the FWI system regarding the temporal aggregation of the model outputs. A positive and robust signal of fire danger increase for Spain was found in the 21st century, more pronounced in the second half of the century. Remarkable increments were described for some critical FWI-derived indicators such as the frequency of events FWI > 30 (FOT30) and length of the fire season. However, both FOT30 and fire season length exhibit a large multi-model spread, increasing for the second and third future time slices considered (2041–2070 and 2071–2100), indicating a high degree of uncertainty in these aspects unseen in previous single-model projections (Giannakopoulos et al., 2009; Moriondo et al., 2006). Mean JJAS (June-July-August-September) FWI conditions and 90th percentile of FWI projected for Spain exhibit a consistent positive signal, accentuated in the latest part of the transient period (2071-2100), with a much lower spread.

Some modifications to the original FWI definition have been introduced in recent times to account for atmospheric instability (Pinto et al., 2020) as an additional fire danger factor of utmost importance to characterise Extreme Meteorological Fire Danger (EMFD). For instance, Bento et al., 2023 found that EMFD would increase significantly in both frequency and intensity by the end of the 21st century in the IP, especially under the RCP 8.5 scenario, with the largest increases occurring in the summer and autumn seasons, using an ensemble of RCMs from the EURO-CORDEX initiative. The north-western region of Iberia, including the north of Portugal and the north-western-to-central Spain are the regions with larger increases in future fire danger. They also find a lengthening of the fire season with an expected extension of the dangerous period to June and, in a lower magnitude, to September.

Overall, these results contributed to the previous lines of evidence pointing to an increase in fire danger conditions in EUMED, and in Spain in particular, with consistent spatial patterns of increased FWI in central and eastern IP, and also a lengthening of the fire season and mean FWI conditions in Atlantic areas.

Human comfort and heat stress

For many impacts such as human health, thermal comfort and labour productivity, as well as for specific sectors (e.g. tourism), the interaction of several variables can enhance their individual effect. Global studies show observed and projected increases of sensible (from increasing air temperature) and latent (through rising humidity) heat in response to anthropogenic GHG forcing of the climate, which lead to larger changes in heat-humidity indices than for air temperature alone (Matthews, 2018). In Europe, air temperature changes are larger in southern Europe than in the north, unlike changes of summer maximum heat stress (combination of high temperature and high humidity) which are more uniform across the continent (Casanueva et al., 2020a). This might be due to the projected decrease in RH in the Mediterranean region, which counterbalances the strong temperature increase and, hence, results in a smaller heat stress change.

From a methodological point of view, having multivariate indices implies examining inter-variable relationships and how the different climate models and downscaling approaches are able to represent them. RCMs present important biases in heat stress indices, for instance, a general underestimation of moderate heat stress events in southern Europe is found (Scoccimarro et al., 2017; Vautard et al., 2021). The contribution of the RCMs to the biases in heat stress is dominant with respect to the GCM contribution, probably due to the strong dependence on physical parameterizations (Vautard et al., 2021). Since many policies (e.g. related to labour productivity) are associated with surpassing absolute thresholds, BA is commonly applied. BA (through EQM and trend-preserving ISIMIP method) of the individual meteorological variables forming a heat stress index (based on dew point temperature and air temperature) is able to improve the representation of the inter-variable relationships just by centering the marginal distributions (Casanueva et al., 2019). Regarding future projections, BA leads to changes (in general, reduction) of the simulated raw signals of heat stress indices, however the uncertainty related to the BA method is generally smaller than or similar to the model uncertainty.

Environmental heat exposure and exceedances of impact-relevant thresholds are projected to increase in the course of the 21st century overall in Europe (Casanueva et al., 2020a; Scoccimarro et al., 2017) and the Mediterranean is one of the regions with the strongest trends in several heat stress indices (Schwingshackl et al., 2021). For instance, for each degree of increased global mean temperature, daily maximum temperature and apparent temperature increase 1.8K/K, the heat index and humidex increase 2.2, WBGT (Wet Bulb Globe Temperature) increases 1.4K/K and UTCI (Universal Thermal Climate Index) increases 1.9K/K in the Mediterranean region.

Summer maximum heat stress in the shade in continental Spain overall may change from 26–29°C in present-day climate to 28–29°C, 28–31°C and 30–32°C in 2070-2099 for the RCP 2.6, RCP 4.5 and RCP 8.5, respectively. Accordingly, summer maximum heat stress in

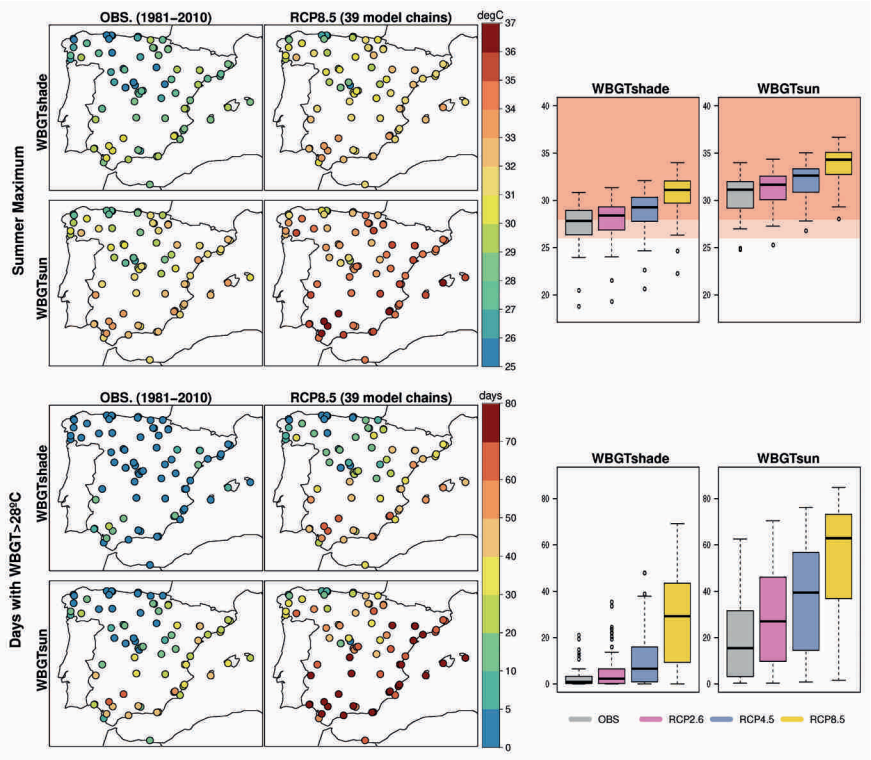

Figure 5.5. Summer maximum heat stress (upper panel) and number of days with heat stress above 28 ºC (lower panel). Maps represent observed and projected values (MME mean for RCP 8.5 in 2070-2099) for heat stress in the shade (WBGTshade) and in the sun (WBGTsun). Boxplots summarise the results for the three RCPs (2.6, 4.5 and 8.5) in 2070-2099 and two WBGT implementations for Spanish stations. Source: Adapted from Casanueva et al., 2020.

the sun is projected to rise from 29–32°C to 30–33°C, 32–34°C and 34–36°C in 2070-2099, respectively for the three scenarios (Figure 5.5). Maximum heat stress is projected to be higher but also more frequent, since extreme heat stress conditions are projected to increase by 5–15, 15–30 and 30–50 days per year in the Mediterranean region by the end of the century with respect to today's climate for the three RCPs, respectively (Casanueva et al., 2020, Figure 5.5). Climate projections are qualitatively consistent among heat stress indices. Particularly, considering humidex, *huge* discomfort (humidex between 40-45) is projected to increase over southern Europe under RCP 8.5, e.g. in south-western Spanish plains (Scoccimarro et al., 2017). Considering the wet bulb temperature (TW), the largest historical increases of critical days (TW above 26°C) in European cities are found in Spain, with Valencia at the top of the ranking consistently across RCMs (Karwat and Franzke, 2021). In Madrid, overall TW values are slightly lower, but still may cross a level of 32°C under RCP 8.5, leading to severe heat stress.

Such heat stress has important consequences in health and economic sectors. Heat-related mortality may increase by about 7.9% per decade in Spain for RCP 8.5 by 2050, which is almost twice the mortality risk trend for RCP 2.6 (Karwat and Franzke, 2021). Regarding labour productivity, by the end of the twenty-first century under RCP 8.5, the amount of working hours lost due to heat stress may reach more than 50% in some locations in Spain, being Seville very affected with 30%, 40% and 57% hours lost due to heat stress for RCP 2.6, RCP 4.5 and RCP 8.5, respectively (MME means for 2070-2100; Casanueva et al., 2020). Spain will be one of most economically harmed countries by excessive heat in the future, moving from national gross domestic product (GDP) losses of about 0.5% in current climate (1981-2010) to 2% in 2040 and 3% in 2060 (García-León et al., 2021).

Along with labour productivity loss, electricity demand and ozone concentrations do not scale linearly with the magnitude of future warming, i.e. largest increases are found during the warmest fortnights given the same warming level (Garrido-Pérez et al., 2023). Thus, as temperatures continue to rise, rearranging summer holidays (i.e. shifting from the second fortnight of August, which is the main summer holiday, to the second fortnight of July, which is the hottest) would be more beneficial in order to reduce of labour productivity losses, electricity demand and ozone concentrations (Garrido-Perez et al., 2023).

Tourism will be one of the most affected sectors by climate change in Spain. Currently, almost the entire Mediterranean exhibits above 90 days per year with *acceptable* conditions (climate index for tourism, CIT, between 4-5) and Spain features up to 60 days per summer with *ideal* climatic conditions in most coastal areas (CIT between 6-7). In the Canary Islands, the coastal regions currently have between 20-30 *excellent* and *ideal* days per month (Tourism Climate Index, TCI, between 80-89 for "excellent" and above 90 for "ideal") and, even during the winter months, more than half of the days can be considered *excellent* for urban tourism (Carrillo et al., 2022a).

Projections for 2075-2094 (under SRES A1B scenario) suggest an important deterioration of summer optimal conditions in Spain (especially affecting beach-based tourism), with an increase of about 30 days of *acceptable* conditions in the Atlantic basin at the expense of a reduction in the number of *ideal* days elsewhere. This will go hand in hand with an overall improvement in the shoulder seasons, e.g. increasing *ideal* conditions as *acceptable* ones decrease in spring (Amengual et al., 2014).

By regions, a northward shift is expected in the climatic assets, leading to excellent climate potentials in central and north Spain, while likely declining in south-western regions during the high seasons (Cardell et al., 2023; Díaz-Poso et al., 2023b). Regarding urban tourism (based on the Holiday Climate Index, HCI:Urban), by mid-century (2041-2060) the regions with the best comfort conditions will continue to be the Balearic Islands, Murcia, Valencia and Andalusia, for RCP 4.5 and RCP 8.5 (Díaz-Poso et al., 2023b). By the end of the century under RCP 8.5, the Balearic Islands and Andalusia (two of the regions receiving the highest number of tourists), are, together with Extremadura and Murcia, the regions with the largest decreases of HCI:Urban (2.91%, 3.33%, 3.75% and 3.34% respectively, compared to 1986-2005, based on the EURO-CORDEX ensemble mean). In contrast, Asturias, Cantabria, La Rioja, Galicia and the Basque Country, will considerably improve urban comfort, with increases of HCI:Urban of 11.27%, 9.67%, 8.27%, 7.13% and 5.86%, respectively (Díaz-Poso et al., 2023b).

In the Canary Islands, projections show an improvement from spring to autumn in the highest areas. However, fewer *excellent* days for tourism (based on TCI) are expected especially in summer in the south of Tenerife and Gran Canaria, and a large part of Fuerteventura and Lanzarote, where most of the hotel infrastructure is located. *Excellent* and *ideal* days may increase in winter and shoulder seasons in the most visited areas (Carrillo et al., 2022a).

By activities, an overall deterioration of the optimal climate conditions for inland activities (i.e. cycling, cultural, football, golf, hiking) is projected in summer, while spring and autumn could benefit from favourable climate conditions (Bafaluy et al., 2014) and a general future increase of excellent climate potentials is expected in winter (Cardell et al., 2023). Only nautical sports could experience an important increase in the annual number of days rated as *ideal*, as it could be practised not only in the peak season (summer) but also in shoulder seasons (Bafaluy et al., 2014). In particular, autumn will become the ideal season for sailing, thus companies dedicated to this sector should explore the expansion of this activity to autumn (Cardell et al., 2023).

There are still some open questions regarding heat stress and human comfort in Spain. Although scenario uncertainty is considered in most studies, only few studies quantify model uncertainty and only some use a large ensemble of RCMs. Future research could benefit from the combined use of RCMs with ESD methods, including those tackling multivariate aspects. Literature covering the Balearic and Canary Islands is sparse; only one paper about the Canary Islands was found in this review, based on a single RCM driven by several GCMs.

Agroclimatic indices

European vineyards account for approximately 52.7% of the total vine cultivation areas worldwide, located mainly in Spain, France, and Italy (Cardell et al., 2019b). In addition to temperatures and precipitation, some agroclimatic indices are defined to characterise climatological conditions in the growing season (Serrano Notivoli and Beguería, 2021). For instance, the Winkler index combines daily maximum and minimum temperatures and provides information on the accumulation of heat during the growing season, the Huglin index (HI) relates to the sum of the temperatures required for vine development and grape ripening, the Biologically Effective Degree-Days (BEDD) accounts for heat accumulation and the hydrothermic index of Branas, Bernon and Levadoux (BBLI) quantifies the influence of temperature and precipitation on the grape yield and wine quality.

Climate change will negatively affect wine grape growing in southern Europe. On the one hand, future increase in temperatures relates to enhanced cumulative thermal stress (over 400°C increase in HI for 2041–2070; Fraga et al., 2013). On the other hand, dry conditions in the growing season are projected to intensify (Fraga et al., 2013). Furthermore, the projected precipitation decrease and higher rates of evapotranspiration due to a warmer climate will likely increase water requirements (Cardell et al., 2019b) and the sector should adapt including crop irrigation or water stress mitigation methods. Results from ENSEMBLES (Fraga et al., 2013) and EURO-CORDEX (Cardell et al., 2019b; Velasco Horcajada, 2023) projections agree qualitatively for Spain. For instance, HI and BEDD, which depend exclusively on temperatures, show a generalised increase across the IP under a GWL of 4 ºC (Velasco Horcajada, 2023). This increase is particularly noticeable in areas

such as the northern plateau and mountainous areas, precisely those regions with lower observed values in present climate. Differences in the climate change signals are driven by the climate model, being the uncertainty associated with the BA method smaller than model uncertainty. The BBLI index (which combines temperature and precipitation) is projected to decrease over large parts of the IP (Velasco Horcajada, 2023). All the above points to a reduction in table quality vines and wine grape production (Cardell et al., 2019b), which could be accentuated due to an enhanced inter-annual variability (Fraga et al., 2013).

For the particular case of wine production in Rías Baixas, increasing trends of Winkler and Huglin indices are projected under SRES A1B scenario, aligned with the observed increasing trend in 1958–2005 (Lorenzo et al., 2013). Under the projected warmer and drier climate in the region, the varietal spectrum of the DO Rías Baixas could change substantially since the suitability for the cultivation of a given cultivar is largely temperature driven.

While the above studies use RCMs, statistical downscaling based on artificial neural networks have been used to project chill and heat accumulations (Egea et al., 2022). Such indices are used to build decision tools that help producers and other stakeholders to design optimal production and economic policies for medium and long term. Chill and heat accumulations are relevant for stone fruit production (i.e., peach, apricot, plum, and sweet cherry) in Spain; e.g. cultivars require specific chill accumulations, otherwise poor flowering, delay in flowering and sprouting, and lack of uniformity in both processes can occur. Future scenarios show a clear decrease of accumulated chill in warm areas, in northern Extremadura and some interior areas of the Mediterranean. As chill accumulation decreases in future scenarios, heat accumulation increases proportionally (Egea et al., 2022). To ensure the adaptive suitability of the different cultivars, a relocation may be needed, and some of the cultivars should be moved to close areas (interior zones in the Mediterranean area or toward Extremadura in the case of the Guadalquivir Valley) where the chilling requirements will be fulfilled even in the future scenarios, and the frost risks are expected to decrease (Egea et al., 2022).

Based on GCMs, projected decreasing trends in chill accumulations are also found in Zaragoza and associated with seven sweet cherry cultivars (Fadón et al., 2023). For three out of the seven species, most GCMs predict medium or low risks by 2050 and 2085 under the RCP 4.5 scenario. Under the RCP 8.5 scenario, particularly by the end of the 21st century, four of the cultivars with high chill needs are expected to not meet their chill requirements very often. Still sweet cherries may adapt to regions with medium- and high-chill profiles (Fadón et al., 2023).

Drought and aridity

Drought and aridity pose great challenges for the economy, ecosystems, and the agricultural sector (Zhou et al., 2019). According to the last report of the IPCC (IPCC, 2023), agricultural and ecological droughts have become more frequent and intense with 0.5 ºC of additional global temperature rise. Therefore, in a global warming world, changes in the patterns of these types of phenomena are expected to occur, making them critical factors for water management (García-Valdecasas Ojeda et al., 2021b), assessments of fire risks (Chaparro et al., 2016; Turco et al., 2013), and the implementation of mitigation and adaptation

strategies to climate change. This is especially important in regions such as the IP and Canary Islands, where there are dry regions with prolonged periods of no precipitation.

Global temperature rise will increase atmospheric evaporative demand (AED), resulting in an increase in global aridity (Asadi Zarch et al., 2017; Sherwood and Fu, 2014, among others). Such conditions will be exacerbated in regions where precipitation is expected to decrease. This is the case of the IP, which, as part of the Mediterranean region, has been identified as a climate change hotspot (Giorgi, 2006). Here, the evidence of the reduction of the water cycle is robust across the future climate scenarios with low uncertainty in the sign of the changes. In this context, studies focused on changes in aridity conditions for the IP suggest a significant reduction in precipitation, especially towards the end of the century and under the business-as-usual scenario (RCP 8.5), with reductions up to 30-40% over southern IP (Carvalho et al., 2022; García-Valdecasas Ojeda et al., 2020a, b). This fact, combined with the enhanced AED, which is more pronounced in this area, is likely to lead to a decrease in surface evapotranspiration due to the depletion of soil water content (García-Valdecasas Ojeda et al., 2020a, b). As an exception, increases in surface evapotranspiration are expected over mountain regions, such as the Pyrenees, but these also resulted in an increase in aridity as the balance between precipitation and evapotranspiration is projected to decrease (Carvalho et al., 2022). The latter is supported by Andrade et al., 2021, who used the Martonne (De Martonne, 1923), Pinna Combinative (Zambakas, 1992), and Erinç (Erinç, 1965) aridity indices to analyse future conditions and found an increase in aridity over the IP in the future. The results from these three indices, which were calculated with a MME of bias-corrected EURO-CORDEX simulations, exhibited more arid conditions from 2041 to 2071 when compared to the recent past (1961-1990) under RCP 4.5 and RCP 8.5, especially in southern peninsular regions. The Canary Islands, moreover, are expected to experience drier conditions due to a precipitation reduction. These changes will be more noticeable under RCP 8.5 and in the southeast of Tenerife and Gran Canaria (Carrillo et al., 2023).

While aridity refers to the long-term average balance of water demand (i.e., evapotranspiration) and water supply (i.e., precipitation), drought is associated with water scarcity over a specific period, and thus, it can be considered as an extreme. Changes in drought conditions are also projected to increase in both frequency and severity in the Mediterranean region. This is especially true for the IP and Canary Islands, where numerous studies, using different methodologies, suggest that drought will worsen in the future. That is, a robust signal concerning the increase of drought hazard is found for this region using both global (e.g., Vicente-Serrano et al., 2020; Vicente-Serrano et al., 2022) and RCMs (Spinoni et al., 2018); based on a few numbers of climate simulations (García-Valdecasas Ojeda et al., 2021b) or supported by RCM/GCM multi-model CORDEX ensembles (Alvarez et al., 2024; Driouech et al., 2020; García-Valdecasas Ojeda et al., 2021a; Spinoni et al., 2020); using different emission scenarios (Soares et al., 2023b; Spinoni et al., 2021), future periods, and warming levels (GWL).

Standardised drought indices, such as the Standardised Precipitation Index (SPI, McKee et al., 1993) and the Standardised Precipitation Evapotranspiration Index (SPEI, Vicente-Serrano et al., 2010), have been widely used to assess drought characteristics. This is primarily due to their multi-scalar character, which allows them to be used

to investigate various types of droughts. Thus, for the IP, the three-month timescale is commonly applied to assess meteorological droughts. 6- or 12-month timescales, however, seems to be better suited for characterising agricultural and hydrological drought, respectively (García-Valdecasas Ojeda et al., 2017). In general, both global and regional studies based on drought indices show a consensus on the expected trend in the IP in terms of drought. All these studies indicate that drought conditions will worsen, with higher emissions scenarios becoming more pronounced by the end of the century. However, the magnitude of the projected changes is highly dependent on a variety of factors that must be considered when assessing drought in a changing climate. On the one hand, the use of combined indices such as the SPEI or the reconnaissance drought index (RDI, Tsakiris et al., 2007), which take the AED into account when monitoring drought events, appear to be critical in arid regions such as the IP and as temperatures rise. Thus, the non-inclusion of this variable in the index could lead to significant errors in the drought characterization (Carrillo et al., 2023), as this variable could be a major driver of drought severity. In this regard, many studies report much more significant changes in drought conditions over the IP when SPEI was used in comparison with projection obtained from SPI (Carrillo et al., 2023; Esteban-Parra et al., 2022; García-Valdecasas Ojeda et al., 2021a; Soares et al., 2023b; Spinoni et al., 2020, 2021). In the same way, the selection of AED formulae could have a significant impact on drought event estimation. Commonly, AED is estimated following one of these equations: (1) Thornthwaite (TH, Thornthwaite, 1948), which is based on mean temperature, (2) Hargreaves (HG, Hargreaves and Samani, 1985), which uses maximum and minimum temperature, and (3) Penman-Monteith (PM, Allen et al., 2006), which includes additional variables such as the net radiation, wind speed, or vapour pressure. Several studies point to PM as one of the most suitable equations to estimate AED for the calculation of drought indices, particularly in the context of climate change (e.g., Donohue et al., 2010). However, it cannot always be applied as PM requires a larger number of hydrometeorological variables for calculation, which are not always available. In this case, HG appears appropriate, despite producing underestimations in windy regions and overestimations in hot-humid climate conditions (Tabari et al., 2013). In any case, it seems to be more appropriate than TH, which overestimates droughts (Han and Singh, 2023) in dry periods especially when extreme temperature occurs. Another important consideration is the selection of the reference period when calculating drought characteristics such as frequency, severity, or duration for preset (Um et al., 2017) and future conditions. This is particularly relevant when projections are used, with expected strong trends in drought-related variables by the end of the century (García-Valdecasas Ojeda et al., 2021a). That is, future drought indices are typically calculated using self-calibrated or relative indices. Self-calibrated indices are calculated over the entire study period (from the recent past to the distant future), whereas relative indices only consider the present-past when adjusting the spatial distribution parameters. Thus, in a study of the impact of the calibration period on the projection of different drought characteristics by calculating the SPEI at a 12-month timescale, García-Valdecasas Ojeda et al., 2021 found that self-calibrated indices show an increase in the frequency and duration of drought events, while relative indices indicate a worsening of drought associated with extremely prolonged events.

Renewable energies

According to the IPCC, 2022, "all global modelled pathways that limit warming to 1.5 ºC with no or limited overshoot, and those that limit warming to 2°C (>67%), involve rapid and deep and in most cases immediate GHG emission reductions in all sectors. Modelled mitigation strategies to achieve these reductions include transitioning from fossil fuels without carbon capture and storage (CCS) to very low- or zero-carbon energy sources, such as renewables or fossil fuels with CCS." To this aim, "in 2050 almost all the electricity should be supplied from zero- or low-carbon sourcer, such as renewable, combined with increased electrification of energy demand." according to the IPCC, 2022. This transition supposes a great challenge across the full energy sector that have, on the other hand, multiple co-benefits, including improvements in air quality and health.

In this framework, the viability, operativity and stability of electricity systems powered predominantly by renewable energies, such as wind and solar, has been the main focus of the studies over Spain in the latest years in order to scientifically support the proper transition and adaptation pathway until the end of the century based on the state-of-the-art climate change scenarios and simulations.

Based on the concept of energy drought (De La Vara et al., 2020; Gutiérrez et al., 2021; Kapica et al., 2024), reflecting periods with low productivity, the studies analysed how the electricity system of Spain, based on wind and solar energies, will evolve along the next century, and how both energy sources could be combined in order to minimise the occurrence of energy drought events (Jerez et al., 2019). Jerez et al., 2019 made a deeper analysis in order to study the temporal complementarity of both energy sources at several time scales.

The main conclusion of all the studies is that a hybrid system, regardless of the climate scenario, might reduce the energy storage requirements and lead to an overall reduction of the drought days along the year compared to a system based on one of them separately. Also, a high share of photovoltaic power, at least 50%, reduces the impact on the total photovoltaic-plus-wind mean production and the temporal variability of the daily production.

4. Regions of special interest

In this section, we consider small-scale, clearly-delimited geographical regions which are typically beyond the skillful scale of large ensembles of regional projections. They also exhibit challenging contrasts (orographic, land-sea, land use, etc.) that often require dedicated analyses. In particular, we consider the case of the Canary Islands and different mountain regions.

Other areas were not considered in detail because of the few studies available. Two particular cases represent important knowledge gaps. One is the Balearic Islands, which are typically covered in studies that focus, in principle, over continental Spain and these islands. However, few conclusions are usually extracted for the islands and the spatial resolution of the downscaling products used (e.g. CORDEX EUR-11 simulations) represent the islands by a few grid-cells unable to properly represent orographic and coastline details. The few dedicated studies available deal primarily with impacts on different sectors, such as tourism (Bafaluy et al., 2014; Torres et al., 2021) or energy (De La Vara et al., 2020). The second

important literature gap identified is urban areas, where climate affects many people. Given that the presence of cities modifies their environment, urban areas require specific climate projections beyond those corresponding to their overall location. Cities are beyond both GCM and RCM skillful scales. The latter may include specific parameterizations (urban canopy models; Garuma, 2018) to account for the effect of cities on regional climate. However, the complexity, or even use, of these urban models varies across RCMs; for instance, within the EURO-CORDEX ensemble. The importance to assess climate change effects on cities has been highlighted by the IPCC, which is currently scoping a Special Report on cities (Bai, 2023), or CORDEX, which endorsed a Flagship Pilot Study (FPS) on Urban environments and Regional Climate Change[1]. The few studies located for this report focus on specific indices (drought, torrentiality, HWs) in a specific city (Andrade et al., 2021b; Cutillas-Lozano et al., 2023; Ventura et al., 2023), although there are studies at European scale which focus on major cities, including Spanish ones (Karwat and Franzke, 2021; Reder et al., 2022). Their results have been included in the sections above.

Results from the scientific literature available for the Canary Islands and several mountain regions are summarised in the sections below.

4.1. Canary Islands

The Canary archipelago consists of 8 small islands (see Chapter 3: Section 8.1). GCMs, due to their coarse resolution, are not able to represent small islands. Their grid cells comprise a very high percentage of sea, with a small contribution from land-based phenomena, and orography is not taken into account. Furthermore, the Canary Islands, due to their location, are not included in the joint European regional climate simulations such as those of the EURO-CORDEX domain, which provides regional climate data at a moderate resolution. All this leads to a scarcity of available data related to climate projections, at an adequate resolution, for the Canary Islands.

Some previous studies on the Canary Islands use CP-RCMs with a 5 km resolution, employing the PGW approach to reproduce the observed geographical distribution of temperature and precipitation (Expósito González et al., 2022; Martí Ezpeleta et al., 2022; Pérez et al., 2014). In addition, data from different climate projections are available on the AEMET website, using ESD methods on a set of stations for the Canary Islands; no gridded data are provided.

More recently, new regional climate simulations have been performed, at a spatial resolution of 3 km, using the results of three GCMs as drivers, which belong to the CMIP5 project. Three 30-year periods were considered, both in the recent past (1980-2009) and in the future (2030-2059 and 2070-2099), using two emission pathways, RCP 4.5 and RCP 8.5. The projections show a significant increase in temperature (around 4.2 ºC by the end of the century for the RCP 8.5 scenario), more pronounced at higher altitudes (Pérez et al., 2022). This behaviour is associated with a reduced lapse rate in the future, that is consistent with wet adiabatic stratification in tropical and subtropical areas. It is important to take this fact into account for ecology studies, which usually estimate a shift to higher altitudes of certain ecosystems to reduce the consequences of climate change, typically assuming a lapse rate

1 https://ms.hereon.de/cordex_fps_urban

similar to the current one. As expected, by the end of the century, a significant increase, close to 30% percentage points for RCP 8.5, in the number of WD (maximum temperature over the 90th percentile, computed for the reference period) was projected. At the same time, the number of cold nights (minimum temperature below the 10th percentile) will be reduced to almost zero. In addition to the possible modification of the synoptic patterns, the increase in temperatures is mainly due to a decrease in TCC and soil moisture, which, in turn, is caused by a decrease in precipitation. This decrease in soil moisture has a direct effect on the reduction in latent heat flux and an increase in sensible heat flux, which leads to a projected rise of the diurnal temperature range. The return times of extremely warm temperatures, calculated in the recent past period with a 20-year return period, also decrease drastically to a few years.

Regarding precipitation, the aforementioned projections predict a considerable decrease, mainly in the higher altitude islands (Acosta-Mora et al., 2022). Simulation results show a general decline in annual precipitation of around 30% by the end of the century in the RCP 8.5 pathway. This decrease is mainly due to a reduction of above 30% in the number of wet days (daily precipitation over 1 mm) in most land areas. Days with heavy precipitation (over 20 mm) will also be reduced by more than 60% in many areas of the islands. An increase in the maximum length of dry spells was projected in most of the territory, as well as a decrease in the maximum length of wet spells. In contrast to extreme temperatures, return times for extreme daily precipitation are expected to increase. A shorter experiment (De Vries et al., 2022), using two ten year periods (1996-2005 and 2090-2099) and a single GCM as boundary conditions, also projected a decrease in heavy hourly precipitation (99.9th percentile computed from all data, wet and dry events). In the highest island, Tenerife, the heavy precipitation is expected to decrease around 4 mm/h in the wettest season (December-January-February), mainly due to a reduction in heavy precipitation events, while the intensity of those events remains very similar.

This decrease in precipitation, as well as the increase in temperature, leads to a worsening of drought conditions in the islands (Carrillo et al., 2023). Both SPI and SPEI were computed using statistical distributions obtained for the 30-year period corresponding to the recent past. Future projections suggest a decrease in the number of drought periods (Figure 5.6), since these will be considerably longer, in some areas extending over almost the entire 30-year period at the end of the century. As in other previous studies, the convenience of using the SPEI index in this region is highlighted, since it also takes evapotranspiration into account. Consistent with the aforementioned, a larger increase in temperature with altitude and a more pronounced decrease in precipitation in the higher elevations of the islands, would lead to more severe future droughts in these areas. In fact, projections show that, by the end of the century, in the RCP 8.5 scenario, almost all of the highlands would be in drought most of the time.

The future change of several fire risk indicators derived from the FWI have been also studied (Carrillo et al., 2022b). The fire season will increase its length, being more noticeable as altitude increases. For example, for Tenerife, the fire season is currently around 166 days (from mid-June to mid-November). However, projections made at the end of the century indicate an extension to around 200 days for RCP 4.5 and 241 days for RCP 8.5 (from the end of March to the end of November). The extreme risk days (FWI > 60) show an average

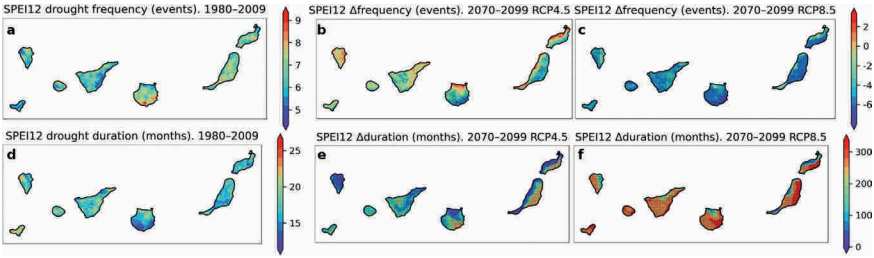

Figure 5.6: Drought frequency (number of drought events in 30 years) (a–c) and mean duration (months) (d–f) for the SPEI index computed at a 12-month time scale. Changes in the frequency and duration of drought events for the future (2070–2099), under RCP 4.5 (b, e) and RCP 8.5 (c, f), relative to the recent past period (1980–2009) (a, d). Dotted grid points correspond to robust future changes. Source: Carrillo et al., 2023.

increase of 58%, reaching 12 days a year, and the area with high risk could increase by 44%. The factor that would have the largest impact on the future worsening of fire risk in the islands would be the reduction of precipitation.

A semi-permanent wind stream, known as the North African Coastal Low-Level Jet (NACLLJ), flows along the northwestern African coast. It is mainly driven by the Azores Anticyclone and the Sahara thermal low. Some studies (Soares et al., 2019b, a), using results from CORDEX-Africa simulations (at 0.44º resolution) and from an atmosphere-ocean coupled model (~25 km atmosphere) project a small increase in the surface wind speed in the area affected by NACLLJ. In the Canary region a decrease of around 0.4 m/s is projected, but it is not statistically significant. Higher resolution PGW simulations (González et al., 2017), using WRF configuration forced by CMIP5 models under RCP 4.5 and RCP 8.5, and ERA-Interim, projected small and not statistically significant changes. However, some seasonal considerable modifications in the 2045-2054 and 2090-2099 periods were observed. A general increase appears for winter over the whole study region. For summer, the five western islands suggest a decline in the central part, and an increase in the north and south coast; in the remaining islands a reinforcement appears in the north and south while a reduction is shown in the north-west coast.

The computational demands of regional climate modelling limit the production of a sufficient number of simulations at a scale appropriate for the Canary Islands to adequately evaluate uncertainties. Moreover, unlike what happens in larger regions, very few research groups are interested in performing such simulations over long periods of time. However, the complexity of the islands' orography, the ocean-land interface and the density of observation sites make the islands a good laboratory for understanding convection permitting simulations. In the future it would be desirable to join efforts of international groups interested in the climate study of different archipelagos, for example through a CORDEX-FPS or other similar initiatives.

4.2. Mountains

Mountain regions are particularly vulnerable to climate change and thus serve as natural global observatories where the most obvious signs of global change are evident (Esteban-Parra et al., 2022). Global warming affects the mountain cryosphere, altering the water cycle through changes in seasonal runoff, and temperature patterns through changes in albedo. These changes have significant implications for water reservoirs, mountain ecosystems, tourism, and other areas. The Mediterranean mountains face a double risk due to their special vulnerability as mountain regions and their location in the Mediterranean basin, which is emerging as a climate change hot spot (Amblar-Francés et al., 2020). To assess the impact of global warming on mountainous regions, high-resolution projections are necessary to properly simulate their complex topography and processes (e.g. water fluxes, snow, albedo, convection). General Circulation Models (GCMs) lack the required spatial resolution, necessitating some type of downscaling. However, downscaling over mountainous regions is particularly challenging for several reasons. Their complex orography requires simulations of extremely fine resolution, difficult to achieve even by Regional Climate Models (RCMs). Additionally, mountain observations are sparse, which is a significant limitation for statistical downscaling, bias adjustment, and model evaluation. In this section, we summarise the main findings on climate projections over Spanish mountains found in recent literature highlighting the main results for each mountain range.

Carvalho et al., 2021 analysed an ensemble of 17 EURO-CORDEX simulations combining 6 GCMs from CMIP5 and 5 bias-corrected RCMs over the Iberian Peninsula (IP), with a spatial resolution of 0.11º. The ensemble was validated over a reference period (1986–2005), and projections were analysed for two future periods (medium-term: 2046–2065, and long-term: 2081–2100) under RCP 8.5. Mean, maximum, and minimum temperatures are projected to substantially increase, around 2.1 ºC, 2.3 ºC, and 1.8 ºC, respectively, in the medium-term, and 4.1 ºC, 4.4 ºC, and 3.8 ºC in the long-term, averaged over the whole domain. These changes are more pronounced for maximum and mean temperatures, especially in inland central areas, the south, the Cantabrian and Pyrenees mountain ranges, and Sierra Nevada. García-Valdecasas Ojeda et al., 2020 studied the same domain with the same resolution, using one RCM driven by two different GCMs from CMIP5, previously bias-corrected. The reference period used was 1980-2014 and changes were calculated for 2071-2100 under RCP 4.5 and RCP 8.5. Both scenarios projected an increase in maximum temperature, more marked in mountainous regions. The projected increase in maximum temperature was found to be greater than in the minimum, resulting in positive values of daily temperature range (DTR). For the Pyrenees and Sierra Nevada, two of the main mountain ranges of the IP, specific studies have been found in the literature (e.g. (Amblar-Francés et al., 2020; Esteban-Parra et al., 2022; Pérez-Palazón et al., 2018).

For precipitation, different studies have projected significant changes in the IP, but the exact spatial distribution of the changes remains uncertain as they are strongly model-dependent, with less agreement between models compared to temperature (Amblar-Francés et al., 2020). Snow is another key component of the water cycle and a crucial element in many ecological, hydrological, and atmospheric processes in cold and mountainous areas. Mountainous regions, especially those located in semi-arid environments, are highly vulnerable to shifts from snowfall to rain. In the IP, a large amount of the total annual

precipitation falls during winter (López-Moreno et al., 2017), resulting in extensive snow-covered areas (Alonso-González et al., 2020). Additionally, the snow-albedo feedback during winter and spring at high altitudes alters soil moisture and subsequently produces different effects through land-atmosphere interaction, i.e., snow hydrological effects (García-Valdecasas Ojeda et al., 2020a). Alonso-González et al., 2020 investigated the sensitivity of the snowpack to increased temperature and short-wave radiation along an elevation gradient (1500-2500 m) over the main mountain ranges of the IP (Cantabrian Range, Central Range, Iberian Range, Pyrenees, and Sierra Nevada). Their results showed remarkable differences in the sensitivity of the duration of the snowpack to temperature increase across the study areas. In general, there was a clear decrease in the sensitivity of the duration of the snowpack to temperature increase with increasing elevation, particularly in colder areas. The effects of variations in precipitation on the sensitivity of the duration of the snowpack decreased markedly with increasing elevation, and the effect of short-wave radiation variability on the duration of the snowpack was less than that caused by variations in temperature, with little effect induced by variation in precipitation. The response of melt rates to warming was negative in most areas at all elevations, suggesting less intense but longer melt seasons.

For other variables such as evapotranspiration, soil moisture, and runoff, only a few studies have been found in the literature. García-Valdecasas Ojeda et al., 2020 found high values for evapotranspiration in the reference climatology over mountainous areas during summer. Evapotranspiration increases at high altitudes, however, are only seen in some models, indicating that the inter-model variability is large for this variable.

Sierra Nevada

Projected changes are more pronounced for maximum and mean temperatures, especially for Sierra Nevada (Carvalho et al., 2021a). In this region, the projected change in mean and maximum temperatures for the long term exceeds 5 ºC in certain areas. García-Valdecasas Ojeda et al., 2020 found that simulations indicate, on average, slight changes in winter precipitation, with significant reductions only over certain high-altitude regions in the southern Iberian Peninsula (Sierra Nevada) by the end of the century under the RCP 8.5 scenario. The increase in temperatures is more significant in summer.

Esteban-Parra et al., 2022 analysed an ensemble of 15 EURO-CORDEX simulations combining 4 GCMs from CMIP5 with 5 RCMs over Sierra Nevada, with a spatial resolution of 0.11º, under RCP 4.5 and RCP 8.5. In the near future (2020-2049), both RCPs show increases of around 1.5 °C and 2 °C compared to the reference period (1980-2009) for maximum and minimum temperatures, respectively. For the long-term future (2070-2099), increases compared to the recent past reach values up to 3 °C and 5.5 °C under RCP 4.5 and RCP 8.5, respectively. Increases in both maximum and minimum temperatures will be more pronounced in summer, followed by autumn, with more moderate changes during winter and spring.

Pérez-Palazón et al., 2018 also focused on Sierra Nevada, using an ensemble of 9 CMIP5 GCMs downscaled with ESD over stations and then interpolated to a 30 m grid with topographic corrections, under RCP 4.5 and RCP 8.5. Trends during 2006-2100 for

maximum temperature are projected at 0.024 ºC/year and 0.062 ºC/year, for minimum temperature 0.010 ºC/year and 0.028 ºC/year, and for mean temperature 0.019 ºC/year and 0.047 ºC/year.

Over Sierra Nevada, precipitation increases from east to west, with approximately 80% occurring between October and April (Esteban-Parra et al., 2022). Climate change projections for precipitation in this massif show a slight decrease in annual mean precipitation for the near future (2020-2049) compared to the recent past (1980-2009), with the highest differences over eastern Sierra Nevada (around –15%) under RCP 8.5 (Esteban-Parra et al., 2022). By the end of the century (2070-2099), differences between RCPs become more pronounced, with RCP 4.5 indicating reductions in precipitation of more than 15% on average, whereas RCP 8.5 shows reductions of up to 35% over the western Sierra Nevada and surrounding areas, with summer seeing the largest reductions. Winter changes are more moderate, with spring and autumn showing transitional behaviour between winter and summer. These results align with those of Pérez-Palazón et al., 2018, who also found a negative precipitation trend in this region, more marked for RCP 8.5 than for RCP 4.5, using statistical downscaling techniques.

Studies on precipitation extremes indicate that drought events are likely to become slightly longer and more frequent in the near future (2020-2049), with the RCP scenario not showing a clear effect on drought conditions during this period. Increases in mean drought duration, on average, by around 2 months and 10 months at 3- and 12-month timescales, respectively, under RCP 4.5, and increases in drought frequency around 2.5 events/year for both timescales are projected (Esteban-Parra et al., 2022). For the far future (2070-2099), according to RCP 4.5, Sierra Nevada is likely to experience an increase in the severity of drought conditions with more frequent and longer-lasting drought events. For drought indices (SPI and SPEI) computed at 12-month timescales, the mean drought duration is projected to reach around 30 months on average. Under RCP 8.5, the length of drought events may increase to around 125 months on average, reaching up to 144 months over western Sierra Nevada (Esteban-Parra et al., 2022). Carvalho et al., 2022 investigated future aridity changes in the Mediterranean under RCP 4.5 and RCP 8.5 using nine bias-corrected high-resolution simulations from the EURO-CORDEX Project. They detected strong decreases in precipitation (up to 30-40% in Sierra Nevada) towards the end of the century (2081-2100) under RCP 8.5, associated with projected decreases in evapotranspiration, resulting in slight reductions in the water balance (precipitation – evapotranspiration).

For Sierra Nevada, Pérez-Palazón et al., 2018 evaluated the influence of future climate scenarios (RCP 4.5 and RCP 8.5) on the snowfall regime at annual and decadal scales for the period 2006-2100. The resulting snowfall regime for each scenario follows a significant decreasing trend associated with the long-term increasing trend in temperature, with higher reductions in the snow domain area. Another important result from this study is the likely impact of climate scenarios on the torrentiality of snowfall, with a decrease in the number of days with snowfall and a significant increase in the global mean snowfall intensity under both RCPs.

For evapotranspiration, future projections under both RCP 4.5 and RCP 8.5 point to an increase during winter, spring, and summer in some parts of Sierra Nevada, especially under RCP 8.5 in winter and spring (García-Valdecasas Ojeda et al., 2020a). Esteban-Parra

et al., 2022 found reductions in surface evapotranspiration during winter and spring over a large part of Sierra Nevada, while several high-altitude points show moderate increases. For summer and autumn, the reduction in evapotranspiration is widespread throughout the mountain and more marked over eastern Sierra Nevada in summer. Changes for the near future are more moderate (values ranging from –10 to 5%) with similar differences between RCPs. Differences in magnitude are more pronounced between scenarios for the far future, with most of the region showing reductions not exceeding 15% under RCP 4.5, while RCP 8.5 shows decreases up to 20% for eastern Sierra Nevada.

Esteban-Parra et al., 2022 found that the total soil moisture content in Sierra Nevada is projected to decrease overall, with general agreement in the sign between models under RCP 8.5. Under RCP 4.5, reductions of up to 6% are projected for the near future compared to the recent past.

Pyrenees

Mean, maximum, and minimum temperature are projected to substantially increase. These changes are more marked for maximum and mean temperatures, and especially for the Pyrenees mountain ranges (Carvalho et al., 2021a). For example, the projected change in the mean and maximum temperatures for the long-term surpasses 5 ºC in certain areas of the Pyrenees. The projected increase in the maximum temperature was found of greater magnitude than in the minimum, resulting in positive values of daily temperature range (DTR) (García-Valdecasas Ojeda et al., 2020a). However, this DTR resulted to be negative during winter in the Pyrenees, probably due to snow depletion. Amblar-Francés et al., 2020 analysed an ensemble of 24 CMIP5 GCMs downscaled with ESD on a 0.05º grid over the Pyrenees, under RCP 4.5, RCP6.0 and RCP 8.5. Daily maximum and minimum temperature are projected to increase during the 21st century for all analysed RCPs. The change is more pronounced for the most emissive scenario (RCP 8.5), for the end of the century, and for maximum temperature where, on average, changes are projected between 4.0 and 6.3 ºC with respect to the reference period (1986–2005). In addition to the projected change in the mean values, also some extremes related to temperature have been analysed in different studies. Carvalho et al., 2021 found that the occurrence of FDs is projected to decrease, particularly in mountainous areas such as the Pyrenees. This reduction ranges between 10 to 45 nights for 2046–2065 and 30–90 nights for 2081–2100. Amblar-Francés et al., 2020 found that the number of WD and WN, as well as the WSDI will increase, especially at the end of the century and for the more emissive scenarios, where the increases probably will be between 10–55 days for WD, 10–40 days for WSDI and 10–55 days for WN. FD shows a decline, more pronounced for the RCP 8.5 and for the end of the century (~ 60 days). Díaz-Poso et al., 2023; Lorenzo et al., 2021 analysed HWs and cold waves, respectively, over the IP using 5 EURO-CORDEX simulations corresponding to the combination of 1 RCM with 5 different GCMs from CMIP5 and with a spatial resolution of 0.11º under RCP 4.5 and RCP 8.5. The near future (2021-2050) was analysed and they found a general significant increase in intensity, frequency, duration and spatial extent of HWs rising to 150% for the Mediterranean coast and the Pyrenees. The annual number of heatwave days showed the highest values located in the Pyrenees, inland and south of the IP. The Maximum Excess Heat Factor (EHFmax) showed changes ranging between 60% and 80% in the RCP 4.5 scenario and was almost 100% across most of the peninsula in the RCP 8.5 scenario

(Pyrenees showing the maximum values). The spatial trend of the number of cold wave days under RCP 4.5 oscillates for the whole domain between 0 and -2 days/decade, except for the main mountain systems, while for RCP 8.5, the negative trend is significant for the whole domain and values below -3 days/decade are generalised, especially in the southern half of the IP and in the Balearic Islands. The lowest values, corresponding to the most significant negative trends, are concentrated in the Pyrenees with -4 days/decade.

Amblar-Francés et al., 2020, applying statistical downscaling techniques using 24 climate models from CMIP5 and three scenarios (RCP 4.5, 6 and 8.5), established that for the Pyrenees future precipitation changes do not exhibit a clear tendency and can even point towards different sense of change, being the uncertainty associated with the models greater than uncertainties due to emission scenarios. In this area, concerning seasonal behaviour, a slight precipitation decline is appreciated in autumn while an increase in summer is observed at the end of the century. Consequently, the surface runoff also will experience changes in these regions. García-Valdecasas Ojeda et al., 2020 found that increases in the surface runoff appear together with an overall reduction in the total runoff in regions of the IP, with the Pyrenees as exception, showing increases in the total runoff in their simulations under RCP 8.5 for the end of the century in winter. For this massif, also notably increases in the spring precipitation appear, particularly under the RCP 8.5, which coincide with the enhanced evapotranspiration that occurs in this region (Carvalho et al., 2022; García-Valdecasas Ojeda et al., 2020a), previously mentioned. Additionally, some studies have focused on projected changes in some precipitation extremes. For the Pyrenees area, there is a large uncertainty about this subject, with no clear tendencies for changes in heavy precipitation or length of drought. Only the number of wet days shows a slight and reduced signal to increase in some isolated zones of the eastern part of the massif and a slight signal to decrease in the northern part (Amblar-Francés et al., 2020).

Evapotranspiration is projected to increase around 20% under the RCP 8.5, which could be related to the temperature increase projected for this area (Carvalho et al., 2022). This means that the water availability can significantly decrease up to 40-50% in the Pyrenees due to an increase of evapotranspiration. This result is in agreement with those from García-Valdecasas Ojeda et al., 2020, who found high evapotranspiration rates in the Pyrenees (up to 25%) for the 2071-2100 period under the RCP 8.5 using two GCMs for conducting DD. They found that future projections under both RCP 4.5 and RCP 8.5, pointed to an increase during winter, spring, and summer in northern mountainous regions (e.g. the Cantabrian Range and the Pyrenees), especially under RCP8.5 in winter and spring.

For the Pyrenees, the study of García-Valdecasas Ojeda et al., 2020, shows projected changes in seasonal snowmelt for the far future (2071-2100) under the RCP 4.5 and RCP 8.5. From this, increased snowmelt in winter and spring is detected under the two scenarios, more apparent under RCP 8.5, associated with an increase in the soil moisture in this massif, and therefore may lead to more evapotranspiration associated with the temperature increases.

For soil water content, high values in the reference climatology over the Pyrenees during summer, and future projections under RCP 8.5, point to an increase in soil moisture content over the Pyrenees during winter (García-Valdecasas Ojeda et al., 2020). Runoff is projected to decrease under RCP 8.5 during spring, summer and autumn over the Pyrenees, and an increase during winter.

Cantabrian Mountains

The overall increases projected for mean, maximum, and minimum temperature are more marked for maximum and mean temperatures, and especially for the Cantabrian mountain range (Carvalho et al., 2021). The occurrence of FDs is projected to decrease (Carvalho et al., 2021). García-Valdecasas Ojeda et al., 2020 investigated climate change projections in the IP for the 2071-2100 period under the RCP 8.5 using two GCMs for conducting DD, finding high evapotranspiration rates in the Cantabrian Range. They are projected to increase under both RCP 4.5 and RCP 8.5, during winter, spring, and summer in the area, especially under RCP8.5 in winter and spring.

5. Conclusions

We have summarised the findings of recent scientific literature regarding future climate change over Spain for different variables and for specific regions of interest, where targeted assessments are required. Figures of specific projected changes are highly dependent on the reference and future periods considered, along with the set of models used to assess those changes. Still, some overall conclusions can be extracted from the above detailed results.

As compared to the previous assessment, we have considered a larger amount of references (more than 200) covering different variables and derived indices. This highlights the substantial increase in scientific literature following the release of global and downscaled projections from various coordinated initiatives, such as CMIP and CORDEX.

The assessment of temperature projections for the Iberian Peninsula reveals that while CMIP6 GCMs have improved in capturing trends in temperature extremes, they still overestimate hot day trends and exhibit significant biases, particularly in seasonal and regional extremes. The region is expected to face severe warming, especially in summer, with temperatures increasing 1.6 times faster than the global average. Downscaling methods, including dynamical and statistical approaches, are crucial for localised projections, although they are not free from biases and uncertainties. Innovations such as deep learning are enhancing downscaling accuracy and physical reliability. Projections indicate a notable rise in the frequency and intensity of heatwaves, with extended summer seasons anticipated by the century's end, especially under high-emission scenarios. Downscaled projections reveal a significant increase in summer mean temperatures over Spain, with a mean rise of 2 ºC under the RCP4.5 scenario and up to 4 ºC under the RCP8.5 scenario by the end of the century. This increase is more pronounced in the interior regions compared to coastal areas. Additionally, the models indicate a rise in temperature extremes, especially during summer months, and an increased frequency of extreme heat events and prolonged heatwaves. Nighttime temperatures are expected to rise significantly, contributing to higher overall temperature averages. Southern Spain is particularly vulnerable, with projections indicating the most pronounced warming. Coastal areas might experience more intense heat and humidity, affecting human comfort and health.

Mean precipitation is projected to decline throughout the century, while precipitation extremes are expected to increase. Additionally, atmospheric rivers' frequency will increase by 50% under high-emission scenarios, with extreme water vapour transports increasing by 20%. The reduction of moisture contribution from the North Atlantic Ocean to Europe and the IP will impact the

precipitation regime, particularly reducing rainfall during winter and autumn by the century's end. These changes will exacerbate water scarcity in already dry areas, contributing to a trend toward more arid climates in Spain.

Both, GCMs and RCMs, exhibit poor performance in simulating observed wind speed changes and multidecadal variability over the IP. GCMs generally project a decline in near-surface wind speed (NSWS) by the end of the century, especially under high anthropogenic forcing scenarios. However, some RCMs indicate an increase in NSWS for the same periods. Due to the large uncertainties, NSWS projections should be approached with caution, necessitating further efforts to improve simulation accuracy. Internal variability remains the main source of uncertainty for future atmospheric circulation projections.

The projected wintertime East Atlantic (EA), Scandinavian (SCA), and East Atlantic-Western Russia (EA-WR) indices do not show significant changes toward their positive or negative phases throughout the 21st century. Depending on the GCMs considered, the North Atlantic Oscillation (NAO) index may remain stable or exhibit a slight trend toward its positive phase. Atmospheric blocking over the IP is expected to become less frequent in winter, with no significant change anticipated in summer. A marked reduction in relative humidity (RH) over the IP is projected for all seasons and climate scenarios, particularly in summer, driven mainly by increased oceanic evaporation.

Environmental heat exposure is projected to rise over the 21st century, with exceedances of impact-relevant thresholds increasing non-linearly with the magnitude of future warming. Optimal summer tourism conditions are expected to deteriorate, with improvements in shoulder seasons and a northward shift. Climate change may reduce the production of some cultivars, including grapes, exacerbated by enhanced inter-annual variability. A projected reduction in precipitation over the southern IP, combined with increased atmospheric evaporative demand (AED), may decrease surface evapotranspiration and increase aridity conditions. Drought conditions are projected to become more frequent and severe, consistent with both global and regional studies.

Climate projections indicate an increase in fire danger conditions, with more frequent and extreme fires and longer danger seasons, extending into June and, to a lesser extent, September. Hybrid systems combining wind and solar energies could help mitigate energy storage requirements and periods of low productivity, such as drought days.

The Canary Islands are expected to experience significant temperature increases, up to 4.2°C by the end of the century under the Radiative Concentration Pattern 8.5 (RCP 8.5) scenario, and a substantial decrease in precipitation by around 30%. This will exacerbate drought conditions, especially at higher altitudes. The fire season will lengthen, with more extreme fire risk days and a larger area susceptible to fires due primarily to reduced precipitation. Despite the high computational demands of high-resolution climate modelling for the Canary Islands, their unique characteristics offer a valuable opportunity for convection-permitting simulations. International collaboration is crucial for advancing climate research in the archipelagos.

Mountain regions, particularly in the Mediterranean, are highly sensitive to climate change, making them crucial observatories for global warming impacts. Global warming disrupts the mountain cryosphere and water cycles, significantly affecting ecosystems and human activities. Accurate climate projections require high-resolution models due to the complex topography of mountainous regions, but this is hindered by the limitations of GCMs and the challenge of downscaling. Studies show significant increases in temperature and varied precipitation projections in Spanish

mountains, with notable sensitivity differences in snowpack across elevations. While projections for other variables like evapotranspiration and soil moisture are less comprehensive, they indicate considerable variability among models.

References

Abaurrea, J., Asín, J., and Cebrián, A. C.: Modelling the occurrence of heat waves in maximum and minimum temperatures over Spain and projections for the period 2031-60, Glob. Planet. Change, 161, 244–260, https://doi.org/10.1016/j.gloplacha.2017.11.015, 2018.

Acosta-Mora, P., Expósito González, F. J., Pérez Darias, J. C., González Fernández, A. J., and Díaz González, J. P.: Análisis de precipitaciones extremas en Canarias a partir de resultados de regionalizaciones estadísticas y dinámicas, Asociación Española de Climatología, 2022.

Allan, R. P., Barlow, M., Byrne, M. P., Cherchi, A., Douville, H., Fowler, H. J., Gan, T. Y., Pendergrass, A. G., Rosenfeld, D., Swann, A. L. S., Wilcox, L. J., and Zolina, O.: Advances in understanding large-scale responses of the water cycle to climate change, Ann. N. Y. Acad. Sci., 1472, 49–75, https://doi.org/10.1111/nyas.14337, 2020.

Allen, R. G., Pruitt, W. O., Wright, J. L., Howell, T. A., Ventura, F., Snyder, R., Itenfisu, D., Steduto, P., Berengena, J., Yrisarry, J. B., Smith, M., Pereira, L. S., Raes, D., Perrier, A., Alves, I., Walter, I., and Elliott, R.: A recommendation on standardized surface resistance for hourly calculation of reference ETo by the FAO56 Penman-Monteith method, Agric. Water Manag., 81, 1–22, https://doi.org/10.1016/j.agwat.2005.03.007, 2006.

Alonso-González, E., López-Moreno, J. I., Navarro-Serrano, F., Sanmiguel-Vallelado, A., Aznárez-Balta, M., Revuelto, J., and Ceballos, A.: Snowpack sensitivity to temperature, precipitation, and solar radiation variability over an elevational gradient in the Iberian mountains, Atmospheric Res., 243, 104973, https://doi.org/10.1016/j.atmosres.2020.104973, 2020.

Álvarez, I., Pereira, H., Lorenzo, M. N., Picado, A., Sousa, M. C., Taboada, J. J., and Dias, J. M.: Drought projections for the NW Iberian Peninsula under climate change, Clim. Dyn., https://doi.org/10.1007/s00382-023-07084-z, 2024.

Amblar Francés, P., Casado Calle, M. J., Pastor Saavedra, A., Ramos Calzado, P., and Rodríguez Camino, E.: Guía de escenarios regionalizados de cambio climático sobre España a partir de los resultados del IPCC-AR5, Agencia Estatal de Meteorología, https://doi.org/10.31978/014-17-010-8, 2017.

Amblar-Francés, M. P., Ramos-Calzado, P., Sanchis-Lladó, J., Hernanz-Lázaro, A., Peral-García, M. C., Navascués, B., Domínguez-Alonso, M., Pastor-Saavedra, M. A., and Rodríguez-Camino, E.: High resolution climate change projections for the Pyrenees region, Adv. Sci. Res., 17, 191–208, https://doi.org/10.5194/asr-17-191-2020, 2020.

Amengual, A., Homar, V., Romero, R., Ramis, C., and Alonso, S.: Projections for the 21st century of the climate potential for beach-based tourism in the Mediterranean, Int. J. Climatol., 34, 3481–3498, https://doi.org/10.1002/joc.3922, 2014.

Andrade, C., Contente, J., and Santos, J. A.: Climate Change Projections of Aridity Conditions in the Iberian Peninsula, Water, 13, 2035, https://doi.org/10.3390/w13152035, 2021a.

Andrade, C., Contente, J., and Santos, J. A.: Climate Change Projections of Dry and Wet Events in Iberia Based on the WASP-Index, Climate, 9, 94, https://doi.org/10.3390/cli9060094, 2021b.

Andrés-Martín, M., Azorín-Molina, C., Shen, C., Fernández-Álvarez, J. C., Gimeno, L., Vicente-Serrano, S. M., and Zha, J.: Uncertainty in surface wind speed projections over the Iberian Peninsula: CMIP6 GCMs versus a WRF-RCM, Ann. N. Y. Acad. Sci., 1529, 101–108, https://doi.org/10.1111/nyas.15063, 2023.

Asadi Zarch, M. A., Sivakumar, B., Malekinezhad, H., and Sharma, A.: Future aridity under conditions of global climate change, J. Hydrol., 554, 451–469, https://doi.org/10.1016/j.jhydrol.2017.08.043, 2017.

Azorín-Molina, C., Vicente-Serrano, S. M., McVicar, T. R., Jerez, S., Sánchez-Lorenzo, A., López-Moreno, J.-I., Revuelto, J., Trigo, R. M., Lopez-Bustins, J. A., and Espírito-Santo, F.: Homogenization and Assessment of Observed Near-Surface Wind Speed Trends over Spain and Portugal, 1961–2011*, J. Clim., 27, 3692–3712, https://doi.org/10.1175/JCLI-D-13-00652.1, 2014.

Azorín-Molina, C., Guijarro, J. A., McVicar, T. R., Trewin, B. C., Frost, A. J., and Chen, D.: An approach to homogenize daily peak wind gusts: An application to the Australian series, Int. J. Climatol., 39, 2260–2277, https://doi.org/10.1002/joc.5949, 2019.

Bafaluy, D., Amengual, A., Romero, R., and Homar, V.: Present and future climate resources for various types of tourism in the Bay of Palma, Spain, Reg. Environ. Change, 14, 1995–2006, https://doi.org/10.1007/s10113-013-0450-6, 2014.

Bai, X.: Make the upcoming IPCC Cities Special Report count, Science, 382, eadl1522, https://doi.org/10.1126/science.adl1522, 2023.

Baño-Medina, J., Manzanas, R., and Gutiérrez, J. M.: Configuration and intercomparison of deep learning neural models for statistical downscaling, Geosci. Model Dev., 13, 2109–2124, https://doi.org/10.5194/gmd-13-2109-2020, 2020.

Baño-Medina, J., Manzanas, R., and Gutiérrez, J. M.: On the suitability of deep convolutional neural networks for continental-wide downscaling of climate change projections, Clim. Dyn., 57, 2941–2951, https://doi.org/10.1007/s00382-021-05847-0, 2021.

Baño-Medina, J., Manzanas, R., Cimadevilla, E., Fernández, J., González-Abad, J., Cofiño, A. S., and Gutiérrez, J. M.: Downscaling multi-model climate projection ensembles with deep learning (DeepESD): contribution to CORDEX EUR-44, Geosci. Model Dev., 15, 6747–6758, https://doi.org/10.5194/gmd-15-6747-2022, 2022.

Baño-Medina, J., Iturbide, M., Fernández, J., and Gutiérrez, J. M.: Transferability and explainability of deep learning emulators for regional climate model projections: Perspectives for future applications, https://doi.org/10.48550/ARXIV.2311.03378, 2023.

Barriopedro, D., García-Herrera, R., Ordóñez, C., Miralles, D. G., and Salcedo-Sanz, S.: Heat Waves: Physical Understanding and Scientific Challenges, Rev. Geophys., 61, e2022RG000780, https://doi.org/10.1029/2022RG000780, 2023.

Bartók, B., Wild, M., Folini, D., Lüthi, D., Kotlarski, S., Schär, C., Vautard, R., Jerez, S., and Imecs, Z.: Projected changes in surface solar radiation in CMIP5 global climate models and in EURO-CORDEX regional climate models for Europe, Clim. Dyn., 49, 2665–2683, https://doi.org/10.1007/s00382-016-3471-2, 2017.

Bartók, B., Tobin, I., Vautard, R., Vrac, M., Jin, X., Levavasseur, G., Denvil, S., Dubus, L., Parey, S., Michelangeli, P.-A., Troccoli, A., and Saint-Drenan, Y.-M.: A climate projection dataset tailored for the European energy sector, Clim. Serv., 16, 100138, https://doi.org/10.1016/j.cliser.2019.100138, 2019.

Bedia, J., Herrera, S., Martín, D. S., Koutsias, N., and Gutiérrez, J. M.: Robust projections of Fire Weather Index in the Mediterranean using statistical downscaling, Clim. Change, 120, 229–247, https://doi.org/10.1007/s10584-013-0787-3, 2013.

Bedia, J., Herrera, S., Camia, A., Moreno, J. M., and Gutiérrez, J. M.: Forest fire danger projections in the Mediterranean using ENSEMBLES regional climate change scenarios, Clim. Change, 122, 185–199, https://doi.org/10.1007/s10584-013-1005-z, 2014.

Bedia, J., Herrera, S., Gutiérrez, J. M., Benali, A., Brands, S., Mota, B., and Moreno, J. M.: Global patterns in the sensitivity of burned area to fire-weather: Implications for climate change, Agric. For. Meteorol., 214–215, 369–379, https://doi.org/10.1016/j.agrformet.2015.09.002, 2015.

Bedia, J., Baño-Medina, J., Legasa, M. N., Iturbide, M., Manzanas, R., Herrera, S., Casanueva, A., San-Martín, D., Cofiño, A. S., and Gutiérrez, J. M.: Statistical downscaling with the downscaleR package (v3.1.0): contribution to the VALUE intercomparison experiment, Geosci. Model Dev., 13, 1711–1735, https://doi.org/10.5194/gmd-13-1711-2020, 2020.

Bento, V. A., Lima, D. C. A., Santos, L. C., Lima, M. M., Russo, A., Nunes, S. A., DaCamara, C. C., Trigo, R. M., and Soares, P. M. M.: The future of extreme meteorological fire danger under climate change scenarios for Iberia, Weather Clim. Extrem., 42, 100623, https://doi.org/10.1016/j.wace.2023.100623, 2023.

Berg, P., Christensen, O. B., Klehmet, K., Lenderink, G., Olsson, J., Teichmann, C., and Yang, W.: Summertime precipitation extremes in a EURO-CORDEX 0.11° ensemble at an hourly resolution, Nat. Hazards Earth Syst. Sci., 19, 957–971, https://doi.org/10.5194/nhess-19-957-2019, 2019.

Boé, J., Somot, S., Corre, L., and Nabat, P.: Large discrepancies in summer climate change over Europe as projected by global and regional climate models: causes and consequences, Clim. Dyn., 54, 2981–3002, https://doi.org/10.1007/s00382-020-05153-1, 2020.

Bonan, G. B. and Doney, S. C.: Climate, ecosystems, and planetary futures: The challenge to predict life in Earth system models, Science, 359, eaam8328, https://doi.org/10.1126/science.aam8328, 2018.

Bony, S., Stevens, B., Frierson, D. M. W., Jakob, C., Kageyama, M., Pincus, R., Shepherd, T. G., Sherwood, S. C., Siebesma, A. P., Sobel, A. H., Watanabe, M., and Webb, M. J.: Clouds, circulation and climate sensitivity, Nat. Geosci., 8, 261–268, https://doi.org/10.1038/ngeo2398, 2015.

Brands, S., Herrera, S., Fernández, J., and Gutiérrez, J. M.: How well do CMIP5 Earth System Models simulate present climate conditions in Europe and Africa?: A performance comparison for the downscaling community, Clim. Dyn., 41, 803–817, https://doi.org/10.1007/s00382-013-1742-8, 2013.

Brands, S., Fernández-Granja, J. A., Fernández Fernández, J., Bedia, J., Casanueva, A., and Taboada Hidalgo, J. J.: Performance of the CMIP6 global climate models over the Iberian Peninsula and relationships with the simulated climate system complexity, Asociación Española de Climatología, 2022.

Brands, S., Fernández-Granja, J. A., Bedia, J., Casanueva, A., and Fernández, J.: A Global Climate Model Performance Atlas for the Southern Hemisphere Extratropics Based on Regional Atmospheric Circulation Patterns, Geophys. Res. Lett., 50, e2023GL103531, https://doi.org/10.1029/2023GL103531, 2023.

Brogli, R., Heim, C., Mensch, J., Sørland, S. L., and Schär, C.: The pseudo-global-warming (PGW) approach: methodology, software package PGW4ERA5 v1.1, validation, and sensitivity analyses, Geosci. Model Dev., 16, 907–926, https://doi.org/10.5194/gmd-16-907-2023, 2023.

Cabos, W., De La Vara, A., Álvarez-García, F. J., Sánchez, E., Sieck, K., Pérez-Sanz, J.-I., Limareva, N., and Sein, D. V.: Impact of ocean-atmosphere coupling on regional climate: the Iberian Peninsula case, Clim. Dyn., 54, 4441–4467, https://doi.org/10.1007/s00382-020-05238-x, 2020.

Cai, W., Li, K., Liao, H., Wang, H., and Wu, L.: Weather conditions conducive to Beijing severe haze more frequent under climate change, Nat. Clim. Change, 7, 257–262, https://doi.org/10.1038/nclimate3249, 2017.

Cannon, A. J.: Reductions in daily continental-scale atmospheric circulation biases between generations of global climate models: CMIP5 to CMIP6, Environ. Res. Lett., 15, 064006, https://doi.org/10.1088/1748-9326/ab7e4f, 2020.

Cardell, M. F., Romero, R., Amengual, A., Homar, V., and Ramis, C.: A quantile–quantile adjustment of the EURO-CORDEX projections for temperatures and precipitation, Int. J. Climatol., 39, 2901–2918, https://doi.org/10.1002/joc.5991, 2019a.

Cardell, M. F., Amengual, A., and Romero, R.: Future effects of climate change on the suitability of wine grape production across Europe, Reg. Environ. Change, 19, 2299–2310, https://doi.org/10.1007/s10113-019-01502-x, 2019b.

Cardell, M. F., Amengual, A., and Romero, R.: Present and future climate potentials for several outdoor tourism activities in Spain, J. Sustain. Tour., 31, 2219–2249, https://doi.org/10.1080/09669582.2022.2096624, 2023.

Careto, J. A. M., Soares, P. M. M., Cardoso, R. M., Herrera, S., and Gutiérrez, J. M.: Added value of EURO-CORDEX high-resolution downscaling over the Iberian Peninsula revisited – Part 1: Precipitation, Geosci. Model Dev., 15, 2635–2652, https://doi.org/10.5194/gmd-15-2635-2022, 2022.

Carrillo, J., González, A., Pérez, J. C., Expósito, F. J., and Díaz, J. P.: Projected impacts of climate change on tourism in the Canary Islands, Reg. Environ. Change, 22, 61, https://doi.org/10.1007/s10113-022-01880-9, 2022a.

Carrillo, J., Pérez, J. C., Expósito, F. J., Díaz, J. P., and González, A.: Projections of wildfire weather danger in the Canary Islands, Sci. Rep., 12, 8093, https://doi.org/10.1038/s41598-022-12132-5, 2022b.

Carrillo, J., Hernández-Barrera, S., Expósito, F. J., Díaz, J. P., González, A., and Pérez, J. C.: The uneven impact of climate change on drought with elevation in the Canary Islands, Npj Clim. Atmospheric Sci., 6, 31, https://doi.org/10.1038/s41612-023-00358-7, 2023.

Carvalho, D., Cardoso Pereira, S., and Rocha, A.: Future surface temperature changes for the Iberian Peninsula according to EURO-CORDEX climate projections, Clim. Dyn., 56, 123–138, https://doi.org/10.1007/s00382-020-05472-3, 2021a.

Carvalho, D., Cardoso Pereira, S., and Rocha, A.: Future surface temperatures over Europe according to CMIP6 climate projections: an analysis with original and bias-corrected data, Clim. Change, 167, 10, https://doi.org/10.1007/s10584-021-03159-0, 2021b.

Carvalho, D., Rocha, A., Costoya, X., de Castro, M., and Gómez-Gesteira, M.: Wind energy resource over Europe under CMIP6 future climate projections: What changes from CMIP5 to CMIP6, Renew. Sustain. Energy Rev., 151, 111594, https://doi.org/10.1016/j.rser.2021.111594, 2021c.

Carvalho, D., Pereira, S. C., Silva, R., and Rocha, A.: Aridity and desertification in the Mediterranean under EURO-CORDEX future climate change scenarios, Clim. Change, 174, 28, https://doi.org/10.1007/s10584-022-03454-4, 2022.

Casanueva, A., Herrera, S., Fernández, J., and Gutiérrez, J. M.: Towards a fair comparison of statistical and dynamical downscaling in the framework of the EURO-CORDEX initiative, Clim. Change, 137, 411–426, https://doi.org/10.1007/s10584-016-1683-4, 2016.

Casanueva, A., Bedia, J., Herrera, S., Fernández, J., and Gutiérrez, J. M.: Direct and component-wise bias correction of multi-variate climate indices: the percentile adjustment function diagnostic tool, Clim. Change, 147, 411–425, https://doi.org/10.1007/s10584-018-2167-5, 2018.

Casanueva, A., Kotlarski, S., Herrera, S., Fischer, A. M., Kjellstrom, T., and Schwierz, C.: Climate projections of a multivariate heat stress index: the role of downscaling and bias correction, Geosci. Model Dev., 12, 3419–3438, https://doi.org/10.5194/gmd-12-3419-2019, 2019.

Casanueva, A., Kotlarski, S., Fischer, A. M., Flouris, A. D., Kjellstrom, T., Lemke, B., Nybo, L., Schwierz, C., and Liniger, M. A.: Escalating environmental summer heat exposure—a future threat for the European workforce, Reg. Environ. Change, 20, 40, https://doi.org/10.1007/s10113-020-01625-6, 2020a.

Casanueva, A., Herrera, S., Iturbide, M., Lange, S., Jury, M., Dosio, A., Maraun, D., and Gutiérrez, J. M.: Testing bias adjustment methods for regional climate change applications under observational uncertainty and resolution mismatch, Atmospheric Sci. Lett., 21, e978, https://doi.org/10.1002/asl.978, 2020b.

Chaparro, D., Piles, M., Vall-llossera, M., and Camps, A.: Surface moisture and temperature trends anticipate drought conditions linked to wildfire activity in the Iberian Peninsula, Eur. J. Remote Sens., 49, 955–971, https://doi.org/10.5721/EuJRS20164950, 2016.

Claro, A., Santos, J. A., and Carvalho, D.: Assessing the Future wind Energy Potential in Portugal Using a CMIP6 Model Ensemble and WRF High-Resolution Simulations, Energies, 16, 661, https://doi.org/10.3390/en16020661, 2023.

Coppola, E., Sobolowski, S., Pichelli, E., Raffaele, F., Ahrens, B., Anders, I., Ban, N., Bastin, S., Belda, M., Belusic, D., Caldas-Alvarez, A., Cardoso, R. M., Davolio, S., Dobler, A., Fernández, J., Fita, L., Fumiere, Q., Giorgi, F., Goergen, K., Güttler, I., Halenka, T., Heinzeller, D., Hodnebrog, Ø., Jacob, D., Kartsios, S., Katragkou, E., Kendon, E., Khodayar, S., Kunstmann, H., Knist, S., Lavín-Gullón, A., Lind, P., Lorenz, T., Maraun, D., Marelle, L., Van Meijgaard, E., Milovac, J., Myhre, G., Panitz, H.-J., Piazza, M., Raffa, M., Raub, T., Rockel, B., Schär, C., Sieck, K., Soares, P. M. M., Somot, S., Srnec, L., Stocchi, P., Tölle, M. H., Truhetz, H., Vautard, R., De Vries, H., and Warrach-Sagi, K.: A first-of-its-kind multi-model convection permitting ensemble for investigating convective phenomena over Europe and the Mediterranean, Clim. Dyn., 55, 3–34, https://doi.org/10.1007/s00382-018-4521-8, 2020.

Coppola, E., Nogherotto, R., Ciarlo', J. M., Giorgi, F., Van Meijgaard, E., Kadygrov, N., Iles, C., Corre, L., Sandstad, M., Somot, S., Nabat, P., Vautard, R., Levavasseur, G., Schwingshackl, C., Sillmann, J., Kjellström, E., Nikulin, G., Aalbers, E., Lenderink, G., Christensen, O. B., Boberg, F., Sørland, S. L., Demory, M., Bülow, K., Teichmann, C., Warrach-Sagi, K., and Wulfmeyer, V.: Assessment of the European Climate Projections as Simulated by the Large EURO-CORDEX Regional and Global

Climate Model Ensemble, J. Geophys. Res. Atmospheres, 126, e2019JD032356, https://doi.org/10.1029/2019JD032356, 2021a.

Coppola, E., Raffaele, F., Giorgi, F., Giuliani, G., Xuejie, G., Ciarlo, J. M., Sines, T. R., Torres-Alavez, J. A., Das, S., Di Sante, F., Pichelli, E., Glazer, R., Müller, S. K., Abba Omar, S., Ashfaq, M., Bukovsky, M., Im, E.-S., Jacob, D., Teichmann, C., Remedio, A., Remke, T., Kriegsmann, A., Bülow, K., Weber, T., Buntemeyer, L., Sieck, K., and Rechid, D.: Climate hazard indices projections based on CORDEX-CORE, CMIP5 and CMIP6 ensemble, Clim. Dyn., 57, 1293–1383, https://doi.org/10.1007/s00382-021-05640-z, 2021b.

Cornes, R. C., Van Der Schrier, G., Van Den Besselaar, E. J. M., and Jones, P. D.: An Ensemble Version of the E-OBS Temperature and Precipitation Data Sets, J. Geophys. Res. Atmospheres, 123, 9391–9409, https://doi.org/10.1029/2017JD028200, 2018.

Cos, J., Doblas-Reyes, F., Jury, M., Marcos, R., Bretonnière, P.-A., and Samsó, M.: The Mediterranean climate change hotspot in the CMIP5 and CMIP6 projections, Earth Syst. Dyn., 13, 321–340, https://doi.org/10.5194/esd-13-321-2022, 2022.

Crook, J. A., Jones, L. A., Forster, P. M., and Crook, R.: Climate change impacts on future photovoltaic and concentrated solar power energy output, Energy Environ. Sci., 4, 3101, https://doi.org/10.1039/c1ee01495a, 2011.

Cusinato, E., Rubino, A., and Zanchettin, D.: Winter Euro-Atlantic Climate Modes: Future Scenarios From a CMIP6 Multi-Model Ensemble, Geophys. Res. Lett., 48, e2021GL094532, https://doi.org/10.1029/2021GL094532, 2021.

Cutillas-Lozano, L. G., López, M. S. C., Velasco, A. P., Andrés-Doménech, I., and Olcina-Cantos, J.: Local-scale regionalisation of climate change effects on rainfall pattern: application to Alicante City (Spain), Theor. Appl. Climatol., 154, 377–402, https://doi.org/10.1007/s00704-023-04565-3, 2023.

Darmaraki, S., Somot, S., Sevault, F., Nabat, P., Cabos Narvaez, W. D., Cavicchia, L., Djurdjevic, V., Li, L., Sannino, G., and Sein, D. V.: Future evolution of Marine Heatwaves in the Mediterranean Sea, Clim. Dyn., 53, 1371–1392, https://doi.org/10.1007/s00382-019-04661-z, 2019.

Davini, P. and D'Andrea, F.: From CMIP3 to CMIP6: Northern Hemisphere Atmospheric Blocking Simulation in Present and Future Climate, J. Clim., 33, 10021–10038, https://doi.org/10.1175/JCLI-D-19-0862.1, 2020.

De La Vara, A., Gutiérrez, C., González-Alemán, J. J., and Gaertner, M. Á.: Intercomparison Study of the Impact of Climate Change on Renewable Energy Indicators on the Mediterranean Islands, Atmosphere, 11, 1036, https://doi.org/10.3390/atmos11101036, 2020.

De La Vara, A., Cabos, W., Sein, D. V., Teichmann, C., and Jacob, D.: Impact of air–sea coupling on the climate change signal over the Iberian Peninsula, Clim. Dyn., 57, 2325–2349, https://doi.org/10.1007/s00382-021-05812-x, 2021.

De León, S. P. and Orfila, A.: Numerical study of the marine breeze around Mallorca Island, Appl. Ocean Res., 40, 26–34, https://doi.org/10.1016/j.apor.2012.12.003, 2013.

De Luca, P. and Donat, M. G.: Projected Changes in Hot, Dry, and Compound Hot-Dry Extremes Over Global Land Regions, Geophys. Res. Lett., 50, e2022GL102493, https://doi.org/10.1029/2022GL102493, 2023.

De Luca, P., Delgado-Torres, C., Mahmood, R., Samso-Cabre, M., and Donat, M. G.: Constraining decadal variability regionally improves near-term projections of hot, cold and dry extremes, Environ. Res. Lett., 18, 094054, https://doi.org/10.1088/1748-9326/acf389, 2023.

De Martonne, E.: Aridité et indices d'aridité, Académie Sci. Comptes Rendus, 182, 1935–1938, 1923.

De Vries, H., Lenderink, G., Van Der Wiel, K., and Van Meijgaard, E.: Quantifying the role of the large-scale circulation on European summer precipitation change, Clim. Dyn., 59, 2871–2886, https://doi.org/10.1007/s00382-022-06250-z, 2022.

Del Jesús, M. and Díez-Sierra, J.: Climate change effects on sub-daily precipitation in Spain, Hydrol. Sci. J., 68, 1065–1077, https://doi.org/10.1080/02626667.2023.2215931, 2023.

Delgado-Torres, C., Verfaillie, D., Mohino, E., and Donat, M. G.: Representation and Annual to Decadal Predictability of Euro-Atlantic Weather Regimes in the CMIP6 Version of the EC-Earth Coupled Climate Model, J. Geophys. Res. Atmospheres, 127, e2022JD036673, https://doi.org/10.1029/2022JD036673, 2022.

Demory, M.-E., Berthou, S., Fernández, J., Sørland, S. L., Brogli, R., Roberts, M. J., Beyerle, U., Seddon, J., Haarsma, R., Schär, C., Buonomo, E., Christensen, O. B., Ciarlo`, J. M., Fealy, R., Nikulin, G., Peano, D., Putrasahan, D., Roberts, C. D., Senan, R., Steger, C., Teichmann, C., and Vautard, R.: European daily precipitation according to EURO-CORDEX regional climate models (RCMs) and high-resolution global climate models (GCMs) from the High-Resolution Model Intercomparison Project (HighResMIP), Geosci. Model Dev., 13, 5485–5506, https://doi.org/10.5194/gmd-13-5485-2020, 2020a.

Demory, M.-E., Berthou, S., Fernández, J., Sørland, S. L., Brogli, R., Roberts, M. J., Beyerle, U., Seddon, J., Haarsma, R., Schär, C., Buonomo, E., Christensen, O. B., Ciarlo`, J. M., Fealy, R., Nikulin, G., Peano, D., Putrasahan, D., Roberts, C. D., Senan, R., Steger, C., Teichmann, C., and Vautard, R.: European daily precipitation according to EURO-CORDEX regional climate models (RCMs) and high-resolution global climate models (GCMs) from the High-Resolution Model Intercomparison Project (HighResMIP), Geosci. Model Dev., 13, 5485–5506, https://doi.org/10.5194/gmd-13-5485-2020, 2020b.

Déqué, M., Somot, S., Sánchez-Gómez, E., Goodess, C. M., Jacob, D., Lenderink, G., and Christensen, O. B.: The spread amongst ENSEMBLES regional scenarios: regional climate models, driving general circulation models and interannual variability, Clim. Dyn., 38, 951–964, https://doi.org/10.1007/s00382-011-1053-x, 2012.

Deser, C. and Phillips, A. S.: A range of outcomes: the combined effects of internal variability and anthropogenic forcing on regional climate trends over Europe, Nonlinear Process. Geophys., 30, 63–84, https://doi.org/10.5194/npg-30-63-2023, 2023.

Deser, C., Phillips, A., Bourdette, V., and Teng, H.: Uncertainty in climate change projections: the role of internal variability, Clim. Dyn., 38, 527–546, https://doi.org/10.1007/s00382-010-0977-x, 2012.

Deser, C., Hurrell, J. W., and Phillips, A. S.: The role of the North Atlantic Oscillation in European climate projections, Clim. Dyn., 49, 3141–3157, https://doi.org/10.1007/s00382-016-3502-z, 2017.

Deser, C., Lehner, F., Rodgers, K. B., Ault, T., Delworth, T. L., DiNezio, P. N., Fiore, A., Frankignoul, C., Fyfe, J. C., Horton, D. E., Kay, J. E., Knutti, R., Lovenduski, N. S., Marotzke, J., McKinnon, K. A., Minobe,

S., Randerson, J., Screen, J. A., Simpson, I. R., and Ting, M.: Insights from Earth system model initial-condition large ensembles and future prospects, Nat. Clim. Change, 10, 277–286, https://doi.org/10.1038/s41558-020-0731-2, 2020.

Díaz-Poso, A., Lorenzo, N., Martí, A., and Royé, D.: Cold wave intensity on the Iberian Peninsula: Future climate projections, Atmospheric Res., 295, 107011, https://doi.org/10.1016/j.atmosres.2023.107011, 2023a.

Díaz-Poso, A., Royé, D., and Martínez-Ibarra, E.: Turismo y Cambio Climático: Aplicación del Holiday Climate Index (HCI:Urban) en España en los meses de verano para mediados y finales de siglo, Investig. Tur., 274–296, https://doi.org/10.14198/INTURI.23493, 2023b.

Díez-Sierra, J., Iturbide, M., Fernández, J., Gutiérrez, J. M., Milovac, J., and Cofiño, A. S.: Consistency of the regional response to global warming levels from CMIP5 and CORDEX projections, Clim. Dyn., 61, 4047–4060, https://doi.org/10.1007/s00382-023-06790-y, 2023.

Díez-Sierra, J., Iturbide, M., Brands, S., Fernández, J., Milovac, J., Cofiño, A. S., Azorín-Molina, C., Vicente-Serrano, S. M., and Gutiérrez, J. M.: Regional response of the Iberian mean and extreme climate to different levels of global warming, 2024.

Directorate-General for Energy (European Commission): EU energy in figures: statistical pocketbook 2021, Publications Office of the European Union, LU, 2021.

Domínguez, M., Romera, R., Sánchez, E., Fita, L., Fernández, J., Jiménez-Guerrero, P., Montávez, J., Cabos, W., Liguori, G., and Gaertner, M.: Present-climate precipitation and temperature extremes over Spain from a set of high resolution RCMs, Clim. Res., 58, 149–164, https://doi.org/10.3354/cr01186, 2013.

Donohue, R. J., McVicar, T. R., and Roderick, M. L.: Assessing the ability of potential evaporation formulations to capture the dynamics in evaporative demand within a changing climate, J. Hydrol., 386, 186–197, https://doi.org/10.1016/j.jhydrol.2010.03.020, 2010.

Dosio, A.: Projections of climate change indices of temperature and precipitation from an ensemble of bias-adjusted high-resolution EURO-CORDEX regional climate models, J. Geophys. Res. Atmospheres, 121, 5488–5511, https://doi.org/10.1002/2015JD024411, 2016.

Driouech, F., ElRhaz, K., Moufouma-Okia, W., Arjdal, K., and Balhane, S.: Assessing Future Changes of Climate Extreme Events in the CORDEX-MENA Region Using Regional Climate Model ALADIN-Climate, Earth Syst. Environ., 4, 477–492, https://doi.org/10.1007/s41748-020-00169-3, 2020.

Dufresne, J.-L. and Bony, S.: An Assessment of the Primary Sources of Spread of Global Warming Estimates from Coupled Atmosphere–Ocean Models, J. Clim., 21, 5135–5144, https://doi.org/10.1175/2008JCLI2239.1, 2008.

Dunn, R. J. H., Willett, K. M., Ciavarella, A., and Stott, P. A.: Comparison of land surface humidity between observations and CMIP5 models, Earth Syst. Dyn., 8, 719–747, https://doi.org/10.5194/esd-8-719-2017, 2017.

Dutta, R., Chanda, K., and Maity, R.: Future of solar energy potential in a changing climate across the world: A CMIP6 multi-model ensemble analysis, Renew. Energy, 188, 819–829, https://doi.org/10.1016/j.renene.2022.02.023, 2022.

Egea, J. A., Caro, M., García-Brunton, J., Gambín, J., Egea, J., and Ruiz, D.: Agroclimatic Metrics for the Main Stone Fruit Producing Areas in Spain in Current and Future Climate Change Scenarios: Implications From an Adaptive Point of View, Front. Plant Sci., 13, 842628, https://doi.org/10.3389/fpls.2022.842628, 2022.

Enríquez-Alonso, A., Sánchez-Lorenzo, A., Calbó, J., González, J.-A., and Norris, J. R.: Cloud cover climatologies in the Mediterranean obtained from satellites, surface observations, reanalyses, and CMIP5 simulations: validation and future scenarios, Clim. Dyn., 47, 249–269, https://doi.org/10.1007/s00382-015-2834-4, 2016.

Enríquez-Alonso, A., Calbó, J., Sánchez-Lorenzo, A., and Tan, E.: Discrepancies in the Climatology and Trends of Cloud Cover in Global and Regional Climate Models for the Mediterranean Region, J. Geophys. Res. Atmospheres, 122, https://doi.org/10.1002/2017JD027147, 2017.

Erinç, S.: An attempt on precipitation efficiency and a new index, İstanbul Üniversitesi Coğrafya Enstitüsü Yayın., 1965.

Espinoza, V., Waliser, D. E., Guan, B., Lavers, D. A., and Ralph, F. M.: Global Analysis of Climate Change Projection Effects on Atmospheric Rivers, Geophys. Res. Lett., 45, 4299–4308, https://doi.org/10.1029/2017GL076968, 2018.

Esteban-Parra, M. J., García-Valdecasas Ojeda, M., Peinó-Calero, E., Romero-Jiménez, E., Yeste, P., Rosa-Cánovas, J. J., Rodríguez-Brito, A., Gámiz-Fortis, S. R., and Castro-Díez, Y.: Climate Variability and Trends, in: The Landscape of the Sierra Nevada, edited by: Zamora, R. and Oliva, M., Springer International Publishing, Cham, 129–148, https://doi.org/10.1007/978-3-030-94219-9_9, 2022.

Expósito González, F. J., Díaz González, J. P., González Fernández, A. J., and Pérez Darias, J. C.: Proyecciones climáticas de índices de temperaturas extremas en Canarias, Asociación Española de Climatología, 2022.

Eyring, V., Bony, S., Meehl, G. A., Senior, C. A., Stevens, B., Stouffer, R. J., and Taylor, K. E.: Overview of the Coupled Model Intercomparison Project Phase 6 (CMIP6) experimental design and organization, Geosci. Model Dev., 9, 1937–1958, https://doi.org/10.5194/gmd-9-1937-2016, 2016.

Fadón, E., Fernández, E., Luedeling, E., and Rodrigo, J.: Agroclimatic requirements and adaptation potential to global warming of Spanish cultivars of sweet cherry (Prunus avium L.), Eur. J. Agron., 145, 126774, https://doi.org/10.1016/j.eja.2023.126774, 2023.

Falquina, R., De La Vara, A., Cabos, W., Sein, D., and Gallardo, C.: Impact of ocean-atmosphere coupling on present and future Köppen-Geiger climate classification in Europe, Atmospheric Res., 275, 106223, https://doi.org/10.1016/j.atmosres.2022.106223, 2022.

Fantini, A., Raffaele, F., Torma, C., Bacer, S., Coppola, E., Giorgi, F., Ahrens, B., Dubois, C., Sánchez, E., and Verdecchia, M.: Assessment of multiple daily precipitation statistics in ERA-Interim driven Med-CORDEX and EURO-CORDEX experiments against high resolution observations, Clim. Dyn., 51, 877–900, https://doi.org/10.1007/s00382-016-3453-4, 2018.

Fernández, J., Frías, M. D., Cabos, W. D., Cofiño, A. S., Domínguez, M., Fita, L., Gaertner, M. A., García-Díez, M., Gutiérrez, J. M., Jiménez-Guerrero, P., Liguori, G., Montávez, J. P., Romera, R., and Sánchez, E.: Consistency of climate change projections from multiple global and regional model intercomparison projects, Clim. Dyn., 52, 1139–1156, https://doi.org/10.1007/s00382-018-4181-8, 2019.

Fernández, J., Casanueva, A., Montávez, J. P., Gaertner, M. Á., Casado, M. J., Manzanas, R., and Gutiérrez, J. M.: Regional climate projections over Spain: Atmosphere. Future climate projections, 45–52 pp., 2017.

Fernández-Álvarez, J. C., Pérez-Alarcón, A., Eiras-Barca, J., Ramos, A. M., Rahimi-Esfarjani, S., Nieto, R., and Gimeno, L.: Changes in Moisture Sources of Atmospheric Rivers Landfalling the Iberian Peninsula With WRF-FLEXPART, J. Geophys. Res. Atmospheres, 128, e2022JD037612, https://doi.org/10.1029/2022JD037612, 2023.

Fernández-Álvarez, J. C., Costoya, X., Pérez-Alarcón, A., Rahimi, S., Nieto, R., and Gimeno, L.: Dynamic downscaling of wind speed over the North Atlantic Ocean using CMIP6 projections: Implications for offshore wind power density, Energy Rep., 9, 873–885, https://doi.org/10.1016/j.egyr.2022.12.036, 2023a.

Fernández-Álvarez, J. C., Pérez-Alarcón, A., Eiras-Barca, J., Rahimi, S., Nieto, R., and Gimeno, L.: Projected changes in atmospheric moisture transport contributions associated with climate warming in the North Atlantic, Nat. Commun., 14, 6476, https://doi.org/10.1038/s41467-023-41915-1, 2023b.

Fernández-Granja, J. A., Casanueva, A., Bedia, J., and Fernández, J.: Improved atmospheric circulation over Europe by the new generation of CMIP6 earth system models, Clim. Dyn., 56, 3527–3540, https://doi.org/10.1007/s00382-021-05652-9, 2021.

Fernández-Granja, J. A., Brands, S., Bedia, J., Casanueva, A., and Fernández, J.: Exploring the limits of the Jenkinson–Collison weather types classification scheme: a global assessment based on various reanalyses, Clim. Dyn., 61, 1829–1845, https://doi.org/10.1007/s00382-022-06658-7, 2023.

Fernández-Montes, S., Gómez-Navarro, J. J., Rodrigo, F. S., García-Valero, J. A., and Montávez, J. P.: Covariability of seasonal temperature and precipitation over the Iberian Peninsula in high-resolution regional climate simulations (1001–2099), Glob. Planet. Change, 151, 122–133, https://doi.org/10.1016/j.gloplacha.2016.09.007, 2017.

Feron, S., Cordero, R. R., Damiani, A., and Jackson, R. B.: Climate change extremes and photovoltaic power output, Nat. Sustain., 4, 270–276, https://doi.org/10.1038/s41893-020-00643-w, 2020.

Findell, K. L., Keys, P. W., Van Der Ent, R. J., Lintner, B. R., Berg, A., and Krasting, J. P.: Rising Temperatures Increase Importance of Oceanic Evaporation as a Source for Continental Precipitation, J. Clim., 32, 7713–7726, https://doi.org/10.1175/JCLI-D-19-0145.1, 2019.

Fosser, G., Kendon, E. J., Stephenson, D., and Tucker, S.: Convection-Permitting Models Offer Promise of More Certain Extreme Rainfall Projections, Geophys. Res. Lett., 47, e2020GL088151, https://doi.org/10.1029/2020GL088151, 2020.

Fraga, H., Malheiro, A. C., Moutinho-Pereira, J., and Santos, J. A.: Future scenarios for viticultural zoning in Europe: ensemble projections and uncertainties, Int. J. Biometeorol., 57, 909–925, https://doi.org/10.1007/s00484-012-0617-8, 2013.

García-Díez, M., Fernández, J., and Vautard, R.: An RCM multi-physics ensemble over Europe: multi-variable evaluation to avoid error compensation, Clim. Dyn., 45, 3141–3156, https://doi.org/10.1007/s00382-015-2529-x, 2015.

García-León, D., Casanueva, A., Standardi, G., Burgstall, A., Flouris, A. D., and Nybo, L.: Current and projected regional economic impacts of heatwaves in Europe, Nat. Commun., 12, 5807, https://doi.org/10.1038/s41467-021-26050-z, 2021.

García-Valdecasas Ojeda, M., Gámiz-Fortis, S. R., Castro-Díez, Y., and Esteban-Parra, M. J.: Evaluation of WRF capability to detect dry and wet periods in Spain using drought indices, J. Geophys. Res. Atmospheres, 122, 1569–1594, https://doi.org/10.1002/2016JD025683, 2017.

García-Valdecasas Ojeda, M., Yeste, P., Gámiz-Fortis, S. R., Castro-Díez, Y., and Esteban-Parra, M. J.: Future changes in land and atmospheric variables: An analysis of their couplings in the Iberian Peninsula, Sci. Total Environ., 722, 137902, https://doi.org/10.1016/j.scitotenv.2020.137902, 2020a.

García-Valdecasas Ojeda, M., Rosa-Cánovas, J. J., Romero-Jiménez, E., Yeste, P., Gámiz-Fortis, S. R., Castro-Díez, Y., and Esteban-Parra, M. J.: The role of the surface evapotranspiration in regional climate modelling: Evaluation and near-term future changes, Atmospheric Res., 237, 104867, https://doi.org/10.1016/j.atmosres.2020.104867, 2020b.

García-Valdecasas Ojeda, M., Romero-Jiménez, E., Rosa-Cánovas, J. J., Yeste, P., Castro-Díez, Y., Esteban-Parra, M. J., Vicente-Serrano, S. M., and Gámiz-Fortis, S. R.: Assessing Future Drought Conditions over the Iberian Peninsula: The Impact of Using Different Periods to Compute the SPEI, Atmosphere, 12, 980, https://doi.org/10.3390/atmos12080980, 2021a.

García-Valdecasas Ojeda, M., Gámiz-Fortis, S. R., Romero-Jiménez, E., Rosa-Cánovas, J. J., Yeste, P., Castro-Díez, Y., and Esteban-Parra, M. J.: Projected changes in the Iberian Peninsula drought characteristics, Sci. Total Environ., 757, 143702, https://doi.org/10.1016/j.scitotenv.2020.143702, 2021b.

Garijo, C. and Mediero, L.: Assessment of Changes in Annual Maximum Precipitations in the Iberian Peninsula under Climate Change, Water, 11, 2375, https://doi.org/10.3390/w11112375, 2019.

Garrido-Perez, J. M., García-Herrera, R., Barriopedro, D., and Ordóñez, C.: Shifting summer holidays in Spain as an adaptation measure to climate change, Sci. Total Environ., 904, 166879, https://doi.org/10.1016/j.scitotenv.2023.166879, 2023.

Garuma, G. F.: Review of urban surface parameterizations for numerical climate models, Urban Clim., 24, 830–851, https://doi.org/10.1016/j.uclim.2017.10.006, 2018.

Gernaat, D. E. H. J., De Boer, H. S., Daioglou, V., Yalew, S. G., Müller, C., and Van Vuuren, D. P.: Climate change impacts on renewable energy supply, Nat. Clim. Change, 11, 119–125, https://doi.org/10.1038/s41558-020-00949-9, 2021.

Giannakopoulos, C., Le Sager, P., Bindi, M., Moriondo, M., Kostopoulou, E., and Goodess, C. M.: Climatic changes and associated impacts in the Mediterranean resulting from a 2 °C global warming, Glob. Planet. Change, 68, 209–224, https://doi.org/10.1016/j.gloplacha.2009.06.001, 2009.

Gil, V., Gaertner, M. A., Gutierrez, C., and Losada, T.: Impact of climate change on solar irradiation and variability over the Iberian Peninsula using regional climate models, Int. J. Climatol., 39, 1733–1747, https://doi.org/10.1002/joc.5916, 2019.

Gil-Guirado, S., Pérez-Morales, A., Pino, D., Peña, J. C., and Martínez, F. L.: Flood impact on the Spanish Mediterranean coast since 1960 based on the prevailing synoptic patterns, Sci. Total Environ., 807, 150777, https://doi.org/10.1016/j.scitotenv.2021.150777, 2022.

Giorgi, F.: Climate change hot-spots, Geophys. Res. Lett., 33, 2006GL025734, https://doi.org/10.1029/2006GL025734, 2006.

González, A., Pérez, J. C., Díaz, J. P., and Expósito, F. J.: Future projections of wind resource in a mountainous archipelago, Canary Islands, Renew. Energy, 104, 120–128, https://doi.org/10.1016/j.renene.2016.12.021, 2017.

González-Abad, J., Hernández-García, Á., Harder, P., Rolnick, D., and Gutiérrez, J. M.: Multi-variable Hard Physical Constraints for Climate Model Downscaling, https://doi.org/10.48550/ARXIV.2308.01868, 2023.

González-Abad, J., Baño-Medina, J., and Gutiérrez, J. M.: Using Explainability to Inform Statistical Downscaling Based on Deep Learning Beyond Standard Validation Approaches, J. Adv. Model. Earth Syst., 15, e2023MS003641, https://doi.org/10.1029/2023MS003641, 2023.

González-Alemán, J. J., Insua-Costa, D., Bazile, E., González-Herrero, S., Marcello Miglietta, M., Groenemeijer, P., and Donat, M. G.: Anthropogenic Warming Had a Crucial Role in Triggering the Historic and Destructive Mediterranean Derecho in Summer 2022, Bull. Am. Meteorol. Soc., 104, E1526–E1532, https://doi.org/10.1175/BAMS-D-23-0119.1, 2023.

Greene, A. M., Goddard, L., and Cousin, R.: Web tool deconstructs variability in twentieth-century climate, Eos Trans. Am. Geophys. Union, 92, 397–398, https://doi.org/10.1029/2011EO450001, 2011.

Gutiérrez, C., Somot, S., Nabat, P., Mallet, M., Corre, L., Meijgaard, E. V., Perpiñán, O., and Gaertner, M. Á.: Future evolution of surface solar radiation and photovoltaic potential in Europe: investigating the role of aerosols, Environ. Res. Lett., 15, 034035, https://doi.org/10.1088/1748-9326/ab6666, 2020.

Gutiérrez, C., De La Vara, A., González-Alemán, J. J., and Gaertner, M. Á.: Impact of Climate Change on Wind and Photovoltaic Energy Resources in the Canary Islands and Adjacent Regions, Sustainability, 13, 4104, https://doi.org/10.3390/su13084104, 2021.

Gutiérrez, J. M., San-Martín, D., Brands, S., Manzanas, R., and Herrera, S.: Reassessing Statistical Downscaling Techniques for Their Robust Application under Climate Change Conditions, J. Clim., 26, 171–188, https://doi.org/10.1175/JCLI-D-11-00687.1, 2013.

Gutiérrez, J. M., Maraun, D., Widmann, M., Huth, R., Hertig, E., Benestad, R., Roessler, O., Wibig, J., Wilcke, R., Kotlarski, S., San Martín, D., Herrera, S., Bedia, J., Casanueva, A., Manzanas, R., Iturbide, M., Vrac, M., Dubrovsky, M., Ribalaygua, J., Pórtoles, J., Räty, O., Räisänen, J., Hingray, B., Raynaud, D., Casado, M. J., Ramos, P., Zerenner, T., Turco, M., Bosshard, T., Štěpánek, P., Bartholy, J., Pongracz, R., Keller, D. E., Fischer, A. M., Cardoso, R. M., Soares, P. M. M., Czernecki, B., and Pagé, C.: An intercomparison of a large ensemble of statistical downscaling methods over Europe: Results from the VALUE perfect predictor cross-validation experiment, Int. J. Climatol., 39, 3750–3785, https://doi.org/10.1002/joc.5462, 2019.

Gutowski Jr., W. J., Giorgi, F., Timbal, B., Frigon, A., Jacob, D., Kang, H.-S., Raghavan, K., Lee, B., Lennard, C., Nikulin, G., O'Rourke, E., Rixen, M., Solman, S., Stephenson, T., and Tangang, F.: WCRP COordinated Regional Downscaling EXperiment (CORDEX): a diagnostic MIP for CMIP6, Geosci. Model Dev., 9, 4087–4095, https://doi.org/10.5194/gmd-9-4087-2016, 2016.

Gutowski, W. J. J., Giorgi, F., Timbal, B., Frigon, A., Jacob, D., Kang, H.-S., Raghavan, K., Lee, B., Lennard, C., Nikulin, G., O'Rourke, E., Rixen, M., Solman, S., Stephenson, T., and Tangang, F.: WCRP COordinated Regional Downscaling EXperiment (CORDEX): a diagnostic MIP for CMIP6, Geosci. Model Dev., 9, 4087–4095, https://doi.org/10.5194/gmd-9-4087-2016, 2016.

Haarsma, R. J., Selten, F. M., and Drijfhout, S. S.: Decelerating Atlantic meridional overturning circulation main cause of future west European summer atmospheric circulation changes, Environ. Res. Lett., 10, 094007, https://doi.org/10.1088/1748-9326/10/9/094007, 2015.

Haarsma, R. J., Roberts, M. J., Vidale, P. L., Senior, C. A., Bellucci, A., Bao, Q., Chang, P., Corti, S., Fučkar, N. S., Guemas, V., von Hardenberg, J., Hazeleger, W., Kodama, C., Koenigk, T., Leung, L. R., Lu, J., Luo, J.-J., Mao, J., Mizielinski, M. S., Mizuta, R., Nobre, P., Satoh, M., Scoccimarro, E., Semmler, T., Small, J., and von Storch, J.-S.: High Resolution Model Intercomparison Project (HighResMIP v1.0) for CMIP6, Geosci. Model Dev., 9, 4185–4208, https://doi.org/10.5194/gmd-9-4185-2016, 2016a.

Haarsma, R. J., Roberts, M. J., Vidale, P. L., Senior, C. A., Bellucci, A., Bao, Q., Chang, P., Corti, S., Fučkar, N. S., Guemas, V., Von Hardenberg, J., Hazeleger, W., Kodama, C., Koenigk, T., Leung, L. R., Lu, J., Luo, J.-J., Mao, J., Mizielinski, M. S., Mizuta, R., Nobre, P., Satoh, M., Scoccimarro, E., Semmler, T., Small, J., and Von Storch, J.-S.: High Resolution Model Intercomparison Project (HighResMIP v1.0) for CMIP6, Geosci. Model Dev., 9, 4185–4208, https://doi.org/10.5194/gmd-9-4185-2016, 2016b.

Han, J. and Singh, V. P.: A review of widely used drought indices and the challenges of drought assessment under climate change, Environ. Monit. Assess., 195, 1438, https://doi.org/10.1007/s10661-023-12062-3, 2023.

Hartmann, D. L., Wallace, J. M., Limpasuvan, V., Thompson, D. W. J., and Holton, J. R.: Can ozone depletion and global warming interact to produce rapid climate change?, Proc. Natl. Acad. Sci., 97, 1412–1417, https://doi.org/10.1073/pnas.97.4.1412, 2000.

Hernanz, A., García-Valero, J. A., Domínguez, M., and Rodríguez-Camino, E.: Evaluation of statistical downscaling methods for climate change projections over Spain: Future conditions with pseudo reality (transferability experiment), Int. J. Climatol., 42, 3987–4000, https://doi.org/10.1002/joc.7464, 2022a.

Hernanz, A., García-Valero, J. A., Domínguez, M., and Rodríguez-Camino, E.: Evaluation of statistical downscaling methods for climate change projections over Spain: Present conditions with imperfect predictors (global climate model experiment), Int. J. Climatol., 42, 6793–6806, https://doi.org/10.1002/joc.7611, 2022b.

Hernanz, A., García-Valero, J. A., Domínguez, M., Ramos-Calzado, P., Pastor-Saavedra, M. A., and Rodríguez-Camino, E.: Evaluation of statistical downscaling methods for climate change projections over Spain: Present conditions with perfect predictors, Int. J. Climatol., 42, 762–776, https://doi.org/10.1002/joc.7271, 2022c.

Hernanz, A., Correa, C., Domínguez, M., Rodríguez-Guisado, E., and Rodríguez-Camino, E.: Comparison of machine learning statistical downscaling and regional climate models for temperature, precipitation, wind speed, humidity and radiation over Europe under present conditions, Int. J. Climatol., 43, 6065–6082, https://doi.org/10.1002/joc.8190, 2023a.

Hernanz, A., Correa, C., Andrés García-Valero, J., Domínguez, M., Rodríguez-Guisado, E., and Rodríguez-Camino, E.: pyClim-SDM: Service for generation of statistically downscaled climate change projections supporting national adaptation strategies, Clim. Serv., 32, 100408, https://doi.org/10.1016/j.cliser.2023.100408, 2023b.

Hernanz, A., Correa, C., Sánchez-Perrino, J., Prieto-Rico, I., Rodríguez-Guisado, E., Domínguez, M., and Rodríguez-Camino, E.: On the limitations of deep learning for statistical downscaling of climate change projections: The transferability and the extrapolation issues, Atmospheric Sci. Lett., 25, e1195, https://doi.org/10.1002/asl.1195, 2024.

Herrera, S., Bedia, J., Gutiérrez, J. M., Fernández, J., and Moreno, J. M.: On the projection of future fire danger conditions with various instantaneous/mean-daily data sources, Clim. Change, 118, 827–840, https://doi.org/10.1007/s10584-012-0667-2, 2013.

Herrera, S., Cardoso, R. M., Soares, P. M., Espírito-Santo, F., Viterbo, P., and Gutiérrez, J. M.: Iberia01: a new gridded dataset of daily precipitation and temperatures over Iberia, Earth Syst. Sci. Data, 11, 1947–1956, https://doi.org/10.5194/essd-11-1947-2019, 2019.

Herrera, S., Soares, P. M. M., Cardoso, R. M., and Gutiérrez, J. M.: Evaluation of the EURO-CORDEX Regional Climate Models Over the Iberian Peninsula: Observational Uncertainty Analysis, J. Geophys. Res. Atmospheres, 125, e2020JD032880, https://doi.org/10.1029/2020JD032880, 2020.

Herrera-Lormendez, P., Douville, H., and Matschullat, J.: European Summer Synoptic Circulations and Their Observed 2022 and Projected Influence on Hot Extremes and Dry Spells, Geophys. Res. Lett., 50, e2023GL104580, https://doi.org/10.1029/2023GL104580, 2023a.

Herrera-Lormendez, P., John, A., Douville, H., and Matschullat, J.: Projected changes in synoptic circulations over Europe and their implications for summer precipitation: A CMIP6 perspective, Int. J. Climatol., 43, 3373–3390, https://doi.org/10.1002/joc.8033, 2023b.

Hertig, E., Maraun, D., Bartholy, J., Pongracz, R., Vrac, M., Mares, I., Gutiérrez, J. M., Wibig, J., Casanueva, A., and Soares, P. M. M.: Comparison of statistical downscaling methods with respect to extreme events over Europe: Validation results from the perfect predictor experiment of the COST Action VALUE, Int. J. Climatol., 39, 3846–3867, https://doi.org/10.1002/joc.5469, 2019.

Hou, X., Wild, M., Folini, D., Kazadzis, S., and Wohland, J.: Climate change impacts on solar power generation and its spatial variability in Europe based on CMIP6, Earth Syst. Dyn., 12, 1099–1113, https://doi.org/10.5194/esd-12-1099-2021, 2021.

Intergovernmental Panel On Climate Change (Ed.): Evaluation of Climate Models, in: Climate Change 2013 – The Physical Science Basis, Cambridge University Press, 741–866, https://doi.org/10.1017/CBO9781107415324.020, 2014a.

Intergovernmental Panel On Climate Change (Ed.): Long-term Climate Change: Projections, Commitments and Irreversibility Pages 1029 to 1076, in: Climate Change 2013 – The Physical Science Basis, Cambridge University Press, 1029–1136, https://doi.org/10.1017/CBO9781107415324.024, 2014b.

Intergovernmental Panel On Climate Change (Ipcc): Climate Change 2021 – The Physical Science Basis: Working Group I Contribution to the Sixth Assessment Report of the Intergovernmental Panel on Climate Change, 1st ed., Cambridge University Press, https://doi.org/10.1017/9781009157896, 2023a.

Intergovernmental Panel On Climate Change (Ipcc) (Ed.): Summary for Policymakers, in: Climate Change 2022 - Mitigation of Climate Change, Cambridge University Press, 3–48, https://doi.org/10.1017/9781009157926.001, 2023b.

Iturbide, M., Bedia, J., Herrera, S., Baño-Medina, J., Fernández, J., Frías, M. D., Manzanas, R., San-Martín, D., Cimadevilla, E., Cofiño, A. S., and Gutiérrez, J. M.: The R-based climate4R open framework for reproducible climate data access and post-processing, Environ. Model. Softw., 111, 42–54, https://doi.org/10.1016/j.envsoft.2018.09.009, 2019.

Iturbide, M., Gutiérrez, J. M., Alves, L. M., Bedia, J., Cerezo-Mota, R., Cimadevilla, E., Cofiño, A. S., Di Luca, A., Faria, S. H., Gorodetskaya, I. V., Hauser, M., Herrera, S., Hennessy, K., Hewitt, H. T., Jones, R. G., Krakovska, S., Manzanas, R., Martínez-Castro, D., Narisma, G. T., Nurhati, I. S., Pinto, I., Seneviratne, S. I., Van Den Hurk, B., and Vera, C. S.: An update of IPCC climate reference regions for subcontinental analysis of climate model data: definition and aggregated datasets, Earth Syst. Sci. Data, 12, 2959–2970, https://doi.org/10.5194/essd-12-2959-2020, 2020.

Iturbide, M., Fernández, J., Gutiérrez, J. M., Pirani, A., Huard, D., Al Khourdajie, A., Baño-Medina, J., Bedia, J., Casanueva, A., Cimadevilla, E., Cofiño, A. S., De Felice, M., Díez-Sierra, J., García-Díez, M., Goldie, J., Herrera, D. A., Herrera, S., Manzanas, R., Milovac, J., Radhakrishnan, A., San-Martín, D., Spinuso, A., Thyng, K. M., Trenham, C., and Yelekçi, Ö.: Implementation of FAIR principles in the IPCC: the WGI AR6 Atlas repository, Sci. Data, 9, 629, https://doi.org/10.1038/s41597-022-01739-y, 2022a.

Iturbide, M., Casanueva, A., Bedia, J., Herrera, S., Milovac, J., and Gutiérrez, J. M.: On the need of bias adjustment for more plausible climate change projections of extreme heat, Atmospheric Sci. Lett., 23, e1072, https://doi.org/10.1002/asl.1072, 2022b.

Jacob, D., Teichmann, C., Sobolowski, S., Katragkou, E., Anders, I., Belda, M., Benestad, R., Boberg, F., Buonomo, E., Cardoso, R. M., Casanueva, A., Christensen, O. B., Christensen, J. H., Coppola, E., De Cruz, L., Davin, E. L., Dobler, A., Domínguez, M., Fealy, R., Fernández, J., Gaertner, M. A., García-Díez, M., Giorgi, F., Gobiet, A., Goergen, K., Gómez-Navarro, J. J., Alemán, J. J. G., Gutiérrez, C., Gutiérrez, J. M., Güttler, I., Haensler, A., Halenka, T., Jerez, S., Jiménez-Guerrero, P., Jones, R. G., Keuler, K., Kjellström, E., Knist, S., Kotlarski, S., Maraun, D., Van Meijgaard, E., Mercogliano, P., Montávez, J. P., Navarra, A., Nikulin, G., De Noblet-Ducoudré, N., Panitz, H.-J., Pfeifer, S., Piazza, M., Pichelli, E., Pietikäinen, J.-P., Prein, A. F., Preuschmann, S., Rechid, D., Rockel, B., Romera, R., Sánchez, E., Sieck, K., Soares, P. M. M., Somot, S., Srnec, L., Sørland, S. L., Termonia, P., Truhetz, H., Vautard, R., Warrach-Sagi, K., and Wulfmeyer, V.: Regional climate downscaling over Europe: perspectives from the EURO-CORDEX community, Reg. Environ. Change, 20, 51, https://doi.org/10.1007/s10113-020-01606-9, 2020a.

Jacob, D., Teichmann, C., Sobolowski, S., Katragkou, E., Anders, I., Belda, M., Benestad, R., Boberg, F., Buonomo, E., Cardoso, R. M., Casanueva, A., Christensen, O. B., Christensen, J. H., Coppola, E., De Cruz, L., Davin, E. L., Dobler, A., Domínguez, M., Fealy, R., Fernández, J., Gaertner, M. A., García-Díez, M., Giorgi, F., Gobiet, A., Goergen, K., Gómez-Navarro, J. J., Alemán, J. J. G., Gutiérrez, C., Gutiérrez, J. M., Güttler, I., Haensler, A., Halenka, T., Jerez, S., Jiménez-Guerrero, P., Jones, R. G., Keuler, K., Kjellström, E., Knist, S., Kotlarski, S., Maraun, D., van Meijgaard, E., Mercogliano, P., Montávez, J. P., Navarra, A., Nikulin, G., de Noblet-Ducoudré, N., Panitz, H.-J., Pfeifer, S., Piazza, M., Pichelli, E., Pietikäinen, J.-P., Prein, A. F., Preuschmann, S., Rechid, D., Rockel, B., Romera, R., Sánchez, E., Sieck, K., Soares, P. M. M., Somot, S., Srnec, L., Sørland, S. L., Termonia, P., Truhetz, H., Vautard, R., Warrach-Sagi, K., and Wulfmeyer, V.: Regional climate downscaling over Europe: perspectives from the EURO-CORDEX community, Reg. Environ. Change, 20, 51, https://doi.org/10.1007/s10113-020-01606-9, 2020b.

Jerez, S., Tobin, I., Vautard, R., Montávez, J. P., López-Romero, J. M., Thais, F., Bartok, B., Christensen, O. B., Colette, A., Déqué, M., Nikulin, G., Kotlarski, S., Van Meijgaard, E., Teichmann, C., and Wild, M.: The impact of climate change on photovoltaic power generation in Europe, Nat. Commun., 6, 10014, https://doi.org/10.1038/ncomms10014, 2015.

Jerez, S., Tobin, I., Turco, M., Jiménez-Guerrero, P., Vautard, R., and Montávez, J. P.: Future changes, or lack thereof, in the temporal variability of the combined wind-plus-solar power production in Europe, Renew. Energy, 139, 251–260, https://doi.org/10.1016/j.renene.2019.02.060, 2019.

Jung, C. and Schindler, D.: A review of recent studies on wind resource projections under climate change, Renew. Sustain. Energy Rev., 165, 112596, https://doi.org/10.1016/j.rser.2022.112596, 2022.

Kapica, J., Jurasz, J., Canales, F. A., Bloomfield, H., Guezgouz, M., De Felice, M., and Kobus, Z.: The potential impact of climate change on European renewable energy droughts, Renew. Sustain. Energy Rev., 189, 114011, https://doi.org/10.1016/j.rser.2023.114011, 2024.

Karnauskas, K. B., Lundquist, J. K., and Zhang, L.: Southward shift of the global wind energy resource under high carbon dioxide emissions, Nat. Geosci., 11, 38–43, https://doi.org/10.1038/s41561-017-0029-9, 2018.

Karwat, A. and Franzke, C. L. E.: Future Projections of Heat Mortality Risk for Major European Cities, Weather Clim. Soc., https://doi.org/10.1175/WCAS-D-20-0142.1, 2021.

Katragkou, E., Sobolowski, S. P., Teichmann, C., Solmon, F., Pavlidis, V., Rechid, D., Hoffmann, P., Fernandez, J., Nikulin, G., and Jacob, D.: Delivering an Improved Framework for the New Generation of CMIP6-Driven EURO-CORDEX Regional Climate Simulations, Bull. Am. Meteorol. Soc., 105, E962–E974, https://doi.org/10.1175/BAMS-D-23-0131.1, 2024.

Klein, S. A., Zhang, Y., Zelinka, M. D., Pincus, R., Boyle, J., and Gleckler, P. J.: Are climate model simulations of clouds improving? An evaluation using the ISCCP simulator, J. Geophys. Res. Atmospheres, 118, 1329–1342, https://doi.org/10.1002/jgrd.50141, 2013.

Kothe, S., Dobler, A., Beck, A., and Ahrens, B.: The radiation budget in a regional climate model, Clim. Dyn., 36, 1023–1036, https://doi.org/10.1007/s00382-009-0733-2, 2011.

Lasher-Trapp, S., Orendorf, S. A., and Trapp, R. J.: Investigating a Derecho in a Future Warmer Climate, Bull. Am. Meteorol. Soc., 104, E1831–E1852, https://doi.org/10.1175/BAMS-D-22-0173.1, 2023.

Legasa, M. N., Manzanas, R., Fernández, J., Herrera, S., Iturbide, M., Moufouma-Okia, W., Zhai, P., Driouech, F., and Gutiérrez, J. M.: Assessing Multidomain Overlaps and Grand Ensemble Generation in CORDEX Regional Projections, Geophys. Res. Lett., 47, e2019GL086799, https://doi.org/10.1029/2019GL086799, 2020.

Li, X., Wagner, F., Peng, W., Yang, J., and Mauzerall, D. L.: Reduction of solar photovoltaic resources due to air pollution in China, Proc. Natl. Acad. Sci., 114, 11867–11872, https://doi.org/10.1073/pnas.1711462114, 2017.

Lionello, P. and Scarascia, L.: The relation between climate change in the Mediterranean region and global warming, Reg. Environ. Change, 18, 1481–1493, https://doi.org/10.1007/s10113-018-1290-1, 2018.

López-Moreno, J. I., Gascoin, S., Herrero, J., Sproles, E. A., Pons, M., Alonso-González, E., Hanich, L., Boudhar, A., Musselman, K. N., Molotch, N. P., Sickman, J., and Pomeroy, J.: Different sensitivities of snowpacks to warming in Mediterranean climate mountain areas, Environ. Res. Lett., 12, 074006, https://doi.org/10.1088/1748-9326/aa70cb, 2017.

López-Romero, J. M., Montávez, J. P., Jerez, S., Lorente-Plazas, R., Palacios-Peña, L., and Jiménez-Guerrero, P.: Precipitation response to aerosol–radiation and aerosol–cloud interactions in regional climate simulations over Europe, Atmospheric Chem. Phys., 21, 415–430, https://doi.org/10.5194/acp-21-415-2021, 2021.

Lorenzo, M. N. and Álvarez, I.: Climate change patterns in precipitation over Spain using CORDEX projections for 2021–2050, Sci. Total Environ., 723, 138024, https://doi.org/10.1016/j.scitotenv.2020.138024, 2020.

Lorenzo, M. N., Taboada, J. J., Lorenzo, J. F., and Ramos, A. M.: Influence of climate on grape production and wine quality in the Rías Baixas, north-western Spain, Reg. Environ. Change, 13, 887–896, https://doi.org/10.1007/s10113-012-0387-1, 2013.

Lorenzo, M. N., Pereira, H., Álvarez, I., and Días, J. M.: Standardized Precipitation Index (SPI) evolution over the Iberian Peninsula during the 21st century, Atmospheric Res., 297, 107132, https://doi.org/10.1016/j.atmosres.2023.107132, 2024.

Lorenzo, N., Díaz-Poso, A., and Royé, D.: Heatwave intensity on the Iberian Peninsula: Future climate projections, Atmospheric Res., 258, 105655, https://doi.org/10.1016/j.atmosres.2021.105655, 2021.

Lucas-Picher, P., Argüeso, D., Brisson, E., Tramblay, Y., Berg, P., Lemonsu, A., Kotlarski, S., and Caillaud, C.: Convection-permitting modeling with regional climate models: Latest developments and next steps, WIREs Clim. Change, 12, e731, https://doi.org/10.1002/wcc.731, 2021.

Maher, N., Milinski, S., Suárez-Gutiérrez, L., Botzet, M., Dobrynin, M., Kornblueh, L., Kröger, J., Takano, Y., Ghosh, R., Hedemann, C., Li, C., Li, H., Manzini, E., Notz, D., Putrasahan, D., Boysen, L., Claussen, M., Ilyina, T., Olonscheck, D., Raddatz, T., Stevens, B., and Marotzke, J.: The Max Planck Institute Grand Ensemble: Enabling the Exploration of Climate System Variability, J. Adv. Model. Earth Syst., 11, 2050–2069, https://doi.org/10.1029/2019MS001639, 2019.

Maraun, D.: Bias Correcting Climate Change Simulations - a Critical Review, Curr. Clim. Change Rep., 2, 211–220, https://doi.org/10.1007/s40641-016-0050-x, 2016.

Maraun, D., Widmann, M., Gutiérrez, J. M., Kotlarski, S., Chandler, R. E., Hertig, E., Wibig, J., Huth, R., and Wilcke, R. A. I.: VALUE : A framework to validate downscaling approaches for climate change studies, Earths Future, 3, 1–14, https://doi.org/10.1002/2014EF000259, 2015.

Maraun, D., Huth, R., Gutiérrez, J. M., Martín, D. S., Dubrovsky, M., Fischer, A., Hertig, E., Soares, P. M. M., Bartholy, J., Pongrácz, R., Widmann, M., Casado, M. J., Ramos, P., and Bedia, J.: The VALUE perfect predictor experiment: Evaluation of temporal variability, Int. J. Climatol., 39, 3786–3818, https://doi.org/10.1002/joc.5222, 2019.

Martí Ezpeleta, A., Lorenzo González, María de las Nieves, Royé, Dominic, and Díaz Poso, Alejandro: Retos del cambio climático: impactos, mitigación y adaptación, Asociación Española de Climatología Agencia Estatal de Meteorología (Ministerio para la Transición Ecológica y el Reto Demográfico), Madrid, 2022.

Martija-Díez, M., López-Parages, J., Rodríguez-Fonseca, B., and Losada, T.: The stationarity of the ENSO teleconnection in European summer rainfall, Clim. Dyn., 61, 489–506, https://doi.org/10.1007/s00382-022-06596-4, 2023.

Martins, J., Rocha, A., Viceto, C., Pereira, S. C., and Santos, J. A.: Future Projections for Wind, Wind Shear and Helicity in the Iberian Peninsula, Atmosphere, 11, 1001, https://doi.org/10.3390/atmos11091001, 2020.

Mateos, D., Sánchez-Lorenzo, A., Antón, M., Cachorro, V. E., Calbó, J., Costa, M. J., Torres, B., and Wild, M.: Quantifying the respective roles of aerosols and clouds in the strong brightening since the early 2000s over the Iberian Peninsula, J. Geophys. Res. Atmospheres, 119, https://doi.org/10.1002/2014JD022076, 2014.

Materia, S., Ardilouze, C., Prodhomme, C., Donat, M. G., Benassi, M., Doblas-Reyes, F. J., Peano, D., Caron, L.-P., Ruggieri, P., and Gualdi, S.: Summer temperature response to extreme soil water conditions in the Mediterranean transitional climate regime, Clim. Dyn., 58, 1943–1963, https://doi.org/10.1007/s00382-021-05815-8, 2022.

Matte, D., Christensen, J. H., and Ozturk, T.: Spatial extent of precipitation events: when big is getting bigger, Clim. Dyn., 58, 1861–1875, https://doi.org/10.1007/s00382-021-05998-0, 2022.

Matthews, T.: Humid heat and climate change, Prog. Phys. Geogr. Earth Environ., 42, 391–405, https://doi.org/10.1177/0309133318776490, 2018.

McKee, T. B., Doesken, N. J., Kleist, J., and others: The relationship of drought frequency and duration to time scales, in: Proceedings of the 8th Conference on Applied Climatology, 179–183, 1993.

McKenna, C. M. and Maycock, A. C.: Sources of Uncertainty in Multimodel Large Ensemble Projections of the Winter North Atlantic Oscillation, Geophys. Res. Lett., 48, e2021GL093258, https://doi.org/10.1029/2021GL093258, 2021.

McVicar, T. R., Roderick, M. L., Donohue, R. J., Li, L. T., Van Niel, T. G., Thomas, A., Grieser, J., Jhajharia, D., Himri, Y., Mahowald, N. M., Mescherskaya, A. V., Kruger, A. C., Rehman, S., and Dinpashoh, Y.: Global review and synthesis of trends in observed terrestrial near-surface wind speeds: Implications for evaporation, J. Hydrol., 416–417, 182–205, https://doi.org/10.1016/j.jhydrol.2011.10.024, 2012.

Meehl, G. A., Senior, C. A., Eyring, V., Flato, G., Lamarque, J.-F., Stouffer, R. J., Taylor, K. E., and Schlund, M.: Context for interpreting equilibrium climate sensitivity and transient climate response from the CMIP6 Earth system models, Sci. Adv., 6, eaba1981, https://doi.org/10.1126/sciadv.aba1981, 2020.

Minola, L., Azorín-Molina, C., and Chen, D.: Homogenization and Assessment of Observed Near-Surface Wind Speed Trends across Sweden, 1956–2013, J. Clim., 29, 7397–7415, https://doi.org/10.1175/JCLI-D-15-0636.1, 2016.

Miralles, D. G., Gentine, P., Seneviratne, S. I., and Teuling, A. J.: Land–atmospheric feedbacks during droughts and heatwaves: state of the science and current challenges, Ann. N. Y. Acad. Sci., 1436, 19–35, https://doi.org/10.1111/nyas.13912, 2019.

Miranda, P. M. A., Alves, J. M. R., and Serra, N.: Climate change and upwelling: response of Iberian upwelling to atmospheric forcing in a regional climate scenario, Clim. Dyn., 40, 2813–2824, https://doi.org/10.1007/s00382-012-1442-9, 2013.

Miró, J. J., Estrela, M. J., Olcina-Cantos, J., and Martín-Vide, J.: Future Projection of Precipitation Changes in the Júcar and Segura River Basins (Iberian Peninsula) by CMIP5 GCMs Local Downscaling, Atmosphere, 12, 879, https://doi.org/10.3390/atmos12070879, 2021.

Molina, M. O., Sánchez, E., and Gutiérrez, C.: Future heat waves over the Mediterranean from an Euro-CORDEX regional climate model ensemble, Sci. Rep., 10, 8801, https://doi.org/10.1038/s41598-020-65663-0, 2020.

Molina, M. O., Careto, J. A. M., Gutiérrez, C., Sánchez, E., and Soares, P. M. M.: The added value of high-resolution EURO-CORDEX simulations to describe daily wind speed over Europe, Int. J. Climatol., 43, 1062–1078, https://doi.org/10.1002/joc.7877, 2023.

Molinié, G., Déqué, M., Coppola, E., Blanchet, J., and Neppel, L.: Sub-chapter 1.3.1. Heavy precipitation in the Mediterranean basin, in: The Mediterranean region under climate change, edited by: Moatti, J.-P. and Thiébault, S., IRD Éditions, 107–114, https://doi.org/10.4000/books.irdeditions.23121, 2016.

Montávez, J. P., Fernández, J., Casanueva, A., Gutiérrez, J. M., and Sánchez, E.: Regional climate projections over Spain: Atmosphere. Present climate evaluation, 39–44 pp., 2017.

Moriondo, M., Good, P., Durao, R., Bindi, M., Giannakopoulos, C., and Corte-Real, J.: Potential impact of climate change on fire risk in the Mediterranean area, Clim. Res., 31, 85–95, 2006.

Moyano, J., Dimas, M., Álvarez, A. J., Barranco, L. M., D, C. R., Portal, E., and Rico, A.: Evaluation of the impact of climate change on water resources and droughts frequency and severity in a small-scale international catchment in the Iberian Peninsula, Int. J. Water, 15, 207–231, https://doi.org/10.1504/IJW.2023.133996, 2023.

Müller, J., Folini, D., Wild, M., and Pfenninger, S.: CMIP-5 models project photovoltaics are a no-regrets investment in Europe irrespective of climate change, Energy, 171, 135–148, https://doi.org/10.1016/j.energy.2018.12.139, 2019.

Müller, R. and Pfeifroth, U.: Remote sensing of solar surface radiation – a reflection of concepts, applications and input data based on experience with the effective cloud albedo, Atmospheric Meas. Tech., 15, 1537–1561, https://doi.org/10.5194/amt-15-1537-2022, 2022.

Muñoz, Á. G., Thomson, M. C., Goddard, L., and Aldighieri, S.: Analyzing climate variations at multiple timescales can guide Zika virus response measures, GigaScience, 5, 41, https://doi.org/10.1186/s13742-016-0146-1, 2016.

Muñoz, Á. G., Yang, X., Vecchi, G. A., Robertson, A. W., and Cooke, W. F.: A Weather-Type-Based Cross-Time-Scale Diagnostic Framework for Coupled Circulation Models, J. Clim., 30, 8951–8972, https://doi.org/10.1175/JCLI-D-17-0115.1, 2017.

Nabat, P., Somot, S., Mallet, M., Sánchez-Lorenzo, A., and Wild, M.: Contribution of anthropogenic sulfate aerosols to the changing Euro-Mediterranean climate since 1980, Geophys. Res. Lett., 41, 5605–5611, https://doi.org/10.1002/2014GL060798, 2014.

Obermann-Hellhund, A., Conte, D., Somot, S., Torma, C. Z., and Ahrens, B.: Mistral and Tramontane wind systems in climate simulations from 1950 to 2100, Clim. Dyn., 50, 693–703, https://doi.org/10.1007/s00382-017-3635-8, 2018.

O'Brien, T. A., Wehner, M. F., Payne, A. E., Shields, C. A., Rutz, J. J., Leung, L. -R., Ralph, F. M., Collow, A., Gorodetskaya, I., Guan, B., Lora, J. M., McClenny, E., Nardi, K. M., Ramos, A. M., Tomé, R., Sarangi, C., Shearer, E. J., Ullrich, P. A., Zarzycki, C., Loring, B., Huang, H., Inda-Díaz, H. A., Rhoades, A. M., and Zhou, Y.: Increases in Future AR Count and Size: Overview of the ARTMIP Tier 2 CMIP5/6 Experiment, J. Geophys. Res. Atmospheres, 127, e2021JD036013, https://doi.org/10.1029/2021JD036013, 2022.

Olmo, M., Cos, J, Muñoz, AG, Altava-Ortiz, V, Barrera-Escoda, A, Campos, D, Soret, A, and Doblas-Reyes, F.: Cross-time scale analysis of year-round synoptic circulation patterns and their impacts on rainfall and temperatures in the Iberian Peninsula, J. Clim. Submitt., 2024.

Ortega, M., Sánchez, E., Gutiérrez, C., Molina, M. O., and López-Franca, N.: Regional winds over the Iberian Peninsula (Cierzo, Levante and Poniente) from high-resolution COSMO-REA6 reanalysis, Int. J. Climatol., 43, 1016–1033, https://doi.org/10.1002/joc.7860, 2023.

Ossó, A., Craig, P., and Allan, R. P.: An assessment of CMIP6 climate signals and biases in temperature, precipitation and soil moisture over Europe, Int. J. Climatol., 43, 5698–5719, https://doi.org/10.1002/joc.8169, 2023.

Ozturk, T., Matte, D., and Christensen, J. H.: Robustness of future atmospheric circulation changes over the EURO-CORDEX domain, Clim. Dyn., 59, 1799–1814, https://doi.org/10.1007/s00382-021-06069-0, 2022.

Palmer, T. E., McSweeney, C. F., Booth, B. B. B., Priestley, M. D. K., Davini, P., Brunner, L., Borchert, L., and Menary, M. B.: Performance-based sub-selection of CMIP6 models for impact assessments in Europe, Earth Syst. Dyn., 14, 457–483, https://doi.org/10.5194/esd-14-457-2023, 2023.

Payne, A. E., Demory, M.-E., Leung, L. R., Ramos, A. M., Shields, C. A., Rutz, J. J., Siler, N., Villarini, G., Hall, A., and Ralph, F. M.: Responses and impacts of atmospheric rivers to climate change, Nat. Rev. Earth Environ., 1, 143–157, https://doi.org/10.1038/s43017-020-0030-5, 2020.

Peral García, C., Navascués Fernández-Victorio, B., and Ramos Calzado, P.: Serie de precipitación diaria en rejilla con fines climáticos, Agencia Estatal de Meteorología, https://doi.org/10.31978/014-17-009-5, 2017.

Pereira, S. C., Carvalho, D., and Rocha, A.: Temperature and Precipitation Extremes over the Iberian Peninsula under Climate Change Scenarios: A Review, Climate, 9, 139, https://doi.org/10.3390/cli9090139, 2021.

Pérez, J. C., Díaz, J. P., González, A., Expósito, J., Rivera-López, F., and Taima, D.: Evaluation of WRF Parameterizations for Dynamical Downscaling in the Canary Islands, J. Clim., 27, 5611–5631, https://doi.org/10.1175/JCLI-D-13-00458.1, 2014.

Pérez, J. C., Expósito, F. J., González, A., and Díaz, J. P.: Climate projections at a convection-permitting scale of extreme temperature indices for an archipelago with a complex microclimate structure, Weather Clim. Extrem., 36, 100459, https://doi.org/10.1016/j.wace.2022.100459, 2022.

Pérez-Palazón, M., Pimentel, R., and Polo, M.: Climate Trends Impact on the Snowfall Regime in Mediterranean Mountain Areas: Future Scenario Assessment in Sierra Nevada (Spain), Water, 10, 720, https://doi.org/10.3390/w10060720, 2018.

Pérez-Zanón, N., Casas-Castillo, M. C., Peña, J. C., Aran, M., Rodríguez-Solà, R., Redaño, A., and Solé, G.: Analysis of synoptic patterns in relationship with severe rainfall events in the Ebre Observatory (Catalonia), Acta Geophys., 66, 405–414, https://doi.org/10.1007/s11600-018-0126-1, 2018.

Perkins-Kirkpatrick, S. E. and Lewis, S. C.: Increasing trends in regional heatwaves, Nat. Commun., 11, 3357, https://doi.org/10.1038/s41467-020-16970-7, 2020.

Pinto, M. M., DaCamara, C. C., Hurduc, A., Trigo, R. M., and Trigo, I. F.: Enhancing the fire weather index with atmospheric instability information, Environ. Res. Lett., 15, 0940b7, https://doi.org/10.1088/1748-9326/ab9e22, 2020.

Prein, A. F.: Thunderstorm straight line winds intensify with climate change, Nat. Clim. Change, 13, 1353–1359, https://doi.org/10.1038/s41558-023-01852-9, 2023.

Quilcaille, Y., Batibeniz, F., Ribeiro, A. F. S., Padrón, R. S., and Seneviratne, S. I.: Fire weather index data under historical and shared socioeconomic pathway projections in the 6th phase of the Coupled Model Intercomparison Project from 1850 to 2100, Earth Syst. Sci. Data, 15, 2153–2177, https://doi.org/10.5194/essd-15-2153-2023, 2023.

Ramon, J., Lledó, L., Torralba, V., Soret, A., and Doblas-Reyes, F. J.: What global reanalysis best represents near-surface winds?, Q. J. R. Meteorol. Soc., 145, 3236–3251, https://doi.org/10.1002/qj.3616, 2019.

Randall, D., Branson, M., Wang, M., Ghan, S., Craig, C., Gettelman, A., and Edwards, J.: A Community Atmosphere Model With Superparameterized Clouds, Eos Trans. Am. Geophys. Union, 94, 221–222, https://doi.org/10.1002/2013EO250001, 2013.

Randall, D. A., Wood, R. A., Bony, S., Colman, R., Fichefet, T., Fyfe, J., Kattsov, V., Pitman, A., Shukla, J., Srinivasan, J., Stouffer, R. J., Sumi, A., and Taylor, K. E.: Climate Models and Their Evaluation, in: Climate Change 2007: The Physical Science Basis. Contribution of Working Group I to the Fourth Assessment Report of the Intergovernmental Panel on Climate Change, Cambridge University Press, Cambridge, United Kingdom and New York, NY, USA, 2007.

Reder, A., Raffa, M., Padulano, R., Rianna, G., and Mercogliano, P.: Characterizing extreme values of precipitation at very high resolution: An experiment over twenty European cities, Weather Clim. Extrem., 35, 100407, https://doi.org/10.1016/j.wace.2022.100407, 2022.

Requena, A. I., Jiménez-Álvarez, A., and García, C.: Assessment of climate change impact on maximum precipitation in Spain, Hydrol. Process., 37, e14803, https://doi.org/10.1002/hyp.14803, 2023.

Riahi, K., Van Vuuren, D. P., Kriegler, E., Edmonds, J., O'Neill, B. C., Fujimori, S., Bauer, N., Calvin, K., Dellink, R., Fricko, O., Lutz, W., Popp, A., Cuaresma, J. C., Kc, S., Leimbach, M., Jiang, L., Kram, T., Rao, S., Emmerling, J., Ebi, K., Hasegawa, T., Havlik, P., Humpenöder, F., Da Silva, L. A., Smith, S., Stehfest, E., Bosetti, V., Eom, J., Gernaat, D., Masui, T., Rogelj, J., Strefler, J., Drouet, L., Krey, V., Luderer, G., Harmsen, M., Takahashi, K., Baumstark, L., Doelman, J. C., Kainuma, M., Klimont, Z., Marangoni, G., Lotze-Campen, H., Obersteiner, M., Tabeau, A., and Tavoni, M.: The Shared Socioeconomic Pathways and their energy, land use, and greenhouse gas emissions implications: An overview, Glob. Environ. Change, 42, 153–168, https://doi.org/10.1016/j.gloenvcha.2016.05.009, 2017.

Roderick, M. L., Rotstayn, L. D., Farquhar, G. D., and Hobbins, M. T.: On the attribution of changing pan evaporation, Geophys. Res. Lett., 34, 2007GL031166, https://doi.org/10.1029/2007GL031166, 2007.

Rössler, O., Fischer, A. M., Huebener, H., Maraun, D., Benestad, R. E., Christodoulides, P., Soares, P. M. M., Cardoso, R. M., Pagé, C., Kanamaru, H., Kreienkamp, F., and Vlachogiannis, D.: Challenges to link climate change data provision and user needs: Perspective from the COST-action VALUE, Int. J. Climatol., 39, 3704–3716, https://doi.org/10.1002/joc.5060, 2019.

Ruffault, J., Curt, T., Moron, V., Trigo, R. M., Mouillot, F., Koutsias, N., Pimont, F., Martin-StPaul, N., Barbero, R., Dupuy, J.-L., Russo, A., and Belhadj-Khedher, C.: Increased likelihood of heat-induced large wildfires in the Mediterranean Basin, Sci. Rep., 10, 13790, https://doi.org/10.1038/s41598-020-70069-z, 2020.

Ruosteenoja, K. and Räisänen, P.: Seasonal Changes in Solar Radiation and Relative Humidity in Europe in Response to Global Warming*, J. Clim., 26, 2467–2481, https://doi.org/10.1175/JCLI-D-12-00007.1, 2013.

Sánchez, E., Rodríguez-Fonseca, B., Bladé, I., Brunet, M., Aznar, R., Cacho, I., Casado, M. J., Gimeno, L., Gutiérrez, J. M., Jordá, G., Lavín, A., López, J. A., Salat, J., and Valero-Garcés, B. L.: Progress in detection and projection of climate change in Spain since the 2010 CLIVAR-Spain regional climate change assessment report, 2017.

Sánchez-Lorenzo, A., Enríquez-Alonso, A., Calbó, J., González, J.-A., Wild, M., Folini, D., Norris, J. R., and Vicente-Serrano, S. M.: Fewer clouds in the Mediterranean: consistency of observations and climate simulations, Sci. Rep., 7, 41475, https://doi.org/10.1038/srep41475, 2017.

San-Miguel-Ayanz, J., Schulte, E., Schmuck, G., Camia, A., Strobl, P., Liberta, G., Giovando, C., Boca, R., Sedano, F., Kempeneers, P., McInerney, D., Withmore, C., Oliveira, S. S. de, Rodrigues, M., Durrant, T., Corti, P., Oehler, F., Vilar, L., and Amatulli, G.: Comprehensive Monitoring of Wildfires in Europe: The European Forest Fire Information System (EFFIS), in: Approaches to Managing Disaster - Assessing Hazards, Emergencies and Disaster Impacts, IntechOpen, https://doi.org/10.5772/28441, 2012.

Santos, F., Gómez-Gesteira, M., de Castro, M., Añel, J. A., Carvalho, D., Costoya, X., and Días, J. M.: On the accuracy of CORDEX RCMs to project future winds over the Iberian Peninsula and surrounding ocean, Appl. Energy, 228, 289–300, https://doi.org/10.1016/j.apenergy.2018.06.086, 2018.

Schmith, T., Thejll, P., Berg, P., Boberg, F., Christensen, O. B., Christiansen, B., Christensen, J. H., Madsen, M. S., and Steger, C.: Identifying robust bias adjustment methods for European extreme precipitation in a multi-model pseudo-reality setting, Hydrol. Earth Syst. Sci., 25, 273–290, https://doi.org/10.5194/hess-25-273-2021, 2021.

Schulte, L. A. and Mladenoff, D. J.: SEVERE WIND AND FIRE REGIMES IN NORTHERN FORESTS: HISTORICAL VARIABILITY AT THE REGIONAL SCALE, Ecology, 86, 431–445, https://doi.org/10.1890/03-4065, 2005.

Schwingshackl, C., Sillmann, J., Vicedo-Cabrera, A. M., Sandstad, M., and Aunan, K.: Heat Stress Indicators in CMIP6: Estimating Future Trends and Exceedances of Impact-Relevant Thresholds, Earths Future, 9, e2020EF001885, https://doi.org/10.1029/2020EF001885, 2021.

Scoccimarro, E., Fogli, P. G., and Gualdi, S.: The role of humidity in determining scenarios of perceived temperature extremes in Europe, Environ. Res. Lett., 12, 114029, https://doi.org/10.1088/1748-9326/aa8cdd, 2017.

Sein, D. V., Mikolajewicz, U., Gröger, M., Fast, I., Cabos, W., Pinto, J. G., Hagemann, S., Semmler, T., Izquierdo, A., and Jacob, D.: Regionally coupled atmosphere-ocean-sea ice-marine biogeochemistry model ROM: 1. Description and validation, J. Adv. Model. Earth Syst., 7, 268–304, https://doi.org/10.1002/2014MS000357, 2015.

Seneviratne, S. I. and Hauser, M.: Regional Climate Sensitivity of Climate Extremes in CMIP6 Versus CMIP5 Multimodel Ensembles, Earths Future, 8, e2019EF001474, https://doi.org/10.1029/2019EF001474, 2020.

Serrano-Notivoli, R. and Beguería, S.: Distribución espacial y tendencias de indicadores agroclimáticos en la España peninsular, Geographicalia, 35–54, https://doi.org/10.26754/ojs_geoph/geoph.2021735204, 2021.

Shahi, N. K., Polcher, J., Bastin, S., Pennel, R., and Fita, L.: Assessment of the spatio-temporal variability of the added value on precipitation of convection-permitting simulation over the Iberian Peninsula using the RegIPSL regional earth system model, Clim. Dyn., 59, 471–498, https://doi.org/10.1007/s00382-022-06138-y, 2022.

Shen, C., Zha, J., Li, Z., Azorin-Molina, C., Deng, K., Minola, L., and Chen, D.: Evaluation of global terrestrial near-surface wind speed simulated by CMIP6 models and their future projections, Ann. N. Y. Acad. Sci., 1518, 249–263, https://doi.org/10.1111/nyas.14910, 2022.

Shepherd, T. G., Boyd, E., Calel, R. A., Chapman, S. C., Dessai, S., Dima-West, I. M., Fowler, H. J., James, R., Maraun, D., Martius, O., Senior, C. A., Sobel, A. H., Stainforth, D. A., Tett, S. F. B., Trenberth, K. E., Van Den Hurk, B. J. J. M., Watkins, N. W., Wilby, R. L., and Zenghelis, D. A.: Storylines: an alternative approach to representing uncertainty in physical aspects of climate change, Clim. Change, 151, 555–571, https://doi.org/10.1007/s10584-018-2317-9, 2018.

Sherman, P., Song, S., Chen, X., and McElroy, M.: Projected changes in wind power potential over China and India in high resolution climate models, Environ. Res. Lett., 16, 034057, https://doi.org/10.1088/1748-9326/abe57c, 2021.

Sherwood, S. and Fu, Q.: A Drier Future?, Science, 343, 737–739, https://doi.org/10.1126/science.1247620, 2014.

Shields, C. A., Rosenbloom, N., Bates, S., Hannay, C., Hu, A., Payne, A. E., Rutz, J. J., and Truesdale, J.: Meridional Heat Transport During Atmospheric Rivers in High-Resolution CESM Climate Projections, Geophys. Res. Lett., 46, 14702–14712, https://doi.org/10.1029/2019GL085565, 2019.

Soares, P. M. M., Lima, D. C. A., Cardoso, R. M., and Semedo, A.: High resolution projections for the western Iberian coastal low level jet in a changing climate, Clim. Dyn., 49, 1547–1566, https://doi.org/10.1007/s00382-016-3397-8, 2017a.

Soares, P. M. M., Lima, D. C. A., Cardoso, R. M., Nascimento, M. L., and Semedo, A.: Western Iberian offshore wind resources: More or less in a global warming climate?, Appl. Energy, 203, 72–90, https://doi.org/10.1016/j.apenergy.2017.06.004, 2017b.

Soares, P. M. M., Lima, D. C. A., Semedo, A., Cardoso, R. M., Cabos, W., and Sein, D. V.: Assessing the climate change impact on the North African offshore surface wind and coastal low-level jet using coupled and uncoupled regional climate simulations, Clim. Dyn., 52, 7111–7132, https://doi.org/10.1007/s00382-018-4565-9, 2019a.

Soares, P. M. M., Lima, D. C. A., Semedo, A., Cabos, W., and Sein, D. V.: Climate change impact on Northwestern African offshore wind energy resources, Environ. Res. Lett., 14, 124065, https://doi.org/10.1088/1748-9326/ab5731, 2019b.

Soares, P. M. M., Johannsen, F., Lima, D. C. A., Lemos, G., Bento, V., and Bushenkova, A.: High resolution downscaling of CMIP6 Earth System and Global Climate Models using deep learning for Iberia, Climate and Earth system modeling, https://doi.org/10.5194/gmd-2023-136, 2023a.

Soares, P. M. M., Careto, J. A. M., Russo, A., and Lima, D. C. A.: The future of Iberian droughts: a deeper analysis based on multi-scenario and a multi-model ensemble approach, Nat. Hazards, 117, 2001–2028, https://doi.org/10.1007/s11069-023-05938-7, 2023b.

Sobolowski, S., Somot, S., Fernández, J., Evin, G., Maraun, D., Kotlarski, S., Jury, M., Benestad, R. E., Teichmann, C., Christensen, O. B., Katharina, B., Buonomo, E., Katragkou, E., Steger, C., Sørland, S., Nikulin, G., McSweeney, C., Dobler, A., Palmer, T., Wilke, R., Boé, J., Brunner, L., Ribes, A., Qasmi, S., Nabat, P., Sevault, F., Oudar, T., and Brands, S.: EURO-CORDEX CMIP6 GCM Selection & Ensemble Design: Best Practices and Recommendations, Zenodo, https://doi.org/10.5281/ZENODO.7673400, 2023.

Solano-Farias, F., García-Valdecasas Ojeda, M., Donaire-Montaño, D., Rosa-Cánovas, J. J., Castro-Díez, Y., Esteban-Parra, M. J., and Gámiz-Fortis, S. R.: Assessment of physical schemes for WRF model in convection-permitting mode over southern Iberian Peninsula, Atmospheric Res., 299, 107175, https://doi.org/10.1016/j.atmosres.2023.107175, 2024.

Somot, S., Sevault, F., Déqué, M., and Crépon, M.: 21st century climate change scenario for the Mediterranean using a coupled atmosphere–ocean regional climate model, Glob. Planet. Change, 63, 112–126, https://doi.org/10.1016/j.gloplacha.2007.10.003, 2008.

Sousa, M. C., de Castro, M., Álvarez, I., Gómez-Gesteira, M., and Días, J. M.: Why coastal upwelling is expected to increase along the western Iberian Peninsula over the next century?, Sci. Total Environ., 592, 243–251, https://doi.org/10.1016/j.scitotenv.2017.03.046, 2017.

Sousa, P. M., Barriopedro, D., García-Herrera, R., Ordóñez, C., Soares, P. M. M., and Trigo, R. M.: Distinct influences of large-scale circulation and regional feedbacks in two exceptional 2019 European heatwaves, Commun. Earth Environ., 1, 48, https://doi.org/10.1038/s43247-020-00048-9, 2020a.

Sousa, P. M., Ramos, A. M., Raible, C. C., Messmer, M., Tomé, R., Pinto, J. G., and Trigo, R. M.: North Atlantic Integrated Water Vapor Transport—From 850 to 2100 CE: Impacts on Western European Rainfall, J. Clim., 33, 263–279, https://doi.org/10.1175/JCLI-D-19-0348.1, 2020b.

Spinoni, J., Vogt, J. V., Naumann, G., Barbosa, P., and Dosio, A.: Will drought events become more frequent and severe in Europe?, Int. J. Climatol., 38, 1718–1736, https://doi.org/10.1002/joc.5291, 2018.

Spinoni, J., Barbosa, P., Bucchignani, E., Cassano, J., Cavazos, T., Christensen, J. H., Christensen, O. B., Coppola, E., Evans, J., Geyer, B., Giorgi, F., Hadjinicolaou, P., Jacob, D., Katzfey, J., Koenigk, T., Laprise, R., Lennard, C. J., Kurnaz, M. L., Li, D., Llopart, M., McCormick, N., Naumann, G., Nikulin, G., Ozturk, T., Panitz, H.-J., Porfirio Da Rocha, R., Rockel, B., Solman, S. A., Syktus, J., Tangang, F., Teichmann, C., Vautard, R., Vogt, J. V., Winger, K., Zittis, G., and Dosio, A.: Future Global Meteorological Drought Hot Spots: A Study Based on CORDEX Data, J. Clim., 33, 3635–3661, https://doi.org/10.1175/JCLI-D-19-0084.1, 2020.

Spinoni, J., Barbosa, P., Bucchignani, E., Cassano, J., Cavazos, T., Cescatti, A., Christensen, J. H., Christensen, O. B., Coppola, E., Evans, J. P., Forzieri, G., Geyer, B., Giorgi, F., Jacob, D., Katzfey, J., Koenigk, T., Laprise, R., Lennard, C. J., Kurnaz, M. L., Li, D., Llopart, M., McCormick, N., Naumann, G., Nikulin, G., Ozturk, T., Panitz, H., Da Rocha, R. P., Solman, S. A., Syktus, J., Tangang, F., Teichmann, C.,

Vautard, R., Vogt, J. V., Winger, K., Zittis, G., and Dosio, A.: Global exposure of population and land-use to meteorological droughts under different warming levels and SSPs : A CORDEX -based study, Int. J. Climatol., 41, 6825–6853, https://doi.org/10.1002/joc.7302, 2021.

Squintu, A. A., Van Der Schrier, G., Van Den Besselaar, E., Van Der Linden, E., Putrasahan, D., Roberts, C., Roberts, M., Scoccimarro, E., Senan, R., and Klein Tank, A.: Evaluation of trends in extreme temperatures simulated by HighResMIP models across Europe, Clim. Dyn., 56, 2389–2412, https://doi.org/10.1007/s00382-020-05596-6, 2021.

Stryhal, J. and Huth, R.: Classifications of winter atmospheric circulation patterns: validation of CMIP5 GCMs over Europe and the North Atlantic, Clim. Dyn., 52, 3575–3598, https://doi.org/10.1007/s00382-018-4344-7, 2019.

Sylla, A., Mignot, J., Capet, X., and Gaye, A. T.: Weakening of the Senegalo–Mauritanian upwelling system under climate change, Clim. Dyn., 53, 4447–4473, https://doi.org/10.1007/s00382-019-04797-y, 2019.

Tabari, H., Grismer, M. E., and Trajkovic, S.: Comparative analysis of 31 reference evapotranspiration methods under humid conditions, Irrig. Sci., 31, 107–117, https://doi.org/10.1007/s00271-011-0295-z, 2013.

Thomson, M. C., Muñoz, Á. G., Cousin, R., and Shumake-Guillemot, J.: Climate drivers of vector-borne diseases in Africa and their relevance to control programmes, Infect. Dis. Poverty, 7, 81, https://doi.org/10.1186/s40249-018-0460-1, 2018.

Torralba, V., Doblas-Reyes, F. J., and González-Reviriego, N.: Uncertainty in recent near-surface wind speed trends: a global reanalysis intercomparison, Environ. Res. Lett., 12, 114019, https://doi.org/10.1088/1748-9326/aa8a58, 2017.

Torres, C., Jordà, G., De Vílchez, P., Vaquer-Sunyer, R., Rita, J., Canals, V., Cladera, A., Escalona, J. M., and Miranda, M. Á.: Climate change and its impacts in the Balearic Islands: a guide for policy design in Mediterranean regions, Reg. Environ. Change, 21, 107, https://doi.org/10.1007/s10113-021-01810-1, 2021.

Trancoso, R., Syktus, J., Allan, R. P., Croke, J., Hoegh-Guldberg, O., and Chadwick, R.: Significantly wetter or drier future conditions for one to two thirds of the world's population, Nat. Commun., 15, 483, https://doi.org/10.1038/s41467-023-44513-3, 2024.

Tsakiris, G., Pangalou, D., and Vangelis, H.: Regional Drought Assessment Based on the Reconnaissance Drought Index (RDI), Water Resour. Manag., 21, 821–833, https://doi.org/10.1007/s11269-006-9105-4, 2007.

Tuel, A. and Eltahir, E. A. B.: Why Is the Mediterranean a Climate Change Hot Spot?, J. Clim., 33, 5829–5843, https://doi.org/10.1175/JCLI-D-19-0910.1, 2020.

Tuel, A., Kang, S., and Eltahir, E. A. B.: Understanding climate change over the southwestern Mediterranean using high-resolution simulations, Clim. Dyn., 56, 985–1001, https://doi.org/10.1007/s00382-020-05516-8, 2021.

Turco, M., Llasat, M. C., Von Hardenberg, J., and Provenzale, A.: Impact of climate variability on summer fires in a Mediterranean environment (northeastern Iberian Peninsula), Clim. Change, 116, 665–678, https://doi.org/10.1007/s10584-012-0505-6, 2013.

Turco, M., Rosa-Cánovas, J. J., Bedia, J., Jerez, S., Montávez, J. P., Llasat, M. C., and Provenzale, A.: Exacerbated fires in Mediterranean Europe due to anthropogenic warming projected with non-stationary climate-fire models, Nat. Commun., 9, 3821, https://doi.org/10.1038/s41467-018-06358-z, 2018.

Um, M.-J., Kim, Y., Park, D., and Kim, J.: Effects of different reference periods on drought index (SPEI) estimations from 1901 to 2014, Hydrol. Earth Syst. Sci., 21, 4989–5007, https://doi.org/10.5194/hess-21-4989-2017, 2017.

Utrabo-Carazo, E., Azorín-Molina, C., Serrano, E., Aguilar, E., Brunet, M., and Guijarro, J. A.: Wind stilling ceased in the Iberian Peninsula since the 2000s, Atmospheric Res., 272, 106153, https://doi.org/10.1016/j.atmosres.2022.106153, 2022.

van der Linden, P., Mitchell, J.F.B.: ENSEMBLES: Climate Change and its Impacts: Summary of research and results from the ENSEMBLES project — European Environment Agency (EEA), 2009.

van Wagner, C.E.: Development and structure of the Canadian Forest Fire Weather Index System, Minister of Supply and Services Canada, Ottawa, 1987.

Vautard, R., Kadygrov, N., Iles, C., Boberg, F., Buonomo, E., Bülow, K., Coppola, E., Corre, L., Van Meijgaard, E., Nogherotto, R., Sandstad, M., Schwingshackl, C., Somot, S., Aalbers, E., Christensen, O. B., Ciarlo, J. M., Demory, M., Giorgi, F., Jacob, D., Jones, R. G., Keuler, K., Kjellström, E., Lenderink, G., Levavasseur, G., Nikulin, G., Sillmann, J., Solidoro, C., Sørland, S. L., Steger, C., Teichmann, C., Warrach-Sagi, K., and Wulfmeyer, V.: Evaluation of the Large EURO-CORDEX Regional Climate Model Ensemble, J. Geophys. Res. Atmospheres, 126, e2019JD032344, https://doi.org/10.1029/2019JD032344, 2021.

Vautard, R., Cattiaux, J., Happé, T., Singh, J., Bonnet, R., Cassou, C., Coumou, D., D'Andrea, F., Faranda, D., Fischer, E., Ribes, A., Sippel, S., and Yiou, P.: Heat extremes in Western Europe increasing faster than simulated due to atmospheric circulation trends, Nat. Commun., 14, 6803, https://doi.org/10.1038/s41467-023-42143-3, 2023.

Vázquez Medina, R.: Future climate evolution in the canary current upwelling system from a regional coupled model, doctoral thesis, 2023.

Vazquez, R., Parras-Berrocal, I., Cabos, W., Sein, D. V., Mañanes, R., and Izquierdo, A.: Assessment of the Canary current upwelling system in a regionally coupled climate model, Clim. Dyn., 58, 69–85, https://doi.org/10.1007/s00382-021-05890-x, 2022.

Vázquez, R., Parras-Berrocal, I. M., Koseki, S., Cabos, W., Sein, D. V., and Izquierdo, A.: Seasonality of coastal upwelling trends in the Mauritania-Senegalese region under RCP8.5 climate change scenario, Sci. Total Environ., 898, 166391, https://doi.org/10.1016/j.scitotenv.2023.166391, 2023.

Velasco Horcajada, J. J.: Idoneidad de técnicas univariantes y multivariantes para la corrección de sesgos en modelos climáticos regionales: aplicación para el cálculo de índices agroclimáticos, Suitability of uni and multi-variate bias correction techniques in regional climate models: applicability to the computation of agroclimatic indices, 2023.

Ventura, S., Miró, J. R., Peña, J. C., and Villalba, G.: Analysis of synoptic weather patterns of heatwave events, Clim. Dyn., 61, 4679–4702, https://doi.org/10.1007/s00382-023-06828-1, 2023.

Vicente-Serrano, S. M., Beguería, S., and López-Moreno, J. I.: A Multiscalar Drought Index Sensitive to Global Warming: The Standardized Precipitation Evapotranspiration Index, J. Clim., 23, 1696–1718, https://doi.org/10.1175/2009JCLI2909.1, 2010.

Vicente-Serrano, S. M., Domínguez-Castro, F., McVicar, T. R., Tomás-Burguera, M., Peña-Gallardo, M., Noguera, I., López-Moreno, J. I., Peña, D., and El Kenawy, A.: Global characterization of hydrological and meteorological droughts under future climate change: The importance of timescales, vegetation-CO_2 feedbacks and changes to distribution functions, Int. J. Climatol., 40, 2557–2567, https://doi.org/10.1002/joc.6350, 2020.

Vicente-Serrano, S. M., Peña-Angulo, D., Beguería, S., Domínguez-Castro, F., Tomás-Burguera, M., Noguera, I., Gimeno-Sotelo, L., and El Kenawy, A.: Global drought trends and future projections, Philos. Trans. R. Soc. Math. Phys. Eng. Sci., 380, 20210285, https://doi.org/10.1098/rsta.2021.0285, 2022.

Wan, H., Wang, X. L., and Swail, V. R.: Homogenization and Trend Analysis of Canadian Near-Surface Wind Speeds, J. Clim., 23, 1209–1225, https://doi.org/10.1175/2009JCLI3200.1, 2010.

Wang, J., Guan, Y., Wu, L., Guan, X., Cai, W., Huang, J., Dong, W., and Zhang, B.: Changing Lengths of the Four Seasons by Global Warming, Geophys. Res. Lett., 48, e2020GL091753, https://doi.org/10.1029/2020GL091753, 2021.

Wild, M., Folini, D., Hakuba, M. Z., Schär, C., Seneviratne, S. I., Kato, S., Rutan, D., Ammann, C., Wood, E. F., and König-Langlo, G.: The energy balance over land and oceans: an assessment based on direct observations and CMIP5 climate models, Clim. Dyn., 44, 3393–3429, https://doi.org/10.1007/s00382-014-2430-z, 2015.

Woolway, R. I., Merchant, C. J., Van Den Hoek, J., Azorín-Molina, C., Nõges, P., Laas, A., Mackay, E. B., and Jones, I. D.: Northern Hemisphere Atmospheric Stilling Accelerates Lake Thermal Responses to a Warming World, Geophys. Res. Lett., 46, 11983–11992, https://doi.org/10.1029/2019GL082752, 2019.

Wu, J., Han, Z.-Y., Yan, Y.-P., Sun, C.-Y., Xu, Y., and Shi, Y.: Future changes in wind energy potential over China using RegCM4 under RCP emission scenarios, Adv. Clim. Change Res., 12, 596–610, https://doi.org/10.1016/j.accre.2021.06.005, 2021.

Zambakas, J.: General climatology, Dep. Geol. Natl. Kapodistr. Univ. Athens Athens Greece, 1992.

Zappa, G., Hoskins, B. J., and Shepherd, T. G.: The dependence of wintertime Mediterranean precipitation on the atmospheric circulation response to climate change, Environ. Res. Lett., 10, 104012, https://doi.org/10.1088/1748-9326/10/10/104012, 2015.

Zeng, Z., Ziegler, A. D., Searchinger, T., Yang, L., Chen, A., Ju, K., Piao, S., Li, L. Z. X., Ciais, P., Chen, D., Liu, J., Azorín-Molina, C., Chappell, A., Medvigy, D., and Wood, E. F.: A reversal in global terrestrial stilling and its implications for wind energy production, Nat. Clim. Change, 9, 979–985, https://doi.org/10.1038/s41558-019-0622-6, 2019.

Zhang, G., Azorín-Molina, C., Shi, P., Lin, D., Guijarro, J. A., Kong, F., and Chen, D.: Impact of near-surface wind speed variability on wind erosion in the eastern agro-pastoral transitional zone of Northern China, 1982–2016, Agric. For. Meteorol., 271, 102–115, https://doi.org/10.1016/j.agrformet.2019.02.039, 2019.

Zhou, S., Zhang, Y., Park Williams, A., and Gentine, P.: Projected increases in intensity, frequency, and terrestrial carbon costs of compound drought and aridity events, Sci. Adv., 5, eaau5740, https://doi.org/10.1126/sciadv.aau5740, 2019.

Zittis, G., Hadjinicolaou, P., Klangidou, M., Proestos, Y., and Lelieveld, J.: A multi-model, multi-scenario, and multi-domain analysis of regional climate projections for the Mediterranean, Reg. Environ. Change, 19, 2621–2635, https://doi.org/10.1007/s10113-019-01565-w, 2019.

Zittis, G., Bruggeman, A., and Lelieveld, J.: Revisiting future extreme precipitation trends in the Mediterranean, Weather Clim. Extrem., 34, 100380, https://doi.org/10.1016/j.wace.2021.100380, 2021.

CHAPTER 6

REGIONAL OCEANIC CLIMATE CHANGE PROJECTIONS AROUND SPAIN

Authors: Paula Camus[1], Jose C. Sánchez-Garrido[2], Gabriel Jordà[3]

[1] Dpto. Ciencias Y Técnicas Del Agua Y Del Medio Ambiente, Universidad de Cantabria, Santander, Spain

[2] Department of Applied Physics, University of Málaga, Málaga, Spain

[3] Spanish Institute of Oceanography, CSIC, Palma, Spain

1. Introduction

Approximately 40% of the world's population lives within the "near coastal zone" (closer than 100 kilometers from the coast) while in Spain the percentage rises up to 60%. Moreover, the ocean holds large biodiversity; present and future food security relies on marine resources; maritime transport is a key element of global and regional economy; and coastal activities are a major contributor to the Spanish economy. Therefore, it is important to analyze the expected evolution of ocean variables in a context of enhanced greenhouse gasses (GHG) concentrations, especially for a region as dependent on the sea as Spain.

Global warming has notorious impacts on the oceans. The heat excess is largely stored in the ocean interior, inducing a warming of the global ocean at all depths . Expected modifications in the wind patterns as well as in the spatial gradients of water density would induce changes in the ocean circulation. In turn, those changes would imply different redistributions of heat and salt, thus modifying the temperature and salinity fields both in the horizontal and the vertical. Moreover, global sea level will rise due to the thermal expansion of the water column and to the addition of mass coming from the continental ice melting and changes in the landwater storage. Spatial gradients of sea level will in turn be also modified by mass redistribution due to changes in the ocean circulation or gravitational effects. Ocean biogeochemistry is also expected to be modified in several ways. The uptake of anthropogenic carbon emission by the ocean leads to seawater acidification. Deoxygenation is exacerbated by the reduction of oxygen (O_2) solubility due to rising seawater temperatures. Enhanced near-surface stratification impedes vertical mixing and property exchanges with the deep ocean and leads to a reduced nutrient supply into the euphotic zone. As a result, net primary production (NPP) could suffer significant changes.

All those alterations projected at global scale will have a significant regional diversity. How the heat and mass excess is redistributed, and subsequently other ocean properties, depends on many factors. Therefore, large variations with respect to global averages are expected at regional scale. In this chapter, projected changes for the main physical and biogeochemical variables around the Iberian Peninsula and the Canary Islands will be analyzed based on the outputs from global and regional ocean models. The results will be presented separately for the Atlantic and the Mediterranean Sea. The reason is that the Mediterranean Sea, due to its semi-enclosed nature and complex surrounding orography, can evolve, up to certain extent, differently from the nearby Atlantic Ocean. Also, the dynamical complexity of the region requires high resolution models to be properly characterized. So, the results obtained from global models (e.g. CMIP models) with horizontal spatial resolutions of 1º-2º have to be taken with caution and it is preferred to rely on regional ocean models (e.g. MedCORDEX models, (Ruti et al., 2016)).

This chapter is organized as follows. First, the projections of ocean circulation changes will be presented, followed by projections of temperature and salinity. Sea level will be addressed afterwards and biogeochemical variables will be analyzed at last.

2. Ocean Circulation

The general circulation in the North Atlantic is characterized by a western boundary current, the Gulf Stream, that flows following the eastern coastlines of the United States, turns eastwards around 40ºN to feed the North Atlantic current (NAC) which crosses the Atlantic Ocean. At about 30°W a bifurcation of the flow occurs and, while the NAC continues its path towards the north-east, the Azores Current (AC) rises toward the south-east. These currents also determine the main circulation around the Iberian Peninsula (IP) and Canary Islands. Additionally, there is the Atlantic Meridional Overturning Circulation (AMOC), which is the name given to the circulation pattern in the North Atlantic that transports warm upper-ocean water northwards in the western part, and cold, deep water southwards in the eastern part. AMOC is part of the global ocean circulation system and changes on it influence global ocean heat content and transport as well as regional sea level. Therefore, a lot of attention has been paid to its future evolution. The IPCC AR6 (Intergovernmental Panel On Climate Change, 2023) reports that, recently, confidence in modeled and reconstructed AMOC has decreased due to new observations and model disagreements. Namely, it has been found that CMIP5 models exhibit large biases in the representation of the AMOC. These are related to biases in the representation of ocean convection, sea ice extent, overflows and freshwater forcing (Deshayes et al., 2014; Wang et al., 2015). As a result, there was a large intermodel spread in CMIP5 modeled transports, which is still present in CMIP6 simulations (10–31 Sv; Weijer et al., 2019).

Regarding future changes, in spite of the differences in overall AMOC strength and characteristics, the model projections reported in the IPCC are qualitatively similar. Results suggest that AMOC will very likely decline over the 21st century for all SSP scenarios. Another relevant aspect is the potential abrupt collapse of the AMOC, which would entail dramatic changes in the European climate (e.g. see the summary of Rahmstorf, 2024). The analysis of CMIP models lead to conclude that there is medium confidence that the decline will not involve an abrupt collapse before 2100. However, two recent studies by (Ditlevsen and Ditlevsen, 2023) and (van Westen et al., 2024) suggest that it is very likely that the collapse will occur during this century. The first one focuses on the detection of early-warning signals of AMOC collapse based on observations. In particular, they have analyzed the increase in variance (i.e. loss of resilience) and increased autocorrelation (i.e. critical slowing down), and have provided statistical significance and data-driven estimators for the time of collapse. (van Westen et al., 2024) have used a different approach. In particular, they have used a state-of-the-art climate model to analyze the processes of an AMOC collapse, and to develop a physics-based and observable early warning signal of AMOC tipping. This, in turn, has been applied to reanalysis products, concluding that that the present-day AMOC is on route to tipping. This collapse would modify many aspects of the marine conditions around the IP but there are no studies analyzing these aspects in detail as far as the AMOC collapse was not considered a short-term plausible scenario up to recently. So, in the following, we focus on the published studies but keeping in mind that they do not consider AMOC collapse.

Concerning the regional characteristics of the circulation around the IP and the Canary Islands, CMIP5 and CMIP6 models show an almost doubling of the surface circulation with a good

agreement in the sign of change in the ensemble (Intergovernmental Panel On Climate Change, 2023). This increase could be induced by the enhancement of the horizontal density gradients (see the temperature and salinity sections below). Those simulations also show significant changes in the surface winds. In particular, the southward winds blowing along the western part of the IP will increase, while the eastward winds blowing along the northern part of the IP will decrease. This will imply an increase of the Ekman Pumping and the upwelling along the western Iberian coasts and the Canary region (~10-20% under scenario SSP5-8.5 for the period 2070-2099), and a decrease of the downwelling in the northern coasts. This is in good agreement with the results of (Gomis et al., 2016) based on the outputs of a small set of regional ocean models.

It has to be noted that most of the information is provided by global models which lack in resolution to spatially resolve the narrow shelves surrounding the IP and the Canary Islands. Therefore, there is large uncertainty on how the local circulation features in these regions will evolve in time.

The circulation in the Western Mediterranean can be characterized as a quasi-permanent two layer system, which is part of the Mediterranean thermohaline circulation (Millot, 1999). At the upper layer (0-150 m, roughly), the inflow of Atlantic waters through the strait of Gibraltar flows along the African coast towards the Strait of Sicily. There, part of the flow recirculates northwards and joins the northern current which flows along the northern and the Iberian slopes in a cyclonic sense. The intermediate layer (150- 600 m, roughly) is characterized by the entrance of Levantine Intermediate waters through the Strait of Sicily which also flows northwards along the continental slopes in a cyclonic sense until it exits through the Gibraltar strait (García Lafuente et al., 2009; Sánchez-Garrido et al., 2011). On top of this circulation pattern, there is a rich field of mesoscale and submesoscale gyres (Isern-Fontanet et al., 2006). Moreover, strong convective events occur in winter in the Northwestern Mediterranean, bringing oxygenated waters towards the intermediate and deeper layers (Somot et al., 2018).

The evolution of the main circulation features under climate change has been little studied and no studies have suggested significant changes in the main features, so far. At sub-basin scale, Adloff et al., 2015, using a small ensemble of simulations based on the same model, suggested a clear change in the Balearic region with the penetration of the Atlantic surface water towards the north, along the Spanish coasts. However this projected change should be interpreted cautiously since the circulation of their historical simulation was not realistic in that small region. De La Vara et al., 2022, using a single run of a global ocean model with increased resolution in the Mediterranean, also projected some changes in the Thyrrenian sea circulation patterns and attributed them to changes in the wind field and the main circulation. Those mechanisms have not been analyzed along the Iberian Mediterranean coasts so far.

More attention has been paid to the projected evolution of the vertical convection in the Western Mediterranean. Most studies point towards a reduction of the winter convection (Adloff et al., 2015; Sannino et al., 2022; Somot et al., 2006; Soto-Navarro et al., 2020). Even if there are discrepancies among models regarding the strength of that reduction, almost all of the simulations show a clear reduction in the averaged maximum MLD, being larger under scenario RCP8.5 (Soto-Navarro et al., 2020). The reduction ranges between 20% and 90% (Adloff et al., 2015; Somot et al., 2006; Soto-Navarro et al., 2020) and some authors have even projected a collapse of the convection under scenario RCP8.5 in 2040-2050 (Parras-Berrocal et al., 2022) or 2060 (Sannino et al., 2022). This collapse would have important implications for the whole Mediterranean thermohaline circulation as it could reduce its intensity up to 40 % (Adloff et al., 2015; Somot et al., 2006), reducing in turn the ventilation of the deeper layers.

The mechanisms behind the reduction of the winter convection are mainly two. First, there is the reduction of the buoyancy loss in winter, and, second, an increase of the stratification which would make the convective events more difficult. Both mechanisms have already been reported for the present climate (Amitai et al., 2017; Josey and Schroeder, 2023; Margirier et al., 2020) and will contribute in the future. However, it seems that, in the future, the dominating mechanism would be the increase of the stratification (Sannino et al., 2022; Somot et al., 2006). Even if the number of strong buoyancy loss events will be reduced in the future, there will still be some strong events. However, the increase of the stratification due to the lightening of the upper layers (driven by the warming), and the heaving of the intermediate layers (driven by the increased salinity) would require stronger buoyancy losses to generate convection.

Another important feature induced by global warming in the Mediterranean circulation would be the change in the fluxes at the Strait of Gibraltar. First, the net water transport will increase to compensate for the projected enhancement of the water loss in the Mediterranean. The enhancement of the evaporation and the reduction of the precipitation and river inputs will make that the Mediterranean basin will increase the water loss through the surface up to 40% (see section on Mediterranean salinity below). Consequently, to compensate that increase, the net water transport will also increase up to 0.02 Sv mainly due to a reduction in the outflow and, to a less extent, an increase in the inflow (Adloff et al., 2015; Parras-Berrocal et al., 2022). The enhancement of the density differences between the inflowing Atlantic waters and the outflowing Mediterranean waters, would presumably also increase the exchange, although no studies have analyzed that extent so far.

Finally, Ser-Giacomi et al., 2020 have analyzed how the mesoscale field would evolve in the future based on a single model simulation under scenario RCP8.5. They have shown that the mean and eddy kinetic energy (MKE and EKE, respectively), would increase up to 25% at the end of the century. They suggest that the increase would be linked to an increase of the available potential energy related to the enhancement of the horizontal density gradients. Their results show that this would affect the whole Mediterranean and, specially the Balearic basin.

3. Temperature

The ensemble of global climate simulations shows an almost linear relationship between global mean temperature rate and global ocean heat content change, with high consistency between CMIP5 and CMIP6 (Jevrejeva et al., 2021). However, the patterns of heat addition and the heat redistribution mechanisms play a key role in shaping the patterns of ocean heat content change. In particular, in the North Atlantic, the pattern of added heat is quite homogeneous, but the redistribution driven by circulation induces a decrease in the heat content along the Iberian coasts and the Canary Islands (about a -25% of the added heat; Bronselaer and Zanna, 2020). As mentioned in the previous section, although most models agree in projecting a slowdown of the AMOC, the details of the projected circulation changes, in terms of strength and location, are rather uncertain. Consequently, the heat redistribution component is also more uncertain than the added heat component in the North Atlantic. In other words, there is high confidence projecting North Atlantic warming for the next decades but there is a certain degree of uncertainty in the regional details.

CMIP projections for the Northeastern Atlantic show a generalized warming which is lowered along the Iberian margin and the Canary region due to the increase of the seasonal upwelling (Figure

6.1). Under scenario SSP585, for the period (2070-2099), CMIP6 models project a sea surface temperature (SST) increase with respect to the period (1955-1984) of 3.0 $\pm$ 0.9 ^{o}C and 2.9 $\pm$ 0.8 ^{o}C in the Cantabrian sea and the Gulf of Cadiz, while they project 2.5 $\pm$ 0.9 ^{o}C and 2.6 $\pm$ 0.7 ^{o}C in the Iberian margin and the Canary area, respectively. Using a regional model, Gomis et al., 2016 showed results that are highly consistent with the general picture provided by Global Climate Models (GCMs). The higher resolution of their model has allowed them to draw a more complex picture about the processes that will determine the evolution of temperature in the region. They have found that near the continental margin, the temperature rise could be partially counteracted by an enhancement of the seasonal upwelling, which is also reproduced by the CMIP6 ensemble. However, the spatial structure of the upwelling signal in the regional model, and therefore of the area with less warming, is more complex, pointing towards a less pronounced effect in the northern part of the Iberian margin. Also, regarding the higher warming in the Gulf of Cadiz, it has to be noted that CMIP6 models typically have a spatial resolution that prevents them from properly solving the dynamical processes that take place in that area. The results of Gomis et al., 2016 suggest that warming patterns in that region are influenced by the advection of water along the continental slopes, which cannot be reproduced by CMIP6 models. Therefore, the CMIP6 results in that region must be taken with caution.

The warming is more pronounced in summer than in winter, specially in the Cantabrian sea and the Gulf of Cadiz where the future warming in summer is 1.4 ^{o}C and 0.7 ^{o}C larger than in winter. Therefore, there will be an increase in the SST seasonal amplitude. This has been attributed to a greater relative shoaling of the mixed-layer depth in summer than in winter (Alexander et al., 2018). In the Iberian margin and the Canary area the summer warming will also be larger than the winter one, but not that much (0.5 ^{o}C and 0.2 ^{o}C, respectively).

The warming pattern in summer will also affect the characteristics of marine heatwaves (MHWs). MHWs have approximately doubled in frequency and have become more intense and longer since the 1980s, mainly due to the increase of summer temperatures (Intergovernmental Panel On Climate Change, 2023) and CMIP models project that this trend will continue. In the NE Atlantic and for the period 2080-2100, the proportion by which the number of MHW days per year will increase relative to pre-industrial times in the Iberian margin and the Canary islands will be up to 10-20 under scenario SSP126 and 60-80 under scenario SSP585.

Regarding the evolution of subsurface temperatures, CMIP6 models project less warming, but the patterns of change at 100 m depth are very consistent with the surface ones (Figure 6.1). The projected warming for the period 2070-2099 with respect to 1955-1984 is 2.1 $\pm$ 0.8 ^{o}C, 2.0 $\pm$ 0.8 ^{o}C, 1.6 $\pm$ 0.9 ^{o}C and 1.8 $\pm$ 0.9 ^{o}C for the Cantabrian sea, the Iberian margin, the Gulf of Cadiz and the Canary area, respectively. At 500 m, the pattern of change in the Northeast Atlantic is more homogeneous, with a SE to NW gradient (Figure 6.1). For the same period and scenario, the projected warming is 2.2 $\pm$ 0.6 ^{o}C, 2.0 $\pm$ 0.5 ^{o}C, 1.7 $\pm$ 0.5 ^{o}C and 1.2 $\pm$ 0.5 ^{o}C.

The future evolution of the temperature in the Mediterranean is determined by the changes in the surface heat fluxes, the heat exchange at the Gibraltar Strait and, to a lesser extent, to changes in the Dardanelles and rivers contribution (Jordà et al., 2017). For the surface heat fluxes, at present estimated as approximately -5 W/m^2 , all projections by global and regional models suggest a change ranging from +25 % to +118 %. This means that some models predict that the Mediterranean Sea could even gain heat through the surface in the future. The magnitude of the changes in surface heat fluxes is tightly correlated with the GHG concentrations of the different

considered scenarios (Adloff et al., 2015; Dubois et al., 2012; Gualdi et al., 2013; Somot et al., 2008, 2006).

Soto-Navarro et al., 2020, using an ensemble of simulations performed by the MedCORDEX ensemble of regional atmosphere-ocean coupled models, have analyzed the contribution of the fluxes through the Strait of Gibraltar. They have shown that all simulations project a warmer inflow of Atlantic water, in good agreement with the projected warming of NE Atlantic, but also a warming of the outflowing waters. Therefore, the net balance can be puzzling. Overall, in the MedCORDEX ensemble most simulations show a net increase in the net heat flux through Gibraltar, although one of the simulations shows a decrease in the net heat flux (i.e. outflowing heat flux larger than inflowing heat flux). Comparing the contribution of the Gibraltar fluxes with the surface fluxes, the results suggest that heat content change in the Mediterranean will be dominated by the decrease in the surface heat loss. Regarding the rivers and the Dardanelles contribution, there are no estimates of their future contribution but it is likely that it will be minor.

As a result, all global and regional simulations project a warmer Mediterranean. The warming rate depends at the first order on both the time horizon and the greenhouse gas emission scenario (Adloff et al., 2015; Mariotti et al., 2015; Shaltout and Omstedt, 2014). Darmaraki et al., 2019 showed that the MedCORDEX ensemble projected a basin average SST increase of 3.1 $\pm$ 0.5 ^{o}C and 1.6 $\pm$ 0.8 ^{o}C under scenario RCP8.5 and RCP4.5 for the period 2070-2100 with respect to the period 1976-2005. This is in good agreement with previous results. Adloff et al., 2015 projected, for the same period, a SST increase of 3.1 ^{o}C, 2.5 ^{o}C and 1.7 ^{o}C under SRES scenarios A2, A1B and B1, respectively. In order to put in context these results, it is interesting to analyze what CMIP6 models project for this region and for the global ocean. SST projections for the western and eastern Mediterranean basins are very close, reaching a 4.0 $\pm$ 0.8 ^{o}C, while the global SST reaches 2.9 $\pm$ 0.8 ^{o}C under scenario SSP585. Therefore, the Mediterranean is expected to be significantly warmer than the global ocean and NE Atlantic. It is worth noting that Kwiatkowski et al., 2020 have shown that, under scenario RCP8.5 and for the same time period, CMIP5 models project a global SST warming of 3.5 $\pm$ 0.8 ^{o}C. This lower projected ocean warming results from a general increase in the climate sensitivity of CMIP6 models relative to those of CMIP5. Therefore, as the most recent MedCORDEX regional ensemble has been forced by CMIP5 simulations, it could be expected that Mediterranean regional projections will produce higher warming rates when forced by CMIP6 simulations.

In spite of not having a total consensus on patterns of the increase in SST, most models show some common features in the Western Mediterranean (e.g. Adloff et al., 2015; Soto-Navarro et al., 2020). Namely, they show less warming close to the Gibraltar Strait which is enhanced northwards along the Iberian eastern margin and reaches maximum values in the Balearic sea, north of the Balearic Islands. This pattern can be found in most simulations and across scenarios. The relatively low warming in the southern part has been attributed to the inflow of Atlantic waters that are less warm than those inside the Mediterranean. The higher values in the Balearic sea, one of the regions showing the highest warming in the Mediterranean, can be attributed to the low renewal time and mixing of the waters in that region (Adloff et al., 2015; Parras-Berrocal et al., 2022). The most recent projections reported by Soto-Navarro et al., 2020 based on the MedCORDEX ensemble, show, for the period 2075-2100 with respect to 1980-2005 under scenario RCP8.5, a SST warming of 3.1 $\pm$ 0.4 ^{o}C, 2.7 $\pm$ 0.4 ^{o}C and 2.3 $\pm$ 0.6 ^{o}C for the Balearic basin, around the Palos cape region and the Alboran sea, respectively.

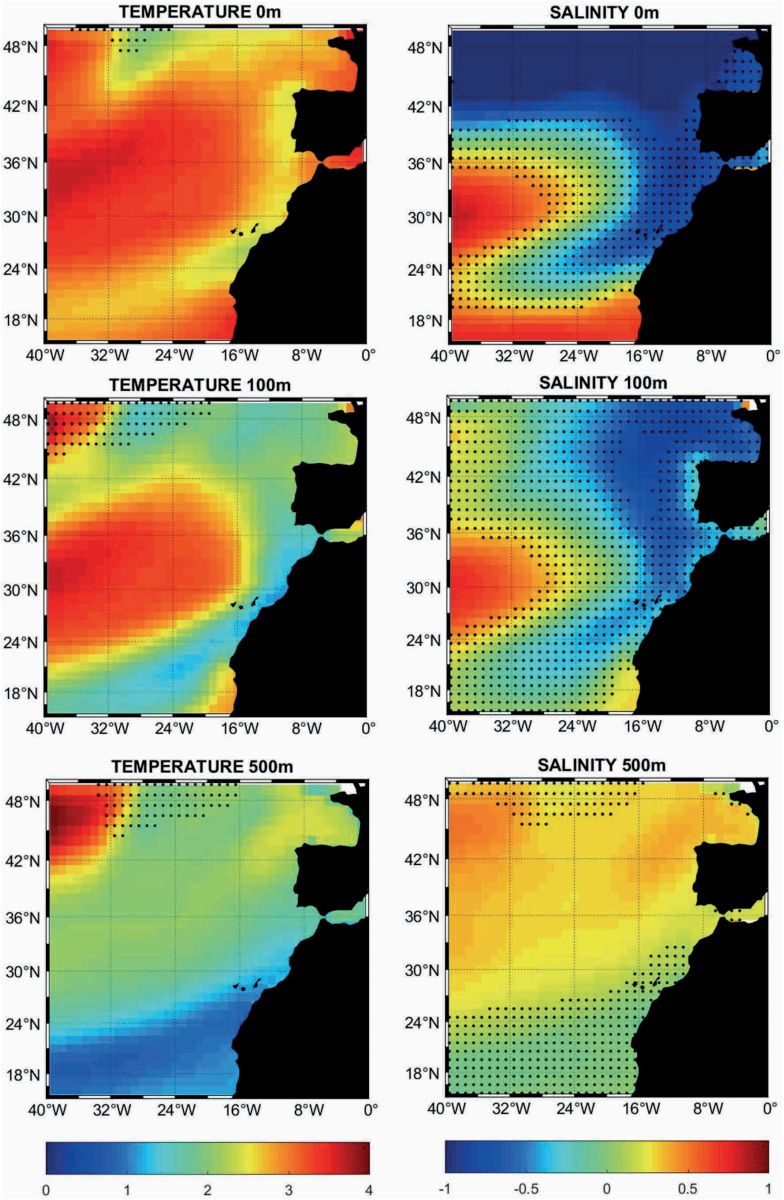

Figure 6.1. CMIP6 ensemble mean projected change (2070-2099 relative to 1985-2014) under SSP5–8.5 scenario temperature (left) and salinity (right) for different layers: surface (top), 100 m (middle) and 500 m (bottom). Dotted areas indicate areas where the ensemble spread is larger than the projected change. Data obtained from the NOAA Climate Change Web Portal (https://psl.noaa.gov/ipcc/cmip6).

Regarding MHWs, Darmaraki et al., 2019 have analyzed the outputs of the MedCORDEX ensemble and found that the models seem to properly simulate MHW properties during the historical period, despite biases in mean and extreme SST. As expected, the increase in the mean SST entails an intensification and more frequency of the events. However, the increase in the seasonal cycle (i.e. more warming in summer than in winter), as well as the increased daily temperature variability, also contributes in about 10-20% to the intensification of MHWs. By 2100 and under RCP8.5, simulations project at least one long-lasting MHW every year, up to three months longer, about 4 times more intense and 42 times more severe than present-day events.

The surface climate change signal is propagated efficiently towards the deeper layers through the Mediterranean thermohaline circulation and more particularly through intermediate and deep water formation processes. There are no studies focusing specifically in the Spanish area, but in the Western Mediterranean, the projections show a strong warming up to 500-600 m. For the period 2075-2100 with respect to 1980-2005 under scenario RCP8.5, Soto-Navarro et al., 2020 have shown a warming of 2.4 $\pm$ 0.4 ºC, 2.2 $\pm$ 0.4 ºC and 0.2 $\pm$ 0.1 ºC in the upper (0-150 m), intermediate (150-600 m) and deep (600 m – bottom) layers, respectively. In the upper layer, the warming is mainly induced by the surface warming and the Atlantic inflow. In the intermediate layer, the dominant factor is the arrival of Levantine intermediate waters, formed in the eastern Mediterranean, through the Sicily Strait. These waters are very warm and salty, and in some models, they can even induce a subsurface maximum warming in the western Mediterranean.

4. Salinity

Global salinity will roughly maintain constant values in the future (i.e. there is no significant input of salt into the global ocean), but regional changes can be expected. Since the 1950s, observed near-surface and subsurface salinity pattern changes have been linked to changing surface freshwater fluxes (Cheng et al., 2020; Zika et al., 2018). However, changes in the ocean circulation also affect salinity, largely on annual to decadal time scales due to the water mass redistribution (Du et al., 2019; Holliday et al., 2020; Liu et al., 2019). In the subpolar North Atlantic, since the early 1990s, the salinity decrease expected from increased Greenland meltwater flux have been compensated by the increase of a northward transport of Atlantic waters entering the subpolar gyre from the South (Dukhovskoy et al., 2019, 2016; Stendardo et al., 2020). Later, after the mid-2010s that trend reversed and the largest freshening recorded in 120 years occurred in the North Atlantic (Holliday et al., 2020).

Regarding future evolution of salinity, CMIP6 projections confirm the SROCC assessment that fresh ocean regions will continue to get fresher and salty ocean regions will continue to get saltier in the 21st century. In particular, the increased influx of fresh water from ice melting will decrease the surface salinity in the subpolar North Atlantic and in the eastern part of the North Atlantic subtropical gyre as projected by CMIP ensembles (Levang and Schmitt, 2020). Also, Sathyanarayanan et al., 2021 point out that besides changes in surface freshwater fluxes, subsurface salinity changes over the upper 1000 m in the Atlantic may be also related to changes in wind stress and circulation, which in turn are related to changes in surface warming. On the other hand, most models project that tropical Atlantic waters will become saltier up to approximately 40ºN. This contrasting evolution between the freshening at high latitudes and the salinity increase in the tropical Atlantic is robust among models. However, the details are model dependent as they depend on the circulation

characteristics (i.e. strength and width of the eastern branch of the subpolar gyre). This increases the uncertainty of salinity evolution around the IP.

For the sea surface salinity (SSS), the CMIP6 projections under SSP5-8.5 scenario show a freshening of the Iberian margin and the Canary region (averaged projected changes between -0.8 and -0.6 psu respectively for the period 2070-2100, see Figure 6.1) with an intermodel spread of 0.8 psu. Seasonal differences in the projected changes are small. At 100 m the projected salinity change has a similar pattern but the freshening is lower, being around -0.5 psu. Close to the western Iberian coasts, some models project an even lower freshening, of -0.2 psu, related to the countereffect of the increased coastal upwelling. I.e. increased upwelling of deep salty waters would reduce the large-scale freshening. At this depth the intermodel spread is about 0.7 psu. At 500 m, there is good agreement among models and most of them project a salinity increase of 0.2-0.3 psu with an intermodel spread lower than 0.15 psu.

Using a regional ocean model forced by three GCMs, Gomis et al., 2016 have shown similar results. Also, thanks to the higher resolution of their model, they have confirmed that, along the Iberian coasts, the eventual salinity increase derived from a more intense upwelling would not be enough to counteract the large-scale freshening.

These results, combined with the projected warming of the upper layers, suggest that in the future the water column will be more stratified, specially around the IP, and a little less around the Canary islands (Kwiatkowski et al., 2020).

Mediterranean basin salinity is determined by the balance between the surface freshwater budget (evaporation, precipitation and river runoff) and the contribution of the exchanges through the Gibraltar Strait and, to a lesser extent, the Black Sea (Jordà et al., 2017). For the first term, the general consensus in all model projections is that the water deficit will increase. Sánchez-Gómez et al., 2009 analyzed the outputs from 12 Regional Climate Models (RCMs) forced by 6 different GCMs under the A1b scenario. Their results showed that the Mediterranean water budget is likely to be significantly altered at the end of this century. Specifically, the regional projections show a 12% increase in the evaporation, a 16% reduction in precipitation, a 24% reduction in the river's runoff, and a 40% reduction in the contribution from the Black Sea. All these changes result in an increase of 40% of water losses. Dubois et al., 2012, using a small ensemble of atmosphere-ocean coupled regional climate models (AORCMs), and Adloff et al., 2015 using a single model, showed similar results. More recently, Soto-Navarro et al., 2020 showed that the MedCORDEX RCM ensemble project an increase in the water deficit of 0.35 ± 0.48 mm/d (0.25 ± 0.17 mm/d) for the period 2075-2100 with respect to 1980-2005 under scenario RCP8.5 (RCP4.5). That would imply an increase of 20% (15%) in the water losses through the surface, although the ensemble spread is large.

Regarding the projections of salt transport through the Gibraltar Strait, they are very uncertain. That transport depends on the magnitude of the water exchange (inflow and outflow) and the salinity of the exchanged waters. There is a large disagreement among models in the magnitude of projected changes in the water exchange. Also, it is not totally clear if the inflowing waters will be saltier or fresher, as it depends on how the GCMs represent the redistribution of melted water in the North Atlantic. In spite of that, Soto-Navarro et al. (2020) made a first attempt to disentangle those components in the MedCORDEX ensemble. They found that the most important terms had opposite effects: the freshening of the inflowing Atlantic would contribute to the reduction of the

basin salinity, while the reduction of the outflow volume transport would increase the salinity of the basin. The salting of the Mediterranean outflow and the reduction of the inflow transport would play a secondary role, although not negligible. Nevertheless, these results must be taken with caution due to the potential inaccuracies in the computations.

Concerning SSS evolution, Adloff et al., 2015 showed that the choice of the GCM used to provide the lateral boundary conditions in the near-Atlantic is a key factor. In their case, the GCM they used provided projections of Atlantic SSS increase of 0.2-0.6 psu, resulting in an increase of Mediterranean SSS of 0.5-0.7 psu. Soto-Navarro et al., 2020 confirmed the sensitivity of Mediterranean SSS to the lateral conditions, especially around the Iberian Peninsula. Most GCMs used to force their RCM ensemble project a freshening of the Atlantic inflow, which, in turn, induced a decrease of 1 psu in the RCMs along the southern coasts under scenario RCP8.5 at the end of the century. In the northeastern part of the Peninsula and the Balearic Islands they project almost no change in SSS. It is worth noting that few GCMs do not project the entrance of fresher waters through the Gibraltar Strait. The RCMs that use those GCMs as boundary conditions project a saltening of western Mediterranean SSS.

For the evolution of intermediate and deep waters, there is much more agreement among models as all project a salinization of those layers. The increase in the water deficit in the eastern Mediterranean leads to an increase of the salinity of the Levantine Intermediate water mass formed in that region. Afterwards, this water mass is advected towards the western basin occupying the intermediate layer. The decrease in the dense water formation rates (see the Temperature section above), also implies a decrease in the advection of relatively fresh water from the surface to the deeper layers, which, in turn, leads to a salinity increase in those layers. As a result, Soto-Navarro et al., 2020 project an increase of 0.25 $\pm$ 0.18 psu (0.21 $\pm$ 0.09 psu) in the 150-600 m layer in the western Mediterranean at the end of the century under scenario RCP8.5 (RCP4.5). For the layer below 600 m they project an increase of 0.10 $\pm$ 0.05 psu (0.10 $\pm$ 0.14 psu).

In summary, the projected increased deficit of surface freshwater implies an increase in the basin salinity, that is not restricted to the upper layer but is also transferred to the intermediate and deeper layers. The Atlantic waters entering in the Mediterranean through Strait of Gibraltar will be fresher although there are large uncertainties about the magnitude of that freshening. These fresher waters would reduce the salinity of the upper layers in the western Mediterranean, especially around the IP. Therefore, the stratification around the Spanish coasts is expected to increase in the upper layers, due to the reduction in salinity and specially due to the projected warming. In the intermediate layers the results are not that robust as projected salting would partially counteract the warming.

5. Sea Level

5.1 Mean Sea Level

Regional projections show that the change in mean sea level exhibits high spatial variability, stemming from the combination of dynamic changes in the ocean, gravitational, rotational, and deformation effects in response to current mass changes, and long-term glacial isostatic adjustment (Slangen et al., 2023). Changes in gravitational and mass components are large-scale, and therefore, their simulation does not require high spatial resolution. The

same does not apply to the dynamic component of sea level, influenced by circulation and mass displacements due to mechanical effects of wind and atmospheric pressure. Although the dynamic component of sea level is a major driver of spatial variability, it is often derived from simulations of GCMs. However, the quality of local-scale information they provide is limited due to their spatial resolution, approximately 1° in CMIP5 models and up to 0.25° in few CMIP6 models. Generally, the resolution of global models has not increased significantly from CMIP5 to CMIP6, with the dynamic ocean component exhibiting similar behavior (Liu et al., 2020). Therefore, to account for small-scale processes, tides, and bathymetric features in coastal areas, high-resolution modeling is necessary, which may also involve a more explicit modeling of processes parameterized in global models.

Dynamic downscaling of GCMs has been applied in the northwest European continental shelf (Chaigneau et al., 2022; Hermans et al., 2020) and the Mediterranean (Sannino et al., 2022). In the study by Hermans et al., 2020, the AMM7 regional model (O'Dea et al., 2017) was used for dynamic downscaling of two CMIP5 global models (MPI-ESM-LR and HadGEM2-ES). The horizontal resolution of AMM7 is 1/15° latitude by 1/9° longitude (nominally 7 by 7 km) and AMM7 has 50 vertical levels with hybrid z-coordinates. Atmospheric surface forcing is obtained from simulations of the Rossby Centre regional atmospheric model RCA4 (Strandberg et al., 2014) at 50 km horizontal resolution within the Euro-CORDEX initiative. Dynamic downscaling was found to provide a better simulation of mean sea level variability on seasonal and interannual scales. Regarding climate change projections, downscaled HadGEM2-ES model provides lower dynamic sea level variations by the end of the century (2074-2099), compared to the historical period (1980–2005), being 15 cm lower in the North Sea and between 3-4 cm along the northern coast of Spain. In the case of GCM MPI-ESM-LR, maximum differences were limited to 2.5 cm in the North Sea, while along the Spanish coast, downscaled projections provided decreases of 3.5 cm, similar between both GCMs. However, these differences between sea level variations in northwest Europe obtained from CMIP5 global models and through dynamic downscaling were within the uncertainty range of the CMIP5 GCM ensemble (Hermans et al., 2020). Bathymetry and land mask differences between global and regional models were the main contributors to these differences.

Chaigneau et al., 2022 performed a dynamic downscaling in the northwest Atlantic at a 1/12 resolution using the NEMO model forced with a 1/4 resolution CMIP6 global model (CNRM-CM6-1-HR), resolving tides, surface atmospheric pressure, and general ocean circulation. A bias correction of the GCM was also conducted to force the regional model during the period from 1950 to 2100 for the SSP1-2.6 and SSP5-8.5 scenarios. Comparisons of sea level projections along the coast showed a limited impact of the increased resolution, thanks to the relatively high resolution of the parent GCM. Regarding bias correction, the effect on projections is small along the coast, except in the Mediterranean Sea, where bias corrections are substantial. Differences in dynamic sea level changes are up to 15 cm larger in bias-corrected projections compared to raw projections in the Alboran Sea, associated with a greater increase in net transport through the Strait of Gibraltar. These differences in dynamic sea level are limited to 3 cm along the southern Spanish Atlantic coasts.

On the other hand, the Mediterranean Sea has the particularity of being a semi-closed sea connected to the Atlantic through the Strait of Gibraltar. Therefore, it is crucial for

ocean models to have high resolution and the capability to resolve water exchanges through the Strait of Gibraltar. Additionally, due to the dynamic complexity within the basin, high-resolution models are required to adequately simulate key processes (Calafat et al., 2012). Conversely, RCMs can capture part of the regional variability but are usually not designed to reproduce the connection with the global ocean, and thus missing a key part of the variability, being local deviations up to 10 cm (Adloff et al., 2018). Projections of the mean sea level in the Mediterranean Sea were generated by Sannino et al., 2022 for the RCP8.5 climate scenario, using an ocean model (MED16, Sannino et al., 2015) with a resolution of 1/16°, further increased at the Gibraltar and Turkish Straits to represent inter-basin water exchanges at the boundaries. The MED16 model was forced using the correspondent regional downscaling experiments performed with the SMHI-RCA4 atmospheric model (Strandberg et al., 2014), constrained by the HadGEM2-ES RCP8.5 for the future scenario at 0.11° resolution (i.e. approx. 12.5 km grid spacing). The study concluded that the mean sea level change across the entire basin fell within the uncertainties obtained from the selected CMIP5 GCM ensemble in Slangen et al., 2014, which excluded models without an open connection between the basin and the Atlantic Ocean. In conclusion, accounting for all components shows that the Mediterranean sea level rise (SLR) will be close to the northeastern Atlantic, where future sea level will be similar (difference lower than 5%) to the global mean sea level. The reason is that regional differences produced by changes in the circulation and mass redistribution almost compensate each other (Slangen et al., 2014). These results are in line with those obtained by Cherif et al., 2020, who concluded that the main contributions to Mediterranean basin-average sea level changes are coming from terrestrial ice melting and the northeastern Atlantic dynamics .

Based on the results of these regional studies, it can therefore be considered that the regional sea level projections from the set of global CMIP6 models considered in the latest IPCC AR6 report may be representative for the Spanish coasts. The latest IPCC AR6 report provided 21st century sea-level projections for five different emission scenarios (Intergovernmental Panel On Climate Change (Ipcc), 2023): SSP1-1.9 ('very low'), SSP1-2.6 ('low'), SSP2-4.5 ('intermediate'), SSP3-7.0 ('high') and SSP5-8.5 ('very high'). Median projected regional sea level changes around Spain are shown in Figure 6.2, with driving factors: global mean thermosteric sea level rise, Greenland Ice Sheet, Antarctic Ice Sheet, low confidence ice-sheet projections, glaciers, land-water storage, ocean dynamic sea level, gravitational, rotational and deformational effects, glacial isostatic adjustment and other drivers of vertical land motion. Since there is no single model that can directly compute all of the contributions to sea level change, the contributions to sea level changes are computed separately and then combined. These projections include all processes that could be assessed with at least medium confidence, thereby excluding ice sheet processes associated with deep uncertainty. For instance, processes related to ice flow are highly uncertain, especially concerning contributions from Antarctica and Greenland. According to the IPCC AR6, high-end projections that consider those sources could increase global mean sea level (GMSL) rise up to over 3 m by 2300 under the very high-emission scenario SSP5-8.5 (Intergovernmental Panel On Climate Change (Ipcc), 2023). Also, a weakening or even a collapse of the AMOC (University of Potsdam and Rahmstorf, 2024), would result, via geostrophic balance, in a dynamic sea-level rise in the Atlantic Ocean with up to 40-50 cm rise around the Iberian and Mediterranean (van Westen et al., 2024).

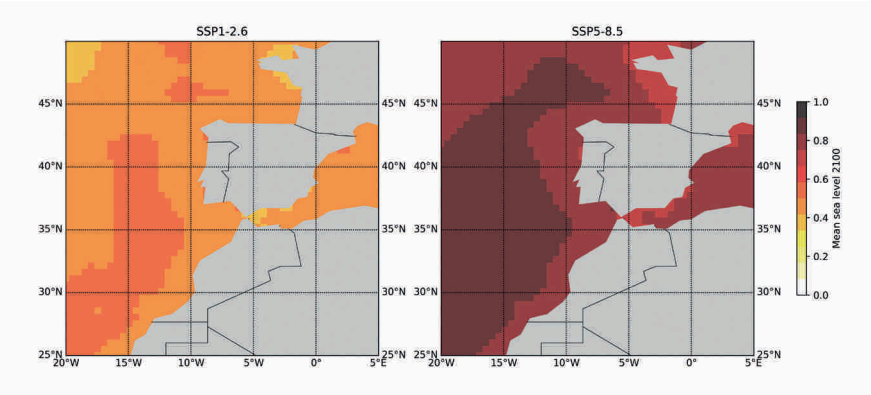

Figure 6.2. Median regional sea level change at 2100 for different scenarios (with respect to 1995–2014) for: (Left) SSP1-2.6; (Right) SSP5-8.5. These changes include all mechanisms that could be assessed with, at least, medium confidence (Intergovernmental Panel On Climate Change (Ipcc), 2023) thereby excluding ice sheet processes associated with deep uncertainty.

A novelty in the AR6 report, compared to previous IPCC reports, is the inclusion of sea level projections stratified by warming levels. Most of the contributors to GMSL are more closely tied to time integrated global surface atmosphere temperature (GSAT) than instantaneous GSAT (Hermans et al., 2020), which means that sea level projections by warming level can only be interpreted if the warming levels are linked to a specific time frame. The warming level projections are defined based on the 2081–2100 GSAT anomaly. Different pathways in GSAT can be followed to reach a certain temperature level, which affects the temporal evolution of the different contributors to sea level change. The sea level projections presented here might include different pathways to the same warming level in 2100, which is reflected in the uncertainty ranges, and should therefore be interpreted as illustrative of sea level scenarios under a certain warming level. Provided that sea level rise around Spain will roughly follow the GMSL rise, it is useful to include here GMSL rise as a function of warming levels (see Table 1).

5.2 Extreme sea levels

The extreme sea levels (ESL) on the coast result from the combined action of changes in mean sea level, astronomical tides, and meteorological tide and waves generated by atmospheric pressure and surface winds. Especially important are the meteorological tides (storm surges), which are changes in water level generated by atmospheric forcing, specifically by the drag of the wind on the sea surface and by variations in the surface atmospheric pressure associated with storms. Storm surges last for periods ranging from a few hours to 2 or 3 days and have spatial scales that are large compared with the water depth. Waves also contribute to sea level extremes through the transfer of momentum due to wave breaking (wave setup) and the ascent of waves on a beach or structure (wave run-

	1.5°C	2.0°C	3.0°C	4.0°C	5.0°C	SSP5-8.5 Low Confidence
Closest SSPs	**SSP1-2.6**	**SSP1-2.6/ SSP2-4.5**	**SSP2-4.5/ SSP3-7.0**	**SSP3-7.0**	**SSP5-8.5**	
Total 2050	0.16–0.24 m	0.17–0.26 m	0.18–0.27 m	0.19–0.28 m	0.22–0.31 m	0.20–0.40 m
Total 2100	0.34–0.59 m	0.40–0.69 m	0.50–0.81 m	0.58–0.92 m	0.69–1.05 m	0.63–1.60 m
Rate 2040–2060	2.9–5.7 mm yr^{-1}	3.7–7.0 mm yr^{-1}	4.6–8.1 mm yr^{-1}	5.0–8.6 mm yr^{-1}	5.7–9.8 mm yr^{-1}	5.6–16.1 mm yr^{-1}
Rate 2080–2100	2.6–6.4 mm yr^{-1}	3.4–8.4 mm yr^{-1}	5.3-–11.6 mm yr^{-1}	7.1–14.3 mm yr^{-1}	8.5–17.0 mm yr^{-1}	8.6–30.1 mm yr^{-1}

Table 6.1: Projections of likely ranges of 21st-century GMSL rise along climate trajectories leading to different increases in GSAT between 1850–1900 and 2081–2100. The SSPs trajectories for which the temperature-level projections are most closely aligned are also included. Adapted from (Intergovernmental Panel On Climate Change 2023).

up) (Dodet et al., 2019). Therefore, sea level extremes are short-term phenomena (hours to days timescale) generated by atmospheric disturbances and tides, but they are also modulated by seasonal, interannual, and long-term variations in both mean sea level and atmospheric forcing.

Changes in mean sea level lead to modifications in the reference level from which extremes reach the coastline. For instance, it has been observed that sea level rise can locally alter astronomical tides (Haigh et al., 2020). However, the main harmonic constituents of tides are not significantly affected along the Spanish coast due to the depth and extent of the continental shelf (Pickering et al., 2017). On the other hand, wave action is also sensitive to changes in water depth in shallow areas. In this regard, a sensitivity analysis of projected changes in waves to variations in mean sea level along the European coasts has been conducted (Chaigneau et al., 2022). In this case, it was also noted that the most significant impact of changes in mean sea level on waves occurs on the extensive continental shelf where shallow water dynamics predominate, especially in areas with macro tides. Therefore, concerning the Spanish coasts, no significant changes in wave patterns were found due to the rise in mean sea level.

Regarding the future changes of meteorological tides, barotropic hydrodynamic models have been employed to simulate their future changes. This can be done either based solely on simulated atmospheric changes from regional or global climate models (Vousdoukas et al., 2018, 2017), or by considering the projected sea level rise imposed on the model as a change in water depth (Muis et al., 2023, 2020). The most recent study, conducted by Muis et al., 2023, simulated sea level due to the combined effect of astronomical and meteorological tides from 1950 to 2050 for the SSP5-8.5 scenario on a global scale. The

model Global Tide and Surge was forced with atmospheric simulations from a set of ~25-km resolution climate models (High Resolution Model Intercomparison Project, HighResMIP, Haarsma et al., 2016) from CMIP6. A decrease in meteorological tide (values corresponding to the 10-year return period) of up to 15% is projected along the south Atlantic coast of the IP by the mid-21st century (with a significant agreement among models in the HighResMIP ensemble). Small changes are expected in mid-latitude extratropical storms, but a northward shift in their trajectories from east to west is predicted (Intergovernmental Panel On Climate Change, 2023), which may explain the projected decrease in meteorological tide.

For the Spanish Mediterranean coast, changes are negligible in the period 2021-2050. However, for the 2071-2100 horizon, decreases on the order of 15% are expected, according to the study by Makris et al., 2023. This projection is based on the RCP8.5 scenario using three regional atmospheric models. Small changes are also projected at the end of the century, with zero changes under scenario RCP4.5 and a slight decrease of 0.02 m under scenario RCP8.5, from a dynamical downscaling of 6 regional climate models (CMCC, CNRM, GUF, ITUbats, ITUclm, and LMD) in the framework of the MedCORDEX initiative using HYPSE model, covering the whole Mediterranean with a spatial resolution of 1/5° (Agulles et al., 2021). In general, a decrease in the number and intensity of storms moving through the Mediterranean is expected by the end of the 21st century, based on the analysis of a set of regional models from Med-CORDEX for the RCP8.5 scenario (Reale et al., 2022), explaining the projected declines. (Vousdoukas et al., 2017) using an ensemble of 8 GCMs, also found a decrease in meteorological tide along the south Atlantic coast of Spain and the eastern Cantabrian Sea, while no significant changes in the Mediterranean region. However, it has to be noted that Mediterranean cyclone activity may not be properly solved in GCMs due to their spatial resolution.

Once projections for the different components of ESL are obtained, two different approaches can be employed for projecting future ESL changes: (i) The static approach, also known as the mean sea level offset, which utilizes historical distributions of tidal, surge, and wave components. It adjusts future ESL distributions based on the rise in mean Relative Sea Level (RSL); (ii) The dynamic approach, which utilizes hydrodynamic and/or wave models driven by projections of atmospheric fields to, in turn, project changes in tidal, storm surge, and wave distributions. These changes are then integrated with RSL projections to project future ESLs.

Here we will first analyze changes in sea level extremes using the static approach, i.e.: considering only the effects of mean sea level rise. In this case, the distribution obtained from fitting historical sea level extremes is combined with projections of sea level rise, taking into account the uncertainty in both and assuming that the historical distribution of extremes is maintained in the future. Projections of changes in extreme sea levels due to sea level rise are typically expressed as an amplification in the probability of a particular extreme sea level event (Hermans et al., 2023; Tebaldi et al., 2021; Vitousek et al., 2017). For example, in the IPCC AR6 (Intergovernmental Panel On Climate Change (Ipcc), 2023) it was projected that the sea level associated with the historical centennial event, an event with a 1% probability of occurring each year (once per century on average), will be exceeded several times per year on the Atlantic Iberian in 2100 even for the more moderate SSP2-4.5 scenario. In the Canary Islands and the Mediterranean coasts, the amplification is projected to be 2-3 times larger, due to lower climatic variability in extremes (Intergovernmental Panel On Climate Change (Ipcc), 2023).

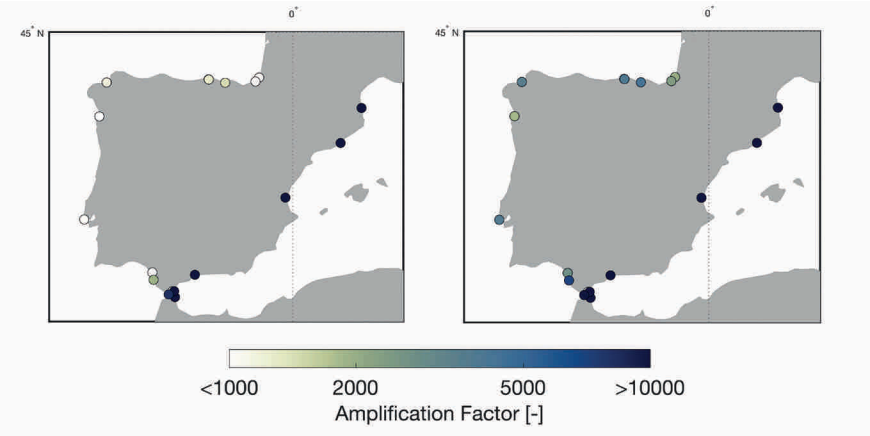

Figure 6.3. Projected median frequency amplification factors of the historical centennial sea level event in 2100 under the SSP2-4.5 and SSP5-8.5 scenario (adapted from Intergovernmental Panel On Climate Change (IPCC, 2023). An amplification factor of 100 means that events occurring every 100 years on average, could occur every year.

Another way of applying this type of approach is, for example, to calculate the sea level rise required for a 10- or 100-fold increase in flood protection standards for coastal infrastructures (Hermans et al., 2023). The increase in sea level would be in the range of a few centimeters to tens of centimeters at many tide gauges in southern Europe, implying that SLR will reduce the level of protection relatively quickly at these locations.

Following the dynamic approach (i.e. considering the linear sum of changes in meteorological tide, wave, and mean sea level rise), the effect of waves on sea level extremes at broad spatial scales, generally global scales, has been primarily assessed using parametric formulations for wave set-up and run-up (Kirezci et al., 2020; Melet et al., 2018; Vousdoukas et al., 2017). In all cases, similar coastal characteristics are assumed across all world coastlines, typically dissipative beaches with a wide range of beach slope values across studies. Projections of meteorological tide and wave conditions are derived from numerical model outputs. For instance, in the studies by Vousdoukas et al., 2018, where they used the DFLOW FM model and the WW3 model for wave generation (Mentaschi et al., 2017), driven by an ensemble of 6 global models for the RCP4.5 and RCP8.5 scenarios. The most recent study, published by Jevrejeva et al., 2023, integrates dynamic simulations of all components of ESL, including mean sea level rise along with levels due to astronomical, meteorological, and wave-induced tides, for the present century under the RCP4.5 and RCP8.5 scenarios. They apply a probabilistic process-based method to calculate regional projections of SLR for each RCP, with SLR projections incorporating increased uncertainties arising from the Greenland and Antarctic ice sheets (Vousdoukas et al., 2018). This worst-case scenario for ESL is calculated as a combination of sea level rise associated with meteorological tide and waves (100-year return period, 95th percentile), astronomical tide (95th percentile), and a low-probability sea level rise scenario (95th percentile). The projected changes in

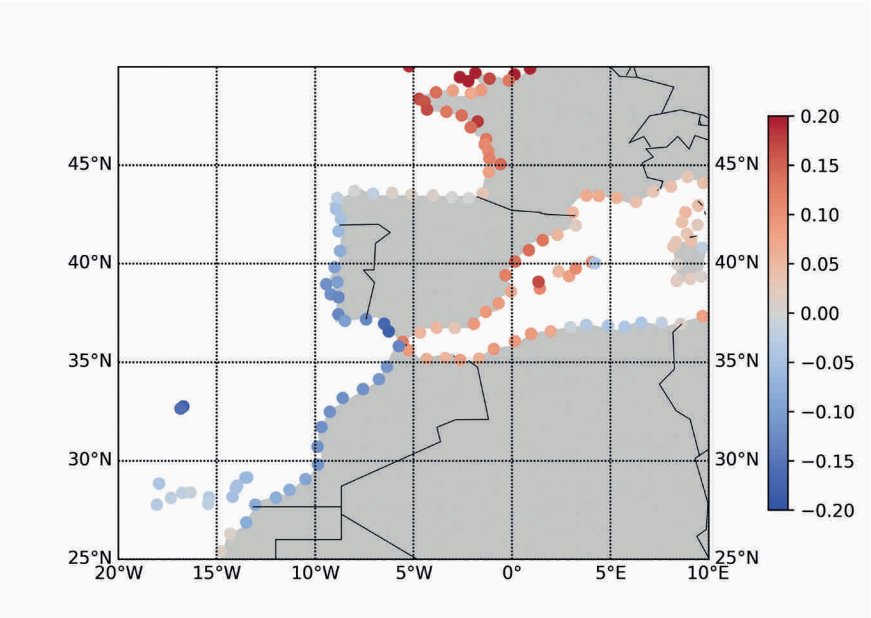

Figure 6.4. Impact of storm surges and waves on changes (increase/decrease) in the 95th percentile of ESL (m) by 2100, relative to baseline period (1980–2014) for the European coastline (adapted from Jevrejeva et al., 2023). This contribution should be added to the mean sea-level rise to obtain the total change of ESL.

low-probability extreme sea levels by 2100, relative to the historical period 1980-2014, are estimated to be around 1.3-1.4 m along the Spanish Atlantic coast, while they range from 1.6-1.8 m for the Mediterranean coast. These increases are based on current ESLs of around 4.5-5.0 m in the Atlantic and 2.5-3.0 m in the Mediterranean (Figure 1 of Jevrejeva et al., 2023). Up to 90% of the changes in ESL by 2100 are explained by future sea-level rise, compared to 10% due to changes in extreme sea levels associated with storm surges and waves. The 95th percentile of regional sea level projections, whose global mean sea level rise is 1.8m by 2100, was used in this study. Changes due to meteorological tide and waves resulting in an average increase of 0.2 m globally. For Spain, decreases in sea level are anticipated due to these components, approximately 0.3 m along the southern Atlantic coast, while increases are projected to be around 0.2 m along the Mediterranean coast and less than 0.1 m along the Cantabrian coast (see Figure 6.4).

6. Biogeochemistry

Anthropogenic climate change will affect biogeochemical cycles in the ocean. Projected global mean changes emerging from the CMIP5 and CMIP6 simulation ensembles include ocean warming, acidification, deoxygenation, decline of near-surface nutrients, and changes of

net primary production (NPP) (Table 1; Bopp et al., 2013; Kwiatkowski et al., 2020). All these environmental changes will pose serious challenges to marine species. Poleward shifts of many marine species unable to acclimate to the rising temperatures have been already observed, leading to reduced biodiversity in the tropics (Chaudhary et al., 2021; Thomas et al., 2012). In addition to temperature, which regulates most biological rates and exerts metabolic constraint on living organisms, acidification and deoxygenation represent additional environmental stressors. Calcifying species, for example, are especially sensitive to acidification, undergoing low growth and high mortality under slight drops of pH. On the other hand, low levels of O_2 can slowdown aerobic metabolism and thereby cause higher mortality of marine species. Augmented interannual variability of these stressors and, especially, extreme events such as ocean heat waves, whose frequency, intensity, and duration are expected to increase in the future, exacerbates their potential impact on marine ecosystems.

Rising seawater temperatures and acidification are particularly widespread and robust future effects across CMIP models. The uptake of anthropogenic carbon emission by the ocean –up to 30% of total emissions– is the main driver of seawater acidification. Global surface pH has declined by 0.1 units since pre-industrial times (Bindoff, N. L., et al., 2007) and this tendency is projected to accelerate during the next decades (Table 6.2). Enhanced near-surface stratification and shrinking of the surface mixed layer depth are other broadly projected consequences of global warming. Stronger stratification impedes vertical mixing and property exchange with the deep ocean, whereas thinner mixed layer depth results in a shallower source of upwelling water. As a result, deep water ventilation slows down and seawater dissolved oxygen is reduced. This deoxygenation process is exacerbated by the warming-induced reduction of O_2 solubility. The largest projected decline in subsurface O_2 occurs at higher latitudes, whereas a moderate increase of O_2 in equatorial regions is predicted by both CMIP5 and CMIP6 models, but with high inter-model uncertainty. It has been speculated that this latter pattern can be related to the poor representation of subsurface ventilation pathways in the equatorial ocean by coarse-resolution models.

Stronger near-surface stratification implies also reduced nutrient supply into the euphotic zone. This is thought to be the primary driver for the projected decline of NPP over much of the tropical and mid-latitude oceans where photosynthesis is largely limited by nutrients availability. In contrast, NPP is projected to increase in light-limited polar and subpolar regions, where weaker vertical mixing and the retreat of sea ice facilitates longer exposure of phytoplankton to light. Overall, a global mean decline of NPP is projected (Table 1), although the magnitude of such decline is highly uncertain across models.

Biochemical trends of the Atlantic waters off Iberia are greatly influenced by North Atlantic patterns (Figure 6.5). The most significant deviations with respect to global trends at upper mid-latitudes in the north Atlantic concern euphotic-zone nutrients and NPP, both declining much faster than globally (-2.5 mmol m^{-3} and -20% under the SSP5-8.5 scenario; see also Figure 6.5a-c). These changes concur with a strong enhancement of stratification and shoaling of the mixed layer depth projected in the region (Figure 6.5d-f), suggesting that the generally proposed mechanism for oligotrophication of low-latitude oceans –i.e., reduced fertilization of the upper ocean by weaker vertical mixing– could be at play in the north Atlantic. The oligotrophication pattern in the North Atlantic decays from north to south so, at regional scale, the Cantabrian Sea appears more sensitive to oligotrophication than the southwest façade of the IP and the Canary Islands. Moving to shorter scales, no significant NPP trend is found in the coastal upwelling region off Portugal and

Variable	Scenario	
	SSP2-4.5	SSP5-8.5
ΔSST (°C)	+2.10 ± 0.43	+3.47 ± 0.78
ΔpH	-0.26 ± 0.00	-0.44 ± 0.01
ΔO_2 (mmol m-3)	-8.14 ± 4.08	-13.27 ± 5.28
ΔNO_3 (mmol m-3)	-0.65 ± 0.32	-1.06 ± 0.45
ΔNPP (%)	-1.13 ± 5.81	-2.99 ± 9.11

Table 6.2. Global average anomalies of sea surface temperature, surface pH, subsurface (100-600 m) dissolved O_2 concentration, upper-ocean (0-100 m) nitrate (NO_3) concentration, and depth-integrated net primary production for the CMIP6 SSP2-4.5 and CMIP6 SSP5-8.5 emission scenarios. Anomalies correspond to 2080-2099 mean values relative to 1970-1899 mean values (adapted from Kwiatkowski et al., 2020).

Northwestern Africa, as noted by the white narrow coastal strip in Figure 6.5b-c. Over such coastal upwelling regions, however, regional downscaling solutions can differ substantially from global solutions (Pozo Buil et al., 2021), thus projections here must be considered with particular caution.

For the rest of biochemical stressors, projected changes of subsurface O_2 and surface pH by the end of the 21st century are -30 mmol m^{-3} and -0.3 in SSP5–8.5 in coastal waters of Iberia and in the Canary Islands (Fig. i,l); the same anomalies are -20 mmol m^{-3} and -0.2 in SSP2–4.5 (Figure 6.5h-k). Changes in pH are practically homogenous in the North Atlantic.

According to the global models from CMIP6, the Mediterranean Sea will be similarly exposed to acidification as the Atlantic Iberian façade, while less than the latter to subsurface deoxygenation (~20 mmol m^{-3} instead of ~30 mmol m^{-3} under SSP5–8.5 scenario; Figure 6.5.i). Near-surface stratification is also projected to strengthen, especially in the Gulf of Lions and in the Levantine basin (Figure 6.5.e-f), suggesting reduced formation of deep and intermediate waters and a slowdown of the Mediterranean overturning circulation, which is in good agreement to the results obtained with regional models (Adloff et al., 2015; Soto-Navarro et al., 2020). In contrast to most oligotrophic systems, the CMIP6 models project NPP increase in the Mediterranean (gC m^{-2} y^{-1} in SSP5–8.5, Figure 6.5.c) despite the associated deficit of upper-ocean fertilization. This suggests more complex interactions in the food web shaping NPP in the Mediterranean, possibly involving zooplankton grazing and/or temperature-effects on phytoplankton metabolic rates.

Although CMIP5 and CMIP6 solutions can provide guidance of potential future biochemical changes of the Mediterranean, the reliability of global projections at regional scales and in the Mediterranean in particular, can be put into question because of the relatively coarse resolution of global models in marginal seas. A few regional physical-biochemical models have been applied to gain insights into potential future changes of Mediterranean biochemistry (see Reale et al., 2022 and references therein). Overall, regional models concur on the Mediterranean becoming warmer at accelerated rate with respect to global ocean, saltier, with stronger near-surface stratification,

and with diminished overturning circulation by the end of century (Soto-Navarro et al., 2020). These changes are expected to be more profound in the Levantine basin due, in part, to its greater isolation from the global ocean. There is no general agreement, however, on how these physical changes will affect primary producers. Using regional models, NPP has been projected to either increase (Reale et al., 2022), remain practically unchanged (Lazzari et al., 2014; Macias et al., 2015), or decrease (Pagès et al., 2020; Richon et al., 2018) by the end of the 21st century, either under RCP8.5 or RCP4.5 climate scenarios. This uncertainty can lie in the different functional responses and parameterizations of phytoplankton metabolic rates to temperature employed by ocean biochemistry models (Reale et al., 2022), combined with the primary role of temperature as environmental stressor in the Mediterranean by its accelerated warming trend. In some models, temperature effects on phytoplankton growth overcome diminished growth by reduced nutrient availability and augmented respiration, resulting in higher NPP. This could be the reason for the positive change of NPP projected for the Mediterranean in CMIP6 (Figure 6.5c). Another identified effect of the accelerated warming of the upper water column in the Mediterranean is the increase of ecosystem respiration (Lazzari et al., 2014; Reale et al., 2022; Solidoro et al., 2022), contributing to global tendencies of deoxygenation and acidification.

7. Conclusions and future perspectives

Global warming has notable impacts on the ocean through many different mechanisms that go beyond the warming of the seawater. Changes in the patterns of almost all ocean fields can be expected as well as global rise of sea level, water temperature, acidification or deoxygenation. The details of those changes depend on complex interactions between different mechanisms. In this chapter, a detailed analysis of global warming impact on the ocean properties around Spain has been presented.

The circulation around the Iberian Atlantic waters and the Canary Islands is expected to be strengthened due to the enhancement of the density gradients and the intensification of winds (Intergovernmental Panel On Climate Change, 2023). The upwelling along the western Iberian coasts and the Canary region will also increase while a decrease of the downwelling in the northern Iberian coasts is also expected. No large changes in the general circulation of the Mediterranean are expected, but a large reduction in the deep water convection in the Western Mediterranean is foreseen (Soto-Navarro et al., 2020) as well as a moderate increase in the mesoscale activity (Ser-Giacomi et al., 2020).

Ocean temperature will increase in all Spanish waters in the whole water column, especially in the Mediterranean. The warming will be higher in summer and the intensity of marine heatwaves will be strongly enhanced. Regarding salinity, a freshening of northeast Atlantic waters is expected due to the advection of waters from the Arctic. In coastal areas, that freshening will be partially damped by the increased coastal upwelling. The salt content in the Mediterranean will increase due to the enhancement of evaporation. However, the salinity in the shallower waters of the Western basin may decrease due to the entrance of fresher Atlantic Waters (Soto-Navarro et al., 2020).

The mean sea level around Spain will roughly follow the same evolution of global mean sea level as regional differences produced by changes in the circulation and mass redistribution almost compensate each other (Slangen et al., 2023). Up to 90% of the changes in the extreme sea levels by 2100 are explained by future sea-level rise, compared to 10% due to changes in extreme

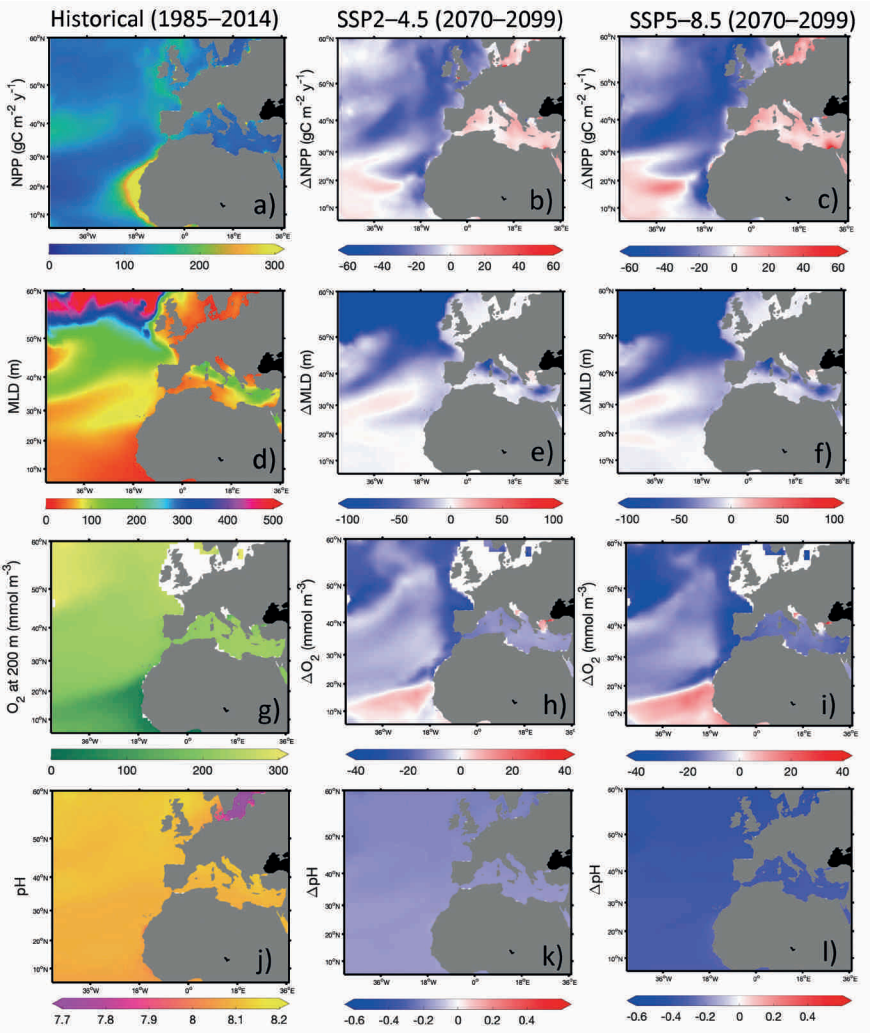

Figure 6.5. Ensemble mean CMIP6 historical climate (1985-2014) and projected 21st century anomalies (2070-2099 relative to 1985-2014 ensemble means) under CMIP6 SSP4–4.5 and SSP5–8.5 experiments for (a-c) net primary production, (d-f) mixing layer depth, (g-i) dissolved oxygen at 200 m depth, and (j-l) surface pH. Data obtained from the NOAA Climate Change Web Portal (https://psl.noaa.gov/ipcc/cmip6).

sea levels associated with storm surges and waves. As a result, historical centennial events are expected to occur several times per year (Jevrejeva et al., 2023).

Surface acidification trends associated with absorption of anthropogenic carbon emissions is a robust feature among models. Furthermore, they project a reduction of dissolved oxygen concentration attributed to enhanced upper-ocean stratification, weaker ventilation of subsurface waters, and warming-induced reduction in O_2 solubility.

The increase of upper-ocean stratification will hinder the nutrients supply from the deep ocean, so a diminished nutrient availability in the euphotic zone can be expected. The net primary production will also be affected, and models project negative changes in the Atlantic sector of the Iberian Peninsula and off the Canary Islands, but with large inter-model uncertainty. This uncertainty probably stems from the complex dependence of plankton metabolism upon seawater temperature and the variety of fashions this is parameterized among the different models. In the Mediterranean, the changes of net primary production are even more uncertain due to the limited number of regional model simulations conducted and the intermodel spread.

All the analyses presented in this chapter have shown that the robustness of the regional ocean projections strongly depends on the region under study as well as the variable of interest. Most studies focusing on the Atlantic region are based on GCMs, although the few studies based on RCMs (Gomis et al., 2016) have pointed out that local processes that are not solved by GCMs (e.g. coastal upwelling) can modulate the large-scale changes. Therefore, more efforts should be devoted to the regional modeling of this region in order to increase the robustness of coastal projections. In the Mediterranean, the importance of regional modeling has been put forward much earlier and more efforts have been made on the regional modeling (e.g. see for instance the MedCORDEX initiative, Ruti et al., 2016), although larger ensembles will also be desirable.

Regarding the robustness of projections for given variables, temperature and mean sea level projections are more robust with large agreements among models. The circulation and surface salinity are more uncertain both in the Atlantic and the Mediterranean, mainly due to the discrepancies among models about the southwards advection of north Atlantic freshwater. A detailed analysis of the mechanism of this advection could help to increase confidence on the projections. The biogeochemical variables are more difficult to simulate as their evolution depends on both physical and biogeochemical processes. Also, the model ensembles are relatively small and model uncertainty, linked to essential biogeochemical processes, is relatively large. So, more work is needed in the model tuning and validation as well on enlarging the ensembles, to increase the confidence of biogeochemical projections around the Spanish waters.

REFERENCES

Adloff, F., Jordà, G., Somot, S., Sevault, F., Arsouze, T., Meyssignac, B., Li, L., Planton, S., 2018. Improving sea level simulation in Mediterranean regional climate models. Clim. Dyn. 51, 1167–1178. https://doi.org/10.1007/s00382-017-3842-3

Adloff, F., Somot, S., Sevault, F., Jordà, G., Aznar, R., Déqué, M., Herrmann, M., Marcos, M., Dubois, C., Padorno, E., Alvarez-Fanjul, E., Gomis, D., 2015. Mediterranean Sea response to climate change in an ensemble of twenty first century scenarios. Clim. Dyn. 45, 2775–2802. https://doi.org/10.1007/s00382-015-2507-3

Agulles, M., Jordà, G., Lionello, P., 2021. Flooding of Sandy Beaches in a Changing Climate. The Case of the Balearic Islands (NW Mediterranean). Front. Mar. Sci. 8, 760725. https://doi.org/10.3389/fmars.2021.760725

Alexander, M.A., Scott, J.D., Friedland, K.D., Mills, K.E., Nye, J.A., Pershing, A.J., Thomas, A.C., 2018. Projected sea surface temperatures over the 21st century: Changes in the mean, variability and extremes for large marine ecosystem regions of Northern Oceans. Elem. Sci. Anthr. 6, 9. https://doi.org/10.1525/elementa.191

Amitai, Y., Ashkenazy, Y., Gildor, H., 2017. Multiple equilibria and overturning variability of the Aegean-Adriatic Seas. Glob. Planet. Change 151, 49–59. https://doi.org/10.1016/j.gloplacha.2016.05.004

Bindoff, N. L., Willebrand, J., Artale, V., Cazenave, A., Gregory, J. M., Gulev, S., Hanawa, K., Le Quere, C., Levitus, S., Nojiri, Y., Shum, C. K., Talley, L. D., Unnikrishnan, A. S., Josey, S. A., Tamisiea, M., Tsimplis, M. and Woodworth, P., 2007. Observations: oceanic climate change and sea level, in Climate change 2007: the physical science basis. Contribution of Working Group I, S. Solomon, D. Qin, M. Manning, Z. Chen, M. Marquis, K. B. Averyt, M. Tignor, and H. L. Miller. ed. Cambridge University Press, Cambridge.

Bopp, L., Resplandy, L., Orr, J.C., Doney, S.C., Dunne, J.P., Gehlen, M., Halloran, P., Heinze, C., Ilyina, T., Séférian, R., Tjiputra, J., Vichi, M., 2013. Multiple stressors of ocean ecosystems in the 21st century: projections with CMIP5 models. Biogeosciences 10, 6225–6245. https://doi.org/10.5194/bg-10-6225-2013

Bronselaer, B., Zanna, L., 2020. Heat and carbon coupling reveals ocean warming due to circulation changes. Nature 584, 227–233. https://doi.org/10.1038/s41586-020-2573-5

Calafat, F.M., Jordà, G., Marcos, M., Gomis, D., 2012. Comparison of Mediterranean sea level variability as given by three baroclinic models. J. Geophys. Res. Oceans 117, 2011JC007277. https://doi.org/10.1029/2011JC007277

Chaigneau, A.A., Reffray, G., Voldoire, A., Melet, A., 2022. IBI-CCS: a regional high-resolution model to simulate sea level in western Europe. Geosci. Model Dev. 15, 2035–2062. https://doi.org/10.5194/gmd-15-2035-2022

Chaudhary, C., Richardson, A.J., Schoeman, D.S., Costello, M.J., 2021. Global warming is causing a more pronounced dip in marine species richness around the equator. Proc. Natl. Acad. Sci. 118, e2015094118. https://doi.org/10.1073/pnas.2015094118

Cheng, L., Trenberth, K.E., Gruber, N., Abraham, J.P., Fasullo, J.T., Li, G., Mann, M.E., Zhao, X., Zhu, J., 2020. Improved Estimates of Changes in Upper Ocean Salinity and the Hydrological Cycle. J. Clim. 33, 10357–10381. https://doi.org/10.1175/JCLI-D-20-0366.1

Darmaraki, S., Somot, S., Sevault, F., Nabat, P., Cabos Narvaez, W.D., Cavicchia, L., Djurdjevic, V., Li, L., Sannino, G., Sein, D.V., 2019. Future evolution of Marine Heatwaves in the Mediterranean Sea. Clim. Dyn. 53, 1371–1392. https://doi.org/10.1007/s00382-019-04661-z

De La Vara, A., Parras-Berrocal, I.M., Izquierdo, A., Sein, D.V., Cabos, W., 2022. Climate change signal in the ocean circulation of the Tyrrhenian Sea. Earth Syst. Dyn. 13, 303–319. https://doi.org/10.5194/esd-13-303-2022

Deshayes, J., Curry, R., Msadek, R., 2014. CMIP5 Model Intercomparison of Freshwater Budget and Circulation in the North Atlantic. J. Clim. 27, 3298–3317. https://doi.org/10.1175/JCLI-D-12-00700.1

Ditlevsen, P., Ditlevsen, S., 2023. Warning of a forthcoming collapse of the Atlantic meridional overturning circulation. Nat. Commun. 14, 4254. https://doi.org/10.1038/s41467-023-39810-w

Dodet, G., Castelle, B., Masselink, G., Scott, T., Davidson, M., Floc'h, F., Jackson, D., Suanez, S., 2019. Beach recovery from extreme storm activity during the 2013–14 winter along the Atlantic coast of Europe. Earth Surf. Process. Landf. 44, 393–401. https://doi.org/10.1002/esp.4500

Du, Y., Zhang, Y., Shi, J., 2019. Relationship between sea surface salinity and ocean circulation and climate change. Sci. China Earth Sci. 62, 771–782. https://doi.org/10.1007/s11430-018-9276-6

Dubois, C., Somot, S., Calmanti, S., Carillo, A., Déqué, M., Dell'Aquilla, A., Elizalde, A., Gualdi, S., Jacob, D., L'Hévéder, B., Li, L., Oddo, P., Sannino, G., Scoccimarro, E., Sevault, F., 2012. Future projections of the surface heat and water budgets of the Mediterranean Sea in an ensemble of coupled atmosphere–ocean regional climate models. Clim. Dyn. 39, 1859–1884. https://doi.org/10.1007/s00382-011-1261-4

Dukhovskoy, D.S., Myers, P.G., Platov, G., Timmermans, M., Curry, B., Proshutinsky, A., Bamber, J.L., Chassignet, E., Hu, X., Lee, C.M., Somavilla, R., 2016. Greenland freshwater pathways in the subArctic Seas from model experiments with passive tracers. J. Geophys. Res. Oceans 121, 877–907. https://doi.org/10.1002/2015JC011290

Dukhovskoy, D.S., Yashayaev, I., Proshutinsky, A., Bamber, J.L., Bashmachnikov, I.L., Chassignet, E.P., Lee, C.M., Tedstone, A.J., 2019. Role of Greenland Freshwater Anomaly in the Recent Freshening of the Subpolar North Atlantic. J. Geophys. Res. Oceans 124, 3333–3360. https://doi.org/10.1029/2018JC014686

García Lafuente, J., Delgado, J., Sánchez Román, A., Soto, J., Carracedo, L., Díaz del Río, G., 2009. Interannual variability of the Mediterranean outflow observed in Espartel sill, western Strait of Gibraltar. J. Geophys. Res. Oceans 114, C10018–C10018. https://doi.org/10.1029/2009jc005496

Gomis, D., Álvarez-Fanjul, E., Jordà, G., Marcos, M., Aznar, R., Rodríguez-Camino, E., Sánchez-Perrino, J.C., Rodríguez-González, J.M., Martínez-Asensio, A., Llasses, J., Pérez, B., Sotillo, M.G., 2016. Regional marine climate scenarios in the NE Atlantic sector close to the Spanish shores. Sci. Mar. 80, 215–234. https://doi.org/10.3989/scimar.04328.07A

Gualdi, S., Somot, S., Li, L., Artale, V., Adani, M., Bellucci, A., Braun, A., Calmanti, S., Carillo, A., Dell'Aquila, A., Déqué, M., Dubois, C., Elizalde, A., Harzallah, A., Jacob, D., L'Hévéder, B., May, W., Oddo, P., Ruti,

P., Sanna, A., Sannino, G., Scoccimarro, E., Sevault, F., Navarra, A., 2013. The CIRCE Simulations: Regional Climate Change Projections with Realistic Representation of the Mediterranean Sea. Bull. Am. Meteorol. Soc. 94, 65–81. https://doi.org/10.1175/BAMS-D-11-00136.1

Haarsma, R.J., Roberts, M.J., Vidale, P.L., Senior, C.A., Bellucci, A., Bao, Q., Chang, P., Corti, S., Fučkar, N.S., Guemas, V., Von Hardenberg, J., Hazeleger, W., Kodama, C., Koenigk, T., Leung, L.R., Lu, J., Luo, J.-J., Mao, J., Mizielinski, M.S., Mizuta, R., Nobre, P., Satoh, M., Scoccimarro, E., Semmler, T., Small, J., Von Storch, J.-S., 2016. High Resolution Model Intercomparison Project (HighResMIP v1.0) for CMIP6. Geosci. Model Dev. 9, 4185–4208. https://doi.org/10.5194/gmd-9-4185-2016

Haigh, I.D., Pickering, M.D., Green, J.A.M., Arbic, B.K., Arns, A., Dangendorf, S., Hill, D.F., Horsburgh, K., Howard, T., Idier, D., Jay, D.A., Jänicke, L., Lee, S.B., Müller, M., Schindelegger, M., Talke, S.A., Wilmes, S., Woodworth, P.L., 2020. The Tides They Are A-Changin': A Comprehensive Review of Past and Future Nonastronomical Changes in Tides, Their Driving Mechanisms, and Future Implications. Rev. Geophys. 58, e2018RG000636. https://doi.org/10.1029/2018RG000636

Hermans, T.H.J., Malagón-Santos, V., Katsman, C.A., Jane, R.A., Rasmussen, D.J., Haasnoot, M., Garner, G.G., Kopp, R.E., Oppenheimer, M., Slangen, A.B.A., 2023. The timing of decreasing coastal flood protection due to sea-level rise. Nat. Clim. Change 13, 359–366. https://doi.org/10.1038/s41558-023-01616-5

Hermans, T.H.J., Tinker, J., Palmer, M.D., Katsman, C.A., Vermeersen, B.L.A., Slangen, A.B.A., 2020. Improving sea-level projections on the Northwestern European shelf using dynamical downscaling. Clim. Dyn. 54, 1987–2011. https://doi.org/10.1007/s00382-019-05104-5

Holliday, N.P., Bersch, M., Berx, B., Chafik, L., Cunningham, S., Florindo-López, C., Hátún, H., Johns, W., Josey, S.A., Larsen, K.M.H., Mulet, S., Oltmanns, M., Reverdin, G., Rossby, T., Thierry, V., Valdimarsson, H., Yashayaev, I., 2020. Ocean circulation causes the largest freshening event for 120 years in eastern subpolar North Atlantic. Nat. Commun. 11, 585. https://doi.org/10.1038/s41467-020-14474-y

Intergovernmental Panel On Climate Change, 2023. Climate Change 2021 – The Physical Science Basis: Working Group I Contribution to the Sixth Assessment Report of the Intergovernmental Panel on Climate Change, 1st ed. Cambridge University Press. https://doi.org/10.1017/9781009157896

Isern-Fontanet, J., García-Ladona, E., Font, J., 2006. Vortices of the Mediterranean Sea: An Altimetric Perspective. J. Phys. Oceanogr. 36, 87–103. https://doi.org/10.1175/JPO2826.1

Jevrejeva, S., Palanisamy, H., Jackson, L.P., 2021. Global mean thermosteric sea level projections by 2100 in CMIP6 climate models. Environ. Res. Lett. 16, 014028. https://doi.org/10.1088/1748-9326/abceea

Jevrejeva, S., Williams, J., Vousdoukas, M.I., Jackson, L.P., 2023. Future sea level rise dominates changes in worst case extreme sea levels along the global coastline by 2100. Environ. Res. Lett. 18, 024037. https://doi.org/10.1088/1748-9326/acb504

Jordà, G., Von Schuckmann, K., Josey, S.A., Caniaux, G., García-Lafuente, J., Sammartino, S., Özsoy, E., Polcher, J., Notarstefano, G., Poulain, P.-M., Adloff, F., Salat, J., Naranjo, C., Schroeder, K., Chiggiato, J., Sannino, G., Macías, D., 2017. The Mediterranean Sea heat and mass budgets: Estimates,

uncertainties and perspectives. Prog. Oceanogr. 156, 174–208. https://doi.org/10.1016/j.pocean.2017.07.001

Josey, S.A., Schroeder, K., 2023. Declining winter heat loss threatens continuing ocean convection at a Mediterranean dense water formation site. Environ. Res. Lett. 18, 024005. https://doi.org/10.1088/1748-9326/aca9e4

Kirezci, E., Young, I.R., Ranasinghe, R., Muis, S., Nicholls, R.J., Lincke, D., Hinkel, J., 2020. Projections of global-scale extreme sea levels and resulting episodic coastal flooding over the 21st Century. Sci. Rep. 10, 11629. https://doi.org/10.1038/s41598-020-67736-6

Kwiatkowski, L., Torres, O., Bopp, L., Aumont, O., Chamberlain, M., Christian, J.R., Dunne, J.P., Gehlen, M., Ilyina, T., John, J.G., Lenton, A., Li, H., Lovenduski, N.S., Orr, J.C., Palmieri, J., Santana-Falcón, Y., Schwinger, J., Séférian, R., Stock, C.A., Tagliabue, A., Takano, Y., Tjiputra, J., Toyama, K., Tsujino, H., Watanabe, M., Yamamoto, A., Yool, A., Ziehn, T., 2020. Twenty-first century ocean warming, acidification, deoxygenation, and upper-ocean nutrient and primary production decline from CMIP6 model projections. Biogeosciences 17, 3439–3470. https://doi.org/10.5194/bg-17-3439-2020

Lazzari, P., Mattia, G., Solidoro, C., Salon, S., Crise, A., Zavatarelli, M., Oddo, P., Vichi, M., 2014. The impacts of climate change and environmental management policies on the trophic regimes in the Mediterranean Sea: Scenario analyses. J. Mar. Syst. 135, 137–149. https://doi.org/10.1016/j.jmarsys.2013.06.005

Levang, S.J., Schmitt, R.W., 2020. Intergyre Salt Transport in the Climate Warming Response. J. Phys. Oceanogr. 50, 255–268. https://doi.org/10.1175/JPO-D-19-0166.1

Liu, B., Liu, J., Ning, L., Sun, W., Yan, M., Zhao, C., Chen, K., Wang, X., 2020. The Role of Samalas Mega Volcanic Eruption in European Summer Hydroclimate Change. Atmosphere 11, 1182. https://doi.org/10.3390/atmos11111182

Liu, C., Liang, X., Ponte, R.M., Vinogradova, N., Wang, O., 2019. Vertical redistribution of salt and layered changes in global ocean salinity. Nat. Commun. 10, 3445. https://doi.org/10.1038/s41467-019-11436-x

Macias, D.M., Garcia-Gorriz, E., Stips, A., 2015. Productivity changes in the Mediterranean Sea for the twenty-first century in response to changes in the regional atmospheric forcing. Front. Mar. Sci. 2. https://doi.org/10.3389/fmars.2015.00079

Makris, C.V., Tolika, K., Baltikas, V.N., Velikou, K., Krestenitis, Y.N., 2023. The impact of climate change on the storm surges of the Mediterranean Sea: Coastal sea level responses to deep depression atmospheric systems. Ocean Model. 181, 102149. https://doi.org/10.1016/j.ocemod.2022.102149

Margirier, F., Testor, P., Heslop, E., Mallil, K., Bosse, A., Houpert, L., Mortier, L., Bouin, M.-N., Coppola, L., D'Ortenzio, F., Durrieu De Madron, X., Mourre, B., Prieur, L., Raimbault, P., Taillandier, V., 2020. Abrupt warming and salinification of intermediate waters interplays with decline of deep convection in the Northwestern Mediterranean Sea. Sci. Rep. 10, 20923. https://doi.org/10.1038/s41598-020-77859-5

Mariotti, A., Pan, Y., Zeng, N., Alessandri, A., 2015. Long-term climate change in the Mediterranean region in the midst of decadal variability. Clim. Dyn. 44, 1437–1456. https://doi.org/10.1007/s00382-015-2487-3

Melet, A., Meyssignac, B., Almar, R., Le Cozannet, G., 2018. Under-estimated wave contribution to coastal sea-level rise. Nat. Clim. Change 8, 234–239. https://doi.org/10.1038/s41558-018-0088-y

Mentaschi, L., Vousdoukas, M.I., Voukouvalas, E., Dosio, A., Feyen, L., 2017. Global changes of extreme coastal wave energy fluxes triggered by intensified teleconnection patterns. Geophys. Res. Lett. 44, 2416–2426. https://doi.org/10.1002/2016GL072488

Millot, C., 1999. Circulation in the Western Mediterranean Sea. J. Mar. Syst. 20, 423–442. https://doi.org/10.1016/S0924-7963(98)00078-5

Muis, S., Aerts, J.C.J.H., Á. Antolínez, J.A., Dullaart, J.C., Duong, T.M., Erikson, L., Haarsma, R.J., Apecechea, M.I., Mengel, M., Le Bars, D., O'Neill, A., Ranasinghe, R., Roberts, M.J., Verlaan, M., Ward, P.J., Yan, K., 2023. Global Projections of Storm Surges Using High-Resolution CMIP6 Climate Models. Earths Future 11, e2023EF003479. https://doi.org/10.1029/2023EF003479

Muis, S., Apecechea, M.I., Dullaart, J., De Lima Rego, J., Madsen, K.S., Su, J., Yan, K., Verlaan, M., 2020. A High-Resolution Global Dataset of Extreme Sea Levels, Tides, and Storm Surges, Including Future Projections. Front. Mar. Sci. 7, 263. https://doi.org/10.3389/fmars.2020.00263

O'Dea, E., Furner, R., Wakelin, S., Siddorn, J., While, J., Sykes, P., King, R., Holt, J., Hewitt, H., 2017. The CO5 configuration of the 7 km Atlantic Margin Model: large-scale biases and sensitivity to forcing, physics options and vertical resolution. Geosci. Model Dev. 10, 2947–2969. https://doi.org/10.5194/gmd-10-2947-2017

Pagès, R., Baklouti, M., Barrier, N., Ayache, M., Sevault, F., Somot, S., Moutin, T., 2020. Projected Effects of Climate-Induced Changes in Hydrodynamics on the Biogeochemistry of the Mediterranean Sea Under the RCP 8.5 Regional Climate Scenario. Front. Mar. Sci. 7, 563615. https://doi.org/10.3389/fmars.2020.563615

Parras-Berrocal, I.M., Vázquez, R., Cabos, W., Sein, D.V., Álvarez, O., Bruno, M., Izquierdo, A., 2022. Surface and Intermediate Water Changes Triggering the Future Collapse of Deep Water Formation in the North Western Mediterranean. Geophys. Res. Lett. 49, e2021GL095404. https://doi.org/10.1029/2021GL095404

Pickering, M.D., Horsburgh, K.J., Blundell, J.R., Hirschi, J.J.-M., Nicholls, R.J., Verlaan, M., Wells, N.C., 2017. The impact of future sea-level rise on the global tides. Cont. Shelf Res. 142, 50–68. https://doi.org/10.1016/j.csr.2017.02.004

Pozo Buil, M., Jacox, M.G., Fiechter, J., Alexander, M.A., Bograd, S.J., Curchitser, E.N., Edwards, C.A., Rykaczewski, R.R., Stock, C.A., 2021. A Dynamically Downscaled Ensemble of Future Projections for the California Current System. Front. Mar. Sci. 8, 612874. https://doi.org/10.3389/fmars.2021.612874

Reale, M., Cabos Narvaez, W.D., Cavicchia, L., Conte, D., Coppola, E., Flaounas, E., Giorgi, F., Gualdi, S., Hochman, A., Li, L., Lionello, P., Podrascanin, Z., Salon, S., Sanchez-Gomez, E., Scoccimarro, E., Sein, D.V., Somot, S., 2022. Future projections of Mediterranean cyclone characteristics using the Med-CORDEX ensemble of coupled regional climate system models. Clim. Dyn. 58, 2501–2524. https://doi.org/10.1007/s00382-021-06018-x

Richon, C., Dutay, J.-C., Dulac, F., Wang, R., Balkanski, Y., 2018. Modeling the biogeochemical impact of atmospheric phosphate deposition from desert dust and combustion sources to the Mediterranean Sea. Biogeosciences 15, 2499–2524. https://doi.org/10.5194/bg-15-2499-2018

Ruti, P.M., Somot, S., Giorgi, F., Dubois, C., Flaounas, E., Obermann, A., Dell'Aquila, A., Pisacane, G., Harzallah, A., Lombardi, E., Ahrens, B., Akhtar, N., Alias, A., Arsouze, T., Aznar, R., Bastin, S., Bartholy, J., Béranger, K., Beuvier, J., Bouffies-Cloché, S., Brauch, J., Cabos, W., Calmanti, S., Calvet, J.-C., Carillo, A., Conte, D., Coppola, E., Djurdjevic, V., Drobinski, P., Elizalde-Arellano, A., Gaertner, M., Galàn, P., Gallardo, C., Gualdi, S., Goncalves, M., Jorba, O., Jordà, G., L'Heveder, B., Lebeaupin-Brossier, C., Li, L., Liguori, G., Lionello, P., Maciàs, D., Nabat, P., Önol, B., Raikovic, B., Ramage, K., Sevault, F., Sannino, G., Struglia, M.V., Sanna, A., Torma, C., Vervatis, V., 2016. Med-CORDEX Initiative for Mediterranean Climate Studies. Bull. Am. Meteorol. Soc. 97, 1187–1208. https://doi.org/10.1175/BAMS-D-14-00176.1

Sánchez-Garrido, J.C., Sannino, G., Liberti, L., García Lafuente, J., Pratt, L., 2011. Numerical modeling of three-dimensional stratified tidal flow over Camarinal Sill, Strait of Gibraltar. J. Geophys. Res. 116, C12026. https://doi.org/10.1029/2011JC007093

Sanchez-Gomez, E., Somot, S., Mariotti, A., 2009. Future changes in the Mediterranean water budget projected by an ensemble of regional climate models. Geophys. Res. Lett. 36, 2009GL040120. https://doi.org/10.1029/2009GL040120

Sannino, G., Carillo, A., Iacono, R., Napolitano, E., Palma, M., Pisacane, G., Struglia, M., 2022. Modelling present and future climate in the Mediterranean Sea: a focus on sea-level change. Clim. Dyn. 59, 357–391. https://doi.org/10.1007/s00382-021-06132-w

Sannino, G., Carillo, A., Pisacane, G., Naranjo, C., 2015. On the relevance of tidal forcing in modelling the Mediterranean thermohaline circulation. Prog. Oceanogr. 134, 304–329. https://doi.org/10.1016/j.pocean.2015.03.002

Sathyanarayanan, A., Köhl, A., Stammer, D., 2021. Ocean Salinity changes in the global ocean under global warming conditions Part 1: Mechanisms in a strong warming scenario. J. Clim. 1–56. https://doi.org/10.1175/JCLI-D-20-0865.1

Semia Cherif, Doblas-Miranda, E., Lionello, P., Borrego, C., Giorgi, F., Iglesias, A., Sihem Jebari, Mahmoudi, E., Moriondo, M., Pringault, O., Rilov, G., Somot, S., Tsikliras, A., Vià, M., Zittis, G., 2020. First Mediterranean Assessment Report - Chapter 2: Drivers of Change. [object Object]. https://doi.org/10.5281/ZENODO.7100601

Ser-Giacomi, E., Jordá-Sánchez, G., Soto-Navarro, J., Thomsen, S., Mignot, J., Sevault, F., Rossi, V., 2020. Impact of Climate Change on Surface Stirring and Transport in the Mediterranean Sea. Geophys. Res. Lett. 47, e2020GL089941. https://doi.org/10.1029/2020GL089941

Shaltout, M., Omstedt, A., 2014. Recent sea surface temperature trends and future scenarios for the Mediterranean Sea. Oceanologia 56, 411–443. https://doi.org/10.5697/oc.56-3.411

Slangen, A.B.A., Carson, M., Katsman, C.A., Van De Wal, R.S.W., Köhl, A., Vermeersen, L.L.A., Stammer, D., 2014. Projecting twenty-first century regional sea-level changes. Clim. Change 124, 317–332. https://doi.org/10.1007/s10584-014-1080-9

Slangen, A.B.A., Palmer, M.D., Camargo, C.M.L., Church, J.A., Edwards, T.L., Hermans, T.H.J., Hewitt, H.T., Garner, G.G., Gregory, J.M., Kopp, R.E., Santos, V.M., Van De Wal, R.S.W., 2023. The evolution of 21st century sea-level projections from IPCC AR5 to AR6 and beyond. Camb. Prisms Coast. Futur. 1, e7. https://doi.org/10.1017/cft.2022.8

Solidoro, C., Cossarini, G., Lazzari, P., Galli, G., Bolzon, G., Somot, S., Salon, S., 2022. Modeling Carbon Budgets and Acidification in the Mediterranean Sea Ecosystem Under Contemporary and Future Climate. Front. Mar. Sci. 8, 781522. https://doi.org/10.3389/fmars.2021.781522

Somot, S., Houpert, L., Sevault, F., Testor, P., Bosse, A., Taupier-Letage, I., Bouin, M.-N., Waldman, R., Cassou, C., Sanchez-Gomez, E., Durrieu De Madron, X., Adloff, F., Nabat, P., Herrmann, M., 2018. Characterizing, modelling and understanding the climate variability of the deep water formation in the North-Western Mediterranean Sea. Clim. Dyn. 51, 1179–1210. https://doi.org/10.1007/s00382-016-3295-0

Somot, S., Sevault, F., Déqué, M., 2006. Transient climate change scenario simulation of the Mediterranean Sea for the twenty-first century using a high-resolution ocean circulation model. Clim. Dyn. 27, 851–879. https://doi.org/10.1007/s00382-006-0167-z

Somot, S., Sevault, F., Déqué, M., Crépon, M., 2008. 21st century climate change scenario for the Mediterranean using a coupled atmosphere–ocean regional climate model. Glob. Planet. Change 63, 112–126. https://doi.org/10.1016/j.gloplacha.2007.10.003

Soto-Navarro, J., Jordá, G., Amores, A., Cabos, W., Somot, S., Sevault, F., Macías, D., Djurdjevic, V., Sannino, G., Li, L., Sein, D., 2020. Evolution of Mediterranean Sea water properties under climate change scenarios in the Med-CORDEX ensemble. Clim. Dyn. 54, 2135–2165. https://doi.org/10.1007/s00382-019-05105-4

Stendardo, I., Rhein, M., Steinfeldt, R., 2020. The North Atlantic Current and its Volume and Freshwater Transports in the Subpolar North Atlantic, Time Period 1993–2016. J. Geophys. Res. Oceans 125, e2020JC016065. https://doi.org/10.1029/2020JC016065

Strandberg, G., Kjellström, E., Poska, A., Wagner, S., Gaillard, M.-J., Trondman, A.-K., Mauri, A., Davis, B.A.S., Kaplan, J.O., Birks, H.J.B., Bjune, A.E., Fyfe, R., Giesecke, T., Kalnina, L., Kangur, M., Van Der Knaap, W.O., Kokfelt, U., Kuneš, P., Lata\\l Owa, M., Marquer, L., Mazier, F., Nielsen, A.B., Smith, B., Seppä, H., Sugita, S., 2014. Regional climate model simulations for Europe at 6 and 0.2 k BP: sensitivity to changes in anthropogenic deforestation. Clim. Past 10, 661–680. https://doi.org/10.5194/cp-10-661-2014

Tebaldi, C., Debeire, K., Eyring, V., Fischer, E., Fyfe, J., Friedlingstein, P., Knutti, R., Lowe, J., O'Neill, B., Sanderson, B., Van Vuuren, D., Riahi, K., Meinshausen, M., Nicholls, Z., Tokarska, K.B., Hurtt, G., Kriegler, E., Lamarque, J.-F., Meehl, G., Moss, R., Bauer, S.E., Boucher, O., Brovkin, V., Byun, Y.-H., Dix, M., Gualdi, S., Guo, H., John, J.G., Kharin, S., Kim, Y., Koshiro, T., Ma, L., Olivié, D., Panickal, S., Qiao, F., Rong, X., Rosenbloom, N., Schupfner, M., Séférian, R., Sellar, A., Semmler, T., Shi, X., Song, Z., Steger, C., Stouffer, R., Swart, N., Tachiiri, K., Tang, Q., Tatebe, H., Voldoire, A., Volodin, E., Wyser, K., Xin, X., Yang, S., Yu, Y., Ziehn, T., 2021. Climate model projections from the Scenario Model Intercomparison Project (ScenarioMIP) of CMIP6. Earth Syst. Dyn. 12, 253–293. https://doi.org/10.5194/esd-12-253-2021

Thomas, M.K., Kremer, C.T., Klausmeier, C.A., Litchman, E., 2012. A Global Pattern of Thermal Adaptation in Marine Phytoplankton. Science 338, 1085–1088. https://doi.org/10.1126/science.1224836

University of Potsdam, Rahmstorf, S., 2024. Is the Atlantic Overturning Circulation Approaching a Tipping Point? Oceanography. https://doi.org/10.5670/oceanog.2024.501

van Westen, R.M., Kliphuis, M., Dijkstra, H.A., 2024. Physics-based early warning signal shows that AMOC is on tipping course. Sci. Adv. 10, eadk1189. https://doi.org/10.1126/sciadv.adk1189

Vitousek, S., Barnard, P.L., Fletcher, C.H., Frazer, N., Erikson, L., Storlazzi, C.D., 2017. Doubling of coastal flooding frequency within decades due to sea-level rise. Sci. Rep. 7, 1399. https://doi.org/10.1038/s41598-017-01362-7

Vousdoukas, M.I., Mentaschi, L., Voukouvalas, E., Verlaan, M., Feyen, L., 2017. Extreme sea levels on the rise along Europe's coasts. Earths Future 5, 304–323. https://doi.org/10.1002/2016EF000505

Vousdoukas, M.I., Mentaschi, L., Voukouvalas, E., Verlaan, M., Jevrejeva, S., Jackson, L.P., Feyen, L., 2018. Global probabilistic projections of extreme sea levels show intensification of coastal flood hazard. Nat. Commun. 9, 2360. https://doi.org/10.1038/s41467-018-04692-w

Wang, D., Gouhier, T.C., Menge, B.A., Ganguly, A.R., 2015. Intensification and spatial homogenization of coastal upwelling under climate change. Nature 518, 390–394. https://doi.org/10.1038/nature14235

Weijer, W., Cheng, W., Drijfhout, S.S., Fedorov, A.V., Hu, A., Jackson, L.C., Liu, W., McDonagh, E.L., Mecking, J.V., Zhang, J., 2019. Stability of the Atlantic Meridional Overturning Circulation: A Review and Synthesis. J. Geophys. Res. Oceans 124, 5336–5375. https://doi.org/10.1029/2019JC015083

Zika, J.D., Skliris, N., Blaker, A.T., Marsh, R., Nurser, A.J.G., Josey, S.A., 2018. Improved estimates of water cycle change from ocean salinity: the key role of ocean warming. Environ. Res. Lett. 13, 074036. https://doi.org/10.1088/1748-9326/aace42

ACRONYMS

20CR – 20th Century Reanalysis

AABW – Antarctic Bottom Water

AAIW – Antarctic Intermediate Water

AC – Azores Current

AED – Atmospheric Evaporative Demand

AEMET – Agencia Estatal de Meteorología/State Meteorological Agency

AL – Atlantic Low

AMO – Atlantic Multidecadal Oscillation

AMOC – Atlantic Meridional Overturning Circulation

AMV – Atlantic Multidecadal Variability

AN – Atlantic El Niño

ANOVA – Analysis of Variance

AO – Arctic Oscillation

AR – Atmospheric Rivers

ARG – Atlantic Ridge

AR6 – Sixth Assessment Report

ARTMIP – Atmospheric Rivers Tracking Method Intercomparison Project

AW – Atlantic Water

B-A – Bölling-Allerød

BA – Bias Adjustment

BBLI – Branas, Bernon and Levadoux Hydrothermic Index

BEDD – Biologically Effective Degree-Days

BLO – Scandinavian Blocking

BNDC – National Climatic Data Bank

BSh – Mid-latitude steppe and desert climate

BWh – Tropical and subtropical desert climate

CCC – cryogenic cave carbonates

CCS – Carbon Capture and Storage

CCUS – Canary Current Upwelling System

CDD – Consecutive Dry Days

CE – Common Era

CESM2 – Community Earth System Model 2CIT-Climate Index for Tourism

CF – Capacity factor

CFSR – Climate Forecast System Reanalysis

CHJ – Júcar Hydrographic Confederation

CIC – Internal Basins of Catalonia

CIW – Cretan Intermediate Water

CLIMPY – Characterization of the evolution of climate and provision of information for adaptation in the Pyrenees

CLIVAR – Climate Variability and Predictability

CMIP – Coupled Model Intercomparison Project

CMIP5 – CMIP Phase 5th

CMIP6 – CMIP Phase 6th

CNN – Convolutional Neural Network

COL – cut-off low

CORDEX – COordinated Regional Climate Downscaling EXperiment

CORDEX FPS – CORDEX Flagship Pilot Study

COSMO – COnsortium for Small-scale Modelling

CP – Circulation Patterns

CP-RCM – Convection-Permitting Regional Climate Model

CSIC – Consejo Superior de Investigaciones Científicas

CTD – Conductivity, Temperature, and Depth

DA – Dark Ages

DC – Drought Code

DD – Dynamical Downscaling

DeepESD – A Deep Learning-based Empirical Statistical Downscaling method

DF6 – Dry spell Frequency exceeding 6 months

DMC – Duff Moisture Code

DO – Dansgaard-Oeschger

DRM – dynamic recycling model

DTR – Daily Temperature Range

E-OBS – daily gridded land-only observational dataset over Europe

EA – East Atlantic

EA-WR – East Atlantic-Western Russia

EAP – East Atlantic Pattern

EBC – Eastern Boundary Current

ECA&D – European Climate Assessment and Dataset project

ECMWF – European Centre for Medium-Range Weather Forecasts

ECV – Essential Climate Variables

EFFIS – European Forest Fire Information System

EHF – Excess Heat Factor

EHFmax – Maximum Excess Heat Factor

EKE – Eddy Kinetic Energy

EMA – Early Middle Ages

EMED – Eastern Mediterranean

EMFD – Extreme Meteorological Fire Danger

EMT – Eastern Mediterranean Transient

ENA – Eastern North Atlantic

ENACW – Eastern North Atlantic Central Water

ENADW – Eastern North Atlantic Deep Water

ENSO – El Niño- Southern Oscillation

EOV – Essential Ocean Variables

EP – Eastern Pacific

EQM – Empirical Quantile Mapping

ERA-Interim – ECMWF atmospheric reanalysis fourth generation

ERA20C – ECMWF twentieth century reanalysis

ERA5 – ECMWF reanalysis fifth generation

ESD – Empirical Statistical Downscaling

ESGCM – Earth System Global Climate Model

ESGF – Earth System Grid Federation

ESL – Extreme Sea Levels

ESM – Earth system Model

ESTOC – European Station for Time series in the Ocean at the Canary Islands

EUCP – European Climate Prediction

EUMED – Mediterranean Europe

EURO-CORDEX – European branch of CORDEX

FAIR – Findability, Accessibility, Interoperability and Reusability

FD – Frost Days

FLEXPART – FLEXible PARTicle dispersion model

FOT30 – Frequency of Events FWI > 30

FPS – Flagship Pilot Study

FWI – Canadian Fire Weather Index

GCM – Global Climate Model

GCMs – General Circulation Atmospheric Models

GHG – Greenhouse Gas

GI – Greenland Interstadial

GMSL – Global Mean Sea Level

GNSS – Global Navigation Satellite System

GOME-2 – Global Ozone Monitoring Experiment 2

GPS – Global Positioning System

GRD – gravity, rotation and deformation

GS – Greenland Stadial

GSAT – Global Surface Air Temperature

GTS – Global Telecommunications System

GWL – Global Warming Level

HCI – Holiday Climate Index

HG – Hargreaves Evapotranspiration

HI – Huglin Index

HighResMIP-High Resolution Model Intercomparison Project

HR – High Resolution

HS1 – Heinrich Stadial 1

HTM – Holocene Thermal Maximum

HW – Heat Wave

HWS – heatwave season

HyMeX IOP12 – Intense Observation Period for the Hydrological Cycle in the Mediterranean Experiment

ICOADS – International Comprehensive Ocean-Atmosphere Data Set

IE – Industrial Era

IP – Iberian Peninsula

IPC – Iberian Poleward Current

IPCC – Intergovernmental Panel on Climate Change

IPCC-AR6-WGI – Working Group I contribution to the Sixth Assessment Report of the Intergovernmental Panel on Climate Change

IPCC-AR6-WGI-Working Group I contribution to the Sixth Assessment Report of the Intergovernmental Panel on Climate Change

IRDs – Ice Rafted Debris

IRI – International Research Institute for Climate and Society Timescale Decomposition Map Room.

ISD – Integrated Surface Database

ISIMIP – The Inter-Sectoral Impact Model Intercomparison Project

ITCZ – Intertropical Convergence Zone

IWV – integrated water vapor

JJA – June-July-August

JJAS – June-July-August-September

JRA25 – Japanese 25-year Reanalysis

ka BP – kilo year before Present, being Present the year 1950 CE

LARS-WG – Long Ashton Research Station Weather Generator

LGM – Last Glacial Maximum

LIA – Little Ice Age

LINCC-UIB – Interdisciplinary Climate Change Laboratory of the University of the Balearic Islands

LIW – Levantine Intermediate Water

LR – Low Resolution

LSW – Labrador Sea Water

LULC – Land Use and Land Cover Changes

MAAT – mean annual air temperature

MAE01 – Mean Absolute Error of the 1st percentile

MAE99 – Mean Absolute Error of the 99st percentile

MCA – Medieval Climate Anomaly

Med-CORDEX – Mediterranean branch of CORDEX

MedNA – Mediterranean and North Atlantic area

MERRA2 – Modern-Era Retrospective Analysis for Research and Applications, Version 2

MHW – Marine Heatwaves

MKE – Mean Kinetic Energy

MM – meridional mode

MME – Multi-Model Ensemble

MODIS – Moderate Resolution Imaging Spectroradiometer

MOPREDAS – MOnthly PREcipitation DAtabase of Spain

MOS – Model Output Statistics

MOTEDAS – MOnthly Temperature Dataset of Spain

MOW – Mediterranean Outflow Water

MSWEP – Multi-Source Weighted-Ensemble Precipitation

MW – Mediterranean Water

mwp – meltwater pulse

NAC – North Atlantic Current

NACLLJ – North African Coastal Low-Level Jet

NADW – North Atlantic Deep Water

NAO – North Atlantic Oscillation

NCAR – National Center for Atmospheric Research

NCEP – National Centers for Environmental Prediction

NOAA – National Oceanic and Atmospheric Administration

NPP – Net Primary Production

NSWS – Near-Surface Wind Speed

OA – Ocean acidification

OBSAM-IME – Socio-environmental Observatory of Menorca-Menorcan Studies Institute / L'Observatori Socioambiental de Menorca-l'Institut Menorquí d'Estudis

OD – Oldest Dryas

OHC – Ocean heat content

OMI – Ozone Monitoring Instrument

OPCC – Observatorio Pirenaico de Cambio Climático

ORL – Organic Rich Layer

P98Wet – 98th Percentile of Wet Days

PDV – Pacific Decadal Variability

PGW – Pseudo-Global Warming

PM – Penman-Monteith Evapotranspiration

PMIP – Paleo Model Intercomparison Project

PNACC – Plan Nacional de Adaptación al Cambio Climático

PP – Perfect Prognosis

RCM – Regional Climate Model

RCP – Representative Concentration Pathways

RDI – Reconnaissance Drought Index

RH – Relative Humidity

RSL – Relative Sea Level

RWP – Roman Warm Period

SAT – Surface Air Temperature

SCA – Scandinavian

SCA – Scandinavian pattern

SCAN – Scandinavian teleconnection pattern

SDII – Simple Daily Intensity Index

SLP – Sea Level Pressure

SLR – Sea Level Rise

SMILES – Single Model Initial-condition Large Ensembles

SO – Southern Oscillation

SON – September-October-November

SPEI – Standardised Precipitation-Evapotranspiration Index

SPI – Standardised Precipitation Index

SPREAD – Spanish PREcipitation At Daily scale

SRES – Special Report Emissions Scenarios

SROCC – Special Report on the Ocean and Cryosphere

SSP – Shared Socioeconomic Pathways

SSR – Surface Solar Radiation

SSS – Sea Surface Salinity

SST – Sea Surface Temperature

SSW – Sudden Stratospheric Warming

SUHI – Surface Urban Heat Island

SWE – snow water equivalent

SWE3 – Southwestern Europe at 3 km resolution

TCC – Total Cloud Cover

TCI – Tourism Climate Index

TH – Thornthwaite Evapotranspiration

THREDDS –Thematic Realtime Environmental Distributed Data Service

TMAS – mean annual ground temperatures

Tmax – Seasonal maximum temperature

Tmin – Seasonal minimum temperature

Tn – Minimum Temperature

TNA – Tropical North Atlantic

TNn – Minimum Annual Temperature

TOA – Top of the Atmosphere

TSI – Total Solar Irradiance

TSNA – tropical–subtropical North Atlantic corridor

TW – Wet Bulb Temperature

Tx – Maximum Temperature

TX35 – Number of days with maximum temperature exceeding 35°C

TXx – Maximum Annual Temperature

UAV – Unmanned Aerial Vehicle

UHI – Urban Heat Island

UTCI – Universal Thermal Climate Index

WAM-2layers – Eulerian Water Accounting Model-2layers

WBGT – Wet Bulb Globe Temperature

WBGTshade – Wet Bulb Globe Temperature in the shade

WBGTsun – Wet Bulb Globe Temperature in the sun

WD – Warm Days

WeMO – Western Mediterranean Oscillation

WeMOi – WeMO index

WG – Weather Generators

WI – Westerly Index

WMDW – Western Mediterranean Deep Water

WMED – Western Mediterranean

WMT – Western Mediterranean Transition

WMW – Western Mediterranean Water

WN – Warm Night

WPD – Wind power density

WR – Weather regimes

WRF – Weather Research and Forecasting

WSDI – Warm Spell Duration

XAI – Explainable Artificial Intelligence

XGB – Extreme Gradient Boost

YD – Younger Dryas